Faculty of Engineering and Science

Environmental Geochemistry of the Lower Baram River, Borneo

PRABAKARAN KRISHNAMURTHY

This thesis is presented for the Degree of
Doctor of Philosophy
of
Curtin University

September 2017

Declaration

To the best of my knowledge and belief this thesis contains no material previously published by any other person except where due acknowledgment has been made. This thesis contains no material which has been accepted for the award of any other degree or diploma in any university.

K. PRABAKARAN

6th September 2017

Acknowledgements

I would like to express my sincere gratefulness to my main Supervisor, A/Prof. Nagarajan Ramasamy, and Co-supervisor Dr. Eswaramoorthi Sellappa Gounder for their support, advices, guidance, suggestions and valuable comments throughout my research. I am truly grateful to my thesis committee Chairperson, A/Prof. Chua Han Bing, for his unwavering support. My sincere thanks to Dr. Merlin Franco Francis, for rendering his kind help, support and guidance, whenever needed. I would like to thank Curtin University, for providing me the Curtin Sarawak Postgraduate Research Fellowship, The Dean, Research and Development and the Dean, Faculty of Engineering and Science, Curtin University for their financial assistance throughout my research.

Special thanks to Dr. Vijith Hamza, for his paramount help and support throughout my research. Words are not enough to express my gratitude for your kindness. My sincere thanks to my dear friend Dr. A. Anand Kumar for his never ending genuine support in all my ups and downs of life. Thank you for being there with me all these days, my friend. My sincere thanks to Dr. Rajamohan, for his kind support and help throughout my research period.

This research would have been impossible without the inspiration and encouragement of my friends and well-wishers. I would like to express my deepest gratitude to my friends Dr. Surya Palani and Mr. V. Jagadeesan for their everlasting love towards me. My heartfelt thanks to Mr. L. Wai-Hwa, Dr. Shameel Mohammed, Mr. Jaison Jeevanandam and Ms. Ninu Krishnan for their kind help in my field works. Earnest thanks to my laboratory technicians Ms. Marilyn Andrew and Ms. Rassti and the laboratory manager, Ms. Helda Puyang Jaufor their moral support in handling the instrumentation facilities and providing the necessary chemicals required during the research period.

My sincere thanks to Mr. Fauzi Hj. Mob, the incharge of the boat for sample collection. I would also like to thank Mr. Eli, Mr. Tonny and Madam Kejan, campus security services for their support in accessing the laboratories after working hours and safety protocols.

Glory to God Almighty for having blessed me with such a wonderful family. Their continuous motivation takes me to achievements, always. Finally, I would like to thank

my HDR friends, department colleagues and staffs and administrative staffs at the Curtin University for their encouragement and support which made my stay and studies more enjoyable.

Frequently used list of abbreviations

AAS	Atomic Absorption Spectrophotometer
AMS	Accelerator Mass Spectrometry
APHA	American Public Health Association
BCF	Bio Concentration Factor
BCR	The Community Bureau of Reference
BDL	Below Detection Limit
BP	Before Present
CF	Contamination Factor
CRM	Certified Reference Material
DO	Dissolved Oxygen
EC	Electrical Conductivity
EC	European Commission
EDLs	Electrodeless Discharge Lamps
EU	European Union
EUCR	European Union Commission Regulation
FAO	Food and Agricultural Organization
FDA	Food and Drug Administration
FSA	Food Standards of Australia
GFAAS	Graphite Furnace Atomic Absorption Spectroscopy
HCL	Hallow Cathode Lamp
IBMK	Iso-Butyl Methyl Ketone
ICP-MS	Inductively Coupled Plasma Mass Spectrometer
I_{geo}	Geo-accumulation Index
MDL	Method Detection Limit
MFR	Malaysian Food Regulations
mg/L	Milligram per Litre
MPL	Maximum Permissible Limit
ND	Not Detected
NTU	Nephelometric Turbidity Unit
OC	Organic Carbon
ORP	Oxidation-Reduction Potential
PCA	Pearson Correlation Analysis

PCA	Principal Component Analysis
POM	Post-Monsoon
RAC	Risk Assessment Code
SEP	Sequential Extraction Procedure
SCS	South China Sea
SPSS	Statistical Package for Social Science
STD	Standard Deviation
SW	South-western
TDS	Total Dissolved Solids
UCC	Upper Continental Crust
PAAS	Post-Archaean Australian Shale
TF	Translocation Factor
USEPA	United State Environmental Protection Authority
USFDA	Food and Drug Administration of the United States
UV-SPEC	Ultra-Violet Spectrometer
WHO	World Health Organization
µg/L	Microgram per Litre
µg/g	Microgram per gram

Abstract

The Baram River is one of the largest rivers in Borneo, the third largest island in the world. The catchment area of the Baram River basin comprises about 22,800 km^2 and receives an annual rainfall of ~ 2500 to 4000 mm/year, and delivers ~50 billion m^3 of fresh water and ~24 million tonnes of sediments annually into the South China Sea. The river basin has a complex geology and is mainly composed of turbidites, Neogene volcanic lavas/tuffs, Miocene intrusives, limestones (Melinau) and Quaternary-Holocene coastal and river alluvium. In order to understand the environmental geochemistry of this complex terrain, seasonal surface water and sediment samples, core sediments, and root, bark and leaves from mangrove trees were collected from the Lower Baram River (Kuala Baram to Marudi). The Provenance analysis and tectonic discrimination diagrams revealed the source rocks are predominantly recycled felsic materials from the sedimentary and meta-sedimentary terrane of the Baram Basin with minor mafic input from Pliocene volcanic rocks. The CIA, PIA and CIW weathering indices and element ratios point to a moderate to high weathering intensity in the source region, however the weathering signal is masked by recycling, thus quartz dilution. Based on detrital Zr grain geochronology, the major provenance area was main range granites of West Malaysia and the Schwaner Mountains of Southern Borneo for the source rocks of the Baram Basin, which have been recycled. The age of the youngest zircons indicates the Usun Apau Plateau also contributed fresh sediments, which have been mixed with the recycled sediments from sedimentary to meta-sedimentary rocks of the Baram Basin.

The factor analytical model revealed that in the monsoon (MON) season water column, adsorption onto Mn-hydroxide floccules was the dominant mechanism controlling trace element behavior in the Lower Baram River. The $Al(OH)_3$ may also have a significant role in trace element transportation. Furthermore, formation of authigenic clay mineral is indicated. During the post-monsoon (POM) season, the incursion of saline water has resulted in the remobilization of Pb, Ni, and Co from the sediments. However, the remobilized Pb and Ni are redistributed between aluminium and Mn-oxyhydroxides, whereas, Co is released to the water column. Water column pH and dissolved oxygen were found to be the dominant factors controlling the levels of orthophosphate and ammoniacal-nitrogen.

In the surface sediments, during the MON season the grain size distribution of the sediments segregate the elements Al, Fe, Mn, K, Sc, Be, V, Ba, Sr, Ni, Rb, Cs, Eu, as one group and discriminate Si, Ag, Zr, Hf as another group. This is the primary mechanism responsible for exerting control over the chemical composition of the sediments. The grouping of Cu, Zn and Sn indicated both natural and anthropogenic sources contribute to the concentrations of these elements. The presence of chromite and powellite minerals in the detrital phase has also been revealed. During the POM season, most of the major and trace elements were associated with clay. Detrital minerals are associated with either granite or hydrothermal veins in the source area contributed to the observed patterns in W, Nb, Ag and Sn. A differential mobility of Na was observed in the sediments, possibly due to the weathering of fresh Na-bearing feldspar from the volcanic rocks of Usun Apau. The sequential extraction of the sediments revealed differing patterns of elemental distribution among various fractions during the MON and POM season. Manganese was the only element with a high concentration in the exchangeable (F1) fraction during both seasons. An average sedimentation rate of 0.21 cm y^{-1} from 2670 to 1970 BP was revealed from the core sediments by neglecting out the reverse age. The observed reverse age may indicate a local slump due to tectonic activity, which may have taken place during the Late Holocene in this region. The whole core represents the source rock rather than the hydrological regime. No major variations of weathering intensity was evident during the deposition of core sediments and this denotes a predominant influence by the detrital input, rather than the fluctuation of redox conditions.

Risk assessment of the surface and core sediments was performed using risk indices such as Contamination Factor (C_f), Geoaccumulation Index (I_{geo}), Pollution Load Index (PLI), ERL-ERM (Effect Range Low – Effect Range Median) and Risk Assessment Code (RAC). The C_f values suggested the surface sediments were contaminated by Cu, Zn, Sn, Cr, Sb and W and the core sediments were contaminated by Cu, Zn, Sn, Pb, Mn, Ni, Co and W. However, based on I_{geo} values the sediments of the Lower Baram River are highly contaminated by Cu and this has been confirmed by other indices. In order to assess the status of bioaccumulation of the elements on the biota, the concentration of elements on different tissues of mangroves was studied and found none of the elements

was above the toxic range in any of the tissues. The ANOVA results suggested there was no significant difference ($P < 0.05$) of BCF values between the tissues for Fe, Mn, Zn and Pb. However, between the same tissues there was a significant difference ($P < 0.05$) for Cu, indicating the active intervention by plant physiology in the translocation of copper. Similar to Cu, the Cd translocation is also controlled by plant physiology.

Contents

List of Tables

List of Figures

Chapter 1. Introduction

Environmental geochemistry is the discipline that examines the chemistry of the solid earth, its aqueous and gaseous components, and life forms to evaluate the actual impact of various contaminants on our planet's ecosystem (Siegel, 2002). To illustrate the full impact of environmental contaminants on a diverse ecosystem, a multidisciplinary research approach is needed. Hence, an integrated environmental study using a combination of chemical and biological based assessments will demonstrate the geochemistry and bioavailability as well as interactive and combined effects of contaminants with regard to numerous environmental factors characterizing a particular location. The dissolved and particulate loads carried by rivers undergo a lot of changes while moving downstream, especially in the estuarine environment by a number of biogeochemical processes. As a result, research on the behavior of the elements, during their transport downstream as well as in the estuaries are important for evaluating the estuarine modification of river input of chemical elements to the ocean.

According to Cameron and Pritchard (1963), “an estuary is a semi enclosed and coastal body of water with free communication to the ocean, and within which ocean water is diluted by freshwater derived from land”. Estuaries play a critical role in the life history and development of many aquatic species and are the most productive marine ecosystems in the world (Underwood & Kromkamp, 1999). They are important feeding, migration and rearing zones for aquatic life and home to a diverse range of plant species. Estuaries support recreational and commercial fisheries, making them significant ecosystems in terms of ecological, environmental and economic value (Chapman & Wang, 2001). However, estuaries are also one of the main recipients of almost all anthropogenic discharges of pollutants, which makes it imperative to undertake studies at the geochemical and biological levels as they play a significant role in the life cycle of several aquatic organisms (Chiffoleau et al., 1994; Kennish, 2002; Amado et al., 2006). The sedimentation processes in estuaries play a major role and influence the river input of trace metals to the sea (Zwolsman & Van Eck, 1999). Estuaries are characterized by strong hydrodynamic and physio-chemical gradients,

which accounts for the variations in the distribution of trace elements between dissolved and particulate species. These modifications along with the fluctuations of the water and total particles discharge, influence the metal fluxes in the estuarine region (Paucot & Wollast, 1997). There is a growing interest in studying the geochemistry of trace metals in rivers and estuaries in order to understand the processes that determine the fate of the metals and to estimate the net riverine contribution to the metal budget of the world oceans (Kraepiel et al., 1997).

1.1 Classification of estuarine systems

Generally the need for habitat classification was developed from merely a scientific debate, such that workers may be familiarized with the terms used in the field, in regards to the politico-socio-management sphere (Elliott & McLusky, 2002). Environmental scientists and managers use classification to understand, protect and manage natural resources (Engle et al., 2007). As estuaries are a valuable recreational, commercial and aesthetic resource, their classification can be a useful tool for coastal resource management and also aids in the transfer of knowledge between estuaries of the same type (Hume & Herdendorf, 1988). Estuarine classification is a broad topic and is based on several criteria. Estuaries have been classified according to several schemes, including topography/geomorphology (Pritchard, 1967; Hume & Herdendorf, 1988), hydrodynamics/ circulation (Stommel & Farmer, 1952; Ketchum, 1954; Pritchard, 1967; Cameron & Pritchard, 1963; Hansen & Rattray, 1966), trophic status (Bricker et al., 1999, 2003; Nobre et al., 2005) and hybrids of the above. Estuaries have traditionally been classified based on their geomorphology and their salinity stratification (Hansen & Rattray, 1966).

1.1.1 Classification of estuaries based on geomorphology

On the basis of geomorphology, estuaries have been classified into four types (Pritchard, 1952). They were drowned river valleys, fjords, bar built estuaries and tectonic estuaries. The description of the types with examples are given in Table 1.1.

Table 1.1 Physiographic classification of estuaries (adopted from Pritchard, 1967)

Type of estuary	Description	Examples
Drowned river valley	Found along coastlines with wide coastal plains; Funnel shaped with exponential increase in cross section towards the mouth. Only a part of the area affected by tides is estuarine based on salinity diluted by freshwater.	Chesapeake Bay, Delaware bay, Thames and Grinode rivers.
Fjord	Generally U-shaped, gouged out by glaciers; Has a characteristic shallow sill near or at their mouth that closes the very deep valley.	Norwegian and British Columbia (Canada) coastlines
Bar-built	Also called coastal lagoons. Offshore barrier sand islands and sand spits build above sea level and extend between headlands in a chain broken by one or more inlets; enclosed area generally elongated relative to shoreline; may be more than one river drainage; reduced tidal action; wind-driven circulation	Pamlico Estuary, USA, Dos Patos lagoon, Brazil.
Tectonic	Coastal indentures formed by faulting or local subsistence, with an excess freshwater Flow	San Francisco Bay, Valdivia river, Chile and Itamaraca, Brazil.

1.1.2 Classification of estuaries based on water stratification and circulation

In addition to geomorphology, estuaries can also be classified based on the water column stratification or salinity vertical structure as a salt wedge, strongly stratified, weakly stratified or vertically mixed (Pritchard, 1955; Cameron & Pritchard, 1963). Considering the buoyant force of the river and competitive mixing from the tidal force, the classification can be made. The description of the classification types with examples are tabulated in Table 1.2.

Table 1.2 Classification of estuaries by water stratification and Circulation

Type of estuary	Description	Examples
Salt wedge	Large river discharge and weak tidal force; the tidal force influences the penetration of salt water up the estuary in the form of a defined wedge whose upstream penetration is greatest during periods of low river flow and least during periods of high river flow.	Mississippi (USA), Rio de la Plata (Argentina), Vellar (India), Ebro (Spain), Pánuco (México), and Itajaí-Açu (Brazil)
Strongly stratified	Moderate to large river discharge and weak to moderate tidal force; the bottom transitional area does not demonstrate the large-scale seasonal movements to upstream and downstream such as in salt wedge estuaries.	Silver Bay (Canada) and Vellar estuary (India)
weakly stratified or partially mixed	Moderate to strong tidal forcing and weak to moderate river discharge; Shows vigorous mean exchange flow when compared to other types of estuaries because of the mixing between riverine and oceanic waters.	Chesapeake Bay system (The James River,US), River Tees and the Thames River (UK)
Vertically mixed estuaries	Strong tidal forcing and weak river discharge; result in vertically mixed estuaries. Mean salinity profiles are virtually uniform and mean flows are unidirectional with depth.	Examples of this type of estuary are scarce, but however, parts of the lower Chesapeake Bay may exhibit this behavior in early autumn.

1.2 Weathering and riverine transport of trace elements

Rivers are responsible for the terrigenous materials supplied from land to ocean (Martin & Meybeck, 1979). Rivers transport eroded materials from the continents to the oceans (Martin & Whitfield, 1983). Transport of riverine suspended sediments has significant effects on the coastal environment and evolution of the delta region and marine production in shelf areas (Zhang, 1999). Rivers play a key role in the global geochemical cycle (Martin & Meybeck, 1979; Ludwig & Probst, 1996; Viers et al., 2009; Oelkers et al., 2011, 2012; Gaillardet et al., 2014). Large tropical rivers around the world are being investigated on a variety of subjects, besides the great complexity of tropical climates and the enormous extent of tropical river basins. Rivers are regarded as

the carriers of extensive chemical signals to the world's oceans, as they play a major role in the transport of materials originating from both natural crustal weathering and anthropogenic processes along the land - sea margins. Both dissolved and particulate compounds characterize riverine material. Dissolved compounds are mainly transported through water across aquatic systems. However, particulate compounds are transported in accordance with flow velocity; or may settle and be remobilized; or transferred based on particle size and shape, riverbed morphology, etc. Thus, in riverine systems, dissolved materials and particulate materials exhibit distinct pathways and transport characteristics.

Among the 110 or more known chemical elements, about 90 are metals plus some metalloids. These metals are categorized as either essential metals, which support normal biological processes or non-essential metals with no known biological function. River discharge contributes to the major input of trace metals to the ocean, apart from windblown dust. Trace element association in dissolved as well as particle and colloidal phases will determine their fate in estuarine processes as well as the ocean. Therefore, studying trace elements and their physiochemical properties in rivers is paramount in understanding their fate in the ocean (Dahlqvist et al., 2007). Asian rivers are responsible for 50% of the seaward sediment influx in the world with poorly developed drainage basins and therefore the study of these less disturbed systems may present insights into weathering and erosion control in aquatic chemistry (Zhang & Huang, 1993). To evaluate the environmental health risks in estuarine and coastal areas, it is critical the chemical and physical processes occurring during the transport pathways are well documented and the fluxes of riverine trace elements are accurately estimated (Hu et al., 2015).

1.2.1 Weathering processes responsible for the release of trace elements from rocks and minerals

The geochemical cycle of elements on the Earth's surface is predominantly controlled by the chemical weathering of crustal rocks. The changes in the Earth's surface and the geochemical cycling of elements are mainly arbitrated to the chemical weathering of rocks. Consumption of atmospheric and/or endogenous carbon dioxide

during chemical erosion causes the extraction of metals from rocks, which are then released into rivers and shallow ground water and is finally discharged into the ocean (Garrels & MacKenzie, 1972). The parent-rock type, topography, climate and biological activity are some of the main variables, which control the rate and nature of chemical weathering. The continental rocks are partially dissolved because of chemical weathering to form soil and this is then followed by mechanical erosion in which soils are physically broken up. The products of both chemical and mechanical denudation of rocks are transported from the continents to oceans by rivers. Weathering aids the mobilization and redistribution of trace elements, which is rather complicated as these elements are influenced by various processes such as dissolution of primary minerals, formation of secondary phases, redox processes, transport of materials, co-precipitation and ion exchange of various minerals (Nesbitt, 1979; Fritz & Ragland, 1980; Nesbitt and Markovics, 1980; Chesworth et al., 1981; Fritz & Mohr, 1984; Harriss & Adams, 1966). The products of weathering can collectively represent the lithology, the degree of physical and chemical weathering experienced by the source area and the subsequent changes during transportation and the deposition processes (Singh et al., 2005; Armstrong et al., 2013; Nagarajan et al., 2017a,b).

Most of the soluble elements are released during the process of chemical weathering of rocks but in the case of silicate rocks, there remains a residue, which is enriched in the insoluble elements. Weathering processes greatly influence the abundance of trace elements in rivers apart from the source rocks. The trace elements, when not depleted by chemical weathering and transport processes and are not influenced by diagenesis, metamorphism etc., their ratio in the particles is expected to be similar to that of the source rock from which they are derived. Hence, the abundance of trace elements in rivers depends not only on their abundance in source rocks but also on the weathering style (Gaillardet et al., 2014). The factors which determine the actual river chemistry include the element partitioning between dissolved and solid phases, water and sediment loads, as well as weathering features of the drainage basin (Zhang et al., 1994). The behavior of trace elements in various weathering environments are presented in Table 1.3. The basic weathering processes are characterized as follows (Kabata-Pendias, 2011):

- Dissolution: minerals are soluble in the aquatic phase
- Hydration: minerals increase their water content
- Hydrolysis: reaction of minerals with water, producing new ions and/or insoluble components
- Oxidation: incorporation of oxygen into the chemical components or increase of the element potential
- Reduction: reactions that are the reverse of oxidation
- Carbonatization: alteration of compounds into carbonates due to the incorporation of CO_2.

Table 1.3 Behavior of Trace Elements in Various Weathering Environments

(Adopted from Kabata-Pendias, 2011)

Degree of Mobility	Environmental Conditions	Trace Elements
High	Oxidizing and acid	B, Br, and I
	Neutral or alkaline	B, Br, F, I, Li, Mo, Re, Se, U, V, W, and Zn
	Reducing	B, Br, and I
Medium	Oxidizing and acid	Li, Cs, Mo, Ra, Rb, Se, Sr, F, Cd, Hg, Cu, Ag, and Zn
	Mainly acid	Ag, Au, Cd, Co, Cu, Hg, and Ni
	Reducing, with variable potential	As, Ba, Cd, Co, Cr, F, Fe, Ge, Li, Mn, Nb, Sb, Sn, Sr, Tl, U, and V
Low	Oxidizing and acid	Ba, Be, Bi, Cs, Fe, Ga, Ge, La, Li, Rb, Si, Th, Ti, and Y
	Neutral or alkaline	Ba, Be, Bi, Co, Cu, Ge, Hf, Mn, Ni, Pb, Si, Ta, Te, and Zr
Very low	Oxidizing and acid	Al, Au, Cr, Fe, Ga, Os, Pt, Rh, Ru, Sc, Sn, Ta, Te, Th, Ti, Y, and Zr
	Neutral or alkaline	Ag, Al, Au, Cu, Co, Fe, Ga, Ni, Th, Ti, Y, and Zr
	Reducing	Ag, As, Au, B, Ba, Be, Bi, Cd, Co, Cu, Cs, Ge, Hg, Li, Mo, Ni, Pb, Re, Se, Te, Th, Ti, U, V, Y, Zn, and Zr

1.2.2 Trace element transport in dissolved form

Water finds its way to the river environment directly from the atmosphere or indirectly from surface runoff, underground water circulation and the discharge. Rock weathering, the decomposition of organic material, wet and dry atmospheric deposition and human induced discharges are the sources of the presence of dissolved and particulate components in river water. The strength of these sources are controlled by a number of complex, often interrelated, environmental factors that operate in an

individual river basin which may include rock lithology, relief, climate, the extent of vegetative cover and the magnitude of pollutant inputs (Chester & Jickells, 2012). Dissolved or soluble fraction of trace elements represents the fraction, which passes a 0.45µm pore size filter (Batley & Gardner, 1977). Trace element abundance in rivers is influenced by their abundance in the continental crust as well as their mobility during weathering and transport. Trace element transport per liter of river water is subjected to the mobility of the element in the weathering transport process and on the annual solid transport by the river. Variations in the dissolved trace element abundance in rivers is greatly influenced by the preferential dissolution of the different types of lithology or minerals (Gaillardet et al., 2014).

Trace element mobility in river water is influenced by a combination of several factors, including; their solubility in water, contribution from non-weathering sources such as atmospheric and/or anthropogenic sources, the ability of the elements to be complexed by fine (<0.2µm) colloidal material, and the affinity of the elements for solids by processes such as adsorption, co-precipitation and solubility equilibrium (Gaillardet et al., 2014). Knowledge of the temporal concentration of dissolved trace elements in rivers is important for flux calculations, for understanding the mechanisms controlling the concentrations of these elements in rivers, and for the design of research and monitoring programs (Shiller, 1997). The global systematics of trace elements in river water is still poorly understood (Gaillardet et al., 2014). Reliable measurements of dissolved trace metal concentrations in rivers is essential for calculating organic chemical mass balances, understanding continental weathering and freshwater chemistry and for assessing anthropogenic chemical perturbations (Shiller & Boyle, 1985).

1.2.3 Trace element transport in particulate form

Rivers transport continental weathering materials to the oceans and particulate fluxes dominate dissolved fluxes for most elements (Oelkers et al., 2011). The transport of trace metals in rivers involves certain chemical mechanisms, which are: dissolving ionic species and inorganic associations, complexing with organic molecules in solution, adsorption on solids, precipitation and co-precipitation on solids (metallic coatings), incorporation in solid biological materials, and incorporation in crystalline structures

(Gibbs, 1973). The average runoff rates in a river affects particle chemistry, with high runoff in a river transporting the most heavily altered particles (Yiğiterhan et al., 2011). Many trace metals adsorb strongly on particles (Balistrieriet al.,1981; Balistrieri & Murray, 1981) and thus they are preferentially associated with particulate matter in rivers (Guieu et al., 1998; Guieu & Martin, 2002). The study of riverbeds and suspended sediments is essential as they represent the mixing of weathering products in drainage basins and provide key information of provenance, tectonic setting and weathering mechanisms (Martin & Meybeck, 1979; Stallard & Edmond, 1983; Wu et al., 2011).

There are two genetically different element – host associations (Chester and Jickells, 2012). They are,

I. Elements associated with the crystalline mineral matrix (the detrital or residual fraction), which are in an environmentally immobile form and largely have their concentrations fixed at the site of weathering.
II. Elements associated with non - crystalline material (the non - detrital or non - residual fraction), which are in environmentally mobile forms and have their concentrations modified by dissolved and particulate reactivity.

The non-detrital fraction contains many elemental associations such as an exchangeable fraction; a carbonate bound fraction, fractions associated with a metal oxide, and an organic matter associated fraction. A variety of techniques are available to partition the elements among these host components and one of the most common involves the sequential leaching or sequential extraction of the primary sample with a number of reagents that are designed progressively to take into solution elements associated with the individual hosts (Chester, 2012).

1.2.4 Role of dissolved and particulate organics in trace elements transport

The dissolved organic carbon (DOC) can be largely the resultant from terrestrial sources (i.e. allochthonous) and consists of high and low molecular weight organic substances such as humic and fulvic acids, which originate from the decomposition of organic matter such as leaves and plant debris and subsequent accumulates in soils (Hedges et al., 1994; Raymond & Bauer, 2001; Bianchi et al.,2007; Mora et al.,2014). The particulate organic carbon (POC) is the result of allochthonous and autochthonous

sources. Allochthonous POC comprises plant debris or litter and humic substances adsorbed onto mineral surfaces, whereas autochthonous POC consists of autotrophic organisms such as phytoplankton, periphyton, bryophytes, etc. of the aquatic community (Minshall, 1978; Mora et al., 2014). The dissolved organic matter (DOM) is comprised from a range of organic molecules, of which humic substances are the primary metal-binding ligands for trace metals including copper and iron (Tipping, 2004). DOM influences the bioavailability of trace metals as they can enable the binding of trace metals and toxic metals. For example, humic substances influence the complexation of aluminium. The complexation of Al^{3+} is weak under lower pH conditions, resulting in detrimental effects to biota. As pH rises, Al is increasingly complexed with DOM, decreasing its toxicity (Tranvik & Von Wachenfeldt, 2009).

1.3 Study Area - The Lower Baram River

Sarawak is one of two Eastern Malaysian states situated immediately to the north of equator lying between latitude 0°50´N and 5°N and longitude 109°36´E and 115°40´E on the northwest coast of the island of Borneo, bordering the Malaysian state of Sabah to the northeast, Indonesia to the south, and surrounding Brunei. Being in a tropical region, Sarawak experiences an equatorial climate with two monsoonal changes (i.e., Northeast and Southwest monsoon). Generally, the climatic conditions are stable in Sarawak throughout the year except for the monsoonal events. The state receives about 3300mm to 4600mm of annual rainfall. The Baram River basin receives an annual rainfall of about 3000 - 4000mm, of that, about 76% of the total rainfall occurs from July to March. The remaining 24% falls from April to June (Nagarajan et al., 2015).

The Baram River is the second longest river in Sarawak, extending to about 466 km in length. The river initially flows westwards through tropical rainforests, and then turns northward to drain into the South China Sea at Miri (near Kuala Baram). Miri is one of the major cities located in the estuarine part of the river and the region is poised for major industrial growth with various hydroelectric power plants planned for the Upper Baram River (Nagarajan et al., 2015). Miri's history of commercial activities related to numerous oil and gas producing companies' dates back to 1910, when the first oil well was drilled. There are also numerous ship building companies, most of which

are based in Kuala Baram. Moreover, there are a number of timber processing and palm oil production industries along the banks of the river, which ultimately adds to the pollution loads of the Baram River estuarine system. To date there is very little available data regarding the pollution status of the Baram River estuarine system and this is the main reason this river was selected as the study site for the proposed study.

Covering a catchment area of about 22,800 km^2, the Baram River discharges an estimated 1590 m^3/s of water and 2.4×10^{10} kg of sediment load per year (Sandal, 1996; Straub & Mohrig, 2009). The rapidly flowing river discharges into the South China Sea resulting in a higher stratification of water column, which has led to the formation of a typical salt wedge estuary. The salt-wedge or highly stratified estuaries are characterized as having a high degree of water column stratification, low tidal range, and high river discharge rates (Stommel, 1953; Pritchard 1967). Depending on the monsoon, the salt wedge varies in stratification (Figure 1.1 and Figure 1.2).

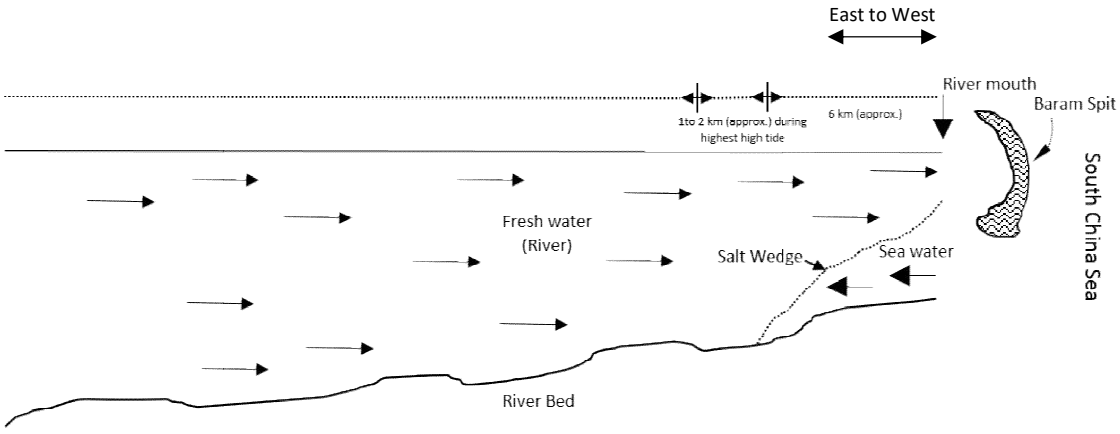

Figure 1.1 Longitudinal cross section of the Baram estuary during peak monsoon

(The force of the river is very high due to flood inflow which restricts the transport of tidal currents to upstream of the river)

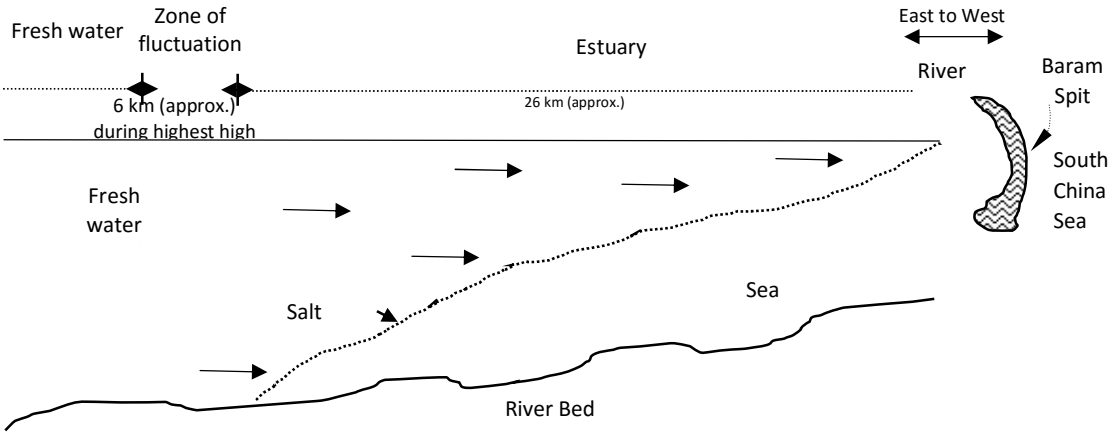

Figure 1.2 Longitudinal cross section of the Baram estuary during non-monsoon

(The absence of flood inflow results in the transport of tidal currents to upstream of the river to some extent when compared to monsoon period)

A total of 32 sampling locations, covering a distance of about 111 Km were selected for the present study starting from the Baram River mouth to Marudi, a riverine town (Figure 1.3). Based on the salinity and mangrove population, which has been observed at the 16th site, there is a zone of transition between the 16th and 17th sites. Sites 17 to 32 represent the freshwater zone. Thus, the selected sampling locations represent both riverine as well as estuarine conditions. Starting from the Baram River mouth, the first 16 sites (BES 01 – BES 16) are in the Baram estuary and the remaining 16 sites, located further upstream as far as Marudi (BES 17 – BES 32) are the Baram River (riverine) sites for the present study (Figure 1.3).

1.4 Geology of the Baram River Basin

The geology of the Baram River basin has been extracted from the geology map (Scale 1:500,000) published by the Geological Society of Malaysia (Figure 1.4). The Baram catchment geology consists predominantly of meta-sedimentary to sedimentary rocks aged from Paleogene to Recent. The upstream region is primarily covered by Oligocene, Miocene and Eocene sediments whereas the downstream region primarily consists of Quaternary River and coastal alluvium as the Baram river month was originally located near Marudi but has extended towards north over the past 5000 years (Caline & Huong, 1992). This is a result of extensive erosion in land and deposition

downstream as the river profile flattens out. The alluvium deposits also include thick peat soils, which is quite common in the lower river section (Anderson, 1964). There are very small minor acid/basic intrusive rocks in the SW part of the River basin (Usun Apau area). Deep water turbidites are common in the eastern part of the basin and nearer to Long Loma. The Miocene to Pliocene sediments are mostly recycled materials (Van Hattum et al., 2013; Nagarajan et al. 2014, 2015, 2017a, b) and recycling is common until today. Structural trend lines are oriented in a NE-SW direction. Geological units and their approximate locations are summarised in Table 1.4. The units are listed in order of increasing age (i.e. with youngest at the top). Limestones are common in the NE part of the study area belonging to the Melinau Limestone Formation and minor exposures are common near Long Loma area.

Figure 1.3 Study area map showing sampling locations

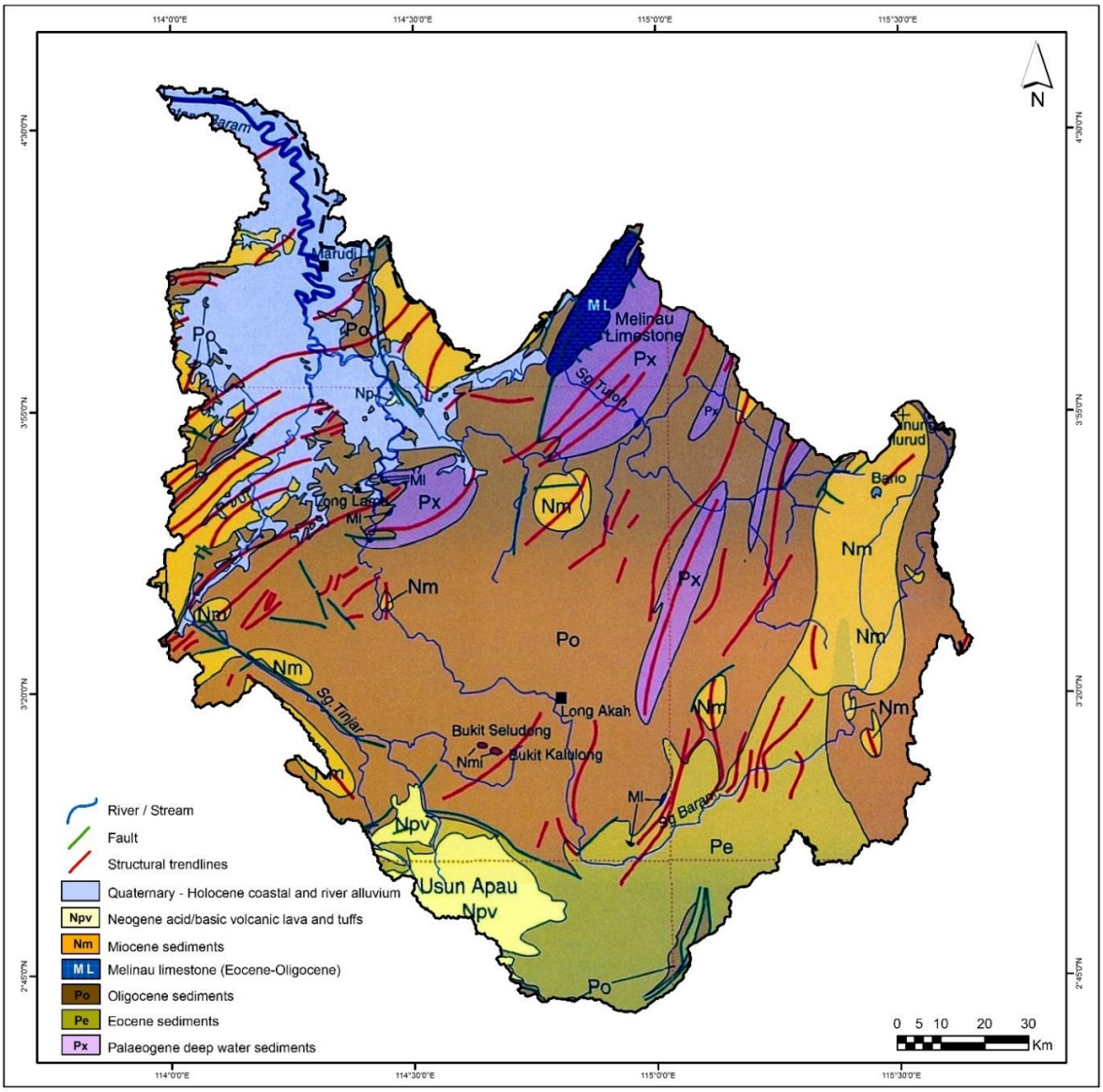

Figure 1.4 Geological map of the Baram River Basin

(Source: 1:500,000 Geological Map of Borneo published by Tate, RB; Geological Society of Malaysia)

Table 1.4 Geological Units of the Baram River Basin

(Extracted from 1:500,000 Geological Map of Borneo published by Tate, RB, Geological Society of Malaysia) and their location details.

Unit Code	Unit Description	Significance in basin	Location
-	Quaternary-Holocene coastal and river alluvium	Intermediate	Downstream of Long Lama
Npv	Neogene acid/basic volcanic lavas and tuffs	Minor	Usun Apau plateau
Nmi	Miocene I type intrusives	Very minor	Bukit Seludong and Bukit Kalulong
Nm	Miocene sediments	Intermediate	Bario, Dulit Range, Long Lama to Marudi to Miri zone
Ml	Melinau Limestone	Minor	Near southernmost point of Baram and Mulu
Po	Oligocene sediments	Major	Mostly upstream of Long Lama and downstream of Sg. Tutoh.
Pe	Eocene sediments	Intermediate	South of Baram
Px	Paleogene deepwater sediments	Intermediate	Several isolated zones

1.5 The significance of the problem

The Baram River is one the world's major rivers with a catchment area of 22,800 km^2. The rainfall intensity in the river basin varies from 2500 to 4000 mm/year. The estimated annual discharge of the Baram River is 1590 m^3/s of fresh water and 24 million tonnes of sediments into the South China Sea (Sandal, 1996; Straub & Mohrig, 2009). Geologically, the river basin mainly consists of sedimentary-meta-sediment rocks of Oligocene to Miocene that have formed under deep marine conditions during earlier geological periods. In addition, neogene acid acid/base volcanic lavas/tuffs, Miocene I type intrusives, limestones (Melinau) and Quatenary-Holocene coastal and river alluviums are exposed in the Baram River Basin. However, a significant section of the upper Baram basin is covered by Oligocene sediments. Due to weathering, the trace elements are leached into the river water. The river water, when it reaches the intertidal zone or, estuarine region, deposits all of the transported metals and organic matter. As the intertidal and shallow sub-tidal sediments of the Baram River consist of mud and

sand (Lambiase et al., 2002), the accumulation and remobilization of these trace elements are primarily affected by sediment texture. The Baram River Delta, which has a sub-aerial area of 300 km^2, has been undergoing erosion since 2000 BP. The diurnal tides with a range of 1.7 m (Sandal, 1996) creates tidal currents within the intertidal zone, which flush out the deltaic sediments and associated trace elements into the South China Sea.

Peat deposits from the Baram River area, Sarawak, are thick and extensive with thicknesses range from 1 to 12 m (Cameron et al., 1989). Thick clay and sand deposits, which were deposited by the pro-gradation of the Baram River, have formed the basis of the peat (Wilford, 1966). The upper reaches of the present Baram River valley are confined by terraced highlands that outline the original coastal embayment that existed during a period with a higher sea level, about 4000-5400 years ago (Wilford, 1962). Since then, the embayment has been filled with sediment as the Baram River delta prograded seaward to the north. It is on this surface the peat deposits have formed (Cameron et al., 1989). This peatland, which has been drained due to the lowering sea-level since 2000 years BP, often are burned, releasing a significant amount of trace metals into the coastal areas. The weathering and leaching of trace elements from turbidites, metal remobilization from the sediments in the intertidal zone by tidal currents and peat fires, all contribute to significant environmental problems. The present study was carried out to understand the geological processes, by reconstructing the history of sediment and metal accumulation, and the results of the study will contribute to the knowledge of trace metal levels observed in different compartments (i.e. water, surface and core sediment, and mangrove plants) of the Baram River and its impact on the estuarine ecosystem. In addition, the provenance, intensity of weathering and maturity of the sediments have also been studied to establish the effect of natural processes under anthropogenic influences.The Sarawak Energy Board (SEB) has proposed construction of 3 dams on the Baram River. The construction of dams will affect the ecosystem of the river by altering the physical characteristics and endurance of reservoir habitats, flow distribution, organic matter, water velocity, water depth and water temperature in the reservoir leading to the subsequent disruption of biota associated with the reservoir (Tiemann et al., 2004). The results from the present

research study can also serve as a baseline data inventory for the local government, environmental managers, researchers and policy makers.

1.6 Objectives

The aim of the present research study is to achieve a comprehensive assessment of metal distribution in different compartments of the Baram River estuarine system and to assess their bioavailability, and potential impact on aquatic biota. For this purpose, the following objectives were identified:

1. To study the geochemistry and distribution of major and trace elements in water and sediment compartments of the Lower Baram River based on standard environmental guidelines.
2. To determine the history of major and trace elements accumulation in sediment cores of the Baram River estuarine system.
3. To study the bioaccumulation of trace elements in different tissues of the mangroves in the Baram River estuarine system.

Chapter 2. Review of Literature

2.1 The behaviour of trace elements in estuaries

The element partition between solution and suspended particles in rivers undergoes drastic changes during estuarine mixing in response to the changes in pH, ionic strength, solution composition, etc. (Li et al., 1984). The biogeochemical and sedimentological processes that are taking place in the estuaries and coastal areas determine the flux and fate of trace metals being transported from the continent to the ocean. Knowledge of these processes is therefore of paramount importance in interpreting the consequences of anthropogenic alteration of discharge, and in evaluating the capacity of the receiving waters to accommodate wastes without detrimental effects (Martin et al., 1993). Physical, chemical, and biological interactions between freshwater and saltwater systems can have profound influences on the transport and fate of trace metals (Ip et al., 2007). The estuarine distribution of trace metals is controlled by complex dynamic processes, which are linked to each estuary's particular physical and geochemical characteristics (Keeney-Kennicutt & Presley, 1986). The complex processes of material exchange with trace metal distribution in estuarine environments can also be affected by anthropogenic inputs (Ip et al., 2007). Knowledge of the geochemical dynamics of estuaries is essential for constructing elemental mass balances for the coastal zone as well as for the ocean as a whole (Shiller & Boyle, 1991).

Due to the presence of strong hydrodynamic and physio-chemical gradients, estuaries account for modifications of the distribution of trace elements between various dissolved and particulate classes. These modifications along with fluctuations of the water and total particles discharged, can influence the fluxes of heavy metals of the estuarine region (Paucot & Wollast, 1997). The trace metal distribution and behaviour within the estuarine mixing zone are basically examined and interpreted in relation to salinity, i.e. if they behave conservatively or not (Garvine, 1975; Martin et al., 1993; Cindrić et al., 2015). Factors such as redox, ionic strength, abundance of adsorbing surfaces, and pH control the fate and transport of trace elements in estuaries (Förstneret al., 1989; Wen et al., 1999; Bradl, 2004). Variations in the estuarine in situ processes specifically, coagulation and flocculation in the estuarine turbidity maximum,

resuspension events of sediments and porewaters, and sedimentation processes greatly influence the partitioning of trace metals between the dissolved and particulate fractions (Santschi et al., 1997). All of these processes are responsible for the complexity of trace metal speciation in estuaries (Boyle et al., 1977; Shiller & Boyle, 1987; Buffle, 1989; Honeyman & Santschi, 1989; Santschi et al., 1997). Larger scale internal and external processes such as storm events, tidal exchanges, wind effects, and inputs from rivers and bordering wetlands also can influence the overall partitioning of metals in estuaries (Bianchi, 2007). Besides hydrodynamic patterns, all estuaries share certain common processes such as adsorption/desorption, flocculation, biological uptake, sediment resuspension, as well as organic/inorganic complexation alongside the competitive effects of major cations/anions, which will explain the spatio-temporal distributions of trace metals in estuaries (Cindrić et al., 2015).

2.1.1 Mechanisms of trace element accumulation in the sediments

a) Flocculation

"Flocculation is a condition in which clays, polymers, or other small charged particles become attached to form a fragile structure called a floc; flocs form because of attractions between negative face charges and positive edge charges (Bianchi, 2007)". During estuarine mixing, dissolved metals come into the particulate phase due to flocculation processes (Boyle et al., 1977; Eckert & Sholkovitz, 1976), which can significantly influence the chemical mass balance between rivers and seas or lakes (Karbassi et al., 2008). Generally elements transported from upstream of the river accumulates or flocculates and settles into the lower estuarine region (Jayaprakash et al., 2014). Trace metal deposition in estuarine regions is mediated by the hydrodynamic setting of the estuarine region, which often has a variable interaction to pH, salinity, water temperature and redox effects (Alagarsamy, 2006; Krom et al., 2009; Fernandes et al., 2011). The dissolved metals removed by flocculation and gained by desorption are two non-biological processes operating in an estuary (Sholkovitz, 1978). Trace metals are removed from the dissolved phase by the process of precipitation of insoluble inorganic compounds and adsorption onto suspended particles; whereas trace metals are retained in the dissolved phase by the complexation/chelation with dissolved organic and

inorganic ligands and/or formation of colloids (Sholkovitz & Copland, 1981; Wen et al., 1999; Jackson et al., 2005).

b) Adsorption and desorption

Adsorption is the attraction of negatively charged metal ions to positively charged surfaces and the distribution of metals between the particulate and the dissolved phase largely depends on the process of adsorption (Förstner & Wittmann, 1979). In estuarine environments, the maximum turbidity zone represents the highest concentrations of suspended particles, total and particulate metal concentrations and very low dissolved metal concentrations due to adsorption. Generally the adsorption of metal ions is increased at higher pH and decreased at lower pH (Bianchi et al., 2007). Both particle reactive (e.g., Pb) and nutrient-like behavior (e.g., Cd) trace metals are removed from surface water through adsorption during their vertical transport through the water column. Most probably, these processes of removal take place in deeper estuaries which are less affected by resuspension events, where particles can become trapped at the pycnocline or redox boundary, as found in the Baltic Sea (Pohl & Hennings, 1999) and Arabian Sea (Nath et al., 1997; Cowie & Levin, 2009).

Fe and Mn hydroxides play an extensive role in the sorptive removal of trace metals in estuaries (Perret et al., 2000; Turner et al., 2004). During estuarine mixing, the partition of metals between the solution and suspended particles is extensively affected by the two most significant counteractive, non-biological processes, which are the desorption of metals from suspended particles and the flocculation of metal humates from solution (Li et al., 1984). As the salinity increases metal desorption from sediments and suspended matter also increases (Mwanuzi & De Smedt, 1999) as a result of the complexation of metals such as Cd with chloride and sulphate forming soluble inorganic complexes (Greger et al., 1995). Particularly, cations such as Ca and Na, compete with metals for adsorption sites displacing both weakly and moderately sorbed metals such as Cr, Cu, Zn and Pb (Fairbrother et al., 2007).

2.2 The partitioning of trace elements in the sediments

In aquatic ecosystem, a minor fraction of metals remains dissolved in water whereas large quantities of free metal ions are stored in sediments. The stored metals are

either retained in the sediments or released back to the water column by various remobilization processes (Neyestani et al., 2016). Sediment bound metals exist in a number of chemical forms, and their physical and chemical behaviors differ in terms of chemical interaction, mobility, biological availability and potential toxicity. Although the overall sediment contamination can be revealed from the total concentrations of metals, it gives inadequate information about the environmental impact of contaminated sediments as the environmental behaviour of metals depends critically on their specific chemical forms and binding states (Arain et al., 2009; Bacon & Davidson, 2008; Marin et al., 1997). Metal accumulation and bioavailability in sediments are influenced by a number of factors such as sediment parameters (mineralogy, texture), metal characteristics, pH, organic matter and oxidation–reduction potential (Buccolieri et al., 2006; El Nemr et al., 2007; Bastami et al., 2015).Hence use of total metal concentration as a criterion to assess the potential effects of particulate metals in natural water systems is clearly flawed (Tessier et al., 1979). Metal bioavailability and subsequent ecotoxicity can be revealed through the knowledge of metal partitioning among different geochemical phases (Galán et al., 2003). Therefore, distinguishing and quantifying metal species in sediments is a vital approach to predict their mobility, bioavailability, and potential environmental toxicity (Gu et al., 2015).

Sequential extraction is an important and ubiquitous method that provides information about the strength of metal binding to particulates and the phase associations of metals in a solid matrix (Tessier et al., 1979; Hass & Fine, 2010; Sutherland, 2010). The mobility, biological availability and potential toxicity of metals in sediments depend on their operational chemical form in sediments. The sequential extraction procedure proposed by Tessier et al., (1979), partitions elements into five operationally-defined geochemical fractions such as exchangeable (F1); carbonates (F2, acid-soluble); Fe and Mn oxides (F3, reducible); organic matter (F4, oxidizable); and residual (F5). Among these, exchangeable and carbonate bound fractions are considered to be bioavailable, and determine the bioaccumulation and biomagnification in an aquatic food web (Hickey & Kittrick, 1984; Tessier & Campbell, 1987; Ma & Rao, 1997; Sundaray et al., 2011; Dhanakumar et al., 2015). Specific metal forms are useful environmental indicators because the fractionation of the total metal contents may

indicate their origin (Fang & Yang, 2010; Hass & Fine, 2010; Koukina et al., 2016). The procedure has also proved very successful in distinguishing between metals originating from anthropogenic sources and metals of geochemical origin (El-Azim & El-Moselhy, 2005).

2.2.1 A review of sequential extraction procedures

In unpolluted soils, trace metals are mainly bound to silicates and primary minerals forming relatively immobile species, whereas in polluted soils trace metals are generally more mobile and confined to other soil or sediment phases. Hence it is important in environmental studies to determine the different ways of binding of trace metals in sedimentary compartment in order to acquire more information on trace metal mobility, as well as on their availability or toxicity, in comparison with the total element content (Rauret, 1998). The partition of sediments into their different specific phases can be achieved by the use of appropriate reagents. Goldberg and Arrhenius (1958), made an attempt to differentiate residual from non-residual metal fractions in deep-sea sediments. This was followed by further attempts by several authors (Chester & Hughes, 1967; Loring, 1976; Agemian & Chau, 1977; Malo, 1977). However, such attempts failed to address the use of a single reagent to totally dissolve all the non-residual fractions and to differentiate organic from inorganic ones (Martin et al., 1987).

The sequential extraction technique is used to study the mobility and dynamics of the operationally determined chemical forms of metals in sediments and their ecological risk for biotic species (Sundaray et al., 2011). The geochemical processes that dictate the mobilization and subsequent potential risks of metals can be easily understood by applying sequential extraction techniques (Yuan et al., 2004). Sequential extraction methods are designed to impose the rational use of a series of more or less selective reagents, which can solubilize successively the different mineralogical fractions thought to be responsible for retaining the larger part of the trace elements (Gleyzes et al., 2002). The sample to be investigated is subjected to a series of reagents, increasing the strength of the extraction at each step, in order to achieve dissolution of trace metals present in different sediment phases. The extractants generally used are inert electrolytes, weak acids, reducing agents, oxidizing agents and strong mineral acids

(Bacon & Davidson, 2008). This sequential set of selective extractions are intended to simulate the various possible natural and anthropogenic modifications of environmental conditions such as pH, redox potential and degradation of organic matter (Rauret, 1998). The use of sequential extractions, although more time consuming, furnishes detailed information about the origin, mode of occurrence, biological and physicochemical availability, mobilization, and transport of trace metals (Tessier et al., 1979).

Of the different sequential extraction schemes proposed to investigate the distribution of metals in soil and sediments, the five-step and six-step extraction schemes developed by Tessier et al. (1979) and Kersten and Förstner (1986) respectively, have been the most widely used and accepted techniques (Yuan et al., 2004). As a follow up of these two basic schemes, several other procedures were also developed with different categories of reagents or operational conditions (Borovec et al., 1993; Campanella et al., 1995; Gómez Ariza et al., 2000). In order to harmonize the existing methods of sequential extraction, the European Community Bureau of Reference (BCR), now the Standards, Measurement and Testing Program, proposed a new sequential extraction process called the BCR method, which replaces the first two steps of the Tessier protocol with a single step (Ure et al., 1992). A revised protocol of the original BCR method was also recommended in the late 1990s in order to overcome the limitations in the original BCR protocol (Rauret et al., 1999). All the sequential extraction procedures have advantages and disadvantages, and the decision which to use should depend on the properties of samples (Gleyzes et al., 2002).

The protocol developed by Tessier et al. (1979), is the most often used and applied technique not only to soils and sediments, but also to atmospheric particulate matter (Segura et al., 2006; Rath et al., 2009; Sundaray et al., 2011; Truzzi et al., 2017). The procedure was originally developed for sediment analysis and later on it was also employed for agricultural and contaminated soils (Barona & Romero, 1997; Flores et al., 1997; Maiz et al., 2000; Sungur et al., 2015; Matong et al., 2016). Many sequential extraction procedures were developed for analyzing soils and sediments, many of which are variants on the Tessier procedure in which the exchangeable metals and those nominally associated with carbonate, Fe-Mn oxides, organic material and silicate residues were extracted with magnesium chloride, sodium acetate-acetic acid, hydroxyl

ammonium chloride, hydrogen peroxide and hydrofluoric perchloric acid, respectively (Davidson et al., 1994). There are several other sequential extraction procedures developed by following the Tessier procedure, and there is now a wide variety of them available based on various sequences of extractants and diverse operational conditions (Oyeyiola et al., 2011; Mittermüller et al., 2016).

2.2.2 Pros and cons of sequential extraction procedures

Sequential extraction procedures were developed to separate more accurately labile (inorganic and organic) from residual phases in order to acquire more insight on the particulate speciation of metals and this approach has been widely used in a variety of disciplines including geochemistry, soil sciences, environmental sciences and pollution studies (Martin et al., 1987). Metals associated with the principal accumulative phases in sedimentary deposits can be determined only with the help of sequential extraction experiments. Sequential extraction experiments are very useful to distinguish pollution sources, evaluate metal mobility and bioavailability and to identify the binding sites of metals for assessing metal accumulation, pollution and transport mechanisms (Filgueiras et al., 2002; Sundaray et al., 2011). The most important aspect of sequential extraction is that it only divides the particulate trace element content of a test sample into portions soluble in particular reagents under particular conditions (Bacon & Davidson, 2008). The approach of sequential extraction has been widely applied to study changing environments such as estuaries, recently deposited sediments or to the biodegradability of particulate elements by living organisms (Martin et al., 1987). Non – residual metal complexes can be separated from residual metals with the help of sequential extraction techniques (Schintu et al., 2016). Sequential extraction procedures are a powerful tool to investigate the geochemistry and geo-availability of potentially toxic harmful elements (PTHE) (García-Ordiales et al., 2016).

Nirel and Morel (1990) published a technical note in the *Water Research Journal* regarding the pitfalls in sequential extraction techniques. The authors discouraged the expanding uncritical use of sequential extractions for measuring the particulate speciation of trace elements. The authors also criticized the ‘operationally defined’ results obtained from sequential extraction procedures are not validated. Furthermore,

the authors added that reagents and kinetics involved in sequential extraction procedures do not mimic the actual natural processes and thus sequential extraction procedures do not provide actual particulate speciation. However, Tessier and Campbell (1991) have stated the 'technical note by Nirel and Morel (1990) was based neither on new experimental facts nor on new ideas'. The authors stressed the sequential extractions are realistic analytical tools that can be useful in the study of sediment geochemistry, provided they are used with proper judgment and care. The authors also pointed out the procedures are worthless when they are used simply to generate numbers and the over-interpretation of the results should be viewed with caution. Trace metals associated with specific mineral phases in environmental solids cannot be quantitatively determined for reasons which include (a) re-distribution of analytes among phases during extraction; (b) non-selectivity of reagents for target phases; (c) incomplete extraction; and (d) precipitation of 'new' mineral phases during extraction (Bacon & Davidson, 2008). Despite all of the limitations, the efficacy of sequential extractions is evident from the considerable insights it has provided over three decades into the environmental behaviour of potentially toxic elements (Bacon & Davidson, 2008). The widely used sequential extraction procedure proposed by Tessier et al. (1979) was actually first used in analyzing the sediment samples collected from the lower reaches of the Yamaska and Saint-Francois rivers (Quebec, Canada). This method was then successfully applied in a number of studies involving the investigation of particulate trace element speciation in riverine and estuarine sediments (Singh et al., 2005; Benson, 2008; Dessai & Nayak, 2009; Frankowski et al., 2010; Sundaray et al., 2011; Mohan et al., 2012; Li et al., 2013; Mittermüller et al., 2016; Cui et al., 2017)

2.3 Trace elements and the mangrove ecosystems

Mangroves refer to a unique group of forested wetlands that dominate 240×10^3 km^2 of the intertidal zone of tropical and subtropical coastal landscapes from river deltas, lagoons and estuarine settings to islands in oceanic environments (Twilley & Day, 2012). Mangroves are a highly productive ecosystem and represents a source of carbon and nutrients to the adjacent lagoonal and coastal systems (Odum & Heald, 1972; Wattayakorn et al., 1990; Woodroffe, 1992). Mangroves in many inter-tidal zones of tropical and subtropical estuaries enhance the accumulation of fine, organic-rich

materials and their associated contaminates (Harbison, 1986; Silva et al., 1990; Lacerda et al., 1991). The majority of mangrove ecosystems are in close proximity to developed areas (Tam & Wong, 2000; MacFarlane & Burchett, 2002; Preda & Cox, 2002). Furthermore, enrichment of metallic contaminants occur through urban and agricultural runoff, industrial effluents, boating and recreational use of water bodies, chemical spills, sewage treatment plants, leaching from domestic garbage dumps and mining operations (Peters et al., 1997). Metal contamination in mangrove ecosystems is a serious threat to mangrove biodiversity due to their persistence, potential toxicity, and bioavailability (Marchand, et al., 2011).

Mangroves are tolerant to high metal fluxes and protect adjacent marine communities by acting as a buffering zone (Peters et al., 1997). Mangrove sediments serve as a sink for trace metals because of their ability to retain trace metals derived from tidal waters and fresh water rivers including storm water runoff (Harbison, 1986; Lacerda et al., 1993; Tam & Wong, 1993, 1996, 2000). Trace metals and/or metalloids contamination poses a serious threat to mangrove ecosystem (Wang et al., 2013). Mangrove sediments may act as a sink or source for trace metals in an aquatic ecosystem with respect to the influence by physiochemical conditions (Keene et al., 2010; Marchand et al., 2006; Nath et al., 2013; Wang et al., 2013; Sappal et al., 2014). The retention of water borne trace metals is favored by the high sulphide and organic matter contents in mangrove environments (Tam & Wong, 1996). These highly productive wetlands are extensively used to rehabilitate coastal developments due to their high sedimentation and stabilized vegetated nature (Daoust et al., 1996; Dominik & Stanley, 1993).

Despite the potential of mangrove rhizosphere sediments to protect coastal marine environments from pollution by sequestering trace metals (Harbison, 1986; Clark et al., 1998), variations in physico-chemical conditions in the environment may trigger a release of accumulated trace metals into the sediment–water interface (Marchand et al., 2006; Keene et al., 2010; Nath et al., 2013). Mangroves are capable of excluding metals or regulating uptake of metals at the root level and limit translocation to the shoot (MacFarlane & Burchett, 2002). A significant amount of metals is exported from the forests to the surrounding communities, counterbalancing the low metal concentrations

(Peters et al., 1997). In order to understand the fate of trace metals in mangrove ecosystem, it is important to study trace metal concentrations in different compartments of the environment and through this it is possible to alert coastal managers of potential impacts upon the detritus driven food web, which can potentially lead to the bioaccumulation of contaminants in organisms (Qiu et al., 2011). Knowledge of the trace metal distribution in the mangrove environment is essential to understand the mechanisms controlling the dispersal, accumulation, and fate of the metals in the mangrove ecosystem (Kumar et al., 2016).

2.3.1 Major mangrove ecosystems of the world

Distribution of mangroves is confined to the inter-tidal region between the sea and land in tropical and subtropical regions of the world between approximately 30° N and 30° S latitude (Giri et al., 2011). Mangroves are the main vegetation type in protected intertidal areas along tropical and subtropical coastlines and they grow in environmental settings ranging from highly humid to extremely arid conditions and in soils, which range from pure clays to peat, sand, or coral rubble (English et al., 1997; Parvaresh et al., 2011). Mangrove forests are built by a small group of 73 species of trees and shrubs and largely restricted to the tropics and a few warm temperate regions (Sandilyan & Kathiresan, 2015), which comprises 2.4% of the Earths total tropical forest (FAO, 2007). Mangroves cover about 150,000 km^2 worldwide, and about 75% of the mangrove forests are concentrated in just fifteen countries - Indonesia, Australia, Brazil, México, Nigeria, Malaysia, Myanmar, Papua New Guinea, Bangladesh, Cuba, India, Guinea Bissau, Mozambique, Madagascar and the Philippines (Giri et al., 2011; Spalding et al., 2010). There are 9 orders, 20 families, 27 genera and roughly 70 species of mangroves spread over an area of about 181 000 km^2 (Spalding et al., 1997). The Indo-West Pacific regions contain the most diverse biogeographical regions of mangroves. Indonesia, Australia, Brazil and Nigeria have roughly 43% of the world's mangrove forests (Alongi, 2002).

The countries with the largest proportions of mangroves are as follows: Indonesia - 4.25 x 10^4 km^2 (Spalding et al., 1997), Brazil – 1.34 x 10^4 km^2 (Spalding et al., 1997), Nigeria – 1.05 x 10^4 km^2 (Saenger & Bellan, 1995), and Australia - 1.00 x

$10^4 km^2$ (Robertson & Duke, 1990). At present, Malaysia is the 6th largest mangrove area in the world and with respect to diversity the country ranks second next to Indonesia (Hamdan et al., 2014). More than half of the total mangrove forest area of 505,386 ha is found in the states of Sabah and Sarawak (Jusoff, 2008; Giri et al., 2011). However, there are about 115,000 ha of intact mangrove in Peninsular Malaysia (Hamdan et al., 2014). Mangroves support a variety of ecosystem services and their ecosystem value can reach up to several thousand US$yr^{-1} ha^{-1} (Walters et al., 2008). Despite their ecosystem value, due to overexploitation, pollution and land conversion mangroves are the most threatened ecosystem worldwide disappearing at the rate of 1 to 2% per year (Duke et al., 2007; Valiela et al., 2001).

2.3.2 Bioaccumulation of trace elements in the mangroves

Mangroves protect the coastal environment from metal contamination by their capacity to sequester or partition metals in their substratum (Jin-Eong, 1995; Harty 1997). But elevated sediment metal concentrations may lead to bioaccumulation and pose a serious threat to mangrove ecosystems (Birch et al., 2015). Mangroves are poor accumulators of trace metals (De Lacerda, 1998). Accumulation of metals in mangroves occur at the root level and the transport to aerial portions of the plant is generally limited (Silva et al., 1990; Chiu & Chou, 1991). The concentration factors (ratio of metal concentrations between tissues and sediments) for heavy metals in mangrove leaves are usually observed to be much lower than one (Rao et al., 1991; Tam & Wong, 1995; Thomas & Fernandez, 1997;Ong Che, 1999). The anaerobic and reduced nature of mangrove sediments along with rich sulphide and organic matter content favors the retention of water-borne heavy metals (Silva et al., 1990; Tam & Wong, 2000) and the subsequent oxidation of sulphides between tides allows metal mobilization and bioavailability (Clark et al., 1998).

Sediments exhibit elevated metal concentrations and they exceed the concentrations in the overlying water in the range 3–5 orders of magnitude (Zabetoglou et al., 2002). In those conditions, the bioavailability of even a minute fraction of the total sediment metal content may pose significant impacts in respect to bioaccumulation in both animal and plant species living in the mangrove environment (Defew et al., 2005). The accumulated metals in mangroves are passed on to detritus food chains in adjacent

coastal waters through the cycling of organic matter through litter production, decomposition, and tidal transport (Ramos et al., 2006). The cycling of trace elements in mangrove environments is a serious problem (Marchand et al., 2006; Pekey, 2006) as excess trace metal adsorption from sediments to mangrove plants may lead to contamination of the food chain (Ahmed et al., 2011). Metal accumulation in mangroves is due to their ability to trap suspended material from the water column (Furukawa et al., 1997), their richness in organic matter (Marchand et al., 2011), and the various diagenetic processes that take place in mangrove sediments (Kristensen et al., 2008), which make them natural biogeochemical reactors (Marchand et al., 2016).

Metal accumulation in mangrove leaf tissues is a serious concern as it enters the food chain through leaf litter transport and leaf consumption (MacFarlane & Burchett, 2002; Machado et al., 2002). Metal absorption and storage occur at the mangrove roots and some metals are translocated upward to other sensitive tissues. The metal concentrations in shoots were observed to be half that of roots (MacFarlane et al., 2007; Zhou et al., 2011; He et al., 2014). Accumulated metal concentrations in mangrove roots tend to be similar to that of the adjacent sediment concentrations and the concentrations were only half the levels in leaf tissues compared to that of the plant's roots (MacFarlane et al., 2007). This phenomena can vary in disturbed environments, the dynamics and balance can be affected and any accumulated metals are mobilized and end up in the flora and coastal food chain (Vannucci, 2001).

Bioaccumulation can be calculated with the help of indices such as biological concentration factor (BCF), translocation factor (TF), and biological accumulation coefficient (BAC) (Pilon-Smits, 2005). The sediment quality parameters are associated with pH, salinity, redox potential, mineral and organic content, resident biota, and the synergistic interactions between these variables influence the bioavailability and toxicity of metals (Martin et al., 2006; Morrissey & Guerinot, 2009). Mangroves regulate essential metals and act as an excluder species for non-essential metals (MacFarlane et al., 2007). Mangroves are tolerant to high levels of metals and this tolerance is thought to be the result of the metals in the sediment being in a form not bio-available, in conjunction with biological mechanisms including exclusion and sequestering processes in root tissue (Chiu & Chou, 1991).

2.4 The study of Provenance analysis

The study of provenance will aid in comprehending all the factors related to the production of sediment, with a precise mention to the composition of the parent rocks as well as the physiography and climate of the source area from which sediment is derived (Weltje & Eynatten, 2004). The study of sedimentary provenance encompasses several of the mainstream geological disciplines such as mineralogy, geochemistry, geochronology, sedimentology, and igneous and metamorphic petrology. Furthermore, through this study it is possible to discern the location and nature of sediment source regions, the associated sediment transport pathways from the source to basin of deposition, and the factors that impact the composition of sedimentary rocks such as climate and tectonic setting, i.e., to unravel the line of descent or lineage of the sediment under investigation (Haughton et al., 1991; Weltje & Eynatten, 2004). The sedimentary processes affecting the rocks, the nature of the provenance, and the geochemical history of certain provenance components can be revealed through geochemical data (McLennan et al., 1993). The reins of provenance sources and the weathering intensity on sediment composition can be understood through geochemical analysis and the use of geochemical indices and associated discriminant diagrams (Descourvieres et al., 2011; Ben-Awuah et al., 2017; Nagarajan et al., 2017a,b). In the present study, the provenance of the sediments was identified by using bivariate, trilinear plots, and discrimination diagrams in order to explore weathering, sorting and recycling of the sediments, through which it is possible to understand the possible combination of source rocks compositions and geochemical processes that control the prevailing geochemical environment of the Lower Baram River.

From the literature review, it is understood that, to study the overall environmental status, the need for conducting comprehensive studies using a combination of chemical and biological based assessments becomes necessary. Further, the study of provenance is necessary in order to discern the source of origin of the major and trace elements of concern.

Chapter 3. Research Methodology

3.1 Sample collection and preparation

A stratified random sampling method was adopted for the present study. In order to study the spatial and temporal variations, surface water and sediment samples were collected at 32 sampling locations from the Baram River mouth to Marudi, a riverine town located about 111km upstream from the Baram River mouth. Surface water and sediment samples (surface sediments from the riverbed) were collected during January (representing the monsoon season) and April (representing the post monsoon season) 2015, in order to assess the spatial and temporal variations of water and sediment quality. Sampling locations were selected to represent the major downstream characteristics of the river such as river meanders, tributary inputs, villages and industrial areas. The sites selected for the study show both estuarine as well as freshwater characteristics.

Water samples were collected using a non-metallic aqua-trap water sampler. Water samples were collected in polyethylene containers, which were acid-washed using nitric acid prior to their use. The samples were filtered through Whatman filter paper (11µ) and stored in a refrigerator until further analysis. Instead of using a 0.45µ filter, the 11µ filter was used in order to measure the quantum of the trace elements being transported in the colloidal form and as natural nanoparticles. For metal determination, samples were acidified to pH < 2 using nitric acid and then stored in a refrigerator until analysis. The physical properties of water such as temperature, pH, salinity, dissolved oxygen, total dissolved solids (TDS), electrical conductivity (EC) and redox potential (Eh) were analyzed in the field by using field water analysis kit (Thermoscientific, USA-Orion star plus). The collected and preserved water samples were also used for determining micronutrients, major/trace ions and trace/heavy metals.

Surface sediment samples were collected by using a grab sampler. The sediments trapped on the center portion of the grab sampler were taken for analysis in order to avoid contamination. Sediment samples were collected both from the riverbed as well as the accumulated sediment at the point bars such as river bends (meanders).Overbank sediments represent the present and past sediment sources from upstream of the

sampling point and are considered to be a more representative sample of the study area, which can be used to determine the main regional and continental geochemical distribution patterns (Ottesen et al., 1989; Macklin et al.,1994; Bølviken et al., 2004). The collected surface sediments were brought to the laboratory in airtight polyethylene bags. The samples were dried in the laboratory oven at 60ºC and homogenized by using a stone mortar and pestle without reducing the size of the grain and were partitioned using the cone and quartering method. The homogenised samples were used for the determination of particle size and the calcium carbonate and organic carbon content. The homogenized sediments were ground to <63 micron size using an agate mortar for the analysis of major trace and Rare Earth Elements (REE).

Sediment cores and mangrove plant samples were collected in September 2015. Leaves, roots and tree bark were collected from the mangrove species S*onneratia caseolaris* (L.) Engl. found along the Baram River estuarine system. This the only observed species in the Baram River estuarine system. Leaf samples were collected following the methodology of MacFarlane et al. (2003). For each site, approximately 20 leaves were collected from three trees. Each individual tree was greater than 3 m tall and of similar health condition. Leaves were collected from the second whorl of the northeast (NE) facing branches of each tree. Leaves of each tree were combined to obtain a composite sample and were stored in an icebox and transported to the laboratory. Leaves were sub-sampled, homogenised and washed in distilled water for immediate photosynthetic pigment determination. Apart from leaves, trunk bark and roots/pneumatophores were also collected from the same trees, subsampled, homogenized and oven dried at 55ºC until they become completely dried and stored for metal analysis.

A total of 10 sediment short cores were collected along the Baram River estuarine system. Of these, four sediment cores were selected for geochemical analyses. They are BSC-01, BSC-06, BSC-07 and BSC-09. All these four cores represent different depositional environment of the study area. The Core BSC-01 was collected at the river mouth, BSC-06 was collected in the mangrove environment, BSC-07 was collected in a meander curve and BSC-09 was collected from the confluence Point of Bakung River with the Baram River. Sediment cores were collected by using a PVC coring tube of

about 60cm in length and 4.5cm in width. The PVC coring tube was gently pushed into the sediment and retrieved back in a sealed position. They were transported in an icebox to the laboratory and kept in a deep freeze until further processing. The core length varied between 35cm and 50cm among the station samples due to variations in the nature of the substratum. The samples were sub-sampled at 4 cm intervals with the help of a PVC spatula. The samples were then oven dried and homogenized by the cone and quartering method for determining organic carbon and calcium carbonate levels. The homogenized samples were ground using agate mortar and pestle, sieved through a 63µm filter and were stored in airtight polypropylene bags for later determination of down core variations of total trace/major elements. Apart from the short cores, one long core of 1.5m was collected using the PVC coring tube in the Kuala Baram area and the sample was subsampled at 4cm intervals and processed as described above for the determining levels of organic carbon, calcium carbonate and downcore variations of total trace/major elements. The industrial activities and the typical environmental characteristics of the study area, the collection of samples, the insitu analysis of water quality parameters and the laboratory processing of samples are listed in Figure 3.2 to Figure 3.5.

3.2 Sample analysis

The collected and preserved water samples were analysed for their micronutrients, major and trace ions and trace/heavy metals by following the standard protocols (Table 3.1). The homogenized sediment samples were used for the determination of the presence of calcium and organic matter by the total combustion (Loss on ignition) method (Heiri et al., 2001). The distribution of metals in sediments were studied by sequential extraction into 5 fractions (F1 – F5) as described by Tessier et al. (1979) (Figure 3.1).The processed surface sediments and sediment cores were used for the determination of major, trace and rare earth elements at the Actlab facility in Canada.

The concentration of metals in the mangrove leaves, trunk bark and roots/pneumatophores was determined by digesting the samples with a hot mixture of concentrated nitric acid and hydrogen peroxide (Krishnamurthy et al., 1976). The

resultant products obtained were analysed for metals using an Atomic Absorption Spectrophotometer (AAS-Perkin Elmer A Analyst 400 with WinLab 32 Software Version 6.5). Fresh leaf samples (5 samples per location) were taken for the determination of photosynthetic pigments by using the method Inskeep and Bloom, (1985), using extraction by N,N-dimethyl formamide (DMF) and further spectrophotometric analysis. 50 mg of fresh of leaf tissue was sliced finely cut by using stainless steel scissors, in order to increase the surface area of tissue exposed to the extractant and placed in a 15 ml amber glass screw cap bottle containing 10 ml DMF. The bottles were placed inside a darkened container in the refrigerator for seven days prior to spectrophotometric determination on a UV/VIS spectrophotometer. Wavelengths chosen for analysis of the photosynthetic pigments were 647, 664 nm for chlorophylls, and 480 nm for carotenoids. Pigment contents were calculated in mg/g dry weight applying the absorption coefficient equations described by Wellburn (1984).

Table 3.1 Methodologies overview

S.No	Analysis	Method	Instrument
A. Water Analysis			
1.	Physico-chemical parameters: Temperature, pH, dissolved oxygen, electrical conductivity, total dissolved solids, salinity, resistivity	In-situ	Thermoscientific, USA-Orion star plus
2.	Dissolved oxygen	-	DO Meter (YSI Pro 20)
3.	Turbidity	-	2100Q Portable turbidimeter
2.	**Major and minor Ions**		
i)	Carbonate (CO_3)	H_2SO_4 Titration (APHA 2005)	
ii)	Bicarbonate ($HCO_{3)}$		
iii)	Chloride (Cl^-)	Mohr's Titration (APHA 2005	
iv)	Sulphate (SO_4)	SulfaVer 4 Method (HACH kits)	UV- Spectrophotometer
v)	Sodium	Photometric	FAAS
vi)	Potassium		
vii)	Calcium		
viii)	Magnesium		
3.	**Nutrients**		
i)	Nitrate Nitrogen (NO_3-N)	Hach Kit	UV- Spectrophotometer
ii)	Orthophosphate (PO_4^{3-})	Hach Kit	UV- Spectrophotometer
iii)	Nitrogen-Ammonia (NH_3-N)	Hach Kit	UV- Spectrophotometer
5.	**Major and Trace elements**		
v)	Major and Trace elements		FAAS
B. Sediment Analysis			
i)	Sequential Extraction of heavy metals	Protocol of Tessier et al. (1979)	FAAS
ii)	Bulk geochemistry	Protocol of Activation laboratories, Canada	ICP and ICP-MS
iii)	Dating of core sediments	^4C dating carried at Beta Analytic Inc. lab USA	AMS
iv)	Zr Dating	Zircon U-Pb dating carried at Actlabs, Canada	Resonetics RESOlution M-50 series 193nm excimer laser ablation system
iv)	Calcium Carbonate	Loss on ignition	Muffle Furnace
v)	Organic Carbon	Loss on ignition	Muffle Furnace
C. Mangroves			
i)	Major and trace elements	Krishnamurthy et al. (1976)	FAAS
ii)	Photosynthetic pigments	Inskeep and Bloom, (1985)	UV- Vis Spectrophotometer

3.2.1 Bulk Geochemistry of Sediments

In total, 64 surface sediment samples with 4 short core and one long core sediment samples were selected for geochemical analysis (i.e. for determination of major, trace and rare earth elements). Geochemical analysis was carried out at Activation Laboratories Ltd, in Canada using the Code 4LITHO (11+) Major Elements Fusion ICP (WRA)/Trace Elements Fusion ICP/MS(WRA4B2) package. The most aggressive fusion technique was employed with a lithium metaborate/tetraborate fusion for the major, trace and REE analysis. The molten bead was digested in a weak nitric acid solution. The fusion ensured the entire sample was dissolved and the analysis was carried out by ICP and ICPMS. Certified reference materials NIST 694, DNC-1, GBW 07113 (for major and trace elements) and NCS DC70009, OREAS 100a, 101a, and 101b (for REE) were used to confirm the accuracy and precision of the analysis. The accuracy and precision of the analysis was better than 5% except for Cs, Tl, (±10%) and Sn (>10%). The list of elements analysed, the method of analyses and the detection limit of each element with the unit is summarized below in Table 3.2.

3.2.2 ^{14}C AMS dating of core sediments

Selected samples were sent to the Beta Analytic Inc. lab in the USA. Samples were cross-checked for accuracy between sample containers and the documentation. They were logged into the database with bar coding for tracking all of the chemical steps concerning date, time and technician. This bar-coding is used in the event of an inquiry so anyone can track the movement of each sample through each chemical step. The submitted material was pretreated physically and chemically to remove contamination.

Table 3.2 Method of analyses and detection limit of each elements

Analyte Symbol	Unit Symbol	Detection Limit	Analysis Method
SiO_2	%	0.01	FUS-ICP
Al_2O_3	%	0.01	FUS-ICP
Fe_2O_3(T)	%	0.01	FUS-ICP
MnO	%	0.001	FUS-ICP
MgO	%	0.01	FUS-ICP
CaO	%	0.01	FUS-ICP
Na_2O	%	0.01	FUS-ICP
K_2O	%	0.01	FUS-ICP
TiO_2	%	0.001	FUS-ICP
P_2O_5	%	0.01	FUS-ICP
LOI	%		FUS-ICP
Total	%	0.01	FUS-ICP
Sc	ppm	1	FUS-ICP
Be	ppm	1	FUS-ICP
V	ppm	5	FUS-ICP
Ba	ppm	3	FUS-ICP
Sr	ppm	2	FUS-ICP
Y	ppm	2	FUS-ICP
Zr	ppm	4	FUS-ICP
Cr	ppm	20	FUS-MS
Co	ppm	1	FUS-MS
Ni	ppm	20	FUS-MS
Cu	ppm	10	FUS-MS
Zn	ppm	30	FUS-MS
Ga	ppm	1	FUS-MS
Ge	ppm	1	FUS-MS
As	ppm	5	FUS-MS
Rb	ppm	2	FUS-MS
Nb	ppm	1	FUS-MS
Mo	ppm	2	FUS-MS
Ag	ppm	0.5	FUS-MS
In	ppm	0.2	FUS-MS
Sn	ppm	1	FUS-MS
Sb	ppm	0.5	FUS-MS
Cs	ppm	0.5	FUS-MS
La	ppm	0.1	FUS-MS
Ce	ppm	0.1	FUS-MS
Pr	ppm	0.05	FUS-MS
Nd	ppm	0.1	FUS-MS
Sm	ppm	0.1	FUS-MS
Eu	ppm	0.05	FUS-MS
Gd	ppm	0.1	FUS-MS
Tb	ppm	0.1	FUS-MS
Dy	ppm	0.1	FUS-MS
Ho	ppm	0.1	FUS-MS
Er	ppm	0.1	FUS-MS
Tm	ppm	0.05	FUS-MS
Yb	ppm	0.1	FUS-MS
Lu	ppm	0.04	FUS-MS
Hf	ppm	0.2	FUS-MS
Ta	ppm	0.1	FUS-MS
W	ppm	1	FUS-MS
Tl	ppm	0.1	FUS-MS
Pb	ppm	5	FUS-MS
Bi	ppm	0.4	FUS-MS
Th	ppm	0.1	FUS-MS
U	ppm	0.1	FUS-MS

3.2.3 Carbonate sediments

Solid carbonates such as shells are most often etched with acid to remove the outer surfaces with potential secondary carbonate. This was not possible for the carbonate sediments collected due to the fine grain nature of the carbonate present. The samples were analyzed for the total inorganic carbon present by placing sample material into a vessel where it was evacuated of all air and then mixed with phosphoric acid to generate CO_2.

3.2.4 Pretreatment and combustion to CO_2 for the organics

The samples were first visually inspected for size, homogeneity, debris, inclusions, clasts, grain size, organic constituents and potential contaminants. They were then dispersed in de-ionized water, homogenized through stirring and sonication and then sieved through a 180μm sieve. The material passing through the sieve was used for the analysis. Each was then bathed in 1.0N HCl at 90°C for a minimum of 1.5 hours to ensure removal of carbonates, followed by serial de-ionized water rinses at 70°C until neutrality was reached. Any debris or micro-rootlets were discarded during these rinses. After drying in an oven at 100°C for 12- 24 hours, concentrated HCl was applied to a representative sub-sample and placed under a microscope to validate the absence of carbonate. Microscopic examination was performed to assess characteristics and to determine the appropriate sub-sample for AMS dating. Each sample was then separately placed into a closed chemistry line, which had been purged of any CO_2 to a level below 10e-^{15} atoms (background levels). The line was filled with 100% oxygen and ignited at >900°C to combust the sample organic carbon to CO_2.

3.2.5 AMS analysis

The CO_2 was dried and introduced into a reaction vessel containing an aliquot of cobalt metal catalyst. Hydrogen was introduced such that when the mixture was heated to 50ºC, the CO_2 cracked to carbon (graphite). The graphite was pressed into a target for measurement in an accelerator mass spectrometer (AMS: Highly customized 250Kev NEC single stage particle accelerator). The AMS was calibrated to provide an accurate ratio of $^{14}C/^{13}C$ between the sample graphite and a modern reference (NIST-4990C, Oxalic acid). Quality assurance samples were reacted simultaneously in the lab and

measured simultaneously in the AMS. The analytical result was obtained as a fraction of the value of the modern reference, corrected for isotopic fractionation using $^{13}C/^{12}C$ ($\delta^{13}C$) and the radiocarbon age calculated according to the conventions cited in Radiocarbon, Volume 19, Number 3, 1977. The QA samples were checked for accuracy and observed to fall within expectations for the laboratory to accept and report the sample results. The acceptance was defined as being within 2 sigma of the known value, based on the total laboratory error known to be within 2 sigma. As always, Conventional Radiocarbon Ages and sigmas are rounded to the nearest 10 years per the conventions of the 1977 International Radiocarbon Conference. When counting statistics produce sigmas lower than ± 30 years, a conservative ± 30 BP is cited for the result.

3.2.6 Zr Dating

Three sand samples collected from the Upper Baram River were used for U-Pb dating of zircons at the Actlabs facility in Canada. Zircon U-Pb dating was carried out using a Resonetics RESOlution M-50 series 193nm excimer laser ablation system equipped with a Laurin Technic Pty S-155 ablation cell. A minimum of 60-70 grains were used for the analysis. A detailed methodology is summarized by Nagarajan et al., 2017b (see. supplementary file).

3.3 Accuracy and precision: for overall study

3.3.1 Apparatus and reagents

All the glassware and plastic containers used in this research were soaked in a solution of 20% HNO_3, left overnight and rinsed thoroughly with distilled water prior to use. All reagents were of analytical grade, purchased from Merck (Darmstadt, Germany) and Fisher Scientific. The Safety Data Sheets (MSDS/SDS) for all the chemicals and instruments were reviewed before starting the experiments. Chemical wastes and reacted solutions were disposed of according to Curtin University, local, state and federal regulations.

3.3.2 Standards solutions

Standard stock metal solutions (1000 mg/L) were purchased from Merck (Darmstadt, Germany). A sub-stock solution of 100 mg/L and 10 mg/L was prepared by

diluting the standard stock solution using (2%) HNO_3 or distilled water according to the recommended instructions documented in the instrumentation protocols. The working standard solution of 0.1 mg/L, 0.5 mg/L, 1.0 mg/L and 2.0 mg/L was prepared by further diluting the sub-stock solution.

3.3.3 Calibration Procedure

For checking the accuracy of the flame atomic absorption spectrometer, the calibration curves for each trace/heavy metal analysis were done to ensure and confirm accuracy and reliability. The calibration curves were made with standard solutions. Normally five working calibration standards were prepared by serial dilution of a sub-stock solution of 100 or 10 mg/L. These working standards were prepared immediately prior to the analysis process. The liner range calibration method was used and the correlation coefficient (R^2) for each metal was determined from the calibration curve and all R^2 were greater than 0.995. The instrument specific conditions for AAS are given in Table 3.3.

3.3.4 Evaluation of analytical performance and quality control

The precision of the analytical performance was validated by measuring the certified standard reference material MESS 3 to check the accuracy of the results. Appropriate quality control and quality assurance samples were collected to provide confidence in the data regarding bias and variability. To check the possible contamination in the samples, equipment blanks were used in order to verify that decontamination procedures and laboratory protocols were adequately followed (Koterba et al., 1995). The overall mean recovery rates for trace/heavy metals ranged between 87% and 105%, and this was found to be satisfactory with the results of the certified values. Analytical control was assured by preparing the reagent blanks and utilizing standard solutions as quality control at every five-sample interval.

Table 3.3 Instrument specific condition of AAS

Element	Wave Length (nm)	Char. Conc[a] (mg/l)	Sensitivity Check[b] (mg/l)	Linear Range[c] (mg/l)	Slit width	Oxidant Flow: Air (L/min)	Acetylene Flow (L/min)	Light Sources[d] (Lamp)
Cadmium	228.80	0.01	0.5	1	2.7	10	2.5	EDLs & HCL
Copper	324.75	0.025	1.3	1.6	2.7	10	2.5	HCL
Cobalt	240.73		7	3.5	1.8	10	2.5	HCL
Iron	248.33	0.04	2	3	1.8	10	2.5	HCL
Lead	283.31	0.18	8	10	2.7	10	2.5	EDLs & HCL
Manganese	279.48	0.016	1	0.6	1.8	10	2.5	HCL
Potassium	766.49	0.02	1	1	2.7	10	2.5	HCL
Zinc	213.86	0.006	0.3	0.75	2.7	10	2.5	HCL

[a]Characteristic conc. is the minimum absorbance value of the instrument

[b] Sensitivity check is the concentration giving approximately 0.2 Absorbance Units (AU)

[c] Linear Range is the maximum absorbance value with the relative noise

[d] Light Source is Electrodeless discharge lamps (EDLs) and Hollow Cathode Lamps (HCLs)

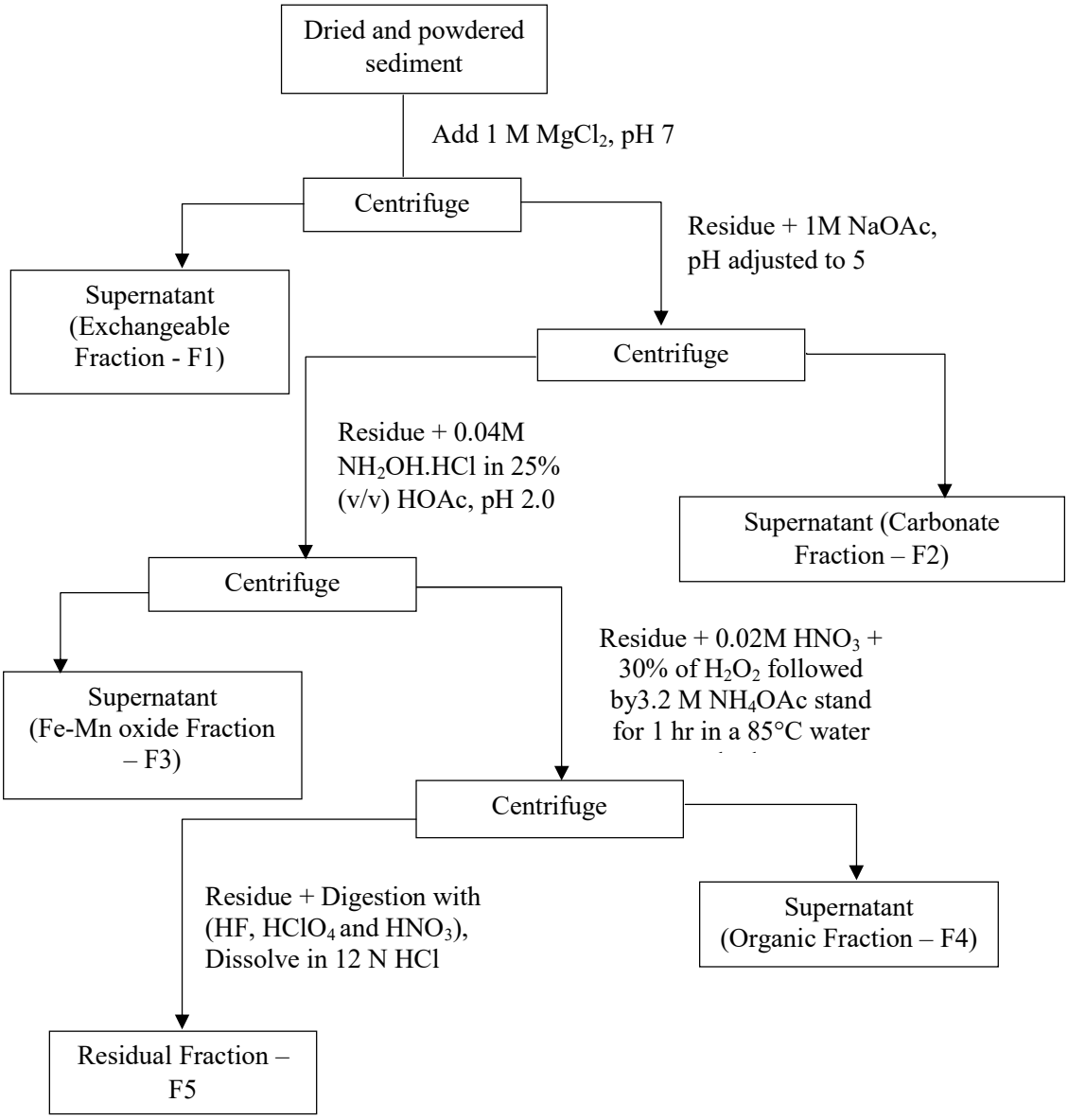

Figure 3.1 Flowchart signifies the sequential extraction of trace metals by Tessier protocol

Figure 3.2 (A, B and C) Industrial activities near the Baram River estuary

Figure 3.3 (A, B and C). Study sites representing typical depositional environments and mixing zones of the Baram River with tributaries

Figure 3.4 (A, B and C). Field sample collection and on field determination of water quality parameters

Figure 3.5 (A, B and C). Sample processing at the laboratory

Chapter 4. Water Chemistry

The climate of the tropical regions, with warm temperatures and high rainfall, favors the physical and chemical weathering of rocks. The prevailing high-energy conditions such as wind, water discharge, etc., can rapidly enhance the removal and transport of solutes and particulates from the source area to the sea in a comparatively shorter residence time as compared to a more temperate climate (Sultan et al., 2011). About 50% of the sediment flux to oceans have been contributed by Asian rivers and most of their drainage basins are comparatively less influenced by industrial activities and therefore the study of these less disturbed river systems can pave the way towards a better understanding of weathering and erosion control over aquatic chemistry (Zhang & Huang, 1993). Therefore, it is pertinent to conduct significant research to study and understand any potentially toxic elemental background concentrations in the tropical watersheds in Asia in order to manage and monitor any changes caused by anthropogenic activities in the future (Sultan et al., 2011). In the present study, various physico-chemical parameters were analyzed in the surface water samples collected from the Lower Baram River in order to understand the geochemistry of the trace elements in the surface water. Major water quality parameters such as temperature, pH, dissolved oxygen, electrical conductivity, total dissolved solids, salinity, resistivity, turbidity, redox potential, major and minor ions, nutrients as well as the major and trace elements were analysed. A Paired T-test was performed in order to comprehend whether the analysed parameters vary significantly ($p<0.05$) between MON and POM seasons (Appendix -1).

4.1 Results

4.1.1 Physicochemical Parameters

The descriptive statistics of the major physicochemical parameters of the surface water for MON and POM seasons are given in Table 4.1 and Table 4.2 respectively. The temperature in the study area ranged from 25.60ºC to 27.80ºC during the MON season with an average of 26.70ºC. During the POM season, the temperature varied from 28.70ºC to 32.00ºC with a mean temperature of 30.10ºC. The temperature fluctuations in the study area varied significantly ($p<0.01$) between

the two seasons. The pH variations between the study sites during the MON season ranged from 4.26 to 6.09 with a mean of 5.81 and during the POM season, it varied from 4.58 to 7.49 with a mean of 6.82. The pH levels observed between the MON and the POM seasons were significantly different ($p<0.01$). The DO level varied from 1.30 mg $L^{-1}$to 5.80 mg $L^{-1}$with an average 4.05 mg L^{-1}during the MON season. However, during the POM, an average level of 4.53 mg $L^{-1}$was observed with the levels varying from 0.40 mg $L^{-1}$to 5.55 mg L^{-1}between sites. Significant differences ($p<0.01$) were detected for the DO levels observed between the two seasons. The observed EC values recorded an average of 43.67 µS cm^{-1} during the MON season. During the POM, EC levels ranged from 39.50 µS cm^{-1} to 9060.00 µS cm^{-1} with an average of 3178.16 µS cm^{-1}. The EC levels varied significantly ($p<0.01$) between the two seasons.

The study sites exhibited TDS levels with an average value of 21.31 mg L^{-1}during the MON season. In the POM, the TDS levels varied from 19.00 mg $L^{-1}$to 4440.00 mg L^{-1} with an average of 1557.22 mg L^{-1}. The TDS levels were found to be significantly different ($p<0.01$) between the two seasons. The salinity was almost nil during the MON season. However, during the POM season the salinity ranged from 0.00‰ to 5.10‰ with an average of 1.64‰. Thus the salinity levels varied significantly between the two seasons ($p<0.01$). The observed resistivity in the surface waters ranged from 0.01 Ω· cm to 99.99 Ω· cm with a mean resistivity of 3.15 Ω· cm during the MON season and varied from 0.00Ω·cmto 0.03 Ω· cm with an average of 0.01 Ω· cm during the POM season. However, no significant differences were found between the resistivity observed between the two seasons. Turbidity in the study area during the MON season ranged from 77.30 NTU to 993.00 NTU with an average turbidity of 627.76 NTU. The turbidity levels went beyond the measurable range at some sites during this season. During the POM season, the turbidity ranged from 45.50NTU to 284.00 NTU with an average value of 112.77 NTU. The turbidity levels showed significant differences ($p<0.01$) between the two seasons. The study sites exhibited redox values ranging from 45.20 mV to 154.40 mV during the MON season. During the POM season redox values ranged from -22.20 mV to 138.00 mV. The observed redox values varied significantly ($p<0.01$) between the two seasons.

Table 4.1 Descriptive statistics of the physicochemical parameters of surface water during MON season

Parameters	Units	N	Minimum	Maximum	Mean	Std. Deviation
Temperature	°C	32	25.60	27.80	26.70	0.64
pH	-	32	4.26	6.09	5.81	0.32
DO	mg L^{-1}	32	1.30	5.80	4.05	0.73
EC	µS cm^{-1}	32	0.00	112.90	43.67	21.99
TDS	mg L^{-1}	32	0.00	55.00	21.31	10.70
Salinity	ppt	32	0.00	0.00	0.00	0.02
Resistivity	Ω·cm	32	0.01	99.99	3.15	17.67
Turbidity	NTU	28	77.30	993.00	627.76	209.67
Redox	mV	32	45.20	154.40	63.59	18.97

Table 4.2 Descriptive statistics of the physicochemical parameters of surface water during POM season

Parameters	Units	N	Minimum	Maximum	Mean	Std. Deviation
Temperature	°C	32	28.70	32.00	30.13	0.72
pH	-	32	4.58	7.49	6.82	0.59
DO	mg L^{-1}	32	0.40	5.55	4.53	0.87
EC	µS cm^{-1}	32	39.50	9060.00	3178.16	3392.73
TDS	mg L^{-1}	32	19.00	4440.00	1557.22	1662.40
Salinity	ppt	32	0.00	5.10	1.64	1.88
Resistivity	Ω·cm	32	0.00	0.03	0.01	0.01
Turbidity	NTU	32	45.50	284.00	114.77	53.63
Redox	mV	32	-22.20	138.00	13.68	32.15

4.1.2 Major and Minor Ions

Major and minor ions such as chloride, carbonate, bicarbonate, sodium, potassium, calcium and magnesium were studied. The descriptive statistics of the major and minor ions observed during the MON and POM seasons are given in Table 4.3 and Table 4.4, respectively. The chloride concentrations in the study area were recorded between 4.00 mg $L^{-1}$to 26.00 mg L^{-1} with an average value of 12.25 mg L^{-1}during the MON season, whereas, an average Cl^- was recorded as 966.63 mg L^{-1}during the POM season. The observed Cl^- concentration varied significantly ($p<0.01$) between the two seasons. Carbonate was not detectable in the surface waters of the Lower Baram for either season. The study sites exhibited bicarbonate levels between 18.30 mg L^{-1} and 42.70 mg L^{-1} with an average of 32.79 mg L^{-1}during

the MON season. During the POM season, the HCO_3^- content ranged from 12.20 mg $L^{-1}$to 54.90 mg $L^{-1}$with an average value of 27.74 mg L^{-1}. The observed bicarbonate levels between the two seasons were significantly different ($p<0.05$).

The concentrations of sodium varied between 2.29 mg L^{-1} to 14.15 mg L^{-1} with an average value of 5.54 mg L^{-1}during the MON season. Whereas in the POM season, it varied from 2.63 mg L^{-1} to 1317.00 mg L^{-1} with an average value of 377.02 mg L^{-1}. Significant variation in the levels of Na ($p<0.01$) were observed between the two seasons. Potassium content varied from 1.82 mg L^{-1} to 10.69 mg L^{-1} with an average value of 4.67 mg L^{-1}during the MON season. In the POM season, K^+ concentrations ranged from 1.61 mg L^{-1} to 279.20 mg L^{-1} with an average value of 61.48 mg L^{-1}. The potassium levels varied significantly ($p<0.01$) between the two seasons. In the present study, Ca^{2+} content in the study sites during MON season ranged from 0.11 mg L^{-1} to 4.33 mg L^{-1} with an average value of 1.87 mg L^{-1}. During the POM season, the calcium levels varied from 0.38 mg L^{-1} to 301.00 mg $L^{-1}$with an average value of 34.43 mg L^{-1}. Significant differences ($p<0.01$) in the levels of Ca^{2+} were observed between the two seasons. Magnesium levels ranged from 2.30 mg L^{-1} to 6.90 mg L^{-1} between sites with an average value of 4.00 mg L^{-1}during the MON season. During the POM season, the levels varied from 1.94 mg L^{-1} to 445.23 mg L^{-1} between sites with an average value of 77.27 mg L^{-1}. Significant differences ($p<0.01$) in the levels of Mg^{2+} were observed between the two seasons.

Table 4.3 Descriptive statistics of the major and minor ions in surface water during MON season

Parameters	Units	N	Minimum	Maximum	Mean	Std. Deviation
Chloride	mg L^{-1}	32	4.00	26.00	12.25	5.99
Carbonate	mg L^{-1}	32	BDL	BDL	BDL	BDL
Bicarbonate	mg L^{-1}	32	18.30	42.70	32.79	6.89
Sodium	mg L^{-1}	32	2.29	14.15	5.54	2.47
Potassium	mg L^{-1}	32	1.82	10.69	4.67	2.23
Calcium	mg L^{-1}	32	0.11	4.33	1.87	1.08
Magnesium	mg L^{-1}	32	2.30	6.90	4.00	0.95

Table 4.4 Descriptive statistics of the major and minor ions in surface water during POM season

Parameters	Units	N	Minimum	Maximum	Mean	Std. Deviation
Chloride	mg L^{-1}	32	BDL	2940.00	966.63	1096.11
Carbonate	mg L^{-1}	32	BDL	BDL	BDL	BDL
Bicarbonate	mg L^{-1}	32	12.20	54.90	27.74	9.15
Sodium	mg L^{-1}	32	2.63	1317.00	377.02	437.62
Potassium	mg L^{-1}	32	1.61	279.20	61.48	77.25
Calcium	mg L^{-1}	32	0.38	301.00	34.43	60.83
Magnesium	mg L^{-1}	32	1.94	445.23	77.27	101.47

4.1.3 Nutrients

Nutrients such as orthophosphate, sulfate, ammoniacal nitrogen and nitrate were studied in the surface waters of the Lower Baram River. The descriptive statistics of the nutrient levels observed during the MON and POM seasons are given in Table 4.5 and Table 4.6, respectively. The orthophosphate content in the study sites recorded an average of 0.24 mg L^{-1} during the MON season. During the POM season, the PO_4^{3-} ranged from 0.15 mg L^{-1} to 0.89 mg L^{-1} with an average of 0.23 mg L^{-1}. However, the PO_4^{3-} content did not vary significantly between seasons. The average sulfate concentrations recorded in the study sites was 1.31 mg L^{-1} during the MON season and during the POM season, was recorded at 131.13 mg L^{-1}. A significant difference ($p < 0.01$) was observed in the sulfate content between the two seasons. Ammoniacal nitrogen was absent in the study area during the MON season. However, during the POM an average value of 9.38 µg L^{-1} was recorded. There was no significant difference between the two seasons. The concentration of nitrate showed an average of 2.50 µg L^{-1} during the MON season and 0.04 mg L^{-1} during the POM season. However, the nitrate concentrations varied significantly ($p < 0.01$) between seasons.

Table 4.5 Descriptive statistics of the nutrient levels in the surface water during MON season

Parameters	Units	N	Minimum	Maximum	Mean	Std. Deviation
Orthophosphate	mg L^{-1}	32	BDL	1.66	0.24	0.30
Sulfate	mg L^{-1}	32	BDL	5.00	1.31	1.53
Ammoniacal Nitrogen	mg L^{-1}	32	BDL	BDL	BDL	BDL
Nitrate	µg L^{-1}	32	BDL	50.00	2.50	9.50

Table 4.6 Descriptive statistics of the nutrient levels in the surface water during POM season

Parameters	Units	N	Minimum	Maximum	Mean	Std. Deviation
Orthophosphate	mg L^{-1}	32	0.15	0.89	0.23	0.13
Sulfate	mg L^{-1}	32	BDL	410.00	131.13	145.12
Ammoniacal Nitrogen	mg L^{-1}	32	BDL	300.00	9.38	53.03
Nitrate	mg L^{-1}	32	BDL	0.29	0.04	0.05

4.1.4 Trace elements concentration

The concentrations of major and trace elements such as Fe, Mn, Al, B, Cu, Zn, Pb, Co, Cd, Cr, Ni and Hg were measured in the surface waters of the Lower Baram River and the descriptive statistics of the analysed elements are presented in Table 4.7 and Table 4.8 for both the MON and POM season, respectively. The average elemental concentrations were patterned in the decreasing order as Al > Fe > Mn > B > Zn > Cr > Ni > Cu > Co > Pb > Cd > Hg and Fe > Al > B > Cr > Ni > Zn > Cu > Mn > Co > Pb > Cd > Hg during the MON and POM seasons, respectively.

Table 4.7 Descriptive statistics of the elements levels in the surface water during MON season

Parameters	Units	N	Minimum	Maximum	Mean	Std. Deviation
Cu	mg L^{-1}	32	0.04	0.15	0.06	0.02
Zn	mg L^{-1}	32	0.03	0.39	0.09	0.08
Pb	µg L^{-1}	32	BDL	78.00	3.75	14.87
Co	mg L^{-1}	32	0.02	0.09	0.03	0.02
Ni	mg L^{-1}	32	0.12	0.27	0.15	0.03
Cd	µg L^{-1}	32	BDL	5.00	1.81	1.45
Mn	mg L^{-1}	32	0.13	3.08	0.38	0.52
Fe	mg L^{-1}	32	3.37	43.26	15.57	12.60
Al	mg L^{-1}	32	0.76	88.17	17.07	24.05
Cr	mg L^{-1}	32	0.17	0.39	0.27	0.06
Hg	µg l^{-1}	32	BDL	1.71	0.28	0.30
B	mg L^{-1}	32	BDL	2.20	0.33	0.44

Table 4.8 Descriptive statistics of the elements levels in the surface water during POM season

Parameters	Units	N	Minimum	Maximum	Mean	Std. Deviation
Cu	mg L^{-1}	32	0.04	0.14	0.06	0.02
Zn	mg L^{-1}	32	0.02	0.15	0.04	0.02
Pb	mg L^{-1}	32	BDL	0.04	0.01	0.02
Co	mg L^{-1}	32	0.02	0.06	0.03	0.01
Ni	mg L^{-1}	32	0.13	0.18	0.15	0.01
Cd	µg L^{-1}	32	BDL	7.00	2.63	2.01
Mn	mg L^{-1}	32	0.06	0.11	0.08	0.01
Fe	mg L^{-1}	32	2.30	10.81	4.89	1.70
Al	mg L^{-1}	32	0.42	6.15	2.28	1.00
Cr	mg L^{-1}	32	0.10	0.26	0.19	0.05
Hg	µg L^{-1}	32	BDL	0.48	0.19	0.12
B	mg L^{-1}	32	BDL	1.60	0.80	0.38

Copper concentration in the study area ranged from 0.04 mg L^{-1} to 0.15 mg L^{-1} with a mean of 0.06 mg L^{-1} during the MON season and 0.04 mg L^{-1} to 0.14 mg L^{-1} with a mean of 0.06 mg L^{-1} during the POM season. There was no significant difference in the concentrations of Cu between seasons. Zinc concentrations were observed to be in the range of 0.03 mg L^{-1} to 0.39 mg L^{-1} with a mean of 0.09 mg L^{-1} in the MON season and 0.02 mg L^{-1} to 0.15 mg L^{-1} with a mean of 0.04 mg L^{-1} during the POM season. There existed a significant difference ($p < 0.01$) of Zn

concentrations between the two seasons. The average Pb concentration during the MON season was found to be 3.75 µg L^{-1} and observed in only 3 sites, and the remaining showed below the detection limit. During the POM season, the average Pb concentration was found to be 0.01 mg L^{-1} and was recorded only in 5 sites. Pb concentrations were significantly different ($p < 0.05$) between the two seasons. Cobalt concentrations ranged from 0.02 mg L^{-1} to 0.09 mg L^{-1} during the MON and 0.02 mg L^{-1} to 0.06 mg L^{-1} during the POM season, with an average of 0.03 mg L^{-1} during both seasons. There was no significant difference between the seasons for Co concentration. Nickel concentration was recorded in the range of 0.12 mg L^{-1} to 0.27 mg L^{-1} in the MON season with an average concentration of 0.15 mg L^{-1} and 0.13 mg L^{-1} to 0.18 mg L^{-1} in the POM season, with an average concentration of 0.15 mg L^{-1}. The observed Ni concentrations for both seasons were not significantly different.

The average Cd concentration was recorded as 1.81µg L^{-1} and 2.63 µg L^{-1} during the MON and POM seasons respectively and was not found to be significantly different seasonally. Manganese concentration was observed in the range of 0.13 mg L^{-1} to 3.08 mg L^{-1} with an average of 0.38 mg L^{-1} in the MON and 0.06 mg L^{-1} to 0.11 mg L^{-1} with an average concentration of 0.08 mg L^{-1} in the POM season. The Mn concentration observed between seasons were significantly ($p<0.01$) different. Iron concentration, was in the range of 3.37 mg L^{-1} to 43.26 mg L^{-1} during the MON and 2.30 mg L^{-1} to 10.81 mg L^{-1} during the POM season. The average was recorded as 15.57 mg L^{-1} and 4.89 mg L^{-1} during the MON and POM season, respectively and varied significantly ($p<0.01$) between seasons. Aluminum concentration was in the range of 0.76 mg L^{-1} to 88.17 mg L^{-1} with a mean concentration of 17.07 mg L^{-1} in the MON season and 0.42 mg L^{-1} to 6.15 mg L^{-1} with a mean concentration of 2.28 mg L^{-1} during the POM season. There existed a significant difference ($p<0.05$) of Al concentrations observed between the two seasons. Chromium concentration ranged between 0.17 mg L^{-1} to 0.39 mg L^{-1} with a mean concentration of 0.27 mg L^{-1} during the MON season. During the POM season the concentration ranged from 0.10 mg L^{-1} to 0.26 mg L^{-1} with a mean concentration of 0.19 mg L^{-1}. The concentration of Cr varied significantly ($p<0.01$) between seasons. The average mercury concentrations were found to be 0.28 µg L^{-1} and 0.19 µg L^{-1} during the MON season and POM season respectively and did not vary significantly between seasons. The average Boron concentrations in the present study was recorded as 0.33 mg L^{-1} and 0.80 mg

L^{-1} during the MON and POM periods respectively and the B content varied significantly ($p < 0.01$) between the seasons.

4.2 Discussion

4.2.1 Geochemistry of trace elements in the Baram river surface water during the MON season

In order to understand the geochemical processes occurring in the water column, factor analysis was carried out. Since the ionic composition of the water column, pH, dissolved oxygen and temperature have always had an interaction with trace elements (Gundersen & Steinnes, 2003; De Souza Machado et al., 2016), they have also been included in this factor model to elucidate the geochemical processes. Further, considering the fact that the units of measurement of all these parameters were not the same, the entire data set was standardised before carrying out the factor analysis. The results are given in Table 4.9.

Factor-1 was loaded with Pb, Zn, Mn, Ni, Cu, Co, Hg and Al. The percent contribution of factor-1 explains 28.16% variance in this factor model. The association of these elements suggests the adsorption of Pb, Zn, Ni, Cu, Co, Hg and Al on Mn hydroxide floccules (Sholkovitz et al., 1978; Means et al., 1978; Johnson, 1986; Dong et al., 2000; Li et al., 2001; Kay et al., 2001; Feng et al., 2007; Zhong & Wang, 2008; Suda & Makino, 2016). The adsorption was neither being influenced by pH, nor by ionic composition of the water column, though it has been very well demonstrated in earlier studies that the pH is the main factor affecting the formation of Mn-hydrous oxides, as well as the adsorption of other elements onto it (Lion et al., 1982; Tipping & Heaton, 1983). Under such an observation, this factor model implies that the Mn-hydrous oxide adsorbed species were being transported from the upstream and not being influenced in the downstream areas by the mere reason that during the MON, the heavy flooding does not permit the intrusion of the saline water into the lower reaches of the river. Such a flooding was observed during the field work. Moreover, this was further authenticated by the observation that none of the samples had a measurable salinity (Table 4.1).

It should be noted here that the trace elements were measured using the 11 µm filtered samples, instead of using the 0.45 µm as in many earlier studies (Karbassi et al., 2008; Stolpe & Hassellov, 2010). This has been done purposefully in order to include the quantum of the trace elements, which were being transported by

the river in the colloidal form (Duarte & Cacador, 2012) and as natural nanoparticles (Wigginton et al., 2007). That being said, we wish to emphasise the Baram River originates in the highlands of Borneo and flows through a dense rainforest carrying along with it many dissolved and particulate organics. The presence of organics, especially humic acids, reduces the water column pH significantly (Oliver et al., 1983), and thereby paves the way for the dissolution of many minerals from this river's sediments (Walther, 1996). After dissolution, the trace elements move to the water column and can form metal-organic complexes (Tipping & Heaton, 1983) and that could play a vital role in transporting these metals into the South China Sea. If the samples were filtered using the 0.45 µm, a significant part of the metal organic complexes could have been removed, and there would be no way to discern the contribution of such metal organic complexes in a metals transport mechanism. At the same time, by filtering through a11 µm filter paper there could be a loss of information on the quantity of purely dissolved metal being transported by the rivers. Nonetheless, the preliminary field work showed that the river water was always turbid with significant suspended sediment concentrations.

Under such a situation, most of the dissolved trace elements are likely to be adhered to these fine particles. These colloidal and natural nanoparticles are potentially reactive in the environment (Duarte & Cacador, 2012), and could easily release the adsorbed trace elements with a slight change in environmental conditions (Hatje et al., 2003). The trace elements bound to various fractions of the sediments were also analyzed furthermore, such a release of trace elements from the colloidal and natural nanoparticles could drastically affect their exchange between the water and sediment column. Moreover, these fine particles themselves could flocculate and settle once they mix with the seawater (Sholkovitz, 1978), transporting all their metal content to the sediments. The presence of such a mechanism can only be revealed if the trace elements bound to the fine particles were included in the analysis as well. There is one other dimension to this problem, in the forested soil the mobilisation of Al has also been reported by several earlier studies (Evans, 1986; Mulder & Stein, 1994; Van Hees et al., 2004). The Al, being amphoteric (Pacioglu et al., 2016), with the capability to form polynuclear complexes and being a good adsorbent as $AlOH_3$ (Palleiro et al., 2017), has a potential to adsorb many trace elements akin to Fe and

Mn-oxyhydroxides[1]. To understand all such processes, and to recognise the individual strength of Fe, Mn and Al oxy-hydroxides, it is essential that, such an information not be lost through filtering by using 0.45 µm. While the results do not represent the true dissolved form of the trace elements, it should also be noted that filtering by using 0.45 µm also has its own problems. One such important problem is the 0.45 µm filtered water does not contain only the purely dissolved form of trace elements; they also contain natural nano particles (Wigginton et al., 2007).

The second problem is that there has been no uniformity in the definition of the cut-off for truly a dissolved form of the trace elements (Karbassi & Nadjafpour, 1996). Thus, the analytical results do not represent the purely dissolved form of the trace elements but at the same time, this methodology is designed to extract whatever key information is essential to understand the trace elements behaviour in the riverine and estuarine environment of a typical tropical rain forest river systems in this case the almighty Baram. The authentication of all our concepts have been proven by three observations: 1) the observation of a high concentration of 88.17mg/l of Al in the confluence of Sungai Bakung with the Baram, 2) the loading of Al with factor 1 along with the trace elements Pb, Zn, Mn, Ni, Co and Hg in this factor model and, 3) the high factor score of 4.96 for the sample collected at the Sungai Bakung-Baram confluence (BES-26). These observations demonstrated that not only the Mn-oxy-hydroxides, but also the Al-species could have a significant role in the transportation of some of the trace elements. While, it has been very well established that Fe-Mn oxy-hydroxides are important carriers for trace elements, this factor

[1]As shown in Table 4.10, for the location BES-26, the factor score was 4.96. All other factor scores were below unity. This is a clear-cut information that Al was being mobilised from the Upper Baram region. In our analytical results, we could not identify a higher concentration of Al, either in the Sungai Bakung or in the Baram, but did at the confluence of the Baram and Sungai Bakung (BES-26). Such an observation can only be explained if Al, was being transported in particulate form through the Baram River and got dissolved when this river water mixed with the highly acidic Sungai Bakung. This is how, very high concentrations of Al (88.17 mg/l) were observed at this confluence point. However, nowhere in the upstream and downstream to this confluence point, could a higher concentration of Al be observed in the water column. Since the water was filtered with 11µ filter paper, Al, whether dissolved or in the particulate form could have been easily measured. The absence of such an observation, points to the authigenic clay mineral formation downstream from this confluence point.

model does not exhibit such a significant role for Fe in this river. Instead, Al has taken the role of Fe. Indeed, it is the strong interaction of Mn-oxyhydroxide surface with Al in the presence of adsorbed organics (Tipping & Heaton 1983), which is thought to play a significant role in the formation of metal-organic complexes - possibly the major carriers of trace elements in this river system.

Table 4.9 Rotated component matrix of water quality parameters during MON season

Parameters	Communality	Component					
		1	2	3	4	5	6
Temperature	0.71	-0.27	**-0.65**	0.08	-0.43	0.09	0.16
pH	0.73	-0.14	-0.05	-0.19	**0.79**	-0.17	-0.12
DO	0.92	-0.11	-0.13	0.08	**0.93**	0.12	0.05
EC	0.95	-0.17	-0.24	**0.90**	-0.20	-0.09	-0.04
Chloride	0.87	0.28	0.06	**0.70**	0.00	**0.54**	0.09
Bicarbonate	0.79	-0.21	0.34	0.03	-0.27	**0.48**	-0.57
Orthophosphate	0.75	0.09	0.09	0.01	-0.24	0.04	**0.82**
Sulfate	0.82	-0.26	**-0.69**	0.42	0.22	0.06	0.23
Nitrate	0.64	-0.09	-0.15	-0.05	0.08	-0.35	**0.69**
Boron	0.60	-0.04	**-0.69**	0.10	0.21	-0.18	-0.19
Pb	0.81	**0.86**	0.07	0.07	-0.11	0.16	0.16
Zn	0.89	**0.84**	0.40	-0.11	-0.06	-0.04	-0.07
Mn	0.95	**0.96**	0.02	-0.05	-0.04	0.10	0.09
Fe	0.87	0.26	**0.78**	-0.28	0.21	-0.14	-0.23
Ni	0.95	**0.90**	0.35	-0.04	-0.06	-0.05	-0.11
Cu	0.83	**0.77**	0.42	-0.15	0.04	-0.07	-0.16
Cr	0.61	-0.06	-0.48	0.49	0.24	-0.17	-0.22
Cd	0.63	0.33	0.59	-0.05	-0.40	-0.05	0.06
Co	0.87	**0.88**	0.18	-0.22	0.02	-0.08	0.12
Na	0.92	-0.21	-0.24	**0.88**	-0.01	0.21	-0.02
K	0.94	0.62	**0.71**	-0.06	-0.14	0.05	-0.13
Ca	0.89	-0.40	-0.21	0.05	-0.15	**0.80**	-0.16
Mg	0.77	0.31	0.07	0.12	0.10	**0.78**	-0.17
Hg	0.82	**0.89**	-0.07	0.03	-0.13	0.07	0.08
Al	0.84	**0.72**	**0.48**	-0.10	-0.01	-0.26	-0.15
Percent variance explained		**28.16**	**16.57**	**11.08**	**9.20**	**8.80**	**7.59**
Total variance explained		**81.39**					
Eigen Value		**Greater than 1**					

Table 4.10 Factor scores for water quality parameters during POM season

Samples	Factor 1	Factor 2	Factor 3	Factor 4	Factor 5	Factor 6
BES 01	-0.39	-0.44	0.09	0.24	-0.19	0.55
BES 02	-0.16	-0.74	1.61	-0.10	-0.50	0.52
BES 03	-0.46	-0.44	1.14	-0.05	0.42	0.89
BES 04	-0.66	-0.18	0.93	0.09	-0.17	-0.08
BES 05	-0.30	-0.18	2.52	0.66	0.25	-0.03
BES 06	0.17	-0.56	-1.24	1.15	3.17	0.29
BES 07	-0.40	-0.18	3.18	0.75	0.01	0.20
BES 08	0.27	-2.21	-0.75	0.12	-1.07	1.65
BES 09	0.02	-1.17	-0.09	0.15	-1.57	-0.17
BES 10	0.04	-1.01	0.46	1.72	1.80	-0.85
BES 11	-0.45	-0.58	-0.70	-0.05	-0.01	-0.07
BES 12	-0.09	-1.49	-0.59	0.12	0.05	0.28
BES 13	-0.86	-0.92	-0.76	-0.76	-0.64	0.40
BES 14	-0.64	-0.86	-1.06	-0.72	1.10	0.65
BES 15	-0.50	-0.97	-0.57	-0.53	0.42	-0.11
BES 16	-0.67	-0.55	-0.86	0.26	-0.62	-0.63
BES 17	-0.61	-0.50	-0.32	0.53	-1.54	-4.19
BES 18	-0.58	0.84	-0.31	-1.02	-0.45	-0.26
BES 19	0.81	1.38	0.31	0.42	-0.68	1.34
BES 20	0.35	0.85	-0.14	-0.02	-1.86	1.33
BES 21	-0.32	1.17	-0.38	0.23	-0.23	-0.07
BES 22	0.17	0.43	-0.55	-0.55	0.31	0.39
BES 23	0.54	0.59	-0.52	-1.46	-0.03	-0.40
BES 24	-0.02	0.56	-0.15	0.35	0.11	-0.92
BES 25	-0.72	0.58	0.96	-4.11	1.07	-0.51
BES 26	**4.96**	-0.69	0.47	-0.81	0.27	-0.90
BES 27	0.07	0.58	-0.63	0.06	0.90	0.17
BES 28	0.73	0.90	-0.73	0.85	-0.67	0.31
BES 29	-0.15	1.05	-0.41	0.21	0.25	0.52
BES 30	0.21	1.28	-0.60	0.80	-0.99	0.75
BES 31	-0.30	2.28	0.19	0.71	1.12	-0.47
BES 32	-0.06	1.16	-0.47	0.79	-0.03	-0.58

Factor 2 explained 16.57% variance in the factor model and was loaded with sulphate, B, Fe, K, Al and temperature. Of these, temperature, sulphate, and boron have negative loading and Fe, K and Al have positive loading. Though the loading of temperature, sulphate, boron and Al are on the lower side, they have been taken into account because only their association provides a meaningful geochemical interpretation. The association of temperature with sulphate implies the temperature

controlled Jarosite dissolution. The Jarosite is a allunite series mineral with the formula $K.Fe_3(SO_4)_2(OH)_6$ and is a member of the aluminium-phosphate-sulphate (APS) minerals with the general formula $AB_3\ (XO_4)_2\ (OH)_6$, where A is a large cation (Na, U, K, Ag, NH_4, Pb, Ca, Ba, Sr, REE's and B is one of the cations in the group Al, Fe, Cu and Zn (Dill, 2001).

Allunite formation can occur at a pH greater than 3.3, and, the main source for Al is the dissolution of aluminium silicates during microbial mediated pyrite oxidation, which releases sulphuric acid (Sánchez-España et al., 2016). The tropical climatic conditions are most suitable for the formation of APS minerals (Dill et al., 2002), and peraluminus parent rocks enriched in sulphur and phosphorous are a prerequisite (For a review, refer Dill, 2001). Though the mineralogical studies were not carried out due to the sophistication involved in the identification of APS minerals, this cannot preclude the chances for its formation in a terrain where volcanic, sedimentary, and metamorphic processes have taken place, and allunite has a very good chance of formation in all these environments (Dill, 2001). Given the fact that the Baram River basin mainly consists of turbidites and shale, which are a rich source for the sedimentary pyrite and its dissolution might release sulphuric acid into the environment resulting in the formation of allunite group of minerals.

These minerals can be transported downstream and their dissolution is indicated by the negative loading of sulphate and boron in the water column whereas, the positive loading of Fe, K and Al should be interpreted as their precipitation to the sediments in the form of authigenic clay minerals. To confirm this hypothesis, the partition coefficient (Kd) of the elements were calculated and a factor model was run and the results are given in Table 4.11. From the results of factor loading of the Kd values of Fe, Al, and SO_4, and temperature and potassium (in the water column), the formation of authigenic clay mineral is inferred (Mackin & Aller, 1986; Mackenzie & Kump, 1995; Rahman, 2016; Church, 2016). The formation of authigenic minerals in the estuarine and coastal areas is a widely disputed topic. Though the objective of this work is not aimed at the exploration of authigenic clay mineral formation, this research proposes the prevalence of such a mechanism in the lower reaches of the Baram River. However, further investigation is necessary towards this end.

Table 4.11 Rotated component matrix for the partition coefficients (Kd) of elements and water quality parameters during MON season

Parameters	Communality	Component					
		1	2	3	4	5	6
Kd - Zn	0.69	0.57	0.12	0.15	0.00	-0.03	0.57
Kd - Mn	0.88	0.10	-0.02	0.89	-0.06	-0.04	0.28
Kd - Fe	0.86	0.86	0.23	0.26	-0.03	-0.06	0.01
Kd - Ni	0.81	0.12	-0.49	0.67	0.03	0.12	-0.29
Kd - Cu	0.77	-0.44	0.09	0.09	0.24	0.05	0.71
Kd - Cr	0.69	-0.55	-0.11	0.54	0.28	-0.07	0.01
Kd - Co	0.78	0.39	0.10	0.71	0.16	0.28	0.06
Kd - Al	0.84	0.87	0.06	0.18	-0.09	0.09	-0.17
pH	0.83	0.04	-0.18	-0.03	-0.88	-0.18	0.04
DO	0.88	0.15	0.11	-0.11	-0.85	-0.05	-0.33
EC	0.88	0.39	0.80	-0.07	0.12	-0.06	0.26
Orthophosphate	0.67	0.01	0.03	-0.06	0.54	-0.46	-0.42
Sulfate	0.80	0.73	0.39	-0.21	-0.16	-0.13	-0.20
Temperature	0.67	0.70	0.12	0.18	0.35	-0.03	0.05
Chloride	0.92	-0.12	0.86	0.02	0.10	0.26	-0.29
Bicarbonate	0.78	-0.19	0.00	0.07	0.10	0.81	0.28
Na	0.89	0.37	0.84	-0.08	-0.04	0.14	0.12
K	0.87	-0.91	0.05	0.01	0.18	0.07	-0.05
Ca	0.80	0.41	0.15	0.25	0.07	0.73	-0.12
Mg	0.85	-0.22	0.25	-0.15	0.03	0.72	-0.45
Percent variance explained		**24.55**	**13.70**	**11.84**	**10.83**	**10.78**	**9.02**
Total variance explained		**80.73**					
Eigen Value		**Greater than 1**					

Factor-3 accounted for 11.08% variance in the data and was loaded with EC, Na and Cl. This implies the influence of seawater in this stretch of the Baram River, where the samples have been collected. Though this was during a MON season with flooding of the river, the loading of these parameters on factor-3 clearly demonstrates that even during the MON season, there is a sea water incursion in the river, though this could not be measured using the salinity probe in the surface waters. This incursion was further confirmed by the factor model given in Table 4.11, where a similar pattern was observed on factor-2, demonstrating the validity of our inference. Further, authigenic clay mineral formation can occur only in the presence of saline water, (Mackenzie & Kump, 1995) which has been already inferred from the factor analytical results. Factor-4 explained 9.20% variance in the data and was loaded with pH and DO, illustrating the role of water column productivity on the pH and dissolved oxygen (Feely et al., 2010). Such water column productivity could be due to phytoplanktons, such as diatoms. The productivity dependence of pH and DO in

the water column can be confirmed by the positive loading of both pH and DO – as the productivity continues to draw down the dissolved CO_2, increase the pH and release O_2 in the water column.

Factor-5 accounted for 8.80 % variance in the data and was loaded with Ca, Mg, Cl and HCO_3. In the natural waters, bicarbonate is present above a pH of 4.5 and carbonate ions are present above a pH of 8.3 (Millero, 1979). Under such a situation, the loading of HCO_3 with Cl^- ions along with Ca and Mg is illustrative of their contribution from the sea water. This indicates the dissolution of Ca/Mg carbonates. But the loading of Cl^- on this factor is indicative of the influence of sea water on such a dissolution. The mechanisms of such a dissolution under the influence of Cl^- ions cannot be easily understood. Factor-6 accounted for 7.59% variance in the factor and was loaded with orthophosphate and nitrate, indicating the remobilisation of the nutrients from the sediments of the water column (Zhang et al., 1997). Such a remobilisation is possible upon the degradation of sedimentary organic matter (Emerson et al., 1980; Nedwell et al., 1994; Morford et al., 2005). Such a degradation is likely to release low molecular weight organics into the water column, (Nedwell et al., 1994; Beck et al., 2008) which may form strong metal organic complexes (Beck et al., 2008) and serve as an important repository for some of the elements like Cu and Zn (Widerlund, 1996). Such an association is also inferred from the factor model in Table 4.11.

4.2.2 Geochemistry of trace elements in the Baram River surface water during POM season

During the POM season, the behaviour of trace elements exhibit a different pattern compared to the MON period as revealed in the factor analysis results (Table 4.12). Six factors accounted for 82.61% variance in this factor model. The first factor accounts for 40.46% variance in the data and was loaded with salinity, Cl^-, SO_4, Pb, Ni, Cd, Na and Ca, whereas Co, Mg and B had moderate positive loading and Temperature , Mn, Cr and Al had moderate negative loadings. At first, it seemed that the incursion of saline water into river water remobilised Pb, Ni, Cd, and Co from the sediments to the water column. However looking at the factor analytical results based on the partition coefficient (Kd) values of the trace elements (Table 4.13), such a remobilisation resulted in the redistribution of Pb and Ni except Co, which was released into the water column. Such a mechanism could be understood by the

loading of Kd-Pb with Kd-Ni with Kd-Mn, where it is understood that the remobilised Pb is adsorbed by Al-hydrous oxides (Kinniburgh et al., 1976; González-Costa et al., 2017) and the remobilised Ni is adsorbed with Mn-oxyhydroxides (González-Costa et al., 2017). The formation of Al-hydroxide and Mn-hydroxide under the influence salinity (Sholkovitz, 1978; Tiihonen, 2016) could be understood by the moderate negative loading of Mn and Al on factor-1 in Table 4.12. With regard to Cr, it could be understood that Cr is removed from the water column and found its way into the sediments - since it exhibits negative loading on factor- 1 as opposed to the positive loading of Kd-Cr on factor- 1 along with salinity. In the case of Cd, the analytical results are not available for the sediments and its fate is unknown. The association of Cd and SO_4 with salinity simply means that they were derived from seawater.

Table 4.12 Rotated component matrix of water quality parameters during POM season

Parameters	Communality	Component					
		1	2	3	4	5	6
Temperature	0.81	**-0.62**	-0.53	0.01	0.20	-0.28	0.17
pH	0.96	0.58	**0.74**	0.16	-0.05	0.19	0.09
DO	0.90	0.25	**0.90**	0.11	0.02	0.10	0.07
Salinity	0.97	**0.91**	0.19	0.30	0.10	0.10	0.05
Chloride	0.98	**0.91**	0.19	0.31	0.09	0.10	0.04
Bicarbonate	0.73	0.55	0.37	0.23	0.44	0.18	-0.09
Orthophosphate	0.95	0.03	**-0.97**	0.02	0.03	-0.04	-0.01
Sulfate	0.98	**0.90**	0.18	0.33	0.09	0.09	0.07
NH_3-N	0.95	0.01	**-0.97**	0.01	-0.01	0.04	0.07
Nitrate	0.76	0.02	0.16	-0.04	-0.08	**0.84**	0.11
Boron	0.79	**0.63**	-0.28	0.31	-0.09	0.38	-0.27
Pb	0.96	**0.94**	0.18	0.23	0.00	0.00	0.01
Zn	0.69	-0.23	0.06	-0.23	-0.07	0.37	**0.66**
Mn	0.75	**-0.58**	-0.44	-0.40	0.05	-0.19	-0.14
Fe	0.74	-0.27	-0.01	**-0.80**	-0.05	0.06	0.14
Ni	0.84	**0.86**	-0.01	-0.24	0.03	-0.18	0.04
Cu	0.54	-0.11	0.07	-0.09	**-0.70**	0.11	-0.12
Cr	0.84	**-0.75**	-0.20	-0.43	0.01	-0.10	-0.20
Cd	0.85	**0.89**	0.04	0.20	0.02	-0.12	0.03
Co	0.70	**0.68**	-0.18	0.35	0.00	-0.08	0.29
Na	0.97	**0.95**	0.17	0.20	0.05	0.02	-0.01
K	0.79	0.60	0.18	**0.60**	0.10	-0.06	0.15
Ca	0.75	**0.84**	0.06	-0.11	-0.06	-0.01	-0.19
Mg	0.78	**0.69**	0.18	0.39	0.19	0.26	0.12
Hg	0.84	-0.08	-0.01	-0.05	**0.89**	0.00	-0.20
Al	0.69	**-0.49**	0.05	-0.15	0.05	0.08	**-0.65**
Percent variance explained		**40.46**	**16.43**	**9.20**	**6.27**	**5.27**	**4.99**
Total variance explained		**82.61**					
Eigen Value		**Greater than 1**					

Table 4.13 Rotated component matrix for the partition coefficients (Kd) of elements and water quality parameters during POM season

Parameters	Communality	Component				
		1	2	3	4	5
Temperature	0.83	-0.70	-0.51	0.26	-0.02	0.12
pH	0.95	0.60	0.73	0.15	-0.04	-0.17
DO	0.94	0.24	0.93	0.16	-0.05	-0.03
EC	0.92	0.90	0.24	0.25	-0.02	0.03
Salinity	0.97	0.93	0.19	0.27	-0.06	0.03
Chloride	0.99	0.93	0.20	0.27	-0.04	0.03
Bocarbonate	0.58	0.64	0.36	0.12	0.18	-0.04
Orthophosphate	0.93	0.01	-0.96	0.07	-0.09	0.04
Sulfate	0.98	0.92	0.19	0.31	-0.06	0.02
Nitrate	0.65	0.15	0.21	-0.24	-0.09	-0.72
Boron	0.68	0.72	-0.24	-0.04	-0.31	-0.01
Na	0.95	0.92	0.17	0.22	-0.10	0.09
K	0.75	0.65	0.18	0.54	0.00	0.09
Ca	0.70	0.81	0.01	-0.20	-0.08	0.07
Mg	0.76	0.79	0.18	0.28	0.09	-0.12
Kd - Pb	0.69	0.40	0.24	0.65	-0.14	-0.18
Kd - Zn	0.73	0.25	-0.04	-0.14	0.06	0.80
Kd - Mn	0.85	0.14	0.25	0.08	0.87	-0.11
Kd - Fe	0.73	0.60	-0.07	0.45	0.39	0.06
Kd - Ni	0.76	-0.25	-0.19	0.02	0.80	0.13
Kd - Cu	0.53	-0.01	0.14	-0.29	-0.38	0.53
Kd - Cr	0.69	0.63	0.14	0.47	0.23	0.07
Kd - Co	0.68	-0.63	0.08	-0.24	0.46	0.07
Kd - Al	0.59	0.16	-0.06	0.74	0.10	-0.01
Percent variance explained		**38.62**	**13.64**	**10.51**	**9.05**	**6.69**
Total variance explained		**78.51**				
Eigen Value		**Greater than 1**				

Factor-2 accounted for 16.43% of variance and was loaded with pH and DO whereas orthophosphate and ammoniacal-nitrogen are negatively loaded. Orthophosphate was remobilized from the sediments only under reducing conditions (Sundby et al., 1986) whereas ammonia is the by-product of anaerobic bacterial degradation of organic matter (Canfield et al., 1993; Baric et al., 2002). Hence, it is imperative that when there is an increase in DO in the water column, the release of orthophosphate and ammoniacal-nitrogen to the water should be diminished. This is how orthophosphate and ammoniacal nitrogen are negatively loaded when DO exhibits positive loading. Such an observation indicates the influence of seawater, whose pH is, in general, higher than the river water pH. Factor-3 accounted for 9.20% of the variance in the factor model and was positively loaded with K and negatively loaded with Fe. The positive loading of K was only moderate. This may

indicate either the loss of K from Fe bearing clay minerals (Craw, 1981) or loss of iron from biotite (Acker & Bricker, 1992). This should be confirmed by further study.

Factor-4 accounted for 6.27% of the total variance and was positively loaded with Hg and negatively loaded with Cu. This cannot be interpreted with the available data. Factor-5 accounted for 5.27% of the total variance and was loaded with nitrate. This indicated nitrification in the water column (Scott & Abumoghli, 1995; Cébron et al., 2003; Strauss et al., 2004). Factor-6 accounted for 4.99% of the total variance and was loaded with Zn and Al exhibited moderate loading. This cannot be interpreted with the available data. However, looking at the factor model in Table 4.13, Kd-Zn was loaded on factor-5 along with nitrate, which exhibited a negative loading. This indicated the Zn toxicity to the nitrification process in water column (Hu et al., 2004; Zarcinas & Rogers, 2002). From the factor analysis results, one important observation was authigenic clay mineral formation could be observed only during the MON season. Explaining such an observation will be the topic for future research.

4.3 Saturation index

The potential for a chemical reaction can be determined by calculating the chemical equilibrium of the water with the mineral phase. The saturation index calculation is used to determine the equilibrium state of the water with respect to a mineral phase (Mackenzie & Garrels 1971; Stumm & Morgan 1981). The saturation index (SI) indicates whether a particular water sample is either saturated or not with respect to a particular mineral. A positive SI indicates the water is being supersaturated with respect to the particular mineral phase and therefore incapable of dissolving more of the mineral and under suitable physico-chemical conditions, the mineral phase in equilibrium may precipitate. A negative index (SI) indicates under saturation condition and dissolution of the mineral phase, while neutral SI is in equilibrium state with the mineral phase. The saturation index for mineral phases during the MON and POM season is tabulated in Table 4.14 and Table 4.15 respectively. It should be noted in the table, the value 999 means the particular samples does not have the gypsum and anhydrite because of the absence of sulphate. Furthermore, a predominant dissolution of the mineral phases was observed from the SI of the Baram River samples during both seasons.

Table 4.14 The saturation index for mineral phases during MON season

Sample	Magnesite	Dolomite	Calcite	Anhydrite	Gypsum	Aragonite
BES-01	-3.5187	-7.056	-3.5797	-5.0784	-4.8658	-3.7222
BES-02	-3.5914	-7.2471	-3.6992	-4.5039	-4.2921	-3.8416
BES-03	-3.4785	-6.9342	-3.4993	-4.6781	-4.4663	-3.6416
BES-04	-3.5946	-7.2132	-3.6622	-4.7847	-4.5729	-3.8045
BES-05	-3.5219	-6.9562	-3.4778	-4.6488	-4.4371	-3.6202
BES-06	-3.2133	-6.368	-3.1929	-4.7632	-4.5476	-3.3358
BES-07	-3.409	-6.8912	-3.5258	-4.3799	-4.1682	-3.6681
BES-08	-3.7825	-7.8632	-4.1237	-4.8747	-4.6625	-4.2661
BES-09	-3.9773	-9.1891	-5.256	-5.8306	-5.6192	-5.3982
BES-10	-3.5129	-6.9323	-3.463	-4.2119	-4.0001	-3.6053
BES-11	-3.4658	-6.998	-3.577	-5.0517	-4.8408	-3.7192
BES-12	-3.5852	-7.2357	-3.6953	-4.6034	-4.3924	-3.8375
BES-13	-3.8388	-7.3479	-3.5556	-4.9052	-4.6955	-3.6976
BES-14	-3.3668	-6.4336	-3.1139	-4.2673	-4.0581	-3.2558
BES-15	-3.4397	-6.8457	-3.4531	-4.507	-4.2978	-3.595
BES-16	-3.5599	-7.0816	-3.566	-5.0849	-4.8736	-3.7082
BES-17	-3.9953	-8.1406	-4.1883	-4.8977	-4.6854	-4.3307
BES-18	-3.4645	-6.8102	-3.3881	999	999	-3.5306
BES-19	-3.3738	-7.0189	-3.6807	999	999	-3.824
BES-20	-3.6086	-8.2618	-4.69	999	999	-4.8332
BES-21	-3.5539	-7.0698	-3.5534	999	999	-3.6964
BES-22	-3.4993	-7.0059	-3.5452	999	999	-3.6881
BES-23	-3.9503	-8.0769	-4.175	999	999	-4.3167
BES-24	-3.9335	-7.8376	-3.9428	999	999	-4.0857
BES-25	-4.9266	-9.7902	-4.9078	999	999	-5.0501
BES-26	-4.0123	-9.0045	-5.0322	999	999	-5.1749
BES-27	-3.1439	-6.5748	-3.4762	999	999	-3.6184
BES-28	-3.3627	-7.8103	-4.4839	999	999	-4.6271
BES-29	-3.4539	-7.1621	-3.7457	999	999	-3.8887
BES-30	-3.5659	-8.0258	-4.4961	999	999	-4.6393
BES-31	-3.3137	-6.7091	-3.4304	999	999	-3.5737
BES-32	-3.5138	-7.1255	-3.6486	999	999	-3.7917

Table 4.15 The saturation index for mineral phases during POM season

Sample	Magnesite	Dolomite	Calcite	Anhydrite	Gypsum	Aragonite
BES-01	-0.7658	-1.0638	-0.3515	-1.2401	-1.0381	-0.4927
BES-02	-0.8188	-1.4722	-0.7097	-1.6721	-1.4722	-0.8505
BES-03	-0.7426	-1.1386	-0.4523	-1.4719	-1.2717	-0.5931
BES-04	-0.8764	-1.7176	-0.8986	-1.6949	-1.4957	-1.0393
BES-05	-0.9738	-2.0359	-1.12	-1.8415	-1.6427	-1.2606
BES-06	-0.6121	-1.4578	-0.9037	-1.9935	-1.7947	-1.0443
BES-07	-0.4267	-1.5931	-1.2227	-2.0392	-1.8394	-1.3635
BES-08	-1.1668	-2.7931	-1.6859	-2.1779	-1.9805	-1.8262
BES-09	-0.5669	-1.4743	-0.9676	-2.0581	-1.8612	-1.1079
BES-10	-1.2067	-2.7208	-1.5754	-2.1105	-1.9146	-1.7156
BES-11	-1.0303	-2.5462	-1.5766	-2.2616	-2.065	-1.7168
BES-12	-1.0966	-2.579	-1.5432	-2.0961	-1.8993	-1.6834
BES-13	-1.1836	-2.4952	-1.3781	-2.0845	-1.8929	-1.5176
BES-14	-0.5116	-1.5969	-1.1465	-2.2477	-2.0511	-1.2866
BES-15	-2.456	-4.385	-1.9934	-2.7474	-2.5532	-2.1332
BES-16	-1.8205	-3.6387	-1.8751	-3.0774	-2.8762	-2.0158
BES-17	-2.8899	-5.3743	-2.5451	-3.8261	-3.628	-2.6853
BES-18	-3.1096	-6.513	-3.4679	-5.2022	-5.0075	-3.6076
BES-19	-2.7595	-5.9701	-3.2697	-5.2356	-5.036	-3.4101
BES-20	-3.1469	-6.7508	-3.6634	-5.4159	-5.2169	-3.8038
BES-21	-3.1336	-6.6682	-3.5948	-5.5914	-5.3928	-3.735
BES-22	-3.1655	-6.8012	-3.6969	-5.4325	-5.2349	-3.8371
BES-23	-3.2291	-6.8819	-3.7156	-5.2789	-5.0828	-3.8556
BES-24	-3.261	-6.8811	-3.684	-5.0416	-4.8465	-3.8238
BES-25	-5.0881	-10.1137	-5.0967	-3.8104	-3.6226	-5.2355
BES-26	-3.3166	-6.9962	-3.7446	-4.9196	-4.7254	-3.8842
BES-27	-3.677	-7.6989	-4.0888	-5.5717	-5.3796	-4.2282
BES-28	-3.2259	-6.9695	-3.808	999	999	-3.9477
BES-29	-3.0125	-6.1483	-3.2023	-4.5533	-4.3607	-3.3417
BES-30	-3.2501	-7.0633	-3.876	-4.9893	-4.7932	-4.0159
BES-31	-3.1636	-6.497	-3.3967	-4.69	-4.4944	-3.5366
BES-32	-3.5586	-7.4112	-3.9165	-4.8407	-4.6456	-4.0563

4.4 Risk assessment Indices

Two indices were used to evaluate the risk in this study, specifically, i) the Contamination index (C_d) and, ii) the heavy metal evaluation index, in order to evaluate the water quality of the Lower Baram River.

4.4.1 The Contamination Index (C_d)

This method was developed by Backman et al. (1998), to evaluate the degree of contamination in the analysed water samples. This index evaluates the combined effects of several quality parameters, which are considered harmful to household water. In this study, the contamination index was calculated for the analysed elements specifically, Fe, Mn, Al, Cu, Zn, Pb, Ni, Cr, Cd, Co and Hg, by using the following equation:

$$C_d \sum_{i=1}^{n} C_{fi}$$

$$C_{fi} = \frac{C_{Ai}}{C_{Ni}} - 1$$

Where,

C_{fi} = contamination factor for the i-th component

C_{Ai} = analytical value for the i-th component

C_{Ni} = upper permissible concentration of the i^{th} component (N denotes the normative value).

The resultant Cd values are grouped into three categories as low (C_d< 1), medium (C_d = 1–3) and high (C_d> 3). The computed contamination index for both the MON and POM seasons were given in Table 4.16. In the present study, all the stations fall into the high contamination category (C_d> 3) during both seasons. The values ranged from 28.49 to 64.64 with a mean of 176.19 during the MON season and 36.29 to 92.60 with a mean of 47.26 during the POM season.

4.4.2 Heavy metal evaluation index (HEI)

This index is used to reveal the overall water quality with respect to heavy metals (Edet & Offiong, 2002). This index is calculated by using the following equation:

$$\mathrm{HEI} = \sum_{i=1}^{n} \mathrm{H_c}/\mathrm{H_{mac}}$$

Where, Hc is the monitored value of the i^{th} parameter, and Hmac is the maximum admissible concentration of the i^{th} parameter. The calculated HEI values for both seasons were given in Table 4.16. The HEI values ranged from 39.49 to 654.36 with a mean of 187.19 during the MON season and 47.29 to 103.60 with a mean of 58.26 during the POM season.

Table 4.16 Risk assessment indices for the Lower Baram water samples

Samples	Contamination index (C_d)		Heavy metal evaluation index (HEI)	
	MON season	POM season	MON season	POM season
BES-01	42.78	51.24	53.78	62.24
BES-02	45.18	92.60	56.18	103.60
BES-03	37.53	54.68	48.53	65.68
BES-04	36.73	52.26	47.73	63.26
BES-05	28.49	50.07	39.49	61.07
BES-06	114.18	58.21	125.18	69.21
BES-07	38.87	42.27	49.87	53.27
BES-08	47.78	41.03	58.78	52.03
BES-09	76.00	45.57	87.00	56.57
BES-10	35.50	52.73	46.50	63.73
BES-11	42.06	36.29	53.06	47.29
BES-12	44.94	37.63	55.94	48.63
BES-13	40.49	39.20	51.49	50.20
BES-14	51.82	40.35	62.82	51.35
BES-15	36.44	46.16	47.44	57.16
BES-16	34.44	41.44	45.44	52.44
BES-17	47.93	46.86	58.93	57.86
BES-18	140.13	52.21	151.13	63.21
BES-19	499.38	44.09	510.38	55.09
BES-20	518.90	39.66	529.90	50.66
BES-21	127.72	41.76	138.72	52.76
BES-22	136.66	41.36	147.66	52.36
BES-23	484.68	48.70	495.68	59.70
BES-24	152.15	43.97	163.15	54.97
BES-25	61.03	40.06	72.03	51.06
BES-26	643.36	43.67	654.36	54.67
BES-27	295.68	47.03	306.68	58.03
BES-28	378.54	51.90	389.54	62.90
BES-29	279.52	40.85	290.52	51.85
BES-30	458.96	45.16	469.96	56.16
BES-31	394.28	57.67	405.28	68.67
BES-32	265.85	45.68	276.85	56.68
Minimum	**28.49**	**36.29**	**39.49**	**47.29**
Maximum	**643.36**	**92.60**	**654.36**	**103.60**
Mean	**176.19**	**47.26**	**187.19**	**58.26**
Std. Dev.	**183.64**	**10.08**	**183.64**	**10.08**

4.5 Comparison with the national water quality standards for Malaysia

The mean values of analysed water quality parameters of the present study were compared with the national water quality standards of Malaysia. The water quality standards of Malaysia consist of five classes, which are tabulated in Table 4.17. Table 4.18 shows that all the elements were within the limits (from class I to class V), except for Fe and Al which fall under class V.

Table 4.17 Water classes and uses

CLASS	USES
Class I	Conservation of natural environment. Water Supply I - Practically no treatment necessary. Fishery I - Very sensitive aquatic species.
Class IIA	Water Supply II - Conventional treatment. Fishery II - Sensitive aquatic species.
Class IIB	Recreational use body contact.
Class III	Water Supply III - Extensive treatment required. Fishery III - Common, of economic value and tolerant species; livestock drinking.
Class IV	Irrigation
Class V	None of the above.

Table 4.18 Water quality standards of Malaysia

Parameters	Units	[a]MAC	National water quality standards for Malaysia						This Study	
			I	IIA	IIB	III	IV	V	MON	POM
pH	-	NA	6.5 - 8.5	6 - 9	6 - 9	5 - 9	5 - 9	_	5.807	6.818
DO	mg/L	NA	7	5 - 7	5 - 7	3 - 5	<3	<1	4.053	4.526
EC	µS/cm	NA	1000	1000	-	-	6000	-	43.674	3178.16
TDS	mg/L	NA	50	1000	-	-	4000	-	21.313	1557.22
Turbidity	NTU	NA	5	50	50	-	-	-	674.166	114.772
Pb	mg/L	0.0015	NA	NA	NA	NA	NA	NA	0.004	0.012
Zn	mg/L	5.0000	NL	5	5	0.4*	2	Above IV	0.093	0.038
Mn	mg/L	0.0500	NL	0.1	0.1	0.1	0.2	Above IV	0.382	0.08
Fe	mg/L	0.2000	NL	1	1	1	5	Above IV	15.567	4.888
Ni	mg/L	0.0200	NL	0.05	0.05	0.9*	0.2	Above IV	0.15	0.153
Cu	mg/L	1.0000	NL	0.02	0.02	-	-	Above IV	0.06	0.063
Cr	mg/L	0.0500	NA	NA		NA	NA	NA	0.269	0.185
Cd	mg/L	0.0030	NL	0.01	0.01	0.01* (0.001)	0.01	Above IV	0.002	0.003
Co	mg/L	1.0000	NA	NA	NA	NA	NA	NA	0.032	0.034
Hg	mg/L	0.0010	NL	0.001	0.001	0.004 (0.0001)	0.002	Above IV	0	0
Al	mg/L	NA	NL	-	-	-0.06	0.5	Above IV	17.065	2.282

[a]MAC- Maximum admissible concentration adapted from Siegel, 2002

*- At hardness 50mg/L $CaCO_3$

Un-Bracketed - Maximum; Bracketed values denoted 24-hour average concentrations

NL- Natural levels or absent

4.6 Summary

- Significant difference ($P < 0.05$) was observed for Temperature, pH, DO, Ec, TDS, Salinity, Turbidity, redox, chloride, HCO_3, Sulfate, Nitrate, Na, K, Ca, Mg, B, Pb, Zn, Mn, Fe, Cr and Al between seasons, whereas, the water column concentrations of PO_4^{3-}, NH_3-N, Ni, Cu, Cd, Co and Hg did not show any significant variations between seasons.
- The water samples were filtered using 11 µm filters, instead of using 0.45 µm filters in order to include the quantum of the trace elements, which were being transported in the colloidal form and as natural nanoparticles in the Lower Baram River.
- During the MON season, it was observed from the factor analytical results, that the adsorption of Pb, Zn, Ni, Cu, Co, Hg and Al on Mn hydroxide floccules has been the dominant mechanism controlling their behavior in the water column of the Lower Baram River. The high concentration of Al (88.17 mg $L^{-1)}$ and a factor score of 4.96 for the sample collected at the Sungai Bakung-Baram confluence point (BES-26) during the MON revealed that apart from Mn-oxyhydroxides, the Al-species could also have a significant role in the transportation of the trace elements. The formation of authigenic clay minerals have also been implicated from this factor model along with a consideration of the partition coefficient of the elements.
- During the POM season, the intrusion of seawater was observed causing the remobilization of Pb, Ni and Co from the sediments. However, the adsorbtion of remobilised Pb and Ni onto Al-hydrous oxides and Mn-oxyhydroxides, respectively was demonstrated by their partition coefficients. Thus, Pb and Ni were redistributed within the sediments during the POM. Contrary to this, the remobilised Co was released into the water column. The factor model also revealed the levels of orthophosphate and ammonical-nitrogen were controlled by the water column pH and dissolved oxygen. Notably, the formation of authigenic clay minerals could onlybe observed during the MON season. The reason for such an observation is a topic for future research.

- A predominant dissolution of the mineral phases was observed from the saturation index of the Lower Baram River samples during the MON and POM seasons. Since the water samples were filtered using 11 µm filters, the water samples showed a high contamination category as revealed from the risk assessment indices. Although the results fall within the Malaysian water quality standards, all the elements were within the limits (class I to class IV), except for Fe and Al which falls under class V.

Chapter 5. Provenance of the River sediments

5.1 Introduction

In this chapter, the first part concentrates on the chemistry of the surface sediments from the river bed collected during the monsoon (MON) and post-monsoon (POM) seasons and a long core collected from the mangrove area near the Baram River mouth. The second part mainly focuses on the chemistry of the sediments of the short cores collected at different depositional settings within the lower part of the Baram River basin.

The mineralogical and geochemical compositions of clastic sediments are controlled by many complex factors such as source rock geology, topography/relief, climatic conditions in the source area and hydraulic processes in the transportation and depositional environment (Weltje & Von Eynattan, 2004). Sediments from the river mouth represent the continental input to the ocean after modification by weathering and transport and their REE characterization is important for understanding them in the marine environments (Song & Choi, 2009). In addition, chemical tracers of fine grained sediments of river can be applied to identify the sources and transport of pollutants to the coastal environment (Song & Choi, 2009). Geochemical elements in particular, relatively immobile elements (e.g. Th, Nb, Sc, Zr etc.) and rare earth elements (REE) are transferred nearly quantitatively throughout the sedimentary processes from the source area to the depositional basins and thus these elements are considered important for sediment geochemistry related studies (Taylor & McLennan, 1985; Condie, 1991; Rollinson, 2014).

The Baram River is the second largest river in Sarawak after the Rajang River and originates in the Kelabit Highlands, near the Iran Mountains of East Kalimantan, which forms the border between Sarawak and Indonesia. The Baram Basin's geomorphology is very dynamic and has been modified over a million years by tectonics, geomorphology and lately by land-use/land-cover in the upstream side. From a provenance point of view, this basin has been delivering relatively similar sediments from the Miocene to the present. The geology of the basin is mostly covered by sedimentary to metasedimentary rock with minor amounts of Pliocene-Pleistocene volcanic rocks and ophiolites. The

tectonic upliftment of Borneo since the Mesozoic has been reported and thus the rapid erosion and sedimentation of sediments in the northern part of Borneo during the Neogene is common and continues until today. This river basin experiences tropical climate with small seasonal variation in temperature and abundant rainfall throughout the year. There has also been reports that, the Baram River system has been building a large shelf edge system volumetrically, which is prone to failure on a scale equivalent to the Brunei Slide (Gee et al., 2007). Thus, studying the geochemistry of the Baram River sediments may identify the depositional settings, paleo-weathering and source area characteristics.

5.2 Results of Surface (MON and POM seasons) and a long core sediments

5.2.1 Major Oxides

The statistical summary of the geochemical results for surface sediments (during MON and POM seasons) and a core sediments sample is presented in Table 5.1 and Table 5.2Amongst the major oxides, SiO_2 and Al_2O_3 was recorded higher as 64.74-85.94Wt.% and 5.65-14.41 Wt.% during the MON season and 63.9-89.69Wt.% and 4.24-14.93 Wt.% during the POM season respectively. Fe_2O_3 was moderately higher but there was not much difference in its concentration between the two seasons (1.86-5.17Wt.% and 1.44-5.26 Wt.% with an average of 4.04Wt.% and 4.07Wt.% during the MON and POM season respectively). K_2O varied from 0.93 to 2.44 Wt. % during the MON and 0.67 to 2.42 Wt. % during the POM season respectively. Na_2O, CaO, MnO and P_2O_5 concentrations were recorded lower (average <0.51Wt. %) for both seasons. The average concentrations of major oxides did not show any major variation between the seasons (maximum variation is 0.05 Wt. % for SiO_2).

The SiO_2 content was recorded lower and the Al_2O_3 content was recorded higher in the core sediments compared to the surface sediments of the Lower Baram River as 62.06-70-94 wt. % and 12.56-15.74 Wt. % respectively. Fe_2O_3 content was recorded higher than the surface sediments as 3.93-5.56 Wt. %. K_2O and MgO content varied between 2.06-2.58 Wt. % and 0.91-1.17 Wt. % respectively. CaO, and P_2O_5 contents were recorded low as 0.15-0.26 Wt. % and 0.06-0.12Wt. % respectively. Na_2O content was recorded between 0.58 and 0.67 Wt. % and TiO_2 varied between 0.72 and 0.81 Wt.

%. Loss of Ignition (LOI) in the core sediments was recorded between 6.76 and 9.74 Wt. % and the average LOI in core sediments (8.41 Wt. %) was comparable to the surface sediments of both seasons (7.78 and 7.95 Wt. % during the MON and POM seasons respectively).

The major oxides were normalized against upper continental crust (UCC; values from McLennan, 2001; (Figure 5.1 a-c) in order to observe enrichment or depletion of particular elemental concentrations. In which, the MON surface sediments (Figure 5.1a) showed high variations in elemental concentrations among the samples compared to the POM season (Figure 5.1b) except one sample, which showed a different concentration. Surface sediments from both seasons showed SiO_2 and TiO_2 content either equal to UCC or relatively higher, whilst Al_2O_3, MgO, CaO, Na_2O, K_2O, and P_2O_5 content showed low to moderate depletion compared to UCC except CaO and Na_2O which were extremely depleted compared to other oxides. During the MON season, sample BES 27 (high MnO) and BES 07 (more depleted values for all the major oxides except SiO_2) showed different characteristics compared to other samples. Similarly, during the POM, BES 03 showed high depletion of all the major oxides compared to UCC except SiO_2 content. The normalized spider plot of core sediments (Figure 5.1c) showed a slight to moderate enrichment of SiO_2, Al_2O_3, Fe_2O_3, and TiO_2 and depletion in MnO, MgO, CaO, Na_2O, K_2O and P_2O_5 concentrations with minimum variations amongst the core samples.

5.3 Trace elements

The trace elements are classified as; transitional trace elements (TTE: Sc, V, Cr, Mn, Co, Ni, Cu, Zn); large ion lithophile elements (LILE; Rb, Cs, Ba, Sr), high field strength elements (HFSE; Zr, Hf, Nb, Y, Th, U, Ta and W) and rare earth elements (REE: La-Lu) based on their geochemical behaviour. The statistical summary of the trace elements are presented together with major oxides and REE's in Table 5.1.

5.3.1 Transitional trace elements (TTE: Sc, V, Cr, Mn, Co, Ni, Cu, Zn, Ga)

The average transitional elements (Sc, V, Cr, Mn, Co, Ni, Cu and Zn) were recorded as similar between the seasons except Cu, Zn, Ni and Cr [(Sc=10.75 and 10.63ppm for the MON and POM respectively), (V=83.88; 84.69ppm), (Mn= 320; 321ppm), (Co=9.84; 10.78ppm)]. Copper and Zn concentration varied significantly

between the MON (Cu=142.81; Zn=123.13ppm) and POM (Cu=56.25ppm; Zn=78.44ppm) seasons. The average Cr and Ni contents increased during the POM (Cr=79.06ppm; Ni=35.00ppm) compared to the MON (Cr=64.69ppm; Ni=27.78ppm) season. Among the TTEs, Cu and Zn content decreased during the POM, whereas Ni and Cr content was recorded higher compared to the MON season. The average Sc, V, Cr, Mn, Co, Ni, Cu, and Zn concentrations were recorded in the core sediments as 12.53ppm, 98.83ppm, 75.28ppm, 349ppm, 10.75ppm, 30.56ppm, 330.83ppm, and 241.39ppm respectively, which were higher than the surface sediment concentrations except for Co, Ni, Cr, which were recorded lower than the POM season average values.

5.3.2 Large Ion Lithophile Elements (LILE: Rb, Cs, Ba, Sr, Be)

Large Ion Lithophile Elements did not show significant variations between the seasons. The average values of Rb, Cs, Ba, Sr and Be was recorded as 90.03ppm, 6.49ppm, 212.75ppm, 57.38ppm, and 1.87ppm during the MON season, and 93.25ppm, 6.81ppm, 212.69ppm, 56.78ppm and 1.61ppm during the POM season, respectively. Sample numbers BES 07 during the MON and BES 03 during the POM season showed the lowest LILE concentration. Similarly, the average content of Rb, Cs, Ba, Sr and Be was observed in the core sediments as 116.4ppm, 7.97ppm, 235.28ppm, 66.61ppm and 2ppm respectively, which was higher than the surface sediments in both seasons.

5.3.3 High Field Strength Elements (HFSE: Zr, Hf, Nb, Ta, Y, Th, U and W)

Zirconium and Hf contents were recorded as 185-808 ppm and 4-17.7 ppm during the MON season and 136-614ppm and 3-14ppm during the POM season, respectively. Zirconium content was recorded higher during the MON season (avg. 275.69 ppm) than in the POM (246.91ppm) season. Niobium and Ta content was recorded lower and similar between the seasons (Nb=4-11ppm; Ta=0.7-1.2 ppm during the MON and Nb=3-11ppm; 0.3-1ppm during the POM season respectively). The average Y, Th, U and W was recorded as 24.69ppm, 10.22ppm, 2.67ppm, and 1.97 ppm during the MON season and 22.91ppm, 10.60ppm, 2.73ppm and 4.81ppm during the POM season, respectively. Zirconium and Hf concentrations were recorded lower in the core sediments compared to the surface sediments during both seasons as 171-243ppm and 4.6-8.2ppm for Zr and Hf, respectively. The average concentrations for Nb, Ta, Y,

Th, U and W in the core sediments were recorded as 10.39ppm, 0.98ppm, 23.92ppm, 12.12ppm, 3.16ppm and 2.36ppm, respectively, which were relatively similar to surface sediments or slightly higher except W concentrations, which were recorded higher in the POM season sediments.

Trace element concentrations of surface (both seasons) and core sediments were normalized against Upper Continental Curst values (McLennan, 2001), where, Cu, As, Ag during both seasons and Sb and W during the POM season showed significant enrichments, whilst Sc, Be, V, Ba, Sr, Rb, Nb, Ga and Tl during the MON season and Sc, Be, V, Ba, Sr, Nb, Sn and Tl during the POM season showed depletion compared to the other elements (Figure 5.1 a-c). Other elements showed significant variations in their concentrations between the stations compared to the UCC values. Sample number BES 07 during the MON (Figure 5.1b) and BES 03 during the POM (Figure 5.1b) season showed lesser concentration of many elements than other sampling stations. The UCC normalized plot of core sediments showed enrichment in Y, Cu, Zn, As, Cs and Pb concentrations and depletion in Co, Ni, Zn, Tl concentrations (Figure 5.1c). W concentrations recorded a 7-fold increase over the UCC in a sample (BES 19) during the MON season and in a core sample (Sample No. 19; depth 76cm). The core sediments more or less resembled the surface sediments, however with some limited variation between the samples or at different depths. Wider variations were observed in Fe_2O_3, MnO, P_2O_5, Cu, Ge, W and Pb concentrations compared to the UCC values. Copper and Ag concentrations were enriched 12-fold higher than the UCC concentration.

5.4 Rare Earth Elements (REE)

The rare earth elements concentrations were recorded uniformly between the seasons and between the samples except sample number BES 27 during the MON and BES 03 during the POM season, respectively, which showed very little REE content than the rest of the samples. The ∑REE concentration varied significantly between the samples as 81.7-156.9ppm during the MON season and 56.2-159.1ppm during the POM seasons, respectively with a similar average of 135.4 and 136ppm, respectively during the MON and POM seasons. A chondrite normalized REE pattern (Figure 5.2a-c) showed LREE enrichment (La/Yb_{CN}: 6.17-8.54 during the MON; 6.54-8.70 during the

POM season), flat HREE (Gd/Yb_{CN}:1.08-1.52 during the MON: Figure 5.2a; 1.12-1.53 during the POM season: Figure 5.2b) and negative Eu anomalies (Eu/Eu*: 0.56-0.80 during the MON; 0.62-0.89 during the POM season). The REE concentration in the most studied samples during the MON and in all the samples during the POM were enriched (except one sample each from both seasons) more than the UCC and PASS. In the case of core sediments (Figure 5.2c), which also showed a similar REE pattern as LREE enrichment (La/Yb_{CN}: 6.84-8.60), flat HREE (Gd/Yb_{CN}:1.27-1.52) and negative Eu anomalies (Eu/Eu*:0.62-0.77). The ∑REE concentration in the core sediments ranged from 139.68 to179.32ppm with an average of 152.20 ppm which was higher than the surface sediments of both seasons, and lower than the average ∑REE content of PAAS (184.77 ppm).

Table 5.1 Statistical summary of Bulk geochemistry of surface sediments of the Lower Baram River during MON and POM seasons

Analyte Symbol	MON				POM			
	Min	**Max**	**Avg.**	**St.Dev.**	**Min**	**Max**	**Avg.**	**St.Dev.**
SiO_2	64.74	85.94	71.36	4.80	63.90	89.69	71.31	4.56
SiO_2 (adj)	72.37	89.74	77.71	3.93	72.10	92.38	77.73	3.74
Al_2O_3	5.65	14.41	11.99	2.01	4.24	14.93	11.98	2.01
Fe_2O_3(T)	1.86	5.17	4.04	0.74	1.44	5.26	4.07	0.65
MnO	0.01	0.10	0.04	0.02	0.01	0.07	0.04	0.01
MgO	0.48	1.09	0.89	0.14	0.32	1.10	0.90	0.15
CaO	0.12	0.69	0.19	0.10	0.12	0.20	0.17	0.02
Na_2O	0.30	0.61	0.49	0.07	0.30	0.64	0.51	0.08
K_2O	0.93	2.44	2.00	0.33	0.67	2.42	1.96	0.34
TiO_2	0.43	0.78	0.68	0.09	0.25	0.80	0.67	0.09
P_2O_5	0.03	0.09	0.07	0.02	0.04	0.10	0.07	0.01
LOI	3.40	10.95	7.78	1.60	3.51	11.48	7.95	1.40
Total	98.78	100.40	99.54	0.50	98.53	100.70	99.63	0.70
ICV	0.61	0.74	0.70	0.02	0.58	0.74	0.70	0.03
SiO_2/Al_2O_3	4.49	15.21	6.29	2.15	4.32	21.15	6.37	2.85
Al_2O_3/TiO_2	12.64	18.87	17.47	1.37	15.26	20.18	17.72	1.09
K_2O/Al_2O_3	0.16	0.18	0.17	0.00	0.15	0.17	0.16	0.01
CIA	74	80	78	1.05	74	81	78	1.25
CIW	86	93	91	1.31	84	94	91	1.50
WIP	13	32	27	4.32	10	33	27	4.39
PIA	83	91	89	1.54	82	93	89	1.75
CIA/WIP	3	7	4	0.82	3	8	4	0.97
Sc	5.0	13.0	10.8	1.9	4.0	14.0	10.6	1.7
Be	1.0	2.0	1.9	0.3	1.0	2.0	1.6	0.5
V	42.0	102.0	83.9	13.9	30.0	106.0	84.7	14.0
Ba	109.0	255.0	212.8	32.9	91.0	254.0	212.7	30.9
Sr	35.0	66.0	57.4	7.5	34.0	70.0	56.8	6.9
Y	17.0	29.0	24.7	2.9	13.0	26.0	22.9	2.5
Zr	185.0	808.0	275.7	132.7	136.0	614.0	246.9	93.5
Cr	50.0	90.0	64.7	9.2	40.0	90.0	79.1	8.6
Co	5.0	18.0	9.8	2.2	4.0	13.0	10.8	1.6
Ni	20.0	40.0	27.8	5.1	20.0	40.0	35.0	5.7
Cu	30.0	410.0	142.8	108.2	30.0	190.0	56.3	29.9
Zn	60.0	250.0	123.1	51.8	60.0	130.0	78.4	12.5
Ga	7.0	16.0	13.3	2.2	4.0	18.0	14.2	2.5
Ge	1.0	2.0	1.1	0.2	1.0	2.0	1.2	0.4
As	5.0	10.0	6.5	1.3	5.0	10.0	7.3	1.2
Rb	42.0	112.0	90.0	15.9	29.0	117.0	93.3	15.8
Nb	4.0	11.0	8.1	1.7	3.0	11.0	8.2	2.1
Mo	2.0	4.0	2.7	1.2	0.00	2.00	0.06	0.35
Ag	0.5	3.3	0.9	0.6	0.5	1.3	0.6	0.2
Sn	2.0	10.0	3.8	2.2	1.0	4.0	3.0	0.6
Sb	0.7	0.9	0.8	0.1	0.9	1.9	1.2	0.2
Cs	2.8	8.2	6.5	1.3	1.9	9.0	6.8	1.3

Analyte Symbol	MON				POM			
	Min	Max	Avg.	St.Dev.	Min	Max	Avg.	St.Dev.
La	17.1	32.7	28.1	3.1	12.0	33.2	28.3	3.6
Ce	33.7	66.0	56.7	6.5	23.2	66.5	56.5	7.2
Pr	3.7	7.2	6.1	0.7	2.7	7.5	6.3	0.8
Nd	14.0	27.1	23.2	2.7	8.7	27.8	23.4	3.2
Sm	2.8	5.5	4.6	0.6	1.8	5.6	4.7	0.6
Eu	0.6	1.2	1.0	0.1	0.5	1.2	1.0	0.1
Gd	2.4	5.1	4.2	0.6	1.7	5.1	4.2	0.5
Tb	0.4	0.8	0.7	0.1	0.3	0.8	0.7	0.1
Dy	2.7	5.0	4.2	0.5	2.1	4.6	4.2	0.4
Ho	0.5	1.1	0.9	0.1	0.4	0.9	0.9	0.1
Er	1.6	3.1	2.5	0.3	1.2	2.8	2.5	0.3
Tm	0.3	0.5	0.4	0.0	0.2	0.4	0.4	0.0
Yb	1.7	3.5	2.5	0.3	1.2	3.0	2.6	0.3
Lu	0.3	0.6	0.4	0.1	0.2	0.5	0.4	0.1
Hf	4.0	17.7	6.4	3.0	3.3	14.4	6.0	2.2
Ta	0.7	1.2	0.9	0.1	0.3	1.0	0.9	0.1
W	1.0	5.0	2.0	0.8	4.0	8.0	4.8	1.4
Tl	0.2	0.5	0.4	0.1	0.2	0.7	0.6	0.1
Pb	11.0	123.0	28.5	24.6	7.0	23.0	15.8	2.5
Th	5.8	12.2	10.2	1.4	4.3	12.3	10.6	1.3
U	1.7	3.8	2.7	0.3	1.3	3.3	2.7	0.3
∑ LREE	71.88	139.63	119.75	13.66	48.87	141.57	120.13	15.42
∑ HREE	9.81	19.36	15.69	1.96	7.29	17.74	15.89	1.75
∑REE	81.69	156.92	135.44	15.49	56.16	159.13	136.02	17.04
LREE/HREE	6.86	8.38	7.65	0.36	6.70	8.65	7.54	0.40
La/Sc	2.23	4.48	2.68	0.45	2.36	3.26	2.68	0.19
La/Co	1.76	4.54	2.95	0.55	2.30	3.32	2.64	0.24
Th/Sc	0.84	1.50	0.96	0.12	0.88	1.22	1.01	0.07
Th/Co	0.65	1.71	1.07	0.18	0.89	1.22	0.99	0.08
Cr/Th	5.17	12.70	6.45	1.39	6.36	9.30	7.51	0.55
Zr/Hf	39.82	47.34	43.37	1.84	35.45	45.40	40.71	2.15
Zr/Sc	15.42	125.00	28.71	23.58	12.00	68.22	24.25	11.21
La/Th	2.59	3.56	2.77	0.18	2.55	2.81	2.67	0.07
Co/Th	0.58	1.54	0.96	0.16	0.82	1.12	1.02	0.08

Table 5.2 Statistical summary of Bulk geochemistry of the long core sediments

Analyte Symbol	Min	Max	Avg	St.Dev
SiO_2	62.06	70.94	67.29	2.40
SiO_2 (adj)	69.832339	77.101481	73.68	1.90
Al_2O_3	12.56	15.74	14.15	0.82
Fe_2O_3(T)	3.93	5.56	4.75	0.43
MnO	0.022	0.045	0.04	0.01
MgO	0.91	1.17	1.05	0.07
CaO	0.15	0.26	0.21	0.03
Na_2O	0.58	0.67	0.63	0.02
K_2O	2.06	2.58	2.33	0.13
TiO_2	0.719	0.809	0.75	0.02
P_2O_5	0.06	0.12	0.09	0.02
LOI	6.76	9.74	8.41	0.79
Total	98.53	100.7	99.72	0.76
SiO_2/Al_2O_3	3.94	5.64	4.78	0.44
Al_2O_3/TiO_2	17.43	20.16	18.74	0.88
K_2O/Al_2O_3	0.16	0.17	0.16	0.00
ICV	0.65	0.71	0.69	0.01
CIA	77.52	78.93	78.25	0.32
CIW	90.29	91.62	90.92	0.30
PIA	88.41	90.00	89.17	0.37
WIP	28.42	35.47	31.78	1.78
CIA/WIP	2.21	2.75	2.47	0.13
Sc	11	14	12.53	0.91
Be	2	2	2.00	0.00
V	86	111	98.83	6.87
Ba	210	259	235.28	12.55
Sr	61	75	66.61	3.74
Y	22	28	23.92	1.23
Zr	171	243	200.08	18.34
Cr	70	80	75.28	5.06
Co	9	13	10.75	0.97
Ni	30	40	30.56	2.32
Cu	120	620	330.83	126.07
Zn	140	380	241.39	59.91
Ga	13	19	16.47	1.59
Ge	1	2	1.17	0.38
As	5	8	6.15	0.99
Rb	99	132	116.39	8.70
Nb	8	12	10.39	1.08
Mo	BDL	BDL	BDL	BDL
Ag	0.6	0.6	0.60	0.00

Analyte Symbol	Min	Max	Avg	St.Dev
Sn	2	4	2.86	0.42
Sb	0.5	0.6	0.56	0.05
Cs	6.9	9.3	7.97	0.61
Hf	4.6	8.2	5.81	0.74
Ta	0.8	1.1	0.98	0.09
W	2	13	2.36	1.84
Tl	0.3	0.5	0.43	0.05
Pb	21	38	28.06	4.15
Th	10.7	14.3	12.12	0.94
U	2.8	3.7	3.16	0.22
La	28.9	36.7	31.41	2.18
Ce	58.9	74.6	63.81	4.49
Pr	6.28	8.42	7.02	0.57
Nd	23.9	31.2	26.21	2.02
Sm	4.6	6.3	5.20	0.40
Eu	0.98	1.33	1.13	0.09
Gd	4.3	5.5	4.73	0.31
Tb	0.7	0.9	0.75	0.07
Dy	4.1	5.6	4.66	0.32
Ho	0.9	1.2	0.93	0.07
Er	2.4	3.5	2.75	0.23
Tm	0.36	0.52	0.41	0.03
Yb	2.5	3.5	2.76	0.21
Lu	0.38	0.53	0.42	0.03
La/Th	2.39	2.85	2.59	0.10
Zr/Sc	12.21	22.09	16.15	2.64
Th/Sc	0.86	1.13	0.97	0.06
La/Sc	2.27	2.69	2.51	0.11
Co/Th	0.72	1.02	0.89	0.07
La/Co	2.59	3.47	2.93	0.19
Th/Co	0.98	1.39	1.13	0.10
Cr/Th	5.51	7.48	6.24	0.57
Zr/Hf	27.44	39.30	34.70	3.23
Y/Ho	21.82	27.78	25.76	1.30

5.5 U-Pb dating of zircon grains

The samples from the study area were mostly mud and thus separating the zircon grains was difficult. Therefore, three selected samples from the upstream Baram River were chosen for zircon dating. The studied zircons were mostly detrital and U-Pb dating revealed three age clusters in the samples from the Upper Baram River sediments

(medium to coarse-grained sediments). The sediments of the Baram River yielded a wide age range for zircon from the detrital zircons extracted. Accordingly, the older zircons are mostly Meso-Paleoproterozoic in age (1300-2440Ma). Out of three samples two samples yield two age clusters as 120 Ma and 240 Ma for sample 1; 238.7 Ma and 223.9 Ma for sample 2 and the third sample yielded the youngest age cluster as 4.5Ma. The younger zircons yielded average age peaks at 240, 224, 120, and 4.5Ma. The conventional U-Pb concordia plots for all zircon grains analysis and the young age zircons are presented in Figure 5.3a-i. Uranium and Th concentrations in the studied zircons were in the range of 47–1815 ppm (avg. 533 ppm) and 21–827 ppm(avg. 148 ppm), respectively. The U/Th ratio varied between 0.68 and 29.6 with an average of 5.0.

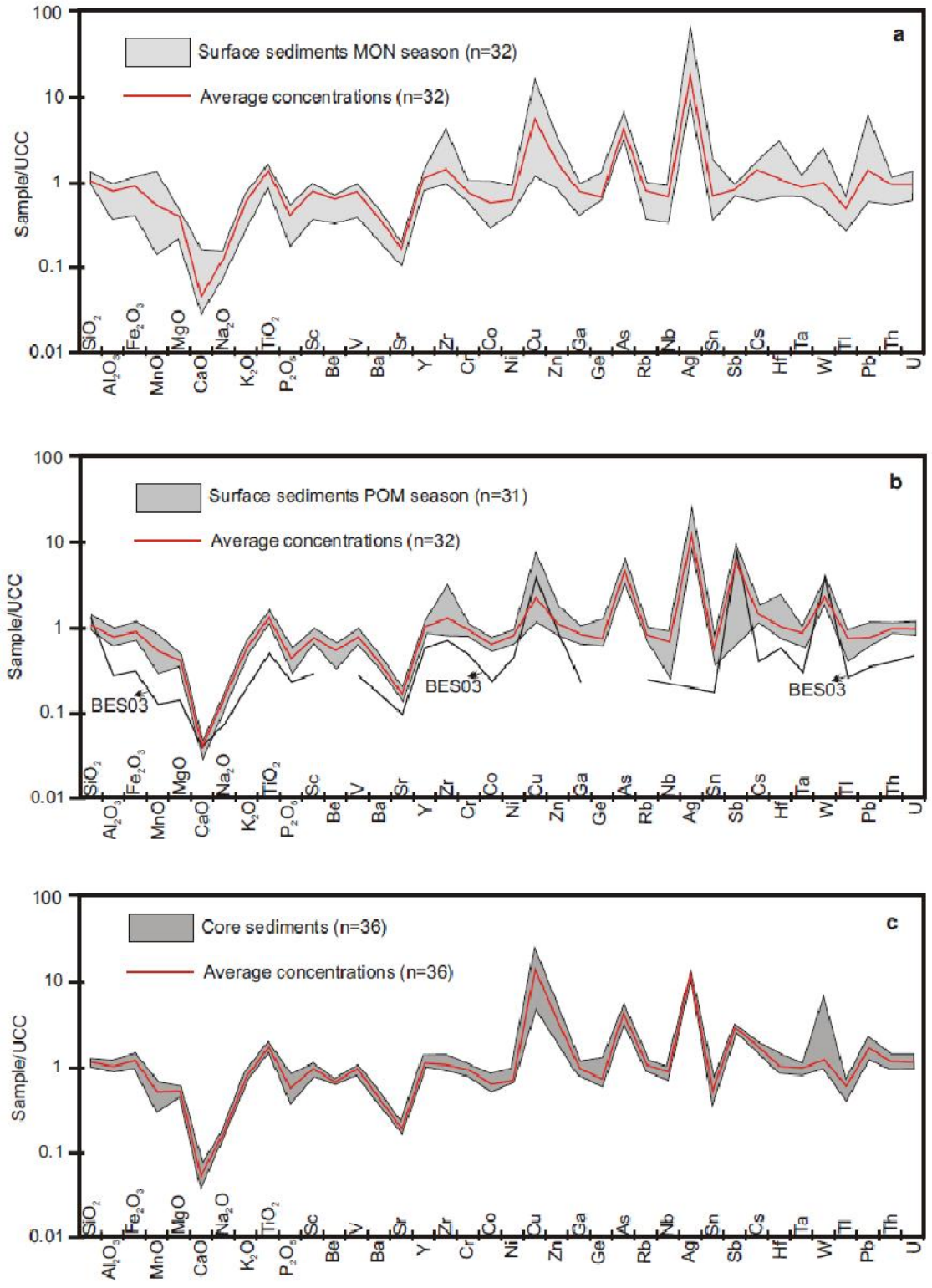

***Figure 5.1a-c. Upper Continental Crust (UCC) normalized spider plot of surface* (a.MON; b.POM) and core sediments (c) from the Lower Baram River**

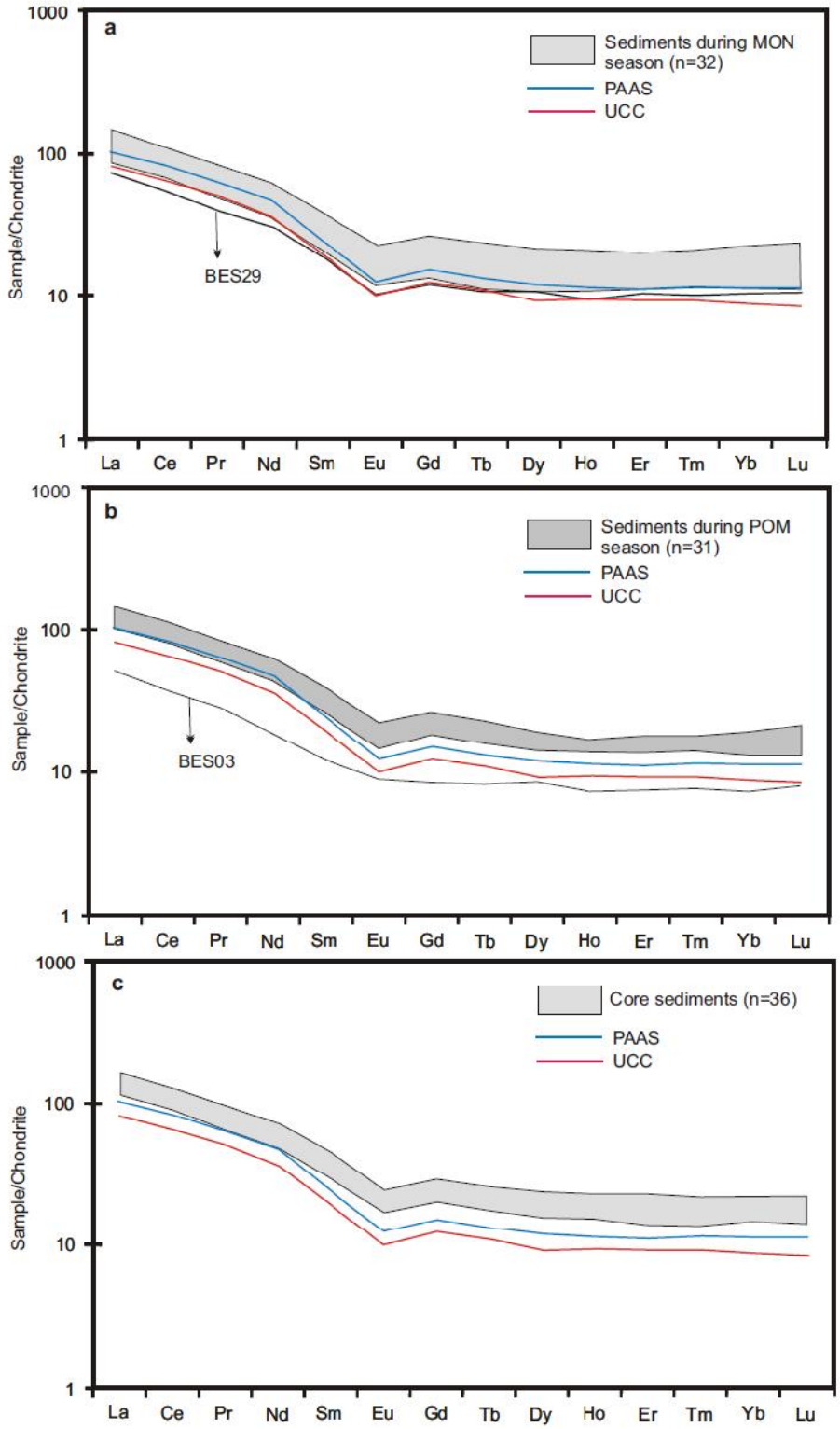

Figure 5.2a-c. Chondrite normalized REE (values from Sun & McDonough, 1989) pattern for the surface **(a.MON; b.POM) and core sediments (c) from the Lower Baram River**

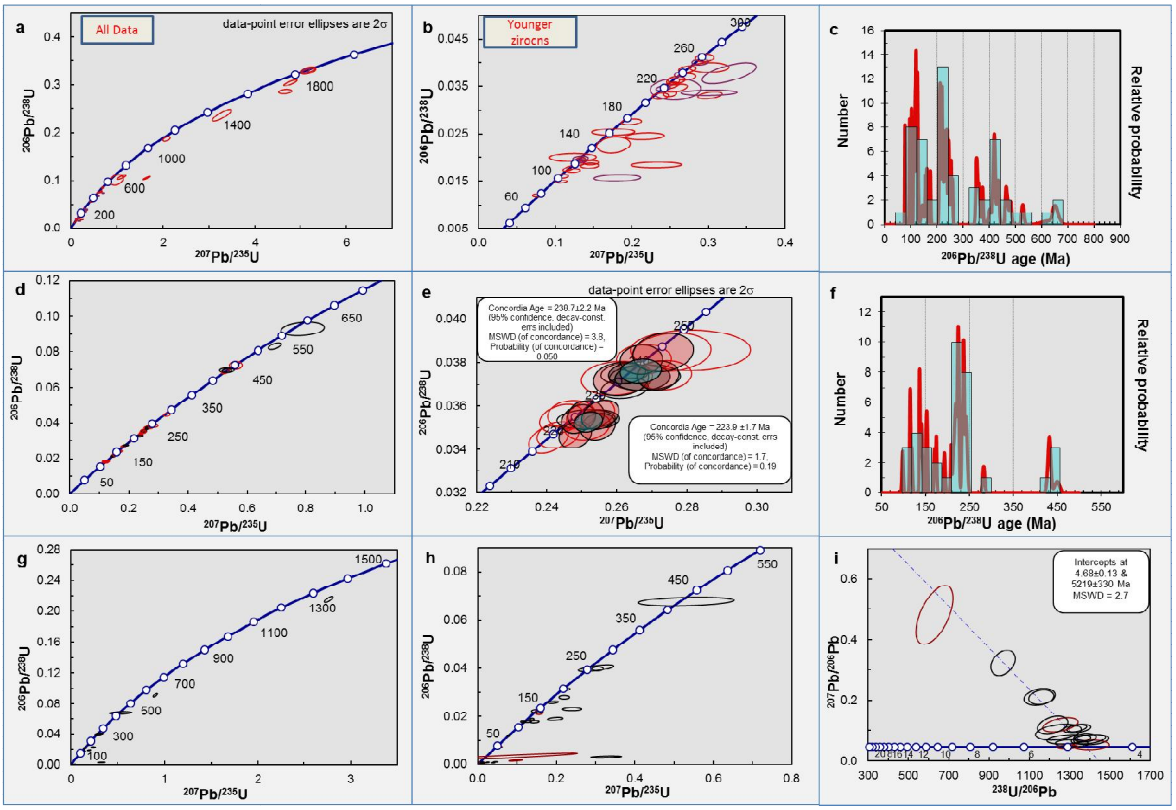

Figure 5.3Conventional U-Pb Concordia plots (total zircons (a, d, g) and young age zircons (b, e, h); data point error ellipses are 2σ) of the U-Pb isotopic analyses results obtained from the laser ablation, and relative frequency plots of youngest zircon ages (c, f, i) obtained from the sediments of the Upper Baram River.

5.6 Discussion

5.6.1 Weathering, sorting and recycling of sediments

The intensity of weathering can be measured for any ancient or recent sediments from different depositional environments by using different geochemical indexes such as a chemical index of alteration (CIA; Nesbitt & Young, 1982), chemical index of weathering (CIW; Harnois, 1988), plagioclase index of alteration (PIA; Fedo et al., 1995), weathering index of Parker (WIP; Parker, 1970), (CIX; Garzanti et al., 2014)and ratios Rb/Sr, Th/U (McLennan et al., 1993) and K_2O/Na_2O (Nesbitt & Young, 1984). In addition, weathering intensity can also be calculated based on single element mobility (i.e. Mg, Ca, Na, Sr, K, Ba) during incongruent weathering of silicates by comparing the single element mobility with the concentration of the non-mobile elements (Ti, Al, Sm, Nd, Th), which have similar magmatic compatibility (Gaillardet et al., 1999; Garzanti et

al., 2013). Gaillardet et al. (1999) used Ti concentration as a non-mobile element against the mobile element with reference to the UCC. However, Ti is preferentially hosted in heavy minerals such as monazite, allanite, titanite, ilmenite and rutile and thus results can be biased (Garzanti et al., 2009). Thus, Garzanti et al. (2013) used Al concentration in order to overcome the samples showing anomalous concentration of heavy mineral due to hydrodynamic processes. αAl values can be quantified for any elements to calculate the bulk mobility of the sediments (Garzanti et al., 2013).

The αAl values were calculated based on Garzanti et al. (2013a) and following a bulk-sediment mobility sequence and is thus illustrated below.

$$\alpha^{Al}_{Ca}>\alpha^{Al}_{Na}>\alpha^{Al}_{Sr}>\alpha^{Al}_{Ba}>\alpha^{Al}_{Mg}>\alpha^{Al}_{K}>\alpha^{Al}_{Rb}>\alpha^{Al}_{Cs} \quad \text{[MON and POM seasons]}$$

$$\alpha^{Al}_{Ca}>\alpha^{Al}_{Na}>\alpha^{Al}_{Sr}>\alpha^{Al}_{Ba}>\alpha^{Al}_{Mg}>\alpha^{Al}_{K}>\alpha^{Al}_{Rb}>\alpha^{Al}_{Cs} \text{ [core sediments]}$$

This sequence is slightly different from what has been observed elsewhere (Gaillardet et al., 2003; Bouchez et al., 2011, Garzanti et al., 2013, 2014). Weathering indices in the samples varied from 74-80 and 74-81 (CIA); 86-93 and 84-94 (CIW); 83-92 and 82-93 (PIA); 13-32 and 10-33 (WIP) for the MON and POM season, respectively. Similarly, core sediments showed the weathering indices ranged as 78-79 for CIA, 90-92 for CIW, 88-90 for PIA and 28-35 for WIP. The WIP index was lower for two samples (BES 07, BES 29) during the MON season, and one sample during the POM season (BES 03) and strongly reflects a quartz dilution (Garzanti et al., 2013a). However, core sediments showed higher WIP values than the surface sediments of both seasons. The calculated αAl values were very similar between the surface sediments of both seasons and core sediments except a small variation for α^{Al}_{Ca} and α^{Al}_{Na}values (Figure 5.4). Significant depletion of mobile elements for both seasons and the core was indicated by high α^{Al} values for Ca, Na and Sr. The loss was less for larger cations such as K, Rb and Ba, which showed smaller α^{Al} values compared to smaller cations (Ca, Na, Sr). The depletion of mobile elements with small ionic radii (Ca, Na, Sr) indicated recycling of siliciclastic and low grade meta-sedimentary source rocks, which initially having poor plagioclases (e.g. Garzanti et al. 2013a). α^{Al} values for Cs show less

mobility than other elements since they are adsorbed to secondary clay minerals (Kronberg et al., 1987; Schneider et al., 2016). The CIA, PIA and CIW weathering indices clearly indicated moderate to high weathering intensity in the source region and the mud sediments of the Lower Baram River were also affected by recycling, which was clearly indicated by the high quartz content particularly during the MON season. In addition to the weathering indices, the surface and core mud sediments were plotted in A-CN-K and A-CNK-FM plots (Figure 5.5a,b and Figure 5.6 a,b), where they are clustered near to the average shale, towards illite and above the feldspar join line in the A-CN-K plot (in molecular proportions), which indicated that the sediments are dominated illite and muscovite types of clay minerals rather than rock-forming mineral feldspars and these sediments have undergone moderate weathering. This was further confirmed by the A-CNK-FM plot (Figure 5.5b; in molecular proportions). The previous study by Liu et al. (2012) considered some selected samples (n=3) from the Baram River in their regional study. Accordingly, the Baram River sediments are richer in illite (range: 75-81%) type of clay than kaolinite (avg. range: 10-13%), chlorite (range: 9-13%) and smectite (range: 0). The feldspar content in these samples was very less, altered to clay minerals and indicated moderate to high weathering intensity.

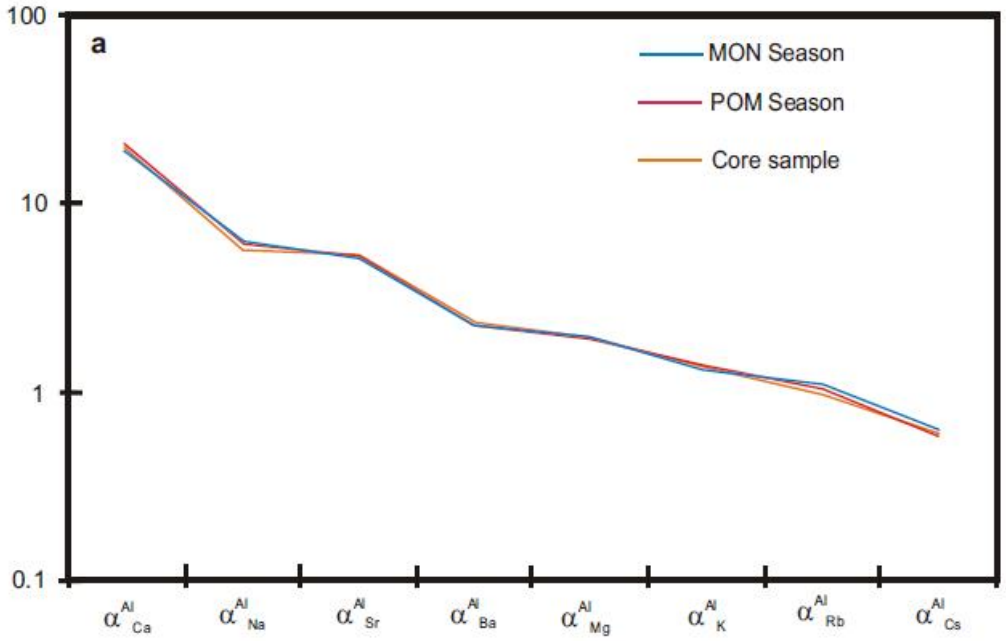

Figure 5.4 Systematic depletion trend of mobile elements relative to non-mobile Al for the sediments of the Lower Baram River (Strongly depleted in smaller cations; i.e., Ca, Na, Sr).

Ancient clastic strata of any large drainage basin might undergone multiple sedimentary cycles (Garzanti et al., 2013, 2014). The mineralogy and chemistry of recent sediments reflects current weathering conditions in addition to the previous weathering and diagenetic histories. Recycled quartzose sediments often show depletion of alkali and alkali earth metals, which is not necessary to be an imprint of weathering (Garzanti et al., 2006; Padoan et al., 2011). Thus, isolating the climatic signal from the composite record is extremely difficult in sedimentary petrology and geochemistry (Cox et al., 1995; Gaillardet et al., 1999; Garzanti et al., 2013, 2014). However, Garzanti et al. (2013) has attempted to differentiate the weathering effect from recycling through proposing a CIA/WIP ratio, which has been used to discriminate between weathering and recycling effects (Garzanti et al., 2014). Accordingly, the first cycle muds have a CIA/WIP ratio between 1 and 2 or lower (e.g. Garzanti et al., 2014), whilst recycled sediments show higher CIA/WIP ratios due to quartz dilution, which reduces the WIP values. Also WIP values remain lower for the polycyclic mud and can be even “0-zero” for the recycled sands (Garzani et al., 2013a). The mud sediments from the Lower Baram River showed the CIA/WIP ratio was between 2.88 and 6.92 during the MON

season (avg. 3.53), 2.80 and 8.40 (avg. 3.58) during the POM season indicating significant recycling effect. The highest values were recorded in the sample BES 07 during the MON season and in BES 03 during the POM season, which showed a higher content of SiO_2 as 89.74 Wt.% (BES 07, MON) and 92.38Wt.% (BES 03, POM) indicating dilution effect of quartz. However, the CIA/WIP ratio for the core sediments were recorded lower than the surface sediments (2.2-2.7; avg.2.5) indicating less quartz dilution by recycling. The WIP values of the sediments were plotted against the CIA values, where the MON sediments showed high effect of quartz dilution, than the POM sediments (Figure 5.7a), whilst core sediments (Figure 5.7b) showed very less effect of quartz dilution which is in agreement with the CIA/WIP ratio. The sorting and recycling effect can be explained effectively using a Zr/Sc Vs. Th/Sc plot (Figure 5.8a,b; McLennan, 1993) since recycling added more heavy minerals (i.e. zircon) to the sediments and thus increased the Zr/Sc ratio. In this plot, there are two characteristic trends; 1) normal compositional variation and 2) zircon addition by recycling. The surface mud sediments of the Lower Baram River were clustered at the end of trend 1 and extended towards trend 2, which indicated the recycling effect and thus zircon enrichment. The MON season samples showed more zircon enrichment (Zr/Sc=15-125; avg. 28.7) than the POM season sediments (Zr/Sc=12-33; avg. 28.3). In the case of core sediments, the recycling effect was less and thus a lower Zr/Sc ratio (12.2-22.1; avg. 16.2) and are plotted in the trend 1, which indicates normal compositional variation.

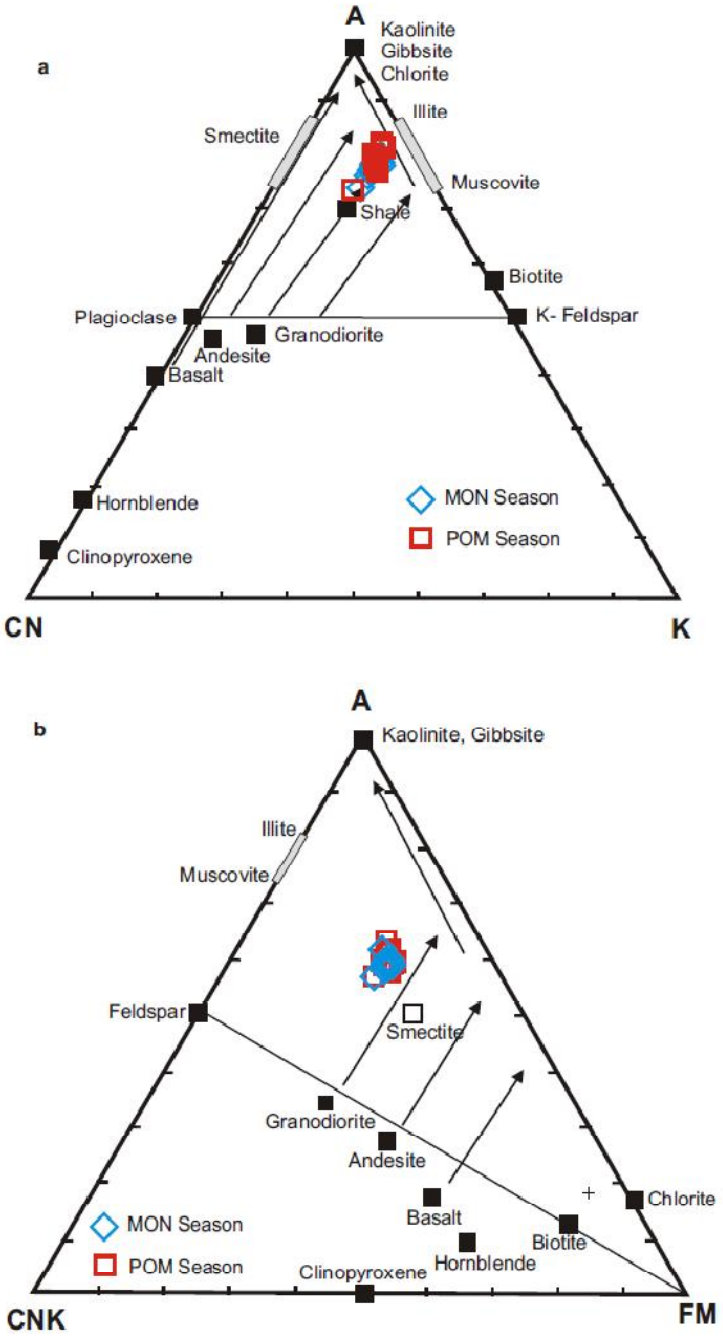

Figure 5.5 (a) A-CN-K and (b) A-CNK-FM (after Nesbitt & Young, 1984; Nesbitt & Wilson, 1992) plots showing the weathering trend for the surface sediments of the Lower Baram River

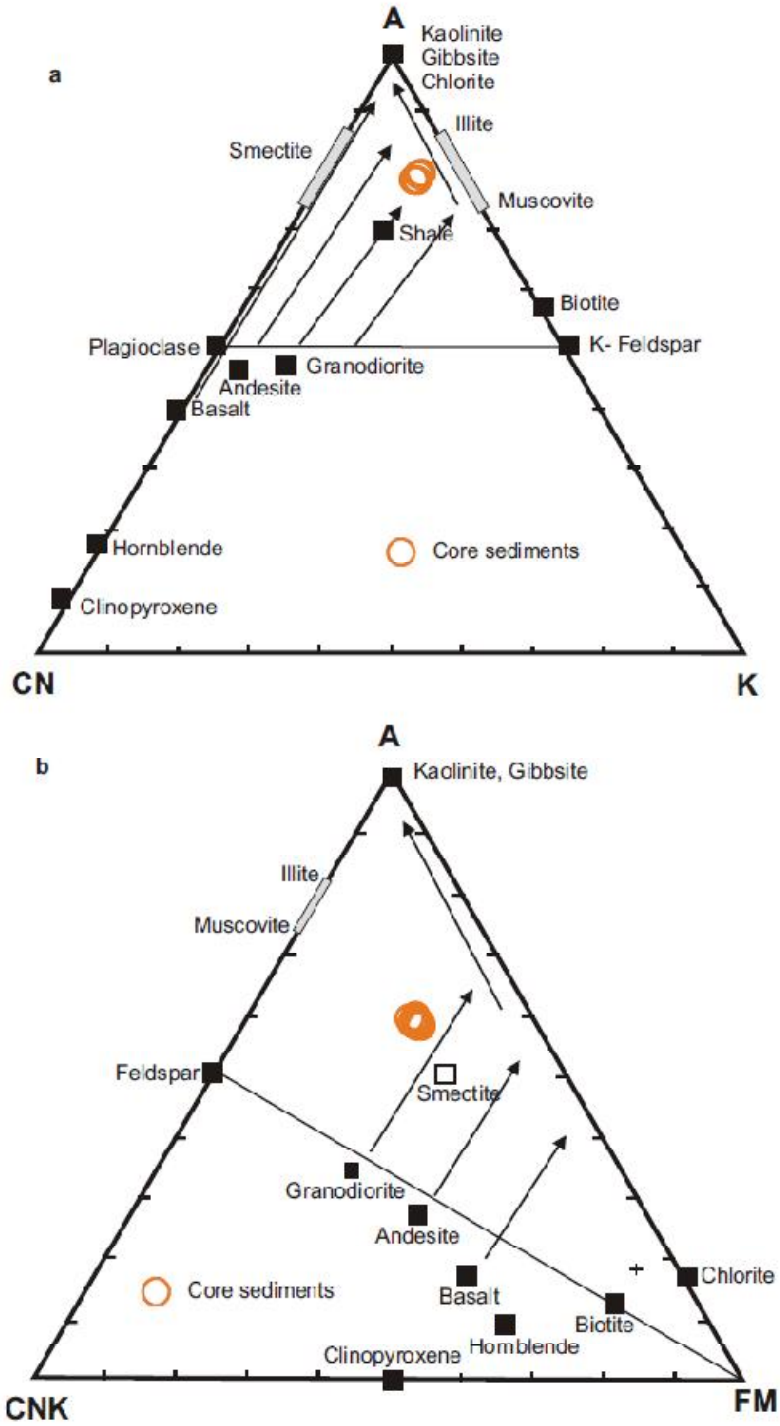

Figure 5.6 a) A-CN-K and (b) A-CNK-FM (after Nesbitt & Young, 1984; Nesbitt & Wilson, 1992) plots showing the weathering trend for the core sediments of the Lower Baram River

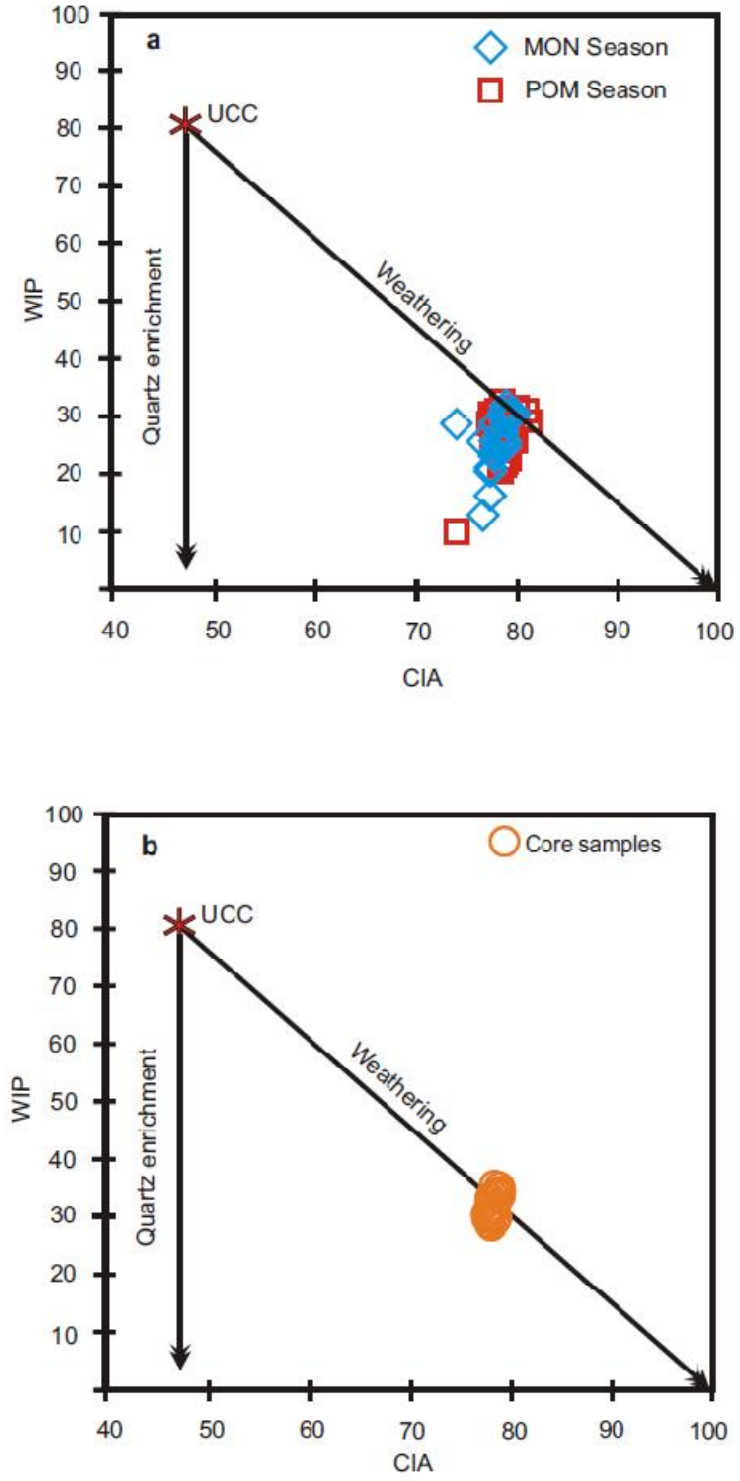

Figure 5.7CIA/WIP biplot (after Garzanti et al. 2013a) shows the enrichment of quartz to some extent in surface sediments (a) than the core sediments (b)

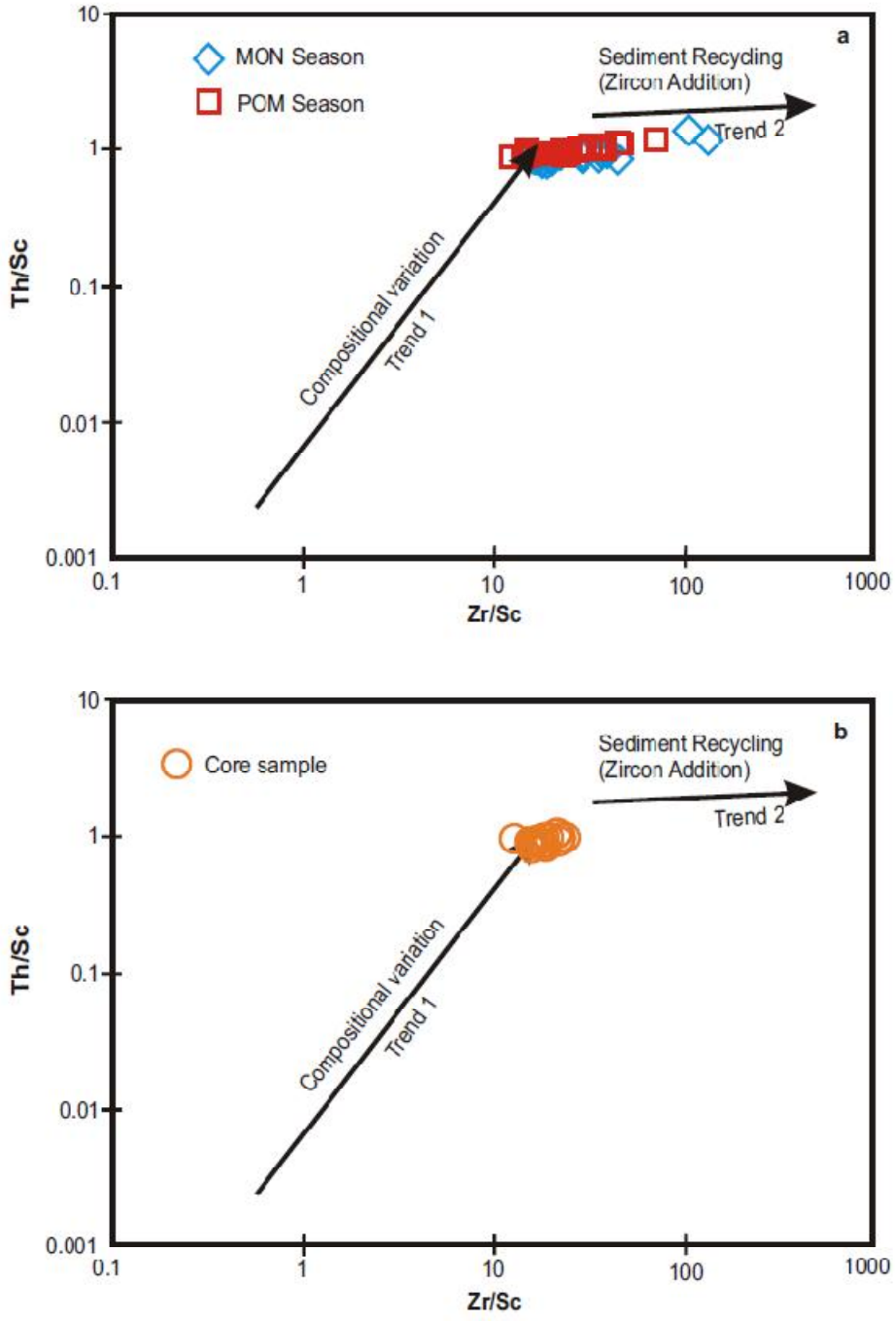

Figure 5.8Th/Sc versus Zr/Sc plot shows the weathering and recycling effect for the surface (a) and core sediments (b) of the Lower Baram River. The addition of zircon due to recycling and sorting is observed in trend 2

5.6.2 Sediment Maturity

The textural maturity can be estimated by the SiO_2/Al_2O_3 ratio, which shows a clear difference between different igneous rocks as 3 and 5 for mafic and felsic igneous rocks whereas compositionally matured sediments have a SiO_2/Al_2O_3 ratio of >5 (Roser et al., 1996). The SiO_2/Al_2O_3 ratio for the surface sediments ranged from 4.5 to 15.2 with an average of 6.3 during the MON season and 4.3-21.2 with an average of 6.4 during the POM season indicated moderate to high maturity. The core sediments also showed the SiO_2/Al_2O_3 ratio between 3.9 and 5.6 with an average of 4.8, which indicated a moderate maturity. The Index of Compositional variability (ICV) index also is used to assess the compositional maturity as they vary significantly between the non-clay minerals and clay minerals (Cox et al., 1995). Non-clay detrital minerals showed higher ICV values (>0.84) than the ICV values of clay minerals (<0.84). The ICV values of the surface sediments from the Lower Baram River ranged between 0.61-0.73 and 0.62-0.74 for the MON and POM season, respectively with an average of 0.70. Similarly, the ICV values of core sediments varied between 0.65-0.71 with an average of 0.69, which indicated the sediments of the Lower Baram River showed moderate maturity and are consisting of a mixture of more clay minerals and less detrital minerals. Also, sediments are not highly matured by recycling. K_2O/Al_2O_3 values of clay were <0.3 and 0.3-0.9 for feldspars (Cox et al., 1995). The average K_2O/Al_2O_3 ratio in the surface mud sediments was 0.17 and 0.16 during the MON and POM season, respectively and core sediments showed the average ratio of 0.16 indicating dominance of clay minerals. According to Garzanti (2017), the sediments do not mature during recycling, instead, the amount of lithic fragment increases and thus mineralogical maturity decreases. Also recycled sediments do not mainly consist of sand grains, but may contain a significant amount of diverse sedimentary rock fragments (i.e. in the silt fraction in this case).

5.7 Provenance

Major oxides based discrimination diagram (Roser & Korsch, 1988) and other diagrams based on trace elemental ratios and concentrations are used to reconstruct the provenance of the mud from the Lower Baram River. The discriminant plot of Roser and Korsch (1988) consists of four provenance fields as felsic igneous provenance,

intermediate igneous provenance, mafic igneous provenance and quartzose sedimentary provenance. The studied mud sediments from both seasons and the core were plotted in the quartzose sedimentary provenance and indicated recycled provenance from the source region (Figure 5.9 a,b). In the Hf Vs. La/Th plot (Figure 5.10 a,b; Floyd & Leveridge, 1987), all the samples were plotted mainly in acidic arc field except some samples showed enrichment in Hf concentration, which indicated the addition of detrital recycled components from old sedimentary terrane/passive margin source, thus enrichment of zircons. The recycled provenance can be further confirmed through the K_2O/Al_2O_3 ratio, which varies between first cycle sediments and redeposited fine grained terrigenous sediments. The redistributed fine grained terrigenous sediments are characterized by a K_2O/Al_2O_3 ratio <0.3 whereas in the clays of first cycle, K is mainly associated with feldspathic clastic grains and thus the K_2O/Al_2O_3 ratio is >0.4 (Cox & Lowe, 1995; Cox et al., 1995). The mud sediments of the Lower Baram River showed aK_2O/Al_2O_3 ratio from 0.16-0.18 during the MON, 0.15-0.17 during the POM and 0.16-0.17 in the core sediments indicated the sediments were redeposited from the sedimentary to the meta-sediment dominated source region (Rajang Group of rocks). However, the compositions of the Lower Baram River mud sediments are felsic to intermediate in nature (mixed provenance) and are comparable to the UCC and PASS. In the bivariate plot of Sc Vs. Th/Sc (Figure 5.11 a,b), where the mud sediments of the Lower Baram River (both surface and core sediments) were plotted between Granite and the UCC indicating felsic intermediate/mixed source rocks rather than mafic or ultramafic dominated source. The K will be preferentially leached compared to Rb during increased weathering and formation of kaolinite. However, both K and Rb are retained on clay minerals by adsorption or cation exchange during initial weathering of fresh source rocks (Nesbitt & Markovics, 1980; Liu et al., 2013). The logarithmic plot of K Vs.Rb can demonstrate the weathering conditions and provenance information. In Rb Vs. K_2O plot (Figure 5.12 a,b), the mud sediments were plotted parallel to a typical differentiated magmatic suite with a K/Rb ratio of 230 (Shaw, 1968). The geochemical ratios such as La/Sc, La/Co, Th/Sc, Th/Co, Cr/Th, Eu/Eu* and $(La/Lu)_{CN}$ of the Lower Baram River mud sediments were compared to the range of sediments from felsic, mafic source rocks (Table 5.3),the UCC and PAAS which were comparable to the range of

felsic to intermediate source rocks and PAAS. The REE pattern normalized against chondrite and PAAS and the size of Eu anomalies, also provided important clues about the source rocks characteristics. The higher LREE/HREE ratios with negative Eu anomalies are the characteristic feature of felsic source rocks whilst lower LREE/HREE ratios with little and/or an absence of Eu anomalies are the characteristic feature of mafic source rocks (Cullers, 1994). In the present study, the higher LREE/HREE ratios (6.86-8.38 during the MON, 6.70-8.65 during the POM season) and significant negative Eu anomalies (Figure 5.2a-c) were attributed to felsic source rock characteristics for the mud sediments of the Lower Baram River. The Zr/Hf ratio also can be used to discriminate the crustal processes and thus can be linked to identify the source rocks for the zircons (Chandrajith et al., 2000). Most crustal rocks have Zr/Hf ratios of close to 40 (Brooks, 1970; Murali et al., 1983). The presence of zircon in the mud sediments can be linked to the higher concentrations of Zr and Hf in the mud sediments. A majority of the studied samples showed higher Zr concentrations (185-808ppm; avg.276 during the MON and 136-614ppm; avg.247ppm during the POM season) than the UCC (Zr=190 ppm) and can be linked to the presence of detrital zircons associated with the finer fractions. The Zr/Hf ratio for mud sediments of the Lower Baram River was recorded as 40-47 during the MON and 36-45 during the POM season, which is comparable to crustal rocks.

The contribution from mafic to ultramafic rocks can be traced by plotting the composition of sediments in the Ni-V-Th*10 ternary plot of Bracciali et al. (2007). In this plot (Figure 5.13 a,b), the mud sediments of the Lower Baram River (both surface and core sediments) plot between felsic and mafic rocks rather than ultramafic rocks. Input from ultramafic rocks increases the Ni concentration in the sediments. In the present study, the Ni content ranged from 20 to 40ppm during the MON and POM seasons in the surface sediments and 30-40ppm in the core sediments, which indicated significant input from ophiolites from the source region, was unlikely. However, some samples may contain some heavy minerals such as chromite in trace amounts (e.g. Nagarajan et al., 2017b; Miocene-Pliocene sediments of Northern Borneo). The recycled sediments may have the mixed characteristics which was confirmed by La-Th-Sc plot (Figure 5.14 a,b; Cullers, 1994), where the sediments of the Lower Baram River plot in

the clay, silt and gravel from mixed sources from the source area (i.e. Rajang group of sediments). Thus, it is clear that the recycled sediments mix with fresh first cycle sediments from mafic to intermediate volcanic rocks exposed in the study area. The mixing model plot (Condie & Wronkiewicz, 1990; Totten et al., 2000) based on Th/Sc vs. Cr/Th was also used to confirm the dominant contribution between the felsic and mafic sources. In this plot (Figure 5.15a,b), the Lower Baram River sediments plot nearer to felsic end member composition, which confirms a felsic rock dominant source region.

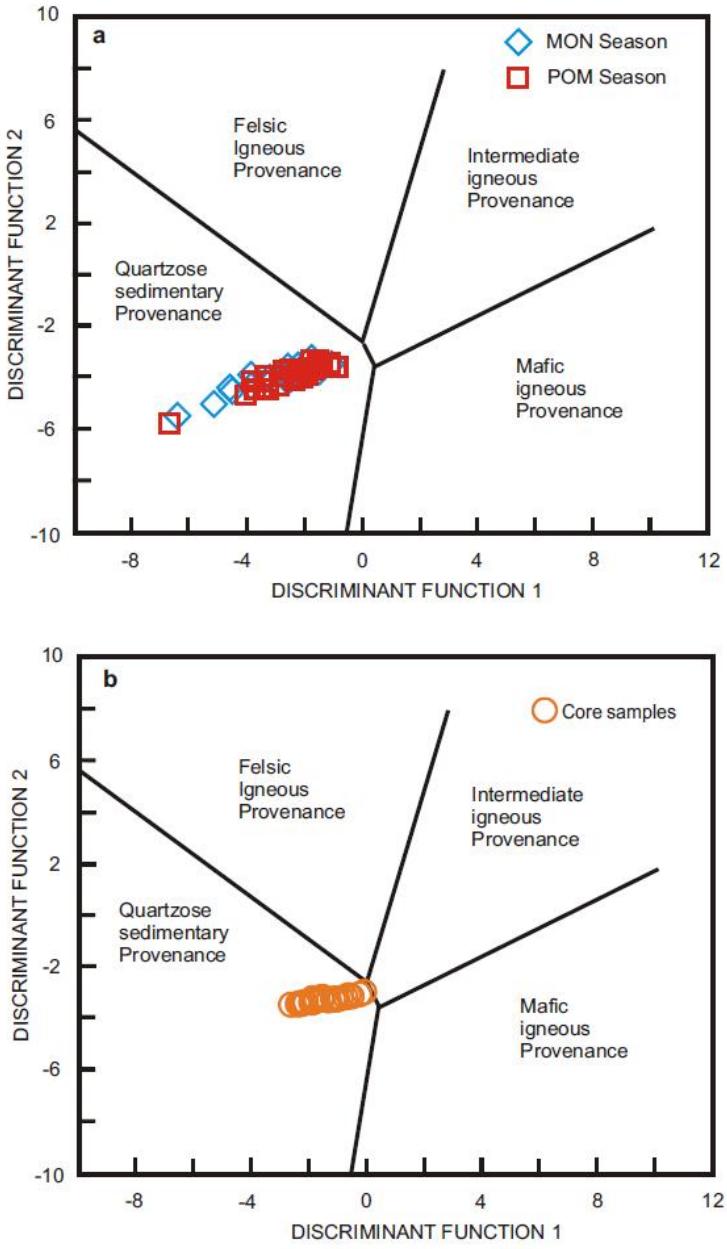

Figure 5.9 Major element provenance discriminant-function diagram for the surface sediments(a) and core sediments (b) of the Lower Baram River (after Roser & Korsch, 1988).

The discriminant function 1 = $(-1.773.TiO_2)$ + $(0.607.Al_2O_3)$ + $(0.760.Fe_2O_3)$ + $(-1.500.MgO)$ + $(0.616.CaO)$ + $(0.509.Na_2O)$ + $(-1.224.K_2O)$ + (-9.090); discriminant function 2 = $(0.445.TiO_2)$ + $(0.070.Al_2O_3)$ + $(-0.250.Fe_2O_3)$ + $(-1.142.MgO)$ +$(0.438.CaO)$ + $(1.475.Na_2O)$ + $(-1.426.K_2O)$ + (-6.861).

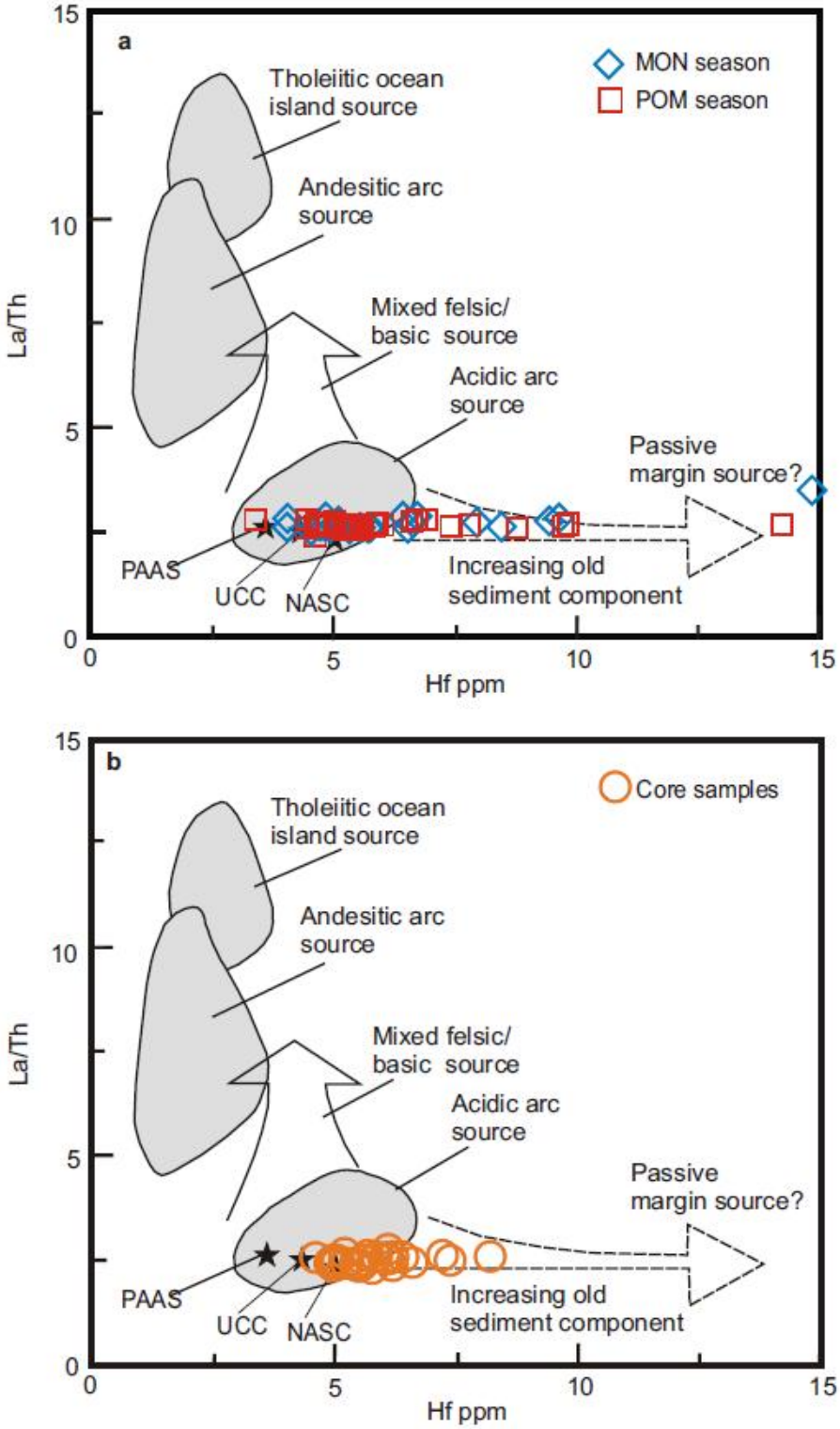

Figure 5.10 Hf vs. La/Th bi-plot of surface (a) and core sediments (b) of the Lower Baram River(after Floyd & Leveridge, 1987).

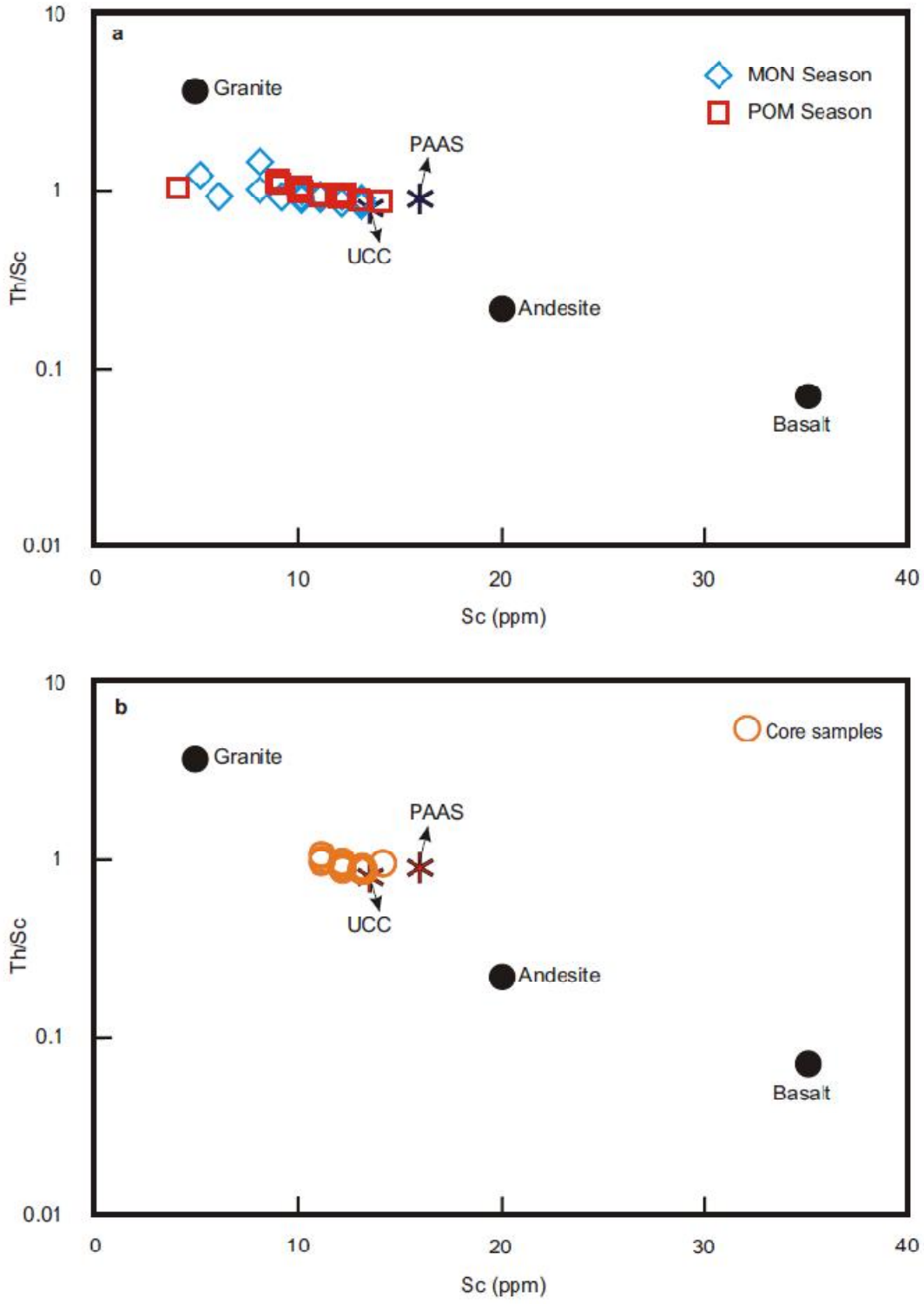

Figure 5.11Th/Sc versus Sc plots show the possible provenance for the surface (a) and core sediments of the Lower Baram River

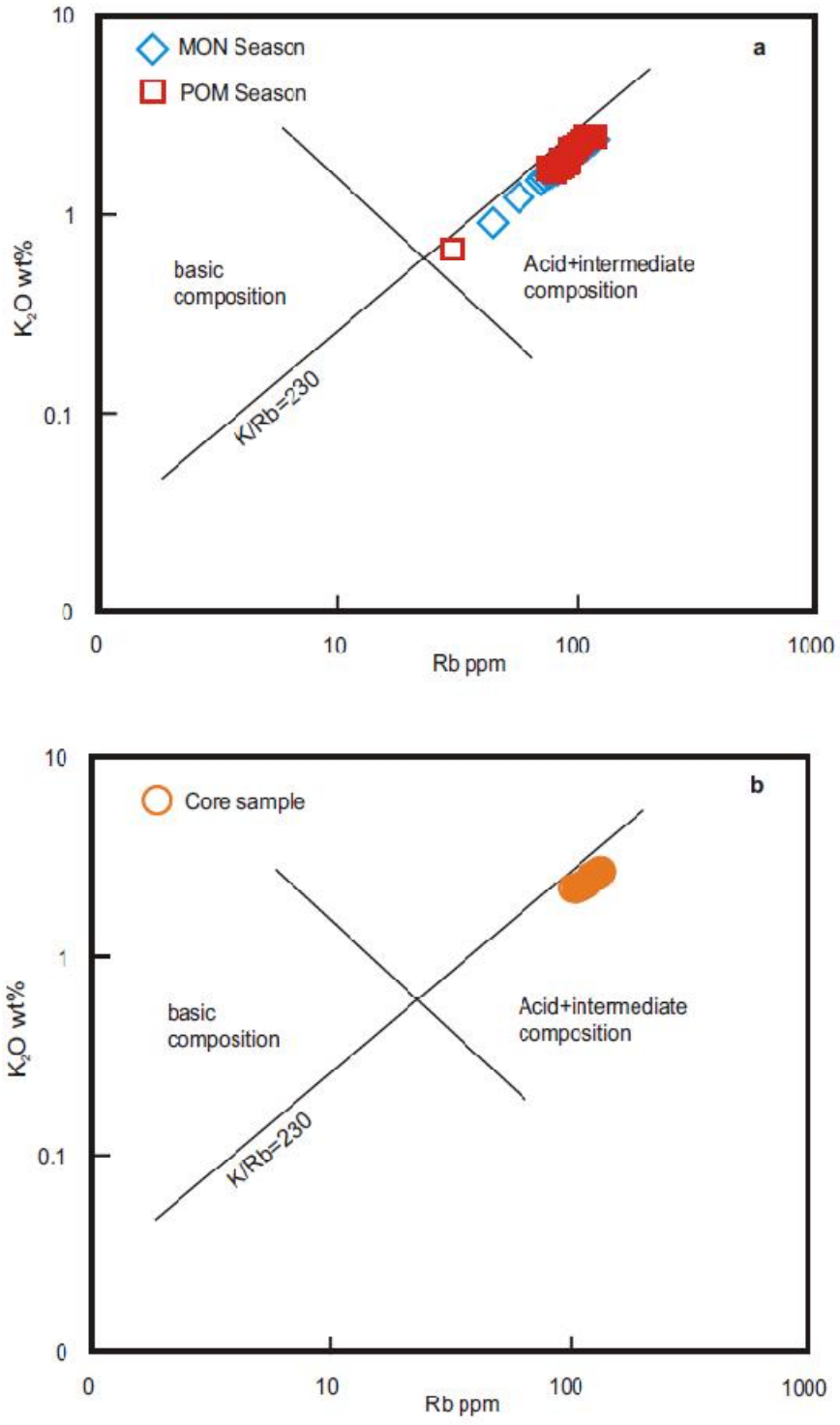

Figure 5.12Rb vs.KwO (Wt.%) plot shows the provenance field relative to K/Rb ratio of 230

(Trend of Shaw, 1968) for the surface (a) and core sediments (b) of the Lower Baram River

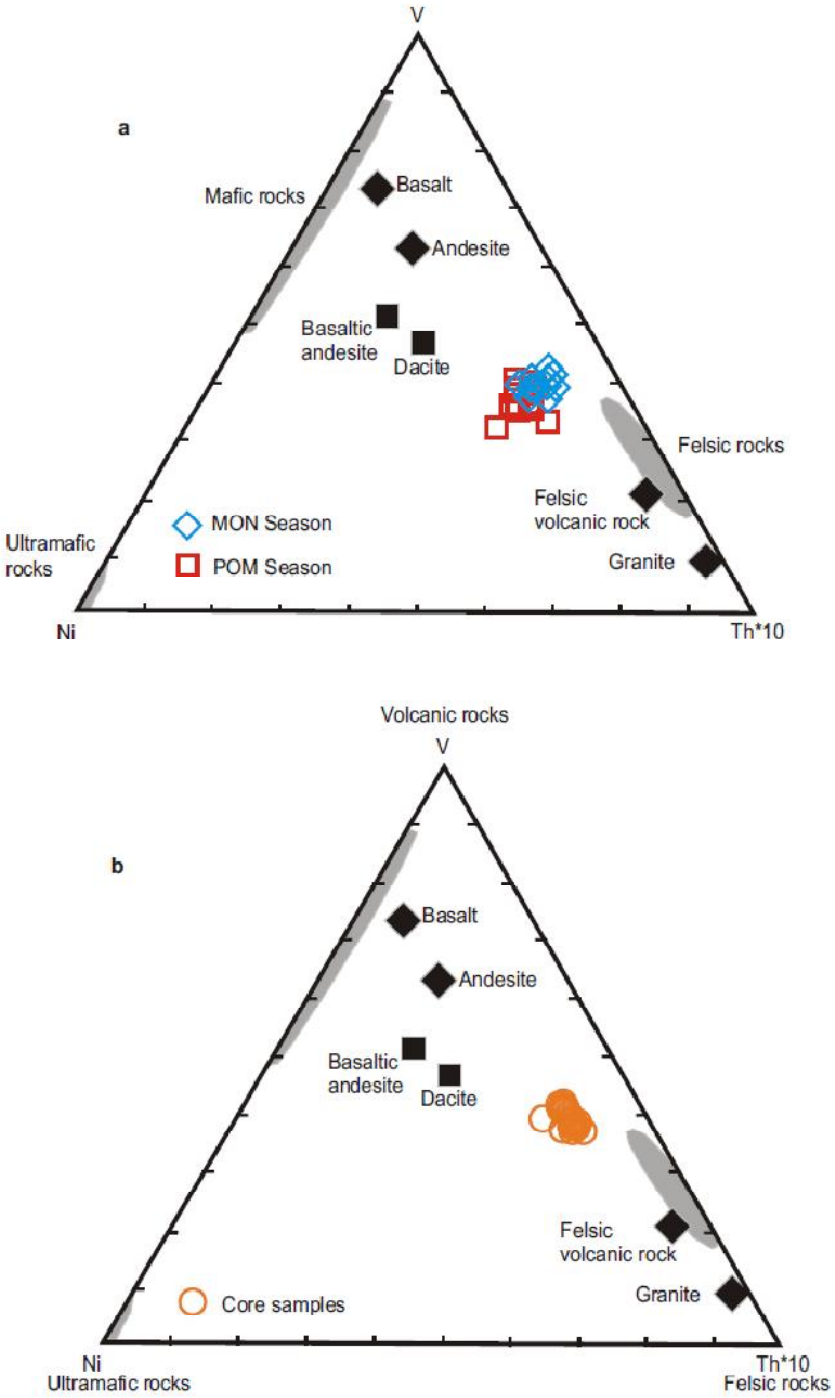

Figure 5.13Ni-Th*10-V plot for the (a) surface sediments b) core sediments of the Lower Baram River

(after Bracciali et al., 2007); (average compositions of basalt, andesite, felsic volcanic rocks and granite from Condie, 1993; basaltic andesite and dacite from the source region (Cullen et al., 2013)

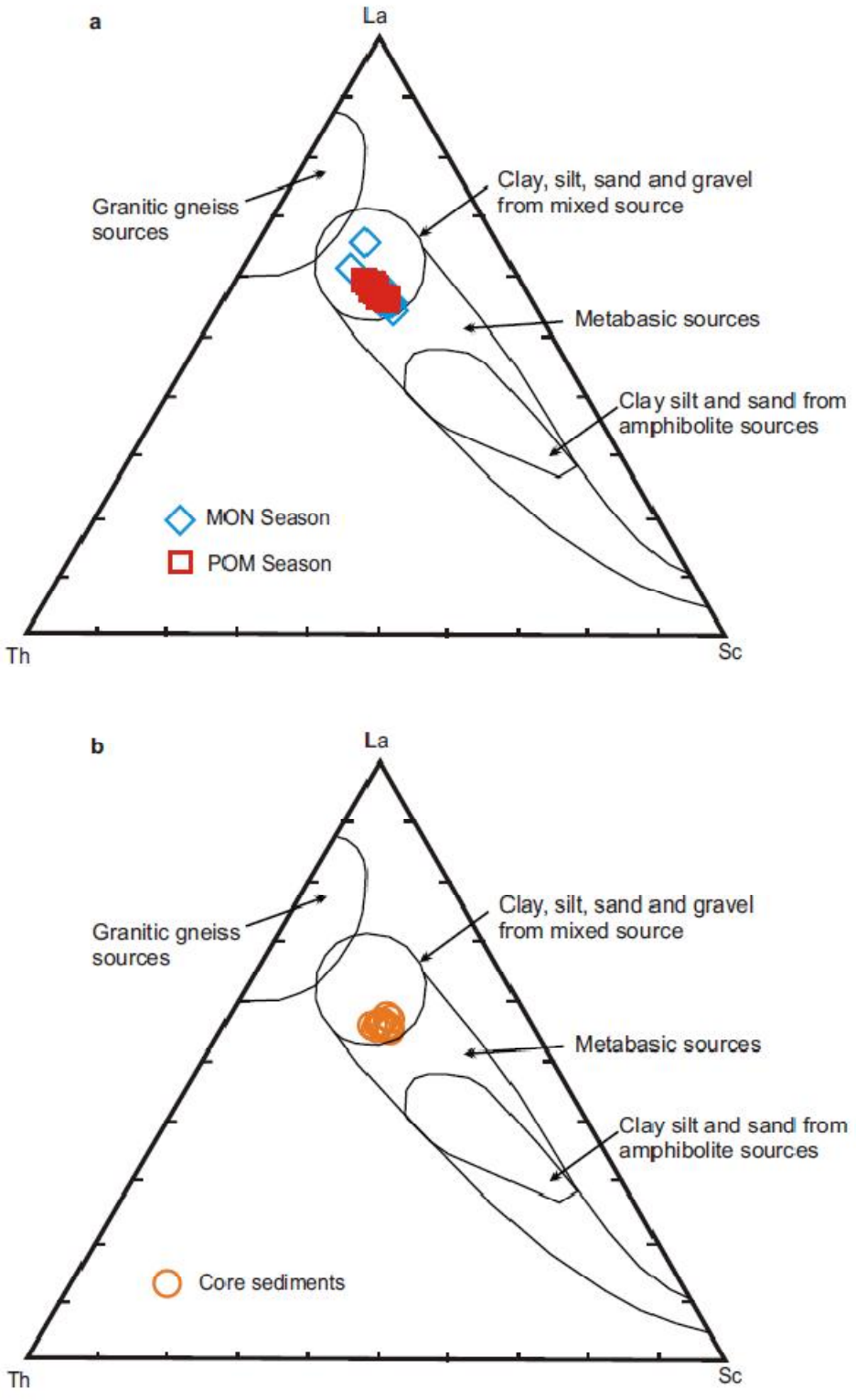

Figure 5.14 La-Th-Sc plot showing the possible provenance field for the surface sediments of Lower Baram River (after Cullers, 1994)

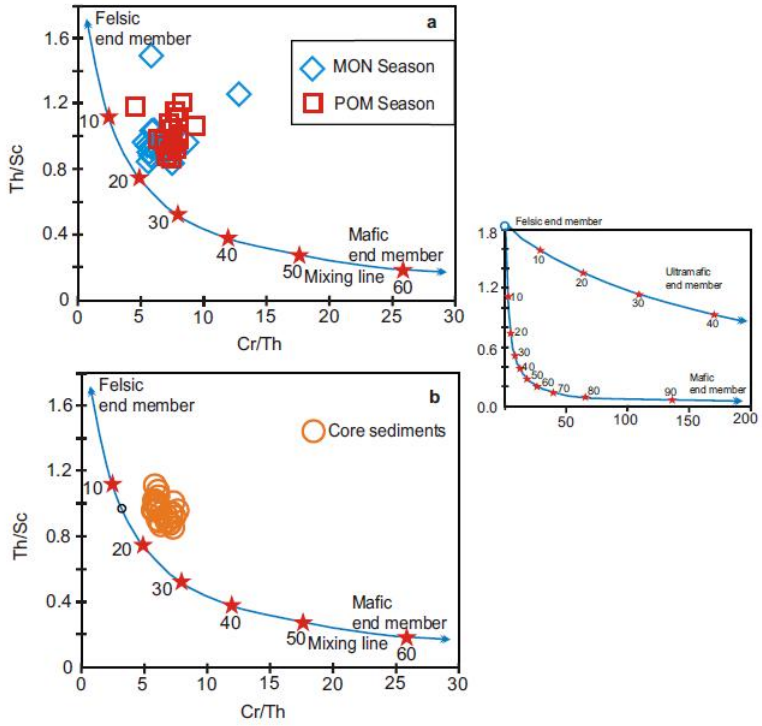

Figure 5.15 Th/Sc versus Cr/Th plot shows the felsic and mafic end member mixing curve

(after Condie & Wronkiewitcz, 1990; Totten et al., 2000). Mixing values are shown in % on the mixing curve represent the mafic end member contribution to the mixing products. The mixing of ultramafic endmember shown on the right side plot.

Table 5.3Range and average of elemental ratios of the surface and long core sediments from the Lower Baram River compared to the ratios in similar fractions derived from felsic rocks, mafic rocks, and background values (UCC and PAAS)

Element ratio	Range of sediments from Baram Estuary [a]			Range of sediments from		UCC [c]	PAAS [c]
	MON (n=32)	POM (n=32)	Core (n=36)	felsic sources [b]	mafic sources [b]		
La/Sc	2.23-4.48 (avg 2.68)	2.36-3.26 (avg 2.68)	2.27-2.69 (avg 2.51)	2.50–16.3	0.43–0.86	2.21	2.40
La/Co	1.76-4.54 (avg 2.95)	2.30-3.32 (avg 2.64)	2.59-3.47 (avg 2.93)	1.80–13.8	0.14–0.38	1.76	1.66
Th/Sc	0.84-1.50 (avg 0.96)	0.88-1.22 (avg 1.01)	0.86-1.13 (avg 0.97)	0.84–20.5	0.05–0.22	0.79	0.90
Th/Co	0.65-1.71 (avg 1.07)	0.89-1.22 (avg 0.99)	0.98-1.39 (avg. 1.13)	0.67–19.4	0.04–1.40	0.63	0.63
Cr/Th	5.17-12.70 (avg 6.45)	6.36-9.30 (avg 7.51)	5.51-7.48 (avg 6.24)	4.00–15.0	25–500	7.76	7.53
$(La/Lu)_{cn}$	5.79-8.70 (avg 7.41)	5.96-8.74 (avg 7.18)	6.89-8.50 (avg 7.71)	3.00–27.0	1.10–7.00	9.73	9.22
Eu/Eu*	0.56-0.80 (avg 0.71)	0.62-0.89 (avg 0.69)	0.62-0.77 (avg 0.70)	0.40–0.94	0.71–0.95	0.65	0.65

[a] This Study
[b]Cullers (1994, 2000); Cullers and Podkovyrov (2000); Cullers et al. (1988).[c]Taylor and McLennan, (1985); McLennan,(2001).

5.8 Results of short core sediments

Four short cores were analysed for their geochemical characteristics, one core each from a mangrove area, BSC-06 (Core 06), a meander, BSC-07 (Core 07) and a confluence point of a tributary of the Baram River, BSC-09 (Core 09) and all were characterized by similar geochemical signatures whilst a core, BSC-01 (core 01) from the mouth of the river/sea boundary showed a distinct variation in its geochemical signature. Based on the similarities and differences between the cores, 3 cores have been discussed together and are compared with a core from the Baram River mouth, unless a detailed individual discussion was needed for each core. The statistical summary of major trace elements and the REE of four short core sediments are summarized in Table 5.4.

5.8.1 Major Oxides

The average SiO_2 content ranged from 69.41-71.01Wt.% in the 3 cores, which was lower than the core 01 SiO_2 content (92.76 Wt.%), the later core increased about 20% in SiO_2 content. The Al_2O_3 content (avg. 2.71Wt. %) was recorded lower in core 01 compared to the other 3 cores (range of averages: 11.85-13.51 Wt. %). All the major oxides were recorded lower in the core 01 sample compared to the three other core samples. Though the three cores have similar geochemical characteristics, Fe_2O_3, CaO and P_2O_5 content in core 09 was not the same as the other two cores. Fe_2O_3, CaO and P_2O_5 content was recorded lower at Fe_2O_3,=2.20 Wt.%, CaO = 0.07 Wt.%, and P_2O_5 = 0.04 Wt.% in core 09 compared to the other 2 cores (average Fe_2O_3 = 4.18 and 4.33 Wt.%; CaO = 0.15 and P_2O_5 = 0.21 Wt.% and 0.08 Wt.% in core 06 and 07 respectively). Loss of Ignition was recorded higher in the three cores ranging from 7.63 to 9.52 Wt. % than in the core 01 (LOI avg.= 2 Wt.%).

Major oxides of the short core sediments were normalized against the UCC and are shown in figure 5.16a-d. All the short core sediments showed enrichment in SiO_2 and depletion of CaO, Na_2O and P_2O_5. Upon comparison between the cores, core 01 sediments were depleted in all the major oxide concentrations except SiO_2 and showed wider variation between the samples, compared to other core sediments. Core 06, 07, and 09 sediments were slightly enriched in Fe_2O_3 (except core 09), and TiO_2 content

compared to the UCC, in addition to SiO_2. Al_2O_3 content was either comparable to the UCC or slightly lower in core 06, 07, and 09 sediments.

5.8.2 Trace elements

Trace elements are classified as transitional trace elements (TTE: Sc, V, Cr, Mn, Co, Ni, Cu, Zn); large ion lithophile elements (LILE; Rb, Cs, Ba, Sr), high field strength elements (HFSE; Zr, Hf, Nb, Y, Th, U, Ta and W) and rare earth elements (REE: La-Lu) based on their geochemical behaviour. The statistical summary of the trace elements in the short core sediments are presented together with major and rare earth elements in Table 5.4.

Table 5.4 Statistical summary of Bulk geochemistry of the short core sediments

Analyte symbol	Baram river mouth during low tide (junction) (Core 01)				The mangrove sediments (Core 06)				At a meander curve (Core 07)				Bakung River meets with Baram River (Core 09)			
	Min	**Max**	**Avg.**	**St.Dev**	**Min**	**Max**	**Avg**	**St.Dev**	**Min**	**Max**	**Avg**	**St.Dev.**	**Min**	**Max**	**Avg**	**St.Dev.**
SiO_2	83.70	95.59	92.76	3.67	67.75	73.08	70.88	1.69	66.06	74.47	69.41	2.40	68.20	73.17	71.01	1.93
SiO_2 (adj)	87.42	96.53	94.94	2.90	75.16	78.68	77.01	1.13	74.83	81.17	77.27	1.94	76.08	79.71	78.14	1.32
Al_2O_3	1.75	7.04	2.71	1.67	11.50	13.11	12.40	0.54	9.97	13.23	11.85	1.07	12.67	14.88	13.51	0.67
Fe_2O_3(T)	0.56	2.29	0.85	0.55	3.72	4.59	4.18	0.27	3.61	4.94	4.33	0.40	1.84	3.47	2.20	0.53
MnO	0.01	0.02	0.01	0.01	0.03	0.05	0.04	0.01	0.04	0.06	0.05	0.01	0.01	0.03	0.02	0.01
MgO	0.16	0.52	0.22	0.12	0.88	1.02	0.95	0.04	0.74	1.00	0.90	0.08	0.75	0.89	0.82	0.05
CaO	0.10	0.18	0.12	0.03	0.13	0.16	0.15	0.01	0.16	0.26	0.21	0.03	0.06	0.11	0.07	0.02
Na_2O	0.27	0.49	0.33	0.06	0.57	0.66	0.61	0.03	0.38	0.56	0.46	0.06	0.55	0.60	0.57	0.02
K_2O	0.31	1.12	0.47	0.25	1.85	2.18	2.04	0.11	1.56	2.26	1.89	0.19	1.73	2.03	1.87	0.10
TiO_2	0.15	0.36	0.20	0.07	0.66	0.75	0.71	0.03	0.52	0.73	0.65	0.07	0.72	0.80	0.75	0.03
P_2O_5	0.02	0.05	0.04	0.02	0.06	0.10	0.08	0.01	0.06	0.09	0.08	0.01	0.02	0.07	0.04	0.02
LOI	1.29	4.65	2.00	1.06	6.60	8.45	7.63	0.69	7.72	12.92	9.52	1.48	7.96	11.16	8.89	1.06
Total	98.64	100.60	99.68	0.73	98.59	100.40	99.67	0.65	98.53	100.60	99.34	0.63	98.99	100.60	99.75	0.57
ICV	0.70	0.96	0.84	0.08	0.68	0.71	0.70	0.01	0.70	0.74	0.72	0.01	0.44	0.56	0.47	0.04
SiO_2/Al_2O_3	11.89	54.62	40.85	12.81	5.17	6.28	5.73	0.37	5.09	7.47	5.91	0.71	4.58	5.78	5.27	0.38
Al_2O_3/TiO_2	9.02	19.50	12.85	3.01	16.36	18.19	17.43	0.55	17.07	19.96	18.31	0.79	16.77	19.29	18.01	0.79
K_2O/Al_2O_3	0.16	0.19	0.18	0.01	0.16	0.17	0.16	0.01	0.15	0.17	0.16	0.01	0.13	0.15	0.14	0.01
CIA	61	76	66	4.34	77	79	78	0.58	77	81	79	1.08	81	82	81	0.43
CIW	69	87	76	5.19	90	91	91	0.50	90	92	91	0.54	92	93	93	0.35
PIA	65	85	72	5.95	88	90	89	0.60	89	91	90	0.72	91	92	91	0.40
WIP	6.08	16.52	8.09	3.24	26.48	29.54	28.18	1.07	22.33	30.21	25.90	2.23	24.40	28.25	25.99	1.19
CIA/WIP	4.58	10.33	8.82	1.72	2.64	2.97	2.78	0.11	2.59	3.55	3.06	0.27	2.90	3.33	3.13	0.14
Sc	1.00	6.00	2.44	1.42	10.00	12.00	10.78	0.67	9.00	12.00	11.00	1.00	11.00	13.00	12.13	0.83
Be	BDL	BDL	BDL	BDL	2.00	2.00	2.00	0.00	1.00	2.00	1.85	0.38	2.00	2.00	2.00	0.00
V	11.00	47.00	17.44	11.57	81.00	94.00	86.67	4.44	67.00	96.00	82.38	9.03	86.00	97.00	91.63	4.17
Ba	60.00	133.00	75.22	22.36	197.00	230.00	217.78	10.80	187.00	241.00	211.08	15.24	208.00	241.00	222.75	10.36
Sr	21.00	42.00	25.00	6.54	54.00	61.00	58.00	2.69	51.00	63.00	56.62	3.40	59.00	66.00	62.63	2.45
Y	5.00	12.00	6.67	2.12	20.00	26.00	23.11	2.03	19.00	28.00	22.77	2.28	23.00	24.00	23.50	0.53
Zr	92.00	246.00	159.67	60.87	157.00	257.00	196.22	32.22	139.00	238.00	193.85	33.45	184.00	231.00	208.25	15.69
Cr	40.00	50.00	43.33	5.00	70.00	80.00	77.78	4.41	60.00	80.00	74.62	7.76	80.00	90.00	85.00	5.35
Co	3.00	6.00	3.56	1.01	10.00	12.00	11.00	0.71	10.00	13.00	11.62	0.96	10.00	18.00	13.13	2.90
Ni	BDL	20.00	20.00	BDL	30.00	40.00	36.67	5.00	30.00	40.00	36.15	5.06	40.00	50.00	42.50	4.63
Cu	80.00	840.00	570.00	285.44	150.00	400.00	247.78	80.28	20.00	30.00	25.38	5.19	170.00	440.00	341.25	85.60
Zn	50.00	390.00	254.44	122.38	130.00	240.00	167.78	33.83	60.00	70.00	66.92	4.80	130.00	280.00	226.25	49.26
Ga	2.00	7.00	3.44	1.42	14.00	16.00	14.89	0.78	11.00	17.00	14.23	1.83	15.00	17.00	16.00	0.76
Ge	1.00	1.00	1.00	0.00	1.00	2.00	1.11	0.33	1.00	2.00	1.31	0.48	1.00	2.00	1.13	0.35
As	BDL	BDL	BDL	BDL	5.00	9.00	6.89	1.17	6.00	9.00	8.08	0.95	5.00	7.00	5.88	0.83
Rb	13.00	51.00	20.78	11.72	89.00	105.00	96.67	5.00	76.00	108.00	92.92	10.27	95.00	103.00	98.63	3.16

Analyte symbol	Baram river mouth during low tide (junction) (Core 01)				The mangrove sediments (Core 06)				At a meander curve (Core 07)				Bakung River meets with Baram River (Core 09)			
	Min	**Max**	**Avg.**	**St.Dev**	**Min**	**Max**	**Avg**	**St.Dev**	**Min**	**Max**	**Avg**	**St.Dev.**	**Min**	**Max**	**Avg**	**St.Dev.**
Nb	2.00	4.00	2.50	0.76	7.00	9.00	8.00	0.71	6.00	10.00	7.69	1.18	8.00	10.00	9.13	0.64
Sn	2.00	11.00	6.44	3.05	2.00	3.00	2.22	0.44	2.00	3.00	2.15	0.38	2.00	4.00	2.50	0.76
Sb	1.00	1.50	1.16	0.15	1.00	1.40	1.20	0.12	0.90	1.30	1.15	0.13	1.10	1.40	1.23	0.13
Cs	0.70	3.50	1.20	0.89	6.60	7.90	7.06	0.44	5.30	8.10	6.82	0.86	7.10	8.00	7.63	0.35
Hf	2.50	5.70	3.91	1.27	4.10	5.90	4.87	0.55	3.30	6.00	4.73	0.90	4.60	5.70	5.26	0.38
Ta	0.20	0.50	0.28	0.11	0.90	0.90	0.90	0.00	0.60	0.90	0.81	0.10	0.90	1.00	0.94	0.05
W	2.00	6.00	3.22	1.09	4.00	4.00	4.00	0.00	3.00	5.00	4.00	0.41	4.00	5.00	4.25	0.46
Tl	0.20	0.30	0.21	0.03	0.50	0.60	0.59	0.03	0.50	0.70	0.58	0.07	0.60	0.70	0.64	0.05
Pb	8.00	23.00	15.67	5.98	16.00	26.00	19.78	3.11	11.00	21.00	15.08	2.63	15.00	23.00	19.13	3.00
Th	2.30	5.90	3.10	1.12	10.30	11.30	10.92	0.29	8.80	12.10	10.59	1.05	11.00	11.70	11.44	0.24
U	0.90	1.70	1.06	0.27	2.60	2.90	2.78	0.10	2.10	2.90	2.61	0.30	2.90	3.10	3.00	0.09
La	8.00	17.60	10.24	3.03	27.40	30.30	28.70	0.82	22.30	31.00	27.56	2.73	29.20	31.50	30.25	0.77
Ce	14.50	33.80	19.32	5.96	54.50	60.00	57.12	1.55	44.40	62.20	54.75	5.55	57.90	62.40	60.30	1.60
Pr	1.64	3.69	2.16	0.64	6.09	6.74	6.42	0.21	5.07	7.03	6.20	0.60	6.60	7.02	6.80	0.18
Nd	5.90	13.90	8.04	2.46	22.30	25.40	23.87	0.94	19.00	26.60	23.47	2.31	24.60	26.50	25.58	0.71
Sm	1.10	2.60	1.48	0.45	4.40	4.90	4.73	0.19	4.00	5.30	4.76	0.35	4.80	5.60	5.20	0.26
Eu	0.22	0.59	0.30	0.12	0.95	1.09	1.03	0.04	0.88	1.17	1.04	0.09	1.00	1.27	1.14	0.09
Gd	0.90	2.10	1.23	0.36	3.90	4.50	4.26	0.17	3.70	5.30	4.42	0.47	4.30	5.20	4.66	0.27
Tb	0.20	0.30	0.21	0.03	0.70	0.80	0.72	0.04	0.60	0.80	0.72	0.07	0.70	0.80	0.76	0.05
Dy	1.00	2.10	1.24	0.34	4.10	4.60	4.38	0.16	3.40	5.00	4.26	0.46	4.30	4.70	4.58	0.18
Ho	0.20	0.40	0.23	0.07	0.80	0.90	0.89	0.03	0.70	1.00	0.85	0.11	0.90	0.90	0.90	0.00
Er	0.60	1.40	0.78	0.25	2.40	2.70	2.59	0.11	2.00	3.00	2.51	0.28	2.50	2.80	2.68	0.09
Tm	0.10	0.21	0.12	0.03	0.37	0.42	0.39	0.02	0.31	0.42	0.38	0.04	0.38	0.43	0.40	0.02
Yb	0.70	1.40	0.83	0.22	2.40	2.80	2.56	0.13	2.00	2.70	2.43	0.27	2.50	2.70	2.61	0.06
Lu	0.11	0.23	0.14	0.04	0.36	0.44	0.41	0.02	0.31	0.43	0.38	0.04	0.40	0.43	0.41	0.01
La/Th	2.98	3.85	3.36	0.25	2.55	2.68	2.63	0.04	2.53	2.71	2.60	0.05	2.60	2.69	2.64	0.03
Zr/Sc	19.17	123.00	76.43	32.14	13.08	25.70	18.32	3.54	11.58	22.80	17.70	3.11	14.15	20.27	17.28	2.03
Th/Sc	0.98	2.40	1.40	0.40	0.94	1.10	1.02	0.05	0.86	1.02	0.96	0.05	0.88	1.04	0.95	0.05
La/Sc	2.93	8.30	4.71	1.47	2.53	2.85	2.67	0.11	2.33	2.72	2.51	0.12	2.30	2.71	2.50	0.14
Co/Th	1.02	1.38	1.17	0.12	0.93	1.07	1.01	0.04	1.01	1.22	1.10	0.05	0.89	1.54	1.15	0.24
La/Co	2.30	3.33	2.89	0.30	2.45	2.87	2.62	0.12	2.15	2.58	2.37	0.11	1.72	2.97	2.39	0.45
Th/Co	0.73	0.98	0.86	0.08	0.93	1.08	1.00	0.04	0.82	0.99	0.91	0.04	0.65	1.12	0.90	0.17
Cr/Th	8.47	18.52	14.82	2.89	6.48	7.41	7.12	0.30	6.45	7.78	7.05	0.39	6.90	7.89	7.43	0.39
Zr/Hf	36.80	43.16	40.16	2.49	36.46	43.56	40.14	2.35	39.07	43.78	41.14	1.53	38.46	41.25	39.58	0.91
$(La/Yb)_N$	7.76	9.21	8.32	0.51	6.91	8.15	7.64	0.35	7.22	8.29	7.72	0.36	7.50	8.23	7.87	0.22
$(Gd/Yb)_N$	1.01	1.39	1.20	0.12	1.21	1.46	1.35	0.08	1.26	1.65	1.48	0.11	1.37	1.62	1.44	0.08
Eu/Eu*	0.61	0.77	0.66	0.06	0.68	0.72	0.70	0.01	0.66	0.72	0.69	0.02	0.66	0.75	0.71	0.03
$(La/Lu)_N$	6.92	9.05	7.82	0.59	6.72	7.90	7.34	0.38	6.93	8.02	7.47	0.27	7.19	8.02	7.62	0.29
∑ LREE	31.36	72.18	41.55	12.64	115.64	128.43	121.88	3.58	95.65	133.17	117.78	11.55	124.58	133.51	129.27	3.35
∑ HREE	4.02	8.14	4.79	1.32	15.03	16.76	16.19	0.54	13.02	18.50	15.96	1.67	15.98	17.73	17.00	0.61
∑REE	35.39	80.32	46.34	13.94	130.67	145.14	138.06	3.97	108.67	150.60	133.75	13.00	140.56	150.63	146.27	3.77
LREE/HREE	7.78	9.60	8.63	0.61	7.14	7.69	7.53	0.18	6.37	7.77	7.39	0.37	7.28	7.80	7.61	0.21

5.8.2.1 Transitional trace elements (TTE: Sc, V, Cr, Mn, Co, Ni, Cu, Zn, Ga)

The average transitional trace elements (Sc, V, Cr, Mn, Co, Ni, Cu and Zn) recorded similar levels between the cores except core 01, which showed lower average values for all the transitional elements as Sc =2 .44 ppm (4 fold lesser); V=17.44 ppm (4 fold lesser); Cr= 43.00 ppm (2 fold lesser), Mn = 70.00 ppm (2-4 fold lesser); Co = 3.56 ppm (3 fold lesser); Ni = 20 ppm (mostly BDL); Ga = 3.44 ppm (4 fold lesser). However, Cu and Zn concentrations were recorded significantly higher in Core 01 sediments (avg. Cu= 570.00 ppm; Zn= 254.44 ppm) than in the other 3 core sediments. Though the 3 cores had a lower Cu and Zn concentration compared to core 1, their concentrations were significantly higher (Cu and Zn in core 06 and 09 was as 247.78 and167.78 ppm; 341.25 and 226.25 ppm, respectively) than the Post Archean Australian shale (Cu = 50 ppm; Zn = 85 ppm). The core 07 sediment showed very low content of Cu and Zn (Cu = 25.38 ppm; Zn = 66.92 ppm) compared to other core sediments and PAAS values.

5.8.2.2 Large Ion Lithophile Elements (LILE: Rb, Cs, Ba, Sr, Be)

Large Ion Lithophile Elements also were recorded lower in Core 01 sediments compared to the other three cores. The average values of Rb, Cs, Ba, Sr and Be was recorded as20.78ppm, 1.20ppm, 75.22ppm, 25.00ppm, and BDL in the core 01 sediments. Except for Be concentrations, the other LILE showed minimum variation between the three cores.

5.8.2.3 High Field Strength Elements (HFSE: Zr, Hf, Nb, Ta, Y, Th, U and W)

The HFSE were depleted in the core 01 sediments and variation in the Zr, Hf and W concentrations were lower also, compared to the other elements in the other short cores. The average concentrations of Zr, Hf, Nb, Ta, Y, Th, U and W in the core 01 sediments were recorded as 159.67 ppm, 3.91 ppm, 2.50 ppm, 0.28 ppm, 6.67 ppm, 3.10 ppm, 1.06 ppm and 3.22 ppm, respectively. Amongst the three other core sediment samples, the HFSE were recorded slightly higher in core 09 sediments which was collected from the confluence point of a tributary with the Baram River. The overall higher concentration of HFSE was recorded in Core 09 sediments as 208.25ppm,

5.26ppm, 9.13ppm, 0.94ppm, 23.50ppm, 11.44ppm, 3.00ppm and 4.25ppm for Zr, Hf, Nb, Ta, Y, Th, U and W, respectively.

The trace element concentrations in four short core sediments were normalized against upper continental curst values (Figure 5.16a-d; McLennan, 2001). All four short core sediments showed very similar trend except Cu, Hf, Sn and As concentrations. As and Sn content was recorded BDL in core 01 sediments and the Cu content was recorded lower in core 07 sediments compared to the other cores. The concentration of trace elements showed wide variation in core 01 sediments compared to the other cores (Core 06, 07, 09), which all showed fewer variations in the elemental concentrations amongst the samples. Cu, Sb, W, As and Zr concentrations were enriched in all the core sediments than in the UCC and the Sr and Sn content was more depleted than in the UCC in the three cores. The core 1 sediments showed depletion in Sr, Co, Ga, Rb, Cs, Ta, and Tl concentrations compared to the UCC. Overall, Cu and Zn concentrations were enriched 5 to 10 fold in core 01, 06 and 09 sediments.

5.9 Rare Earth Elements (REE)

The REE concentrations was recorded uniformly between the cores except core 01 sediments, which showed very less REE content compared with the rest of the core samples. As expected, core 01 sediments showed a wider distribution of REE concentrations as well as core 07 sediments, when compared to the other two core sediments, which showed less variation amongst the samples. The average ∑REE concentration varied significantly between cores with levels as 46.34 ppm, 138.06 ppm, 133.75 ppm, and 146.27 ppm in cores 01, 06, 07 and 09, respectively. The ∑REE concentration in the core sediments was lower than the average ∑REE content of PAAS (184.77ppm). The chondrite normalized REE pattern (Figure 5.17a-d) showed LREE enrichment (La/Yb_{CN}:7.76-9.21; 6.91-8.15; 7.22-8.29; 7.50-8.23 in core 01, 06, 07, and 09, respectively), flat HREE (Gd/Yb_{CN}:1.01-1.39; 1.21-1.46; 1.26-1.65; 1.37-1.62 in core 01, 06, 07, and 09, respectively) and negative Eu anomalies (Eu/Eu*:0.61-0.77; 0.68-0.72; 0.66-0.72; 0.66-0.75). The REE concentration in the samples of cores 06, 07 and 09 was enriched than the UCC and PAAS. Core 01 sediments showed lesser REE

content when compared to the UCC, PAAS and other sediment cores. However, the average chondrite normalized REE trend was similar amongst all the core sediments.

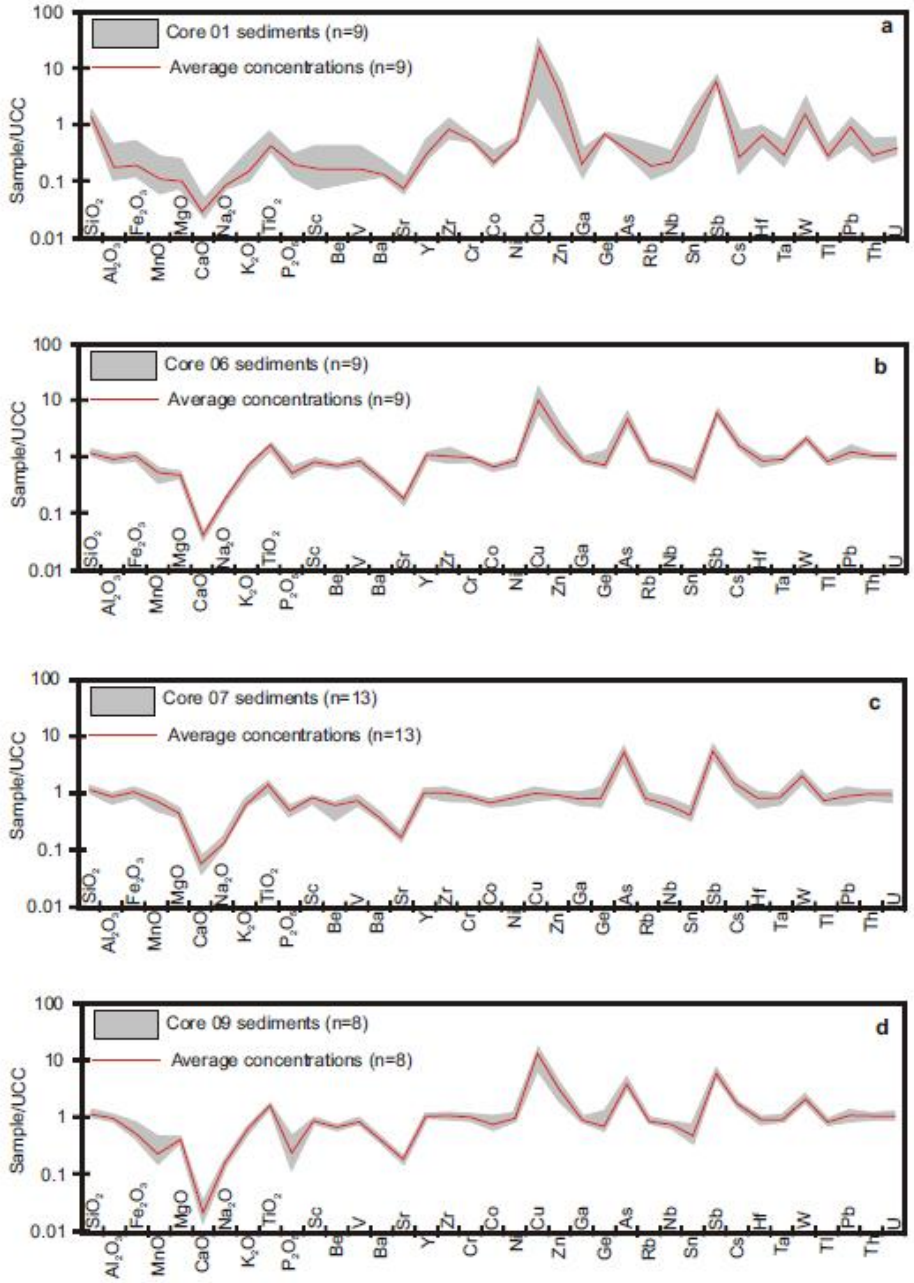

Figure 5.16a-d. Upper Continental Crust (UCC) normalized spider plot of core sediments

(a.core 01; b. core 06; c. core 07 and d. core 09) from the Lower Baram River

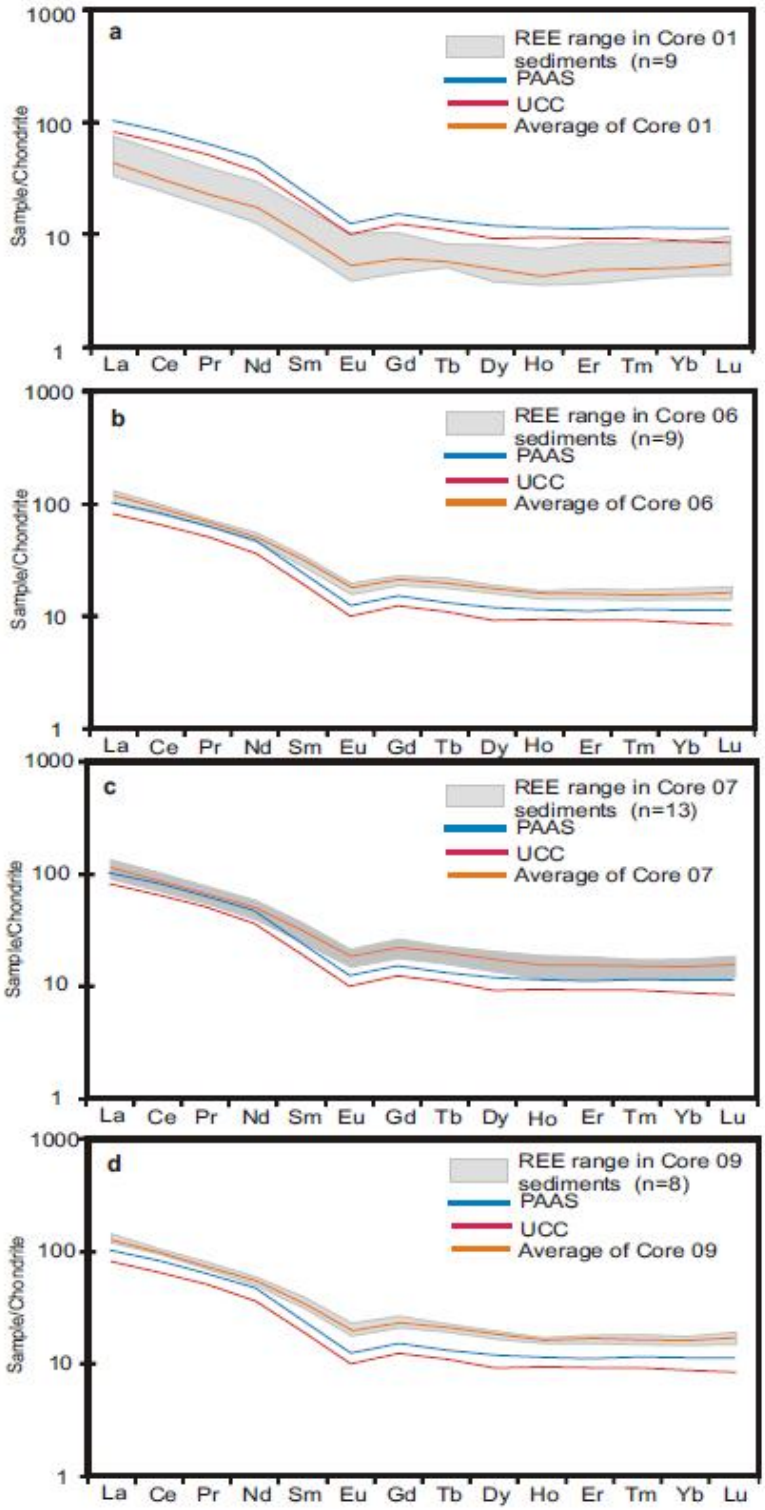

Figure 5.17 a-d. Chondrite normalized REE (Sun & McDonough, 1989) pattern for core sediments

(a. core 01; b. core 06; c. core 07 and d. core 09) from the Lower Baram River

5.10 Discussion

5.10.1 Weathering, sorting and recycling of sediments

As stated above, the weathering intensity of short core sediments were assessed based on weathering indexes such as CIA, CIW, PIA, WIP and based on single element mobility (i.e. Mg, Ca, Na, Sr, K, Ba). Based on Garzanti et al. (2013) Al concentrations are used for assessing short core sediments in order to overcome the samples showing anomalous concentration of heavy minerals due to hydrodynamic processes and the αAl values were quantified for the selected elements to calculate the bulk mobility of the sediments (Garzanti et al., 2013).

The αAl values were calculated based on Garzanti et al. (2013a) and the following bulk-sediment mobility sequence was observed for the short core sediments.

$$\alpha^{Al}_{Ca}>\alpha^{Al}_{Sr}>\alpha^{Al}_{Na}>\alpha^{Al}_{Mg}>\alpha^{Al}_{K}>\alpha^{Al}_{Ba}>\alpha^{Al}_{Rb}>\alpha^{Al}_{Cs} \quad \text{[core 01]}$$

$$\alpha^{Al}_{Ca}>\alpha^{Al}_{Sr}>\alpha^{Al}_{Na}>\alpha^{Al}_{Ba}>\alpha^{Al}_{Mg}>\alpha^{Al}_{K}>\alpha^{Al}_{Rb}>\alpha^{Al}_{Cs} \quad \text{[core 06]}$$

$$\alpha^{Al}_{Ca}>\alpha^{Al}_{Na}>\alpha^{Al}_{Sr}>\alpha^{Al}_{Ba}>\alpha^{Al}_{Mg}>\alpha^{Al}_{K}>\alpha^{Al}_{Rb}>\alpha^{Al}_{Cs} \text{[core 07]}$$

$$\alpha^{Al}_{Ca}>\alpha^{Al}_{Na}>\alpha^{Al}_{Sr}>\alpha^{Al}_{Ba}>\alpha^{Al}_{Mg}>\alpha^{Al}_{K}>\alpha^{Al}_{Rb}>\alpha^{Al}_{Cs} \text{[core 09]}$$

Among the four individual core sediments, cores 07 and 09 showed a similar pattern to the bulk sediments from the MON and POM season and long core sediments, whilst core 01 and core 06 showed a different pattern of mobility where, Sr had the second highest mobility after Ca (Figure 5.18). These sequences are slightly different from what is observed elsewhere (Gaillardet et al., 2003; Bouchez et al., 2011, Garzanti et al., 2013, 2014). Though there is a variation in overall trend, a typical element mobility sequence is observed as having a higher loss in smaller cations such as Ca, Na, and Sr, and a lower loss of larger cations such as K, Rb, and Cs (Nesbitt & Markovics, 1980; Schneider et al., 2016). The cores from the meander and confluence point of the tributary showed a similar mobility trend than the cores from the mangrove area (core 06) and the river mouth/sea junction (core 01).

Weathering indices in the short core sediments varied significantly between the cores as, CIA=61-76; 77-79; 77-81 and 81-82 in core 01, 06, 07 and 09, respectively; CIW= 69-87; 90-91;90-92 and 92-93 in core 01, 06, 07 and 09, respectively; and PIA=65-85; 88-90; 89-91 and 91-92 in cores 01, 06, 07 and 09,respectively. These values indicate that the core 01 sediments showed low to moderate weathering, cores 06 and 07 showed moderate weathering and core 09 showed moderate to intensive weathering. The WIP index is lower in the core 01 sediments (6.08-16.52) than in the other three cores, which strongly reflect quartz dilution (Garzanti et al., 2013a; Figure 5.19) due to recycling. The other three cores showed an average WIP value of 28 (core 06), and 26 (core 07 and 09). The calculated αAl values were very similar between the core sediments except for a major variation ofα^{Al}_{Ca} and α^{Al}_{Na} values. Significant depletion of mobile elements in core sediments is indicated by high α^{Al} values for Ca, Na and Sr. As stated above, the loss is less for larger cations such as K, Rb and Ba, which shows lesser α^{Al} values compared to smaller cations (Ca, Na, Sr). These values indicate recycling of siliciclastic and low grade meta-sedimentary source rocks, which initially have poor plagioclases. α^{Al} values for Cs showed less mobility than other elements as it was observed in the surface sediments during both seasons, this indicates that they are adsorbed to secondary clay minerals (Kronberg et al., 1987; Schneider et al., 2016). The CIA, PIA and CIW weathering indices clearly indicated moderate to high weathering intensity in the source region and core 01 sediments were highly affected by recycling, which was clearly indicated by the high SiO_2 content. In addition to the weathering indices, core sediments were plotted in A-CN-K and A-CNK-FM plots (Figure 5.20 a,b), where they were plotted along the weathering trend from granodiorite and towards illite, which indicates the sediments were dominated by illite and muscovite types of clay minerals rather than rock forming mineral feldspars. In addition, the provenance can be inferred from the samples plotted in the plot through projection back to the source rocks. Upon projection, the source rocks are comparable to intermediate felsic rocks. Amongst the core sediments, core 01 sediments showed low to moderate weathering and other core sediments were moderately weathered. In the A-CN-K plot (Figure 5.20a) core 01 sediments plot along the weathering values, less weathered than other core sediments indicates less clay minerals. Also in the A-CNK-FM plot (Figure

5.20b) core 01 sediments showed somewhat different characteristics and plotted along the weathering trend whilst other core sediment showed moderate weathering and are enriched in clay minerals more than core 01 sediments.

Garzanti et al. (2013) has differentiated the weathering effect from recycling through the CIA/WIP ratio, which is used to discriminate weathering and recycling effects (Garzanti et al., 2014) in the short core sediments. The first cycle muds have a CIA/WIP ratio between 1 and 2 or lower (e.g. Garzanti et al., 2014), whilst recycled sediments show higher CIA/WIP ratios due to quartz dilution, which reduces the WIP values. This may lead WIP values to reduce drastically for the polycyclic mud and can be even "0" for the recycled sands (Garzani et al., 2013a). The sediments of the core 01 sample showed the CIA/WIP ratio between 4.58 and 10.33, which was higher than the CIA/WIP ratio recorded in core 06 (2.64-2.97), core 07 (2.59-3.55) and core 09 (2.90-3.33) sediments, indicating that the recycling effect is greater in core 01 sediments than other cores and enrichment of quartz. However, the CIA/WIP ratio of the other three core sediments were recorded lower than the core 01 sediments (avg. 2.78; 3.06 and 3.13 in core 06, 07, 09 sediments, respectively) indicating less quartz dilution by recycling(Figure 5.19a).

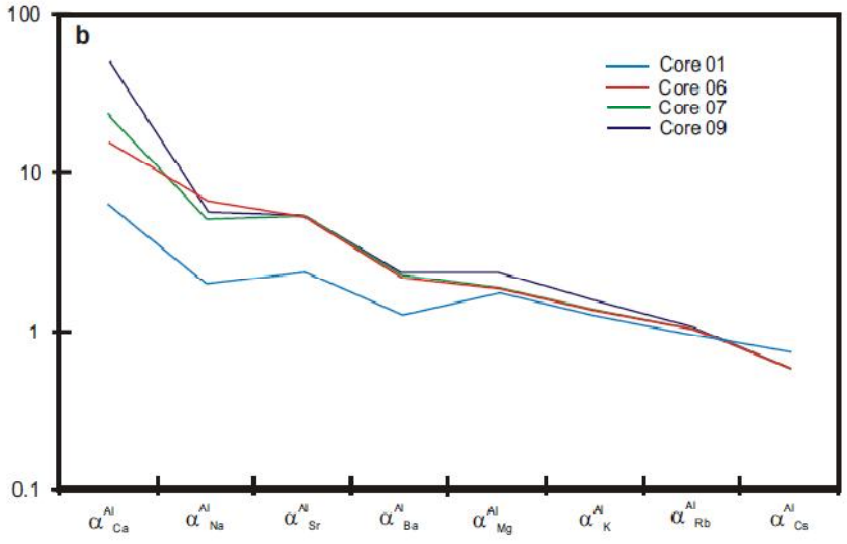

Figure 5.18 Systematic depletion trend of mobile elements relative to non-mobile Al for the short core sediments of the Lower Baram River (Strongly depleted in smaller cations; i.e., Ca, Na, Sr)

The sorting and recycling effect in the short core sediments was also explained using the Zr/Sc Vs. Th/Sc plot (Figure 5.19b; McLennan, 1993), in which, recycled sediments plot along the trend 2 due to addition of heavy minerals (i.e. zircon) to the sediments and thus increases the Zr/Sc ratio. Normal compositional variation can be observed when the sediments plot along trend 1 in the plot. The cores 06, 07, and 09 sediments are clustered at the end of trend 1 (less effect, and/or no addition of heavy minerals), whereas core 1 sediments are extended towards trend 2, which indicates the recycling effect, and thus zircon enrichment (Figure 5.19b).

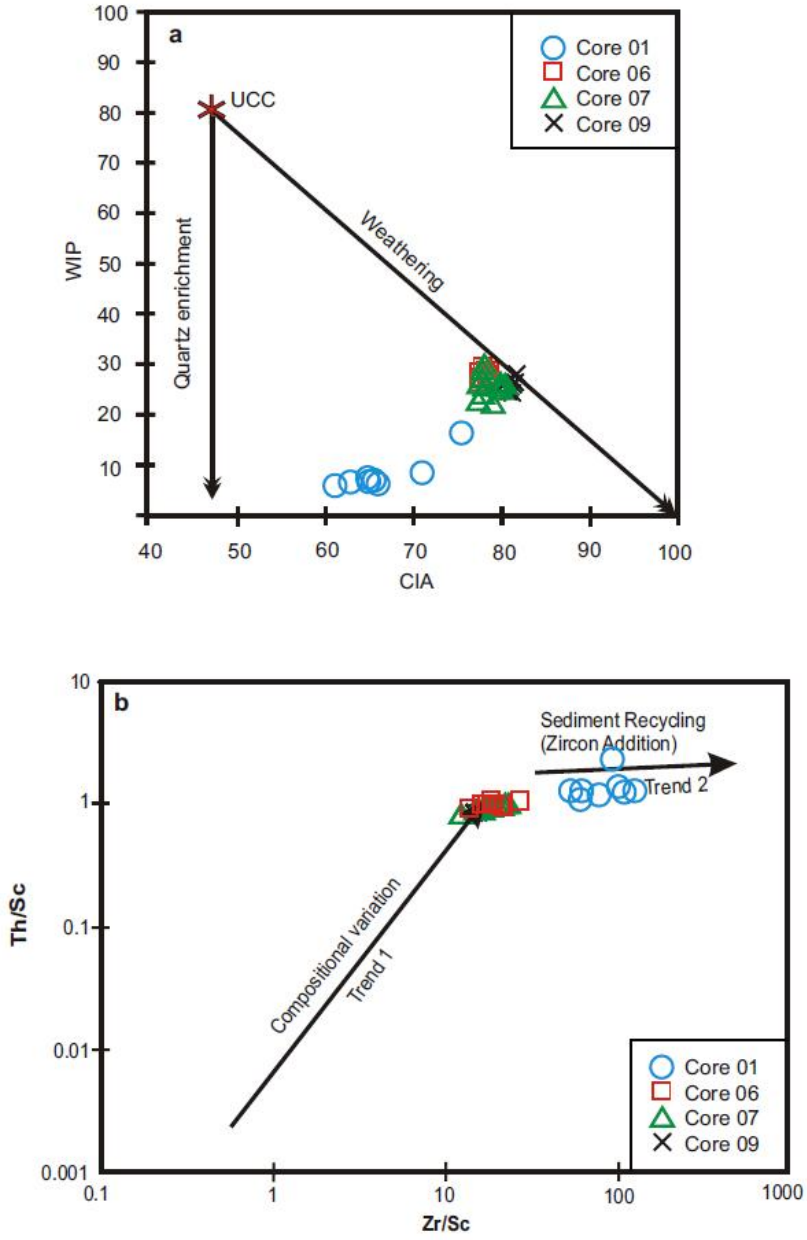

Figure 5.19 a) CIA/WIP biplot (after Garzanti et al., 2013a) shows the enrichment of quartz in core 01 sediments (b) Th/Sc versus Zr/Sc plot shows the weathering and recycling effect for the short core sediments from the Lower Baram River. The addition of zircon due to recycling and sorting is observed in trend 2.

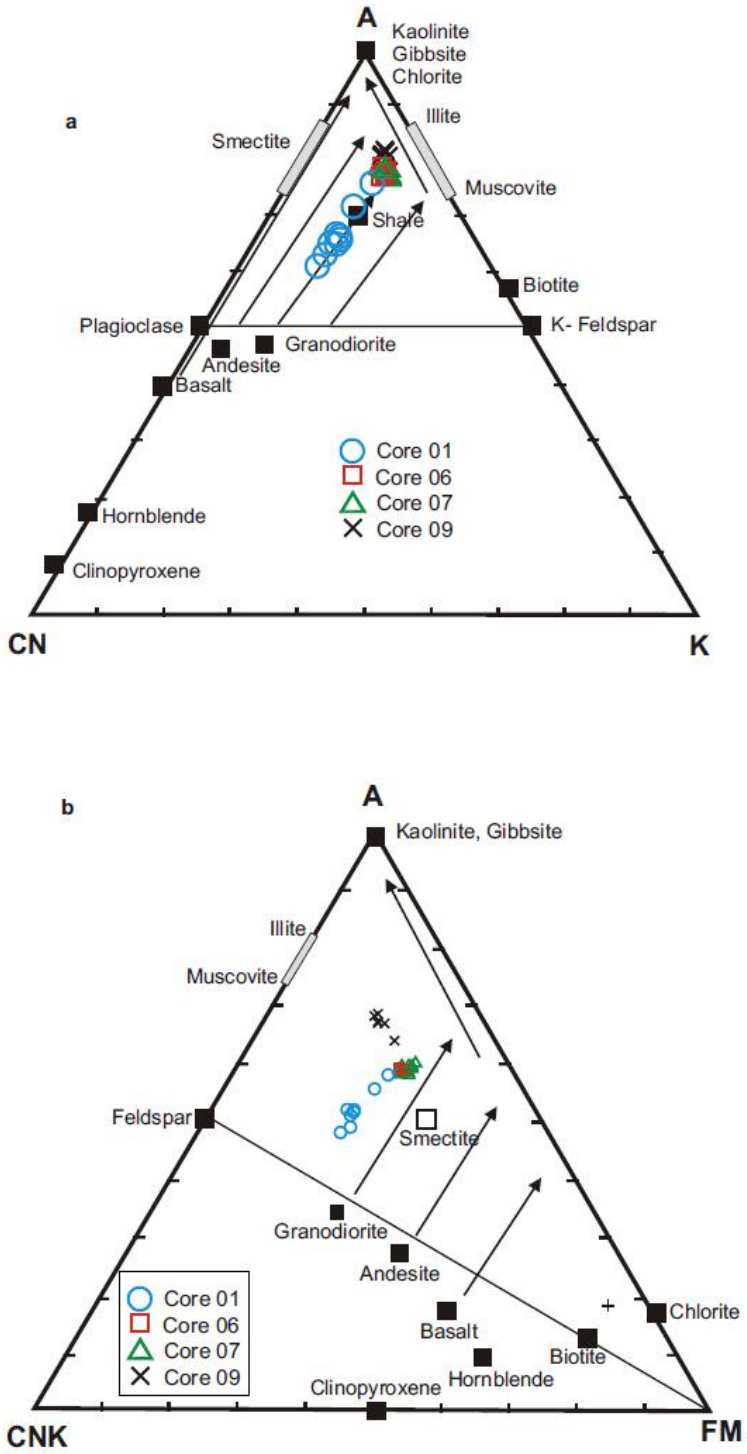

Figure 5.20 a) A-CN-K and b) A-CNK-FM (after Nesbitt & Young, 1984; Nesbitt & Wilson, 1992) plots showing the weathering trend for the siliciclastic sediments of the Lower Baram River.

5.10.2 Sediment Maturity

The textural maturity of short core sediments is estimated through the SiO_2/Al_2O_3 ratio, ICV and the K_2O/Al_2O_3 ratio. The SiO_2/Al_2O_3 ratio for the core sediments ranged from 11.89-54.62 for core 01; 5.17-6.28 for core 06; 5.09-7.47 for core 07 and 4.58-5.78 for core 09, indicating moderate to high maturity (SiO_2/Al_2O_3 ratio for matured sediments is >5; Roser et al., 1996). The Index of Compositional Variability (ICV) ranged from 0.70-0.96 (avg. 0.84) for core 01; 0.68-0.71 (avg.0.71) for core 06; 0.70-074 (avg.0.72) for core 07 and 0.44-0.56 (avg. 0.47) for core 09, indicating core 01 sediments are rich in non-clay minerals whilst other cores are enriched in clay minerals (ICV> and <0.84 for non-clay minerals and clay minerals respectively; Cox et al., 1995). Similarly, the ICV values of core sediments indicated moderate to high maturity and consisted of a mixture of more clay minerals and less detrital minerals. The core 01 sediments were highly matured by recycling, which was comparable to individual elemental mobility values and CIA/WIP ratios (Figure 5.19a). K_2O/Al_2O_3 values in the short core sediments were observed as 0.16-0.19 for core 01; 0.16-0.17 for core 06; 0.15-0.17 for core 07 and 0.13-0.15 for core 09, indicating dominance of clay minerals over detrital minerals in the core sediments of 06, 07 and 09.than core 01 sediments.

5.10.3 Provenance

The chemistry of short core sediments are plotted in major oxides based discrimination diagram (Roser & Korsch, 1988) and other diagrams based on trace elemental ratios and concentrations to reconstruct the provenance. In the discriminant plot (Figure 5.21a) of Roser and Korsch (1988) the short core was plotted in the quartzose sedimentary provenance indicating recycled provenance from the source region. Core 01 sediments were plotted separately from the rest of the core sediments indicating a greater recycling effect, which was further supported by α^{Al}values and CIA/WIP ratios. In the Hf vs. La/Th plot (Figure 5.21b; Floyd & Leveridge, 1987), all the samples were plotted mainly in acidic arc field except for samples from core 01 which were plotted in the mixture felsic and mafic source materials. Based on the discriminant function diagram (Figure 5.21a), the Th/Sc vs Zr/Sc plot (Figure 5.19b) and the CIA vs WIP (Figure 5.19a) plot, the core 01 sediments were highly affected by the recycling effect and resulted in an addition of more quartz and zircon minerals.

However, in the Hf Vs. La/Th plot (Figure 5.21b), these sediments do not show enrichment of Hf concentration, which may in fact be quartz dilution effected by recycling. The recycled provenance of the short core sediments can be further confirmed through the K_2O/Al_2O_3 ratio, which varies between first cycle sediments and redeposited fine grained terrigenous sediments. The redistributed fine grained terrigenous sediments are characterized by K_2O/Al_2O_3 ratio of <0.3 (Cox & Lowe, 1995; Cox et al., 1995) and is well supported by the K_2O/Al_2O_3 ratio of the short core sediments (avg. K_2O/Al_2O_3 ratio = 0.18; 0.16; 0.16 and 0.14 for core 01, 06, 07 and 09, respectively). In the bivariate plot of Sc Vs.Th/Sc (Figure 5.22a), the short core sediments of the Lower Baram River were plotted between Granite and the UCC indicating felsic intermediate/mixed source rocks rather than a mafic or ultramafic source. However, core 01 sediments were plotted closer to granite due to enrichment of quartz by the recycling effect. In the Rb Vs. K_2O plot (Figure5.22b), the short core sediments are plotted parallel to a typically differentiated magmatic suite with a K/Rb ratio of 230 (Shaw, 1968), except the core 01 sediments, which are plotted in the basic composition due to the recycling effect and dominance non-clay minerals (enrichment of detrital minerals; i.e. quartz, zircon, chromite and rutile etc.) The less influence of ultramafic source rocks was confirmed by the Ni-V-Th triplot (Figure 5.23a) and mixed provenance is suggested by the La-Th-Sc trilinear plot (Figure 5.23b). The intermediate nature of sediments may be related to a mixture of felsic and mafic rocks. In the La-Th-Sc plot (Figure 5.23 b), the short core sediments plotted in the field of clay, silt and gravel from mixed source rocks. Further, the contribution of a dominant source are extracted from the Cr/Th vs Th/Sc plot (Figure 5.24) where the short core sediments plotted close to felsic endmember, except core 01, which deviated towards ultramafic endmember, indicating possible detrital minerals from an ultramafic source (i.e. chromites). The geochemical ratios such as La/Sc, La/Co, Th/Sc, Th/Co, Cr/Th, Eu/Eu* and $(La/Lu)_{CN}$ of the short core sediments were compared to the range of sediments from felsic, mafic source rocks, the UCC and PAAS. These were comparable to the range of felsic to intermediate source rocks and PAAS (Table 5.5), indicating a mixed source. The higher LREE/HREE ratios with negative Eu anomalies are the characteristic feature of felsic source rocks whilst lower LREE/HREE ratios with little and/or an absence of Eu anomalies are the

characteristic feature of mafic source rocks (Cullers, 1994). The higher LREE/HREE ratios (7.78-9.60; 7.14-7.69; 6.37-7.77 and 7.28-7.80 for cores 01, 06, 07 and 09, respectively) and significant negative Eu anomalies were attributed to felsic source rock characteristics for the sediments of the Lower Baram River, which is in agreement with the surface sediments collected during both the MON and POM seasons and in the long core sediments.

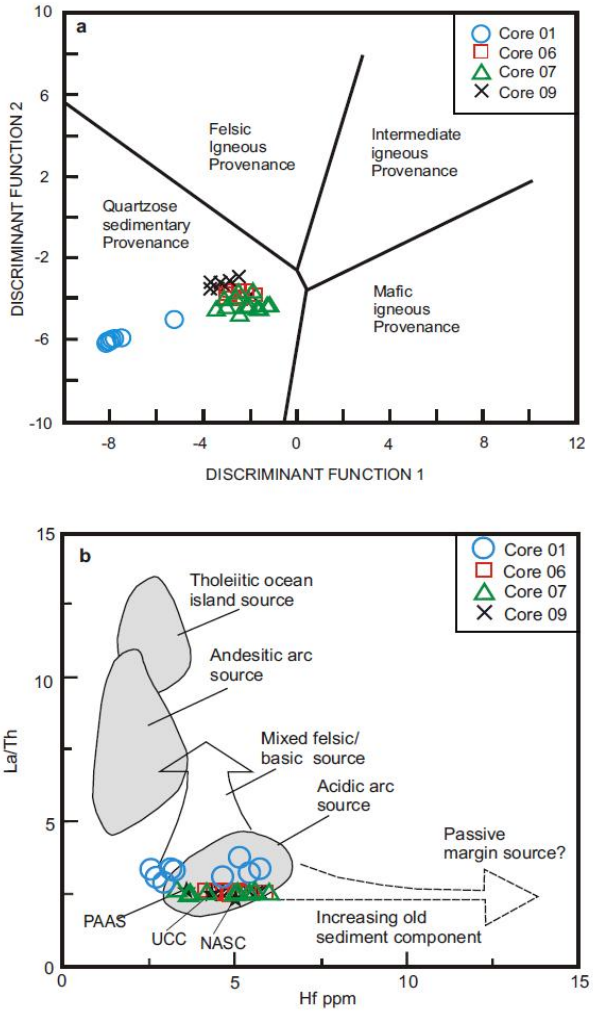

Figure 5.21 a. Major element provenance discriminant-function diagram for the surface and core sediments of the Lower Baram River (after Roser & Korsch 1988).

The discriminant functions are the following: discriminant function 1 = (−1.773.TiO_2) + (0.607.Al_2O_3) + (0.760.Fe_2O_3) + (−1.500.MgO) + (0.616.CaO) + (0.509.Na_2O) + (−1.224.K_2O) + (−9.090); discriminant function 2 = (0.445.TiO_2) + (0.070.Al_2O_3) + (−0.250.Fe_2O_3) + (−1.142.MgO) + (0.438.CaO) + (1.475.Na_2O) + (−1.426.K_2O) + (−6.861). Figure5.21b. Hf vs. La/Th bi-plot for short core sediments from the Lower Baram River (after Floyd & Leveridge, 1987).

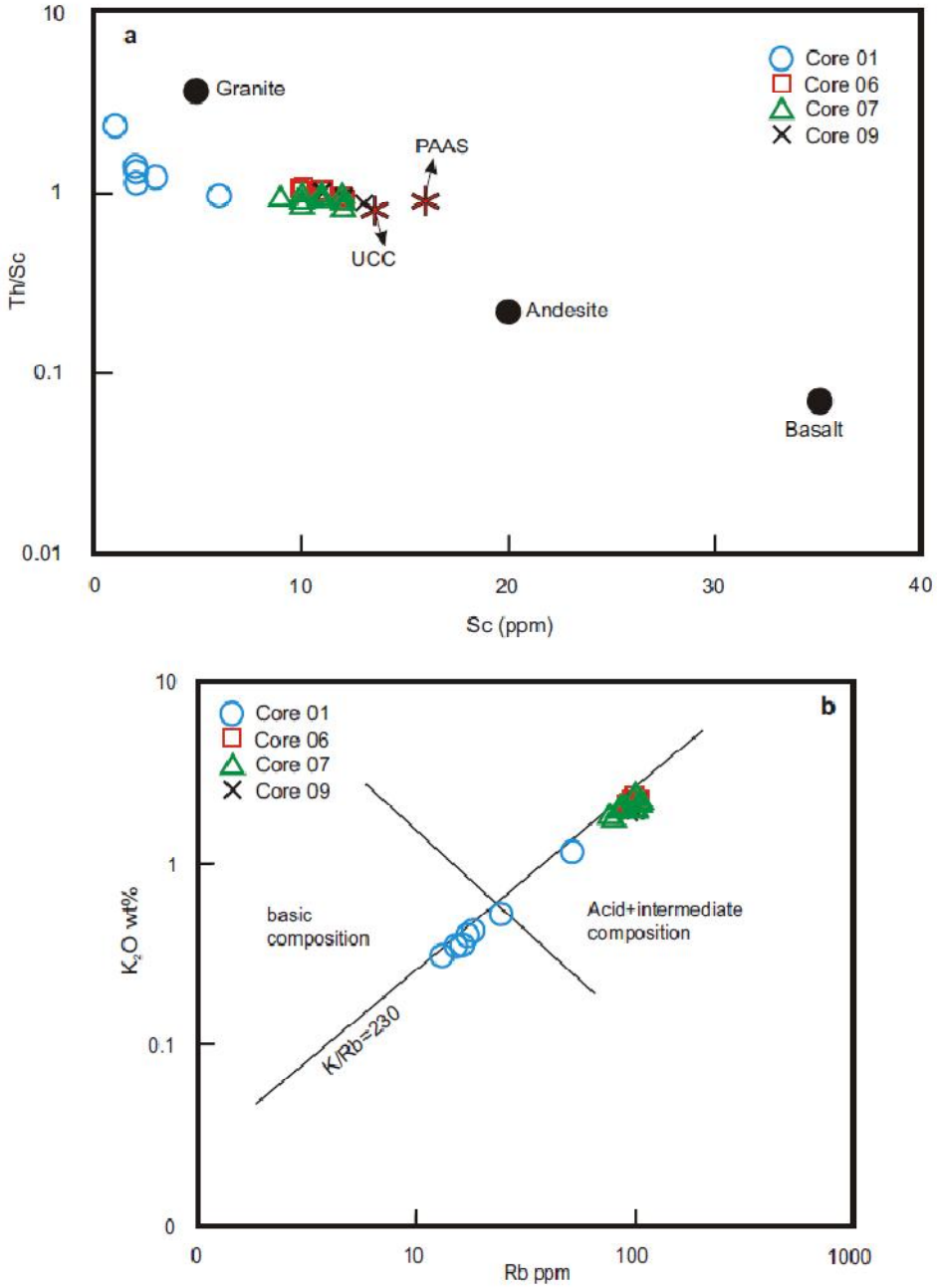

Figure 5.22a. Th/Sc versus Sc plot shows the possible provenance for the short core sediments of the Lower Baram River, 22b. Rb vs. KwO (Wt.%) plot shows the provenance field relative to K/Rb ratio of 230 (trend of Shaw, 1968) for the short core sediments of the Lower Baram River

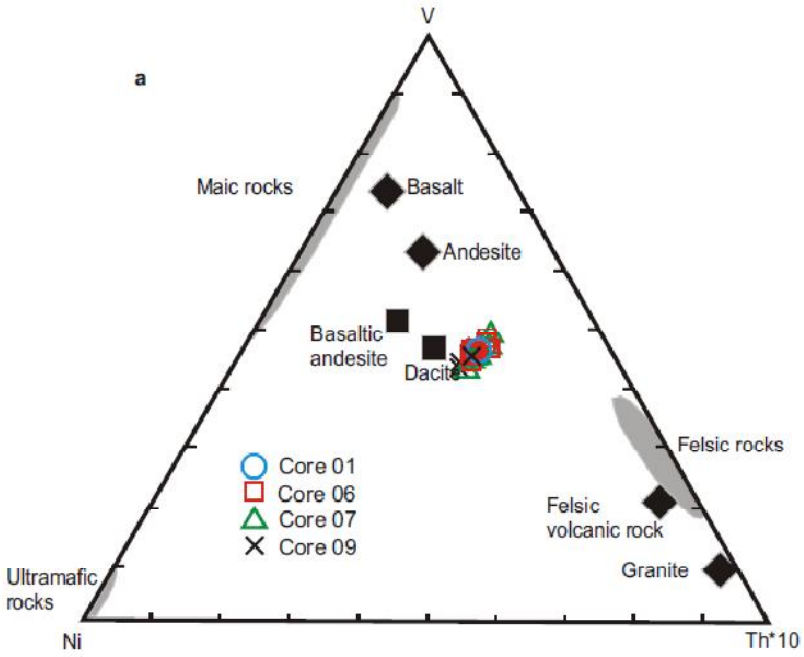

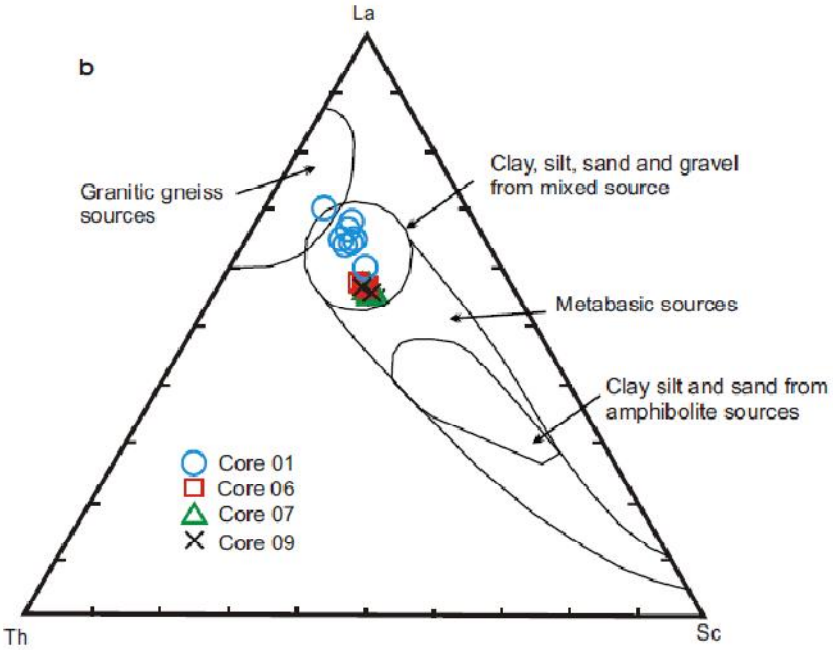

Figure 5.23a. Ni-Th*10-V plot for the short core sediments of the Lower Baram River (average compositions of basalt, andesite, felsic volcanic rocks and granite from Condie, 1993; basaltic andesite and dacite from the source region (Cullen et al., 2013); Figure 5.23b. La-Th-Sc plot showing the possible provenance field for the short core sediments of the Lower Baram River (after Cullers, 1994)

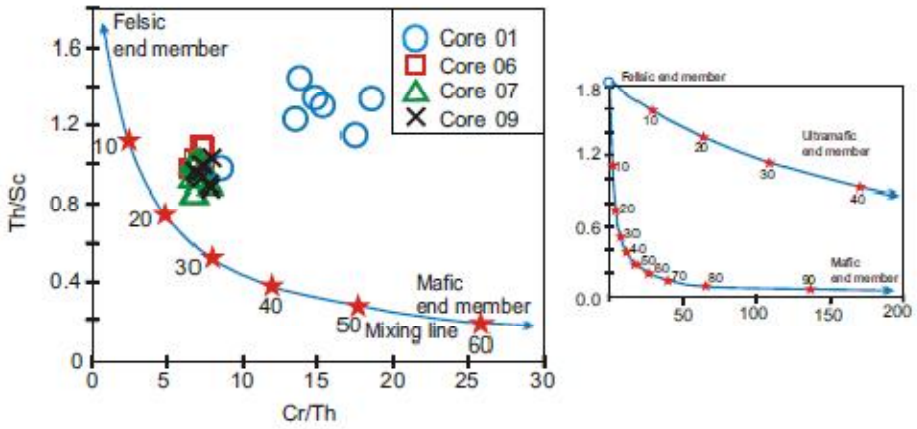

Figure 5.24 Th/Sc versus Cr/Th plot shows the felsic and mafic end member mixing curve. (after Condie & Wronkiewitcz, 1990; Totten et al., 2000) for the short core sediments. Mixing values are shown in % on the mixing curve represent the mafic end member contribution to the mixing products. The mixing of ultramafic end member shown on the right side plot.

Table 5.5 Range and average of elemental ratios of the short core sediments from the Lower Baram River compared to the ratios in similar fractions derived from felsic rocks, mafic rocks, and background values (UCC and PAAS)

Element ratio	Range of core sediments from Baram River, Estuary and Sea[a]				Range of sediments from		UCC [c]	PAAS [c]
	Core 01 (Sea+River junction)	Core 06 (mangroves, estuary)	Core 07 (At meander river)	Core 09 (confluence point of tributary)	felsic sources [b]	mafic sources [b]		
La/Sc	2.93-8.30	2.53-2.85	2.33-2.72	2.30-2.71	2.50–16.3	0.43–0.86	2.21	2.40
La/Co	2.30-3.33	2.45-2.87	2.15-2.58	1.72-2.74	1.80–13.8	0.14–0.38	1.76	1.66
Th/Sc	0.98-2.40	0.94-1.10	0.86-1.02	0.88-1.04	0.84–20.5	0.05–0.22	0.79	0.90
Th/Co	0.73-0.98	0.93-1.08	0.82-0.99	0.65-1.12	0.67–19.4	0.04–1.40	0.63	0.63
Cr/Th	8.47-18.52	6.48-7.41	6.45-7.78	6.90-7.89	4.00–15.0	25–500	7.76	7.53
$(La/Lu)_{cn}$	6.92-7.98	6.72-7.90	6.93-8.02	7.19-8.02	3.00–27.0	1.10–7.00	9.73	9.22
Eu/Eu*	0.61-0.77	0.68-0.72	0.67-0.72	0.66-0.75	0.40–0.94	0.71–0.95	0.65	0.65

5.10.4 Possible provenance area

The Baram River catchment area mainly consists of sedimentary to meta-sedimentary (regional metamorphosed) rocks with a subordinate amount of felsic to mafic volcanic rocks such as andesite and basaltic rocks from the Usun Apau Plateau, and micro-tonalite at Bt.Kalulong (Pliocene-Pleistocene age). Overall, these sedimentary to meta-sedimentary rocks are grouped as the Rajang Group of sediments, which are the

principal source rocks for the Baram River sediments and are significantly influenced by the tectonic and climate events.

The age clusters recorded from the detrital zircons of the Baram River sediments was comparable to the age clusters of the possible source areas such as the Schwaner Mountains in Southern Borneo and main range granites of Peninsular Malaysia. However, the older zircon ages might be related to more distal sources such as the Indo-Australian plate (Van Hattum et al., 2013; Nagarajan et al., 2017b). The Schwaner Mountains have yielded mostly Cretaceous ages whilst plutons from the Malaysia Peninsular have yielded more Triassic ages (Williams et al., 1988; Witts et al., 2012; Van Hattum et al., 2013; Li et al., 2015). The Central belt and Eastern province of the Malaysia Peninsular have yielded comparable ages of present study zircon ages. These Cretaceous and Triassic age clusters were also observed from the zircons extracted from the Miocene-Pliocene sandstones of the Tukau Formation (Nagarajan et al., 2017b). The younger age clusters ~4.5Ma, can be compared to Pliocene volcanic rocks exposed in the catchment area of the Baram River Basin. There are three volcanic mountains exposed in the central part of Borneo, the Hose Mountain Plateau, Linau-Balui Plateau and Usun Apau Plateau. The first two plateaus are exposed in the Rajang River basin and the Usun Apau plateau is exposed within the Baram River Basin. This plateau covers about 906 km^2 with small dissected volcanoes peaking at 1372m and this plateau separates the headwaters of the Rajang and Baram Rivers along with the Tinjar Fault (Cullen et al., 2013; Mathew et al., 2016). The volcanic rocks of Usun Apau and Linau Balui volcanics have been studied by Cullen et al. (2013) for their age, chemistry and petrography. The Usun Apau plateau with an average elevation of 1000m and flat-lying volcanic rocks non-conformably overlie the Paleogene deformed flysch of the Rajang-Crocker Group (Cullen et al., 2013). The reported rocks are hypersthene bearing dacites, andesites and basalts (Campbell, 1956; Kirk, 1968; Tate, 2001; Hutchison, 2005) and the reported age indicates Pliocene to Pleistocene magmatic activity. The reported plateau argon ages for the biotites from andesites and dacites were 3.90±0.04Ma and 3.84±0.06Ma, respectively. However, overlie lava flows show an age of 4.11±0.07Ma, based plagioclase separate from dacite. Based on this study, two distinct magmatic episodes have been reported. The youngest zircon age cluster from a sample (Sample

number 235) collected from a tributary of the Baram River near Usun Apau plateau has shown the zircon age of ~4.5Ma. But no zircon ages are reported for the Pliocene-Pleistocene volcanic rocks of central Borneo. This younger age cluster of zircons can be compared to the evolved phase (older phase then basalts: Cullen et al., 2013) of the Usun Apau plateau. The age clusters observed in the present study confirms the mixture of fresh igneous rocks source with the recycled sediments from the Rajang Group as it was derived from the elemental geochemistry. Based on the zircon age study, it can be concluded that the sediments are derived from the main range granites of Peninsular Malaysia during the Triassic and the Schwaner Mountain during the Cretaceous for the Rajang group of sediments, which have been recycled since the Miocene age to the northern part of Borneo. During the Pliocene, the volcanic rocks became exposed or these fresh rocks contributing sediments to some extent, mixed with the recycled sediments of the Rajang Group, and formed the Holocene to Recent Baram Delta sediments and thus, mixed provenance has been established based on the geochemical study.

Chapter 6. Chemistry of Surface sediments

6.1 Geochemistry and distribution of the major and trace elements and REE's in the surface sediments

Elements discharged into rivers were dispersed between the overlying water column and the bed sediments during their course of transport. Thus, sediment chemistry is concerned with the study of the distribution of chemical elements in bulk as well as in different fractions (Marmolejo-Rodríguez et al., 2007). The underlying geochemical processes in an environment can be revealed by studying the distribution of the trace elements. Surface sediments are the storehouse of information about the current environmental conditions. The sediments reflect the geochemical nature of the river basin and are capable of elucidating the overall character of the material transported by rivers from adjacent land areas, derived from shoreline erosion, carried by marine currents from external sources, produced in situ by organisms, and contributed by human activities (Rubio et al., 2000). Since the surface sediments are very recently deposited, they are also better candidates to understand the short term geochemical processes. They are also useful in deciphering early diagenetic reaction (Fernandes, 1997). In the present study, the major, trace and rare earth elements were anlaysed in the surface sediments collected during two seasons in order to decipher the underlying geochemical processes and the distribution and mobility of the potentially toxic trace elements were studied by sequential extraction in order to determine the relative occurrence of the elements in labile forms. The descriptive summary of the analysed major, trace and rare-earth elements during the MON and POM season (in ppm) are given in Table 6.1 and Table 6.2, respectively. A Paired T-test was performed in order to comprehend whether the analysed parameters vary significantly ($p<0.05$) between the MON and POM seasons (Appendix-2). Among the analysed elements, only 11 elements specifically, Y, Cr, Ni, Cu, Zn, As, Ag, Sb, W, Tl, Pb were found to exhibit significant ($p < 0.05$) variations between the seasons. Therefore, all the other elements were considered to remain compositionally similar, irrespective of the seasons.

Table 6.1 Descriptive statistics of the major, trace and REE's during MON season

Elements	N	Minimum	Maximum	Mean	Std. Deviation
Si	32	302620.65	401717.93	333582.71	22414.53
Al	32	29902.62	76264.92	63458.72	10643.27
Fe	32	13009.39	36160.53	28254.78	5190.22
Mn	32	85.19	805.43	320.43	139.60
Mg	32	2894.88	6573.79	5390.20	859.18
Ca	32	857.64	4931.43	1340.06	688.63
Na	32	2225.58	4525.34	3662.93	502.35
K	32	7720.48	20255.90	16587.63	2728.79
Ti	32	2571.89	4652.19	4098.21	531.45
P	32	130.92	392.77	302.76	65.52
Sc	32	5.00	13.00	10.75	1.93
Be	32	0.00	2.00	1.81	0.47
V	32	42.00	102.00	83.87	13.94
Ba	32	109.00	255.00	212.75	32.86
Sr	32	35.00	66.00	57.37	7.51
Y	32	17.00	29.00	24.68	2.91
Zr	32	185.00	808.00	275.68	132.74
Cr	32	50.00	90.00	64.68	9.15
Co	32	5.00	18.00	9.84	2.24
Ni	32	0.00	40.00	23.43	11.24
Cu	32	30.00	410.00	142.81	108.18
Zn	32	60.00	250.00	123.12	51.77
Ga	32	7.00	16.00	13.34	2.19
Ger	32	1.00	2.00	1.06	0.24
As	32	0.00	10.00	4.50	3.26
Rb	32	42.00	112.00	90.03	15.86
Nb	32	4.00	11.00	8.06	1.70
Mo	32	0.00	4.00	0.25	0.84
Ag	32	0.00	3.30	0.85	0.59
Sn	32	2.00	10.00	3.78	2.23
Sb	32	0.00	0.900	0.15	0.32
Cs	32	2.80	8.20	6.49	1.25
La	32	17.10	32.70	28.09	3.06
Ce	32	33.70	66.00	56.65	6.46
Pr	32	3.69	7.22	6.14	0.72
Nd	32	14.00	27.10	23.24	2.74
Sm	32	2.80	5.50	4.59	0.57
Eu	32	0.59	1.240	1.02	0.14
Gd	32	2.40	5.10	4.20	0.56
Tb	32	0.40	0.80	0.68	0.10
Dy	32	2.70	5.000	4.21	0.54
Ho	32	0.50	1.10	0.85	0.11
Er	32	1.60	3.10	2.46	0.30
Tm	32	0.25	0.49	0.37	0.04
Yb	32	1.70	3.50	2.50	0.31
Lu	32	0.26	0.57	0.39	0.05
Hf	32	4.00	17.70	6.35	2.97
Ta	32	0.70	1.20	0.87	0.12
W	32	0.00	5.00	1.84	0.88
Tl	32	0.20	0.50	0.36	0.07
Pb	32	11.00	123.00	28.53	24.58
Th	32	5.80	12.20	10.22	1.44
U	32	1.70	3.80	2.66	0.33

Table 6.2 Descriptive statistics of the major, trace and REE's during POM season

Elements	N	Minimum	Maximum	Mean	Std. Deviation
Si	32	298694.16	419246.93	333334.38	21293.22
Al	32	22440.20	79017.02	63379.34	10612.59
Fe	32	10071.79	36790.01	28449.31	4525.71
Mn	32	77.44	503.39	321.40	82.47
Mg	32	1929.92	6634.10	5452.40	885.69
Ca	32	857.64	1429.40	1199.35	149.40
Na	32	2225.58	4747.90	3785.80	614.50
K	32	5562.07	20089.87	16273.73	2802.26
Ti	32	1492.78	4778.09	4039.57	559.55
P	32	174.56	436.42	316.40	64.63
Sc	32	4.00	14.00	10.62	1.69
Be	32	0.00	2.00	1.56	0.56
V	32	30.00	106.00	84.68	13.95
Ba	32	91.00	254.00	212.68	30.94
Sr	32	34.00	70.00	56.78	6.92
Y	32	13.00	26.00	22.90	2.51
Zr	32	136.00	614.00	246.90	93.53
Cr	32	40.00	90.00	79.06	8.56
Co	32	4.00	13.00	10.78	1.58
Ni	32	20.00	40.00	35.00	5.68
Cu	32	30.00	190.00	56.25	29.91
Zn	32	60.00	130.00	78.43	12.47
Ga	32	4.00	18.00	14.21	2.54
Ger	32	0.00	2.00	1.12	0.49
As	32	0.00	10.00	6.84	2.15
Rb	32	29.00	117.00	93.25	15.77
Nb	32	0.00	11.00	7.90	2.51
Mo	32	0.00	2.00	0.06	0.35
Ag	32	0.00	1.30	0.41	0.35
Sn	32	1.00	4.00	2.96	0.64
Sb	32	0.90	1.90	1.23	0.20
Cs	32	1.90	9.00	6.80	1.30
La	32	12.00	33.20	28.26	3.55
Ce	32	23.20	66.50	56.45	7.21
Pr	32	2.66	7.45	6.30	0.79
Nd	32	8.70	27.80	23.39	3.16
Sm	32	1.80	5.60	4.72	0.62
Eu	32	0.51	1.22	0.99	0.12
Gd	32	1.70	5.10	4.21	0.53
Tb	32	0.30	0.80	0.70	0.08
Dy	32	2.10	4.60	4.22	0.43
Ho	32	0.40	0.90	0.85	0.09
Er	32	1.20	2.80	2.54	0.28
Tm	32	0.19	0.43	0.39	0.04
Yb	32	1.20	3.00	2.55	0.30
Lu	32	0.20	0.51	0.40	0.05
Hf	32	3.30	14.40	6.04	2.16
Ta	32	0.30	1.00	0.86	0.14
W	32	4.00	8.00	4.81	1.35
Tl	32	0.20	0.70	0.56	0.11
Pb	32	7.00	23.00	15.78	2.54
Th	32	4.30	12.30	10.59	1.30
U	32	1.30	3.30	2.72	0.31

During the MON season, Yttrium concentration varied between 17 ppm to 29 ppm and during the POM the concentration ranged from 13 ppm to 26 ppm. The average Y concentration observed during the MON season (24.68 ppm) was higher than the concentration recorded in the POM season (22.90 ppm). The chromium concentration varied from 50 ppm to 90 ppm during the MON from 40 ppm to 90 ppm during the POM season. The POM season recorded a higher average Cr concentration of 79.06 ppm than in the MON season (64.68 ppm). The maximum concentration of nickel during the MON season was found to be 40.00 ppm. Ni was recorded below the detection limit in 5 sample sites. During the POM season Ni concentration ranged from 20ppm to 40 ppm. The average concentration of Ni was recorded higher in the POM season (35 ppm) than in the MON season (23.43 ppm). Copper concentrations varied from 30 ppm to 410 ppm during the MON season and during the POM season the concentration ranged between 30 ppm to 190 ppm. The average concentration of Cu was higher in the MON season (142.81 ppm) than in the POM season (56.25 ppm). The maximum level of As observed during the MON season was 10 ppm. Among the 32 sample sites, As was recorded below the detection limit in 10 sites. During the POM season the maximum concentration of As was recorded as 10 ppm and was recorded below the detection limit in 2 sites. The mean As concentration was 4.5 ppm during the MON which was lower than the average concentration of 6.84 during the POM season.

The maximum concentration of Ag observed during MON season is 3.30 ppm whereas in the POM season it is recorded as 1.30 ppm. Ag levels is recorded below the detection limit in 2 sites during MON season at 11 sites during POM season. The average concentration of Ag is higher during MON season (0.85 ppm) than the POM season (0.41 ppm). During MON season, the maximum concentration of Sb is recorded as 0.90 ppm and Sb is recorded below the detection limit in 26 locations out of 32 sampled sites. However, during POM, the concentration of Sb ranges from 0.90 ppm to 1.90 ppm. The average concentration of Sb is higher in the POM season (1.23 ppm), than the POM season (0.15 ppm). The highest recorded concentration of W recorded MON season is 5 ppm and is found below the detection limit in 2 sampling sites. However, during POM season, the concentration ranges from 4 ppm to 8 ppm. The average W concentration is lower in the MON season (1.84 ppm), when compared to

POM season (4.81 ppm). The concentration of Tl observed during MON season ranges from 0.20 ppm to 0.50 ppm. During POM season, the Tl concentration ranges from 0.20 ppm to 0.70 ppm. The average concentration of Tl observed during MON season is 0.36 ppm which is lower than the average Tl concentration of 0.56 ppm observed during POM season. Lead concentration during MON season varies between 11 ppm and 123 ppm and during POM season Pb ranges from 7 ppm to 23 ppm. The average concentration of Pb observed during MON season (28.53 ppm) is higher than the average concentration observed during POM season (15.78 ppm).

6.1.1 Factor analytical results for the elements in surface sediments collected during the MON season

Factor analysis was carried out using the major, trace and REE data to further understand the underlying geochemical processes responsible for the observed variation in their concentrations. The factor analytical results of the surface sediments for the MON period are given in Table 6.3. The communality values of Ca and Be were low in this factor model. However, the model results are applicable to all other elements. The varimax rotated component matrix with 7 factors having Eigen value > 1 explained 91.62% of the total variance in the data. The first factor showed positive loading of Al, Fe, Mg, K, Sc, Be, V, Ba, Sr, Ni, Rb, Cs, Eu, and negative loading of Si, Ag, Zr, and Hf and explains the differentiation of the elements based on the grain size. Negative loading of Si with other elements indicated a quart dilution effect. During recycling, quartz and heavy mineral concentrations increase in sediments, which is well supported by close negative loading of Si, Zr, Hf and Ag, etc. Other elements (except Ca, Cr, Cu, Zn, Ge, Nb, Sn, Sb, Pb, V, W, and some HREEs) were moderate to highly loaded on factor-1, indicating their association with clay minerals. The REEs are controlled by two mechanisms: i) their association with clay minerals and ii) their association with detrital heavy minerals such as rutile, zircon, etc. Thus, factor-1 and factor-2 represents the clay and detrital minerals and their grain size. On factor-2, only moderate loadings could be observed for Na, Ti, P, Y, Zr, Ag and Hf whereas all rare earth elements (La to Lu and Th and U) exhibited very good loadings with the exception of Eu, which was highly loaded on factor-1.

On factor-3, the association of Cu, Zn, Pb and Sn indicated both natural and anthropogenic sources contributed to the concentrations of these elements in the Lower Baram River. Source rocks are rich in these elements, but, when compared with upstream concentrations, these elements, particularly Cu, Zn and Pb were enriched in the estuary, indicating additional input through anthropogenic sources. Nb and Ta showed high positive loading under factor 4, in addition, W and Sb also showed moderate positive loading. Nb, and Ta have similar ionic radii and geochemical behavior, mainly associated with rutile and other Ti minerals (Zhao & Zheng, 2015). The positive relationship of Nb and Ta can be related to the presence of niobian rutile. However, both Nb and Ta did not show any relationship with Ti which confirms that niobian rutile and/or other Ti minerals were not controlling their concentration in the sediments. These elements do not substitute for common rock forming minerals and behave incompatibly during crystallization (Linnen & Cuney, 2005). Thus, these elements may be associated with fractionated granitic to pegmatitic rocks (Cerny, 1991; Belkasmi et al., 2000; Johan & Johan, 2005) since peraluminous granites are the major source for the lithophile elements during petrogenesis (Cerny & Ercit, 2005; Sial et al., 2011; Simons et al., 2017).

On factor-5, Ge was loaded along with a moderate loading of Cr. This was due to the presence of chromite as a detrital mineral. Ge is common in many rocks, i.e. sulphide ores, iron ores and some oxide minerals (chromite, magnetite, rutile, etc.), granites, diabase, basalts, coal, etc. Chromites from the detrital phase has been reported in the Miocene sediments of Northwest Boneo, which have been recycled from the source region of the present study. Thus the positive loading of Cr and Ge in factor 5, is controlled by the presence of accessory heavy minerals (rutile and chromite) in the sediments (Nagarajan et al., 2014, 2015, 2017a, b). Similarly, Mo was loaded on factor 6 along with Ca and implied the use of fertilizers and pesticides in this region for agricultural purposes. Foliar application of fertilizers and pesticides is often practiced by farmers to increase yields and physiological potential of seeds. Mo is added with Ca in foliar applications for improving nitrogen metabolism in crops (Costa et al., 2014). However, the use of such fertilizers by farmers in this region is not well known and hence this factor may also be inferred as a natural molybdenum bearing complex

($CaMoO_4$) called powellite associated with Mo-bearing hydrothermal deposits (South West Borneo). Powellite generally has a high stability in a pH of 5 to 6 and may occur as detrital minerals in a high pH condition. In addition, traces of Mo is common in gold placers being present in pulverulent molybdate. Factor 7 is explained by weak positive loading of Mn and Sb. This association indicates the association of Sb in Mn-oxyhydroxides. Particularly Sb is loaded in three factors such as factor 1 (clay minerals) factor 4 detrital minerals and factor 7. It can be related to the presence of some coal fragments if they are bound to organic and/or inorganic matter, which may be related to either pyrite (stibnite) or siderite minerals. Otherwise, it may be dispersed within organic matter (Dai et al. 2012). Coals of Borneo are rich in chalcophile elements (As, Cu, Pb, Sb and Zn) and do not show any relationship with sulphur (Sia & Abdullah, 2012).

Table 6.3 Varimax rotated component matrix factor model of the surface sediments collected during MON season

Element	Communality	1	2	3	4	5	6	7
Si	0.97	**-0.93**	-0.28	-0.10	-0.03	-0.11	-0.10	0.03
Al	0.98	**0.93**	0.31	0.08	0.10	0.05	0.01	-0.03
Fe	0.96	**0.91**	0.30	0.13	0.07	0.09	0.09	0.10
Mn	0.89	0.58	0.18	0.31	0.25	0.09	0.18	**0.58**
Mg	0.98	**0.92**	0.36	-0.01	0.04	0.04	0.00	0.01
Ca	0.77	0.17	0.09	-0.12	0.06	0.13	**0.83**	0.11
Na	0.89	**0.62**	**0.51**	-0.32	-0.05	-0.27	-0.25	-0.05
K	0.98	**0.93**	0.31	0.12	0.05	0.04	0.05	-0.05
Ti	0.98	0.78	**0.57**	-0.08	0.14	-0.01	-0.02	-0.10
P	0.81	**0.77**	0.40	-0.09	0.07	-0.05	-0.12	0.15
Sc	0.97	**0.90**	0.35	0.13	0.09	0.01	0.07	0.05
Be	0.77	**0.85**	0.18	-0.02	0.04	-0.12	0.01	0.00
V	0.99	**0.92**	0.34	0.10	0.11	0.07	0.02	0.03
Ba	0.96	**0.91**	0.27	0.20	0.11	0.03	0.04	-0.03
Sr	0.97	**0.90**	0.39	0.01	0.03	0.02	0.12	-0.02
Y	0.93	0.59	**0.69**	0.04	0.18	-0.05	0.08	-0.24
Zr	0.98	**-0.83**	0.51	-0.08	0.05	0.12	0.11	-0.05
Cr	0.85	0.02	0.39	0.16	0.45	**0.67**	0.02	0.13
Co	0.93	0.71	0.26	0.23	0.29	0.09	0.12	0.44
Ni	0.86	**0.81**	0.14	0.00	0.38	0.00	0.19	-0.06
Cu	0.94	0.11	-0.19	**0.93**	-0.12	0.12	-0.05	0.04
Zn	0.94	0.27	-0.17	**0.90**	-0.09	0.13	0.00	-0.05
Ga	0.98	0.92	0.33	0.10	0.13	0.05	0.07	-0.01
Ger	0.67	0.13	-0.05	-0.04	0.14	**0.79**	-0.04	0.01
As	0.74	0.74	0.14	0.21	0.17	0.14	0.22	0.18
Rb	0.99	**0.92**	0.31	0.12	0.15	0.05	0.06	-0.05
Nb	0.93	0.43	0.15	0.13	**0.79**	0.09	0.12	-0.23
Mo	0.80	0.08	0.04	0.37	0.05	-0.26	**0.75**	-0.15
Ag	0.95	**-0.79**	**0.54**	-0.12	0.01	0.11	0.02	0.11
Sn	0.81	0.12	-0.14	**0.85**	0.22	0.00	-0.04	0.12
Sb	0.90	-0.33	-0.15	0.12	0.63	0.13	-0.15	**0.57**
Cs	0.98	**0.91**	0.35	0.12	-0.03	0.08	0.03	0.08
La	0.98	0.57	**0.77**	-0.06	0.05	0.22	0.14	-0.05
Ce	0.98	0.58	**0.76**	-0.05	0.04	0.19	0.13	-0.05
Pr	0.96	0.58	**0.76**	-0.01	0.06	0.18	0.11	0.01
Nd	0.98	0.61	**0.75**	0.00	0.06	0.15	0.14	-0.02
Sm	0.97	0.60	**0.74**	0.05	0.07	0.15	0.14	0.11
Eu	0.95	**0.82**	**0.47**	0.09	0.15	0.13	0.13	-0.01
Gd	0.97	0.61	**0.74**	0.00	0.00	0.16	0.05	0.16
Tb	0.88	0.57	**0.72**	-0.11	0.00	0.03	0.03	0.17
Dy	0.97	0.52	**0.82**	-0.09	0.01	-0.01	-0.03	0.16
Ho	0.97	0.34	**0.91**	-0.08	0.04	-0.05	0.01	0.05
Er	0.97	0.33	**0.91**	-0.09	0.08	-0.08	-0.04	0.06
Tm	0.96	0.22	**0.94**	-0.09	0.11	-0.02	-0.06	0.03
Yb	0.96	0.08	**0.96**	-0.16	0.06	-0.03	0.00	0.05
Lu	0.94	-0.03	**0.95**	-0.14	0.10	-0.02	0.05	0.00
Hf	0.98	**-0.83**	0.49	-0.08	0.12	0.13	0.12	-0.04
Ta	0.86	0.07	0.20	-0.14	**0.85**	0.19	-0.05	0.18
W	0.59	0.33	0.05	0.08	**0.67**	0.05	0.13	0.04
Tl	0.85	0.77	0.28	0.10	0.30	0.25	0.17	-0.05
Pb	0.83	0.13	-0.16	**0.78**	0.12	-0.30	0.27	0.04
Th	0.98	0.64	**0.73**	0.06	0.02	0.08	0.09	-0.12
U	0.96	0.09	**0.94**	-0.15	0.09	0.05	0.02	-0.18
Percent variance explained		**56.23**	**16.05**	**7.06**	**4.88**	**3.00**	**2.44**	**1.97**
Total variance explained		91.63						
Eigen value		Greater than 1						

6.1.2 Factor analytical results for the elements in surface sediments collected during the POM season

The factor analytical results pertaining to the data of the surface sediments during the POM period are given in Table 6.4. During this season, the communality value for Ge is very low and this factor model does not properly explain its variability. The factor results indicate factor-1 is negatively loaded with Si and positively loaded with major and trace elements (Al, Fe, Mn, Mg, K, Ti, P, Cr, Co, Ni, Rb, Nb, Sn, Sr, Ba, V, Be, Sc, REEs), indicating the association of these elements with clay majority of trace and REE with the clay. Also observed was a gradational change in the factor loading from LREE to HREE between factor-1 and factor-2. Such a fractionation of REE was linked with secondary minerals. Furthermore, Th was also loaded with factor-1. Such an association between LREE and Th is found to be due to the coherent behaviour of LREE and Th during weathering, transport and diagenesis (McLennan et al., 1980). Moreover, on factor-2, the following elements exhibited high positive loading: Ag, Cr, Hf, U, Y, Zr, Cr, Zr, Hf, U, and many of the HREE (Ho, Er, Tm, Yb, Lu) were moderately loaded. Such an association indicates the segregation of heavy minerals. On factor3, W was negatively loaded, while a moderate loading was observed for Nb, Ag and Sn. This implies the presence of a detrital mineral associated with either granite or, hydrothermal veins in the source area (Noli et al., 1996). The mineral cassiterite (SnO_2) has impurities such as Fe, Ta, Nb, Zn, W, Mn, Sc, Ge and Ga, and has been reported from the Crocker-Rajang group of sediments (Van-Hattum et al., 2013) and the Miocene sediments (Nagarajan et al., 2015). In addition, detrital cassiterite may be recycled from the source region or, derived from tin bearing granites (Van-Hattum et al., 2013; Nagarajan et al., 2015). On factor-4, Ca and Mn are associated indicating the variability in Mn concentration in the river sediment was due to its carbonate fraction. Na was highly loaded on factor 5 and was not associated with any other component implying the differential mobility of Na compared to its peers, during weathering of fresh Na-bearing feldspar from the volcanic rocks (Usun Apau) exposed in the source region. Factor-6 was loaded with Cu and Zn, indicating both natural and anthropogenic sources contributed to the concentrations of these elements in the Lower Baram River as elucidated in factor -3 of the monsoon season. Factor 7 was loaded with As and a

moderate negative loading of Mo. Such an association can be related to the dissolution of pyrite containing Mo and As. With such a dissolution, the As and Mo exhibited differential mobility, and became accumulated in the sediments due to the prevailing redox conditions.

Table 6.4 Varimax rotated component matrix factor model of the surface sediments collected during POM season

Element	Communality	1	2	3	4	5	6	7
Si	0.97	**-0.96**	-0.13	-0.07	-0.08	-0.12	0.02	-0.04
Al	0.99	**0.97**	0.14	0.02	0.00	0.15	0.02	-0.02
Fe	0.99	**0.90**	0.15	0.03	0.34	0.18	-0.01	0.01
Mn	0.95	0.56	0.16	-0.03	**0.78**	-0.08	-0.01	0.01
Mg	0.99	**0.91**	0.13	0.19	0.14	0.29	-0.04	0.05
Ca	0.94	0.07	-0.09	-0.32	**0.91**	-0.03	0.05	-0.04
Na	0.97	0.43	0.15	0.12	-0.10	**0.85**	-0.10	0.05
K	0.98	**0.93**	0.13	0.14	0.03	0.28	0.00	0.02
Ti	0.97	**0.85**	0.40	0.04	0.02	0.28	-0.01	0.07
P	0.83	**0.77**	0.02	-0.45	-0.13	0.00	-0.11	0.09
Sc	0.98	**0.96**	0.13	0.11	0.14	0.09	0.00	0.00
Be	0.80	**0.84**	-0.04	0.08	0.20	0.21	0.08	-0.10
V	0.98	**0.97**	0.13	0.06	0.06	0.10	-0.05	0.02
Ba	0.97	**0.93**	0.15	0.08	0.08	0.28	0.01	0.00
Sr	0.95	**0.92**	0.06	0.06	0.03	0.32	0.03	-0.01
Y	0.91	0.47	**0.64**	-0.21	0.08	0.48	0.06	-0.03
Zr	0.95	-0.32	**0.80**	0.14	-0.02	-0.30	0.31	-0.06
Cr	0.92	**0.61**	**0.61**	0.41	0.04	-0.08	0.07	-0.07
Co	0.98	**0.79**	0.22	0.20	0.47	0.10	-0.20	0.03
Ni	0.74	**0.72**	0.05	0.31	0.15	0.05	-0.11	-0.32
Cu	0.93	-0.26	0.13	0.09	-0.06	-0.14	**0.91**	0.02
Zn	0.95	0.27	0.31	0.13	0.10	0.07	**0.87**	-0.05
Ga	0.98	0.94	0.19	0.23	0.05	0.07	-0.04	0.03
Ge	0.52	0.44	0.18	0.43	-0.13	0.16	-0.18	-0.19
As	0.87	0.48	0.19	0.51	0.07	0.20	-0.14	**0.53**
Rb	0.99	**0.96**	0.16	0.18	0.06	0.07	-0.06	0.04
Nb	0.96	**0.68**	0.21	**0.64**	-0.08	-0.05	0.02	0.18
Mo	0.89	0.07	0.00	-0.27	0.08	-0.01	0.00	**-0.90**
Ag	0.83	-0.32	**0.61**	**0.55**	0.04	-0.18	0.11	0.08
Sn	0.84	0.51	0.32	**0.56**	0.04	-0.11	0.30	0.25
Sb	0.84	-0.06	-0.06	-0.81	0.28	-0.06	-0.27	-0.14
Cs	0.99	**0.97**	0.11	0.18	0.03	-0.03	-0.03	0.04
La	0.99	**0.87**	0.44	0.18	0.03	-0.02	0.04	0.01
Ce	0.99	**0.89**	0.43	0.13	0.05	-0.01	0.02	0.00
Pr	0.99	**0.87**	0.43	0.20	0.06	0.00	0.02	-0.01
Nd	0.99	**0.87**	0.43	0.19	0.07	0.02	0.01	0.00
Sm	0.97	**0.85**	0.43	0.16	0.13	0.04	0.02	0.09
Eu	0.95	**0.89**	0.23	0.12	0.28	0.12	-0.02	-0.04
Gd	0.95	**0.80**	0.47	0.08	0.25	0.14	-0.04	0.10
Tb	0.90	**0.74**	0.48	0.18	0.15	0.23	-0.07	0.04
Dy	0.96	**0.68**	0.61	0.11	0.14	0.26	-0.04	0.10
Ho	0.92	0.57	**0.69**	0.14	0.17	0.21	-0.13	0.12
Er	0.98	**0.62**	**0.71**	0.04	0.04	0.26	-0.05	0.13
Tm	0.91	0.57	**0.75**	-0.01	0.05	0.19	-0.01	-0.01
Yb	0.95	0.54	**0.76**	0.15	-0.02	0.22	0.10	0.03
Lu	0.94	0.42	**0.81**	0.19	0.03	0.23	0.15	0.02
Hf	0.96	-0.28	**0.79**	0.21	-0.02	-0.35	0.30	-0.03
Ta	0.93	**0.72**	0.36	0.46	0.00	0.18	0.01	0.20
W	0.79	-0.24	-0.11	**-0.84**	0.05	-0.04	-0.01	-0.11
Tl	0.89	**0.69**	0.17	0.59	-0.10	0.00	-0.06	0.16
Pb	0.78	0.50	0.47	-0.08	0.51	0.06	0.02	-0.20
Th	0.98	**0.84**	0.49	0.12	0.10	0.06	0.02	-0.03
U	0.98	0.50	**0.85**	0.11	-0.04	0.06	0.07	0.03
Percent variance explained		**62.38**	**11.55**	**7.22**	**3.92**	**3.12**	**2.43**	**1.98**
Total variance explained		**92.59**						
Eigen value		**Greater than 1**						

6.2 Determining the partitioning mobility of trace elements in the Lower Baram River sediments by sequential extraction

The potential impacts of trace metal contamination on sediment geochemistry is a major concern. The mobility and bioavailability of the heavy metals cannot be revealed through the assessment of total metal concentrations in the environment (Nemati et al., 2011). The partitioning behavior and the binding strength of trace elements determine their bioavailability and bioaccumulation in the environment (Eggleton & Thomas, 2004). The potential impacts of trace metal contamination can be revealed through a more precise understanding of the chemical forms in which a metal is present in sediments (Liu & Shen, 2014). The toxic effects and bio-geochemical pathways can be better understood through the determination of these chemical forms (Quevauviller, 1998). This can be achieved through speciation studies, which is vital in terms of evaluating the processes of downstream transport, deposition and release under changing environmental conditions (Li et al., 2000; Krupadam et al., 2006). Knowledge about the trace element origin, mobilization, biological availability and toxicity can be achieved through speciation studies (Tessier et al., 1979; Rauret, 1998; Amiard et al., 2007).

Metals in sediments are associated with various compartments specifically adsorbed on clay surfaces or iron and manganese oxyhydroxides, present in lattice of secondary minerals like carbonates, sulphates or oxides, occluded in amorphous materials such as iron and manganese oxyhydroxide, complexed with organic matter or present in lattice of primary minerals such as silicates (Tessier et al., 1979; Schramel et al., 2000; Gismera et al., 2004; Wang et al., 2010). Metals in sediments are mainly associated with silicates and primary minerals and therefore have limited mobility. However, when these metals are from other anthropogenic external origins, they are associated with other sediment phases, such as carbonates, oxides, hydroxides and sulfides, which show greater mobility (Heltai et al., 2005; Passos et al., 2010). The historical input of metal contaminants, their digenetic transformation within the sediments and the reactivity of heavy metal species of both natural and anthropogenic origin can be revealed through sequential extraction techniques (Sundaray et al., 2011). These sequential procedures for studying metal speciation are arranged depending on the

nature of samples and the kind of metals studied, using Tessier et al. (1979) as the archetype procedure (Medici et al., 2011). Metals bound in carbonate and exchangeable, Fe–Mn oxide, and organic fractions are most likely to mobilize from sediments if oxygen or geochemical conditions change in the surface water (Tessier et al., 1979) and hence are more available in the food chain (Maiz et al., 2000). In order to avail adequate information about the mobility and bioavailability of certain trace elements, specifically, Cd, Co, Cu, Fe, Mn, Pb, and Zn, the first four fractions (i.e. the mobile fractions) in the sequential extraction procedure proposed by Tessier et al., (1979) were carried out in the present study. However, due to analytical discrepancies, the amount of elements associated with the residual fraction (F5) is evaluated as the difference between the total element concentration and the sum of the fractions of the elements extracted from mobile fractions (F1 to F4). The distribution of the analysed elements in different fractions during both seasons is depicted in Figure 6.1 and Figure 6.2 respectively and their mean concentration in fractions during both seasons are given in Table 6.5 and Table 6.6 respectively. The partitioning of the analysed elements between these fractions during both seasons are patterned in the descending order as follows.

MON season:

Cd: F3>F4>F1>F2>F5

Co: F3>F4>F5>F2>F1

Cu: F4>F2>F1>F3>F5

Fe: F5>F3>F4>F2>F1

Mn: F1>F5>F3>F2>F4

Pb: F3>F5>F4>F2>F1

Zn: F5>F3>F1>F2>F4

POM season:

Cd: F4>F3>F1>F2>F5

Co: F3>F4>F5>F1>F2

Cu: F4>F5>F2>F3>F1

Fe: F5>F3>F4>F2>F1

Mn: F1>F5>F3>F4>F2

Pb: F3>F4>F5>F1>F2

Zn: F5>F3>F4>F1>F2

Figure 6.1 The percentage distribution of trace elements between different fractions during MON season

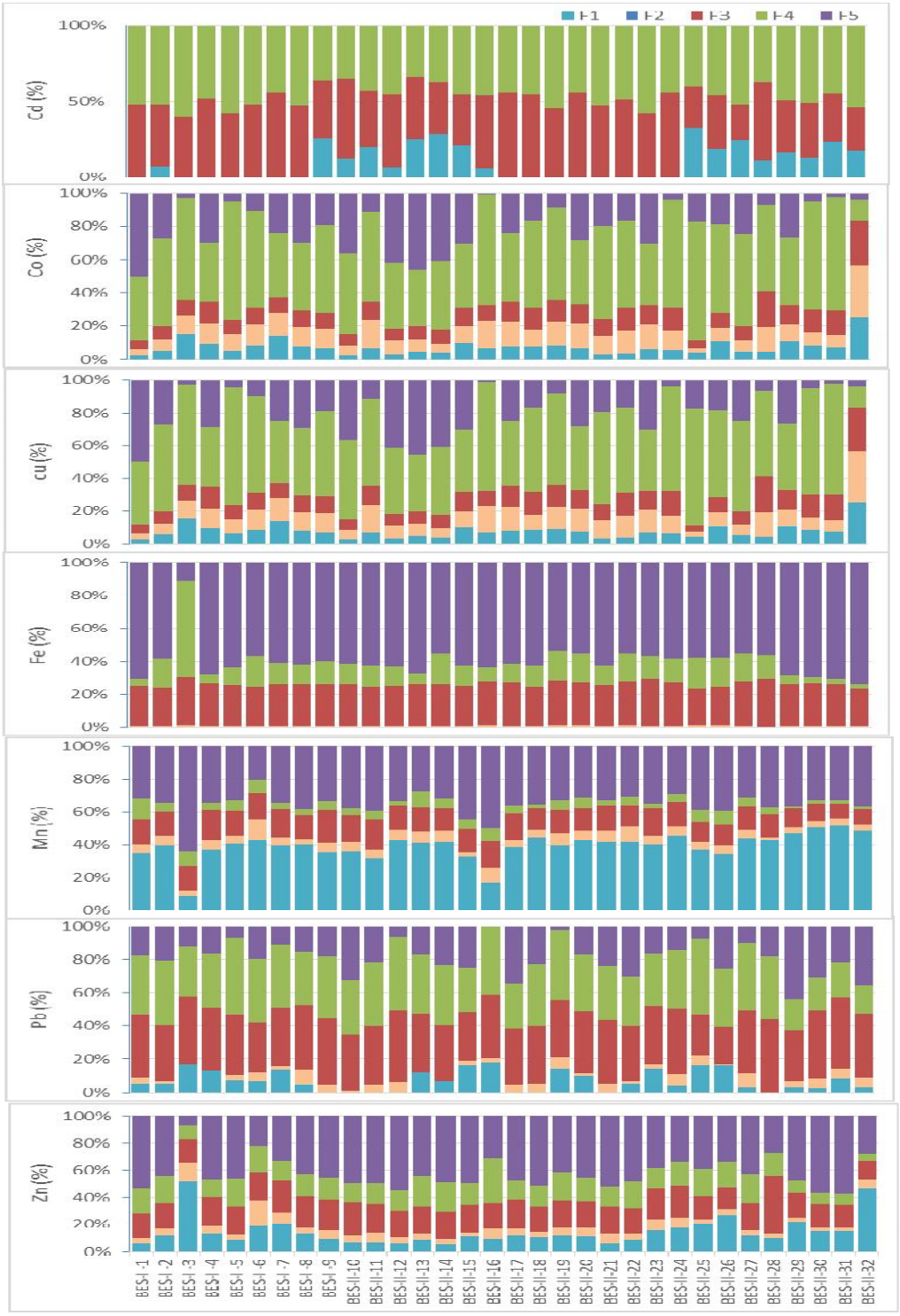

Figure 6.2 The percentage distribution of trace elements between different fractions during POM season

Table 6.5 Trace element concentrations in different fractions in the surface sediments during MON season

Element	F1			F2			F3			F4			F5		
	Min	Max	Mean	Min	Max	Mean	Min	Max	Mean	Min	Max	Mean	Min	Max	Mean
Cd	0.00	0.08	0.008	0.00	0.13	0.007	0.02	0.18	0.11	0.03	0.15	0.08	0	0	0
Co	0.00	2.20	0.80	0.00	3.06	0.96	2.43	7.57	4.78	0.82	3.73	2.04	0.10	7.69	1.82
Cu	0.30	130.01	28.64	2.14	130.99	37.05	3.26	63.64	22.61	9.29	142.03	45.98	3.22	223.98	21.55
Fe	0.00	111.70	14.70	73.90	489.40	257.007	5075.50	12290.10	9047.05	142.70	6078.40	1838.62	8150.17	27601.23	19715.17
Mn	20.60	266.80	132.41	1.20	190.90	37.38	26.20	277.70	75.19	1.70	39.80	11.48	10.97	499.65	113.85
Pb	0.00	20.76	2.12	0.00	22.74	3.35	4.94	46.99	13.47	0.50	25.76	5.38	1.03	11.53	5.53
Zn	1.10	136.70	26.74	2.43	72.55	16.42	15.11	98.67	31.79	3.08	16.50	9.08	3.91	160.70	44.29

Table 6.6 Trace element concentrations in different fractions in the surface sediments during POM season

Element	F1			F2			F3			F4			F5		
	Min	Max	Mean	Min	Max	Mean	Min	Max	Mean	Min	Max	Mean	Min	Max	Mean
Cd	0.00	0.14	0.03	0.00	0.00	0.00	0.06	0.18	0.12	0.09	0.19	0.13	0	0	0
Co	0.54	2.80	1.22	0.00	1.69	1.03	1.54	7.80	4.18	1.54	5.25	3.10	0.02	3.39	1.31
Cu	1.05	47.57	5.38	1.49	60.19	7.31	2.13	50.54	6.95	11.60	79.97	28.35	0.67	21.78	10.11
Fe	BDL	112.80	15.47	40.40	314.40	179.17	3001.30	11937.00	7896.87	758.60	6511.30	3970.30	1139.50	24244.86	19037.49
Mn	7.10	239.90	139.94	2.50	103.40	21.92	12.20	377.70	60.01	5.80	276.00	35.45	51.01	209.16	120.89
Pb	0.00	3.14	1.12	0.00	1.51	0.59	2.90	9.89	5.70	2.06	9.39	5.39	0.05	7.01	3.11
Zn	4.30	61.49	11.97	1.55	18.77	4.53	10.62	38.07	16.03	5.98	26.17	12.89	4.35	45.90	33.00

6.2.1 Fraction 1 (Exchangeable Fraction)

Fraction 1 represents the elements, which are weakly adsorbed and retained on the soil surface by weak electrostatic interactions and can be easily released by ion-exchange processes (Gleyzes at al., 2002; Rao et al., 2008). Metals in this fraction can be easily remobilized by changes in the ionic composition, influencing adsorption–desorption reactions, or lowering of pH (Krishnamurti et al., 1995; Arunachalam et al., 1996; Narwal et al., 1999; Ahnstrom & Parker 2001). The elements associated with this fraction during the MON season were arranged in decreasing order as Mn (35.33%) > Zn (18.42%) >Cu (14.38%) > Co (7.73%) > Pb (5.17%) >Cd (2.83%) >Fe (0.06%) and during the POM as Mn (39.20%) >Zn (14.76%) > Co (11.61%) > Cu (7.56%) > Cd (10.74%) > Pb (7.19%) > Fe (0.05%). It was observed that the percentage of manganese and Zinc was high in exchangeable fractions during both seasons along with Cu during the MON and Co during the POM, which also showed significant amounts in the F1 fraction (>10%).

The relatively high labile amount of Mn should not be attributed to a possible anthropogenic source as this element shows a tendency to be present in less thermodynamically stable phases in the sediments (Tessier et al., 1979; Sakan et al., 2009). The relative predominance of Mn in the exchangeable fraction is attributed to the fact that this element is being reduced in river sediments (Martínez-Santos et al., 2015). The distribution of Fe in exchangeable fraction was less than 1%, which is geochemically insignificant as observed by Zhang et al. (1988) and Sundaray et al. (2011).

6.2.2 Fraction 2 (Bound to Carbonates)

Fraction 2 represents the elements associated with the lattice of carbonates and this is a loosely bound phase accountable to change with environmental conditions such as a change in pH. Carbonate can be an important adsorbent for many metals in aquatic systems where organic matter and Fe–Mn oxides are less abundant (Stone & Droppo 1996). Elements associated with this fraction during the MON season were arranged in descending order as Cu (19.84%) > Zn (11.36%) > Mn (8.70%) > Co (8.36%) > Pb (6.24%) > Cd (2.24%) > Fe (0.85%) and during the POM season as Cu (11.06%) > Co > (9.52%) > Zn (5.69%) > Mn (5.56%) > Pb (3.65%) > Fe (0.59%) > Cd (BDL). It is

observed that Cu and Zn showed significant (>10%) F2 percentage during the MON season whereas during the POM season only Cu showed a significant presence in this fraction, indicating comparatively less metal adsorption of carbonate minerals during the POM season. This could be the result of the greater affinity of the analysed elements towards dissolved organic matter and lower affinity towards adsorption of calcium carbonate (Šurija & Branica, 1995).

6.2.3 Fraction 3 (Bound to Fe and Mn hydroxides)

Iron and manganese oxides are excellent scavengers of metals. Metal scavenging by these secondary oxides, present as coatings on mineral surfaces or as fine discrete particles, can occur by any or a combination of, the following mechanisms: co-precipitation, adsorption, surface complex formation, ion exchange and penetration of the lattice (Rao et al., 2008; Hall et al., 1996). In the present study, elements associated with this fraction during the MON season were arranged in decreasing order as Cd (51.69%) > Pb (47.21%) > Co (45.73%) > Fe (29.56%) > Zn (26.52%) > Mn (22.25%) > Cu (16.19%) and during the POM as Cd (43.38%) > Co (38.51%) > Pb (35.85%) > Fe (25.47%) > Zn (20.48%) > Mn (14.57%) > Cu (11.07%). It is observed that all the analysed elements showed significant manifestation in this fraction during both seasons. This kind of accumulation of hazardous trace elements in the reducible fractions was observed in various other studies showing Fe-Mn-oxyhydroxides are important scavengers of these metals in sediments and they play an important role in controlling their mobility in the environment (Álvarez et al., 2006; Davidson et al., 2006; Kumar & Ramanathan, 2015). The potentially toxic elements such as Cd, Pb and Co have been found associated with Fe and Mn oxides suggesting formation of stable phases of these elements in sediments (Ramos et al., 1994). Also under reducing environmental conditions there is a high probability that these elements will become mobilized, which may be caused most likely by deep burial and a subsequent increase in the reducing environment (Sheikh et al., 2014). Moreover, Zn showed greater affinity to this fraction during both seasons. The association of Zn with Fe-Mn oxides has been reported in various studies (Fernandes 1997; Ma & Rao, 1997; Ramos et al., 1999; Li et al., 2001). The adsorption of Zn onto Fe-Mn oxides possesses higher stability constants when compared to that of carbonates (Li et al., 2001). Likewise, Fe and Mn oxides are the

main carriers of Zn from the fluvial environment to the logoonal environment (Fernandes, 1997).

6.2.4 Fraction 4 (Bound to organic matter)

This fraction represents the elements, which are incorporated in many forms of organic matter including living organisms, organic coatings on inorganic particles and biotic detritus (Gleyzes at al., 2002). Organic matter content in sediments is comprised mainly of complex polymeric material known as fulvic and humic substances which possess inherent high metal adsorptive capacity and, to a lesser degree, other products such as carbohydrates, proteins, peptides, amino acids, fats, waxes and resins (Pickering et al., 1986). The elements associated with this fraction during the MON season were arranged in decreasing order as Cd (43.23%) > Cu (32.84%) > Co (21.04%) > Pb (15.28%) > Zn (7.89%) > Fe (5.96%) > Mn (3.52%) and during the POM as Cu (49.75%) > Cd (47.17%) > Pb (34.02%) > Co (28.18%) > Zn (16.53%) > Fe (13.67%) > Mn (5.37%). Furthermore, Cu dominated in this fraction during both seasons, which could be attributed to the affinity of Cu for organic matter and sulfidic phases to form metal sulfides (Sheikh et al., 2014). In addition, Cu possesses a distinct tendency for complexation with sediment organic matter due to its high affinity to humic substances (Jain et al., 2007; Pacifico et al., 2007; Davutluoglu et al., 2011). A change in the redox potential in this area may stimulate the release of Cu such as the re-suspension and oxidation of the sulfidic sediments into overlying oxic waters (Morgan et al., 2012), possibly during storms or dredging activities (Sheikh et al., 2014).

6.2.5 Fraction 5 (Residual fraction - Bound to mineral matrix)

Primary and secondary minerals containing elements in the crystalline lattice constitute the bulk of this fraction and the elements confined in the residual fraction are strongly bound in the crystal structure of minerals and, cannot be easily mobilized under normal prevailing conditions found in nature (Gleyzes et al., 2002; Varol, 2011; Moyo et al. 2015). Generally the elements bound to this fraction are chemically stable and biologically inactive (Singh et al., 2005). The elements associated with this fraction during the MON season were arranged in decreasing order as Fe(63.56%) > Zn(35.82%) > Mn(30.20%) > Pb(26.11%) > Co(17.14%) > Cu(16.75) > Cd(BDL) and during the

POM as Fe(60.22%) > Zn(42.45%) > Mn(35.30%) > Cu(20.56%) > Pb(19.29%) > Co(12.18%) > Cd(BDL). All the analysed elements except Cd had significant (>10%) affinity in this fraction implying that elements have the strongest association with the crystalline structures of the minerals and they are stable under natural conditions with a lower transfer ability (Nemati et al., 2009; Ma et al., 2016). Apart from major elements such as Fe and Mn, the trace element Zn is found to be associated with residual fraction in an appreciable portion. This indicates that Zn is chiefly bound to silicates and the release of Zn through dissociation in the study area is improbable. The high levels of Zn in the residual fraction and relatively lower levels in the exchangeable fraction could be interpreted as Zn can be easily absorbed and utilized by organisms, clay minerals and silicates in the aquatic environment (Gupta & Chen, 1975; Pizarro et al., 2003; Iwegbue et al., 2007; Ma et al., 2016).

6.3 Factor Analysis

6.3.1 Monsoon Season

Factor analytical results were obtained through SPSS software using PCA extraction and varimax rotation. Eight factors with Eigen values greater than 1 were found for the data pertaining to the MON season and the factor model explained about 86.82% of the variance in the data (Table 6.7). The first factor was loaded with Fe (F3), Al_2O_3, Fe_2O_3, MgO, Na_2O, K_2O, TiO_2 and P_2O_5 along with negative loading of SiO_2. This implied the detrital clay was coated with Iron hydrous oxide. The Factor 2 was loaded with Cd (F4), Co (F4), Fe (F4), Pb (F4), and Zn (F4) implying the factor was associated with pyrite. The Factor 3 was loaded with Cu (F1), Cu (F2), Cu (F3), Pb (F1), Pb (F2) and Zn (F1) indicating the chalcophile nature of elements, which are common in the shale and mudstone beds of turbidities in the source region. Fe (F1) and water pH was loaded on factor 4, thus signifying the flocculation of dissolved Iron. Low pH increases the activity of H^+, Fe^{3+} Al^{3+} and OH^- and the cations compete with heavy metals for negative sorption sites in the sediments (Shafie et al., 2014). Factor 5 was loaded with Cu (F4) and Zn (F3) indicating the replacement or ion exchange of Cu and Zn associated with pyrite. Cd (F2) and CaO were loaded on factor 6 representing the accumulation of Cd on the calcium carbonate surface. Factor 7 was loaded only with Fe

(F2) indicating the conversion of Fe-oxide to Fe-carbonate due to organic matter oxidation. Factor-8 was loaded only with calcium carbonate.

Table 6.7 Varimax rotated component matrix factor model of the elements in different fractions in surface sediments collected during MON season

Parameters	Communality	1	2	3	4	5	6	7	8
Cd (F1)	0.64	-0.03	0.37	0.58	0.24	0.05	0.06	0.25	0.23
Cd (F2)	0.92	-0.33	-0.13	-0.08	-0.09	-0.09	**0.87**	-0.03	0.12
Cd (F3)	0.81	0.18	-0.21	0.00	-0.21	0.37	0.39	0.62	-0.11
Cd (F4)	0.80	0.06	**0.82**	0.23	-0.05	0.00	0.05	-0.20	-0.15
Co (F1)	0.89	0.09	0.35	0.51	-0.34	0.01	-0.17	0.59	0.04
Co (F2)	0.90	-0.10	0.65	0.04	0.14	0.19	0.57	0.25	-0.12
Co (F3)	0.76	0.55	-0.09	-0.14	0.33	0.40	0.34	0.17	-0.10
Co (F4)	0.93	0.14	**0.88**	0.27	-0.14	-0.06	-0.08	0.14	-0.12
Cu (F1)	0.94	-0.05	0.22	**0.91**	-0.11	-0.05	-0.06	-0.10	-0.18
Cu (F2)	0.94	0.02	0.41	**0.79**	0.23	0.16	-0.03	-0.24	-0.10
Cu (F3)	0.89	0.05	0.38	**0.83**	0.22	0.09	0.01	-0.02	-0.04
Cu (F4)	0.92	-0.03	0.48	0.35	-0.04	**0.73**	-0.13	-0.12	0.05
Fe (F1)	0.83	-0.18	-0.06	-0.16	**-0.85**	-0.02	-0.11	0.12	0.16
Fe (F2)	0.83	0.29	-0.21	-0.11	-0.07	0.10	-0.05	**-0.81**	0.13
Fe (F3)	0.85	**0.79**	-0.22	0.07	0.18	0.04	0.29	-0.21	0.13
Fe (F4)	0.95	0.03	**0.89**	0.26	-0.22	-0.11	-0.07	0.17	0.01
Mn (F1)	0.87	0.53	0.45	0.11	0.54	-0.23	-0.11	0.06	0.07
Mn (F2)	0.65	0.10	0.44	-0.11	0.23	0.20	0.27	-0.19	-0.48
Mn (F3)	0.78	0.36	-0.23	-0.10	0.15	0.45	0.55	0.23	-0.08
Mn (F4)	0.80	0.03	0.58	0.07	-0.03	0.66	-0.08	0.12	-0.03
Pb (F1)	0.90	-0.24	0.11	**0.70**	-0.45	0.06	-0.05	0.34	0.09
Pb (F2)	0.89	-0.15	0.46	**0.72**	0.14	0.09	0.00	0.31	0.08
Pb (F3)	0.89	0.02	0.47	0.60	0.26	0.33	-0.02	0.33	0.16
Pb (F4)	0.94	0.05	**0.81**	0.40	0.17	-0.01	-0.06	0.29	0.12
Zn (F1)	0.82	-0.22	-0.07	**0.79**	-0.22	0.13	-0.21	0.12	-0.13
Zn (F2)	0.90	0.05	0.62	0.55	0.25	0.23	0.13	-0.26	-0.15
Zn (F3)	0.95	-0.10	-0.19	0.21	-0.05	**0.92**	0.07	-0.02	-0.03
Zn (F4)	0.91	0.17	**0.88**	0.27	-0.04	0.09	-0.09	0.00	-0.04
pH	0.89	-0.16	-0.47	-0.09	**0.79**	0.02	-0.05	0.04	0.07
Organic Carbon	0.70	0.39	0.10	-0.06	-0.41	0.32	-0.10	0.15	0.48
$CaCO_3$	0.79	0.16	-0.15	-0.15	0.01	-0.04	0.06	-0.23	0.81
SiO_2	-0.97	**-0.95**	-0.25	0.04	0.06	-0.04	-0.05	0.01	-0.02
Al_2o_3	0.98	**0.97**	0.18	-0.01	-0.03	0.02	0.01	0.01	-0.01
Fe_2O_3	0.98	**0.95**	0.18	0.04	0.19	0.00	0.05	-0.03	0.03
MnO	0.81	0.56	0.43	0.05	0.50	-0.12	0.02	0.18	0.10
MgO	0.98	**0.98**	0.04	-0.05	0.04	0.07	0.00	-0.03	0.03
CaO	0.87	0.19	0.09	-0.08	0.07	-0.04	**0.90**	0.00	-0.07
Na_2O	0.82	**0.81**	-0.32	-0.19	-0.03	-0.04	-0.13	0.03	-0.01
K_2O	0.98	**0.97**	0.19	0.00	-0.01	0.01	0.02	0.00	-0.04
TiO_2	0.93	**0.94**	-0.02	-0.15	-0.04	-0.09	0.01	0.00	0.04
P_2O_5	0.82	**0.87**	0.00	-0.04	-0.01	-0.01	-0.15	-0.14	0.12
Percent variance explained		**22.80**	**18.24**	**14.23**	**7.79**	**6.99**	**6.98**	**6.12**	**3.67**
Total variance explained		**86.82**							
Eigen value		**Greater than 1**							

6.3.2 Post-Monsoon Season

Data pertaining to the POM season yielded nine factors with Eigen values greater than 1 explaining 88.83% of the total variance (Table 6.8). Factor 1 was loaded with Fe

(F3), Al_2O_3, Fe_2O_3, MgO, K_2O, TiO_2 and P_2O_5 along with negative loading of SiO_2, implying the detrital clay coated with organics or iron oxide complex. Factor 2 was loaded with Co (F3), Mn (F3), Pb (F3), MnO and CaO, which represents the coating of Mn-oxide on calcium carbonate particles and adsorption of trace elements. Cu (F1), Cu (F2), Cu (F3) and Zn (F1) were loaded on factor 3 suggesting the chalcophile nature of elements. Factor 4 was loaded with Co (F1), and showed negative loading of water pH and salinity, thus, explaining the remobilization of Co due to complexation with chloride or an increase in ionic strength (Tovar-Sánchez et al., 2004; Chen & Lu, 2008). Co (F4), Mn (F4), and Zn (F4) were loaded on factor 5 implying the complexation of Co and Zn with Mn coated organics. Factor 6 was loaded only with Mn (F2), indicating the formation of Mn-carbonate by organic matter oxidation. Factor 7 was loaded only with Fe (F4) implying a source from pyrite. Factor 8 and Factor 9 showed the loading of Pb (F2) and Cu (F4) respectively, which represents carbonate bound Pb and organically complexed Cu, respective of each fraction.

Table 6.8 Varimax rotated component matrix factor model of the elements in different fractions in surface sediments collected during POM season

Parameters	Communality	1	2	3	4	5	6	7	8	9
Cd (F1)	0.63	0.29	-0.26	0.00	0.22	0.12	-0.63	-0.02	-0.06	0.12
Cd (F3)	0.89	0.41	0.39	-0.27	0.01	0.35	0.32	0.26	-0.33	-0.29
Cd (F4)	0.78	0.20	-0.12	-0.10	0.25	0.44	-0.03	0.59	0.31	-0.09
Co (F1)	0.88	0.19	-0.28	0.14	**0.72**	0.16	-0.20	-0.07	0.05	0.40
Co (F2)	0.84	0.10	0.03	-0.13	-0.26	0.15	0.52	0.02	0.64	-0.18
Co (F3)	0.95	0.51	**0.78**	-0.17	-0.13	0.07	0.04	0.10	-0.07	-0.09
Co (F4)	0.97	0.36	0.09	-0.24	-0.09	**0.83**	0.07	0.25	-0.03	-0.08
Cu (F1)	0.97	-0.21	-0.11	**0.94**	0.03	-0.11	0.02	-0.11	0.00	0.04
Cu (F2)	0.99	-0.14	0.04	**0.98**	0.02	-0.03	0.06	-0.07	0.04	-0.06
Cu (F3)	0.99	-0.11	0.13	**0.97**	0.08	-0.11	-0.02	-0.08	0.02	-0.01
Cu (F4)	0.93	-0.11	0.07	0.09	0.12	-0.05	0.11	0.02	0.02	**0.94**
Fe (F1)	0.94	0.29	-0.56	-0.10	0.51	0.02	-0.33	0.26	-0.17	0.26
Fe (F2)	0.79	0.15	-0.40	0.00	0.33	0.65	0.27	0.07	0.03	-0.04
Fe (F3)	0.97	**0.72**	0.63	-0.17	0.10	0.15	0.00	0.07	0.01	-0.03
Fe (F4)	0.83	0.08	-0.09	-0.21	0.06	0.00	0.22	**0.81**	-0.23	0.08
Mn (F1)	0.85	0.42	0.61	-0.01	0.35	-0.28	0.02	-0.14	0.28	-0.01
Mn (F2)	0.82	0.29	-0.02	0.03	-0.17	0.30	**0.73**	0.14	0.15	0.22
Mn (F3)	0.95	0.25	**0.78**	0.07	-0.04	-0.02	-0.24	0.31	-0.33	0.04
Mn (F4)	0.90	-0.04	0.09	-0.08	-0.09	**0.85**	-0.06	-0.36	-0.16	-0.01
Pb (F1)	0.60	0.00	-0.42	0.03	0.19	0.50	-0.08	0.04	-0.16	0.32
Pb (F2)	0.80	0.04	0.04	0.07	0.19	-0.26	0.05	-0.04	**0.82**	0.06
Pb (F3)	0.90	0.29	**0.71**	0.06	0.06	-0.13	-0.10	-0.20	0.45	0.20
Pb (F4)	0.91	0.56	0.27	-0.25	-0.14	0.33	0.04	0.51	0.27	-0.06
Zn (F1)	0.97	-0.22	-0.21	**0.89**	0.13	-0.15	0.02	-0.02	-0.05	0.20
Zn (F2)	0.90	-0.05	-0.13	0.43	-0.33	0.11	0.65	0.25	-0.04	0.29
Zn (F3)	0.93	0.35	0.69	0.26	-0.24	-0.07	-0.05	0.34	-0.29	0.07
Zn (F4)	0.91	0.32	0.05	-0.16	-0.10	**0.79**	0.17	0.33	-0.06	-0.02
pH	0.85	-0.16	0.00	-0.11	**-0.81**	0.07	0.31	-0.16	-0.11	-0.14
Salinity	0.88	0.10	-0.24	-0.08	**-0.89**	0.04	0.07	0.01	-0.07	0.12
Organic carbon	0.77	0.65	-0.04	-0.20	-0.12	0.35	-0.02	0.24	-0.07	0.32
$CaCO_3$	0.86	0.65	0.20	-0.16	0.56	0.03	-0.10	-0.13	-0.14	-0.13
SiO_2	0.98	**-0.95**	-0.13	0.09	-0.15	-0.17	0.00	-0.06	-0.02	-0.04
Al_2o_3	0.97	**0.96**	0.11	-0.08	0.09	0.08	-0.01	0.13	0.01	0.04
Fe_2O_3	0.99	**0.89**	0.39	-0.11	0.08	0.12	0.04	0.01	0.09	-0.02
MnO	0.96	0.47	**0.76**	-0.07	0.27	0.09	0.12	-0.15	0.18	-0.04
MgO	0.98	**0.95**	0.19	-0.12	-0.07	0.12	0.00	0.04	0.06	0.00
CaO	0.78	-0.04	**0.78**	-0.14	0.19	0.00	0.23	-0.23	0.04	0.01
Na_2O	0.94	0.68	-0.09	-0.15	-0.64	-0.01	0.03	-0.06	0.05	-0.16
K_2O	0.98	**0.97**	0.11	-0.10	-0.07	0.09	-0.03	0.09	0.05	0.05
TiO_2	0.95	**0.94**	0.14	0.00	-0.03	0.03	-0.07	0.04	0.11	-0.17
P_2O_5	0.75	**0.71**	-0.05	-0.27	0.34	-0.05	0.09	0.06	-0.22	-0.07
Percent variance explained		**23.97**	**13.90**	**10.91**	**9.79**	**9.17**	**5.67**	**5.65**	**5.32**	**4.45**
Total variance explained		**88.83**								
Eigen value		**Greater than 1**								

6.5 Summary

- From the results of the paired T-test, among 53 analysed elements, 11 elements specifically, Y, Cr, Ni, Cu, Zn, As, Ag, Sb, W, Tl, Pb were found to exhibit significant ($p < 0.05$) variations between the seasons whereas, all the other elements remained compositionally similar, irrespective of the seasons.
- In the surface sediments, during the MON the grain size distribution of the sediments segregate the Al, Fe, Mn, K, Sc, Be, V, Ba, Sr, Ni, Rb, Cs, Eu, as one group and discriminate Si, Ag, Zr, Hf as another group, due to the grain size effect. This is the primary mechanism responsible for exerting control over the chemical composition of the sediments. The association of Cu, Zn, Pb and Sn indicates both natural and anthropogenic sources have contributed to the concentrations of these elements in the Lower Baram River. Source rocks are rich in these elements but when compared with the Upper Baram concentrations, these elements, particularly Cu, Zn and Pb have been enriched in the Lower Baram, indicating additional input from anthropogenic sources. The presence of chromite (as a source of Cr) and powellite (as a source of Mo) minerals in the detrital phase is also indicative of this factor model.
- During the POM the majority of the major and trace elements (Al, Fe, Mn, Mg, K, Ti, P, Cr, Co, Ni, Rb, Nb, Sn, Sr, Ba, V, Be, Sc, REEs) were found to be associated with clay. Furthermore, the fractionation of LREE and HREE was found to prevail, and Th was found to be associated with LREE. Such an association is explained as due to the coherent behaviour of Th and LREE during weathering, transportation and diagenesis. The segregation of the heavy minerals [Ag, Cr, Hf, U, Y, Zr, Cr, Zr, Hf, U, and many of the HREE (Ho, Er, Tm, Yb, Lu)] were also found to influence the sediment chemistry. Detrital minerals associated with either granite or, hydrothermal veins in the source area contributed to the observed patterns in W, Nb, Ag and Sn. The variability in the Mn concentration was found to be affected by sedimentary carbonates. A differential mobility of Na was observed from the sediments, possibly due to the weathering of fresh Na-bearing feldspar from the volcanic rocks of Usun Apau. Similar to the MON season, the Cu and Zn continued to be associated with, and

were thought to have been influenced by both natural and anthropogenic processes.

- The portioning of elements between various fractions has been analyzed by sequential extraction of the sediments and a contrasting pattern of elemental distribution among various fractions during the MON and POM was observed. Manganese was the only element with a high concentration in the exchangeable (F1) fraction during both seasons. Moreover, high levels of exchangeable-Mn in the sediments were expected to play a major role in trace elements adsorption, precipitation and transport mechanisms in the Lower Baram River.

Chapter 7. Geochemistry of core sediments: Downcore geochemical variations

7.1 Introduction

This chapter mainly concentrates on the downcore variations of the selected geochemical elements in terms of variations in weathering, detrital input, paleo-oxygenation, and the sedimentation rate based on the geochemistry and ^{14}C AMS dating. A sediment core from the Baram River mouth was extracted to study the downcore variations of weathering, provenance and trace element distribution in addition to the sedimentation pattern in the NW Borneo region during the Late Holocene. Caline and Huong reconstructed the paleogeographic condition of the Baram River delta based on satellite pictures, aerial photographs in combination with ^{14}C dating of peat deposits and literature review (Caline & Huong, 1992). According to their study, the estuarine deposits formed in the inner bay, south of Marudi (near to inner end of our sampling point, BM-140) at about 5,400 years BP. At about 5000 years BP, peat accumulation proceeded following the stabilization of mudflats by seawater tolerant mangroves. At the same time fluvial/tidal channel belts were prograded to the outer bay, north of Marudi. At about 4000 years BP, Pleistocene sand patches were reworked by longshore currents to the adjacent delta plain and a coastal barrier system gradually closed the outer bay and peats accumulated rapidly. At about 3000 BP the progradation of the lower deltaic plain was controlled by the three main distributaries, which regularly recycled the relic sand patch. In addition, a mangrove belt was developed in a series of lagoons limited by inactive and newly formed barriers. At about 2000 years BP, the river networks became a central distributary (Baram) with two secondary distributaries, the Miri and Belait Rivers. Moreover, abandonment of the meander belt north of Lambir Hills was related to moderate upliftment/tilting of the area, which is supported by the presence of an active fault. The overall geomorphological changes from 5400-2000 years BP have developed a mid-Holocene facies sequence as estuarine sediments (deposited during an early transgressive phase ~5400 BP; south of the bottle neck) and is overlain by deltaic sediments deposited during the later regressive phase (recent deltaic origin) (Staub & Esterle, 1994) with a slower sea-level rise and rapid sediment input. The deltaic

deposition led to rapid progradation of the coast. According to Caline and Huong (1992), the present configuration of the Baram delta system developed about 2000 years BP (Staub & Esterle, 1994). The core locations' present day depositional environment is a riverbank mangrove system but the area was a deltaic environment at about 2000 years BP. The authors have concluded at present, the coast is retrograding once more. Many studies have used core sediments to record the sedimentation pattern, geochemical accumulation, weathering trends, pollution records and paleoclimate records etc. (Fedo et al., 1996; Nath et al., 2000; Keshav & Achyuthan, 2015). With this interesting background, our study expanded to explore the down-core geochemical variation in the Lower Baram River region.

7.2 Results

A complete data set of the core is presented in Chapter-5 (Table 5.2) and selected elements are considered to interpret the downcore variations. The major elements' concentration followed a decreasing order of Si>Al>Fe>K>Mg>Na>Ti>Ca>P, which showed Si was predominant followed by Al, Fe and K. The trace elements followed the decreasing order of Cu>Mn>Zn>Ba>Zr>Rb>V>Cr>Sr>Ni>Pb>Th>Co>Nb>U and showed a positive trend with Al, Fe, and K except Cu, Zn, Zr, and Pb. The organic carbon ranged from 2.94 to 5.81% and $CaCO_3$ ranged from 1.58 to 4.06% with an average of 4.23% and 2.70%, respectively. Silt and mud concentrations were recorded in the range of 48-75% for silt and 25-52% for mud with an average of 61 and 39%, respectively. Based on the silt:mud ratio the core sediments were divided into 3 units: Unit 1 (depth 144cm -116cm), Unit 2 (116-72cm) and Unit 3 (72-0cm). The AMS ^{14}C derived from the core sediments are presented in Table 7.1. The ^{14}C AMS age was determined at 5 depth intervals: 0-4cm, 36-40cm, 76-80cm, 116-120cm and 140-144cm and the sedimentation rates calculated by discarding the reverse age for the three units were 0.34 cm y^{-1},0.16, and 0.28 for the depth intervals 144-121cm, 120-41cm and 41-0cm respectively.

Table 7.1 Depth details and AMS ^{14}C derived dates of Core BM-140 from the Lower Baram River

Sample Interval (cm)	Beta Lab ID	Sediment fraction	Measured radiocarbon age (BP)	Conventional Radiocarbon Age (BP)	2 sigma calibration range (BP)
0-4	440172	Organic	2030±30	1970±30	1990 - 1870
36-40	440174	Organic	2170±30	2110±30	2150 - 1995
76-80	440175	Organic	2000±30	1940±30 Not used for sedimentation rate	1945-1825
116-120	440177	Organic	2660±30	2600±30	2760-2720
140-144	440178	Organic	2740±30	2670±30	2840-2825 2795-2750

7.2.1 Down core variation of the elements

The downcore variation was minor for many elements and ratios; however, a clear trend was observed (Figure 7.1). All the major elements increased from 144cm to 120cm followed by a decrease of up to 40cm and further enrichment towards the top of the core whilst Si showed an opposite trend. Cu and Zn showed a uniform pattern except at the bottom of the core where Zn was recorded higher than Cu and the trend was the opposite of Cu. Similarly, V, Rb, Sr, Th, U and Ba showed a uniform positive trend compared to other elements whereas, Zr and Si showed a negative trend to these trace elements. Mn showed a wider variation and an overall decline towards the top of the core. Many elements (Al, Fe, Mg, Ca, K, Ti P, V, Sr, Co, Rb, and Nb) recorded their lowest concentrations at a depth of 36 cm and the highest concentrations were at a depth of either 128cm (Al, Fe, Mg, Ti, V, Sr, Rb) of 124cm (Ca, K, Ba, Pb, Th, U). However Cu and Zn showed a clear opposite trend with the highest concentrations recorded at 36cm and the lowest concentrations at 136cm together with Si and Zr, which showed the lowest content at 128 cm. Chromium, Ni, Pb and Co showed either uniform or a more fluctuated trend and thus was not comparable to the other elements. This could be overcome by normalizing their concentrations against Al since normalization will compensate the granulometric and mineralogical effects in elemental concentrations (Ho et al., 2012).

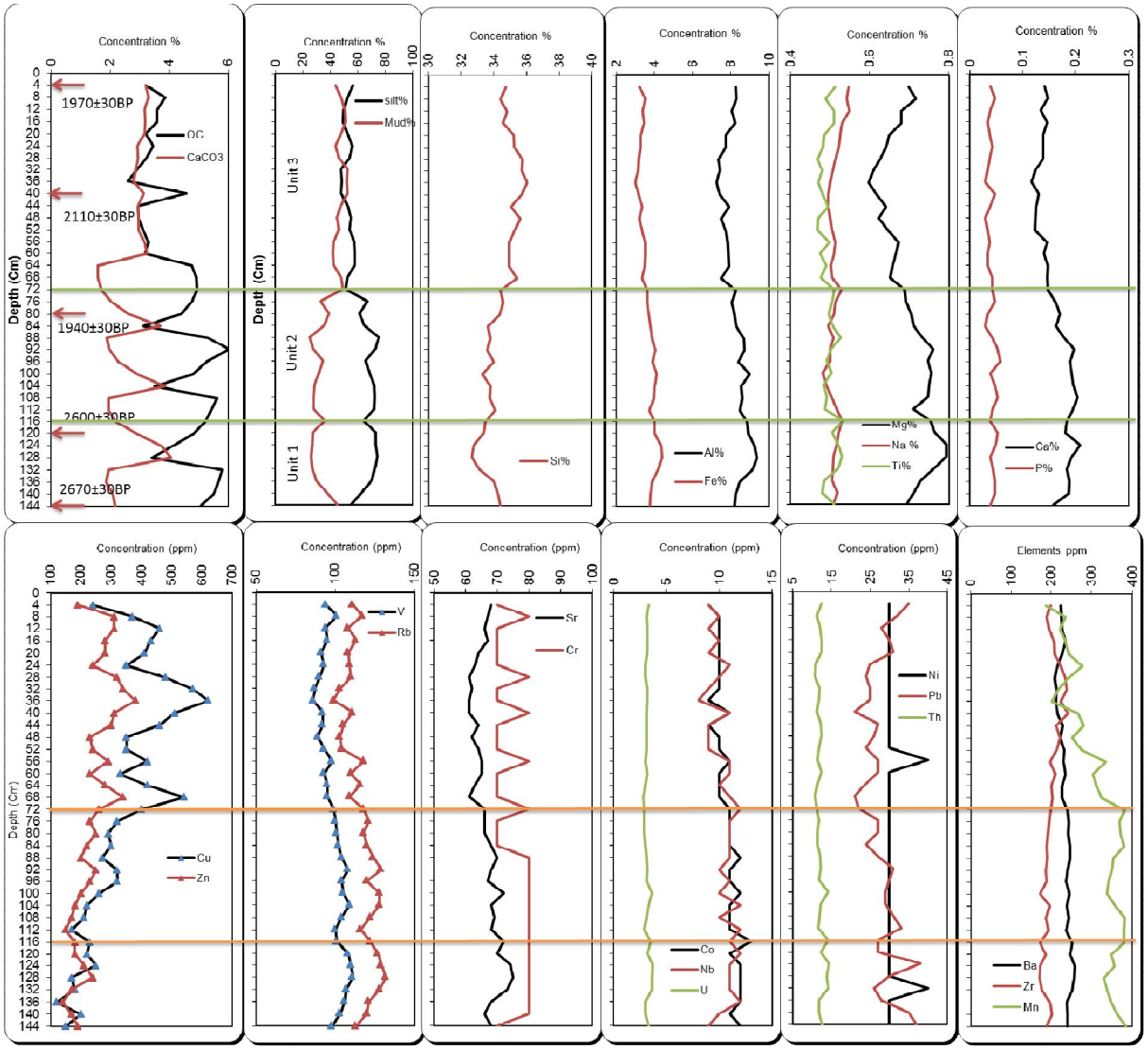

Figure 7.1 Down core variations of the $CaCO_3$, OC, Major and Trace elements for the core sediments of the Lower Baram River

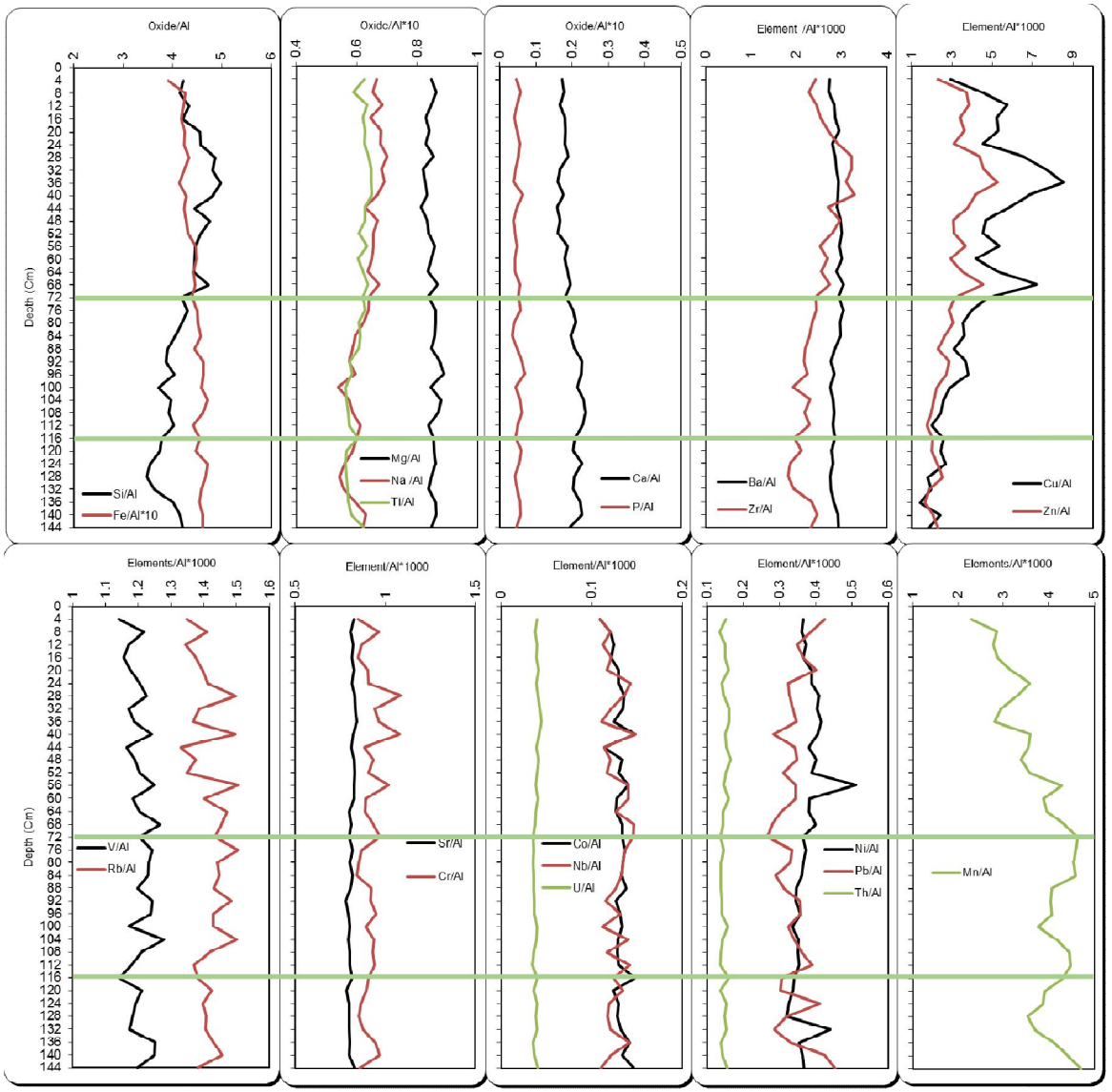

Figure 7.2 Down core variations of the Al normalised major and trace elements for the core sediments of the Baram River

7.3 Discussion

7.3.1 Sedimentation Rate

The radiocarbon ages determined for the core at the depth intervals were 1970 ± 30 BP at 4cm, 2110 ± 30 BP at 40cm, 2600 ± 30 BP at 120cm and 2670 ± 30 BP at 144 cm with a reverse age as 1940 ± 30 BP at 80 cm depth, respectively. The sedimentation rates varied from 0.34cm y^{-1} from 2670 BP to 2600 BP; 0.16cm y^{-1} from 2600 BP to 2110 BP;0.28 cm y^{-1} from 2110 BP to 1970 BP (Figure 7.3). The reverse age was not considered for calculating sedimentation rates of the core sediments. The reverse age at the 80cm depth, may indicate a local slump due to tectonic activity during the Late Holocene. The overall average sedimentation rate was 0.21 cm y^{-1} from 2670 to 1970 BP. The youngest age sediments were not preserved in the study area and indicates either the sediments may be washed away by natural processes or erosion due to dredging activity at the river mouth. Since the core sediments are disturbed by natural processes the sediments become mixed between older and younger sediments and thus, cannot be directly linked to paleoclimate.

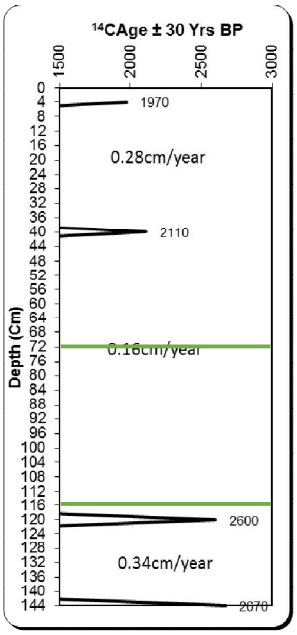

Figure 7.3 Depth Vs radiocarbon dates of the core sediments shows the sedimentation rate over the depositional period

7.3.2 Down core variation of the geochemical normalization by Al

High Si content can be related to quartz and K and Al can be related to clay minerals (Buckley & Cranston, 1991). The Si/Al ratio showed an increasing trend in unit 2 and a declining trend in unit 1, whereas in unit 3 initially declined followed by an increase. The same trend was recorded for Zr/Al, Cu/Al and Zn/Al. Na/Al, Ca/Al, P/Al, Ba/Al, Sr/Al and Th/Al showed minimum variation throughout the depth. Moreover, Cu and Zn showed maximum values at a depth of 36 cm, which is related to enrichment of Si/Al and indicates the effect of recycling. In this case, the Cu and Zn were mainly associated with the detrital fraction of parent rock occurring as lithic fragments rather than associated with the suspended fraction (clay).

7.3.3 Correlation matrix

The correlation matrix was given in (Appendix-3). SiO_2 showed a strong negative correlation with all major elements except Na_2O and P_2O_5 and trace elements except Y, Ni, Sn, Nb, and Ta indicated quartz dilution effect (Bern, 2009) by enrichment of quartz by recycling. Similarly Si showed a positive relationship Cu (r=0.75) and Zn (r=0.64) and indicates their detrital origin. Lithic fragment meta-shales from the source area were associated with fine silt fraction and thus their association with Si. Similarly, Al showed a positive relationship with Fe_2O_3, MnO, MgO, CaO, K_2O, TiO_2, Sc, V, Ba, Sr, Cr, Co, Ga, As, Rb, Nb, Cs, LREEs, Th, and U. This relationship indicates their association with aluminous clay minerals such as illite, Fe-illite clay, kaolinite and smectite, etc. In general, these elements are incorporated into clay minerals during weathering, while Ca, and Na tend to be leached (Nesbitt & Markovics, 1980; Fedo et al., 1996; Selvaraj et al., 2006; 2016). This can be confirmed by the α^{Al} values of the elements, in which, Ca and Na showed a high mobility in the studied samples. In addition, these elements are related to the provenance and thus related to detrital input. Therefore, Si related elements are controlled by silt to fine sand grain size whilst Al related elements are related to clay minerals in the Baram River core sediments. Ti showed a positive relationship with Sr, Sc, Rb, Ba and to a minor extent to LREEs (r=0.53), and a negative correlation with Zr (r=0.58), which indicates their association with clay minerals (illite) rather than detrital minerals (rutile, anatase) (Ratcliffe et al., 2004); however rutile is a common heavy mineral in the sediments of the Upper Baram

River. P_2O_5 showed a moderate positive relationship with CaO and LOI supports that Ca is partly associated with apatite, also P is associated with illite and mixed clay minerals, which was confirmed by their weak to moderate positive relationship with K_2O, MgO, Rb, V, Ga etc. Zr showed a negative correlation with many other elements and showed a positive relationship with Hf (r=0.64), Cu (r=0.70), and Zn (r=0.58). REEs, particularly LREEs and selected HREES showed a moderate to strong positive correlation with Al_2O_3, Fe_2O_3, MgO, K_2O, Rb, Ba (r= ~>0.6) which indicated their association with clay minerals. However, Th and U showed a strong positive correlation with all the REEs, which indicated heavy minerals such as allanite and monazite were controlling REE concentrations of these sediments in addition to clay minerals. In addition, Zr showed a negative correlation with LREEs, which indicated zircon does not contribute any REEs. The HREE was mainly correlated with Y, Sr, Th and U in addition to their weak positive relationship with Al Fe, K, etc., indicating REE was not only controlled by the clay minerals. Similarly, phosphates also did not control the REE concentrations.

7.3.4 Influence of the Paleo-weathering

Weathering is primarily influenced by temperature and rainfall (Gaillardet et al., 1999; Selvaraj et al., 2016) and thus enhancement of the weathering of source rocks in a humid tropical and subtropical climate exceeds that of arid and polar climates (Selvaraj & Chen, 2006). However, the intensity of chemical weathering is controlled by several interplaying factors in which, climatic conditions and time availability are critical (Drever, 1994; Garzanti et al., 2013). Downcore variation of weathering intensity is assessed by different weathering indices such as CIA (Nesbitt & Young, 1982), WIP (Parker, 1970) and geochemical ratios such as Rb/Sr (McLennan et al., 1993), Al/Na ratios (Selvaraj & Chen, 2006) and K/Al (Yarincik et al., 2000).

Based on the constructed downcore variation plots of geochemical ratios and weathering indices, there was no major variation in the weathering intensity in the source region during the deposition of these sediments. However, the minor variation in the weathering intensity was clearly documented by these indices and ratios (Figure 7.7). CIA values ranged from 77.7-79 with an average of 78 and a minimum fluctuation throughout the depth. Other geochemical ratios showed clear variations such as Rb/Sr

and Al/Na, which showed a similar trend as CIA. An increase in weathering intensity leaches more of the Sr and Na compared to Rb and Al and, therefore, the Rb/Sr and Al/Na ratios increased in the weathered profile (Ma et al., 2000). These ratios showed a declining trend between the depths of 120cm and 40cm whilst in the bottom and top of the core some fluctuation was seen. The K/Al ratio can be used as a proxy for the illite/kaolinite ratio in which illite represents physical weathering dominance whilst kaolinite represents intensive chemical weathering in temperate-arid and tropical-humid climate respectively (Bonatti & Gartner, 1973; Selvaraj et al., 2016). The K/Al ratio ranged from 0.25-0.27 with an average of 0.26 and did not follow the CIA, which indicated a dominance of illite, which leads to physical weathering rather than intensive chemical weathering as CIA has suggested. The K/Al ratios showed relatively constant values towards downcore, which indicated that there was no drastic fluctuations in illite (e.g. Hofer et al., 2013). The Rb/Sr ratio was >1 which also supports that illite dominates over kaolinite (Rb/Sr >1 for illite minerals; Chaudhuri & Brookings, 1979). Also, this inference is supported by a previous study by Liu et al. (2012), who found more illite content in the Baram River sediments (75-81%) than kaolinite (10-13%). In this case, the recycling effect was more dominated than weathering as discussed in Chapter-5. The composition of these sediments originated from the source rocks where steep topographic relief and rapid erosion (limited weathering) supports the inference. The Al/Na ratios varied between 14.03 and 18.62 indicating a moderate dissolution of plagioclase and/or due to the recycling effect, which had leached the Na concentration. WIP is suitable for weathering profiles on heterogeneous and homogenous parent rocks (Price et al., 2003). However, its application to highly weathered materials (i.e. bauxites) is uncertain (Eswaran et al., 1973; Price et al., 2003). According to Garzanti et al. (2013a), to discriminate between weathering and recycling effects, WIP can be combined with CIA and α values since the WIP value linearly decreases when quartz is added to the sediment whereas CIA and α values are unaffected by the quartz dilution. WIP values and CIA/WIP ratios showed a negative trend where the CIA/WIP ratio constantly increased from 124 cm to 36 cm (CIA/WIP ratio = 2.2 to 2.7; mainly in unit 2) followed by a decline towards the top of the core, which indicated recycling was significant between ~ 2600 year BP to 2110 years BP.

7.3.5 Elemental Mobility – downcore variation

The individual elements' bulk mobility is discussed in detail in Chapter-5, and thus only downcore variations are discussed here. Ca and Na showed higher mobility compared to other major elements. Ca and Na showed a negative trend to each other (Figure 7.4). Ca showed a higher mobility towards the top of the core whilst Na showed a lower mobility towards the top. Sr next to Ca and Na showed a higher mobility, however the trend was more or less constant. Mg and Ba showed a moderate mobility and were relatively uniform throughout the core depth. K followed by Rb showed the least mobility and their mobility did not change significantly throughout the core depth. Cesium did not show any mobility and showed the $\alpha^{Al}Cs$ values <1 and was uniform throughout the core.

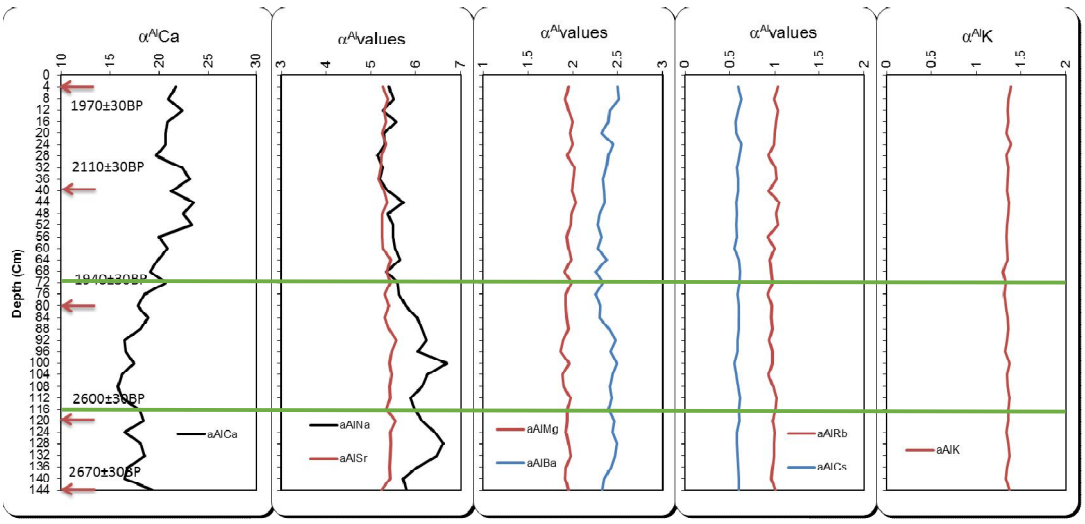

Figure 7.4 Downcore variation of individual element mobility

7.3.6 Influence of the detrital input

Elements controlled by detrital flux from the provenance area can be easily checked by constructing cross plots between trace elements and aluminum or titanium, which are generally immobile during diagenesis (Calvert & Pedersen, 1993; Tribovillard et al., 2006). Elements such as Fe, Mg, Ca, K, Ti, Sc, V, Ba, Sr, Cr, Co, Ga, Rb, Cs, Th and U showed moderate positive correlation with Al_2O_3 and K_2O, which indicated their association with aluminous clay minerals such as illite, kaolinite and/or smectite. Similarly, Zr, Cu, Zn, and Si showed a moderate to strong negative correlation with Al_2O_3, which indicated these elements were not controlled by clay minerals but rather

related to detrital minerals. It is interesting to note that Cu and Zn showed a positive relationship with Si and Zr which could be related to detrital input and/or by recycling and sorting. The sedimentary to meta-sedimentary lithic fragments may be enriched with a sand/silt fraction and may be sorted and enriched in detrital minerals rather than being associated with aluminous clay minerals. Accordingly, positive shifts were recorded for Si/Al, Cu/Al, Zn/Al at depths of 8cm, 12cm, 36cm, 68cm and 96cm (Figure 7.2). However, the trend was uniform throughout the core sample, which could be related to the local slump effect recorded at the middle of the core (80cm).

Elements such as Zr, Hf, Ti, Nb and Ta are easily affected by the sorting process (Zhao & Zheng, 2015). Zr and Hf have relatively similar ionic radii (0.84 and 0.83 Å, respectively) and results similar geochemical behavior, mainly hosted in zircon. Ti, Nb, and Ta also have similar ionic radii and geochemical behavior as Zr and Hf and are mainly associated with rutile and other Ti minerals (Zhao & Zheng, 2015). The heavy minerals such as zircon and rutile from the provenance area may have suffered from hydraulic sorting (grain size effect) during transportation. Overall Zr and Hf showed enrichments between 116cm and 40 cm, which were comparable to the sorting effect. However, Si also showed a similar trend, which indicated a combined effect of recycling and sorting. Also, it should be noted that Ti/Al showed an opposite trend compared to Zr/Al (Figure 7.6) which indicated either variation in the proportion of rutile and zircon minerals in the sediments or Ti was not only associated with heavy minerals, but also associated with clay minerals, which can be confirmed by their association with Al, K, Rb, etc. Nb and Ta did not show any clear trend and did not clearly match with either Zr or Ti, which indicated these elements were not controlled by rutile and/or sorting, instead they were related to clay minerals. Nb showed moderate positive correlation with Al_2O_3, Fe_2O_3, MnO, Ba, which indicated their partial association with clay minerals rather than with heavy minerals such as zircon or rutile.

The ∑REE varied significantly from unit 1 to unit 3. With depths of 144 to 100cm (unit 3 and part of unit 2) recorded the ∑REE relatively equivalent to average shale (173ppm; Taylor & McLennan, 1985) but the 100cm sample from the middle of unit 3 (40cm) showed a declining trend, followed by an increasing trend. ∑REE and ∑LREE closely matched but ∑HREE showed some minor variations at certain depths.

Enrichment of ∑REE occurred at a depth of 96cm, at a depth of 116cm was comparable to enrichment of mud and at a depth of 112cm silt increased and ∑REE decreased, however this trend was consistent throughout the core (Figure 7.5). However, there was not much change in the La/Yb_{CN} ratio and chondrite normalized REE pattern (Figure 7.5) between the 3 units, which indicated that there was no change in the source rocks/area but the ∑REE was relatively affected by hydrodynamic processes and grain size.

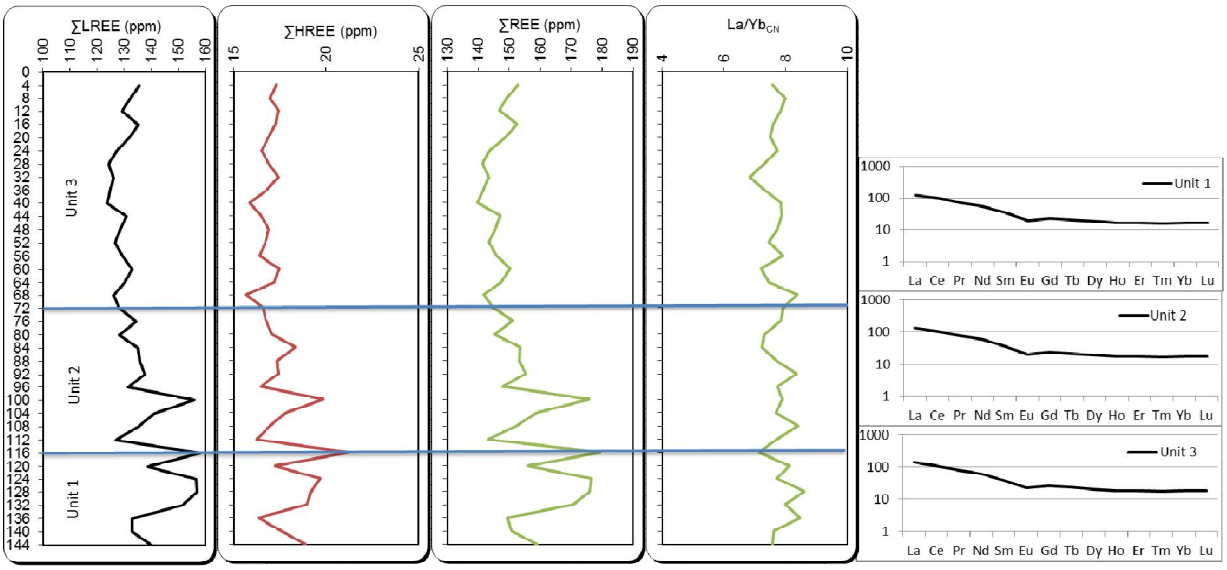

Figure 7.5 Downcore variation of ∑LREE, ∑HREE and ∑REE and chondrite normalized REE pattern for the 3 units.

7.3.7 Paleo-redox condition

The redox condition of the depositional systems can be elucidated by using redox sensitive elements (Mn, Fe, U, V, Cr, Cu, Zn, Mo, Ce etc.) and some geochemical ratios such as V/Cr (Ernst, 1970, Bjorlykke, 1974; Dill, 1986, Jones & manning, 1994), Ni/Co (Dypvik, 1984; Dill, 1986; Jones & Manning, 1994), U/Th (Jones & Manning, 1994; Nath et al., 1997), Cu/Zn (Hallberg, 1976), Ce anomaly (Ce/Ce*; Elderfield & Greaves, 1982) and Mn* ratio (Bellanca et al., 1996) and have been used in many depositional systems to address the paleo oxygenation conditions (Jones & Manning, 1994; Rimmer, 2004; Nagarajan et al., 2007; 2011; Mir, 2015; Madhavaraju et al., 2016). At the same time, these trace elements did not deviate much from the PAAS, which is mainly of

detrital provenance and thus not eligible to be used for paleo-environmental study (e.g. U, Ba and rarely V and Mo; Jones & Manning, 1994; Tribovillard et al., 2006). However, the geochemical ratios such as U/Th or V/Cr should be used with caution since the elements (U or V) are strongly influenced by oxygenation whilst the other elements (Th or Cr) are not, and which are commonly influenced by detrital flux from the provenance area (Potter et al., 2005). In such a situation, Mo concentration can be used to study the oxygenation conditions since it has a strong affinity with dissolved sulfide and thus gets enriched in the bottom sediments by precipitation of Mo sulfide under euxinic conditions (Crusius et al., 1996). Jones and Manning established the boundary values of some geochemical ratios, which are statistically significant and reliable. Accordingly, a V/Cr ratio below and above 2 indicates oxic and anoxic conditions, respectively. Ni/Co, Authigenic U values below and above 5 indicates oxic and anoxic conditions, respectively. The core sediments from the Baram River mouth showed the V/Cr <2, U/Th <1.25, Ni/Co <5, and authigenic U <5, while low Cu/Zn values indicated an oxic depositional environment (Figure 7.7). The Ce/Ce* ratio varied between 0.99 and 1.01 with an average of 1 and was comparable to average shales with no variation at any depth which indicated the core sediments were highly influenced by the detrital input rather than the fluctuation of redox conditions.

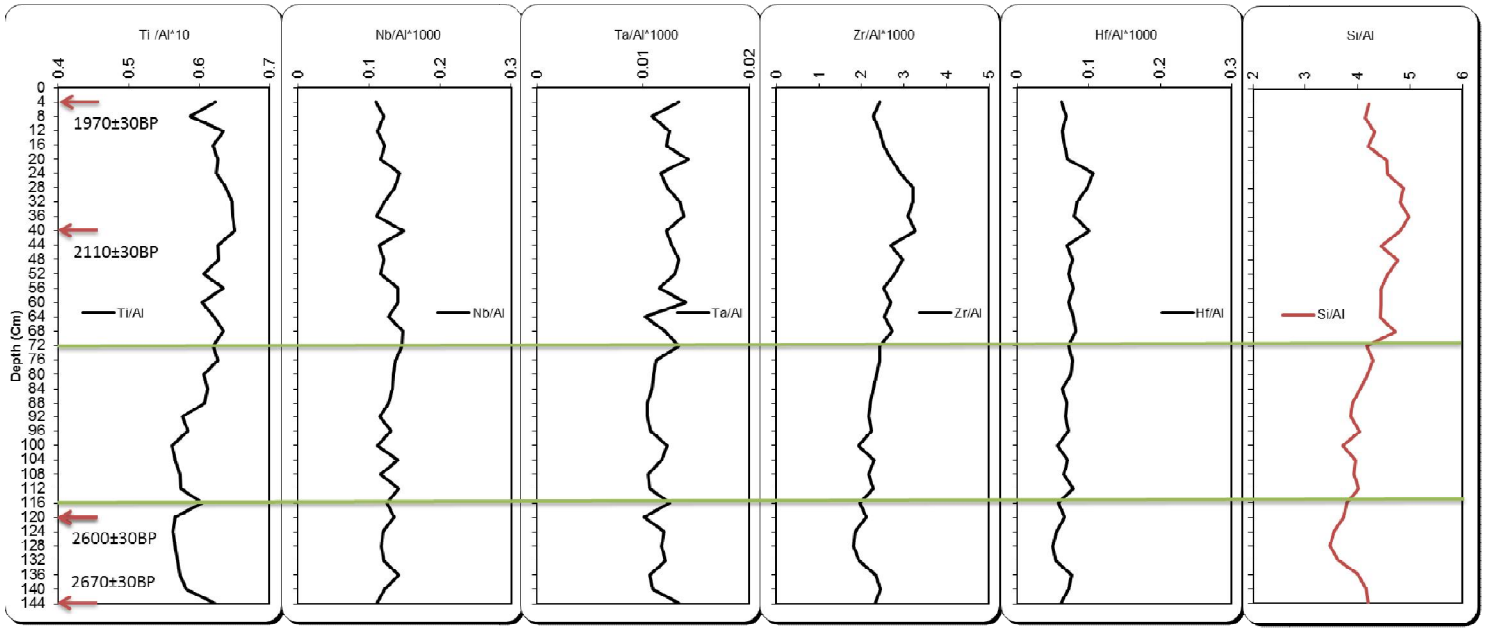

Figure 7.6 Comparison of HFSE down core variations with Si%

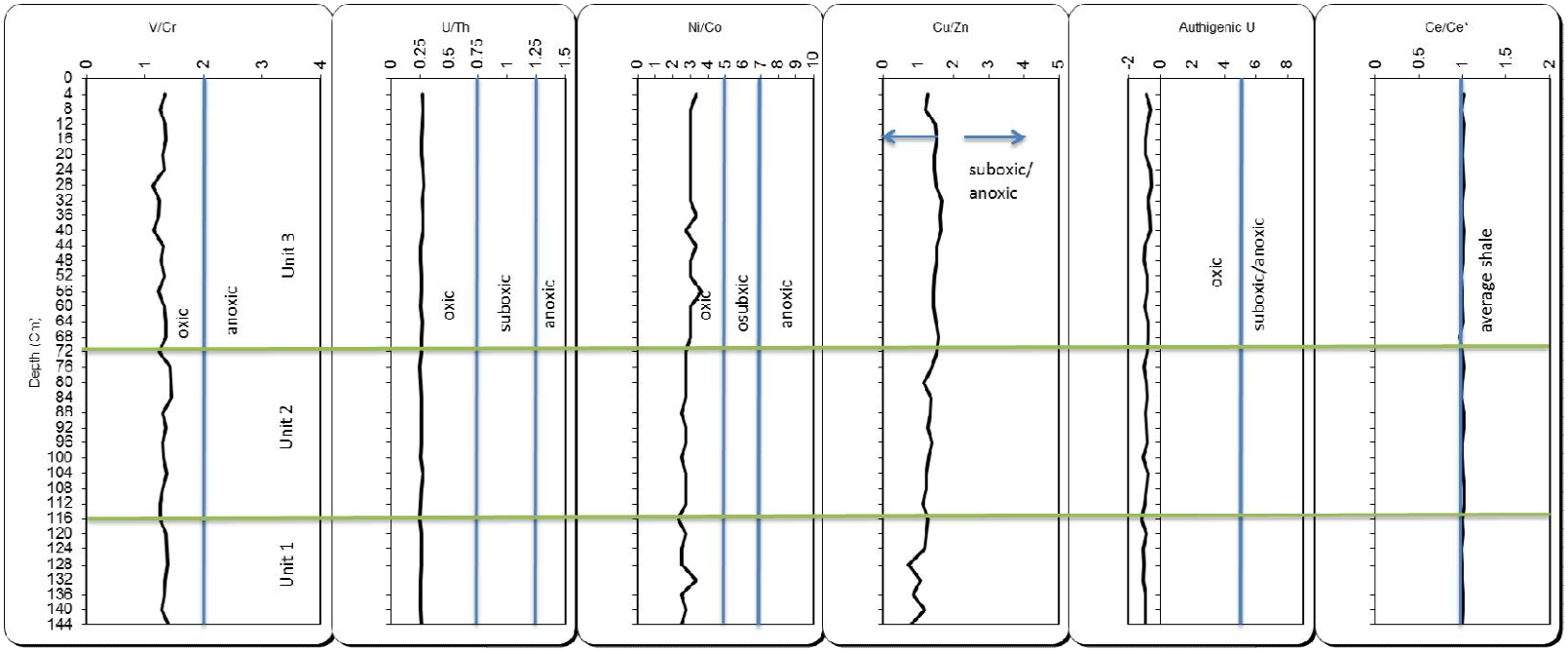

Figure 7.7 Down-core variations of redox sensitive geochemical ratios for the core sediments from the Lower Baram River

7.4 Summary

- Based on the silt:mud ratio, the core sediments were divided into 3 units as Unit 1 (depth 144cm -116cm), Unit 2 (116-72cm) and Unit 3 (72-0cm).
- The radiocarbon age determined at 5 different depth intervals of the core sediments was as follows: 1970 ± 30 BP at 4cm, 2110 ± 30 BP at 40cm, 2600 ± 30 BP at 120cm and 2670 ± 30 BP at 144cm with a reverse age as 1940 ± 30 BP at a depth of 80cm. The calculated average sedimentation rate was 0.21 cm y^{-1} from 2670 to 1970 BP by neglecting out the reverse age. The observed reverse age may indicate a local slump due to tectonic activity taken place during the Late Holocene in this region. The most recent sediments were not preserved in the study area which may point to the fact either the sediments were washed away by natural process or may have been eroded due to dredging activity at the river mouth.
- The whole core represented the source rock rather than the hydrological regime. Mud fraction controls the chemistry of the majority of elements except for Cu and Zn, which are controlled by the silt fraction, which can be linked to lithic fragments of shale and mudstone in the silt fraction evidenced by recycling. Through the correlation matrix it is evident that the elements associated with Si are controlled by silt to fine sand grain size, whereas the elements associated with Al are related to clay minerals.
- The downcore variation of geochemical ratios and weathering indices points to the fact that there was no major variation in the weathering intensity of the source region during deposition. However, minor variations were evident. It was the recycling effect that dominated over the weathering effect of these sediments.
- Ca and Na were highly mobile compared to other elements in the core sediments. The sediments represented an oxic depositional environment. The core sediments denoted a predominant influence by the detrital input, rather than the fluctuation of redox conditions.

Chapter 8. Risk Assessment of the Lower Baram River sediments

Assessing sediment contamination by trace elements in aquatic environments is an important concern due to the toxicity, persistence and bio-magnification effects of accumulated elements beyond purported "permissible limits". When these elements exceed beyond certain concentrations in sediments, they are capable of inducing toxic effects on living organisms (Macfarlane & Burchett, 2000). Aquatic sediments not only act as the main sink for trace elements, but also are potential secondary sources of pollutants in aquatic environments when river conditions change (Singh et al., 2005). Knowledge of sediment quality demands significant concern because sediments are not only essential for acting as a reservoir of pollutants, but also directly interact with other factors across multiple spatial and temporal scales (Bartoli et al., 2012; Erftemeijer et al., 2012; Fu et al., 2014) of which heavy metals are significant parameters (Liao et al., 2017). Accumulated heavy metals in sediments may pollute the overlying water resulting in sub-lethal effects or death in local fish populations as well as accumulate in crops through irrigation (Pekey et al., 2004). Furthermore, they can be released to the water through sediment resuspension, adsorption or desorption reactions, reduction or oxidation reactions and the degradation of organisms (Feng et al., 2007; Dong et al., 2012). These processes substantially increase the dissolved concentration of metals, which impose potential threats to the ecosystem and human health (Liao et al., 2017).

Knowledge of the contamination characteristics of trace elements are essential in terms of watershed ecosystem health management (Casas et al., 2003; Sakan et al., 2009). Thus, a monitoring approach towards trace elements in aquatic ecosystems is essential in order to assess temporal trends in their distribution, the level of their contamination, and their toxic effects on organisms (Audry et al., 2004; Lee et al., 2008; Choi et al., 2011; Hwang et al., 2016). Hence, there is a need for sediment quality indicators to assess the risks of contamination and toxicity posed by the trace/heavy metals in the aquatic environment (Duodu et al., 2016). The calculation of environmental quality indices are an effective tool for transforming the raw

environmental data into more generic information for non-specialists (Dung et al., 2013). This conversion provides information to decision makers for ranking and prioritizing the contaminated areas for further investigation (Caeiro et al., 2005). Many sediment quality indices are being used by researchers worldwide in order to assess the sediment quality of aquatic ecosystems of which contamination factor, index of geo-accumulation (*Igeo*), pollution load index (PLI), effect range low (ERL), effect range median (ERM) and risk assessment code (RAC) were used for the present study. The risk assessment indices were calculated using the average elemental concentrations of the Upper Baram River bulk sediments (<2mm size), as the background value (Table 8.1). The values are available for both seasons (MON and POM). However, for the POM season, in addition to the upstream bulk sediment data, the average elemental concentrations are also available for the upstream fine fraction of sediments (<63µm), which was used for the calculation of risk indices in the surface sediments collected during the POM season as well as the core sediments. Since the Lower Baram River sediments are muddy in nature, the fine fraction chemistry was more suitable than the bulk fraction.

Table 8.1 Descriptive statistics of the considered elements for risk assessment in the Upstream Baram River sediments

Elements	Bulk Upstream (MON) (<2mm)			Bulk Upstream (POM) (<2mm)			fine Upstream POM season (<63 mic)		
	Min	Max	Avg	Min	Max	Avg	Min	Max	Avg
Al	11273.03	99075.60	**48387.56**	6827.33	82033.75	**47207.54**	25086.45	81292.80	**63019.62**
Fe	4546.30	104354.96	**33644.45**	2867.66	86589.43	**30996.06**	9792.02	46092.44	**29014.32**
Mn	54.21	743.48	**310.92**	46.47	1053.27	**314.11**	116.17	557.61	**304.46**
Cu	10.00	130.00	**25.71**	10.00	170.00	**36.72**	10.00	30.00	**19.52**
Zn	30.00	210.00	**71.72**	30.00	160.00	**78.14**	30.00	100.00	**66.35**
Pb	5.00	37.00	**16.43**	6.00	68.00	**16.38**	8.00	21.00	**15.95**
V	16.00	141.00	**68.05**	11.00	116.00	**64.56**	34.00	118.00	**83.92**
Cr	20.00	160.00	**59.59**	20.00	110.00	**50.15**	70.00	190.00	**88.75**
Co	2.00	21.00	**9.21**	1.00	19.00	**8.60**	5.00	15.00	**10.34**
Sr	15.00	92.00	**45.63**	10.00	91.00	**44.32**	32.00	90.00	**60.83**
Ni	20.00	80.00	**34.44**	20.00	60.00	**34.57**	20.00	50.00	**32.81**
As	5.00	22.00	**10.30**	5.00	25.00	**9.90**	5.00	22.00	**7.12**
Ag	0.50	0.80	**0.58**	0.50	1.30	**0.73**	0.50	3.60	**1.30**
Sn	1.00	9.00	**2.10**	1.00	8.00	**2.13**	2.00	3.00	**2.69**
Sb	0.50	1.30	**0.77**	0.50	1.30	**0.76**	1.10	2.00	**1.46**
W	1.00	2.00	**1.55**	1.00	3.00	**1.51**	4.00	8.00	**4.53**

8.1 Surface sediments

8.1.1 Contamination Factor (C_f)

Contamination factor is the ratio of an element at the sampling site to the background value of the same element. Contamination factor is a simple and single index indicator used to evaluate trace element contamination (Duodu et al., 2016). It is calculated by the equation proposed by Hakanson, (1980).

$$C_f = C_m / B_m$$

Where C_m is the concentration of the element in the sampling site and B_m is the background concentration of the element. The contamination factor is classified into four groups as low ($CF<1$), moderate ($1 \leq CF < 3$), considerable ($3 \leq CF \leq 6$) and very high ($CF>6$).

The contamination factor (C_f) was calculated for some selected elements specifically, Fe, Mn, Al, Cu, Zn, Pb, Cr, Co, Ni, V, Sr, As, Ag, Sn, Sb and W for both seasons. The statistical summary of the elements, which were considered for risk assessment in the surface sediments of the Lower Baram River are given in Table 8.2. The range and mean of the calculated C_f of each element for the MON and POM season is tabulated in Table 8.3and Table 8.4 and in Table 8.5for the post- monsoon <63µm and represented in Figure 8.1, Figure 8.3 and Figure 8.5 (based on the POM <63µm background), respectively. Additionally, the site wise illustrations of C_f is given as boxplots in Figure 8.2, Figure 8.4 and Figure 8.6 (based on the POM<63µm background), respectively.

Table 8.2 Descriptive statistics of the considered elements for risk assessment in the surface sediments of the Lower Baram River during MON and POM seasons

		MON				POM			
Elements	**N**	**Minimum**	**Maximum**	**Mean**	**Std. Deviation**	**Minimum**	**Maximum**	**Mean**	**Std. Deviation**
Al	32	29902.63	76264.93	63458.73	10643.27	22440.20	79017.03	63379.34	10612.60
Fe	32	13009.40	36160.53	28254.79	5190.23	10071.79	36790.02	28449.32	4525.72
Mn	32	85.19	805.44	320.43	139.61	77.45	503.40	321.40	82.48
Cu	32	30.00	410.00	142.81	108.19	30.00	190.00	56.25	29.92
Zn	32	60.00	250.00	123.13	51.77	60.00	130.00	78.44	12.47
Pb	32	11.00	123.00	28.53	24.58	7.00	23.00	15.78	2.55
V	32	42.00	102.00	83.88	13.94	30.00	106.00	84.69	13.96
Cr	32	50.00	90.00	64.69	9.15	40.00	90.00	79.06	8.56
Co	32	5.00	18.00	9.84	2.24	4.00	13.00	10.78	1.58
Ni	32	BDL	40.00	23.44	11.25	34.00	70.00	56.78	6.92
Sr	32	35.00	66.00	57.38	7.52	20.00	40.00	35.00	5.68
As	32	BDL	10.00	4.50	3.26	BDL	10.00	6.84	2.16
Ag	32	BDL	3.30	0.85	0.60	BDL	1.30	0.42	0.35
Sn	32	2.00	10.00	3.78	2.24	1.00	4.00	2.97	0.65
Sb	32	BDL	0.90	0.15	0.33	0.90	1.90	1.24	0.20
W	32	BDL	5.00	1.84	0.88	4.00	8.00	4.81	1.35

Table 8.3 Descriptive statistics of contamination factor of analyzed elements in the surface sediments during MON season

Elements	Number of samples (N)	Minimum	Maximum	Mean	Std. Deviation
Fe	32	0.38	1.07	0.84	0.15
Mn	32	0.27	2.59	1.03	0.44
Al	32	0.61	1.57	1.31	0.22
Cu	32	1.16	15.94	5.55	4.20
Zn	32	0.83	3.48	1.71	0.72
Pb	32	0.66	7.48	1.73	1.49
Cr	32	0.83	1.51	1.08	0.15
Co	32	0.54	1.95	1.06	0.24
Ni	27	0.58	1.16	0.80	0.14
V	32	0.61	1.49	1.23	0.20
Sr	32	0.76	1.44	1.25	0.165
As	22	0.48	0.97	0.63	0.12
Ag	30	0.87	5.73	1.58	1.00
Sn	32	0.95	4.76	1.80	1.06
Sb	6	0.91	1.17	1.06	0.12
W	30	0.64	3.22	1.26	0.49

During the MON season, the mean C_f of the elements can be understood in decreasing order as Cu>Sn>Pb>Zn>Ag>Al>W>Sr>V>Cr>Co>Sb>Mn>Fe>Ni>As. Considering the mean C_f, it was found the Lower Baram River sediments were considerably contaminated by Cu and moderately contaminated by Sn, Pb, Zn, Ag, Al, W, Sr, V, Cr, Co, Sb and Mn. However, while considering site wise variation, out of 32 locations, Cu contamination in 12 sites representing 37.5% of the study area were found to be very high, while 7 sites (21.88%) showed considerable contamination with 13 sites (40.63%) showing moderate contamination. For Sn, 4 sites (12.5%) were found to have experienced considerable contamination, while 14 (43.75%) sites experienced moderate contamination and the remaining 14 sites (43.75%) showed low (C_f<1) contamination. In the case of Pb, 11 sites (34.38%) showed moderate contamination, 5 sites (15.63%) showed considerable contamination with 1 site being very highly contaminated. The C_f of Pb was found to be low (C_f<1) in 15 sites, representing 46.88% of the study area. In the case of Zn, 26 sites (81.25%) showed moderate contamination

with 1 site showing considerable contamination while the remaining 5 sites (15.63%) showed low (C_f<1) contamination. For Ag, 24 sites representing 75% of the study area showed moderate contamination with 2 sites showing considerable contamination and 4 sites showing low contamination. However, Ag was found below the detection limits in the remaining 2 sites.

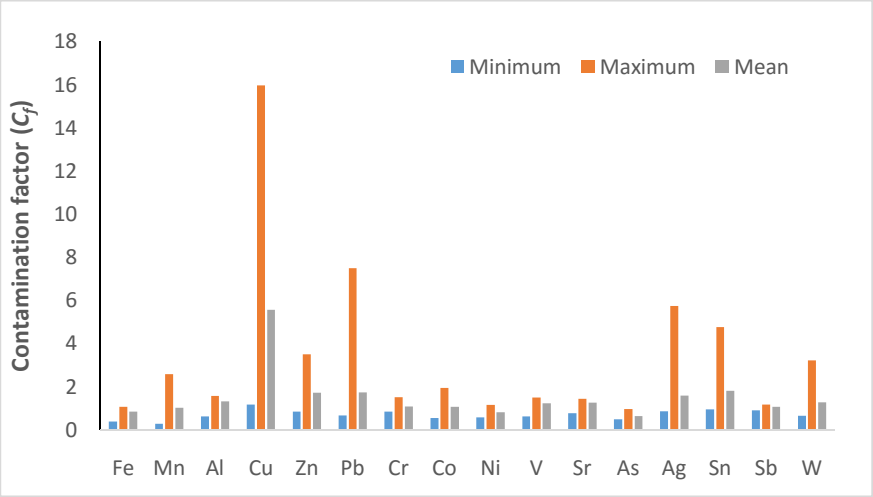

Figure 8.1 Contamination factor of analysed elements in the surface sediments during MON season

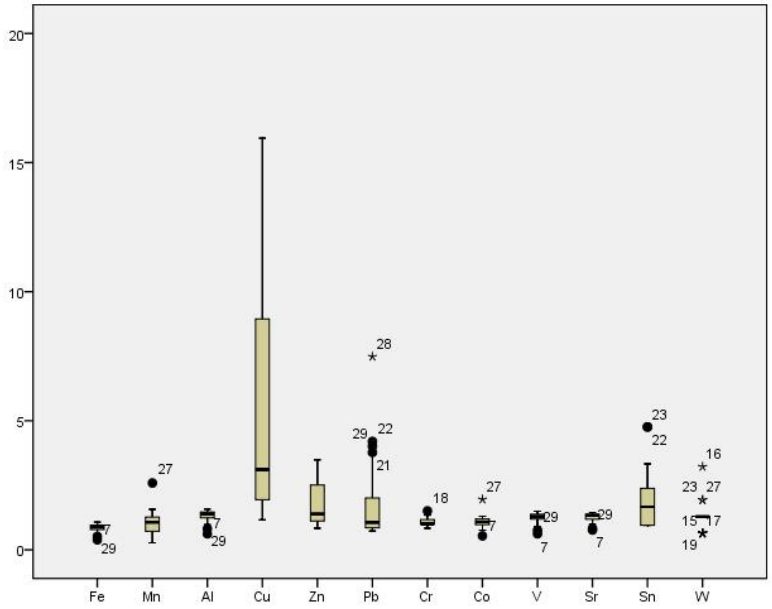

Figure 8.2 Box plot of contamination factor for the elements during MON season

About 29 sites, representing 90.63% of the study area showed moderate contamination for Al, Sr and Cr with the remaining 3 sites (9.38%) showing low contamination. For W, 23 sites (71.88%) showed moderate contamination with 1 site showing considerable contamination and 6 sites (18.75%) showing C_f<1, and thus low contamination. However, W was found below the detection limit in the remaining 2 sites (6.25%). In the case of V, 28 sites (87.5%) showed moderate contamination with the remaining 4 sites (12.5%) showing low (C_f<1) contamination. For Co, 20 sites (62.5%) showed moderate contamination while the remaining 12 sites (37.5%) showed low contamination. For Sb, 4 sites (12.5%) showed moderate contamination, 2 sites (6.25%) showed low contamination, but was found below the detection limit in the remaining 26 sites which represented 81.25% of the total study area. For Mn, 18 sites (56.25%) showed moderate contamination while the C_f of the remaining 14 sites (43.75%) were found to be less than 1 indicating low contamination. For Fe, the C_f of 30 sites (93.75%) were found below 1 with only 2 sites (6.25%) showing moderate contamination. In the case of Ni, in 26 sites (81.25%) the contamination was found to be low with 1 site showing moderate contamination while Ni content was recorded below the detection limit in the remaining 5 sites. For As, 22 sites (68.75%) showed low contamination and 10 other sites showed below the detection limit.

During the POM season, the mean C_f values for the analysed elements were found to be in decreasing order as W> Sb> Cr> Cu> Sn> Al> V> Sr> Co> Mn> Ni> Zn> Pb> Fe> As> Ag. From the mean C_f, the study area was determined to be considerably contaminated by W and moderately contaminated by Sb, Cr, Cu, Sn, Al, V, Sr, Co, Mn, Ni and Zn. While considering site wise, W contamination was found to be considerable in 10 sites (31.25%) and moderate in the rest of 22 sites (68.75%). Sb showed moderate contamination in all 32 sites. In the case of Cr, Al, V, Sr and Co, out of 32 sites, 31 sites (96.88%) showed moderate contamination with the exception of one site, which showed low contamination. For Mn, 18 sites (56.25%) showed moderate contamination while the remaining 14 sites (43.75%) showed low contamination. For Ni, 17 sites (53.13%) showed moderate contamination and for the remaining 15 sites (46.88%) the Mn contamination was low. In the case of Zn, 20 sites (62.5%) showed

moderate contamination while the remaining 12 sites (37.5%) showed low contamination. Cu contamination was recorded as moderate at 28 sites (87.5%), while three sites (9.38%) showed low contamination with 1 site being considerably contaminated. In the case of Sn, out of 32 sites 27 sites (84.38%) were moderately contaminated by Sn with five sites (15.63%) demonstrated low contamination. 22 sites (68.75%) exhibited low contamination for Pb with the rest of the 10 sites (31.25%) indicating moderate contamination. For Fe, the C_f of 23 sites (71.88 %) was found to be low while the remaining 9 sites (28.13%) showed moderate contamination. In case of As, the contamination was found to be low at 29 sites (90.63%) with 1 site moderately contaminated. However, in two sites As concentration was recorded below the detection limit. The C_f values of Ag appeared low (C_f<1) at 17 sites (53.13%) and moderate in 4 sites (12.50%). In the remaining 11 sites (34.38%) Ag concentration was recorded below the detection limit.

Table 8.4 Descriptive statistics of contamination factor of analyzed elements in the surface sediments during POM season

Elements	Number of samples (N)	Minimum	Maximum	Mean	Std. Deviation
Fe	32	0.35	1.27	0.98	0.16
Mn	32	0.25	1.65	1.06	0.27
Al	32	0.36	1.25	1.01	0.17
Cu	32	1.54	9.73	2.88	1.53
Zn	32	0.90	1.96	1.18	0.19
Pb	32	0.44	1.44	0.99	0.16
Cr	32	0.45	1.01	0.89	0.10
Co	32	0.39	1.26	1.04	0.15
Ni	32	0.61	1.22	1.07	0.17
V	32	0.36	1.26	1.01	0.17
Sr	32	0.56	1.15	0.93	0.11
As	30	0.70	1.40	1.03	0.17
Ag	21	0.39	1.00	0.49	0.16
Sn	32	0.37	1.49	1.10	0.24
Sb	32	0.62	1.30	0.85	0.14
W	32	0.88	1.77	1.06	0.30

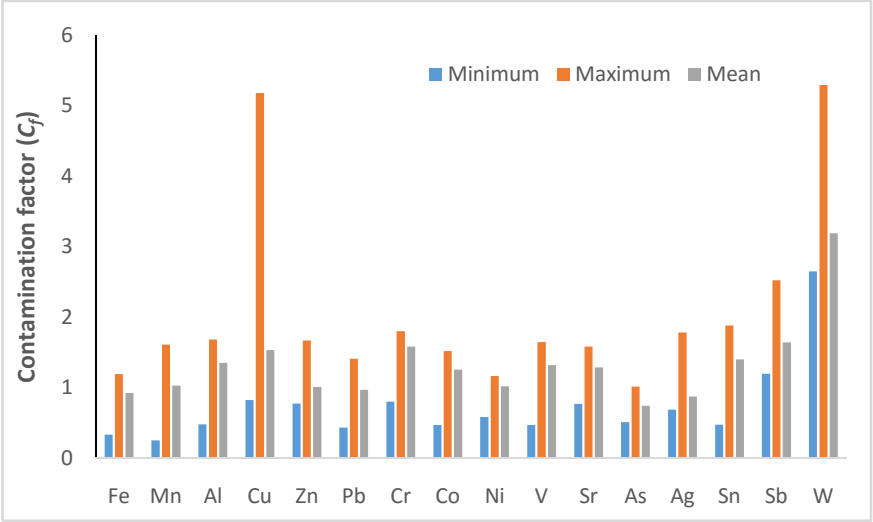

Figure 8.3 Contamination factor of analysed elements in the surface sediments during POM season

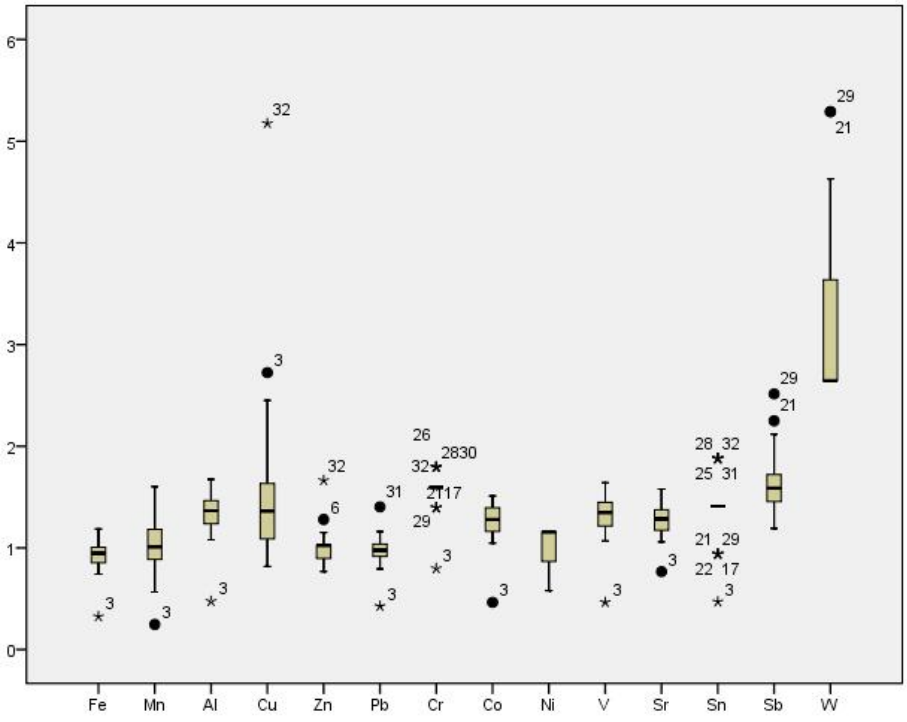

Figure 8.4 Box plot of contamination factor for the elements during post- monsoon season

The C_f values were also calculated by using the average elemental concentration of the upstream fine sediments (<63m) as the background value, and it was found that the mean C_f value of the analysed elements were in the order of

Cu>Zn>Sn>Ni>W>Mn>Co>As>V>Al>Pb>Fe>Sr>Cr>Sb>Ag. Based on the mean C_f values, the study area was moderately contaminated by Cu, Zn, Sn, Ni, W, Mn, Co, As, V and Al. While considering site wise, Cu contamination was found to be moderate at 20 sites (62.5%), while 11 sites (34.38%) showed considerable contamination with one site being very highly contaminated. In the case of Zn, 30 sites (93.75%) showed moderate contamination while the remaining two sites showing low contamination. For Sn, out of 32 sites 27 sites (84.38%) were moderately contaminated with five sites (15.63%) showing low contamination. For Ni, 17 sites (53.13%) showed moderate contamination and the remaining 15 sites (46.88%) showed low contamination. In the case of W, the contamination was moderate in 10 sites (31.25%) and low in the rest of the 22 sites (68.75%). For Mn, 11 sites (34.38%) showed moderate contamination while the remaining 21 sites (65.63%) showed low contamination. For Co, 22 sites (68.75%) showed moderate contamination with the remaining 10 sites (31.25%) showing low contamination. In the case of As, 14 sites (43.75%) showed moderate contamination with 16 sites (50%) showing low contamination and it was found below the detection limit in 2 sites. For V, the contamination was found to be moderate at 28 sites (87.5%) and low in 4 sites (12.5%). For Al, Fe and Pb, 17 sites (53.13%) were moderately contaminated while in the remaining 15 sites (46.88%), the contamination remained low. For Sr, the C_f of 10 sites (31.25 %) was found to be moderate while the remaining 22 sites (68.75%) displayed low contamination. For Cr and Sb, the contamination was found to be low at 28 sites (87.5%) and moderate in four sites (12.5%). The C_f of Ag was low (C_f<1) at 20 sites (53.13%) and moderate in one site. In the remaining 11 sites (34.38%), Ag was below the detection limit.

Table 8.5 Descriptive statistics of contamination factor of analyzed elements in the surface sediments during POM season (Fine sediments <63µm background)

Elements	Number of samples (N)	Minimum	Maximum	Mean	Std. Deviation
Fe	32	0.35	1.27	0.98	0.16
Mn	32	0.25	1.65	1.06	0.27
Al	32	0.36	1.25	1.01	0.17
Cu	32	1.54	9.73	2.88	1.53
Zn	32	0.90	1.96	1.18	0.19
Pb	32	0.44	1.44	0.99	0.16
Cr	32	0.45	1.01	0.89	0.10
Co	32	0.39	1.26	1.04	0.15
Ni	32	0.61	1.22	1.07	0.17
V	32	0.36	1.26	1.01	0.17
Sr	32	0.56	1.15	0.93	0.11
As	30	0.70	1.40	1.03	0.17
Ag	21	0.39	1.00	0.49	0.16
Sn	32	0.37	1.49	1.10	0.24
Sb	32	0.62	1.30	0.85	0.14
W	32	0.88	1.77	1.06	0.30

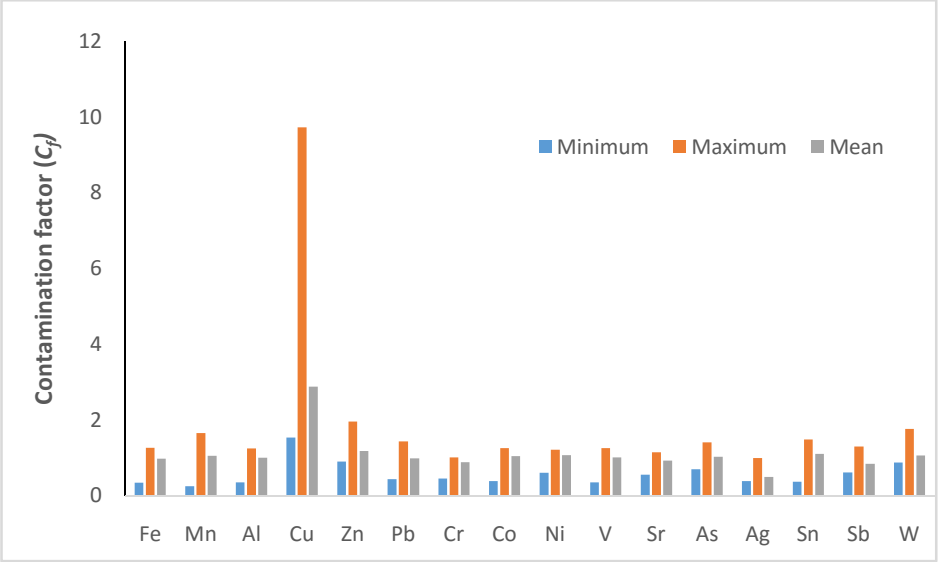

Figure 8.5 Contamination factor of analysed elements in the surface sediments during POM season (Fine sediments <63µm background)

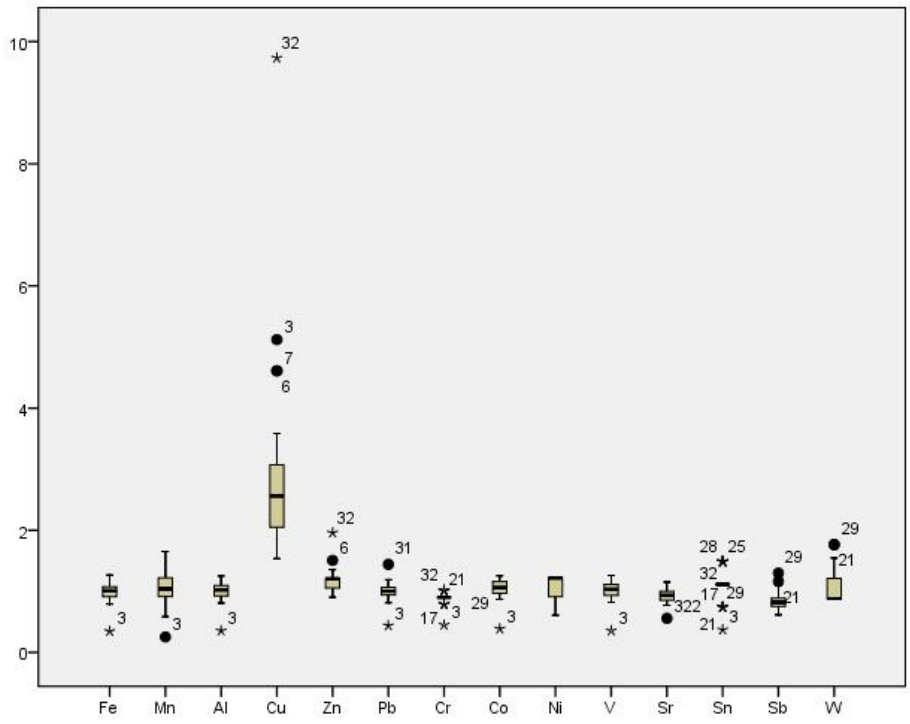

Figure 8.6 Box plot of contamination factor for the elements during post- monsoon season (Fine sediments <63µm background)

8.1.2 Geo-accumulation Index (I_{geo})

The geo-accumulation Index was originally proposed by Muller (1969), which allows for the identification and classification of the pollution status of sediments at seven levels from uncontaminated to extremely contaminated (Table 8.6). The geo-accumulation index is calculated by using the following equation

$$I_{geo} = \log2 (C_n/1.5\ B_n)$$

Where, C_n is the measured concentration of trace elements in the sediments of a sampling site, B_n is the geochemical background value of the element and 1.5 is the background matrix correction factor due to lithogenic effects (Loska et al., 1997; Ghrefat & Yusuf, 2006; Gonzáles-Macías et al., 2006; Chen et al., 2007).

Table 8.6 Ranges of Geo-accumulation Index (I_{geo}) class

Class	Igeo	Pollution Status
1	<0	Uncontaminated
2	0-1	Uncontaminated to moderately contaminated
3	1-2	Moderately contaminated
4	2-3	Moderately contaminated to strongly contaminated
5	3-4	Strongly contaminated
6	4-5	Strongly to extremely contaminated
7	5-6	Extremely contaminated

The geo-accumulation index was calculated for some selected elements specifically, Fe, Mn, Al, Cu, Zn, Pb, Cr, Co, Ni, V, Sr, As, Ag, Sn, Sb and W in the sediments for both seasons. The range and mean of the calculated I_{geo} of each element for the MON and POM season are tabulated in Table 8.7 and Table 8.8 and in Table 8.9 (for the POM fine sediments <63µm as background) and represented in Figure 8.7, Figure 8.9 and in Figure 8.11(for the POM fine sediments <63µm as background), respectively. Additionally, the site wise illustrations of I_{geo} is presented as boxplots in Figure 8.8, Figure 8.10 and in Figure 8.12 (for the POM fine sediments <63µm background), respectively.

During the MON season, the calculated mean I_{geo} of the analysed elements decreased in the following order as Cu> Zn> Sn> Ag> Al> Sr> V> W> Cr> Sb> Co> Mn> Fe> Ni> As> Pb. Considering the mean I_{geo} values, the Lower Baram River sediments were moderately contaminated by Cu, and uncontaminated to moderately contaminated by Zn and Sn. The site wise variation revealed for Cu, 12 sites (37.5%) fell under I_{geo} class 2 indicating uncontaminated to moderately contaminated, 7 sites (21.88%) fell under I_{geo} class 3 indicating moderate contamination, 9 sites (28.13%) fell under I_{geo} class 4 indicating moderate contamination to strong contamination, while 3 sites (9.38%) fell under I_{geo} class 5 indicating strong contamination at these sites. Only one site remained uncontaminated (I_{geo} <1) by Cu.

In the case of Zn, 12 (37.5%) sites fell under the uncontaminated to moderately contaminated class while 19 sites (59.38%) fell under the uncontaminated class (class1) with only 1 site falling under I_{geo} class 3 indicating moderate contamination . For Sn, 17 sites (53.13%) remained uncontaminated with 11 sites (34.38%) falling under I_{geo} class 2

indicating uncontaminated to moderately contaminated, whereas 4 sites (12.5%) were moderately contaminated. For Pb, 27 sites (84.38%) remained uncontaminated while 5 sites (12.5%) were in the uncontaminated to moderately contaminated category and with one site possessing I_{geo} class 3 indicating moderate contamination at this site. For Mn, 29 sites (90.63%) remained uncontaminated while only 3 sites (9.38%) fell under I_{geo} class 2 indicating an uncontaminated to moderately contaminated situation. For Al, 27 sites (84.38%) were found to be uncontaminated with five sites (15.63%) showing uncontaminated to moderately contaminated levels. In the case of Cr and Co, 31 sites (96.88%) remained uncontaminated with only one site falling under the uncontaminated to moderately contaminated category. The I_{geo} of all the other elements for all the sites fell under I_{geo} class 1 (I_{geo}<0) indicating no contamination by these elements in the study area.

Table 8.7 Descriptive statistics of geo-accumulation index (I_{geo}) of analyzed elements in the surface sediments during MON season

Elements	Number of sample (N)	Minimum	Maximum	Mean	Std. Deviation
Fe	32	-1.96	-0.48	-0.87	0.31
Mn	32	-2.45	0.79	-0.68	0.66
Al	32	-1.28	0.07	-0.22	0.29
Cu	32	-0.36	3.41	1.48	1.11
Zn	32	-0.84	1.22	0.08	0.58
Pb	32	-2.34	1.15	-1.30	0.93
Cr	32	-0.84	0.01	-0.48	0.20
Co	32	-1.47	0.38	-0.53	0.33
Ni	27	-1.37	-0.37	-0.92	0.28
V	32	-1.28	0.00	-0.31	0.28
Sr	32	-0.97	-0.05	-0.27	0.21
As	22	-1.63	-0.63	-1.27	0.28
Ag	30	-0.79	1.94	-0.09	0.64
Sn	32	-0.66	1.67	0.06	0.75
Sb	6	-0.72	-0.36	-0.51	0.18
W	30	-1.22	1.10	-0.34	0.53

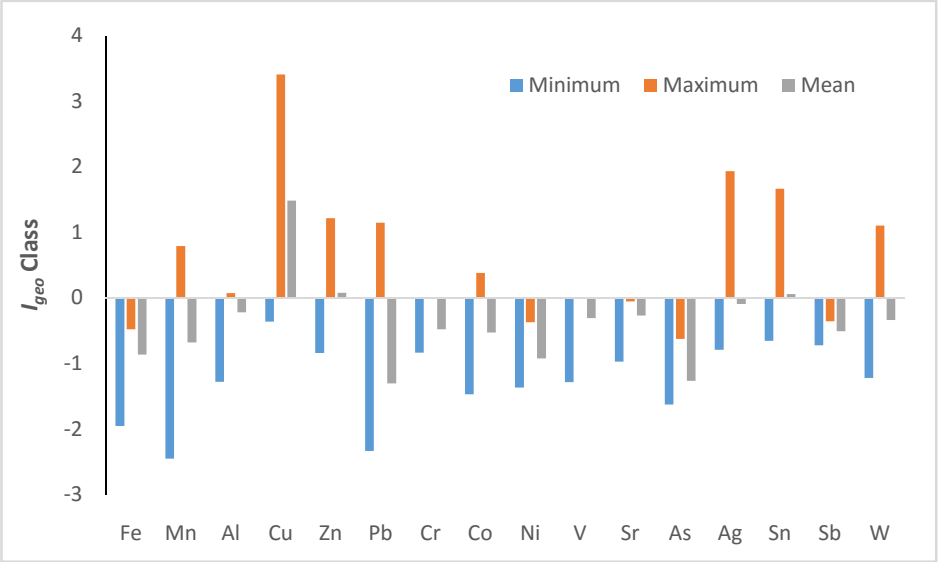

Figure 8.7 Geo-accumulation index of analysed elements in the surface season during MON season

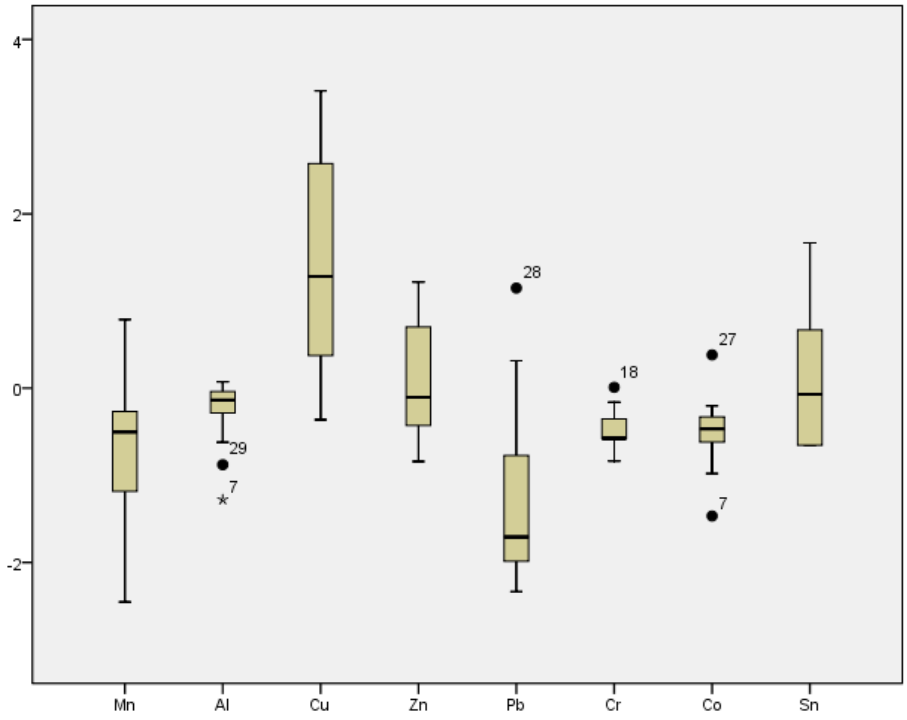

Figure 8.8 Box plot geo-accumulation index for the elements during MON season

During the POM season, the calculated mean of I_{geo} of the elements can be arranged in decreasing order as W> Sb> Cr> Cu> Sn> Al> V> Sr> Co> Ni> Zn> Mn> Pb> Fe> Ag> As. From the mean I_{geo} values, the sediments during this season were found to be moderately contaminated by W, and uncontaminated to moderately contaminated by Sb and Cr. However, while considering the site wise variation, for W, 22 sites (68.75%) fell under I_{geo} class 2 (uncontaminated to moderately contaminated) while the remaining 10 sites (31.25%) fell under I_{geo} class 3 (moderately contaminated). For Sb, 10 sites (31.25%) remained uncontaminated while the remaining 22 sites (68.75%) came under class 2, indicating an uncontaminated to moderately contaminated situation. For Cr, 28 sites (87.5%) showed an uncontaminated to moderately contaminated condition while the remaining sites (12.5%) were uncontaminated. In the case of Cu, 20 sites (62.5%) remained uncontaminated while 11 sites (34.38%) showed an uncontaminated to moderately contaminated condition with one site showing moderate contamination. For Sn, Al and V, 27 sites (84.38%) remained uncontaminated while the remaining five sites (15.63%) showed an uncontaminated to moderately contaminated situation. For the case of Sr and Co, 30 sites (93.75%) stayed uncontaminated while the remaining 2 sites (6.25%) fell under I_{geo} class 2 indicating an uncontaminated to moderately contaminated condition. For Zn and Mn, 31 sites (96.88%) remained uncontaminated with only one site showing an uncontaminated to moderately contaminated condition. The I_{geo} of all the other elements (Fe, Pb, Ni, As and Ag) for all the sites fell under I_{geo} class 1 (I_{geo}<0) indicating no contamination by these elements in the study area.

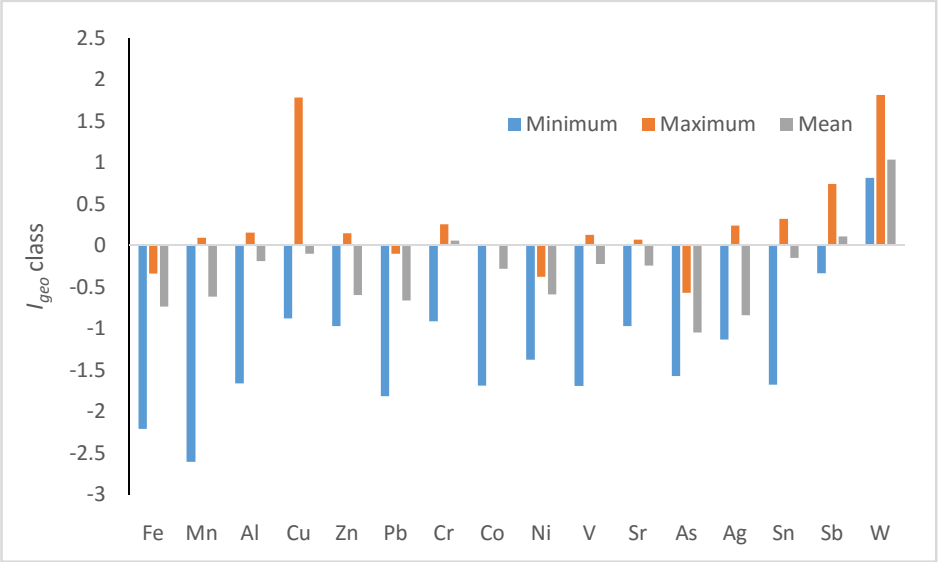

Figure 8.9 Geo-accumulation index of analysed elements in the surface sediments during POM season

Table 8.8 Descriptive statistics of geo-accumulation index (I_{geo}) of analyzed elements in the surface sediments during POM season

Elements	Number of samples (N)	Minimum	Maximum	Mean	Std. Deviation
Fe	32	-2.21	-0.34	-0.73	0.31
Mn	32	-2.61	0.10	-0.62	0.48
Al	32	-1.66	0.16	-0.19	0.32
Cu	32	-0.88	1.79	-0.10	0.56
Zn	32	-0.97	0.15	-0.60	0.21
Pb	32	-1.81	-0.10	-0.66	0.27
Cr	32	-0.91	0.26	0.06	0.20
Co	32	-1.69	0.01	-0.28	0.29
Ni	32	-1.38	-0.38	-0.59	0.25
V	32	-1.69	0.13	-0.22	0.31
Sr	32	-0.97	0.07	-0.24	0.19
As	30	-1.57	-0.57	-1.05	0.26
Ag	21	-1.13	0.24	-0.84	0.39
Sn	32	-1.67	0.33	-0.15	0.39
Sb	32	-0.33	0.75	0.11	0.21
W	32	0.82	1.82	1.04	0.36

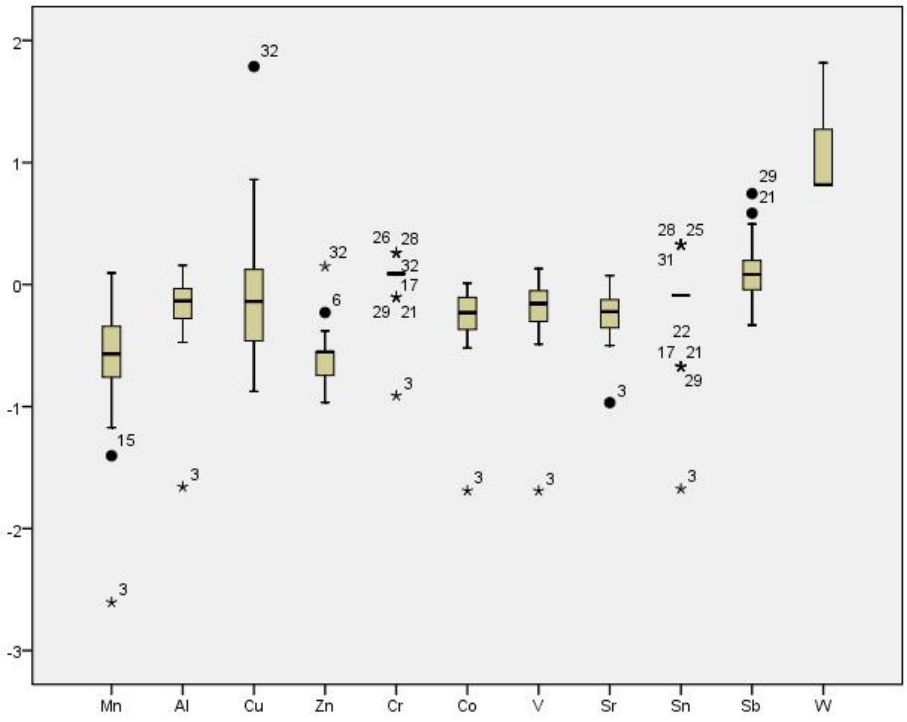

Figure 8.10 Box plot geo-accumulation index for the elements during POM season

When the geo-accumulation index was calculated for some of the selected elements specifically, Fe, Mn, Al, Cu, Zn, Pb, Cr, Co, Ni, V, Sr, As, Ag, Sn, Sb and W for the POM by using the average elemental concentration observed in the upstream fine sediments (<63µm) as the background value, the calculated mean I_{geo} of the analysed elements decreased in the following order as Cu>Zn>Sn>Ni>W>Co>Mn>As>V>Al>Pb>Fe>Sr>Cr>Sb>Ag. Considering the mean I_{geo}, the Lower Baram River sediments were found to be uncontaminated to moderately contaminated by Cu and remained uncontaminated by all the other elements. However, while considering the site wise variation, for Cu, 20 sites (62.5%) fell under 0-1 I_{geo} class indicating an uncontaminated to moderately contaminated situation, 11 sites (34.38%) fell under 1-2 I_{geo} class indicating moderate contamination with only one site falling under 2-3 I_{geo} class indicating moderate contamination to strong contamination. For Zn, 30 sites (93.75%) remained uncontaminated with only two sites (6.25%) showing an uncontaminated to moderately contaminated condition. For Mn, 31 sites (96.88%) were uncontaminated with only one site showing an uncontaminated to moderately contaminated situation. In the case of W, 26 sites (81.25%) remained unaffected with six sites (18.75%) showing an uncontaminated to moderately contaminated situation. The sites remained uncontaminated by all the other elements (I_{geo}< 1).

Table 8.9 Descriptive statistics of geo-accumulation index (I_{geo}) of analyzed elements in the surface sediments during POM season (Fine sediments <63m background)

Elements	Number of samples (N)	Minimum	Maximum	Mean	Std. Deviation
Fe	32	-2.11	-0.24	-0.64	0.31
Mn	32	-2.56	0.14	-0.57	0.48
Al	32	-2.08	-0.26	-0.60	0.32
Cu	32	0.04	2.70	0.82	0.56
Zn	32	-0.73	0.39	-0.36	0.21
Pb	32	-1.77	-0.06	-0.62	0.27
Cr	32	-1.74	-0.57	-0.76	0.20
Co	32	-1.96	-0.26	-0.55	0.29
Ni	32	-1.30	-0.30	-0.51	0.25
V	32	-2.07	-0.25	-0.60	0.31
Sr	32	-1.42	-0.38	-0.70	0.19
As	30	-1.10	-0.10	-0.57	0.26
Ag	21	-1.96	-0.59	-1.67	0.39
Sn	32	-2.01	-0.01	-0.48	0.39
Sb	32	-1.28	-0.21	-0.84	0.21
W	32	-0.77	0.24	-0.55	0.36

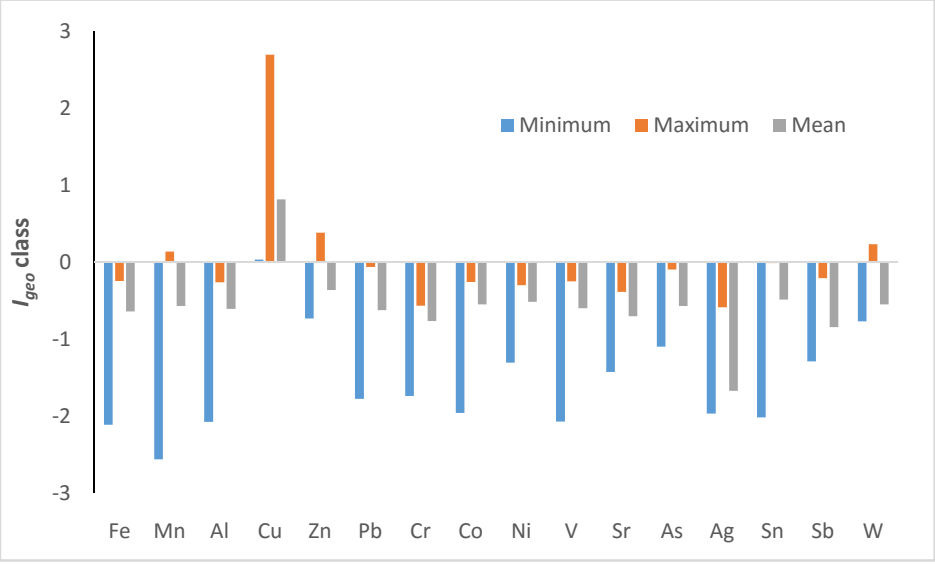

Figure 8.11 Geo-accumulation index of analysed elements in the surface sediments during POM season (Fine sediments < 63µm background)

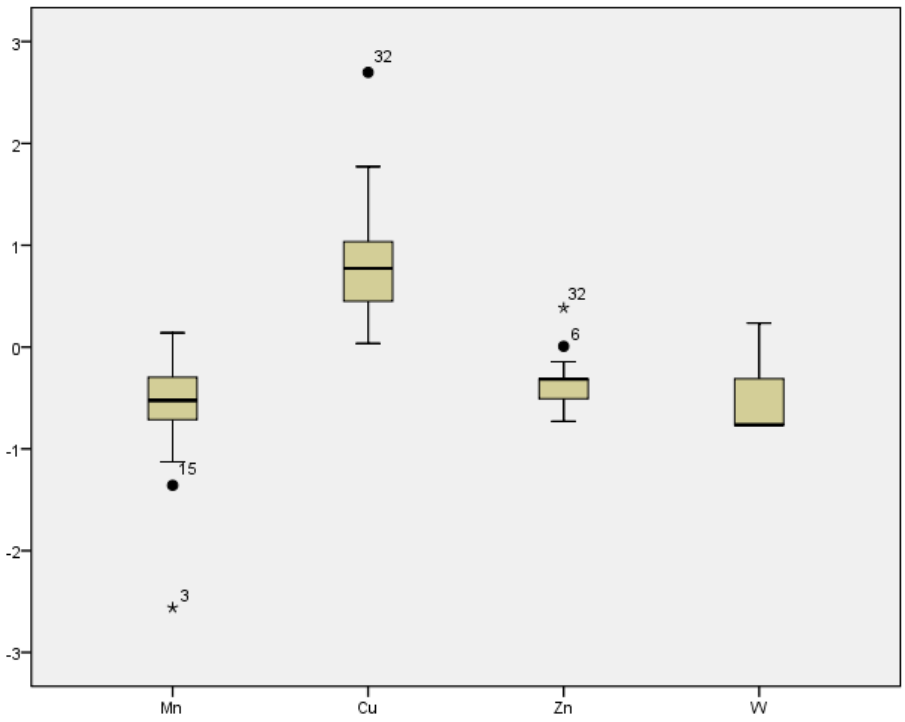

Figure 8.12 Box plot geo-accumulation index for the elements during POM season (Fine sediments <63µm background)

8.1.3 Pollution load Index (PLI)

The Pollution Load Index (PLI) was proposed by Tomlinson et al. (1980), which integrates all the studied elements in one index. This index is calculated through the Contamination Factor (*Cf*) of each studied element. For the entire sampling site, PLI has been determined as the n_{th} root of the product of the n *Cf* by using the following equation

$$PLI = (Cf_1 \times Cf_2 \times Cf_3 \times \cdots \times Cf_n)^{1/n}$$

Where *Cf* is the contamination factor and n is the number of metals. This empirical index provides a simple, comparative means for assessing the level of trace/heavy metal pollution. When PLI > 1, it means pollution exists; otherwise, if PLI < 1, there is no pollution (Varol et al., 2011).

The pollution load index (PLI), was calculated for some elements specifically, Fe, Mn, Cu, Zn, Pb, Cr, Co, Ni, V, Sr, As, Ag, Sn, Sb and W for both seasons. The site wise variation in the PLI during the MON and POM seasons are represented in Figure

8.13 and Figure, respectively and in Figure 8.15 (for the POM using an average of fine sediments <63µm from upstream as background). Site wise variations are illustrated as box plots in Figure 8.16.

During the MON season, 29 sites representing 90.63% of the total study area showed PLI>1, indicating the collective enrichment of the considered elements in the study area at these sites. The remaining three sites exhibited PLI values below one (PLI<1), indicating these sites were unaffected by the elemental concentrations. During the POM season, 31 sites representing 96.88% of the total study area showed a PLI>1, indicating these sites were affected by the enrichment of the considered elements. However, when the PLI was calculated by using the average elemental concentration observed in the upstream fine sediments (<63µm) as the background value during the POM season, 28 sites representing 87.50% of the total study area showed a PLI>1, indicating these sites were affected by the enrichment of the considered elements. However, 6 sites (18.75%) remained unaffected. Moreover, the recorded PLI values > 1 were mainly influenced by Cu followed by Zn and were in agreement with *Cf* and I_{geo} values.

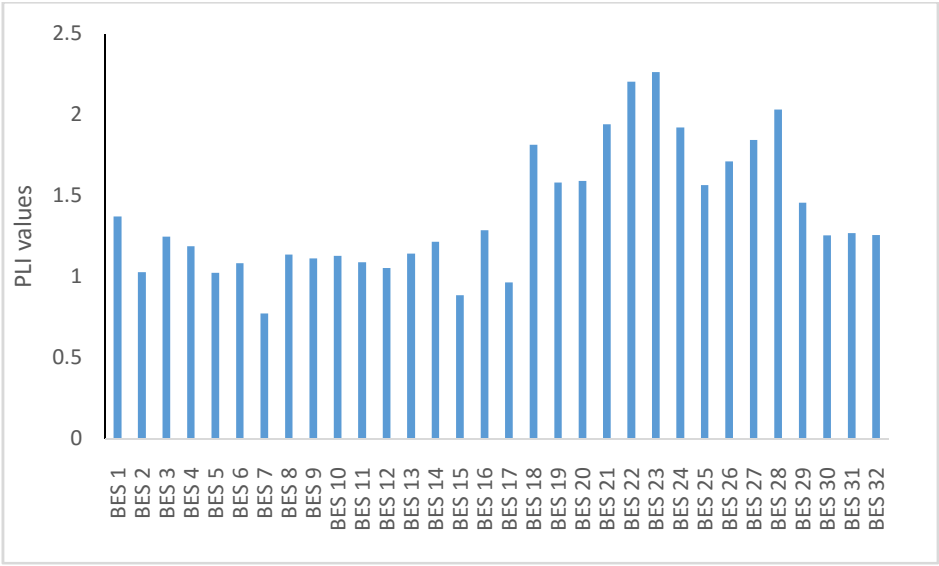

Figure 8.13Pollution load index (PLI) of Surface sediments of analysed elements during MON season

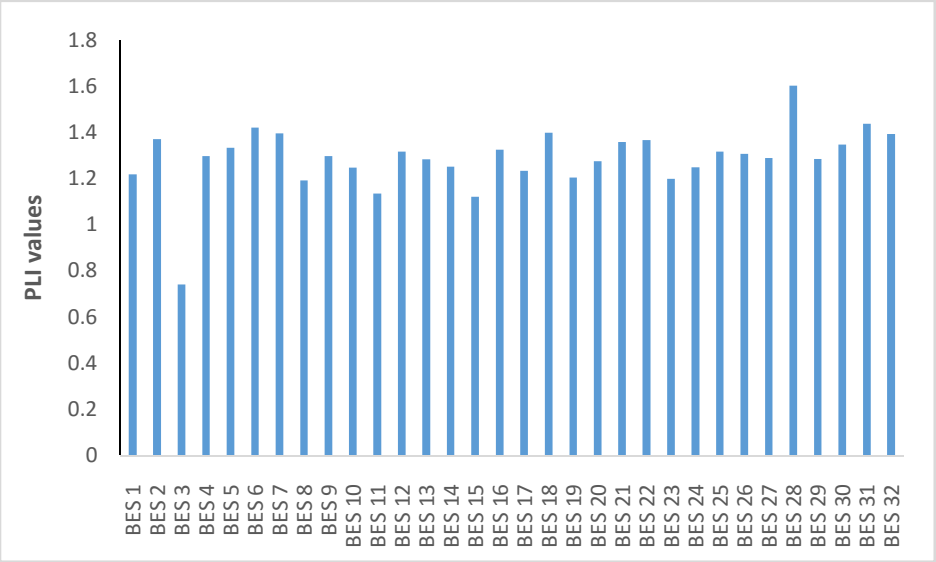

Figure 8.14 Pollution load Index (PLI) of analysed samples in the surface sediments during POM season

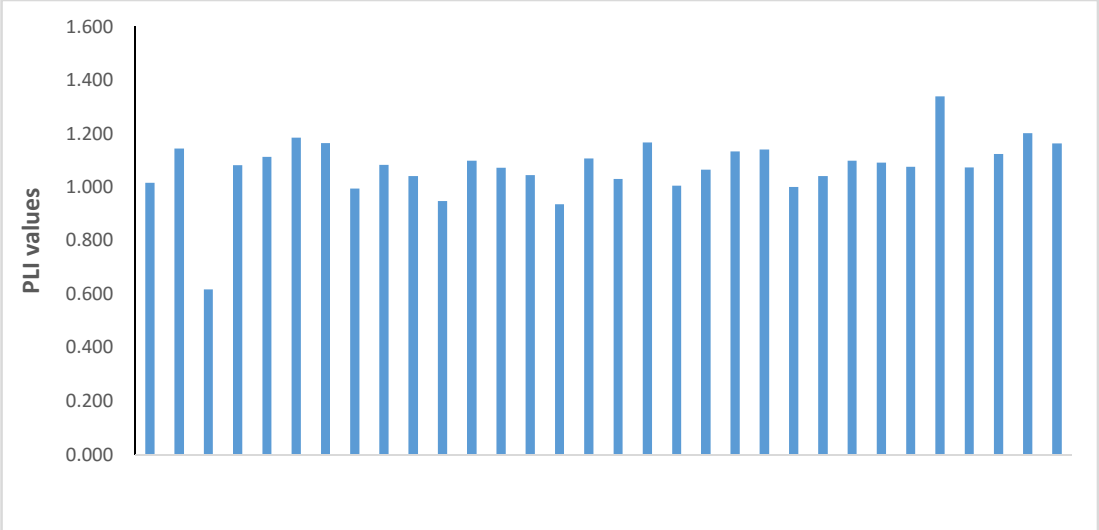

Figure 8.15 Pollution load Index (PLI) of analysed samples in the surface sediments based on average fine sediments (<63µm) as background value during POM season

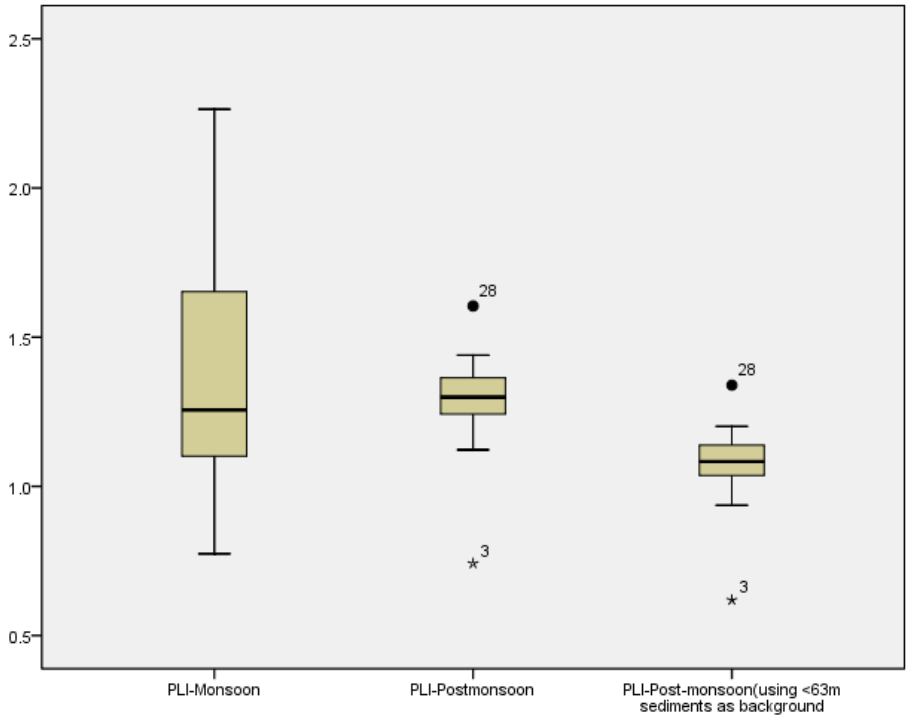

Figure 8.16 Box plot of Pollution load index for surface sediments

8.1.4 Effect-Range Low (ERL) and Effect – Range Median (ERM)

The Effect Range Low (ERL) and Effect Range Median (ERM) is a sediment quality guideline developed by Long et al. (1995), in order to understand and elucidate the effects of observed trace element levels on living organisms. The ERL and ERM of the selected trace elements of the present study are tabulated in Table 8.10 andTable 8.11 and represented in Figure 8.17 and Figure 8.18, respectively.

According to Long et al. (1995), the element concentrations, less than ERL (<ERL) are considered to have little or no adverse biological effects. If the element concentrations are equal to or above ERL and below ERM (ERL-ERM) this represents possible biological effects and is in a range within which effects would occasionally occur. However, if the element concentrations exceeds the ERM (>ERM), values represent the probable effects and is in a range within which the effects would frequently occur.

During the MON season, Cu showed the highest possible effect (81% ERL-ERM) indicating occasional adverse biological effects to living organisms followed by

Ni (62.5% ERL-ERM), Zn (37.5% ERL-ERM), Ag (25% ERL-ERM), Pb (18.75% ERL-ERM), As and Cr (3.125% ERL-ERM). Of the analysed elements, only the concentrations of Cu exceeds ERM (15.625% >ERM) representing a probable effect, which may pose frequent threats to the sediment dwelling living organisms.

Table 8.10 Guideline values and biological effects of trace elements in the surface sediments during monsoon season

Elements	Guidelines (µg g^{-1})		Percent (ratios) incidence of effects		
	ERL	ERM	<ERL	ERL-ERM	>ERM
As	8.2	70	(31/32)96.88	(1/32) 3.13	0
Cr	81	370	(31/32) 96.88	(1/32) 3.16	0
Cu	34	270	(1/32) 3.13	(26/32) 81.25	(5/32) 15.625
Pb	46.7	218	(26/32) 81.25	(6/32) 18.75	0
Ni	20.9	51.6	(12/32) 37.50	(20/32) 62.50	0
Ag	1	3.7	(24/32) 75.00	(8/32) 25.00	0
Zn	150	410	(20/32) 62.50	(12/32) 37.50	0

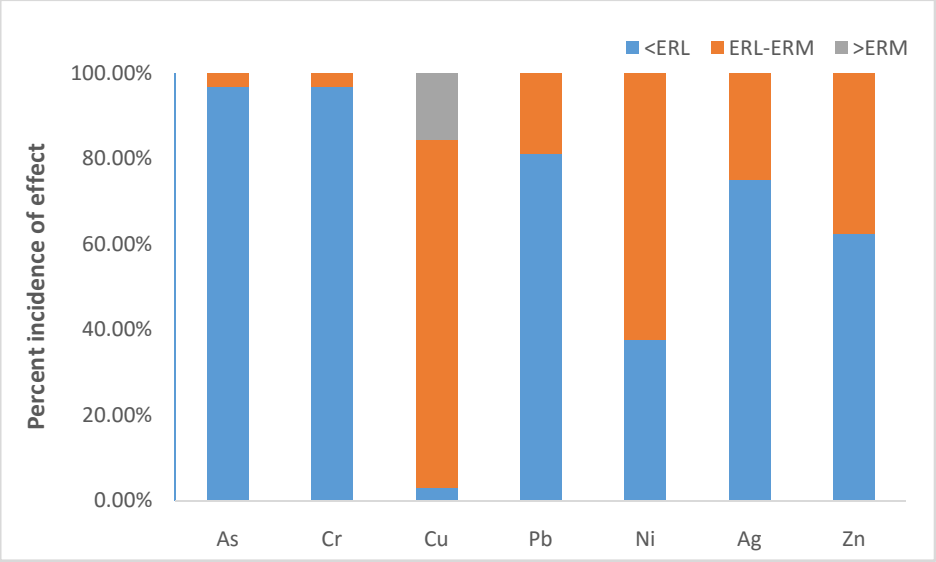

Figure 8.17 Biological effects of trace elements in the surface sediments during MON season

During the POM season, Ni showed the highest possible effect (96.875% ERL-ERM) indicating occasional adverse biological effects to living organisms followed by Cu (90.625% ERL-ERM), As and Cr (12.5% ERL-ERM) and Ag (25% ERL-ERM). Pb

and Zn fell under the safe category (<ERL). None of the elements posed a probable (>ERM) effect to the living organisms during the POM season.

Table 8.11 Guideline values and biological effects of trace elements in the surface sediments during POM season

Elements	Guidelines (µg g^{-1})		Percent (ratios) incidence of effects		
	ERL	ERM	<ERL	ERL-ERM	>ERM
As	8.2	70	(28/32) 87.5	(4/32) 12.5	0
Cr	81	370	(28/32) 87.5	(4/32) 12.5	0
Cu	34	270	(3/32) 9.375	(29/32) 90.625	0
Pb	46.7	218	(32/32) 100	0	0
Ni	20.9	51.6	(1/32) 3.125	(31/32) 96.875	0
Ag	1	3.7	(30/32) 93.75	(2/32) 6.25	0
Zn	150	410	(32/32) 100	0	0

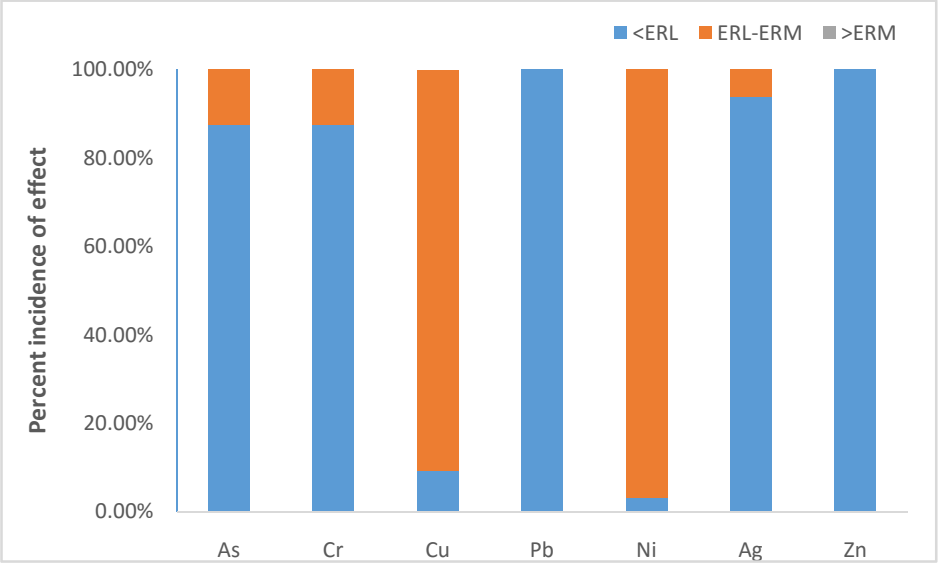

Figure 8.18 Biological effects of trace elements in the surface sediments during POM season

8.2 Risk Assessment code (RAC)

The elements in the sediments are bound to different fractions with different strengths that can be delineated by the sequential extraction procedure. The risk assessment code is defined as the elements associated with carbonates and exchangeable fractions in the sequential extraction process (% of F1 and F2 fractions). Through the

RAC, it is possible to assess the availability of metals in sediments by applying a scale to the percentage of metals in the exchangeable and carbonate fractions (Table-8.10). Assessment of the RAC is important because the fractions introduced by anthropogenic activities are characterized by the exchangeable and bound to carbonate fractions, which are weakly bonded elements that could equilibrate with the aqueous phase and thus become more rapidly bioavailable (Sundaray et al., 2011). In the present study, the RAC was determined by the classification defined by Perin et al. (1985), which is tabulated below in Table 8.12.

The site wise estimation of the RAC for the MON and POM seasons are tabulated in Table 8.13 and Table 8.14, respectively. Mn exhibited high risk during both seasons followed by Cu and Zn. The riverine sites (BES-17 to BES-32) possessed a higher risk code when compared to the estuarine sites (BES-01 to BES-16**)** during both seasons.

Table 8.12 Risk assessment code (RAC) classification described by Perin et al. (1985)

Category	**Risk**	**Percentage of elements in carbonate and exchangeable fractions**
1	No risk	<1
2	Low risk	1-10
3	Medium risk	11-30
4	High risk	30-50
5	Very high risk	>50

Table 8.13 Site-wise risk assessment code (RAC) during MON season

Site	Cd	Co	Cu	Fe	Mn	Pb	Zn
BES 1	N	L	H	V	V	L	H
BES 2	N	L	H	V	V	L	H
BES 3	N	L	M	V	V	N	M
BES 4	N	L	M	V	V	L	M
BES 5	N	L	H	V	V	L	H
BES 6	N	L	M	V	V	L	M
BES 7	N	L	M	V	M	L	M
BES 8	N	L	L	V	V	L	M
BES 9	N	L	L	V	V	N	M
BES 10	N	L	M	V	V	N	M
BES 11	N	L	L	V	V	N	L
BES 12	N	L	L	V	V	N	L
BES 13	N	L	M	V	V	N	M
BES 14	N	L	L	V	V	N	M
BES 15	N	L	M	V	V	N	M
BES 16	N	L	M	V	V	N	M
BES 17	N	L	M	V	V	N	M
BES 18	N	L	V	V	V	N	H
BES 19	N	L	V	V	V	N	V
BES 20	N	L	V	V	V	N	V
BES 21	N	L	V	V	V	M	V
BES 22	N	L	V	V	V	M	V
BES 23	N	L	V	V	V	M	V
BES 24	N	L	V	V	V	M	V
BES 25	N	L	V	V	V	L	H
BES 26	N	L	V	V	V	L	V
BES 27	N	L	H	V	V	L	H
BES 28	N	L	V	V	V	H	M
BES 29	N	L	V	V	V	M	V
BES 30	N	L	M	V	V	L	M
BES 31	N	L	M	V	V	L	M
BES 32	N	L	M	V	V	N	M

NR-No Risk; LR-Low Risk; MR- Medium Risk; HR-High Risk; VHR-Very High Risk

Table 8.14 Site-wise risk assessment code (RAC) during POM season

Site	Cd	Co	Cu	Fe	Mn	Pb	Zn
BES 1	N	L	L	V	V	L	L
BES 2	N	L	L	V	V	L	M
BES 3	N	L	M	V	L	L	H
BES 4	N	L	M	V	V	L	M
BES 5	N	L	L	V	V	L	L
BES 6	N	L	M	V	V	L	M
BES 7	N	L	M	V	V	L	M
BES 8	N	L	L	V	V	L	M
BES 9	N	L	L	V	V	N	M
BES 10	N	L	L	V	V	N	L
BES 11	N	L	L	V	V	N	L
BES 12	N	L	L	V	V	N	L
BES 13	N	L	L	V	V	L	L
BES 14	N	L	L	V	V	L	L
BES 15	N	L	L	V	V	L	L
BES 16	N	L	M	V	V	L	M
BES 17	N	L	L	V	V	N	M
BES 18	N	L	L	V	V	L	M
BES 19	N	L	L	V	V	L	M
BES 20	N	L	M	V	V	L	M
BES 21	N	L	L	V	V	L	M
BES 22	N	L	L	V	V	L	M
BES 23	N	L	M	V	V	L	M
BES 24	N	L	L	V	V	L	M
BES 25	N	L	L	V	V	L	M
BES 26	N	L	M	V	V	L	M
BES 27	N	L	L	V	V	L	M
BES 28	N	L	M	H	V	N	M
BES 29	N	L	M	V	V	L	M
BES 30	N	L	L	V	V	L	M
BES 31	N	L	L	V	V	L	M
BES 32	N	L	V	V	V	L	V

NR-No Risk; LR-Low Risk; MR- Medium Risk; HR-High Risk; VHR-Very High Risk

8.3 Core Sediments

In the present study, four short cores (around 50cm) and one long core (around 1.5m) were analysed for some trace elements and the analysed trace elements were subjected to a risk assessment calculation using risk indices such as contamination factor (C_f), geo-accumulation index (I_{geo}) and pollution load index (PLI) and the results are presented in this section.

8.3.1 Short Cores

About 10 short cores were collected for the present study, out of which 4 sediment cores were selected for the geochemical analysis. They were BSC 01, BSC 06, BSC 07 and BSC 09. The descriptive statistics of the considered elements for risk assessment from these four short cores are given in Table 8.15. The average elemental concentrations of the upstream fine fraction sediments (<63µm), was used as the background value for the calculation of risk indices in the core sediments. Table 8.16 could be referred for the entire short core section hereafter, in order to understand the respective depth of each outlier samples in box plots.

Table 8.15 Descriptive statistics of the considered elements for risk assessment in the short core sediments of the Lower Baram River

	BSC 01					BSC 06				
Elements	**N**	**Minimum**	**Maximum**	**Mean**	**Std. Deviation**	**N**	**Minimum**	**Maximum**	**Mean**	**Std. Deviation**
Al	9	9261.88	37259.20	14348.56	8837.38	9	60863.75	69384.68	65627.00	2870.91
Fe	9	3916.81	16016.95	5945.16	3881.05	9	26018.80	32103.84	29205.09	1866.68
Mn	9	38.72	162.64	69.70	38.72	9	201.36	348.51	287.41	45.07
Cu	9	80.00	840.00	570.00	285.44	9	150.00	400.00	247.78	80.28
Zn	9	50.00	390.00	254.44	122.38	9	130.00	240.00	167.78	33.83
Pb	9	8.00	23.00	15.67	5.98	9	16.00	26.00	19.78	3.11
V	9	11.00	47.00	17.44	11.57	9	81.00	94.00	86.67	4.44
Cr	9	40.00	50.00	43.33	5.00	9	70.00	80.00	77.78	4.41
Co	9	3.00	6.00	3.56	1.01	9	10.00	12.00	11.00	0.71
Sr	9	21.00	42.00	25.00	6.54	9	54.00	61.00	58.00	2.69
Ni	9	BDL	20.00	2.22	6.67	9	30.00	40.00	36.67	5.00
As	9	BDL	BDL	BDL	BDL	9	5.00	9.00	6.89	1.17
Ag	9	BDL	0.60	0.07	0.20	9	BDL	0.50	0.11	0.22
Sn	9	2.00	11.00	6.44	3.05	9	2.00	3.00	2.22	0.44
Sb	9	1.00	1.50	1.16	0.15	9	1.00	1.40	1.20	0.12
W	9	2.00	6.00	3.22	1.09	9	4.00	4.00	4.00	0.00

Elements	BSC 07					BSC 09				
	N	Minimum	Maximum	Mean	Std. Deviation	N	Minimum	Maximum	Mean	Std. Deviation
Al	13	52766.23	70019.78	62728.34	5687.62	8	67055.98	78752.40	71475.21	3539.37
Fe	13	25249.42	34551.84	30317.60	2828.10	8	12869.51	24270.22	15396.20	3684.46
Mn	13	278.81	472.42	381.27	52.92	8	85.19	255.57	121.98	55.04
Cu	13	20.00	30.00	25.38	5.19	8	170.00	440.00	341.25	85.60
Zn	13	60.00	70.00	66.92	4.80	8	130.00	280.00	226.25	49.26
Pb	13	11.00	21.00	15.08	2.63	8	15.00	23.00	19.13	3.00
V	13	67.00	96.00	82.38	9.03	8	86.00	97.00	91.63	4.17
Cr	13	60.00	80.00	74.62	7.76	8	80.00	90.00	85.00	5.35
Co	13	10.00	13.00	11.62	0.96	8	10.00	18.00	13.13	2.90
Sr	13	51.00	63.00	56.62	3.40	8	59.00	66.00	62.63	2.45
Ni	13	30.00	40.00	36.15	5.06	8	40.00	50.00	42.50	4.63
As	13	6.00	9.00	8.08	0.95	8	5.00	7.00	5.88	0.83
Ag	13	BDL	0.50	0.08	0.19	8	BDL	0.50	0.13	0.23
Sn	13	2.00	3.00	2.15	0.38	8	2.00	4.00	2.50	0.76
Sb	13	0.90	1.30	1.15	0.13	8	1.10	1.40	1.23	0.13
W	13	3.00	5.00	4.00	0.41	8	4.00	5.00	4.25	0.46

Table 8.16 Depth profile of short cores with respect to outliers in boxplots

Box plot outliers	Depth (Cm)			
	BSC-01	**BSC-06**	**BSC-07**	**BSC-09**
1	0 - 4	0 - 4	0 - 4	0 - 4
2	4 - 8	4 - 8	4 - 8	4 - 8
3	8 - 12	8 - 12	8 - 12	8 - 12
4	12 - 16	12 - 16	12 - 16	12 - 16
5	16 - 20	16 - 20	16 - 20	16 - 20
6	20 - 24	20 - 24	20 - 24	20 - 24
7	24 - 28	24 - 28	24 - 28	24 - 28
8	28 - 32	28 - 32	28 - 32	28 - 32
9	32 - 36	32 - 36	32 - 36	NA
10	NA	NA	36 - 40	NA
11	NA	NA	40 - 44	NA
12	NA	NA	44 - 48	NA
13	NA	NA	48 - 54	NA

NA-Not Applicable.

8.3.1.1 Contamination Factor (C_f)

BSC -01

The C_f in BSC-01 was calculated for various elements *specifically,* Fe, Mn, Al, Cu, Zn, Pb, Cr, Co, Ni, V, Sr, As, Ag, Sn, Sb and W. The mean calculated C_f value of the analyzed elements can be patterned in the decreasing order as Cu>Zn>Sn>Pb>Sb>W>Cr>Sr>Co>Mn>Al>V>Fe>Ni>Ag>As. Among the analysed elements, the down core variations of the C_f for Cu showed very high contamination (C_f >6) except for one subsample at 4-8cm, which exhibited considerable contamination. In the case of Zn, the calculated C_f values were low at the top (0-8 cm) and further down core it showed considerable contamination. The core exhibited low to considerable contamination for Sn and low to moderate contamination for Pb, Sb and W. The C_f values of all the other elements further down core were recorded as low (C_f<1). Ag and Ni were recorded below the detection limits further down core and As was completely absent in this site. The box plot representation of C_f values of selected elements from this site is illustrated in Figure 8.19.

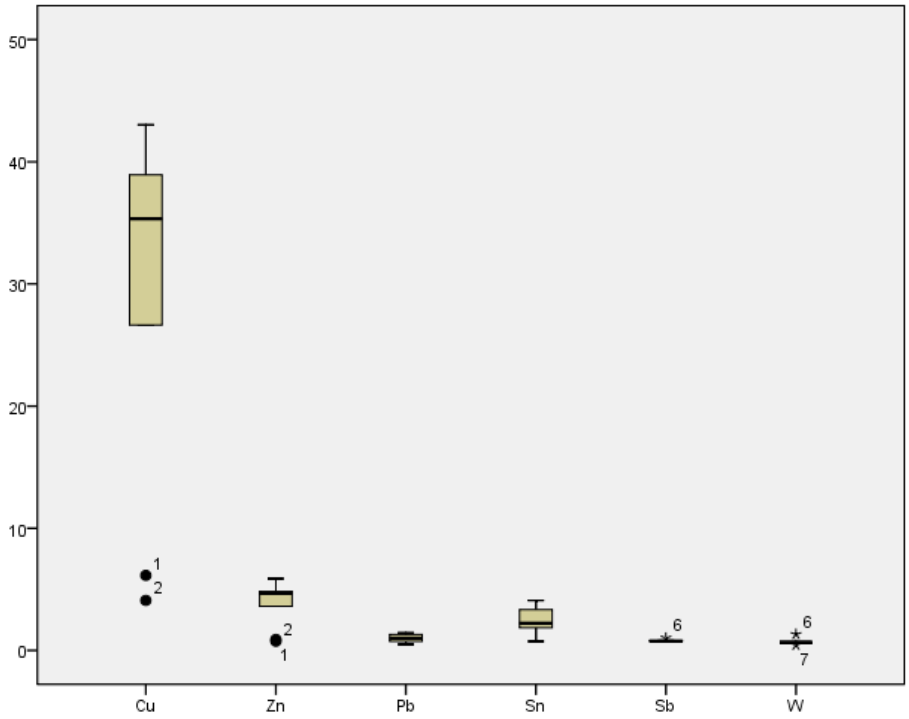

Figure 8.19 Box plot of contamination factor (C_f) of elements observed in BSC-01

BSC-06

The C_f values in BSC-06 were calculated for various elements *specifically,* Fe, Mn, Al, Cu, Zn, Pb, Cr, Co, Ni, V, Sr, As, Ag, Sn, Sb and W. The mean calculated C_f of the analyzed elements can be patterned in decreasing order as Cu> Zn> Pb> Ni> Co> Al>V>Fe>As>Sr>Mn>W>Cr>Sn>Sb>Ag. The core exhibited moderate to considerable contamination by Zn towards down core. Moderate contamination was observed for Pb and low to moderate contamination was observed for Ni, Co, Al, V, Fe, As, Sr and Mn at this site. Ag content was recorded below the detection limits further down core. The C_f values of all the other elements further down core were low (C_f<1). The box plot illustrated the contamination factor of the selected elements from this site (Figure 8.20).

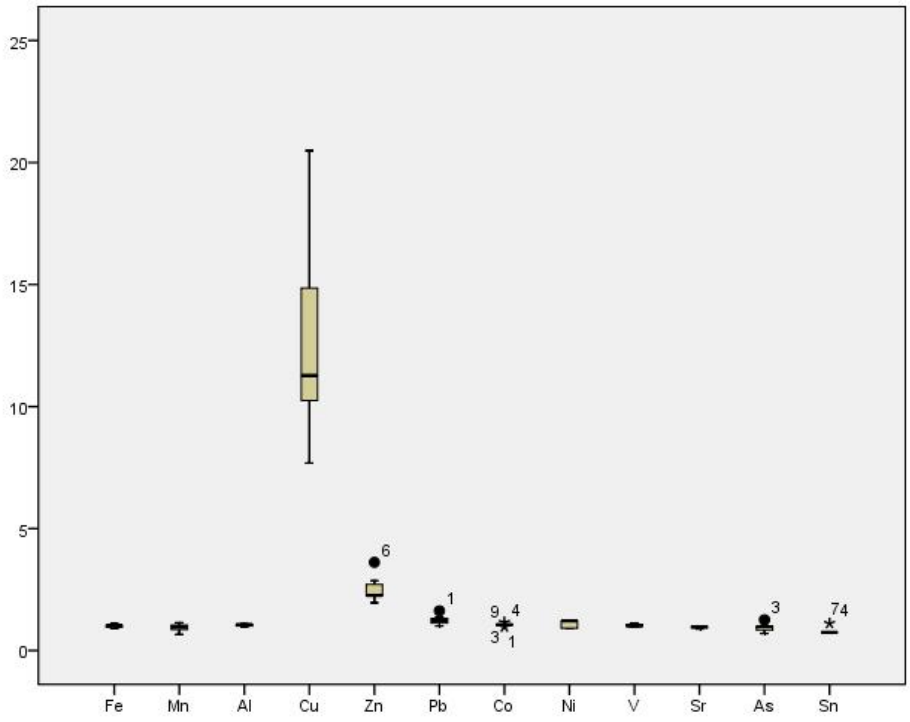

Figure 8.20 Box plot of contamination factor (C_f) of elements observed in BSC-06

BSC-07

The C_f values in BSC-07were calculated for the following elements, Fe, Mn, Al, Cu, Zn, Pb, Cr, Co, Ni, V, Sr, As, Ag, Sn, Sb and W. The mean calculated C_f values of the analyzed elements can be patterned in decreasing order as Cu> Mn> As> Co> Ni> Fe>Zn>Al>V>Pb>Sr>W>Cr>Sn>Sb>Ag. Among the analysed elements, the C_f values

of Cu were classified as moderate further down the core. The core exhibited low to moderate contamination towards Mn, As, Co, Ni, Fe, Zn, Al, V, Pb, Sr, W and Sn. Similar to previous sites, Ag was found below the detection limits further down core. The C_f values of Cr and Sb further down core were low (C_f<1). The C_f values of the studied elements are illustrated as box plot in Figure 8.21.

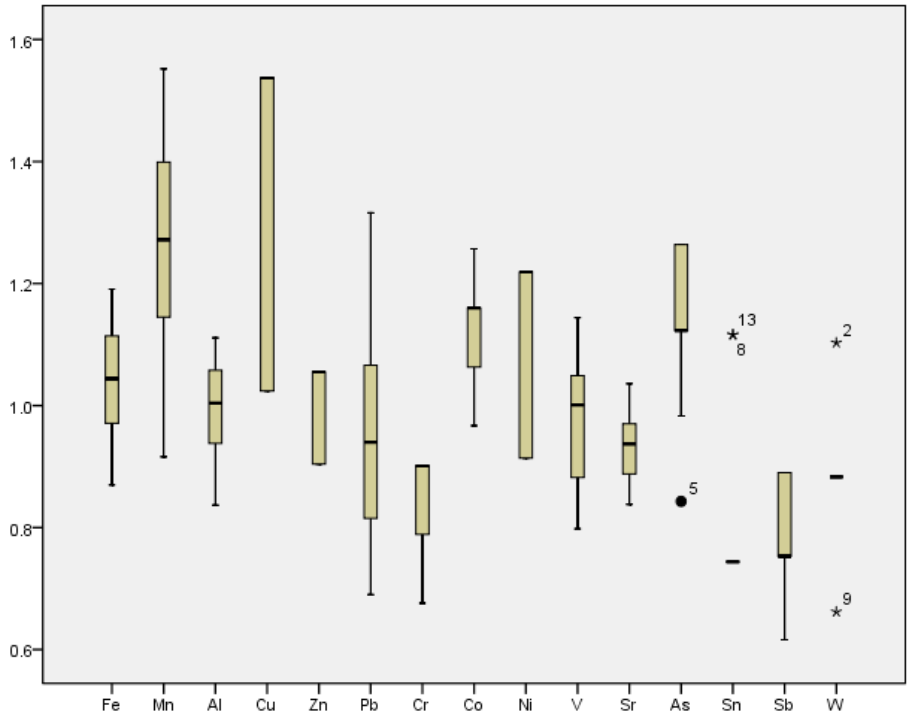

Figure 8.21 Box plot of contamination factor (C_f) of elements observed in BSC-07

BSC-09

The C_f values in BSC-09 were calculated for the elements, Fe, Mn, Al, Cu, Zn, Pb, Cr, Co, Ni, V, Sr, As, Ag, Sn, Sb and W. The mean calculated C_f values of the analyzed elements can be patterned in the decreasing order as Cu> Zn> Ni> Co> Pb> Al>V>Sr>Cr>W>Sn>Sb>As>Fe>Mn>Ag. Among the analysed elements, the C_f values of Cu were very high (C_f>6). Moderate to considerable contamination by Zn and moderate contamination by Ni, Al and V was observed. The site exhibited low to moderate contamination by Co, Pb, Sr, Cr, W and Sn. Ag content was recorded below the detection limits further down core as in the previous sites. The C_f values of all the

other elements further down core were low (C_f<1). The C_f values of the selected elements are illustrated as box plots in Figure 8.22.

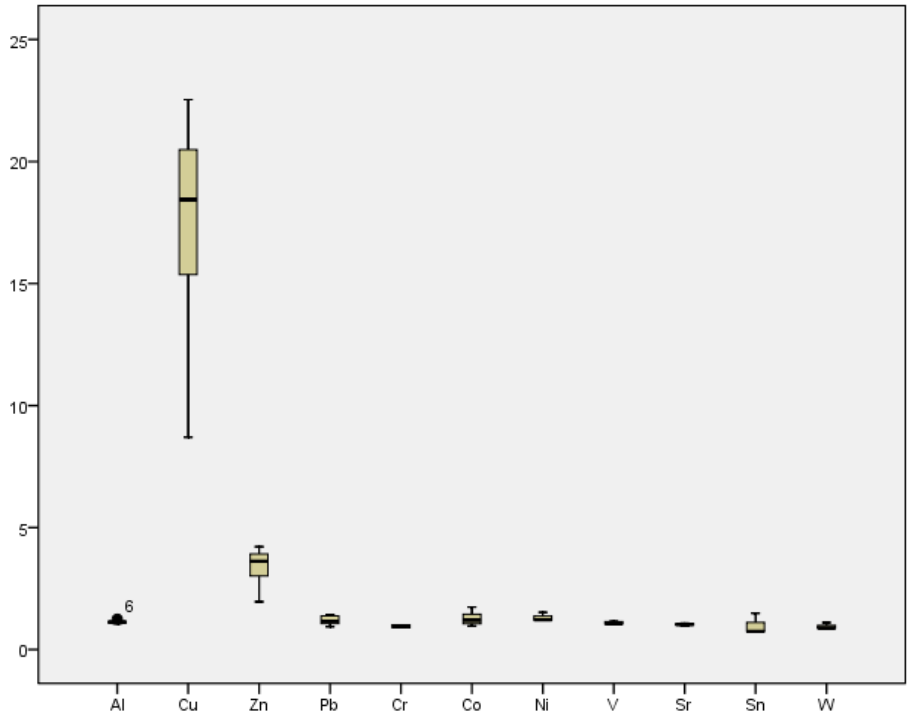

Figure 8.22 Box plot of contamination factor (C_f) of elements observed in BSC-09

8.3.1.2 Geo-accumulation factor (I_{geo})

BSC-01

The I_{geo} values were calculated for the analysed elements , Fe, Mn, Al, Cu, Zn, Pb, Cr, Co, Ni, V, Sr, As, Sn, Sb and W, and the mean I_{geo} values of the analysed elements can be arranged in the decreasing order as Cu> Zn> Sn> Pb> Sb> W> Cr> Sr> Co>Mn>Al>V>Fe>Ni>As>Ag. Among the analysed elements, the I_{geo} of Cu ranged from class 3 (moderately contaminated) to class 6 of I_{geo} (strongly to extremely contaminated). In the case of Zn and Sn, the I_{geo} values ranged from class 1 (uncontaminated) to class 3 (moderately contaminated). However, the sediments remained uncontaminated by the rest of the elements (I_{geo}<1). The I_{geo} values of Cu, Zn and Sn are illustrated as boxplot in Figure 8.23.

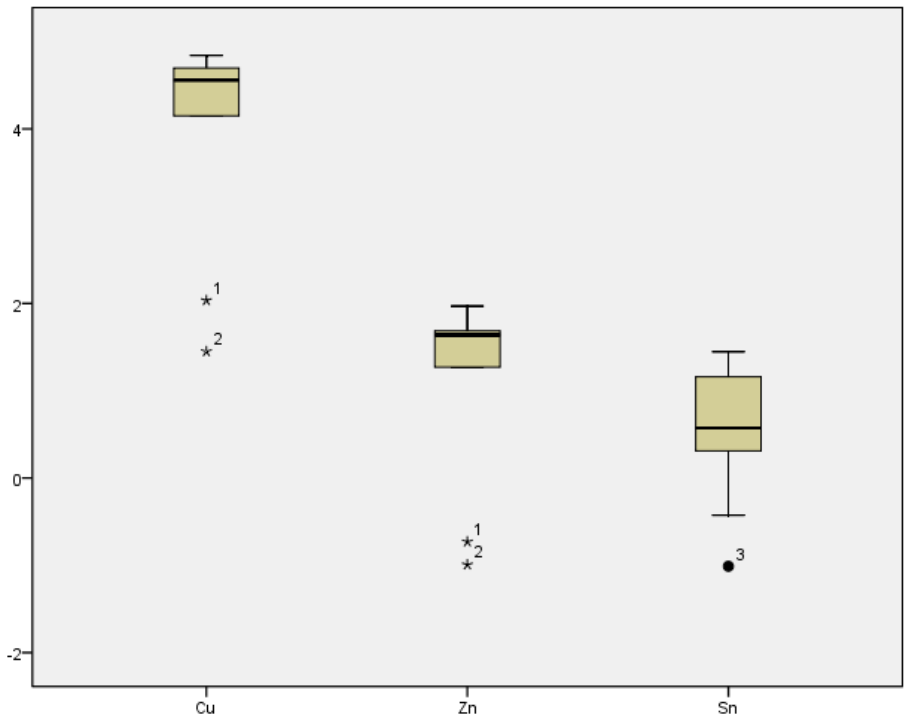

Figure 8.23 Box plot of geo-accumulation index (I_{geo}) of elements observed in BSC-01

BSC-06

The I_{geo} values were calculated for some of the analysed elements *specifically,* Fe, Mn, Al, Cu, Zn, Pb, Cr, Co, Ni, V, Sr, As, Sn, Sb and W, in the BSC-06 core sediments and the mean I_{geo} of the analysed elements can be arranged in decreasing order as Cu>Zn>Pb>Ni>Co>Al>V>Fe>As>Sr>Mn>W>Cr>Sb>Sn>Ag. Based on the I_{geo} values, the site BSC-06 can be categorized as moderately to strongly contaminated by Cu, uncontaminated to moderately contaminated by Zn and Pb and remained uncontaminated by the rest of the considered elements. The I_{geo} values of the elements and their contamination in this core are illustrated as boxplot in Figure 8.24.

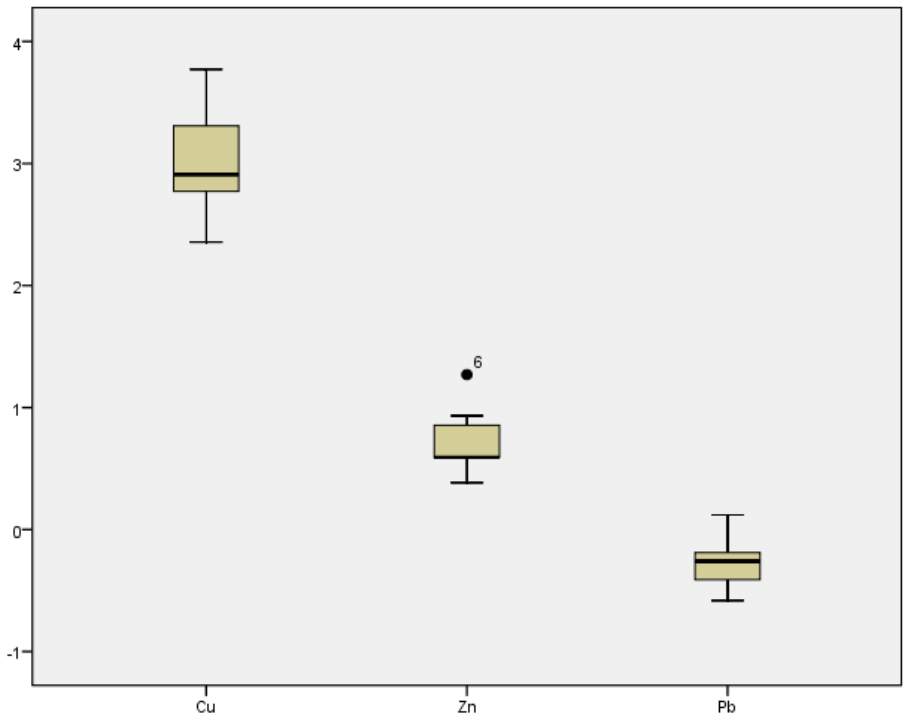

Figure 8.24 Box plot of geo-accumulation index (I_{geo}) of elements observed in BSC-06

BSC-07

The I_{geo} values were calculated for the following analysed elements, Fe, Mn, Al, Cu, Zn, Pb, Cr, Co, Ni, V, Sr, As, Sn, Sb and W in the sediments of BSC-07 core and the average I_{geo} values can be arranged in decreasing order as Cu> Mn> As> Co> Ni> Fe>Zn>Al>V>Pb>Sr>W>Cr>Sn>Sb>Ag. This core was slightly contaminated by Cu and Mn and all the other analysed elements fell under class-1 (I_{geo}<1), indicating the site was not contaminated by the rest of the considered elements. The I_{geo} of Cu and Mn is illustrated as boxplot in Figure 8.25.

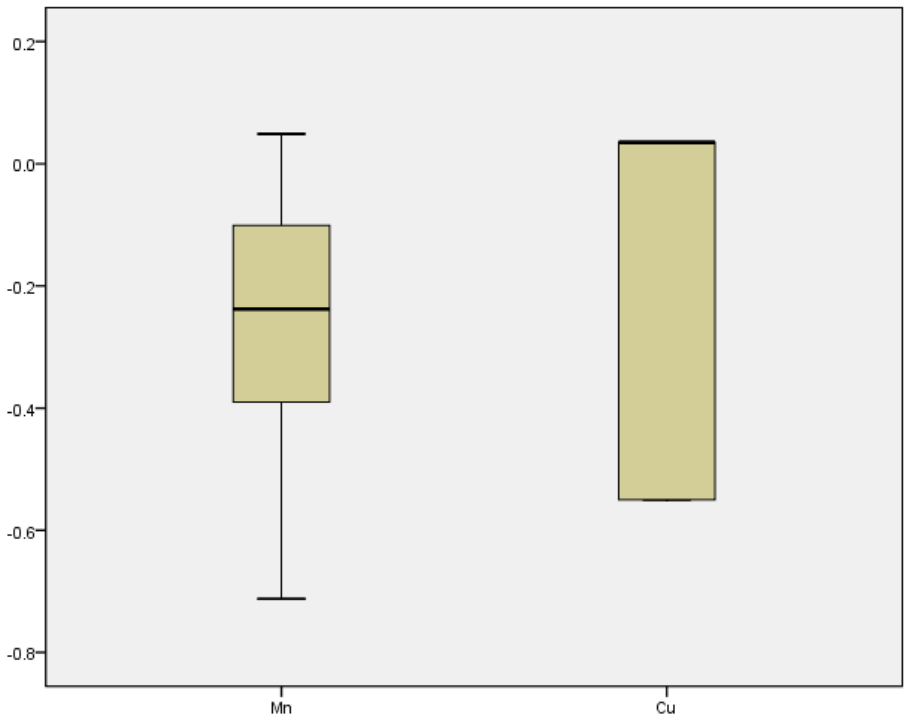

Figure 8.25 Box plot of geo-accumulation index (I_{geo}) of elements observed in BSC-07

BSC-09

The I_{geo} values were also calculated for some of the analysed elements *specifically,* Fe, Mn, Al, Cu, Zn, Pb, Cr, Co, Ni, V, Sr, As, Ag, Sn, Sb and W in the core BSC-09 and the mean I_{geo} of the analysed elements can be arranged in decreasing order as Cu>Zn>Ni>Co>Pb>Al>V>Sr>Cr>W>Sn>Sb>As>Fe>Mn>Ag. Among the analysed elements, the I_{geo} of Cu ranged from class 4 (moderately contaminated to strongly contaminated) to class 5 (strongly contaminated). The sediments of this core were uncontaminated to moderately contaminated by Zn, Ni and Co. The core sediment (BSC-09) remained uncontaminated by the rest of the elements (I_{geo}<1). The I_{geo}values of Cu, Zn, Ni and Co in the core BSC-09 are illustrated as boxplot in Figure 8.26.

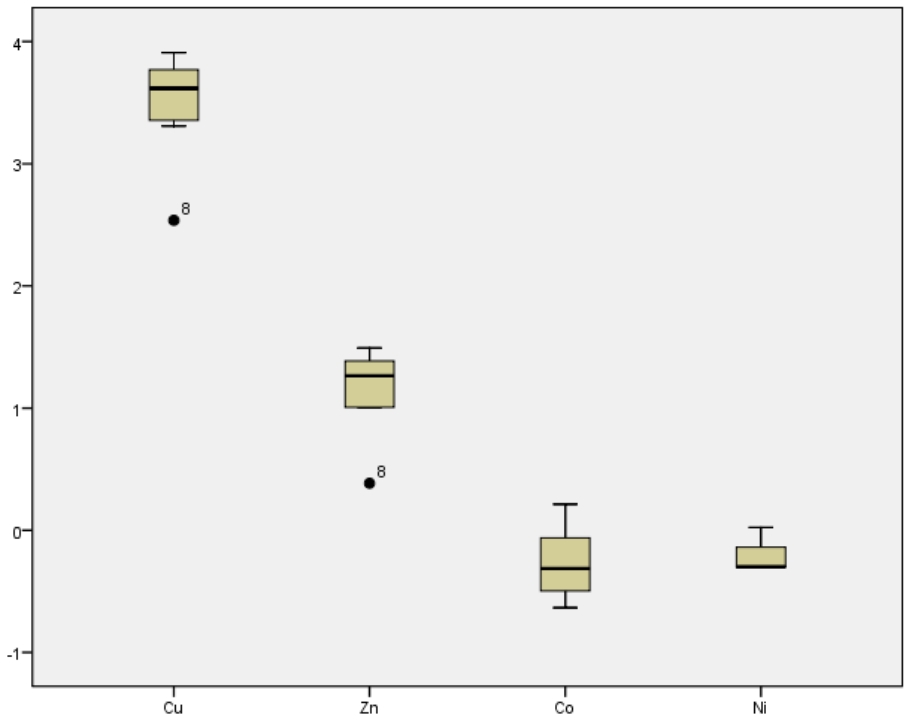

Figure 8.26 Box plot of geo-accumulation index (I_{geo}) of elements observed in BSC-09

8.3.1.3 Pollution Load Index (PLI)

The pollution load index (PLI), was calculated in all the short cores specifically, BSC-01, BSC-06, BSC-07 and BSC-09 for some selected elements such as, Fe, Mn, Cu, Zn, Pb, Cr, Co, V, Sr, Sn, Sb and W. In the case of BSC-01, the PLI of the sample at a depth of 24 cm was shown above 1 (PLI=1.240), indicating partial enrichment of the elements. For BSC-06 and BSC-09 the PLI of all subsamples further downcore were above 1 indicating combined enrichment of the selected elements in these sites. However, for BSC-07, some subsamples showed enrichment of the selected elements. The downcore variations of the PLI of all the short cores are illustrated in Figure 8.27.

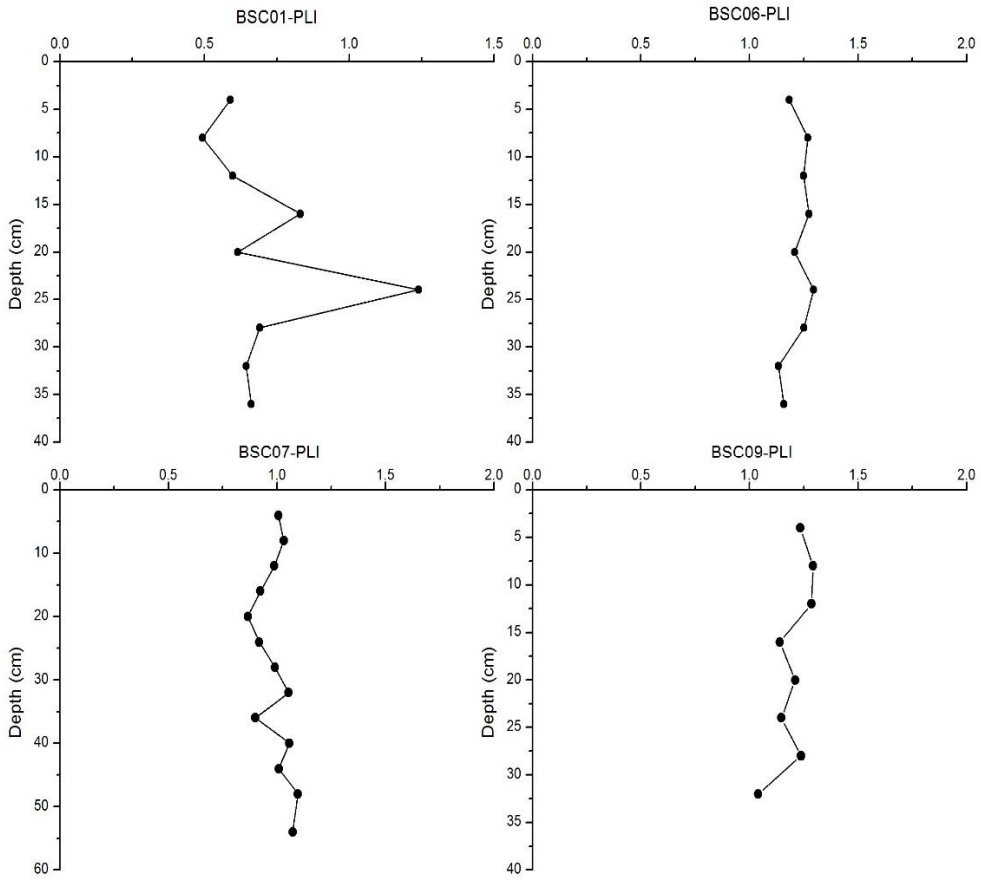

Figure 8.27 Down core variation of pollution load index (PLI) of elements in short core sediments of the Lower Baram River

8.3.2 Long Core

8.3.2.1 Contamination factor (C_f)

The C_f values in core BM-140 was calculated for the elements, Fe, Mn, Al, Cu, Zn, Pb, Cr, Co, Ni, V, Sr, As, Ag, Sn, Sb and W. The descriptive statistics of the elements are given in Table **8.17**. The mean calculated C_f values of the analyzed elements can be patterned in decreasing order as Cu> Zn> Pb> Al> V> Fe> Sr> Sn> Co>Mn>Ni>Cr>W>As>Ag>Sb. Among the analysed elements, the down core variations of the C_f values for Cu was considerable to high (C_f>6). Zn showed moderate to considerable contamination whereas Pb, Al, V and Sr showed moderate contamination. The core sediments BM-140 exhibited low to moderate contamination for Fe, Sn, Co Mn, W and As. The C_f values of all the other elements further down core were low (C_f<1). The C_f value of the elements and the contamination level are illustrated as boxplot in Figure 8.28.

Table 8.17 Descriptive statistics of the considered elements for risk assessment in the long core sediments (BM 140) of the Lower Baram River

Elements	N	Minimum	Maximum	Mean	Std. Deviation
Al	36	66474.00	83304.00	74862.53	4359.81
Fe	36	27488.00	38888.00	33219.00	3019.72
Mn	36	170.00	349.00	286.08	54.05
Cu	36	120.00	620.00	330.83	126.07
Zn	36	140.00	380.00	241.39	59.91
Pb	36	21.00	38.00	28.06	4.15
V	36	86.00	111.00	98.83	6.87
Cr	36	70.00	80.00	75.28	5.06
Co	36	9.00	13.00	10.75	0.97
Sr	36	61.00	75.00	66.61	3.74
Ni	36	30.00	40.00	30.56	2.32
As	36	BDL	8.00	2.22	3.05
Ag	36	BDL	0.60	0.05	0.17
Sn	36	2.00	4.00	2.86	0.42
Sb	36	BDL	0.60	0.08	0.20
W	36	2.00	13.00	2.36	1.84

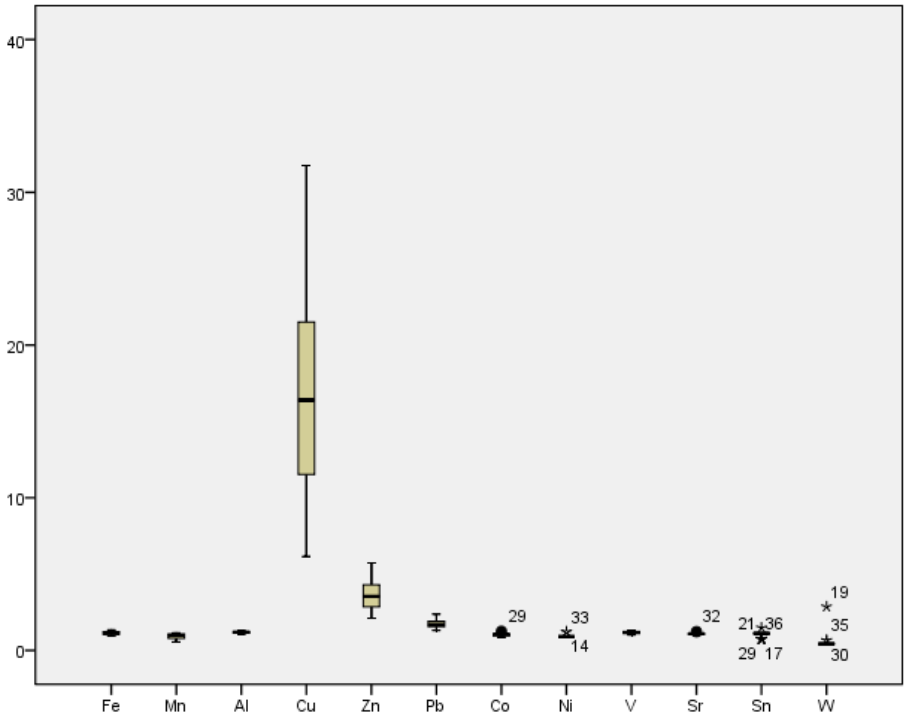

Figure 8.28 Box plot of contamination factor of elements observed in BM 140

Note: Respective depth of outliersamples

14(52-56cm); 17(64-68cm); 19(72-76cm); 21(80-84cm); 29(112-116cm); 30(116-120cm); 32(124-128cm); 33(128-132cm); 35(136-140cm); 36(140-144cm);

8.3.2.2 Geo-accumulation factor (I_{geo})

The geo-accumulation factor (I_{geo}) was calculated for the analysed elements, Fe, Mn, Al, Cu, Zn, Pb, Cr, Co, Ni, V, Sr, As, Sn, Sb and W. The mean I_{geo} of the analysed elements can be arranged in decreasing order as Cu> Zn> Pb> Al> V> Fe> Sr>Sn>Co>Ni>Mn>Cr>W>As>Ag>Sb. Among the elements studied, the I_{geo} values of Cu ranged from class 4 (moderately contaminated to strongly contaminated) to class 5 (strongly contaminated). The I_{geo} values of Zn ranged from class 2 (uncontaminated to moderately contaminated) to class 3 (moderately contaminated) whereas Pb and W ranged from uncontaminated (Class 1) to moderately contaminated class (Class 2). The I_{geo} of all the other elements were low (I_{geo}< 0). The I_{geo} of the selected elements are illustrated in Figure 8.29.

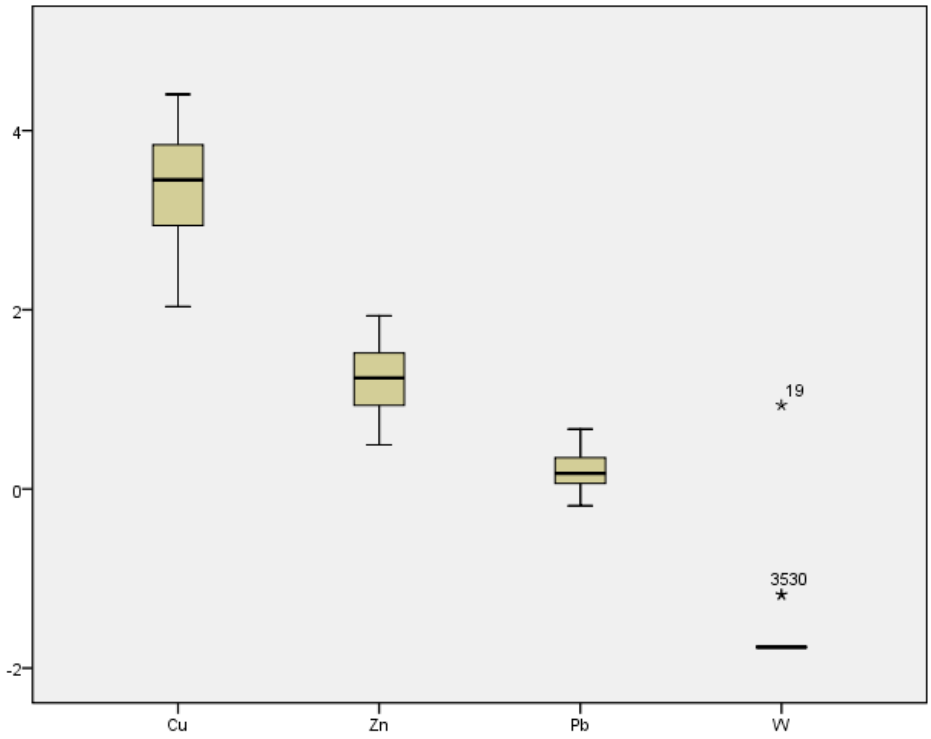

Figure 8.29 Box plot of geo-accumulation index (I_{geo}) of elements observed in BM-140

Note: Respective sample depth of outliers:

19(72-76cm); 30(116-120cm); 35(136-140cm)

8.3.2.3 Pollution Load Index (PLI)

The pollution load index (PLI), was calculated for the elements, Fe, Mn, Al, Cu, Zn, Pb, Cr, Co, V, Sr, Sn, Sb and W. The PLI value of all the subsamples along the downcore were above 1 (PLI>1), indicating combined enrichment of the studied elements in the site. The downcore variation of the pollution load index is shown in Figure 8.30.

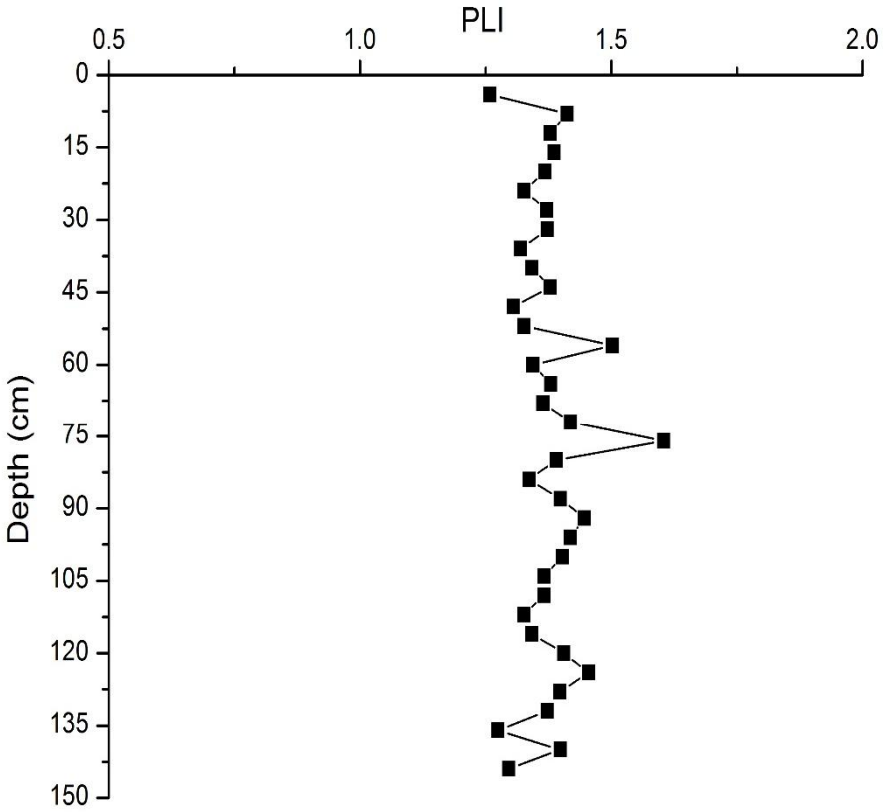

Figure 8.30 Down core variation of pollution load index (PLI) at the long core BM-140

8.4 Summary

- The Lower Baram River sediment quality was evaluated by using various risk assessment indices such as contamination factor (C_f), index of geo-accumulation (I_{geo}), pollution load index (PLI), effect range low (ERL)-effect range median (ERM), and risk assessment code (RAC).
- The risk assessment indices were calculated using the average elemental concentrations of the upstream Baram River bulk sediments (<2mm size), as the back ground value. The values are available for both seasons (the MON

and POM). However, for the POM season, in addition to the upstream bulk sediment data, the average elemental concentrations are also available for the upstream fine fraction sediments (<63µm), which was also used for the calculation of risk indices in the surface sediments collected during the POM season as well as the core sediments. Since the Lower Baram River sediments are muddy in nature, the fine fraction chemistry was more suitable than the bulk fraction.

- Risk assessment indices revealed that during the MON season the Lower Baram River surface sediments were contaminated by Cu, Zn and Sn. During the POM the surface sediments were contaminated by Cu, Cr, Sb and W. The short core sediments were contaminated by Cu, Zn, Sn, Pb, Mn, Ni and Co. The long core sediments were contaminated by Cu, Zn, Pb and W.
- Considering the Pollution Load Index (PLI), during the MON and POM season around ~90% of the sampling sites showed a PLI > 1, indicating enrichment of the elements. The PLI of BSC-01 and BSC-07 showed partial enrichment and BSC-06 and BSC-09 showed complete enrichment. The long core (BM-140) sediments were found to be enriched by the elements selected for risk assessment.

Chapter 9. The bioaccumulation of elements in the mangroves of the Baram River estuarine system

9.1 Introduction

During the Pleistocene, there existed the last glacial maximum (LGM) during which the sea level stood low. Glacio-eustatic lowering of the present day sea level by a minimum of 120 m during the LGM resulted in the complete exposure of the Sunda Shelf, joining mainland Southeast Asia to Sumatra, Java, Borneo and Palawan (Bird et al., 2005). The size of the South China Sea shrank when the Gulf of Thailand and the continental shelf east of Peninsular Malaysia and north of Borneo became exposed. This exposed continent has been called 'Sundaland' (Molengraaff, 1921). The LGM was followed by the melting of large ice caps due to a warming climate, resulting in global marine transgressions that influenced the sedimentary evolution and geochemical character of the coastal lowlands (Preda & Cox, 2002). During the Holocene highstand, the sea level reached its maximum height at around 5,400 yr B.P., and the seacoast was near Marudi (Caline & Huong, 1992). Now Marudi is a town located about 110 km upstream from the Baram River mouth. It is evident from the pollen studies that there were mangroves near Marudi during the Mid-Holocene (Anderson & Muller, 1975). Since then, the sea level has gradually receded and has resulted in the loss of mangroves due to the change in the salinity regime. Then the raised peat bogs have formed over the mangrove sediments (Anderson & Muller, 1975).

The sea level has cycled around eight times in this region, and there has been growth and decimation of mangroves in response to these marine transgression and regression events (Hunt et al., 2012; Hunt & Rushworth, 2005; Woodroffe, 1990). At present, we observed only *Sonneratia caseolaris* in the study area apart from the mangrove palm *Nypa fruticans*. The absence of other mangrove species can be attributed to their adaptation to thrive in comparatively high salinity conditions (Anderson & Muller, 1975; Hunt & Rushworth, 2005). Accompanying the salinity fluctuations has been wide ranging environmental conditions that exert significant control over the physicochemical characteristics of the water column and the sediments. The changing physicochemical environment has affected flocculation,

precipitation and remobilization of many trace elements delivered by the river into the estuarine and coastal regions.

The estuarine region is a major repository for many trace elements and geochemical processes. Historically oscillating sea levels affected not only the growth and proliferation of mangroves but also the accumulation and remobilization of trace elements into their environment. Although the effect of salinity on the growth of mangroves is well defined, research on the interaction of trace elements with the mangrove ecosystem is limited. Understanding such interactions is vital to modeling the mangrove ecosystem of the past, present and into the future. These geochemical processes in combination with the changing environmental conditions (arising due to fluctuating sea levels) may affect the mangrove ecosystem. Thus, the accumulation pattern of trace metals in plant tissues such as root, bark and leaves of *Sonneratia caseolaris* was studied. The results are expected to be useful in understanding the interaction of trace elements within the mangrove ecosystem.

9.2 Trace element concentration in mangrove plants

The root, bark and leaves of the mangrove species *Sonneratia caseolaris* (L.) Engl. were collected from six sites located within the estuarine boundary. The trace element (Fe, Mn, Co, Cu, Zn and Pb) concentration of root/pneumatophore, bark, and leaves of this mangrove species were measured and the results are presented in Table 9.1. The trace element's levels among the plant tissues showed no significant difference except for Cu ($p<0.05$) and Cd ($p<0.01$) (Appendix-4). The accumulation of metals in the mangrove tissues exhibited the same pattern as that of their background sediment metal concentrations (Fe > Mn > Zn > Cu > Pb > Co). This result was an indication that the metal accumulation in the mangrove was proportional to their concentration in the river sediments. The total concentration of Cd in the sediments was not analysed, though its level in the mangrove tissues is known.

The elemental concentrations in the mangrove tissues are in the order: root > bark > leaves for Cd, Pb and Zn, and root > leaves > bark for Co, Cu, Fe and Mn. The levels of Co in the mangrove tissues were comparatively higher than that of Cd, but was absent in the bark. However, very low concentrations of Cd were present in all the mangrove tissues. Cobalt was absent in the bark, present in only one site in the leaves, but present in all the root samples except for one sample (CR-01). These

observations showed the metal uptake by the mangroves was dependent on the nature of the metal, and the characteristics of the mangrove species (Chowdhury & Maiti, 2016). Since practically all metal uptake occurs through the roots, there should be a mechanism by which the metal accumulation in various tissues of the mangrove is controlled.

Earlier studies indicated that the roots showed greater metal accumulation than the above ground parts (MacFarlane & Burchett, 2000; 2002; MacFarlane et al., 2003). The inherent capacity of metal accumulation in the mangrove roots tissue is due to its ability to trap metals in their cell walls or, root epidermis thus preventing further metal transport (Sousa et al., 2008; MacFarlane & Bruchett, 2000). Thus, the presence of Co only in the roots/pneumatophores is an indication that apart from metal accumulation, the roots also regulate the uptake of Co.

During metal uptake, the free metal ions around the roots are depleted, leading to the dissociation of metal complexes resulting in the enhanced diffusional flux or, increased uptake of metals (Degryse et al. 2006; Lutts & Lefevre, 2015). Metal accumulation leads to deposition of unknown substances onto root vessels, resulting in their constriction and blockage of the vascular system that affects further metal transport and results in the sequestration of metals at the root level (Wong et al., 1988). Under waterlogged conditions, the formation of iron-plaque on the root surface acts as a physical barrier through immobilisation. Thus, iron-plaque serves as an efficient absorber of metals at the root level, leading to the retention of metals at the root surface (Lutts & Lefevre, 2015). After uptake by the root, translocation of metals from the root to plant shoots is restricted in most of the plants. The movement of metals is restricted within the root cell wall, resulting in their accumulation (Caetano et al., 2008; Sousa et al., 2008). Such a mechanism protects the sensitive aerial organs of plants from contaminants (Silva et al., 1990; Chiu & Chou, 1991; MacFarlane et al., 2003; Machado et al., 2005). To assess the toxicity of the trace elements, their concentrations in the tissues of mangroves were compared with the recommended limits generalised for various species by Kabata-Pendias and Pendias (1992). The results showed none of the examined elements was above this toxic range in any of the tissue.

Table 9.1 Trace element concentrations in the mangrove Sonneratia caseolaris (L.) Engl. collected from the Baram River estuarine region

Sample Sites	Cd (µg/g)			Co (µg/g)			Cu (µg/g)			Fe (µg/g)		
	Leaves	**Bark**	**Roots**	**Leaves**	**Bark**	**Roots**	**Leaves**	**Bark**	**Roots**	**Leaves**	**Bark**	**Roots**
CR 01	BDL	0.11	0.13	BDL	BDL	BDL	2.92	1.81	3.80	203.49	239.99	519.15
CR 02	0.08	0.10	0.12	BDL	BDL	1.38	3.29	1.28	3.21	330.08	145.22	886.67
CR 03	0.08	0.10	0.15	BDL	BDL	1.44	3.02	1.64	3.56	266.85	168.12	1052.63
CR 04	0.10	0.10	0.27	0.295	BDL	3.17	4.28	3.77	7.37	455.46	271.86	7328.40
CR 05	0.10	0.10	0.20	BDL	BDL	1.25	3.26	1.50	8.30	446.06	180.94	802.97
CR 06	0.09	0.10	0.12	BDL	BDL	1.16	2.91	1.02	2.96	333.52	227.91	689.96
Mean ± Std. Err	**0.09 ± 0.005**	**0.01± 0.002**	**0.17± 0.023**	**NA**	**NA**	**1.68± 0.38**	**3.28± 0.21**	**1.84± 0.40**	**4.87± 0.95**	**339.25± 40.29**	**205.67± 19.77**	**1879.96± 1092.16**
Toxic levels*	5-30			15-50			20-100			-		

Sample Sites	Mn (µg/g)			Pb (µg/g)			Zn (µg/g)		
	Leaves	**Bark**	**Roots**	**Leaves**	**Bark**	**Roots**	**Leaves**	**Bark**	**Roots**
CR 01	42.56	57.65	71.67	0.99	0.76	1.78	8.08	5.40	9.75
CR 02	138.96	94.86	170.37	1.46	0.99	1.58	9.09	2.86	8.91
CR 03	134.90	95.98	176.66	1.02	0.92	1.85	8.41	2.55	8.38
CR 04	181.69	101.74	282.63	1.35	4.06	5.53	9.84	87.63	13.96
CR 05	280.86	171.00	304.29	1.00	0.80	3.39	11.52	2.83	30.95
CR 06	121.93	87.74	176.54	0.83	0.73	1.92	7.85	2.19	7.72
Mean ± Std. Err	**150.15± 32.05**	**101.49± 15.29**	**197.03± 34.67**	**1.11± 0.10**	**1.38± 0.54**	**2.68± 0.63**	**9.13± 0.56**	**17.24± 14.08**	**13.28± 3.65**
Toxic levels*	400-1000			30-300			100-400		

* Represents the excessive or toxic concentrations of trace elements in mature leaf tissue generalised for various species (Kabata-Pendias & Pendias, 1992)

9.3 Bioconcentration factor (BCF)

The bio-concentration factor is the quantitative expression of the accumulation of trace elements in mangrove plant parts or tissues. Essentially, it is the ability of mangroves to absorb contaminant from the sediment. It is the relative measure of the ratio of trace element concentration in the mangrove tissues to that of the sediment. The following equations were adopted in the present study for the calculation of bioconcentration factors.

Bioconcentration factor for the leaf: $BCF_{Leaf} = C_{Leaf}/C_{Sediment}$

Bioconcentration factor for the bark: $BCF_{Bark} = C_{Bark}/C_{Sediment}$

Bioconcentration factor for the root: $BCF_{Root} = C_{Root}/C_{Sediment}$

Where C_{Leaf}, C_{Bark} and C_{Root} are the trace element concentrations in leaf, bark and root, respectively and, $C_{Sediment}$ is the trace element concentrations in the mangrove sediment. The bioconcentration factors based on the total (Table 9.5) and mobile fraction (Table 9.6) of the trace elements were calculated. These BCF values were not significantly different between the tissues and the sites, except for Cu and Cd (Appendix-5). The BCF of both the total and mobile fraction of Cu showed a significant difference ($P < 0.05$) between plant tissues and the sites. Whereas, Cd showed a significant difference ($P < 0.01$) between plant tissues and the sites for the mobile fraction it was not analysed in the total fraction.

There has been an increasing number of studies on both, the ecology and ecotoxicology of mangrove ecosystems around the world (Bayen, 2012; de Almeida Duarte et al., 2017; Prabakaran et al., 2017). There has been an increasing interest in these studies due to the environment in which these mangroves are growing has been subjected to several stresses. They are i) sea level rise; ii) river contamination; iii) the potential of mangrove ecosystems to absorb increasing levels of CO_2 in the atmosphere; iv) the ability of mangrove ecosystems to reduce the effect of coastal erosion and in preventing the calamities caused by tsunamis, v) the unique ecosystem provided by the mangroves for innumerable fauna endemic to this ecosystem and its role in the maintenance of biodiversity; vi) the use of mangrove plant parts for medicinal purposes and vii) its use for the substance of life by the local people. There may be other uses, which are not currently known or partially known like the 'ecosystem services' of mangroves. However, as outlined in the objectives of this thesis, our aim is limited to the study of ecotoxicology with particular relevance to some of the selected trace elements. These trace elements have both beneficial and

detrimental effects on the biological system. In other words, the ecosystem has evolved to adapt itself only to the trace level of these elements. When this concentration exceeds the normal background value, then the mangroves develop stress. An increasing environmental concentration of the elements invariably results in a higher level of uptake. Then, the mangroves adapt to this situation by adopting the "exclusion mechanism" (MacFarlane & Burchett, 2002), whereby the excess trace element is dislodged from the plant tissue or, saved in a form and in a tissue or part of a tissue where it will have the least effect on its physiology. The induction of metallothionein or other enzyme systems such as the oxidative enzyme system are such kind of mechanisms adopted by mangroves.

Thus, metal uptake by the mangrove is controlled by i) the environmental concentration of the metal and its speciation; ii) the membrane permeability of the mangrove root system that not only controls but also enhances the uptake of essential trace elements by releasing extra-cellular enzymes, iii) the effectiveness of the "exclusion mechanism" that operates within the mangroves; iv) the environmental factors that exert control over a) the metals concentration in the environment, b) its uptake by the plant, and c) influence the physiological functions of the plant itself. This research has made an attempt to understand all these processes using the calculated values of BCF to apply ANOVA (Appendix 5-8). The advantage of this method is it is simple to comprehend and carry out, but the limitations are that everything depends on our ability to understand and make the statistical inference. While studies that are more detailed can be carried out in future research, this study's scope is only understanding the processes implied by the statistical relationships inferred from ANOVA. To understand more clearly the inferences, the research presents the summary of the principles, based on which the conclusions are made. While doing so, we have deviated from the usual way of calculating the bioconcentration factor (BCF) from the instantaneous surface sediment concentrations of the trace elements.

For example, we have considered the average background concentration of the trace elements in the surface sediments as well as their depth distribution in shallow core sediments (around 40 cm in depth). Based on this we have computed the BCF values instead of taking the instantaneous surface sediment concentration. The second modification is we have considered the estuarine concentration of the trace

elements in the water column for the calculation of the BCF. More details are presented in the following paragraphs:

I. We have not considered the instantaneous collection of surface sediments along with mangrove tissues (root/pneumatophores, bark and leaves), because the instantaneous sediment concentration of trace elements was not representative of the sediment characteristics as these would vary throughout the year. The study needed to calculate the normal background concentration of the trace elements in the study area. In the transition zone of the estuarine region, many geochemical processes are persistent. For example, changes in ionic interaction, ionic strength or salinity, pH, dissolved oxygen and compositional changes of water column chemistry. These changes tend to flocculate the dissolved trace elements resulting in their accumulation in the bottom sediments along with the clay minerals. Since the prevailing hydrodynamics of the environment significantly influence the physicochemical characteristics of the estuarine system, such an accumulation of trace elements and clay minerals are complex and often localised to optimal environmental conditions. Such an environment results in the anomalous concentration of certain trace elements, and those values should be eliminated for calculating their background levels. Potential normalizers such as Al, Ti, Sc and Cs are used for this purpose. These elements are mostly conservative in nature. Additionally, the trace element/normaliser ratio represents the source area and is considered homogeneous throughout the sediment column provided there is no local influence. Thus, these normalisers should provide a proper background value for any other trace element, which is non-conservative, and its concentration in the sediment is affected by local physicochemical environment. This calculation of background values of every trace element involves constructing a least-square fit line with confidence and prediction intervals for a P value of 0.05 (i.e., the confidence interval is 95%). The confidence interval denotes the probability band within which the trace element/normaliser ratio shall fall (at 95% confidence interval) for the data used to generate the best-fit line. The prediction interval defines the probability band, within which the trace element/normaliser ratio shall fall for any predicted concentration of the trace

element based on this linear least square fit line for any observed level of the normaliser in the sediments. Thus, the points that fall outside the prediction band are outliers, while the points that fall out of the confidence band but remain within the prediction band are the tail ends (5% both on the left and right) of the "normal distribution" that the data at hand is supposed to follow. Such a normalisation cannot be done by the combined data of the two seasonal samples because such a combination may affect the detection of outliers. Consequently, the outlier detection has to be carried out independently for the two different seasons in which the sampling was undertaken. Therefore, the outliers were determined separately during each season for each element. After eliminating these outliers, the background value of a particular trace element can be calculated by averaging its concentration over the two seasons. Such a combination of two seasonal data for averaging is necessary because the mangrove environment is exposed to this average background concentration of a particular trace element throughout the year. Thus, only this calculated background level described above for a particular trace element should be used in the calculation of various potential risk indices concerning trace element toxicity to the mangroves.

II. The other amendment was vested with the calculation of BCF values based on the concentration of trace elements in two shallow cores of about 40 cm. One core (BSC-06) was collected at around 10 km from the Baram river mouth (where salinity was ~5 ‰) and another core (BSC-01) at the boundary of the river along the coast (where salinity was around ~10 ‰; Table 9.8 and Table 9.9). Similarly, using the water column concentration of the trace elements, the BCF values were calculated (Table 9.7).

The basis of such a calculation of BCF lies in the fact that the rhizosphere of the mangrove is not only taking the trace elements from the surface sediments but also from deeper within the sediment column as well as from the water column. All mangrove ecosystems grow only in the estuarine region where flocculation, precipitation and remobilization of trace elements are a common observation (Sholkovitz 1979; Turner 1996; Saulnier & Mucci 2000; Du Laing et al., 2009). The

remobilised trace elements existing within the pore water has an excellent chance of being taken up by the mangrove root system. Moreover, the pore water concentrations of trace elements may be higher than their bulk concentration in the water column due to their release by the early diagenetic reactions from the sediments by the dissolution of iron-manganese hydrous oxides. The iron-manganese hydrous oxides are important carriers of trace elements due to their adsorption characteristics, and preferentially form a coating on the fine-grained particles and clays (Singh et al., 1984). The typical feature of such an adsorption process is that they concentrate the trace elements.

Thus, BCF values calculated using instantaneous and surface sediment concentrations of trace elements is not only misleading but also often erroneous. Apart from this, whatever trace elements present in the sediments should first be dissolved in the water to be later taken up by the plant. This mechanism also applies to the trace element uptake by the root system from the sediments. Therefore, trace element accumulation in the mangroves is not only governed by its concentration in the surface sediments but also its distribution in the deeper sediments surrounding the rhizosphere. Moreover, the water column chemistry just above the sediment-water interface, where the concentration gradient drives metal flux across the sediment-water interface, is also influenced by trace element remobilization.

Consequently, to account for all these mechanisms, we have calculated the BCF values using the concentration of trace elements in i) the surface sediments, ii) shallow core sediments and, iii) the water column. Accordingly, for each trace element, we have three sets of estimated BCF values. Then, which one is correct? Nothing is wrong as far as there is a relationship between the trace element content of the mangrove tissues and the medium from which it was ingested. Having done all these calculations, we have tried to infer the medium from which these trace elements might have been taken up. As a result, we have used all these calculated sets of BCF values to understand the effects of plant physiology and the impact of environmental factors on the uptake of trace elements by the mangroves. By doing this, we can identify the medium from which the trace elements might have been absorbed by the mangroves. The logic behind such an application is described here.

Case-1: First we calculated ANOVA to determine whether there was a significant difference between the trace element concentrations of the

root/pneumatophore, bark and, leaves (Appendix-4, and Table 9.12). If such a difference exists, then this is primarily due to the physiological effects of the plant. If there was no difference, then the plant physiology does not differentiate the trace element accumulation in the root, bark and the leaves.

Case-2: We then calculated the BCF values by taking the surface sediment and plant tissue concentrations of the trace elements (Appendix-5 & 6). If the estimated BCF values followed the same pattern as that of case-1, then there was no influence of surface sediments on the trace element distribution pattern in various tissues of the mangroves. However, if there was a difference of pattern between case-1 and case-2, then this may be due to the effect of surface sediments. This can be confirmed by comparing the BCF values obtained using the core sediments (Table 9.12), as well as the water column (Table 9.12), and subjecting the results to the ANOVA as follows.

Case-3: The core BSC-01 location is just at the point of interface between the river and seashore. However, this does not mean entirely marine conditions exist, as the large volume of freshwater from the Baram River does not permit salinity levels to rise significantly even far into the South China Sea. Compared to the core BSC-06 location, this is an environment of somewhat higher salinity and is often modulated and influenced by the currents and waves that prevail along the coastline. Any significantly different pattern of BCF results (case-2 vs. case-3) obtained for a particular trace element between the core locations BSC-01 and BSC-06 would imply the influence of environmental conditions on the uptake of the trace elements by the mangroves.

Case-4: We have now calculated the BCF values using surface water concentrations of trace elements and compared them with the ANOVA results obtained under cases 1, 2 and 3 (Table 9.12, Apendix-5). If the surface water based BCF values (case-4) follow the same pattern as that of the elemental relationship within the tissues (case-1) but differs from case-2 and case-3, then trace element content of surface and core sediments do not have a significant influence on metals accumulation in the mangrove tissues.

Instead, if the water column based BCF values (case-4) differ from case-1, then the trace element concentration of the water column does not have a significant influence on metals accumulation in the mangrove tissues. Such a possibility can arise due to the early diagenetic reactions that may profoundly affect the mobility of the trace elements from the sediments. To confirm this, however, we need to explore the pattern of ANOVA results obtained under cases 2 and 3 and compare it with the pattern from case-1.

9.4 The calculated background concentration of the elements considered for the study

The background concentration of trace elements in the sediments of the Baram River mangrove ecosystem is given in Table 9.2. The trace element levels in the mangrove sediments exhibited the following order Fe>Mn>Zn>Cu>Pb>Co.

Table 9.2 Background concentrations of selected trace elements in the total fraction

Trace element	Concentration (ppm ± SE)
Fe	27478.27 ± 998.68
Mn	267.71 ± 16.30
Co	9.69 ± 0.38
Cu	57.59 ± 4.57
Zn	80.00 ± 2.22
Pb	14.43 ± 0.41

The trace element concentrations observed in the sediments of the mangrove environment was compared with earlier studies (Table 9.3). For the most part, the levels of the trace elements in the present study are lower than most of the reported values. However, the levels were relatively higher than reported in a few other studies. The eco-toxicological indicators specifically, Effect Range Low (Low), Effect Range Median (ERM), Lowest Effect Level (LEL) and Severe Effect Level (SEL) revealed the concentrations of all the trace elements are lower, except copper. Copper exceeds the eco-toxicological values of Effect Range Low (ERL) and Lowest Effect Level (LEL), indicating copper enrichment in the study area. Furthermore, these values are comparatively higher than the unpolluted sediments reported in the study of Salomons and Förstner (1984).

Table 9.3 The average trace element concentrations in the Baram mangrove sediments and some mangrove wetlands around the world

Location	**Trace element (µg/g)**						**References**
	Fe	**Mn**	**Co**	**Cu**	**Zn**	**Pb**	
Baram mangrove sediments, Borneo	27478	267.705	9.69	57.586	80	14.429	This study
Pichavaram, India	-	-	-	43.4	93	11.2	Ramanathan et al., (1999)
Mai Po, Hong Kong	-	-	-	78.5	240	79.2	Tam and Wong (2000)
Hawksbury, Australia	-	-	-	18.9	94	26.4	MacFarlane (2002)
Newington, Australia	-	-	-	71.3	229.9	121.9	MacFarlane et al., (2003)
Guanabara Bay, Brazil	-	-	-	98.6	483	160.8	Machado et al., (2002)
Sungei Buloh, Singapore	-	-	-	7.06	51.24	12.28	Cuong et al., (2005)
Punta Mala Bay, Panama	9827	295	-	56.3	105	78.2	Defew et al., (2005)
Peninsular Malaysia	-	-	-	320	4.30	83.0	Nazli and Hashim (2010)
Hainan Island, China	-	-	-	18	57	19	Qiu et al., (2011)
Lothain Island, Sunderban, India	-	611.76	25.80	38.0	84.23	28.67	Banerjee et al., (2012)
Farasan Islands, Saudi Arabia	-	-	-	112	57.2	45.2	Usman et al., (2013)
Nansha Mangroves, South China	-	880	-	113	159	55.3	Wu et al., (2014)
Indian Sunderban	29746	901	9.51	47.64	62.85	25.44	Chowdhury et al., (2017)
Eco-toxicological Values							
Unpolluted Sediments	-	770	-	33	95	19	Salomons and Förstner (1984)
Effect Range Low (ERL)	-	-	-	34	150	46.7	Long et al., (1995)
Effect Range Median (ERM)	-	-	-	270	410	218	Long et al., (1995)
Lowest Effect Level (LEL)	-	460	-	26	120	31	USEPA, (2001)
Severe Effect Level (SEL)	-	1110	-	110	820	250	USEPA, (2001)

9.5 Metal fractionation studies in the mangrove environment of the Baram River estuarine system

The bioavailability of the trace elements is dependent on its particulate speciation in the sediments. Thus, the BCF values calculated using bulk sediment concentration of the trace elements might be misleading. Such a dependency arises from the influence of solubility on minerals dissolution and further release of the trace elements under the given environmental conditions (Tessier et al., 1979). Knowledge on the particulate speciation of the trace elements (Cu, Zn, Pb, Cd and Co) and their carrier phases (Fe- and Mn-oxides) in the sediments were obtained by sequential extraction (Tessier et al., 1979). Among the five fractions (exchangeable, carbonate-bound, Fe-Mn oxides-bound, organic-bound and, residual), the residual fraction is immobile, and was not considered in this study. The results are given in Table 9.4. The elemental concentration in different fractions of the Baram River sediments has the following order:

Fe: F3 > F4 > F2 > F1

Mn: F1 > F3 > F2 > F4

Cu: F4 > F3 > F2 > F1

Zn: F3 > F1 > F4 > F2

Co: F3 > F4 > F2 > F1

Pb: F3 > F4 > F1 > F2

Cd: F3 > F4 > F1 > F2

Where, F1 = exchangeable fraction, F2 = carbonate-bound fraction, F3 = iron-manganese oxides-bound fraction, F4 = organic-bound fraction.

Of these, Cu (F4 > F3 > F2 > F1) and Mn (F1 > F3 > F2 > F4) have a distinct distribution pattern with most of their labile fraction being in the F4 and F1 fraction, respectively. Zn also exhibited a unique pattern (F3 > F1 > F4 > F2) from other trace elements with its highest concentration in the Fe-Mn oxides-bound (F3) fraction. Pb and Cd had a similar pattern (F3 >F4 > F1 >F2) with most of their labile fraction being in the Fe-Mn oxides-bound fraction.

Among all these fractions, the F1 fraction seemed to play a dominant role in plant uptake. For example, the mobile fraction of Cu, defined as the sum of F1 + F2 + F3 + F4, was 48 µg/g. While the mobile fraction of Zn, was 53 µg/g. At the same

time, the F1 fraction of Cu was 6.5 µg/g while for Zn it was 13 µg/since, in general, the order of elemental mobility from the sediments follows the order F1 > F2 > F3 > F4, the exchangeable fraction is easily available to the plant. Commensurate with this intake, the accumulation of Zn is greater in the plant than for Cu. However, it should be noted that the physiological control of the plant was not taken into account to derive at this conclusion. As illustrated in Table 9.12, the plant physiology influences the rate of accumulation of Cu but not for Zn. A combination of both these facts clearly explains the higher levels of Zn in the mangroves.

Table 9.4 Fractionation of trace elements in Baram mangrove sediments

Trace element	Concentration (ppm ± SE)				
	F1 (Exchangeable)	F2 (Bound to carbonate)	F3 (Bound to Fe-Mn oxides)	F4 (organic bound)	Total mobile
Fe	15.58 ± 3.13	230.95 ± 17.95	8474.54 ± 364.46	2367.70 ± 379.80	11088.76 ± 428.19
Mn	105.05 ± 9.37	26.35 ± 3.84	70.60 ± 9.33	24.81 ± 8.96	226.80 ± 18.93
Co	0.69 ± 0.09	0.88 ± 0.12	4.59 ± 0.22	2.304 ± 0.186	8.47 ± 0.37
Cu	6.53 ± 1.71	7.59 ± 1.19	8.05 ± 1.12	25.81 ± 3.04	47.97 ± 6.15
Zn	13.04 ± 2.16	5.65 ± 0.69	24.22 ± 2.84	10.08 ± 0.78	52.99 ± 4.52
Pb	0.97 ± 0.19	0.35 ± 0.09	6.27 ± 0.29	3.52 ± 0.46	11.14 ± 0.49
Cd	0.02 ± 0.01	0.01 ± 0.01	0.12 ± 0.01	0.09 ± 0.01	0.24 ± 0.01

9.6 The bioconcentration factor based on total trace element content of the sediments

The bioconcentration factor based on total metal concentrations is presented in Table 9.5. The bioconcentration factor for root tissue (BCF_{Root}) ranged from 0.02 - 0.27 for Fe, 0.27 - 1.14for Mn, 0.12 - 0.33 for Co, 0.05 - 0.14 for Cu, 0.10 - 0.39 for Zn and 0.11 - 0.38 for Pb. The average BCF_{Root} values for Fe, Mn, Co, Cu, Zn and Pb were 0.07, 0.74, 0.17, 0.09, 0.17 and 0.19, respectively. The bioconcentration factors of bark (BCF_{Bark}) ranged from 0.01 - 0.01 for Fe, 0.22- 0.64 for Mn, 0.02- 0.07 for Cu, 0.03- 1.1 for Zn and 0.05 - 0.28 for Pb. The average BCF_{Bark} were 0.01, 0.38, 0.03, 0.22, and 0.10 for Fe, Mn, Cu, Zn and Pb, respectively. As Co was completely absent in the bark, the BCF_{Bark} for Co could not be calculated. Meanwhile, the observed bioconcentration values for leaf (BCF_{Leaf}) was in the range of 0.01- 0.02 for Fe, 0.16- 1.05 for Mn, 0.03 for Co, 0.51 - 0.07 for Cu, 0.10- 0.14 for Zn and 0.06- 0.10 for Pb. The average BCF_{Leaf} values for Fe, Mn, Co, Cu, Zn and Pb were found

to be 0.01, 0.56, 0.03, 0.06, 0.11 and 0.08, respectively. Co was present in only one sample location (CR-04) in the leaf of the mangroves.

9.7 The bioconcentration factor based on mobile fraction of trace element content in the sediments

The bioconcentration factor calculated with respect to mobile fraction (Table 9.6)in the root (BCF_{Root}) ranged from 0.05 to 0.66 for Fe, 0.32 to 1.34 for Mn, 0.14 to 0.37 for Co, 0.06 to 0.17 for Cu, 0.15 to 0.58 for Zn and 0.14 to 0.50 for Pb and 0.51 to 1.12 for Cd. The average BCF_{Root} values for Fe, Mn, Co, Cu, Zn, Pb and Cd were 0.17, 0.87, 0.20, 0.10, 0.25, 0.24 and 0.69, respectively. The bioconcentration factors of bark (BCF_{Bark}) ranged from 0.01 to 0.03 for Fe, 0.25 to 0.75 for Mn, 0.02 to 0.08 for Cu, 0.04 to 1.65 for Zn, 0.07 to 0.37 for Pb and 0.40 to 0.46 for Cd. The average values of BCF_{Bark} were 0.02, 0.45, 0.04, 0.33, 0.12 and 0.41 for Fe, Mn, Cu, Zn, Pb and Cd, respectively. As Co was completely absent in bark tissues, the BCF_{Bark} for Co could not be computed. Meanwhile, the observed bioconcentration values for leaf (BCF_{Leaf}) was in the range of 0.02 to 0.04 for Fe, 0.19 to 1.24 for Mn, 0.04 for Co, 0.06 to 0.09 for Cu, 0.15 to 0.22 for Zn, 0.07 to 0.13 for Pb and 0.31 to 0.41 for Cd. The average BCF_{Leaf} values for Fe, Mn, Co, Cu, Zn, Pb and Cd were found to be 0.03, 0.66, 0.04, 0.07, 0.17, 0.10 and 0.36, respectively. Co was present in only one site (CR-04) in the leaves of the mangroves, and absent in all the other sites.

The average bioconcentration factor for the elements in the mangrove tissues was< 1 for both total and mobile phases of trace elements, indicating a lower metal concentration in the mangroves than in the sediments. The Mn showed comparatively higher bioconcentration factors compared to other elements. At two sampling locations the BCF_{Root} values of Mn were> 1 (CR 04: 1.06 for bulk and, 1.25for mobile fraction; CR 05: 1.14 for bulk and 1.34 for the mobile fraction). Higher BCF_{Leaf} values for Mn were observed in the sampling location CR-05 (1.05 for bulk, and 1.24 for the mobile fraction) and a higher BCF_{Bark} value was observed for Zn in site CR-04 (1.10 for bulk, and 1.65 for the mobile fraction). It should be noted that the BCF values calculated using the mobile fraction of the elements are always higher than the values calculated using the total concentration. This difference is because the mobile fraction is always a part of the total elemental concentration in the sediments and the residual fraction (or, immobile fraction) of an

element in the sediments is never be available to the plant. Therefore, it is always imperative to calculate the BCF values based on the mobile fraction of the elements. Among the mobile fraction, the exchangeable fraction is more prone to be taken up by the plant, as it is easily mobilised from the sediments whenever a slight change in pH or salinity occurs.

When considering the mobile fraction, cadmium has the highest average BCF values next to that of Mn. The BCF_{Root} value for Cd was 1.12 at CR-04, indicating Cd accumulation in the mangrove roots. The bioconcentration factors within the mangrove tissues followed the order of root > leaves > bark for the elements Fe, Mn, Co, Cu. For Zn the BCF values were in the order, bark > root > leaves and root > bark > leaves in the case of Pb and Cd.

Table 9.5 Bioconcentration factors in the mangrove Sonneratia caseolaris (Engl.) collected from the Baram River estuarine region based on total metal concentrations

Samples	Fe			Mn			Co		
	BCF_{Root}	BCF_{Bark}	BCF_{Leaves}	BCF_{Root}	BCF_{Bark}	BCF_{Leaves}	BCF_{Root}	BCF_{Bark}	BCF_{Leaves}
CR 01	0.02	0.01	0.01	0.27	0.22	0.16	BDL	BDL	BDL
CR 02	0.03	0.01	0.01	0.64	0.35	0.52	0.14	BDL	BDL
CR 03	0.04	0.01	0.01	0.66	0.36	0.50	0.15	BDL	BDL
CR 04	0.27	0.01	0.02	1.06	0.38	0.68	0.33	BDL	0.03
CR 05	0.03	0.01	0.02	1.14	0.64	1.05	0.13	BDL	BDL
CR 06	0.03	0.01	0.01	0.66	0.33	0.46	0.12	BDL	BDL
Average	**0.07**	**0.01**	**0.01**	**0.74**	**0.38**	**0.56**	**0.17**	**BDL**	**0.03**

Samples	Cu			Zn			Pb		
	BCF_{Root}	BCF_{Bark}	BCF_{Leaves}	BCF_{Root}	BCF_{Bark}	BCF_{Leaves}	BCF_{Root}	BCF_{Bark}	BCF_{Leaves}
CR 01	0.07	0.03	0.05	0.12	0.07	0.10	0.12	0.05	0.07
CR 02	0.06	0.02	0.06	0.11	0.04	0.11	0.11	0.07	0.10
CR 03	0.06	0.03	0.05	0.11	0.03	0.11	0.13	0.06	0.07
CR 04	0.13	0.07	0.07	0.18	1.10	0.12	0.38	0.28	0.09
CR 05	0.14	0.03	0.06	0.39	0.04	0.14	0.24	0.06	0.07
CR 06	0.05	0.02	0.05	0.10	0.03	0.10	0.13	0.05	0.06
Average	**0.09**	**0.03**	**0.06**	**0.17**	**0.22**	**0.11**	**0.19**	**0.10**	**0.08**

Table 9.6 Bioconcentration factors in the mangrove Sonneratia caseolaris (Engl.) collected from the Baram River estuarine region based on metal concentrations in mobile fractions

Samples	Fe			Mn			Co			Cu		
	BCF_{Root}	BCF_{Bark}	BCF_{Leaves}	BCF_{Root}	BCF_{Bark}	BCF_{Leaves}	BCF_{Root}	BCF_{Bark}	BCF_{Leaves}	BCF_{Root}	BCF_{Bark}	BCF_{Leaves}
CR 01	0.05	0.02	0.02	0.32	0.25	0.19	BDS	BDL	BDS	0.08	0.04	0.06
CR 02	0.08	0.01	0.03	0.75	0.42	0.61	0.16	BDL	BDS	0.07	0.03	0.07
CR 03	0.10	0.02	0.02	0.78	0.42	0.60	0.17	BDL	BDS	0.07	0.03	0.06
CR 04	0.66	0.03	0.04	1.25	0.45	0.80	0.37	BDL	0.04	0.15	0.08	0.09
CR 05	0.07	0.02	0.04	1.34	0.75	1.24	0.15	BDL	BDS	0.17	0.03	0.07
CR 06	0.06	0.02	0.03	0.78	0.39	0.54	0.14	BDL	BDS	0.06	0.02	0.06
Average	**0.17**	**0.02**	**0.03**	**0.87**	**0.45**	**0.66**	**0.20**	**BDL**	**0.04**	**0.10**	**0.04**	**0.07**

Samples	Zn			Pb			Cd		
	BCF_{Root}	BCF_{Bark}	BCF_{Leaves}	BCF_{Root}	BCF_{Bark}	BCF_{Leaves}	BCF_{Root}	BCF_{Bark}	BCF_{Leaves}
CR 01	0.18	0.10	0.15	0.16	0.07	0.09	0.56	0.46	BDL
CR 02	0.17	0.05	0.17	0.14	0.09	0.13	0.52	0.41	0.32
CR 03	0.16	0.05	0.16	0.17	0.08	0.09	0.61	0.40	0.31
CR 04	0.26	1.65	0.19	0.50	0.37	0.12	1.12	0.40	0.41
CR 05	0.58	0.05	0.22	0.30	0.07	0.09	0.84	0.41	0.41
CR 06	0.15	0.04	0.15	0.17	0.07	0.07	0.51	0.41	0.36
Average	**0.25**	**0.33**	**0.17**	**0.24**	**0.12**	**0.10**	**0.69**	**0.41**	**0.36**

Table 9.7Bioconcentration factors in the mangrove Sonneratia caseolaris (Engl.) collected from the Baram River estuarine region based on element concentrations in surface water

Samples	Fe			Mn			Cu			Zn		
	BCF_{Root}	BCF_{Bark}	BCF_{Leaves}	BCF_{Root}	BCF_{Bark}	BCF_{Leaves}	BCF_{Root}	BCF_{Bark}	BCF_{Leaves}	BCF_{Root}	BCF_{Bark}	BCF_{Leaves}
CR 01	114.18	52.78	44.76	511.30	411.27	303.65	72.03	34.39	55.41	261.35	144.89	216.72
CR 02	195.01	31.94	72.60	1215.38	676.67	991.33	60.89	24.29	62.33	239.06	76.59	243.69
CR 03	231.51	36.98	58.69	1260.23	684.67	962.33	67.49	31.08	57.30	224.81	68.50	225.62
CR 04	1611.78	59.79	100.17	2016.24	725.82	1296.15	139.75	71.60	81.22	374.53	2350.11	263.98
CR 05	176.60	39.80	98.11	2170.74	1219.85	2003.55	157.43	28.45	61.76	830.14	75.91	308.86
CR 06	151.75	50.13	73.35	1259.40	625.90	869.82	56.15	19.39	55.25	206.91	58.73	210.61
Average	**413.47**	**45.24**	**74.61**	**1405.55**	**724.03**	**1071.14**	**92.29**	**34.87**	**62.21**	**356.13**	**462.46**	**244.91**

Samples	Pb			Cd			Co		
	BCF_{Root}	BCF_{Bark}	BCF_{Leaves}	BCF_{Root}	BCF_{Bark}	BCF_{Leaves}	BCF_{Root}	BCF_{Bark}	BCF_{Leaves}
CR 01	132.09	56.47	73.16	53.01	42.90	BDL	BDL	BDL	BDL
CR 02	117.21	73.04	108.51	48.69	38.84	30.37	43.55	BDL	BDL
CR 03	137.35	67.91	75.91	57.66	38.01	29.53	45.28	BDL	BDL
CR 04	410.34	301.21	100.38	105.01	37.68	38.82	99.71	BDL	9.30
CR 05	251.38	59.21	73.88	78.63	38.16	38.33	39.25	BDL	BDL
CR 06	142.15	54.14	61.42	47.84	38.38	33.78	36.68	BDL	BDL
Average	**198.42**	**102.00**	**82.21**	**65.14**	**38.99**	**34.17**	**52.89**	**BDL**	**BDL**

Table 9.8 Bioconcentration factors in the mangrove Sonneratia caseolaris (Engl.) collected from the Baram River estuarine region based on total metal concentrations in short core (BSC-01) (River Mouth)

Core Subsamples	Depth (cm)	Fe			Mn			Co		
		BCF_{Root}	BCF_{Bark}	BCF_{Leaves}	BCF_{Root}	BCF_{Bark}	BCF_{Leaves}	BCF_{Root}	BCF_{Bark}	BCF_{Leaves}
BSC-01-I	0-4	0.12	0.05	0.05	0.93	0.74	0.55	BDL	BDL	BDL
BSC 01-II	4-8	0.13	0.06	0.05	0.93	0.74	0.55	BDL	BDL	BDL
BSC 01-III	8-12	0.12	0.05	0.05	1.16	0.93	0.69	BDL	BDL	BDL
BSC 01-IV	12-16	0.08	0.04	0.03	0.93	0.74	0.55	BDL	BDL	BDL
BSC 01-V	16-20	0.12	0.06	0.05	1.32	1.06	0.79	BDL	BDL	BDL
BSC 01-VI	20-24	0.03	0.02	0.01	0.44	0.35	0.26	BDL	BDL	BDL
BSC 01-VII	24-28	0.13	0.06	0.05	1.85	1.49	1.10	BDL	BDL	BDL
BSC 01-VIII	28-32	0.12	0.06	0.05	1.85	1.49	1.10	BDL	BDL	BDL
BSC 01-IX	32-36	0.11	0.05	0.04	1.85	1.49	1.10	BDL	BDL	BDL
Average	-	**0.11**	**0.05**	**0.04**	**1.25**	**1.01**	**0.74**	**BDL**	**BDL**	**BDL**

Core Subsamples	Depth (cm)	Cu			Zn			Pb		
		BCF_{Root}	BCF_{Bark}	BCF_{Leaves}	BCF_{Root}	BCF_{Bark}	BCF_{Leaves}	BCF_{Root}	BCF_{Bark}	BCF_{Leaves}
BSC-01-I	0-4	0.03	0.02	0.02	0.16	0.09	0.14	0.08	0.03	0.04
BSC 01-II	4-8	0.05	0.02	0.04	0.20	0.11	0.16	0.09	0.04	0.05
BSC 01-III	8-12	0.01	0.00	0.01	0.04	0.02	0.03	0.22	0.10	0.12
BSC 01-IV	12-16	0.01	0.00	0.00	0.03	0.02	0.03	0.15	0.06	0.08
BSC 01-V	16-20	0.01	0.00	0.00	0.03	0.02	0.03	0.22	0.10	0.12
BSC 01-VI	20-24	0.01	0.00	0.00	0.03	0.01	0.02	0.11	0.05	0.06
BSC 01-VII	24-28	0.01	0.00	0.00	0.03	0.02	0.02	0.10	0.04	0.06
BSC 01-VIII	28-32	0.01	0.00	0.00	0.03	0.02	0.03	0.15	0.06	0.08
BSC 01-IX	32-36	0.01	0.00	0.01	0.04	0.02	0.03	0.08	0.03	0.04
Average	-	**0.01**	**0.01**	**0.01**	**0.07**	**0.04**	**0.05**	**0.13**	**0.06**	**0.07**

Table 9.9 Bioconcentration factors in the mangrove Sonneratia caseolaris (Engl.) collected from the Baram River estuarine region based on total metal concentrations in short core (BSC-06) (upstream mangrove area)

Core Subsamples	Depth (cm)	Fe			Mn			Co		
		BCF_{Root}	BCF_{Bark}	BCF_{Leaves}	BCF_{Root}	BCF_{Bark}	BCF_{Leaves}	BCF_{Root}	BCF_{Bark}	BCF_{Leaves}
BSC-06-I	0-4	0.03	0.01	0.01	0.88	0.44	0.61	0.12	BDL	BDL
BSC 06-II	4-8	0.02	0.01	0.01	0.56	0.28	0.38	0.11	BDL	BDL
BSC 06-III	8-12	0.02	0.01	0.01	0.53	0.26	0.37	0.10	BDL	BDL
BSC 06-IV	12-16	0.02	0.01	0.01	0.60	0.30	0.41	0.10	BDL	BDL
BSC 06-V	16-20	0.02	0.01	0.01	0.58	0.29	0.40	0.11	BDL	BDL
BSC 06-VI	20-24	0.02	0.01	0.01	0.65	0.32	0.45	0.11	BDL	BDL
BSC 06-VII	24-28	0.02	0.01	0.01	0.51	0.25	0.35	0.11	BDL	BDL
BSC 06-VIII	28-32	0.03	0.01	0.01	0.67	0.33	0.46	0.11	BDL	BDL
BSC 06-IX	32-36	0.03	0.01	0.01	0.69	0.34	0.48	0.12	BDL	BDL
Average	**-**	**0.02**	**0.01**	**0.01**	**0.63**	**0.31**	**0.44**	**0.11**	**BDL**	**BDL**

Core Subsamples	Depth (cm)	Cu			Zn			Pb		
		BCF_{Root}	BCF_{Bark}	BCF_{Leaves}	BCF_{Root}	BCF_{Bark}	BCF_{Leaves}	BCF_{Root}	BCF_{Bark}	BCF_{Leaves}
BSC-06-I	0-4	0.01	0.00	0.01	0.04	0.00	0.04	0.07	0.03	0.03
BSC 06-II	4-8	0.01	0.00	0.01	0.04	0.00	0.04	0.09	0.03	0.04
BSC 06-III	8-12	0.02	0.01	0.02	0.06	0.01	0.06	0.10	0.04	0.04
BSC 06-IV	12-16	0.01	0.01	0.01	0.05	0.01	0.05	0.10	0.04	0.04
BSC 06-V	16-20	0.02	0.01	0.02	0.06	0.01	0.06	0.09	0.04	0.04
BSC 06-VI	20-24	0.01	0.00	0.01	0.03	0.00	0.03	0.10	0.04	0.04
BSC 06-VII	24-28	0.02	0.01	0.02	0.05	0.01	0.05	0.11	0.04	0.05
BSC 06-VIII	28-32	0.02	0.01	0.02	0.05	0.01	0.05	0.12	0.05	0.05
BSC 06-IX	32-36	0.01	0.00	0.01	0.04	0.00	0.04	0.12	0.05	0.05
Average	**-**	**0.01**	**0.01**	**0.01**	**0.05**	**0.01**	**0.05**	**0.10**	**0.04**	**0.04**

9.8 Translocation factors

The translocation factor is the quantitative expression of trace element transport from mangrove roots to other parts. The translocation factor also explains the phyto-extraction capacity, which is the ability of the plant to extract contaminants from their tissues. The translocation factor was calculated from the following equation:

Translocation factor for the leaf: $TF_{Leaf} = C_{Leaf}/C_{Root}$

Translocation factor for the bark: $TF_{Bark} = C_{Bark}/C_{Root}$

Where, C_{Leaf}, C_{Bark} and C_{Root} are the trace element concentrations in leaf, bark and root, respectively. A translocation factor > 1 indicates preferential partitioning of metals to the shoots (Phaenark et al., 2009;Chowdhury et al., 2016).

The translocation factors for TF_{Leaf} and TF_{Bark} are presented in Table 9.10 and Table 9.11, respectively. Zn exhibited a relatively higher TF_{Leaf} translocation factor than other elements. The average TF_{Leaf} translocation factor showed the following pattern: Zn (0.83)>Cu (0.77)>Mn (0.74)>Cd (0.54)>Pb (0.50)>Fe (0.35)>Co (0.09). The site CR-02 showed a higher translocation factor of 1.02 for Cu, and 1.02 for Zn. The sites CR-03 and CR-06 also showed TF_{Leaf} values of 1.00 and 1.01, respectively for Zn indicating preferential partitioning of these particular elements to the leaves.

The TF_{Bark} values showed the following pattern Zn (1.31)>Cd (0.65)>Mn (0.55) >Pb (0.48)>Cu (0.40)>Fe (0.23). Cobalt was completely absent in the bark of the mangroves, and hence the TF_{Bark} values for Co were not detected (ND). The site CR-04 showed a very high translocation factor of 6.28 for Zn. Such a high concentration of Zn was observed in *Avicennia marina* and more details are given in MacFarlane and Burchett (1999). This high value represents the inherent capacity of phytoextraction of the bark from the mangrove of that particular site. The reasons for such a localised high phytoextraction capacity are unknown. The values of all other sites are less than unity.

Table 9.10 Translocation factor (TF_{Leaf}) in the mangrove Sonneratia caseolaris (L.) Engl. collected from the Baram estuarine region

Samples	Cd	Co	Cu	Fe	Mn	Pb	Zn
CR 01	BDL	BDL	0.77	0.39	0.59	0.55	0.83
CR 02	0.62	BDL	1.02	0.37	0.82	0.93	1.02
CR 03	0.51	BDL	0.85	0.25	0.76	0.55	1.00
CR 04	0.37	0.09	0.58	0.06	0.64	0.25	0.71
CR 05	0.49	BDL	0.39	0.56	0.92	0.29	0.37
CR 06	0.71	BDL	0.98	0.48	0.69	0.43	1.02
Average	**0.54**	**0.09**	**0.77**	**0.35**	**0.74**	**0.50**	**0.83**

Table 9.11 Translocation factor (TF_{Bark}) in the mangrove Sonneratia caseolaris (Engl.) collected from the Baram estuarine region

Samples	Cd	Co	Cu	Fe	Mn	Pb	Zn
CR 01	0.81	BDL	0.48	0.46	0.80	0.43	0.55
CR 02	0.80	BDL	0.40	0.16	0.56	0.62	0.32
CR 03	0.66	BDL	0.46	0.16	0.54	0.49	0.31
CR 04	0.36	BDL	0.51	0.04	0.36	0.73	6.28
CR 05	0.49	BDL	0.18	0.23	0.56	0.24	0.09
CR 06	0.80	BDL	0.35	0.33	0.50	0.38	0.28
Average	**0.65**	**BDL**	**0.40**	**0.23**	**0.55**	**0.48**	**1.31**

9.9 Analysis of variance (ANOVA) between Bioconcentration factors (BCF) based on surface sediments and core sediments

The BCFdata (Table 9.5 to Table 9.9) were subjected to ANOVA to determine whether there was a significant ($P < 0.05$) difference between these values. The ANOVA results are given in Appendix-4-8 and the summary of the results are presented in Table 9.12.

9.10 Significance of BCF values within root, bark and leaves

There is no significant difference ($P < 0.05$) of BCF values amongst the tissues for Fe, Mn, Zn and Pb. This then implies the plant physiology does not differentiate the accumulation of these elements in different tissues. However, between the tissues there was a significant difference ($P < 0.05$) for Cu, indicating the active intervention by plant physiology in the translocation of copper. Similar to Cu, the Cd translocation is also controlled by plant physiology. However, the bulk

sediment analysis for Cd in the sediments was not done. Hence, it has not been considered for further discussion. It is noted here though Mn, Zn and Cd are being accumulated in the plant, their translocation was active within the mangroves and no significant differences were observed in their accumulation in various tissues.

9.10.1 The accumulation of iron in mangrove tissues:

The calculated BCF values among the sites in the bark and leaves are different when the surface sediment concentrations and core sediment concentrations are considered. At the BSC-01 location, there was a significant difference (denoted as "S" in Table 9.12 under the column BCF_{Bark} and BCF_{Leaves}), but at the BSC-06 location, there was no significant difference. Since iron is not significantly different between the tissues, a significant difference at the BSC-01 location implies there was a differential uptake of iron from the surface and bottom sediments. However, from the available data, the study could not confirm whether surface or bottom sediments were the source of Fe for the mangroves. For the same reason, a non-significant difference at the BSC-06 location implied there was no differential uptake of iron from the surface and bottom sediments. Because rhizosphere spreads from the surface to the bottom sediments, such a difference was mainly due to early diagenetic reactions within the sediments that affected the mobility of iron. On the surface, iron is expected to be in the oxidised form, and its bioavailability should be limited compared to the bottom sediments where early diagenetic reactions might release Fe^{2+} ions to the pore water and facilitate its uptake into the mangroves. Such a conclusion can be ascertained because there was a significant difference in the BCF values of bark and leaves for both locations (BSC-01 and BSC-06) when the surface water concentration of Fe was used for computation. When there was no differentiation of iron among the tissues (i.e., translocation of Fe is active), a non-significant difference at the BSC-06 location but a significant difference for all other values (i.e, BCF_{Bark} of BSC-01, BCF_{Leaves} of BSC-01 - BCF values calculated using surface sediment concentration of Fe; BCF_{Bark} of BSC-01 and BSC-06, BCF_{Leaves} of BSC-01, BSC-06 - BCF values calculated using surface water concentration of Fe) this would tend to imply that only at this location did the surface and bottom sediment characteristics remain the same. The BSC-06 location is in a comparatively low salinity region (salinity: 5.4‰) towards upstream. Under such conditions, there should be no difference in the mobility of iron from both surface and bottom

sediments due to the prevailing low pH (~5 to 6) conditions in the river water. Consequently, the availability of dissolved iron should be greater and that is the reason why there was a higher Fe concentration in the mangrove roots at the BSC-06 location. Therefore, we had a non-significant difference for the calculated values of BCF for bark and leaves at the BSC-06 location. Whereas, the mixing up of seawater with the river water and the presence of waves, currents and tides at the BSC-01 location might have resulted in the flocculation and precipitation of dissolved iron, and were flushed out from the surface sediments. Therefore, greater differences might exist between the surface and bottom sediment concentrations of iron. Therefore, the BCF values calculated for surface and core sediments varied significantly at this location. Similar arguments are applicable for the BCF values calculated using the water column concentration of Fe. The overall picture in this investigation is that, under low pH and in a low salinity region, the surface sediment concentration of Fe can be used for the calculation of BCF; but, in a comparatively higher salinity region, the calculation of the BCF, based on the core sediment concentration is the more suitable estimate.

9.10.2 The accumulation of manganese in mangrove tissues

There exists a significant difference in the BCF values of Mn for root and bark tissues between sites when the surface and core sediment concentrations are considered for the calculation of BCF. At the BSC-01 location, there was a significant difference, but at the BSC-06 location, there was no significant difference, similar to iron. However, there was a noticeable difference between the bioaccumulation of Fe and Mn. For iron, the significant difference was observed between BCF_{Bark} and BCF_{Leaves}. However, in the case of Mn, the difference occurred between the BCF_{Root} and BCF_{Bark}.

However, the tissue concentrations of Mn did not vary significantly between different tissues and sites. Nevertheless, the BSC-01 location exhibited a significant difference implying the differential uptake of Mn from the surface and bottom sediments. From the existing data, it is not possible to discern whether the surface or bottom sediments were the source of Mn for the mangroves. For the same reason, a non-significant difference at the BSC-06 location implied there was no differential uptake of Mn from the surface and bottom sediments. As seen previously in the case of Fe, the early diagenetic reactions facilitate the uptake of Mn into the mangroves.

When the surface water concentration of Mn was used for computation, the BCF values varied significantly for all the tissues for both locations (BSC-01 and BSC-06). The non-significance of Mn concentrations in all the tissues and sites implied the active translocation of Mn. A non-significant difference at the BSC-06 location but a significant difference at all other values meant the surface and core sediment characteristics were not the same. This then implied the physiology of mangroves play a predominant role in the accumulation of Mn under varying environmental conditions.

9.10.3 The accumulation of copper in mangrove tissues

The BCF values for Cu calculated between the sites in all the tissues were significantly different when the surface and core sediment concentrations were considered. When the surface water concentrations were used for the computation of BCF, the same trend repeated (i.e. a significant difference of BCF between tissues at the locations BSC-01 and BSC-06). This pattern indicated the environment did not exert a significant control in the accumulation of Cu in the mangroves but rather the effective regulation of the mangrove plant controlled the accumulation of Cu. Moreover, such a conclusion was very clear as the Cu concentrations varied significantly ($P < 0.05$) between different tissues and sites.

9.10.4 The accumulation of zinc in mangrove tissues

The BCF values for Zn calculated between the sites in roots and leaves were significantly different when the surface and core sediment concentrations were considered at both the locations (BSC-01 and BSC-06). However, the BCF_{Bark} values were not significantly different. When the surface water concentrations were used for computation of BCF for Zinc, the same exact pattern was repeated for BSC-01 and BSC-06. The Zn concentrations between the tissues did not vary significantly among all the sites. Such a trend implies that irrespective of different levels of Zn in the water, surface and core sediments, all of them have the same effect on the accumulation of Zn in the mangroves. However, the non-significant variation of BCF_{Bark} implied the accumulation of Zn in the bark as evidenced from the translocation factor of > 1 ($TF_{bark} = 1.31$).

9.10.5 The accumulation of lead in mangrove tissues

The BCF values of Pb calculated for all the tissues did not show any significant difference at the BSC-01location. At the BSC-06 location, there was a significant difference for BCF_{Root} and BCF_{Leves}, but the BCF_{Bark} showed no significant difference. However, the tissue concentrations of Pb did not vary significantly between different tissues and sites. Nevertheless, at the BSC-06 location, a significant difference was observed for BCF_{Root} and BCF_{Leaves}, implying the differential uptake of Pb from the surface and bottom sediments. As a result, it was impossible to determine whether the surface or core sediments were responsible for Pb uptake in mangrove plants. For the same reason, a non-significant difference at the BSC-01 location implied there was no differential uptake of Pb from the surface and bottom sediments. As seen previously in the case of Fe and Mn the early diagenetic reactions facilitated the uptake of Pb by the mangroves. When the surface water concentration of Pb was used for computation, the BCF values varied significantly for all the tissues for both locations (BSC-01 and BSC-06). The non-significance of Pb concentrations in all the tissues and sites indicated its efficient translocation within the plant. The non-significant difference at the BSC-01 location but a significant difference at all other locations implies the surface and core sediment characteristics are not the same. This suggests the physiology of mangroves plays a predominant role in the accumulation of Pb, under varying environmental conditions.

Table 9.12 Results of Analysis of variance (ANOVA) performed in the present study

ANOVA Results	Fe			Mn			Cu			Zn			Pb		
	BCF_{Root}	BCF_{Bark}	BCF_{Leaves}	BCF_{Root}	BCF_{Bark}	BCF_{Leaves}	BCF_{Root}	BCF_{Bark}	BCF_{Leaves}	BCF_{Root}	BCF_{Bark}	BCF_{Leaves}	BCF_{Root}	BCF_{Bark}	BCF_{Leaves}
Surface sediment BCF vs BCF of															
Core 1	NS	S	S	S	S	NS	S	S	S	S	NS	S	NS	NS	NS
Core 6	NS	NS	NS	NS	NS	NS	S	S	S	S	NS	S	S	NS	S

S-Significant; NS- Not significant

ANOVA Results	Fe			Mn			Cu			Zn			Pb		
	BCF_{Root}	BCF_{Bark}	BCF_{Leaves}	BCF_{Root}	BCF_{Bark}	BCF_{Leaves}	BCF_{Root}	BCF_{Bark}	BCF_{Leaves}	BCF_{Root}	BCF_{Bark}	BCF_{Leaves}	BCF_{Root}	BCF_{Bark}	BCF_{Leaves}
Surface water BCF vs BCF of															
Core 1	NS	S	S	S	S	S	S	S	S	S	NS	S	S	S	S
Core 6	NS	S	S	S	S	S	S	S	S	S	NS	S	S	S	S

S-Significant; NS- Not significant

ANOVA – Element concentrations between all tissues-all sites					
Fe	**Mn**	**Cu**	**Zn**	**Pb**	**Cd**
NS	NS	S	NS	NS	S

S-Significant; NS- Not significant

ANOVA – BCF between all tissues-all sites						
Elements	**Fe**	**Mn**	**Cu**	**Zn**	**Pb**	**Cd**
BCF of metals based on						
Total Fraction	NS	NS	S	NS	NS	NA
Mobile Fraction	NS	NS	S	NS	NS	S

S-Significant; NS- Not significant; NA-Not available

9.11 Comparison with some similar studies around the world

The level of trace elements in different tissues of mangroves specifically, root/pneumatophores, bark and leaves and the calculated BCF and TF were compared with similar studies from elsewhere in the world. The results are discussed forthwith.

9.11.1 Iron (Fe)

Iron is an essential element for plants and is mainly involved in photosynthesis, nitrogen fixation, and chloroplast development. In the present study, the Fe concentration ranged from 203.49 µg g^{-1} to 455.46µg g^{-1} with a mean of 339.25µg g^{-1}in the leaves. In the case of bark, it ranged from 145.22 µg g^{-1} to 271.86 µg g^{-1} with a mean of 205.67 µg g^{-1}, and, in the root/pneumatophores, it ranged from 519.15 µg g^{-1} to 7328.40 µg g^{-1} with a mean of 1879.96 µg g^{-1}. The BCF for Fe ranged from 0.02 to 0.27 with a mean of 0.07 for BCF_{Root}, the range was from 0.01 to 0.01 with a mean of 0.01 for BCF_{Bark} and 0.01 to 0.01 with a mean of 0.01for BCF_{Leaves}. The TF were 0.06 to 0.56 with a mean of 0.35 for TF_{Leaf} and, 0.04 to 0.46 with a mean of 0.23 for TF_{Bark}. A member of the same genus, *Sonneratia apetala* in the Indian Sundarban wetland, was found to be a hyper-accumulator, with the Fe concentration of about 1376.70µg g^{-1} in the pneumatophore (Chowdhury et al., 2017). The Fe accumulation in the Indian Sundarban is comparatively lower than the Fe levels in the roots/pneumatophore of *Sonneratia caseolaris* in the present study, which was found to be 1879.96 µg g^{-1}. Iron content was found to be very high in the twigs of *Sonneratia caseolaris* from Kerala, India, which ranged from 1200 to 5940 µg g^{-1} (Thomas & Fernandez, 1997).

The *Sonneratia apetala* displayed a higher BCF of about 10.70 for Fe in the contaminated sites of the Indian Sundarban wetland and was found to be a promising candidate for phyto-remediation (Chowdhury et al., 2016). However, the calculated BCF values of *Sonneratia caseolaris* of the present study were greater.

9.11.2 Manganese (Mn)

Mn is also an essential element for plants. It is involved in the photo production of oxygen in chloroplasts and is associated with nitrate reduction. In the present study, Mn concentration in the leaves of *Sonneratia caseolaris* ranged from 42.56 µg g^{-1} to 280.86 µg g^{-1} with a mean of 150.15 µg g^{-1} whereas in the bark it

varied from 57.65 µg g^{-1} to 171.00 µg g^{-1} with an average of 101.49 µg g^{-1}. In the case of the root/pneumatophore tissue, the Mn concentration ranged from 71.67 µg g^{-1} to 304.29µg g^{-1} with an average of 197.03 µg g^{-1}. Similar to that of Fe, the roots of the mangrove plant of the present study showed relatively higher concentrations when compared to other tissues, thus concurring with the above discussion. The bioconcentration factors for Mn ranged from 0.27 to 1.14 with an average of 0.74 for BCF_{Root}, 0.22 to 0.64 with a mean of 0.38 for BCF_{Bark} and 0.16 to 1.05 with an average of 0.56 for BCF_{Leaves}. The translocation factors were 0.59 to 0.92 with an average of 0.74 for leaves and 0.36 to 0.80 with an average of 0.55 for bark.

The comparatively higher concentration of manganese was observed in the twigs of the same *Sonneratia caseolaris* from Kerala, India (258 µg g^{-1} to 1793 µg $^{-1}$, Thomas & Fernandez, 1997). Similarly, a several times higher concentration of Mn was observed in the mature leaves of *Sonneratia apetala* from the Indian Sundarban wetland (Chowdhury et al., 2016). However, a relatively lower concentration of Mn (root: 185.00 µg g^{-1}, stem: 119.00 µg g^{-1} and leaves: 87.60 µg g^{-1}) was observed in *Sonneratia apetala* of the Nansha mangrove, in Southern China (Wu et al., 2014). In the Indian Sundarban mangroves, *Sonneratia apetala* recorded high BCF values for Mn (2.34 in leaves, 1.44 in bark and 1.04 in the pneumatophore). The same plant also exhibited a higher TF of 2.34 for Mn, which was greater than in the present study. In the present study, the BCF exceeded 1 in the root/pneumatophore tissues for two sites CR-04 (1.06) and CR-05 (1.14), and in the leaf tissue of CR-05 (1.05). However, the TF remained close to 1 (0.92) in the CR-05 location. While the TF value of close to 1, indicated the active translocation of Mn from root to above ground biomass in *Sonneratia caseolaris*. A good candidate for phyto-remediation should have a BCF and TF greater than 1 (Yoon et al., 2006; Usman et al., 2013). Thus, the genus *Sonneratia* can be used as a potential accumulator species for Mn (Chowdhury et al., 2017).

9.11.3 Copper (Cu)

Cu is an essential element, necessary for mangrove growth (Marchand et al., 2016). It is directly involved in the photosynthesis 1 and photosynthetic electron transport (Maksymiec, 1998). In the present study, Cu concentration in the leaves of *Sonneratia caseolaris* ranged from 2.91 µg $g^{-1}$to 4.28 µg g^{-1} with a mean of 3.28 µg g^{-1},whereas in the bark the concentration ranged from 1.02 µg g^{-1} to 3.77 µg g^{-1} with

a mean of 1.84 µg g^{-1}. In the root/pneumatophores tissue, Cu concentration varied between 2.96 µg $g^{-1}$and 8.30 µg g^{-1} with a mean of 4.87µg g^{-1}. The bio-concentration factors for Cu ranged from 0.05 to 0.14 with an average of 0.09 for BCF_{Root}, from 0.02 to 0.66with an average of 0.03 for BCF_{Bark} and from 0.05 to 0.07 with an average of 0.06 for BCF_{Leaves}. The translocation factors were 0.39 to 1.02 with a mean of 0.77 for leaves and 0.18 to 0.51 with a mean of 0.40 for bark.

The concentration of Cu in the leaves of *S. caseolaris,* studied in the Futian mangrove forest, China was found to be 15.04µg g^{-1}, which was much higher than the present study. Furthermore, Cu in the leaves of *S. caseolaris* remained stable and was not affected by severe pollution (He et al., 2014). The leaves of *S. caseolaris* from Hainan Island, China, showed a Cu concentration of 6.60µg g^{-1} representing a higher concentration than the present study (Lian et al., 1999). The accumulation abilities of Cu in three mangrove species decreased in the following sequence: *S. caseolaris>S. apetala>K. candel* (Zan et al., 2002; review by Zhang et al., 2014). Cu concentration in the leaves of *S. caseolaris* from Peninsular Malaysia was found to be 26.80µg g^{-1}, which was also much higher than the present study (Nazli & Hashim, 2010). *S. apetala* being a hyper-accumulator adsorbed about 25.89µg g^{-1} in its pneumatophores tissue however, besides this higher concentration the low BCF can be attributed to the metal uptake restriction mechanism of mangroves and/ or by low bioavailability of Cu in the sediment (Chowdhury et al. 2017). Copper concentrations from the *S.apetala* collected from the Nansha mangrove was found to be 13.00µg g^{-1}, 3.18 µg g^{-1} and 2.66 µg g^{-1} in the roots, stem and leaves, respectively with a BCF of 0.06, which was comparable to the present study (Wu et al., 2014). The low BCF was explained by the exclusion mechanisms adopted by mangroves in order to avoid excessive metal uptake (MacFarlane et al., 2003).

9.11.4 Zinc (Zn)

Zinc plays a core role in plant physiology. It is an integral component of enzyme systems in higher plants and is the only element present in 6 enzyme classes (Auld, 2001; Broadley et al., 2007). In the present study, Zn concentration in the leaves of *Sonneratia Caseolaris* was found to be in the range of 7.85 µg g^{-1} to 11.52 µg g^{-1} with a mean of 9.13 µg g^{-1}, whereas in case of bark it varied between 2.19 µg $g^{-1}$and 87.63 µg g^{-1} with a mean of 17.24 µg g^{-1}. In the root/pneumatophore tissue, Zn concentration ranged from 7.72µg $g^{-1}$and 30.95µg $g^{-1}$with a mean of 13.28µg g^{-1}.

The BCF for Zn ranged from 0.10 and 0.39 with a mean of 0.17 for BCF_{Root}, 0.03 to 1.10 with a mean of 0.22 for BCF_{Bark} and 0.10 to 0.14 with a mean of 0.11for $BCF_{Leaves.}$ The translocation factors were 0.37 to 1.02 with a mean of 0.83 for leaves and 0.09 to an unusual higher value of 6.28 with a mean of 1.31 for Bark.

Zinc concentration in the leaves of *S. caseolaris* collected from Hainan Island was found to be 36.00µg g^{-1} with a BCF_{leaf} of 1.30 (Lian et al., 1999), which is much higher than the present study. Similarly, a trend was observed in *S. caseolaris* collected from Kerala, India where Zn concentration varied between 41.00 µg g^{-1} to 67.00µg g^{-1} (Thomas & Fernandez, 1997). The fine roots, thick roots, branch and leaves of *S. apetala* from the Futian mangrove swamp, South China was analysed for Zn which resulted in concentrations of 190.00 µg g^{-1}, 25.00 µg g^{-1}, 11.00 µg g^{-1} and 40.00 µg g^{-1} (Wang et al., 2013), which was also somewhat higher than the present study. However, Zn in the leaves of *Sonneratia caseolaris* was 5.90 µg g^{-1} collected from Peninsular Malaysia (Nazli & Hashim, 2010), was lower than in the present study. The accumulation trend of Zn by three mangrove species decreased in the following sequence. S.*caseolaris* >*S.apetala* >*K.candel in* South China (Zan et al., 2002; review by Zhang et al., 2014).

The leaf concentration of Zn in *S. caseolaris* from the Futian mangrove forest was found to be 71.64 (He et al., 2014), which is many times higher than the present study. Zn concentration in the roots, stems and leaves of *S. apetala* from the Nasha mangrove, South China was found to be 19.10 µg g^{-1}, 10.10 µg g^{-1} and 17.60 µg g^{-1}, which was also marked higher than the present study. Apart from the accumulation, the average BCF for this study was almost similar to all the compared studies. However, at one site CR 04, Zn concentration was recorded as 87.63 in the bark tissue, which was greater than the background sediment concentration of the present study. Mangroves can accumulate metals at a magnitude of several times greater than the surrounding sedimentary environment (MacFarlane, 2002). The mean BCF_{Bark} was recorded as 1.10 and the translocation from root to bark was found to be 1.31 whereas the translocation of Zn from root to leaves was found to be 0.83, which exceeded the results at one site and showed effective transport of Zn from root to above ground parts in the present study. A member of the same genus, *Sonneratia apetala* from the Indian Sundarban mangrove wetland was found to possess a TF of about 9.95 for Zn making it a good candidate for phytoremediation (Chowdhury et al., 2016).

9.11.5 Lead (Pb)

Lead is a non-essential element in plants. Lead through aerosol emissions makes its way into plants either directly by above-ground shoot parts or is taken up from the soil through the root system (Wierzbicka, 1995). In addition to anthropogenic influence, there are natural sources of Lead (Holl & Hampp, 1975). In the present study, the concentration of Pb in the leaves of *Sonneratia Caseolaris* ranged between 0.83 µg g^{-1} and 1.46 µg g^{-1} with a mean of 1.11 µg g^{-1}, whereas in the case of bark it ranged from 0.73µg $g^{-1}$and 4.06 µg g^{-1} with a mean of 1.38 µg g^{-1}. In the root/pneumatophores tissue, the Pb concentration varied from 1.58 µg $g^{-1}$and 5.53µg g^{-1} with a mean of 2.68 µg g^{-1}. The BCF for Pb ranged from 0.38 to 0.11 with a mean of 0.19 for BCF_{Root}, 0.28 to 0.05 with a mean of 0.10 for BCF_{Bark} and 0.10 to 0.06 with a mean of 0.08 for BCF_{Leaves}. The translocation factors were 0.25 to 0.93 with a mean of 0.50 for leaves and 0.24 to 0.73 with a mean of 0.48 for bark. The concentration of Pb in the fine root, thick root, branch and leaves of *Sonneratia apetala* in the Futian mangrove forest, South China were found to be 40.10 µg g^{-1}, 4.10 µg g^{-1}, 0.50 µg g^{-1} and 0.70 µg g^{-1}, respectively (Wang et al., 2013), which was slightly higher than the present study. However, the BCF remained low in the present study indicating the regulating mechanisms adopted by mangroves. However, the same mangrove species, *S. apetala* from the Indian Sundarban wetland displayed a high BCF of 18.01 for Pb (Chowdhury et al., 2016) which was several times higher than the present study. Pb concentrations in the leaves of *Sonneratia caseolaris,* collected from the Futian mangrove forest recorded 0.44 µg g^{-1} (Wu et al., 2014) and from Hainan Island, China was recorded at 0.03 (Lian et al., 1999) and these values were lower than the present study. However, higher Pb levels were observed from the leaves of *S. caseolaris* from Peninsular Malaysia, which was 35.5 µg g^{-1} (Nazli & Hashim, 2010) and from Kerala, India, which ranged between 25.00 µg $g^{-1}$and 125.00 µg g^{-1} in the twigs (Thomas & Fernandez, 1997). Accumulating patterns of Pb in three mangrove species decreased in the following sequence: *S. caseolaris* >*S.apetala* >*K. candel* (Zan et al., 2002; review by Zhang et al., 2014). The low TF and BCF for Pb in the present study indicates the mangrove have adopted an exclusion mechanism for Pb.

9.11.6 Cobalt (Co)

Cobalt is involved in the symbiotic nitrogen fixation in plants. In the present study, cobalt was completely absent in bark tissues. Co was also absent in all the leaf tissues except for one site at CR 04, which recorded 0.30 µg g^{-1}. However, in root samples cobalt was present except for one site CR 01, where Co was absent. In the remaining sites Co in root samples varied between 1.16 µg $g^{-1}$and 3.17 µg $g^{-1}$with a mean of 1.68 µg g^{-1}.The BCF for cobalt in the roots of *S. caseolaris* ranged from 0.12 and 0.33with a mean of 0.17. The cobalt concentration from the twigs of *Sonneratia caseolaris* collected from Kerala, India was found to be in the range of 34.10 µg g^{-1} to 68.20µg g^{-1}, (Thomas & Fernandez, 1997), which was fairly higher than the present study.

9.11.7 Cadmium (Cd)

In the present study, the concentration of Cd in the leaves of *Sonneratia Caseolaris* ranged between 0.08 µg $g^{-1}$and 0.10µg g^{-1} with a mean of 0.09µg g^{-1}. However, Cd was BDL at CR 01. In the case of bark, it ranged from 0.10 µg g^{-1} to 0.11 µg g^{-1} with a mean of 0.10 µg g^{-1}. In the root/pneumatophores tissue Cd concentration varied from 0.12 µg g^{-1} to 0.27 µg g^{-1} with a mean of 0.17 µg g^{-1}. Total Cd data was not available for sedimentary compartment. Hence, the BCF was calculated in line with the available mobile fractions Cd data in sedimentary compartment. The BCF for Cd ranged from 0.51 to 1.12 with a mean of 0.69 for BCF_{Root} 0.40 to 0.46 with a mean of 0.41 for BCF_{Bark} and 0.31 to 0.41 with a mean of 0.36for $BCF_{Leaves.}$ The TF were 0.37 to 0.71 with a mean of 0.54 for leaves and 0.36 to 0.81 with a mean of 0.65 for bark. Cadmium concentration in the leaves of *Sonneratia caseolaris* from Peninsular Malaysia was found to be 1.00 µg g^{-1} (Nazli & Hashim, 2010) which was higher than the present study. Cd concentration in the leaves of *Sonneratia caseolaris* collected from the Futian mangrove forest, China was found to be 0.04 µg g^{-1}, (He et al., 2014) which was lower than the present study. Cd was not detected in *Sonneratia apetala* collected from the Nansha mangroves, South China (Wu et al., 2014). The Cd BCF_{Root} value of *Sonneratia caseolaris* from the Futian National Nature Reserve, China, was found to be 0.09 which was much lower than the present study, with the TF (0.57) being similar to the present study (Li et al., 2016).

9.12 Effect of accumulated leaf trace element concentrations on the photosynthetic pigments of *Sonneratia caseolaris*

Heavy metals are reported to be phytotoxic, which can cause multiple inhibitory effects on photosynthesis at several structural and metabolic levels (Clijsters & Van Assche, 1985; Prasad & Strzalka, 1999). Heavy metals inhibit the total chlorophyll and chlorophyll a/b ratio in higher plants (Sheoran et al., 1990). Metal accumulation in the mature leaves of mangroves have a severe impact on the net photosynthesis (Barua & Jana, 1986; Burzynski & Buczek 1989; Padmaja et al., 1990; Gadallah 1995; Ouzounidou, 1994; Prasad, 1995; MacFarlane et al., 2003; Chowdhury et al., 2015). In aquatic plants, trace metals were found to substitute the central atom of chlorophyll thereby preventing the photosynthetic light-harvesting in the affected chlorophyll molecules, resulting in a breakdown of photosynthesis (Kupper et al., 1996). Heavy metal mediated changes in photosynthetic pigments impairs the photosynthetic apparatus and capacity of affected plants, thus, resulting in the subsequent decline in the carbon assimilation, reduced growth, survival, reproduction, and the production of carbon based products, which may be transferred along the estuarine food chain via detrital export (Vangronsveld & Clijsters, 1994; MacFarlane 2002). Changes in photosynthetic pigments can serve as an excellent biomarker of metal exposure that can possibly provide early warning signs for plants stress before the onset of visual damage (MacFarlane, 2002). Metal induced stress in mangrove plants results in the decreased chlorophyll content in mangrove plants (MacFarlane & Burchett, 2001; Huang & Wang, 2010).

The photosynthetic pigments observed in the leaves of *Sonneratia caseolaris* is presented in Table 9.13. The Pearson correlation coefficient extracted between the photosynthetic pigments and accumulated trace elements in the leaves are presented in Table 9.14. No significant relationship was found between the accumulated leaf metals and the photosynthetic pigments except for Cd. Cd showed significant ($P < 0.05$) positive correlation with Chlorophyll b and negative correlation with the Chlorophyll a/b ratio. Increased concentrations of Cd result in the reduction of the photosynthetic rate in plants (Sheoran et al., 1990). Cadmium is known to inhibit the photosynthetic apparatus, decreases the activity of photosystem II, causes degradation of the chloroplast inner structure and destroys the structure of the light harvesting chlorophyll a/b protein complex II (Baszynski, 1986; Krupa, 1988). However, no significant correlation was found in the case of other metals with

photosynthetic pigments. Similar to the present study, MacFarlane (2002), found no significant relationship between the accumulated leaf metals and photo pigments in the mangrove, *Avicennia marina* from the Sydney estuaries, Australia. The photo pigments may have been influenced by other biotic and abiotic factors, which were not examined here in the present study.

Table 9.13 Photosynthetic pigments in the leaves of Sonneratia caseolaris from the Baram River estuarine system

Samples	Chlorophyll a (mg/g)	Chlorophyll b (mg/g)	Chlorophyll (a+b) (mg/g)	Chlorophyll a/b ratio (mg/g)	Carotenoids (mg/g)
CR 01	0.637	0.015	0.652	41.716	0.178
CR 02	0.678	0.171	0.85	3.955	0.159
CR 03	0.755	0.224	0.979	3.374	0.179
CR 04	1.011	0.328	1.34	3.083	0.214
CR 05	0.609	0.175	0.785	3.477	0.168
CR 06	0.769	0.226	0.994	3.405	0.197
Mean ± Std. Err	**0.743 ± 0.060**	**0.190 ± 0.042**	**0.933 ± 0.096**	**9.835 ± 6.377**	**0.182 ± 0.008**

Table 9.14 Correlation coefficient between photosynthetic parameters and trace element accumulation in the leaves of Sonneratia caseolaris from the Baram River estuarine system

	Cd	Cu	Fe	Mn	Pb	Zn
Chlorophyll a	0.427	0.789	0.429	0.038	0.350	-0.056
Chlorophyll b	0.868*	0.676	0.705	0.494	0.296	0.250
Chlorophyll (a+b)	0.641	0.780	0.570	0.238	0.344	0.074
Chlorophyll a/b	-0.966**	-0.348	-0.679	-0.673	-0.239	-0.376
Carotenoids	0.235	0.561	0.315	-0.065	-0.090	-0.163

*Correlation is significant at 0.05 level (2-tailed), **Correlation is significant at 0.01 level (2-tailed)

9.13 Summary

- The root, bark and leaves of the mangrove species *Sonneratia caseolaris* (L.) Engl. were collected from six locations within the Baram estuary. The major and trace element (Fe, Mn, Co, Cu, Zn and Pb) concentrations of root/pneumatophore, bark, and leaves of this mangrove species were measured.
- To assess the toxicity, element concentrations in different tissues of mangroves were compared with the recommended limits generalised for various species by Kabata-Pendias, (1992). The results showed that none of the elements was above this toxic range in any of the tissues.
- The bio-concentration factor (BCF) was calculated by not only using the concentration of trace elements in the surface sediments but also by using the elemental concentrations in the shallow core sediments and the water column. The basis of such a calculation of BCF lies in the fact that the rhizosphere of the mangrove does not only take the trace elements from the surface sediments but also from deeper within the sediment column as well as from the water column.
- In order to understand the trace element uptake processes in mangroves, the calculated values of BCF have been subjected to analysis of variance (ANOVA) and the mechanisms of trace element uptake are inferred from the statistical relationships implied from ANOVA. The ANOVA results suggest, there was no significant difference ($P < 0.05$) of BCF values between the tissues for Fe, Mn, Zn and Pb. However, between these same tissues there was a significant difference ($P < 0.05$) for Cu, indicating the active intervention by plant physiology in the translocation of copper. Similar to Cu, the Cd translocation is also controlled by plant physiology. In the case of Zn, it is inferred that, regardless of different levels of Zn in the water, surface and core sediments, all have the same effect on the accumulation of Zn in the mangroves. However, the non-significant variation of BCF_{Bark} implied the accumulation of Zn in the bark as evidenced from the translocation factor>1 ($TF_{bark} = 1.305$).
- There was no significant relationship found between the accumulated leaf metals and the photosynthetic pigments, except for Cd. This suggests the photo

pigments may have been influenced by other biotic and abiotic factors which was not examined in the present study.

Chapter 10. Conclusions

Borneo is the third largest island in the world, encompassing two Malaysian States, (Sabah and Sarawak) and situated in the equatorial region. The Baram River in the State of Sarawak is one of the largest rivers in Borneo; the other large rivers are the Rajang and Mahakam (in Indonesia). The Baram River basin has an aerial extension of about 22,800 km^2 and receives an annual rainfall of around 2500 to 4000 mm/year, and delivers ~50 billion m^3 of fresh water and ~24 million tonnes of sediments annually into the South China Sea. The river basin is composed of turbidites, which are a storehouse of many trace elements. Apart from turbidites, Neogene volcanic lavas/tuffs, Miocene intrusives, limestones (Melinau) and Quaternary-Holocene coastal and river alluvium are exposed in the Baram river basin, making this river basin a highly complex geopark. What is the response of this highly complex terrain under changing climatic conditions and human influences? The first step towards answering this question lies in the study of sediment geochemistry as this is the storehouse of historical information. In addition, this study was carried out in the lower reaches of the Baram has provided a birds-eye view of the environmental status of this river basin. This study made an attempt to understand the source of the sediments (provenance), the weathering, elemental mobility, toxicity and biological availability (of trace elements). Seasonal surface water and sediment samples (during the monsoon and post monsoon), core sediments from different depositional conditions and root, bark and leaves of mangroves were collected from the Lower Baram River region (river mouth at Kuala Baram to Marudi town). In order to understand the river basin geochemistry and its environmental impact, various discrimination diagrams, weathering indices, elemental ratios, toxicity risk indices, and bio-concentration and translocation factors in the mangroves were studied. From the results, the following conclusions have been derived:

The provenance analysis revealed a mixed source from the source area where mostly sedimentary and meta-sedimentary rocks derived most part of the sediments as a recycled nature in addition to minor mafic input. The zircon age clusters of the Baram River sediments are comparable to the age clusters of the likely source areas specifically, the Schwaner Mountains from Southern Borneo and main range granites of Peninsular Malaysia. However, the older zircon might be related to more distal sources

such as the Indo-Australian plate. The Central belt and Eastern province of Peninsular Malaysia have yielded zircon with comparable ages as the present study. The younger clusters ~4.5Ma can be compared with Pliocene volcanic rocks exposed in the catchment area of the Baram River Basin. The Usun Apau plateau is the only volcanic feature located within the Baram River Basin. The age clusters observed in the present study have confirmed the mixture of fresh igneous rock source with the recycled sediments from the Rajang group as it was derived from the elemental geochemistry. Based on the zircon age study, the sediments derived from the main range granites of Peninsular Malaysia (Triassic) and Schwaner Mountain (Cretaceous) to form the Rajang Group of rocks, which have been recycled since the Miocene age to the northern part of Borneo. During the Pliocene, the volcanic rocks exposed or these fresh rocks, contributed sediments to some extent and mixed with the recycled sediments of the Rajang Group and formed the Holocene to Recent Baram Delta sediments and thus, a mixed provenance has been established based on the geochemical study.

The water column chemistry and the geochemical processes were found to be different during the MON and POM seasons. Factor analytical results revealed that during the MON, the adsorption of Pb, Zn, Ni, Cu, Co, Hg and Al on Mn hydroxide floccules was the dominant mechanism controlling their behaviour in the water column of the Lower Baram River. The adsorption was neither being influenced by pH, nor by ionic composition of the water column, though it has been very well demonstrated in earlier studies that the pH was the main factor affecting the formation of Mn-hydrous oxides, as well as the adsorption of other elements onto it. With such an observation, this factor model implies the Mn-hydrous oxide adsorbed species were being transported from the upstream and not being influenced in the downstream areas because during the MON, the heavy flooding does not permit the intrusion of the saline water into the lower reaches of the river. The high concentration of Al and a factor score of 4.96 for the sample collected at Sungai Bakung-Baram confluence (BES-26) during the MON demonstrated apart from Mn-oxyhydroxides, the Al-species could have a significant role in the transportation of some of the trace elements. This factor model along with a consideration of the partition coefficient of the elements, demonstrated the dissolution of aluminium-phosphate-sulphate (APS) minerals with the general formula AB_3

$(XO_4)_2(OH)_6$ [where A is a large cation (Na, U, K, Ag, NH_4, Pb, Ca, Ba, Sr, REE's and B is one of the cations in the group Al, Fe, Cu and Zn), and the formation of authigenic clay minerals. The salinity incursion was also found to prevail during this season though it was not discernible through a salinometer. During the POM season, the incursion of saline water has resulted in the remobiisation of Pb, Ni and Co from the sediments. However, Al-hydrous oxides and Mn-oxyhydroxides adsorbed the remobilized Pb and Ni, respectively as illustrated by their partition coefficients. Thus, Pb and Ni were redistributed within the sediments during the POM. Contrary to the above, the remobilised Co was released to the water column. The factor model also demonstrated the levels of orthophosphate and ammonical-nitrogen were controlled by the water column pH and dissolved oxygen. The loss of K from the Fe-bearing clay minerals or, a loss of iron from biotite was also revealed. The authigenic clay mineral formation can be observed only during the MON season. The reason for such an observation will have to wait for future research to answer.

The surface sediments during the MON and the grain size distribution of the sediments controls many elements (i.e) Al, Fe, Mn, K, Sc, Be, V, Ba, Sr, Ni, Rb, Cs, Eu, as one group and discriminates against another group, specifically, Si, Ag, Zr, Hf . This is the primary mechanism responsible for exerting control over the chemical composition of the sediments. The grouping of Cu, Zn and Sn indicated both natural and anthropogenic sources contribute to the concentrations of these elements in the Lower Baram River, and the association of Nb and Ta pointed to the fact these elements may be associated with fractionated granitic to pegmatitic rocks. The factor model also indicated the presence of chromite and powellite minerals in the detrital phase. During the POM, most of the major and trace elements (Al, Fe, Mn, Mg, K, Ti, P, Cr, Co, Ni, Rb, Nb, Sn, Sr, Ba, V, Be, Sc, REEs) were found to be associated with clay. Furthermore, the fractionation of LREE and HREE was found to prevail, and Th was found to be associated with LREE. Such an association is explained as due to the coherent behaviour of Th and LREE during weathering, transportation and diagenesis. The segregation of heavy minerals [Ag, Cr, Hf, U, Y, Zr, Cr, Zr, Hf, U, and many of the HREE, Ho, Er, Tm, Yb, Lu] were also found to influence the sediment chemistry. Detrital minerals associated with either granite or, hydrothermal veins in the source area

may contribute to the observed patterns in W, Nb, Ag and Sn. The variability in Mn concentration is found to be affected by sedimentary carbonates. A differential mobility of Na was observed from the sediments, possibly due to the weathering of fresh Na-bearing feldspar from the volcanic rocks of Usun Apau. Similar to the MON season, the Cu and Zn still continue to be associated, and were thought to be derived from both natural and anthropogenic sources. The dissolution of pyrite released Mo and As, and they were found to be differentially mobile, and accumulated in the sediments due to prevailing redox conditions.

The sequential extraction of the sediments revealed differing patterns of elemental distribution among various fractions during the MON and POM seasons. Manganese is the only element highly associated with the exchangeable (F1) fraction during both seasons. The high levels of exchangeable-Mn in the sediments were expected to play a major role in trace element adsorption, precipitation and transport mechanisms. Moreover, the elemental concentration in different fractions, and between the elements, exhibited seasonal variations. The factor model for the MON season revealed the formation of iron hydrous oxide coating on detrital clay as the main process. The association of Cd (F4), Co (F4), Fe (F4), Pb (F4), and Zn (F4) implied they are associated with pyrite. The chalcophile nature of Cu, Pb and Zn was explained by the association of Cu (F1), Cu (F2), Cu (F3), Pb (F1), Pb (F2) and Zn (F1). These elements are common in the sedimentary and meta-sedimentary rocks exposed in the source region. The flocculation of dissolved iron as an influence on the water column pH was also revealed. The incorporation of Cd within the carbonates was illustrated by the association of Cd (F2) and CaO. The factor model also explained the conversion of Fe-oxide into Fe-carbonate due to organic matter oxidation within the sediments.

During the POM the association of Fe(F3) with major components of the sediments (Al_2O_3, Fe_2O_3, MgO, K_2O, TiO_2 and P_2O_5) along with negative loading of SiO_2 indicated the coating of iron oxide onto detrital clay. But such a coating of Fe-oxide on the clay particles does not influence the variability of trace elements. However, the association of Co (F3), Mn (F3), Pb (F3), MnO and CaO, does represent adsorption of Co and Pb by Mn-oxide coated onto the calcium carbonate particles. Such a difference in the observed ability of Fe and Mn-oxides towards adsorption of trace

elements was mainly dependent on the redox chemistry of Fe and Mn in the sediments under prevailed environmental conditions in the system. The chalcophile elements Cu and Zn [especially the fractions Cu (F1), Cu (F2), Cu (F3) and Zn (F1)] are grouped together. This factor model also revealed the exchangeable fraction of [Co (F1)] was being positively influenced by water column pH, and negatively influenced by salinity. Such behaviour illustrates the remobilisation of Co from the sediments due to complexation with chloride under increasing salinity or in ionic strength. Thus, during the POM season, the sediments act as a source of Co for the coastal area. The model also revealed an association of Co (F4) and Zn (F4) with Mn (F4), implying the complexation of Co and Zn with organically complexed Mn. It is important to realize the trace element interaction with organic matter is enhanced in the presence of Fe-Mn oxides. The formation of Mn-carbonate during bacterial oxidation of organic matter is indicated by the loading of Mn (F2) on an individual factor. Similar to this, the organic-bound-Fe [Fe (F4)] was separately loaded, pointing to the presence of Fe-pyrite in the sediments. Such formation of Fe-pyrite is a common observation during the anoxic degradation of organic matter and the increased alkalinity during this reaction results in the formation of Mn-carbonates in the sediments. The carbonate-bound Pb (F2), and Fe-Mn oxides-bound Cu [Cu (F4)] have loaded on separate factors. It should be noted here except for the Cu (F4) fraction, all other fractions of Cu were loaded together, possibly reflecting the fact the organically-complexed Cu have a different behaviour altogether from other fractions. Similar behaviour is applicable to the carbonate-bound fraction of Pb (F2).

The downcore variations of the selected geochemical elements in terms of variations in weathering, detrital input, paleo-oxygenation, and sedimentation rate based on the geochemistry and ^{14}C AMS dating was studied from one long core of about 144cm extracted from the study area. The average sedimentation rate of 0.21 cm y^{-1} from 2670 to 1970 BP was revealed from the core sediments by neglecting out the reverse age, observed at the 80cm depth. The observed reverse age may indicate a local slump due to tectonic activity during the Late Holocene in this region. The whole core represents the source rock rather than the hydrological regime. No major variations of weathering intensity was evidenced during the deposition of core sediments and denotes

a predominant influence by the detrital input, rather than the fluctuation of redox conditions.

The factor model helped to unravel the geochemical processes responsible for the observed variability of the concentrations of various elements while the risk assessment provided an index to assess whether the level of trace elements were within the acceptable limit. Consequently, the Contamination Factor (C_f), Geoaccumulation Index (I_{geo}), Pollution Load Index (PLI), ERL-ERM (Effect Range Low – Effect Range Median) and Risk Assessment Code (RAC) were assessed in the sediments for the selected elements specifically, Fe, Mn, Cu, Zn, Pb, Cr, Co, V, Sr, Sn, Sb and W. Similarly, the Bioconcentration Factor (BCF) and Translocation Factor (TF) were computed for the mangroves. The following conclusions were derived from these analyses. An overall assessment of C_f and I_{geo} indices revealed during MON, Cu, Zn and Sn contaminated the Lower Baram River surface sediments. During the POM the surface sediments were contaminated by Cu, Cr, Sb and W. Considering the Pollution Load Index, during the MON and POM around ~90% of the sampling sites showed the PLI > 1, indicating enrichment of the elements. However, during the MON, only Cu showed a higher possible effect on biota. As per the RAC, Mn exhibited a higher risk during both seasons followed by Cu and Zn. When the short-core sediment Contamination Factor (C_f) and I_{geo} indices were considered, the elements Cu, Zn, Sn, Pb, Mn, Ni and Co showed contamination. The PLI of BSC-01 and BSC-07 showed partial enrichment and BSC-06 and BSC-09 showed complete enrichment. The elements Cu, Zn, Pb and W as revealed by the C_f and I_{geo} indices contaminated the long core (BM-140) sediments. With regard to the PLI, the entire long core sediments were enriched by the elements studied for risk assessment. When assessing the status of the mangroves in comparison with the recommended limits generalised for various species, none of the elements were above the toxic range in any of the tissues. From the results of the ANOVA, the BCF values from the mangrove tissues for Fe, Mn, Zn and Pb exhibited no significant difference. However, in the case of Cu, there was a significant difference ($P < 0.05$) in the various mangrove tissues, indicating the active intervention by plant physiology in the translocation of copper. Similarly, the translocation of Cd was also found to have been controlled by plant physiology. Also, from the results of Pearson correlation

coefficient there was no significant relationship found between the accumulated leaf metals and the photosynthetic pigments, except for Cd. This indicated the photo pigments may have been influenced by other biotic and abiotic factors which was not examined in the present study.

10.1 Recommendations and future works

Considering the changing environmental conditions and increasing human activities, within the context of the present work the following future research works are recommended:

- Examining the clay mineralogy in the study area can be done since the mineralogical properties of the Lower Baram sediments will reflect the geological history of transport, paleo-climate, sediment maturity and tectonic processes occurring throughout the river basin.
- Isotope studies of the undisturbed cores and various biological materials in the cores in this river basin will serve as indicators, integrators, and tracers of nutrient sources, land use, and biogeochemical reactions occurring in this region over a period of time.
- Studying the geochemical characteristics of the source rocks in the Baram River Basin would aid in further geochemical explorations.
- Estuarine modelling can be done in order to predict the long-term impact of this river basin in response to changing climatic conditions and the influence of increasing anthropogenic activities. In addition, predictive models of trace element transport to the ocean can also be done in the Baram River estuarine system.
- Only mangroves were studied for bioaccumulation in the present study. The study could be extended to include a wider range of biota across different trophic levels in order to understand the overall response of the biota in line with the changing environmental conditions in the river basin. Likewise, human risk assessment through consumption and trophic transfer of toxic elements through the food chain could be assessed.
- The flux of metal transport by the Baram River to the South China Sea can be quantified and the influence of this input on the health of the coral reef ecosystem can be studied. The metal transport mechanisms and pathways in the ocean and the subsequent effect on the fragile biotic components could be carried out in detail, which can pave the way for ecosystem-based management of the rivers, estuaries and coastal areas in this region.

- The Geochemical fingerprinting approach could be adopted to study the influence of the Baram River sediments on the Miri-Sibuti coral reef ecosystem.

References

Acker, J. G., & Bricker, O. P. (1992). The influence of pH on biotite dissolution and alteration kinetics at low temperature. *Geochimica et Cosmochimica Acta*, *56*(8), 3073-3092.

Agemian, H., & Chau, A. S. Y. (1977). A study of different analytical extraction methods for nondetrital heavy metals in aquatic sediments. *Archives of Environmental Contamination and Toxicology*, *6*(1), 69–82.

Ahmed, K., Mehedi, Y., Haque, R., & Mondol, P. (2011). Heavy metal concentrations in some macrobenthic fauna of the Sundarbans mangrove forest, south west coast of Bangladesh. *Environmental Monitoring and Assessment*, *177*(1–4), 505–514.

Ahnstrom, Z. A. S., & Parker, D. R. (2001). Cadmium reactivity in metal-contaminated soils using a coupled stable isotope dilution-sequential extraction procedure. *Environmental Science and Technology*, *35*(1), 121–126.

Alongi, D. M. (2002). Present state and future of the world's mangrove forests. *Environmental Conservation*, *29*(3), 331–349.

Álvarez, J.M., Lopez-Valdivia, L.M., Novillo, J., Obrador, A.,&Rico, M.I. (2006). Comparison of EDTA and sequential extraction tests for phytoavailability prediction of manganese and zinc in agricultural alkaline soils. *Geoderma*,*132*(3), 450–463.

Amado, L. L., Robaldo, R. B., Geracitano, L., Monserrat, J. M., & Bianchini, A. (2006). Biomarkers of exposure and effect in the Brazilian flounder *Paralichthys orbignyanus* (Teleostei: Paralichthyidae) from the Patos Lagoon estuary (Southern Brazil). *Marine Pollution Bulletin*, *52*(2), 207–213.

Amiard, J. C., Geffard, A., Amiard-Triquet, C., & Crouzet, C. (2007). Relationship between the lability of sediment-bound metals (Cd, Cu, Zn) and their bioaccumulation in benthic invertebrates. *Estuarine, Coastal and Shelf Science*, *72*(3), 511-521.

Anderson, J. A. R. (1964). The structure and development of the peat swamps of Sarawak and Brunei. *The Journal of Tropical Geography*, *18*.

Anderson, J. A. R., & Muller, J. (1975). Palynological study of a Holocene peat and a Miocene coal deposit from NW Borneo. *Review of Palaeobotany and Palynology*, *19*(4), 291-317.

Arain, M. B., Kazi, T. G., Jamali, M. K., Baig, J. A., Afridi, H. I., Jalbani, N., & Sarfraz, R. A. (2009). Comparison of Different Extraction Approaches for Heavy Metal Partitioning in Sediment Samples. *Pedosphere*, *19*(4), 476–485.

Armstrong-Altrin, J. S., Nagarajan, R., Madhavaraju, J., Rosalez-Hoz, L., Lee, Y. I., Balaram, V., & Avila-Ramírez, G. (2013). Geochemistry of the Jurassic and Upper Cretaceous shales from the Molango Region, Hidalgo, eastern Mexico: Implications for

source-area weathering, provenance, and tectonic setting. *Comptes Rendus Geoscience*, *345*(4), 185-202.

Arunachalam, J., Emons, H., Krasnodebska, B., & Mohl, C. (1996). Sequential extraction studies on homogenized forest soil samples. *Science of the Total Environment*, *181*(2), 147–159.

Audry, S., Schäfer, J., Blanc, G., & Jouanneau, J. M. (2004). Fifty-year sedimentary record of heavy metal pollution (Cd, Zn, Cu, Pb) in the Lot River reservoirs (France). *Environmental Pollution*, *132*(3), 413-426.

Auld, D. S. (2001). Zinc coordination sphere in biochemical zinc sites. *Biometals*, *14*(3-4), 271-313.

Backman, B., Bodiš, D., Lahermo, P., Rapant, S., & Tarvainen, T. (1998). Application of a groundwater contamination index in Finland and Slovakia. *Environmental Geology*, *36*(1-2), 55-64.

Bacon, J. R., & Davidson, C. M. (2008). Is there a future for sequential chemical extraction? *The Analyst*, *133*(1), 25–46.

Balistrieri, L. S., & Murray, J. W. (1981). The surface chemistry of goethite (alpha - FeOOH) in major ion seawater. *American Journal of Science*, *281*(6), 788-806.

Balistrieri, L., Brewer, P. G., & Murray, J. W. (1981). Scavenging residence times of trace metals and surface chemistry of sinking particles in the deep ocean. *Deep Sea Research Part A. Oceanographic Research Papers,28*(2), 101–121.

Banerjee, K., Senthilkumar, B., Purvaja, R., & Ramesh, R. (2012). Sedimentation and trace metal distribution in selected locations of Sundarbans mangroves and Hooghly estuary, northeast coast of India. *Environmental Geochemistry and Health*, *34*(1), 27-42.

Baric, A., Kuspilic, G. & Matijevic, S., (2002). Nutrient (N, P, Si) fluxes between marine sediments and water column in coastal and open Adriatic. In *Nutrients and Eutrophication in Estuaries and Coastal Waters* (pp. 151-159). Springer Netherlands.

Barona, A., & Romero, F. (1997). Relationships among metals in the solid phase of soils and in wild plants. *Water, Air, and Soil Pollution*, *95*(1–4), 59–74.

Bartoli, G., Papa, S., Sagnella, E., & Fioretto, A. (2012). Heavy metal content in sediments along the Calore River: relationships with physical–chemical characteristics. *Journal of Environmental Management*, *95*, S9-S14.

Barua, B., & Jana, S. (1986). Effects of heavy metals on dark induced changes in Hill reaction activity, chlorophyll and protein contents, dry matter and tissue permeability in detached *Spinacia oleracea* leaves. *Photosynthetica*, *20*, 74-76.

Bastami, K. D., Neyestani, M. R., Shemirani, F., Soltani, F., Haghparast, S., & Akbari, A. (2015). Heavy metal pollution assessment in relation to sediment properties in the

coastal sediments of the southern Caspian Sea. *Marine Pollution Bulletin*, *92*(1–2), 237–243.

Baszyński, T. (1986). Interference of Cd^{2+} in functioning of the photosynthetic apparatus of higher plants. *Acta Societatis Botanicorum Poloniae*, *55*(2), 291-304.

Batley, G. E., & Gardner, D. (1977). Sampling and storage of natural waters for trace metal analysis. *Water Research*, *11*(9), 745–756.

Bayen, S. (2012). Occurrence, bioavailability and toxic effects of trace metals and organic contaminants in mangrove ecosystems: a review. *Environment international*, *48*, 84-101.

Beck, M., Dellwig, O., Liebezeit, G., Schnetger, B. & Brumsack, H.J.(2008). Spatial and seasonal variations of sulphate, dissolved organic carbon, and nutrients in deep pore waters of intertidal flat sediments. *Estuarine, Coastal and Shelf Science*, *79*(2), 307-316.

Belkasmi, M., Cuney, M., Pollard, P. J., & Bastoul, A. (2000). Chemistry of the Ta-Nb-Sn-W oxide minerals from the Yichun rare metal granite (SE China): genetic implications and comparison with Moroccan and French Hercynian examples. *Mineralogical Magazine*, *64*(3), 507-523.

Bellanca, A., Claps, M., Erba, E., Masetti, D., Neri, R., Silva, I. P., & Venezia, F. (1996). Orbitally induced limestone/marlstone rhythms in the Albian—Cenomanian Cismon section (Venetian region, northern Italy): Sedimentology, calcareous and siliceous plankton distribution, elemental and isotope geochemistry. *Palaeogeography, Palaeoclimatology, Palaeoecology*, *126*(3-4), 227-260.

Ben-Awuah, J., Padmanabhan, E., & Sokkalingam, R. (2017). Geochemistry of Miocene sedimentary rocks from offshore West Baram Delta, Sarawak Basin, Malaysia, South China Sea: implications for weathering, provenance, tectonic setting, paleoclimate and paleoenvironment of deposition. *Geosciences Journal*, *21*(2), 167-185.

Benson, N. U., Udosen, E. D., & Akpabio, O. (2008). Interseasonal distribution and partitioning of heavy metals in subtidal sediment of Qua Iboe Estuary and associated Creeks, Niger Delta (Nigeria). *Environmental Monitoring and Assessment*, *146*(1–3), 253–265.

Bern, (2009). Soil chemistry in lithologically diverse datasets: the quartz dilution effect.Applied Geochemistry,24(8), 1429-1437.

Bianchi, T. S., Wysocki, L. A., Stewart, M., Filley, T. R., & McKee, B. A. (2007). Temporal variability in terrestrially-derived sources of particulate organic carbon in the lower Mississippi River and its upper tributaries. *Geochimica et Cosmochimica Acta*, *71*(18), 4425–4437.

Bianchi, T.S.(2007). *Biogeochemistry of Estuaries*. Oxford University Press.

Birch, G., Nath, B., & Chaudhuri, P. (2015). Effectiveness of remediation of metal-contaminated mangrove sediments (Sydney estuary, Australia). *Environmental Science and Pollution Research*, *22*(8), 6185–6197.

Bird, M.I., Taylor, D.,& Hunt, C. (2005). Palaeoenvironments of insular Southeast Asia during the Last Glacial Period: A savanna corridor in Sundaland? *Quaternary Science Rev*iews*24*(20), 2228–2242.

Bjørlykke, K. (1974). Geochemical and mineralogical influence of Ordovician Island Arcs on epicontinental clastic sedimentation. A study of Lower Palaeozoic sedimentation in the Oslo Region, Norway. *Sedimentology*, *21*(2), 251-272.

Bølviken, B., Bogen, J., Jartun, M., Langedal, M., Ottesen, R. T., & Volden, T. (2004). Overbank sediments: a natural bed blending sampling medium for large-scale geochemical mapping. *Chemometrics and Intelligent Laboratory Systems*, *74*(1), 183-199.

Bonatti, E., & Gartner, S. (1973). Caribbean climate during Pleistocene ice ages. *Nature*, *244*(5418), 563-565.

Borovec, Z., Tolar, V., & Mráz, L. (1993). Distribution of some metals in sediments of the central part of the Labe (Elbe) River: Czech Republic. *Ambio*, 200-205.

Bouchez, J., Gaillardet, J., France-Lanord, C., Maurice, L., &Dutra-Maia, P. (2011). Grain size control of river suspended sediment geochemistry: Clues from Amazon River depth profiles. *Geochemistry, Geophysics, Geosystems*, *12*(3).

Boyle, E. A., Edmond, J. M., & Sholkovitz, E. R. (1977). The mechanism of iron removal in estuaries. *Geochimica et Cosmochimica Acta*, *41*(9), 1313–1324

Bracciali, L., Marroni, M., Luca, P., & Sergio, R. (2007). Geochemistry and petrography of Western Tethys Cretaceous sedimentary covers (Corsica and Northern Apennines): from source areas to configuration of margins. *Geological Society of America Special Papers*, *420*, 73-93.

Bradl, H. B. (2004). Adsorption of heavy metal ions on soils and soils constituents. *Journal of Colloid and Interface Science*, *277*(1), 1-18.

Bricker, S. B., Clement, C. G., Pirhalla, D. E., Orlando, S. P., & Farrow, D. R. (1999). *National estuarine eutrophication assessment: effects of nutrient enrichment in the nation's estuaries*. US National Oceanographic and Atmospheric Administration, National Ocean Service, Special Projects Office and the National Center for Coastal Ocean Science.

Bricker, S. B., Ferreira, J. G., & Simas, T. (2003). An integrated methodology for assessment of estuarine trophic status. *Ecological Modelling*, *169*(1), 39-60.

Broadley, M.R., White, P.J., Hammond, J.P., Zelko, I., Lux, A., (2007). Zinc in plants: Tansley review. *New Phytol*.

Brooks, C. K. (1970). The concentrations of zirconium and hafnium in some igneous and metamorphic rocks and minerals. *Geochimica et Cosmochimica Acta*, *34*(3), 411-416.

Buccolieri, A., Buccolieri, G., Cardellicchio, N., Dell'Atti, A., Di Leo, A., & Maci, A. (2006). Heavy metals in marine sediments of Taranto Gulf (Ionian Sea, southern Italy). *Marine chemistry*, *99*(1), 227-235.

Buckley, D. E., & Cranston, R. E. (1991). The use of grain size information in marine geochemistry. *Principles, Methods and Applications of particle size analysis, Syvitski, JM (Ed.), Cambridge Univ. Press, New York. Geological Survey of Canada Contribution*, *12689*, 311-331.

Buffle, J. (1989). Complexation Reactions in Aquatic Systems; Analytical Approach. In Ellis Horwood Ltd (Vol. 17, pp. 230–230).

Burzynski, M., & Buczek, J. (1989). Interaction between cadmium and molybdenum affecting the chlorophyll content and accumulation of some heavy metals in the second leaf of *Cucumis sativus* L. *Acta Physiologiae Plantarum (Poland)*.

Caeiro, S., Costa, M. H., Ramos, T. B., Fernandes, F., Silveira, N., Coimbra, A., ...& Painho, M. (2005). Assessing heavy metal contamination in Sado Estuary sediment: an index analysis approach. *Ecological indicators*, *5*(2), 151-169.

Caeiro, S., Vaz-Fernandes, P., Martinho, A. P., Costa, P. M., Silva, M. J., Lavinha, J. & Costa, M. H. (2017). Environmental risk assessment in a contaminated estuary: An integrated weight of evidence approach as a decision support tool. *Ocean and Coastal Management*, *143*, 51-62.

Caetano, M., Vale, C., Cesário, R., & Fonseca, N. (2008). Evidence for preferential depths of metal retention in roots of salt marsh plants. *Science of the Total Environment*, *390*(2), 466-474.

Caline, B., & Huong, J. (1992). New insight into the recent evolution of the Baram Delta from satellite imagery. *Geological Society of Malaysia Bulletin*, *32*, 1-13.
Calvert, S. E., & Pedersen, T. F. (1993). Geochemistry of recent oxic and anoxic marine sediments: implications for the geological record. *Marine Geology*, *113*(1-2), 67-88.

Cameron, C. C., Esterle, J. S., & Palmer, C. A. (1989). The geology, botany and chemistry of selected peat-forming environments from temperate and tropical latitudes. *International Journal of Coal Geology*, *12*(1–4), 105–156.

Cameron, W.M. & Pritchard, D.W., (1963). Estuaries. In: Hill, M.N. (Ed.), The*Sea: Ideas and Observations on Progress in the Study of the Seas.* Interscience, London.

Campanella, L., D'Orazio, D., Petronio, B. M., & Pietrantonio, E. (1995). Proposal for a metal speciation study in sediments. *Analytica Chimica Acta*, *309*(1–3), 387–393.

Campbell, C.J., (1956). Geology of the Usun Apau area. British Borneo Geological Survey Annual Report. pp. 86-120.

Canfield, D.E., Thamdrup, B. & Hansen, J.W.(1993). The anaerobic degradation of organic matter in Danish coastal sediments: iron reduction, manganese reduction, and sulfate reduction. *Geochimica et Cosmochimica Acta*, *57*(16), 3867-3883.

Casas, J. M., Rosas, H., Solé, M., & Lao, C. (2003). Heavy metals and metalloids in sediments from the Llobregat basin, Spain. *Environmental Geology,44*, 325–332.

Cébron, A., Berthe, T. & Garnier, J., (2003). Nitrification and nitrifying bacteria in the lower Seine River and estuary (France). *Applied and Environmental Microbiology*, *69*(12), 7091-7100.

Černý P. (1991). Rare-element granitic pegmatites. Part 1: Anatomy and internal evolution of pegmatite deposits. Part 2: Regional to global environments and petrogenesis. *Geoscience Canada*, *18*, 49-81.

Černý, P., & Ercit, T. S. (2005). The classification of granitic pegmatites revisited. *The Canadian Mineralogist*, *43*(6).

Chandrajith, R., Dissanayake, C. B., & Tobschall, H. J. (2000). Sources of stream sediments in the granulite terrain of the Walawe Ganga Basin, Sri Lanka, indicated by rare earth element geochemistry. *Applied Geochemistry*, *15*(9), 1369-1381.

Chapman, G. J. C., & Kromkamp, J. (1999). Primary Production by Phytoplankton and Microphytobenthos in Estuaries. *Advances in Ecological Research*, *29*(C), 93–153.

Chapman, P. M., & Wang, F. (2001). Assessing sediment contamination in estuaries. *Environmental Toxicology and Chemistry*, *20*(1), 3–22.

Chaudhuri, S., & Brookins, D. G. (1979). The Rb and Sr systematics in acid-leached clay minerals. *Chemical Geology*, *24*(3), 231-242.

Chen, C. W., Kao, C. M., Chen, C. F., & Dong, C. D. (2007). Distribution and accumulation of heavy metals in the sediments of Kaohsiung Harbor, Taiwan. *Chemosphere*, *66*(8), 1431-1440.

Chen, L., & Lu, S. (2008). Sorption and desorption of radiocobalt on montmorillonite—effects of pH, ionic strength and fulvic acid. *Applied Radiation and Isotopes*, *66*(3), 288-294.

Chester, R. & Jickells, T. (2012).*The Transport of Material to the Oceans: The Fluvial Pathway, in Marine Geochemistry*. John Wiley & Sons, Ltd, Chichester, UK.

Chester, R., & Hughes, M. J. (1967). A chemical technique for the separation of ferro-manganese minerals, carbonate minerals and adsorbed trace elements from pelagic sediments. *Chemical Geology*, *2*, 249–262.

Chesworth, W., Dejou, J., & Larroque, P. (1981). The weathering of basalt and relative mobilities of the major elements at Belbex, France. *Geochimica et Cosmochimica Acta*, *45*(7), 1235–1243.

Chiffoleau, J.-F., Cossa, D., Auger, D., & Truquet, I. (1994). Trace metal distribution, partition and fluxes in the Seine estuary (France) in low discharge regime. *Marine Chemistry*, *47*(2), 145–158.

Chiu, C. Y., & Chou, C. H. (1991). The distribution and influence of heavy metals in mangrove forests of the Tamshui estuary in Taiwan. *Soil Science and Plant Nutrition*, *37*(4), 659-669.

Choi, H. G., Moon, H. B., Choi, M., & Yu, J. (2011). Monitoring of organic contaminants in sediments from the Korean coast: spatial distribution and temporal trends (2001–2007). *Marine pollution bulletin*, *62*(6), 1352-1361.

Chowdhury, A., & Maiti, S. K. (2016). Identification of metal tolerant plant species in mangrove ecosystem by using community study and multivariate analysis: a case study from Indian Sunderban. *Environmental Earth Sciences*, *75*(9), 744.

Chowdhury, R., Favas, P. J., Jonathan, M. P., Venkatachalam, P., Raja, P., & Sarkar, S. K. (2017). Bioremoval of trace metals from rhizosediment by mangrove plants in Indian Sundarban Wetland. *Marine Pollution Bulletin*.

Chowdhury, R., Favas, P. J., Pratas, J., Jonathan, M. P., Ganesh, P. S., & Sarkar, S. K. (2015). Accumulation of trace metals by mangrove plants in Indian Sundarban Wetland: prospects for phytoremediation. *International Journal of Phytoremediation*, *17*(9), 885-894.

Chowdhury, R., Lyubun, Y., Favas, P. J., & Sarkar, S. K. (2016). Phytoremediation Potential of Selected Mangrove Plants for Trace Metal Contamination in Indian Sundarban Wetland. In *Phytoremediation* (pp. 283-310). Springer International Publishing.

Church, T.M., (2016). Marine Chemistry in the Coastal Environment: Principles, Perspective and Prospectus. *Aquatic Geochemistry*, *22*(4), 375-389.

Cindrić, A. M., Garnier, C., Oursel, B., Pižeta, I., & Omanović, D. (2015). Evidencing the natural and anthropogenic processes controlling trace metals dynamic in a highly stratified estuary: The Krka River estuary (Adriatic, Croatia). *Marine Pollution Bulletin*, *94*(1–2), 199–216.

Clark, M. W., McConchie, D., Lewis, D. W., & Saenger, P. (1998). Redox stratification and heavy metal partitioning in Avicennia-dominated mangrove sediments: a geochemical model. *Chemical Geology*, *149*(3–4), 147–171.

Clijsters, H., & Van Assche, F. (1985). Inhibition of photosynthesis by heavy metals. *Photosynthesis research*, *7*(1), 31-40.

Condie, K. C. (1991). Another look at rare earth elements in shales. *Geochimica et Cosmochimica Acta*, *55*(9), 2527-2531.

Condie, K. C. (1993). Chemical composition and evolution of the upper continental crust: contrasting results from surface samples and shales. *Chemical Geology*, *104*(1-4), 1-37.

Condie, K. C., & Wronkiewicz, D. J. (1990). The Cr/Th ratio in Precambrian pelites from the Kaapvaal Craton as an index of craton evolution. *Earth and Planetary Science Letters*, *97*(3-4), 256-267.

Costa, D. S., Barbosa, R. M., Oliveira, J. S., &Sa, M. E. (2014). Foliar Application of Calcium and Molybdenum in Common Bean Plants: Yield and Seed Physiological Potential. *Agricultural Sciences*, *5*(11), 1037-1045.

Cowie, G. L., & Levin, L. A. (2009). Benthic biological and biogeochemical patterns and processes across an oxygen minimum zone (Pakistan margin, NE Arabian Sea). *Deep Sea Research Part II: Topical Studies in Oceanography*, *56*(6), 261-270.

Cox, R., & Lowe, D. R. (1995). A conceptual review of regional-scale controls on the composition of clastic sediment and the co-evolution of continental blocks and their sedimentary cover. *Journal of Sedimentary Research*, *65*(1).

Cox, R., Lowe, D. R., & Cullers, R. L. (1995). The influence of sediment recycling and basement composition on evolution of mudrock chemistry in the southwestern United States. *Geochimica et Cosmochimica Acta*, *59*(14), 2919-2940.

Craw, D., (1981). Oxidation and microprobe-induced potassium mobility in iron-bearing phyllosilicates from the Otago schists, New Zealand. *Lithos*, *14*(1), 49-57.

Crusius, J., Calvert, S., Pedersen, T., & Sage, D. (1996). Rhenium and molybdenum enrichments in sediments as indicators of oxic, suboxic and sulfidic conditions of deposition. *Earth and Planetary Science Letters*, *145*(1-4), 65-78.

Cui, J. L., Luo, C. L., Tang, C. W. Y., Chan, T. S., & Li, X. D. (2017). Speciation and leaching of trace metal contaminants from e-waste contaminated soils. *Journal of Hazardous Materials*, *329*, 150-158.

Cullen, A., Macpherson, C., Taib, N. I., Burton-Johnson, A., Geist, D., Spell, T., & Banda, R. M. (2013). Age and petrology of the Usun Apau and Linau Balui volcanics: Windows to central Borneo's interior. *Journal of Asian Earth Sciences*, *76*, 372-388.

Cullers, R. L. (1994). The controls on the major and trace element variation of shales, siltstones, and sandstones of Pennsylvanian-Permian age from uplifted continental blocks in Colorado to platform sediment in Kansas, USA. *Geochimica et Cosmochimica Acta*, *58*(22), 4955-4972.

Cullers, R. L. (2000). The geochemistry of shales, siltstones and sandstones of Pennsylvanian–Permian age, Colorado, USA: implications for provenance and metamorphic studies. *Lithos*, *51*(3), 181-203.

Cullers, R. L., & Podkovyrov, V. N. (2000). Geochemistry of the Mesoproterozoic Lakhanda shales in southeastern Yakutia, Russia: implications for mineralogical and provenance control, and recycling. *Precambrian Research*, *104*(1), 77-93.

Cullers, R. L., Basu, A., & Suttner, L. J. (1988). Geochemical signature of provenance in sand-size material in soils and stream sediments near the Tobacco Root batholith, Montana, USA. *Chemical Geology*, *70*(4), 335-348.

Cuong, D. T., Bayen, S., Wurl, O., Subramanian, K., Wong, K. K. S., Sivasothi, N., & Obbard, J. P. (2005). Heavy metal contamination in mangrove habitats of Singapore. *Marine Pollution Bulletin*, *50*(12), 1732-1738.

Dahlqvist, R., Andersson, K., Ingri, J., Larsson, T., Stolpe, B., & Turner, D. (2007). Temporal variations of colloidal carrier phases and associated trace elements in a boreal river. *Geochimica et Cosmochimica Acta*, *71*(22), 5339–5354.

Dai, S., Wang, X., Seredin, V. V., Hower, J. C., Ward, C. R., O'Keefe, J. M., ... & Xue, W. (2012). Petrology, mineralogy, and geochemistry of the Ge-rich coal from the Wulantuga Ge ore deposit, Inner Mongolia, China: new data and genetic implications. *International Journal of Coal Geology*, *90*, 72-99.

Daoust, R. J., Moore, T. R., Chmura, G. L., & Magenheimer, J. F. (1996). Chemical evidence of environmental changes and anthropogenic influences in a Bay of Fundy saltmarsh. *Journal of Coastal Research*, *12*(2), 520–533.

Davidson, C. M., Thomas, R. P., Mcvey, S. E., Perala, R., Littlejohn, D., & Ure, A. M. (1994). Evaluation of a Sequential Extraction Procedure for the Speciation of Heavy-Metals in Sediments. *Analytica Chimica Acta,291*(3), 277–286.

Davidson, C. M., Urquhart, G. J., Ajmone-Marsan, F., Biasioli, M., da Costa Duarte, A., Díaz-Barrientos, E., ...& Rodrigues, S. (2006). Fractionation of potentially toxic elements in urban soils from five European cities by means of a harmonised sequential extraction procedure. *Analytica Chimica Acta*, *565*(1), 63-72.

Davutluoglu, O. I., Seckin, G., Ersu, C. B., Yilmaz, T., & Sari, B. (2011). Heavy metal content and distribution in surface sediments of the Seyhan River, Turkey. *Journal of Environmental Management*, *92*(9), 2250-2259.

de Almeida Duarte, L. F., de Souza, C. A., Pereira, C. D. S., & Pinheiro, M. A. A. (2017). Metal toxicity assessment by sentinel species of mangroves: In situ case study integrating chemical and biomarkers analyses. *Ecotoxicology and Environmental Safety*, *145*, 367-376.

De Lacerda, L. D. (2002). *Mangrove ecosystems: function and management*. Springer Science and Business Media.

De Lacerda, L.D. (1998). Trace metals in mangrove plants: why such low concentrations? In: *De Lacerda, L.D., Diop, H.S. (Eds.), Mangrove Ecosystem Studies in Latin America and Africa. UNESCO*, pp. 171–178.

De Souza Machado, A. A., Spencer, K., Kloas, W., Toffolon, M., & Zarfl, C. (2016). Metal fate and effects in estuaries: a review and conceptual model for better understanding of toxicity. *Science of the Total Environment*, *541*, 268-281.

Defew, L. H., Mair, J. M., & Guzman, H. M. (2005). An assessment of metal contamination in mangrove sediments and leaves from Punta Mala Bay, Pacific Panama. *Marine Pollution Bulletin*, *50*(5), 547-552.

Degryse, F., Smolders, E., & Parker, D. R. (2006). Metal complexes increase uptake of Zn and Cu by plants: implications for uptake and deficiency studies in chelator-buffered solutions. *Plant and Soil*, *289*(1-2), 171-185.

Descourvieres, C., Douglas, G., Leyland, L., Hartog, N., & Prommer, H. (2011). Geochemical reconstruction of the provenance, weathering and deposition of detrital-dominated sediments in the Perth Basin: The Cretaceous Leederville Formation, south-west Australia. *Sedimentary Geology*, *236*(1), 62-76.

Dessai, D. V. G., & Nayak, G. N. (2009). Distribution and speciation of selected metals in surface sediments, from the tropical Zuari estuary, central west coast of India. *Environmental Monitoring and Assessment*, 158(1–4), 117–137.

Dhanakumar, S., Solaraj, G., & Mohanraj, R. (2015). Heavy metal partitioning in sediments and bioaccumulation in commercial fish species of three major reservoirs of river Cauvery delta region, India. *Ecotoxicology and Environmental Safety*, 113, 145–151.

Dill, H. (1986). Metallogenesis of early Paleozoic graptolite shales from the Graefenthal Horst (northern Bavaria-Federal Republic of Germany). *Economic Geology*, *81*(4), 889-903.

Dill, H. G. (2001). The geology of aluminium phosphates and sulphates of the alunite group minerals: a review. *Earth-Science Reviews*, *53*(1), 35-93.

Dill, H. G., Pöllmann, H., Bosecker, K., Hahn, L., & Mwiya, S. (2002). Supergene mineralization in mining residues of the Matchless cupreous pyrite deposit (Namibia)—a clue to the origin of modern and fossil duricrusts in semiarid climates. *Journal of Geochemical Exploration*, *75*(1), 43-70.

Dominik, J., & Stanley, D. J. (1993). Boron, beryllium and sulfur in Holocene sediments and peats of the Nile delta, Egypt: Their use as indicators of salinity and climate. *Chemical Geology*, *104*(1), 203–216.

Dong, A., Zhai, S., Zabel, M., Yu, Z., Zhang, H., & Liu, F. (2012). Heavy metals in Changjiang estuarine and offshore sediments: responding to human activities. *Acta Oceanologica Sinica*, *31*(2), 88-101.

Dong, D., Nelson, Y.M., Lion, L.W., Shuler, M.L. & Ghiorse, W.C., (2000). Adsorption of Pb and Cd onto metal oxides and organic material in natural surface coatings as

determined by selective extractions: new evidence for the importance of Mn and Fe oxides. *Water Research*, 34(2), 427-436.

Drever, J. I. (1994). The effect of land plants on weathering rates of silicate minerals. *Geochimica et Cosmochimica Acta*, *58*(10), 2325-2332.

Du Laing, G., Rinklebe, J., Vandecasteele, B., Meers, E., & Tack, F. M. (2009). Trace metal behaviour in estuarine and riverine floodplain soils and sediments: a review. *Science of the Total Environment*, *407*(13), 3972-3985.

Duarte, B., & Caçador, I. (2012). Particulate metal distribution in Tagus estuary (Portugal) during a flood episode. *Marine Pollution Bulletin*, *64*(10), 2109-2116.

Duke, N. C., Meynecke, J. O., Dittmann, S., Ellison, A. M., Anger, K., Berger, U., ...& Koedam, N. (2007). A world without mangroves?. *Science*, *317*(5834), 41-42.

Dung, T. T. T., Cappuyns, V., Swennen, R., & Phung, N. K. (2013). From geochemical background determination to pollution assessment of heavy metals in sediments and soils. *Reviews in Environmental Science and Bio/Technology*, *12*(4), 335-353.

Duodu, G. O., Goonetilleke, A., & Ayoko, G. A. (2016). Comparison of pollution indices for the assessment of heavy metal in Brisbane River sediment. *Environmental Pollution*, *219*, 1077-1091.

Dypvik, H. (1984). Geochemical compositions and depositional conditions of Upper Jurassic and Lower Cretaceous Yorkshire clays, England. *Geological Magazine*, *121*(5), 489-504.

Eckert, J. M., & Sholkovitz, E. R. (1976). The flocculation of iron, aluminium and humates from river water by electrolytes. *Geochimica et Cosmochimica Acta*, *40*(7), 847–848.

Edet, A. E., & Offiong, O. E. (2002). Evaluation of water quality pollution indices for heavy metal contamination monitoring. A study case from Akpabuyo-Odukpani area, Lower Cross River Basin (southeastern Nigeria). *GeoJournal*, *57*(4), 295-304.

Eggleton, J., & Thomas, K. V. (2004). A review of factors affecting the release and bioavailability of contaminants during sediment disturbance events. *Environment international*, *30*(7), 973-980.

El Nemr, A. M., El Sikaily, A., & Khaled, A. (2007). Total and leachable heavy metals in muddy and sandy sediments of Egyptian coast along Mediterranean Sea. *Environmental Monitoring and Assessment*, *129*(1–3), 151–168.

El-Azim, H. A., & El-Moselhy, K. M. (2005). Determination and partitioning of metals in sediments along the Suez Canal by sequential extraction. *Journal of Marine Systems*, *56*(3–4), 363–374.

Elderfield, H., & Greaves, M. J. (1982). The rare earth elements in seawater. *Nature*, *296*, 214-219.

Elliott, M., & McLusky, D. S. (2002). The need for definitions in understanding estuaries. *Estuarine, Coastal and Shelf Science*, *55*(6), 815-827.

Emerson, S., Jahnke, R., Bender, M., Froelich, P., Klinkhammer, G., Bowser, C. & Setlock, G., (1980). Early diagenesis in sediments from the eastern equatorial Pacific, I. Pore water nutrient and carbonate results. *Earth and Planetary Science Letters*, 49(1), pp.57-80.

Engle, V. D., Kurtz, J. C., Smith, L. M., Chancy, C., & Bourgeois, P. (2007). A classification of US estuaries based on physical and hydrologic attributes. *Environmental Monitoring and Assessment*, *129*(1), 397-412.

English, S. S., Wilkinson, C. C., & Baker, V. V. (1997). *Survey manual for tropical marine resources*. Australian Institute of Marine Science.

Erftemeijer, P. L., Riegl, B., Hoeksema, B. W., & Todd, P. A. (2012). Environmental impacts of dredging and other sediment disturbances on corals: a review. *Marine Pollution Bulletin*, *64*(9), 1737-1765.

Ernst, W. G. (1970). Tectonic contact between the Franciscan mélange and the Great Valley sequence - Crustal expression of a late Mesozoic Benioff zone. *Journal of Geophysical Research*, *75*(5), 886-901.

Eswaran, H., & Heng, Y. Y. (1976). The weathering of biotite in a profile on gneiss in Malaysia. *Geoderma*, *16*(1), 9-20.

Eswaran, H., Stoops, G., &De Paepe, P. (1973). A contribution to the study of soil formation on Isla Santa Cruz, Galápagos. *Pedologie*, *23*, 100-122.

Evans, A., (1986). Effects of dissolved organic carbon and sulfate on aluminum mobilization in forest soil columns. *Soil Science Society of America Journal*, 50(6), 1576-1578.

Fairbrother, A., Wenstel, R., Sappington, K., & Wood, W. (2007). Framework for Metals Risk Assessment. *Ecotoxicology and Environmental Safety*, *68*(2), 145–227.

Fang, G. C., & Yang, H. C. (2010). Heavy metals in the River sediments of Asian countries of Taiwan, China, Japan, India, and Vietnam during 1999–2009. *Environmental Forensics*, *11*(3), 201-206.

FAO. (2007). The world's mangroves 1980-2005. *FAO Forestry Paper*, *153*, 89.

Fedo, C. M., Eriksson, K. A., & Krogstad, E. J. (1996). Geochemistry of shales from the Archean (~ 3.0 Ga) Buhwa Greenstone Belt, Zimbabwe: implications for provenance and source-area weathering. *Geochimica et Cosmochimica Acta*, *60*(10), 1751-1763.

Fedo, C. M., Nesbitt, H. W., & Young, G. M. (1995). Unraveling the effects of potassium metasomatism in sedimentary rocks and paleosols, with implications for paleoweathering conditions and provenance. *Geology*, *23*(10), 921-924.

Feely, R.A., Alin, S.R., Newton, J., Sabine, C.L., Warner, M., Devol, A., Krembs, C. & Maloy, C., (2010). The combined effects of ocean acidification, mixing, and respiration

on pH and carbonate saturation in an urbanized estuary. *Estuarine, Coastal and Shelf Science*, *88*(4), 442-449.

Feng, J., Yang, Z., Niu, J., & Shen, Z. (2007). Remobilization of polycyclic aromatic hydrocarbons during the resuspension of Yangtze River sediments using a particle entrainment simulator. *Environmental Pollution*, *149*(2), 193-200.

Feng, X.H., Zhai, L.M., Tan, W.F., Liu, F. & He, J.Z., (2007). Adsorption and redox reactions of heavy metals on synthesized Mn oxide minerals. *Environmental Pollution*, 147(2), 366-373.

Fernandes, H. M. (1997). Heavy metal distribution in sediments and ecological risk assessment: the role of diagenetic processes in reducing metal toxicity in bottom sediments. *Environmental Pollution*, *97*(3), 317-325.

Fernandes, L., Nayak, G. N., Ilangovan, D., & Borole, D. V. (2011). Accumulation of sediment, organic matter and trace metals with space and time, in a creek along Mumbai coast, India. *Estuarine, Coastal and Shelf Science*, *91*(3), 388–399.

Fernandes, R. (2006). Distribution and seasonal variation of trace metals in surface sediments of the Mandovi estuary, west coast of India. *Estuarine Coastal and Shelf Science*, *67*(1–2), 333–339.

Filgueiras, A. V, Lavilla, I., & Bendicho, C. (2002). Chemical sequential extraction for metal partitioning in environmental solid samples. *Analytical and Bioanalytical Chemistry*, *374*(1), 103–108.

Flores, L., Blas, G., Hernandez, G., & Alcala, R. (1997). Distribution and sequential extraction of some heavy metals from soils irrigated with wastewater from Mexico City. *Water, Air, and Soil Pollution*, *98*(1-2), 105-117.

Floyd, P. A., & Leveridge, B. E. (1987). Tectonic environment of the Devonian Gramscatho basin, south Cornwall: framework mode and geochemical evidence from turbiditic sandstones. *Journal of the Geological Society*, *144*(4), 531-542.

Förstner, U., & Wittmann, G. T. (1979). Metal transfer between solid and aqueous phases. In *Metal Pollution in the Aquatic Environment* (pp. 197-270). Springer Berlin Heidelberg.

Förstner, U., Ahlf, W., & Calmano, W. (1989). Studies on the transfer of heavy metals between sedimentary phases with a multi-chamber device: combined effects of salinity and redox variation. *Marine Chemistry*, *28*(1-3), 145-158.

Frankowski, M., Zioła-Frankowska, A., Kowalski, A., & Siepak, J. (2010). Fractionation of heavy metals in bottom sediments using Tessier procedure. *Environmental Earth Sciences*, *60*(6), 1165–1178.

Fritz, S. J., & Mohr, D. W. (1984). Chemical alteration in the micro weathering environment within a spheroidally-weathered anorthosite boulder. *Geochimica et Cosmochimica Acta*, *48*(12), 2527–2535.

Fritz, S. J., & Ragland, P. C. (1980). Weathering rinds developed on plutonic igneous rocks in the North Carolina piedmont. *American Journal of Science*,*280*, 546-559.

Fu, J., Zhao, C., Luo, Y., Liu, C., Kyzas, G. Z., Luo, Y. & Zhu, H. (2014). Heavy metals in surface sediments of the Jialu River, China: their relations to environmental factors. *Journal of Hazardous Materials*, *270*, 102-109.

Furukawa, K., Wolanski, E., & Mueller, H. (1997). Currents and Sediment Transport in Mangrove Forests. *Estuarine, Coastal and Shelf Science*, *44*(3), 301–310.

Gadallah, M. A. A. (1995). Effects of cadmium and kinetin on chlorophyll content, saccharides and dry matter accumulation in sunflower plants. *Biologia Plantarum*, *37*(2), 233.

Gaillardet, J., Dupré, B., Louvat, P., & Allegre, C. J. (1999). Global silicate weathering and CO_2 consumption rates deduced from the chemistry of large rivers. *Chemical Geology*, *159*(1), 3-30.

Gaillardet, J., Viers, J., & Dupré, B. (2003). Trace elements in river waters. *Treatise on geochemistry*, *5*, 605.

Gaillardet, J., Viers, J., & Dupré, B. (2014). Trace elements in river waters. *Treatise on Geochemistry*: Second Edition. Volume 7: Surface and Groundwater, Weathering and Soils.

Galán, E., Gómez-Ariza, J. L., González, I., Fernández-Caliani, J. C., Morales, E., & Giráldez, I. (2003). Heavy metal partitioning in river sediments severely polluted by acid mine drainage in the Iberian Pyrite Belt. *Applied Geochemistry*, 18(3), 409–421.

García-Ordiales, E., Covelli, S., Esbrí, J. M., Loredo, J., & Higueras, P. L. (2016). Sequential extraction procedure as a tool to investigate PTHE geochemistry and potential geoavailability of dam sediments (Almadén mining district, Spain). *Catena*, 147, 394–403.

Garrels, R. M., & MacKenzie, F. T. (1972). A quantitative model for the sedimentary rock cycle. *Marine Chemistry*, *1*(1), 27-41.

Garvine, R. W. (1975). The distribution of salinity and temperature in the Connecticut River estuary. *Journal of Geophysical Research*, *80*(9), 1176-1183.

Garzanti, E. (2017). The maturity myth in sedimentology and provenance analysis. *Journal of Sedimentary Research*, *87*(4), 353-365.

Garzanti, E., Andò, S., & Vezzoli, G. (2009). Grain-size dependence of sediment composition and environmental bias in provenance studies. *Earth and Planetary Science Letters*, *277*(3), 422-432.

Garzanti, E., Andò, S., Vezzoli, G., Megid, A. A. A., & El Kammar, A. (2006). Petrology of Nile River sands (Ethiopia and Sudan): sediment budgets and erosion patterns. *Earth and Planetary Science Letters*, *252*(3), 327-341.

Garzanti, E., Limonta, M., Resentini, A., Bandopadhyay, P. C., Najman, Y., Andò, S., & Vezzoli, G. (2013a). Sediment recycling at convergent plate margins (Indo-Burman ranges and Andaman–Nicobar Ridge). *Earth-Science Reviews*, *123*, 113-132.

Garzanti, E., Padoan, M., Andò, S., Resentini, A., Vezzoli, G., & Lustrino, M. (2013). Weathering and relative durability of detrital minerals in equatorial climate: sand petrology and geochemistry in the East African Rift. *The Journal of Geology*, *121*(6), 547-580.

Garzanti, E., Padoan, M., Setti, M., López-Galindo, A., & Villa, I. M. (2014). Provenance versus weathering control on the composition of tropical river mud (southern Africa). *Chemical Geology*, *366*, 61-74.

Gee, M. J. R., Uy, H. S., Warren, J., Morley, C. K., & Lambiase, J. J. (2007). The Brunei slide: a giant submarine landslide on the North West Borneo Margin revealed by 3D seismic data. *Marine Geology*, *246*(1), 9-23.

Ghrefat, H., & Yusuf, N. (2006). Assessing Mn, Fe, Cu, Zn, and Cd pollution in bottom sediments of Wadi Al-Arab Dam, Jordan. *Chemosphere*, *65*(11), 2114-2121.

Gibbs, R. J. (1973). Mechanisms of trace metal transport in rivers. *Science*, *180*(4081), 71–73.

Giri, C., Ochieng, E., Tieszen, L. L., Zhu, Z., Singh, A., Loveland, T. Duke, N. (2011). Status and distribution of mangrove forests of the world using earth observation satellite data. *Global Ecology and Biogeography*, 20(1), 154–159.

Gismera, M. J., Lacal, J., da Silva, P., Garcıa, R., Sevilla, M. T., & Procopio, J. R. (2004). Study of metal fractionation in river sediments. A comparison between kinetic and sequential extraction procedures. *Environmental Pollution*, *127*(2), 175-182.

Gleyzes, C., Tellier, S., & Astruc, M. (2002). Fractionation studies of trace elements in contaminated soils and sediments: a review of sequential extraction procedures. *TrAC Trends in Analytical Chemistry*, *21*(6), 451-467.

Goldberg, E. D., & Arrhenius, G. O. S. (1958). Chemistry of Pacific pelagic sediments. *Geochimica et Cosmochimica Acta*, 13(2), 153-212.

Gómez Ariza, J. L., Giráldez, I., Sánchez-Rodas, D., & Morales, E. (2000). Metal sequential extraction procedure optimized for heavily polluted and iron oxide rich sediments. *Analytica Chimica Acta*, 414(1–2), 151–164.

González-Costa, J. J., Reigosa, M. J., Matías, J. M., & Fernández-Covelo, E. (2017). Analysis of the Importance of Oxides and Clays in Cd, Cr, Cu, Ni, Pb and Zn Adsorption and Retention with Regression Trees. *PloS one*, *12*(1), e0168523.https://doi.org/10.1371/journal.pone.0168523.

Gonzalez-Macias, C., Schifter, I., Lluch-Cota, D. B., Mendez-Rodriguez, L., & Hernandez-Vazquez, S. (2006). Distribution, enrichment and accumulation of heavy

metals in coastal sediments of Salina Cruz Bay, Mexico. *Environmental Monitoring and Assessment*, *118*(1), 211-230.

Green, T. H. (1995). Significance of Nb/Ta as an indicator of geochemical processes in the crust-mantle system. *Chemical Geology*, *120*(3), 347-359.

Greger, M., Kautsky, L., & Sandberg, T. (1995). A tentative model of Cd uptake in Potamogeton pectinatus in relation to salinity. *Environmental and Experimental Botany*, *35*(2), 215–225.

Gu, Y. G., Lin, Q., Yu, Z. L., Wang, X. N., Ke, C. L., & Ning, J. J. (2015). Speciation and risk of heavy metals in sediments and human health implications of heavy metals in edible nekton in Beibu Gulf, China: A case study of Qinzhou Bay. *Marine Pollution Bulletin*, *101*(2), 852–859.

Guieu, C., & Martin, J.-M. (2002). The Level and Fate of Metals in the Danube River Plume. Estuarine, *Coastal and Shelf Science*, *54*(3), 501–512.

Guieu, C., Martin, J. M., Tankere, S. P. C., Mousty, F., Trincherini, P., Bazot, M., & Dai, M. H. (1998). On trace metal geochemistry in the Danube River and western Black Sea. *Estuarine Coastal and Shelf Science*, *47*(4), 471–485.

Gundersen, P. & Steinnes, E.(2003). Influence of pH and TOC concentration on Cu, Zn, Cd, and Al speciation in rivers. *Water Research*, 37(2), 307-318.

Gupta, S. K., & Chen, K. Y. (1975). Partitioning of trace metals in selective chemical fractions of nearshore sediments. *Environmental letters*, *10*(2), 129-158.

Hakanson, L. (1980). An ecological risk index for aquatic pollution control. A sedimentological approach. *Water Research*, *14*(8), 975-1001.

Hall, G. E. M., Gauthier, G., Pelchat, J. C., Pelchat, P., & Vaive, J. E. (1996). Application of a sequential extraction scheme to ten geological certified reference materials for the determination of 20 elements. *Canadian Journal of Analytical Atomic Spectrometry*, *11*(9), 787–796.

Hallberg, R. O., & Халлберг, P. O. (1976). A Geochemical Method for Investigation of Paleoredox Conditions in Sediments/Геохимический метод исследований условий палеоредокса в осадках. *Ambio Special Report*, 139-147.

Hamdan, O., Aziz, H. K., & Hasmadi, I. M. (2014). L-band ALOS PALSAR for biomass estimation of Matang mangroves, Malaysia. *Remote Sensing of Environment*, *155*, 69-78.

Hansen, D. V., & Rattray, M. (1966). New dimensions in estuary classification. *Limnology and Oceanography*, *11*(3), 319-326.

Harbison, P. (1986). Mangrove muds-A sink and a source for trace metals. *Marine Pollution Bulletin*, *17*(6), 246–250.

Harnois, L. (1988). The CIW index: a new chemical index of weathering. *Sedimentary Geology*, *55*(3-4), 319-322.

Harriss, R. C., & Adams, J. A. S. (1966). Geochemical and mineralogical studies on the weathering of granitic rocks. *American Journal of Science*, *264*(2), 146–173.

Harty, C. (1997). *Mangroves in New South Wales and victoria: forests of the tidal zone in terperate australia*. Vista Publications.

Hass, A., & Fine, P. (2010). Sequential Selective Extraction Procedures for the Study of Heavy Metals in Soils, Sediments, and Waste Materials—a Critical Review. *Critical Reviews in Environmental Science and Technology*, *40*(5), 365–399.

Hatje, V., Payne, T.E., Hill, D.M., McOrist, G., Birch, G.F. & Szymczak, R. (2003). Kinetics of trace element uptake and release by particles in estuarine waters: effects of pH, salinity, and particle loading. *Environment International*, *29*(5), 619-629.

Haughton, P. D. W., Todd, S. P., & Morton, A. C. (1991). Sedimentary provenance studies. *Geological Society, London, Special Publications*, *57*(1), 1-11.

He, B., Li, R., Chai, M., & Qiu, G. (2014). Threat of heavy metal contamination in eight mangrove plants from the Futian mangrove forest, China. *Environmental Geochemistry and Health*, *36*(3), 467–476.

Hedges, J. I., Cowie, G. L., Richey, J. E., Quay, P. D., Benner, R., Strom, M., & Forsberg, B. R. (1994). Origins and processing of organic matter in the Amazon River as indicated by carbohydrates and amino acids. *Limnology and oceanography*, *39*(4), 743-761.

Heiri, O., Lotter, A. F., & Lemcke, G. (2001). Loss on ignition as a method for estimating organic and carbonate content in sediments: Reproducibility and comparability of results. *Journal of Paleolimnology*, 25(1), 101–110.

Heltai, G., Percsich, K., Halász, G., Jung, K., & Fekete, I. (2005). Estimation of ecotoxicological potential of contaminated sediments based on a sequential extraction procedure with supercritical CO 2 and subcritical H 2 O solvents. *Microchemical journal*, *79*(1), 231-237.

Hickey, M. G., & Kittrick, J. A. (1984). Chemical Partitioning of Cadmium, Copper, Nickel and Zinc in Soils and Sediments Containing High Levels of Heavy Metals1. *Journal of Environmental Quality*, *13*, 372–376.

Ho, H. H., Swennen, R., Cappuyns, V., Vassilieva, E., & Van Tran, T. (2012). Necessity of normalization to aluminum to assess the contamination by heavy metals and arsenic in sediments near Haiphong Harbor, Vietnam. *Journal of Asian Earth Sciences*, *56*, 229-239.

Hofer, G., Wagreich, M., & Neuhuber, S. (2013). Geochemistry of fine-grained sediments of the Upper Cretaceous to Paleogene Gosau Group (Austria, Slovakia):

implications for paleoenvironmental and provenance studies. *Geoscience Frontiers*, *4*(4), 449-468.

Holl, W., & Hampp, R. (1975). Lead and plants. *Residue Reviews*, *54*, 79-111.
Honeyman, B. D., & Santschi, P. H. (1989). A Brownian-pumping model for oceanic trace metal scavenging: Evidence from Th isotopes. *Journal of Marine Research*, *47*(4), 951–992.

Hu, B., Li, J., Bi, N., Wang, H., Yang, J., Wei, H., … Li, S. (2015). Seasonal variability and flux of particulate trace elements from the Yellow River: Impacts of the anthropogenic flood event. *Marine Pollution Bulletin*, *91*(1), 35–44.

Hu, Z., Chandran, K., Grasso, D. & Smets, B.F.(2004). Comparison of nitrification inhibition by metals in batch and continuous flow reactors. *Water Research*, *38*(18), 3949-3959.

Huang, G. Y., & Wang, Y. S. (2010). Expression and characterization analysis of type 2 metallothionein from grey mangrove species (*Avicennia marina*) in response to metal stress. *Aquatic Toxicology*, *99*(1), 86-92.

Hume, T. M., & Herdendorf, C. E. (1988). A geomorphic classification of estuaries and its application to coastal resource management - a New Zealand example. *Ocean and Shoreline Management*, *11*(3), 249-274.

Hunt, C. O., & Rushworth, G. (2005). Pollen taphonomy and airfall sedimentation in a tropical cave: the West Mouth of The Great Cave of Niah in Sarawak, Malaysian Borneo. *Journal of Archaeological Science*, *32*(3), 465-473.

Hunt, C. O., Gilbertson, D. D., & Rushworth, G. (2012). A 50,000-year record of late Pleistocene tropical vegetation and human impact in lowland Borneo. *Quaternary Science Reviews*, *37*, 61-80.

Hutchison, C. S. (2005). *Geology of North-West Borneo: Sarawak, Brunei and Sabah*. Elsevier.

Hwang, D. W., Kim, S. G., Choi, M., Lee, I. S., Kim, S. S., & Choi, H. G. (2016). Monitoring of trace metals in coastal sediments around Korean Peninsula. *Marine Pollution Bulletin*, *102*(1), 230-239.

Inskeep, W.P. & Bloom, P.R. (1985). Extinction coefficients of chlorophyll a and b in N,N-dimethylformamide and 80% acetone. *Plant Physiology*,*77*, 483–485.

Ip, C. C. M., Li, X.-D., Zhang, G., Wai, O. W. H., & Li, Y.S. (2007). Trace metal distribution in sediments of the Pearl River Estuary and the surrounding coastal area, South China. *Environmental Pollution*, *147*(2), 311–323.

Iwegbue, C. M., Eghwrudje, M. O., Nwajei, G. E., & Egboh, S. H. O. (2007). Chemical speciation of heavy metals in the Ase River sediment, Niger Delta, Nigeria. *Chemical Speciation & Bioavailability*, *19*(3), 117-127.

Jackson, B. P., Ranville, J. F., Bertsch, P. M., & Sowder, A. G. (2005). Characterization of colloidal and humic-bound Ni and U in the "dissolved" fraction of contaminated sediment extracts. *Environmental Science and Technology*, *39*(8), 2478-2485.

Jain, C. K., Malik, D. S., & Yadav, R. (2007). Metal fractionation study on bed sediments of Lake Nainital, Uttaranchal, India. *Environmental Monitoring and Assessment*, *130*(1-3), 129-139.

Jayaprakash, M., Viswam, A., Gopal, V., Muthuswamy, S., Kalaivanan, P., Giridharan, L., & Jonathan, M. P. (2014). Bioavailable trace metals in micro-tidal Thambraparani estuary, Gulf of Mannar, SE coast of India. *Estuarine, Coastal and Shelf Science*, *146*, 42-48.

Jin-Eong, O. (1995). The ecology of mangrove conservation and management. *Hydrobiologia*, *295*(1–3), 343–351.

Johan, Z., & Johan, V. (2005). Accessory minerals of the Cínovec (Zinnwald) granite cupola, Czech Republic: indicators of petrogenetic evolution. *Mineralogy and Petrology*, *83*(1), 113-150.

Johnson, C.A. (1986). The regulation of trace element concentrations in river and estuarine waters contaminated with acid mine drainage: The adsorption of Cu and Zn on amorphous Fe oxyhydroxides. *Geochimica et Cosmochimica Acta*, *50*(11), 2433-2438.

Jones, B., & Manning, D. A. (1994). Comparison of geochemical indices used for the interpretation of palaeoredox conditions in ancient mudstones. *Chemical Geology*, *111*(1-4), 111-129.

Jusoff, K. (2008). Geospatial information technology for conservation of coastal forest and mangroves environment in Malaysia. *Computer and Information Science*, *1*(2), 129.

Kabata-Pendias, A. (1992). Trace metals in soils in Poland—occurrence and behaviour. *Soil Science*, *140*, 53-70.

Kabata-Pendias, A. (2011). *Trace elements in soils and plants*. CRC Press.

Karbassi, A. R., & Nadjafpour, S. (1996). Flocculation of dissolved Pb, Cu, Zn and Mn during estuarine mixing of river water with the Caspian Sea. *Environmental Pollution*, *93*(3), 257-260.

Karbassi, A. R., Monavari, S. M., Bidhendi, G. R. N., Nouri, J., & Nematpour, K. (2008). Metal pollution assessment of sediment and water in the Shur River. *Environmental Monitoring and Assessment*, *147*(1-3), 107.

Karbassi, A. R., Nouri, J., Mehrdadi, N., & Ayaz, G. O. (2008). Flocculation of heavy metals during mixing of freshwater with Caspian Sea water. *Environmental Geology*, *53*(8), 1811–1816.

Kay, J.T., Conklin, M.H., Fuller, C.C. & O'Day, P.A., (2001). Processes of nickel and cobalt uptake by a manganese oxide forming sediment in Pinal Creek, Globe Mining District, Arizona. *Environmental Science and Technology*, *35*(24), 4719-4725.

Keene, A. F., Johnston, S. G., Bush, R. T., Burton, E. D., & Sullivan, L. A. (2010). Reactive trace element enrichment in a highly modified, tidally inundated acid sulfate soil wetland: East Trinity, Australia. *Marine Pollution Bulletin*, *60*(4), 620–626.

Keeney-Kennicutt, W. L., & Presley, B. J. (1986). The geochemistry of trace metals in the Brazos River estuary. *Estuarine, Coastal and Shelf Science*, *22*(4), 459–477.

Kennish, M. J. (2002). Environmental threats and environmental future of estuaries. *Environmental Conservation*, *29*(1), 78–107.

Kersten, M., & Förstner, U. (1986). Chemical fractionation of heavy metals in anoxic estuarine and coastal sediments. *Water Science and Technology*, *18*(4–5), 121–130.

Keshav, N., & Achyuthan, H. (2015). Late Holocene continental shelf sediments, off Cuddalore, East coast, Bay of Bengal, India: geochemical implications for source-area weathering and provenance. *Quaternary International*, *371*, 209-218.

Ketchum, B. H. (1954). Relation between circulation and planktonic populations in estuaries. *Ecology*, *35*(2), 191-200.

Kinniburgh, D.G., Jackson, M.L. & Syers, J.K. (1976). Adsorption of alkaline earth, transition, and heavy metal cations by hydrous oxide gels of iron and aluminum. *Soil Science Society of America Journal*, *40*(5), 796-799.

Kinsman, B. (1965). *Wind waves: their generation and propagation on the ocean surface*. Courier Corporation.

Kirk, H. J. C. (1968). *The igneous rocks of Sarawak and Sabah* (Vol. 5). US Government Printing Office.

König, S., Münker, C., Schuth, S., & Garbe-Schönberg, D. (2008). Mobility of tungsten in subduction zones. *Earth and Planetary Science Letters*, *274*(1), 82-92.

Koterba M.T.,Wilde, F.D.,& Lapham, W.W. (1995). Groundwater data collection protocols and procedures for the national water quality assessment program—collection and documentation of water quality samples and related data. *US Geological Survey, OpenFile Report*, 95–399, p 113.

Koukina, S. E., Lobus, N. V., Peresypkin, V. I., Dara, O. M., & Smurov, A. V. (2016). Abundance, distribution and bioavailability of major and trace elements in surface sediments from the Cai River estuary and Nha Trang Bay (South China Sea, Vietnam). *Estuarine, Coastal and Shelf Science*. https://doi.org/10.1016/j.ecss.2016.03.005

Kraepiel, A. M. L., Chiffoleau, J.-F., Martin, J.-M., & Morel, F. M. M. (1997). Geochemistry of trace metals in the Gironde estuary. *Geochimica et Cosmochimica Acta*, *61*(7), 1421–1436.

Krishnamurti, G. S. R., Huang, P. M., Van Rees, K. C. J., Kozak, L. M., & Rostad, H. P. W. (1995). Speciation of particulate-bound cadmium of soils and its bioavailability. *Analyst*, *120*(3), 659–665.

Krishnamurty, K. V., Shpirt, E., & Reddy, M. M. (1976). Trace metal extraction of soils and sediments by nitric acid-hydrogen peroxide. *Atomic Absorption Newsletter*, *15*(3), 68.

Kristensen, E., Bouillon, S., Dittmar, T., & Marchand, C. (2008). Organic carbon dynamics in mangrove ecosystems: a review. *Aquatic Botany*, *89*(2), 201-219.

Krom, M. D., Carbo, P., Clerici, S., Cundy, A. B., & Davies, I. M. (2009). Sources and timing of trace metal contamination to sediments in remote sealochs, N.W. Scotland. *Estuarine, Coastal and Shelf Science*, *83*(2), 239–251.

Kronberg, B. I., Nesbitt, H. W., & Fyfe, W. S. (1987). Mobilities of alkalis, alkaline earths and halogens during weathering. *Chemical geology*, *60*(1-4), 41-49.

Krupa, Z. (1988). Cadmium-induced changes in the composition and structure of the light-harvesting chlorophyll a/b protein complex II in radish cotyledons. *Physiologia Plantarum*, *73*(4), 518-524.

Krupadam, R. J., Smita, P., & Wate, S. R. (2006). Geochemical fractionation of heavy metals in sediments of the Tapi estuary. *Geochemical Journal*, *40*(5), 513-522.

Kumar, A., & Ramanathan, A. L. (2015). Speciation of selected trace metals (Fe, Mn, Cu and Zn) with depth in the sediments of Sundarban mangroves: India and Bangladesh. *Journal of Soils and Sediments*, *15*(12), 2476-2486.

Kumar, A., Ramanathan, A. L., Prasad, M. B. K., Datta, D., Kumar, M., & Sappal, S. M. (2016). Distribution, enrichment, and potential toxicity of trace metals in the surface sediments of Sundarban mangrove ecosystem, Bangladesh: a baseline study before Sundarban oil spill of December, 2014. *Environmental Science and Pollution Research*, *23*(9), 8985–8999.

Küpper, H., Küpper, F., & Spiller, M. (1996). Environmental relevance of heavy metal-substituted chlorophylls using the example of water plants. *Journal of Experimental Botany*, *47*(2), 259-266.

Küpper, H., Zhao, F. J., & McGrath, S. P. (1999). Cellular compartmentation of zinc in leaves of the hyperaccumulator *Thlaspi caerulescens*. *Plant physiology*, *119*(1), 305-312.

Lacerda, L. D., Carvalho, C. E. V, Tanizaki, K. F., Ovalle, A. R. C., & Rezende, C. E. (1993). The biogeochemistry and trace metals distribution of mangrove rhizospheres. Biotropica, 25(3), 252–257.

Lacerda, L. D., Rezende, C. E., Aragon, G. T., & Ovalle, A. R. (1991). Iron and chromium transport and accumulation in a mangrove ecosystem. *Water, Air, & Soil Pollution*, *57*(1), 513-520.

Lambiase, J. J., Rahim, A. A. B. A., & Peng, C. Y. (2002). Facies distribution and sedimentary processes on the modern Baram Delta: Implications for the reservoir sandstones of NW Borneo. *Marine and Petroleum Geology*, *19*(1), 69–78.

Lee, M., Bae, W., Chung, J., Jung, H.S. & Shim, H., (2008). Seasonal and spatial characteristics of seawater and sediment at Youngil bay, southeast coast of Korea. *Marine Pollution Bulletin*, 57, 325–334

Li, R., Chai, M., Guo, M., & Qiu, G. Y. (2016). Sediment accumulation and mercury (Hg) flux in *Avicennia marina* forest of Deep Bay, China. *Estuarine, Coastal and Shelf Science*, *177*, 41-46.

Li, S., Yang, X., & Sun, W. (2015). The Lamandau IOCG deposit, southwestern Kalimantan Island, Indonesia: Evidence for its formation from geochronology, mineralogy, and petrogenesis of igneous host rocks. *Ore Geology Reviews*, *68*, 43-58.

Li, X., Shen, Z., Wai, O.W. & Li, Y.S.(2001). Chemical forms of Pb, Zn and Cu in the sediment profiles of the Pearl River Estuary. *Marine Pollution Bulletin*, 42(3), 215-223.

Li, X., Wai, O. W., Li, Y. S., Coles, B. J., Ramsey, M. H., & Thornton, I. (2000). Heavy metal distribution in sediment profiles of the Pearl River estuary, South China. *Applied Geochemistry*, *15*(5), 567-581.

Li, X., Wang, Y., Li, B., Feng, C., Chen, Y., & Shen, Z. (2013). Distribution and speciation of heavy metals in surface sediments from the Yangtze estuary and coastal areas. *Environmental Earth Sciences*, *69*(5), 1537–1547.

Li, Y. H., Burkhardt, L., & Teraoka, H. (1984). Desorption and coagulation of trace elements during estuarine mixing. *Geochimica et Cosmochimica Acta*, *48*(10), 1879-1884.

Lian, Y., Xu, J., Lin, P., Meguro, S., & Kawachi, S. (1999). Five heavy metals in propagules of ten mangrove species of China. *Journal of wood science*, *45*(4), 343-347.

Liao, C., Taylor, A. R., Kenney, W. F., Schlenk, D., & Gan, J. (2017). Historical record and fluxes of DDTs at the Palos Verdes Shelf Superfund site, California. *Science of the Total Environment*, *581*, 697-704.

Linnen, R.L. & Cuney, M. (2005). Granite-related rare-element deposits and experimental constrains on Ta–Nb– W–Sn–Zr–Hf mineralization. In: *Linnen, R.L., Samson, I.M. (Eds.), Rare-element Geochemistry and Mineral Deposits*. Geological Association of Canada. GAC Short Course Notes, 17, pp. 45–68.

Lion, L. W., Altmann, R. S., & Leckie, J. O. (1982). Trace-metal adsorption characteristics of estuarine particulate matter: evaluation of contributions of iron/manganese oxide and organic surface coatings. *Environmental Science & Technology*, *16*(10), 660-666.

Liu, E., & Shen, J. (2014). A comparative study of metal pollution and potential eco-risk in the sediment of Chaohu Lake (China) based on total concentration and chemical speciation. *Environmental Science and Pollution Research*, *21*(12), 7285-7295.

Liu, J., Xiang, R., Chen, Z., Chen, M., Yan, W., Zhang, L., & Chen, H. (2013). Sources, transport and deposition of surface sediments from the South China Sea. *Deep Sea Research Part I: Oceanographic Research Papers*, *71*, 92-102.

Liu, Z., Wang, H., Hantoro, W. S., Sathiamurthy, E., Colin, C., Zhao, Y., & Li, J. (2012). Climatic and tectonic controls on chemical weathering in tropical Southeast Asia (Malay Peninsula, Borneo, and Sumatra). *Chemical Geology*, *291*, 1-12.

Liu, Z., Zhao, Y., Colin, C., Stattegger, K., Wiesner, M.G., Huh, C.A., Zhang, Y., Li, X., Sompongchaiyakul, P., You, C.F. & Huang, C.Y. (2016). Source-to-sink transport processes of fluvial sediments in the South China Sea. *Earth-Science Reviews*, *153*, 238-273.

Long, E. R., Macdonald, D. D., Smith, S. L., & Calder, F. D. (1995). Incidence of adverse biological effects within ranges of chemical concentrations in marine and estuarine sediments. *Environmental Management*, *19*(1), 81-97.

Loring, D. H. (1976). The distribution and partition of zinc, copper, and lead in the sediments of the Saguenay fjord. Canadian Journal of Earth Sciences, *13*(7), 960–971. https://doi.org/10.1139/e76-098

Loska, K., Cebula, J., Pelczar, J., Wiechuła, D., & Kwapuliński, J. (1997). Use of enrichment, and contamination factors together with geoaccumulation indexes to evaluate the content of Cd, Cu, and Ni in the Rybnik water reservoir in Poland. *Water, Air, and Soil Pollution*, *93*(1-4), 347-365.

Ludwig, W., & Probst, J. L. (1996). Predicting the oceanic input of organic carbon by continental erosion. *Global Biogeochemical Cycles*, *10*(1), 23–41.

Lutts, S., & Lefèvre, I. (2015). How can we take advantage of halophyte properties to cope with heavy metal toxicity in salt-affected areas?. *Annals of botany*, *115*(3), 509-528.

Lutts, S., Lefevre, I., Delpérée, C., Kivits, S., Dechamps, C., Robledo, A., & Correal, E. (2004). Heavy metal accumulation by the halophyte species Mediterranean saltbush. *Journal of Environmental Quality*, *33*(4), 1271-1279.

Ma, L. Q., & Rao, G. N. (1997). Chemical fractionation of cadmium, copper, nickel, and zinc in contaminated soils. *Journal of Environmental Quality*, *26*(1), 259-264.

Ma, X., Zuo, H., Tian, M., Zhang, L., Meng, J., Zhou, X. & Liu, Y. (2016). Assessment of heavy metals contamination in sediments from three adjacent regions of the Yellow River using metal chemical fractions and multivariate analysis techniques. *Chemosphere*, *144*, 264-272.

Ma, Y., Liu, C., & Huo, R. (2000). Strontium isotope systematics during chemical weathering of granitoids: importance of relative mineral weathering rates. International *Journal of Goldschmidt Conference Abstract*, *5*, 657.

MacFarlane, G. R. (2002). Leaf biochemical parameters in *Avicennia marina* (Forsk.)

Vierh as potential biomarkers of heavy metal stress in estuarine ecosystems. *Marine Pollution Bulletin*, *44*(3), 244-256.

MacFarlane, G. R., & Burchett, M. D. (1999). Zinc distribution and excretion in the leaves of the grey mangrove, *Avicennia marina* (Forsk.) Vierh. *Environmental and Experimental Botany*, *41*(2), 167-175.

MacFarlane, G. R., & Burchett, M. D. (2000). Cellular distribution of copper, lead and zinc in the grey mangrove, *Avicennia marina* (Forsk.) Vierh. *Aquatic Botany*, *68*(1), 45-59.

Macfarlane, G. R., & Burchett, M. D. (2001). Photosynthetic pigments and peroxidase activity as indicators of heavy metal stress in the grey mangrove, *Avicennia marina* (Forsk.) Vierh. *Marine Pollution Bulletin*, *42*(3), 233-240.

MacFarlane, G. R., & Burchett, M. D. (2002). Toxicity, growth and accumulation relationships of copper, lead and zinc in the grey mangrove *Avicennia marina* (Forsk.) Vierh. *Marine Environmental Research*, *54*(1), 65–84

MacFarlane, G. R., Koller, C. E., & Blomberg, S. P. (2007). Accumulation and partitioning of heavy metals in mangroves: A synthesis of field-based studies. *Chemosphere*, *69*(9), 1454–1464.

MacFarlane, G. R., Pulkownik, A., & Burchett, M. D. (2003). Accumulation and distribution of heavy metals in the grey mangrove, *Avicennia marina* (Forsk.) Vierh.: biological indication potential. *Environmental Pollution*, *123*(1), 139-151.

Machado, W., Gueiros, B. B., Lisboa-Filho, S. D., & Lacerda, L. D. (2005). Trace metals in mangrove seedlings: role of iron plaque formation. *Wetlands Ecology and management*, *13*(2), 199-206.

Machado, W., Silva-Filho, E. V., Oliveira, R. R., & Lacerda, L. D. (2002). Trace metal retention in mangrove ecosystems in Guanabara Bay, SE Brazil. *Marine Pollution Bulletin*, 44(11), 1277–1280.

Mackenzie, F. T., & Garrels, R. M. (1971). *Evolution of sedimentary rocks*. Norton.

Mackenzie, F.T. & Kump, L.R. (1995). Reverse weathering, clay mineral formation, and oceanic element cycles. *Science,* 270(5236), 586.

Mackin, J.E. & Aller, R.C. (1986). The effects of clay mineral reactions on dissolved Al distributions in sediments and waters of the Amazon continental shelf. *Continental Shelf Research*, 6(1-2), pp.245-262.

Macklin, M. G., Ridgway, J., Passmore, D. G., & Rumsby, B. T. (1994). The use of overbank sediment for geochemical mapping and contamination assessment: Results from selected English and Welsh floodplains. *Applied Geochemistry*, *9*(6), 689–700.

Madhavaraju, J., Löser, H., Lee, Y. I., Santacruz, R. L., & Pi-Puig, T. (2016). Geochemistry of Lower Cretaceous limestones of the Alisitos Formation, Baja California, Mexico: Implications for REE source and paleo-redox conditions. *Journal of South American Earth Sciences*, *66*, 149-165.

Maiz, I., Arambarri, I., Garcia, R., & Millan, E. (2000). Evaluation of heavy metal availability in polluted soils by two sequential extraction procedures using factor analysis. *Environmental Pollution*, *110*(1), 3-9.

Maksymiec, W. (1998). Effect of copper on cellular processes in higher plants. *Photosynthetica*, *34*(3), 321-342.

Malo, B. A. (1977). Partial extraction of metals from aquatic sediments. *Environmental Science & Technology*, *11*(3), 277-282.

Marchand, C., Albéric, P., Lallier-Vergès, E., & Baltzer, F. (2006). Distribution and characteristics of dissolved organic matter in mangrove sediment pore waters along the coastline of French Guiana. *Biogeochemistry*, *81*(1), 59–75.

Marchand, C., Allenbach, M., & Lallier-Vergès, E. (2011). Relationships between heavy metals distribution and organic matter cycling in mangrove sediments (Conception Bay, New Caledonia). *Geoderma*, *160*(3–4), 444–456.

Marchand, C., Fernandez, J. M., & Moreton, B. (2016). Trace metal geochemistry in mangrove sediments and their transfer to mangrove plants (New Caledonia). *Science of the Total Environment,* 562, 216–227.

Marchand, C., Lallier-Vergès, E., Baltzer, F., Albéric, P., Cossa, D., & Baillif, P. (2006). Heavy metals distribution in mangrove sediments along the mobile coastline of French Guiana. *Marine Chemistry*, *98*(1), 1–17.

Marin, B., Valladon, M., Polve, M., & Monaco, A. (1997). Reproducibility testing of a sequential extraction scheme for the determination of trace metal speciation in a marine reference sediment by inductively coupled plasma-mass spectrometry. *Analytica Chimica Acta*, *342*(2–3), 91–112.

Marmolejo-Rodríguez, A. J., Prego, R., Meyer-Willerer, A., Shumilin, E., & Cobelo-García, A. (2007). Total and labile metals in surface sediments of the tropical river-estuary system of Marabasco (Pacific coast of Mexico): Influence of an iron mine. *Marine Pollution Bulletin*, *55*(10), 459-468.

Martin, J. M., & Meybeck, M. (1979). Elemental mass-balance of material carried by major world rivers. Marine Chemistry, 7(3), 173–206.

Martin, J. M., & Whitfield, M. (1983). The significance of the river input of chemical elements to the ocean. In *Trace metals in sea water* (pp. 265-296). Springer US.

Martin, J. M., Nirel, P., & Thomas, A. J. (1987). Sequential extraction techniques: Promises and problems. *Marine Chemistry*, *22*(2–4), 313–341.

Martin, J., Guan, D., Elbaz-Poulichet, F., Thomas, A., & Gordeev, V. (1993). Preliminary assessment of the distributions of some trace elements (arsenic, cadmium, copper, iron, nickel, lead, iron, and zinc) in a pristine aquatic environment: The Lena River Estuary (Russia), *Marine Chemistry,43*(1–4), 185–199.

Martin, R. R., Naftel, S. J., Macfie, S. M., Jones, K. W., Feng, H., & Trembley, C. (2006). High variability of the metal content of tree growth rings as measured by synchrotron micro x-ray fluorescence spectrometry. *X-Ray Spectrometry*, *35*(1), 57–62.

Martínez-Santos, M., Probst, A., García-García, J., & Ruiz-Romera, E. (2015). Influence of anthropogenic inputs and a high-magnitude flood event on metal contamination pattern in surface bottom sediments from the Deba River urban catchment. *Science of the Total Environment*, *514*, 10-25.

Mathew, M. J., Menier, D., Siddiqui, N., Kumar, S. G., & Authemayou, C. (2016). Active tectonic deformation along rejuvenated faults in tropical Borneo: Inferences obtained from tectono-geomorphic evaluation. *Geomorphology*, *267*, 1-15.

Matong, J. M., Nyaba, L., & Nomngongo, P. N. (2016). Fractionation of trace elements in agricultural soils using ultrasound assisted sequential extraction prior to inductively coupled plasma mass spectrometric determination. *Chemosphere*, *154*, 249-257.

McLennan, S. M. (1993). Weathering and global denudation. *The Journal of Geology*, *101*(2), 295-303.

McLennan, S. M. (2001). Relationships between the trace element composition of sedimentary rocks and upper continental crust. *Geochemistry, Geophysics, Geosystems*, *2*(4).

McLennan, S. M., Hemming, S., McDaniel, D. K., & Hanson, G. N. (1993). Geochemical approaches to sedimentation, provenance, and tectonics. *Geological Society of America Special Papers*, *284*, 21-40.

McLennan, S. M., Nance, W. B., & Taylor, S. R. (1980). Rare earth element-thorium correlations in sedimentary rocks, and the composition of the continental crust. *Geochimica et Cosmochimica Acta*, *44*(11), 1833-1839.

Means, J.L., Crerar, D.A., Borcsik, M.P. & Duguid, J.O. (1978). Adsorption of Co and selected actinides by Mn and Fe oxides in soils and sediments. *Geochimica et Cosmochimica Acta*, 42(12), pp.1763-1773.

Medici, L., Bellanova, J., Belviso, C., Cavalcante, F., Lettino, A., Ragone, P. P., & Fiore, S. (2011). Trace metals speciation in sediments of the Basento River (Italy). *Applied Clay Science*, *53*(3), 414-442.

Millero, F.J. (1979). The thermodynamics of the carbonate system in seawater. *Geochimica et Cosmochimica Acta*, 43(10), 1651-1661.

Minshall, G. W. (1978). Autotrophy in stream ecosystems. *BioScience*, *28*(12), 767–771.

Mir, A. R. (2015). Rare earth element geochemistry of Post-to Neo-archean shales from Singhbhum mobile belt, Eastern India: implications for tectonic setting and paleo-oxidation conditions. *Chinese Journal of Geochemistry*, *34*(3), 401-409.

Mittermüller, M., Saatz, J., & Daus, B. (2016). A sequential extraction procedure to evaluate the mobilization behavior of rare earth elements in soils and tailings materials. *Chemosphere*, *147*, 155-162.

Mohan, M., Augustine, T., Jayasooryan, K. K., Shylesh Chandran, M. S., & Ramasamy, E. V. (2012). Fractionation of selected metals in the sediments of Cochin estuary and Periyar River, southwest coast of India. *Environmentalist*, *32*(4), 383–393.

Mokievsky, V. O., Tchesunov, a. V., Udalov, a. a., & Toan, N. D. (2011). Quantitative distribution of meiobenthos and the structure of the free-living nematode community of the mangrove intertidal zone in Nha Trang bay (Vietnam) in the South China Sea. *Russian Journal of Marine Biology*, *37*(4), 272–283.

Molengraaff, G. A. F. (1921). Modern deep-sea research in the East Indian Archipelago. *The Geographical Journal*, *57*(2), 95-118.

Mora, A., Laraque, A., Moreira-Turcq, P., & Alfonso, J. A. (2014). Temporal variation and fluxes of dissolved and particulate organic carbon in the Apure, Caura and Orinoco rivers, Venezuela. *Journal of South American Earth Sciences*, *54*, 47–56.

Morford, J.L., Emerson, S.R., Breckel, E.J. & Kim, S.H. (2005). Diagenesis of oxyanions (V, U, Re, and Mo) in pore waters and sediments from a continental margin. *Geochimica et Cosmochimica Acta*, *69*(21), 5021-5032.

Morgan, B., Rate, A. W., & Burton, E. D. (2012). Water chemistry and nutrient release during the resuspension of FeS-rich sediments in a eutrophic estuarine system. *Science of the Total Environment*, *432*, 47-56.

Morrissey, J., & Guerinot, M. Lou. (2009). Iron uptake and transport in plants: The good, the bad, and the ionome. *Chemical Reviews*, *109*(10), 4553–4567.

Moyo, S., McCrindle, R., Mokgalaka, N., & Myburgh, J. (2015). Heavy metal partitioning in sediments from rivers flowing through coal fields in Mpumalanga, South Africa. *CLEAN–Soil, Air, Water*, *43*(6), 892-900.

Mulder, J. & Stein, A.(1994). The solubility of aluminum in acidic forest soils: long-term changes due to acid deposition. *Geochimica et Cosmochimica acta*, *58*(1), 85-94.

Muller, G.(1969). Index of geoaccumulation in sediments of the Rhine River. *Geojournal*, *2*, 108–118.

Murali, A. V., Parthasarathy, R., Mahadevan, T. M., & Das, M. S. (1983). Trace element characteristics, REE patterns and partition coefficients of zircons from different geological environments—a case study on Indian zircons. *Geochimica et Cosmochimica Acta*, *47*(11), 2047-2052.

Mwanuzi, F., & De Smedt, F. (1999). Heavy metal distribution model under estuarine mixing. *Hydrological Processes*, 13(5), 789–804.

Nagarajan, R., Armstrong-Altrin, J. S., Kessler, F. L., Hidalgo-Moral, E. L., Dodge-Wan, D., & Taib, N. I. (2015). Provenance and tectonic setting of Miocene siliciclastic sediments, Sibuti Formation, northwestern Borneo. *Arabian Journal of Geosciences*, *8*(10), 8549-8565.

Nagarajan, R., Jonathan, M. P., Roy, P. D., Muthusankar, G., & Lakshumanan, C. (2015). Decadal evolution of a spit in the Baram river mouth in eastern Malaysia. *Continental Shelf Research*, *105*, 18-25.

Nagarajan, R., Madhavaraju, J., Armstrong-Altrin, J. S., & Nagendra, R. (2011). Geochemistry of Neoproterozoic limestones of the Shahabad Formation, Bhima Basin, Karnataka, southern India. *Geosciences Journal*, *15*(1), 9-25.

Nagarajan, R., Madhavaraju, J., Nagendra, R., Armstrong Altrin, J. S., & Moutte, J. (2007). Geochemistry of Neoproterozoic shales of the Rabanpalli Formation, Bhima Basin, Northern Karnataka, southern India: implications for provenance and paleoredox conditions. *Revista Mexicana de Ciencias Geológicas*, *24*(2).

Nagarajan, R., Roy, P. D., Jonathan, M. P., Lozano, R., Kessler, F. L., & Prasanna, M. V. (2014). Geochemistry of Neogene sedimentary rocks from Borneo Basin, East Malaysia: Paleo-weathering, provenance and tectonic setting. *Chemie der Erde-Geochemistry*, *74*(1), 139-146.

Nagarajan, R., Roy, P. D., Kessler, F. L., Jong, J., Dayong, V., & Jonathan, M. P. (2017b). An integrated study of geochemistry and mineralogy of the Upper Tukau Formation, Borneo Island (East Malaysia): Sediment provenance, depositional setting and tectonic implications. *Journal of Asian Earth Sciences*, *143*, 77-94.

Nagarajan,R., Armstrong-Altrin,J.S.,Kessler, F.L., &Jong, J. (2017a) Petrological and geochemical constraints on provenance, paleo-weathering and tectonic setting of clastic sediments from the Neogene Lambir and Sibuti Formations, NW Borneo. In*Sediment Provenance: influences on compositional change from source to sink*(pp.123-153). Elsevier Amsterdam, Netherlands.

Narwal, R. P., Singh, B. R., & Salbu, B. (1999). Association of cadmium, zinc, copper, and nickel with components in naturally heavy metal-rich soils studied by parallel and sequential extractions. *Communications in Soil Science & Plant Analysis*, *30*(7-8), 1209-1230.

Nath, B. N., Bau, M., Rao, B. R., & Rao, C. M. (1997). Trace and rare earth elemental variation in Arabian Sea sediments through a transect across the oxygen minimum zone. *Geochimica et Cosmochimica Acta*, *61*(12), 2375-2388.

Nath, B. N., Kunzendorf, H., & Pluger, W. L. (2000). Influence of provenance, weathering, and sedimentary processes on the elemental ratios of the fine-grained fraction of the bedload sediments from the Vembanad Lake and the adjoining

continental shelf, southwest coast of India. *Journal of Sedimentary Research*, *70*(5), 1081-1094.

Nath, B., Birch, G., & Chaudhuri, P. (2013). Trace metal biogeochemistry in mangrove ecosystems: A comparative assessment of acidified (by acid sulfate soils) and non-acidified sites. *Science of the Total Environment*, 463–464, 667–674.

Nazli, M. F., & Hashim, N. R. (2010). Heavy metal concentrations in an important mangrove species, *Sonneratia caseolaris*, in Peninsular Malaysia. *Environment Asia*, *3*(Special Issue), 50-55.

Nedwell, D. B., Parkes, R. J., Upton, A. C., & Assinder, D. J. (1994). Seasonal fluxes across the sediment—water interface, and processes within sediments. In *Understanding the North Sea system* (pp. 141-151). Springer Netherlands.

Nemati, K., Bakar, N. K. A., & Abas, M. R. (2009). Investigation of heavy metals mobility in shrimp aquaculture sludge—comparison of two sequential extraction procedures. *Microchemical Journal*, *91*(2), 227-231.

Nemati, K., Bakar, N. K. A., Abas, M. R., & Sobhanzadeh, E. (2011). Speciation of heavy metals by modified BCR sequential extraction procedure in different depths of sediments from Sungai Buloh, Selangor, Malaysia. *Journal of hazardous materials*, *192*(1), 402-410.

Nesbitt, H. (1979). Mobility and fractionation of REE during wearhering of a granodiorite. *Nature*, *279*, 206–210.

Nesbitt, H. W., & Markovics, G. (1980). Chemical processes affecting alkalis and alkaline earths during continental weathering. *Geochimica et Cosmochimica Acta*, *44*(11), 1659-1666.

Nesbitt, H. W., & Wilson, R. E. (1992). Recent chemical weathering of basalts. *American Journal of Science*, *292*(10), 740-777.

Nesbitt, H. W., & Young, G. M. (1982). Early Proterozoic climates and plate motions inferred from major element chemistry of lutites. *Nature*, *299*(5885), 715-717.

Nesbitt, H. W., & Young, G. M. (1984). Prediction of some weathering trends of plutonic and volcanic rocks based on thermodynamic and kinetic considerations. *Geochimica et Cosmochimica Acta*, *48*(7), 1523-1534.

Neyestani, M. R., Bastami, K. D., Esmaeilzadeh, M., Shemirani, F., Khazaali, A., Molamohyeddin, N., ...& Firouzbakht, M. (2016). Geochemical speciation and ecological risk assessment of selected metals in the surface sediments of the northern Persian Gulf. *Marine pollution bulletin*, *109*(1), 603-611.

Nirel, P. M. V., & Morel, F. M. M. (1990). Pitfalls of sequential extractions. *Water research*, *24*(8), 1055-1056.

Nobre, A. M., Ferreira, J. G., Newton, A., Simas, T., Icely, J. D., & Neves, R. (2005). Management of coastal eutrophication: integration of field data, ecosystem-scale simulations and screening models. *Journal of Marine Systems*, *56*(3), 375-390.

Noli, A., De Girolamo, P., & Sammarco, P. (1996). Parametri meteomarini e dinamica costiera: oceanografia e chimica, biologia e geologia marina, clima meteomarino, dinamica dei sedimenti e apporti continentali. *Il Mare del Lazio. Ass. Opere e reti di servizi e mobilita, Regione Lazio, Roma, Italia: Universita degli Studi di La Sapienza*.

Odum, W. E., & Heald, E. J. (1972). Trophic analyses of an estuarine mangrove community. *Bulletin of Marine Science*, *22*(3), 671–738.

Oelkers, E. H., Gislason, S. R., Eiriksdottir, E. S., Jones, M., Pearce, C. R., & Jeandel, C. (2011). The role of riverine particulate material on the global cycles of the elements. *Applied geochemistry*, *26*, S365-S369.

Oelkers, E. H., Jones, M. T., Pearce, C. R., Jeandel, C., Eiriksdottir, E. S., & Gislason, S. R. (2012). Riverine particulate material dissolution in seawater and its implications for the global cycles of the elements. *Comptes Rendus Geoscience*, *344*(11), 646-651.

Oliver, B.G., Thurman, E.M. & Malcolm, R.L. (1983). The contribution of humic substances to the acidity of colored natural waters. *Geochimica et Cosmochimica Acta*, *47*(11), 2031-2035.

Ong Che, R. G. (1999). Concentration of 7 heavy metals in sediments and mangrove root samples from Mai Po, Hong Kong. *Marine Pollution Bulletin*, *39*(1), 269-279.

Ottesen, R. T., Bogen, J., Bølviken, B., & Volden, T. (1989). Overbank sediment: a representative sample medium for regional geochemical mapping. *Journal of Geochemical Exploration*, *32*(1–3), 257–277.

Ouzounidou, G. (1994). Copper-induced changes on growth, metal content and photosynthetic function of *Alyssum montanum* L. plants. *Environmental and Experimental Botany*, *34*(2), 165-172.

Oyeyiola, A. O., Olayinka, K. O., & Alo, B. I. (2011). Comparison of three sequential extraction protocols for the fractionation of potentially toxic metals in coastal sediments. *Environmental Monitoring and Assessment*, *172*(1–4), 319–327.

Pacifico, R., Adamo, P., Cremisini, C., Spaziani, F., & Ferrara, L. (2007). A geochemical analytical approach for the evaluation of heavy metal distribution in lagoon sediments. *Journal of Soils and Sediments*, *7*(5), 313-325.

Pacioglu, O., Cornut, J., Gessner, M.O. & Kasprzak, P. (2016). Prevalence of indirect toxicity effects of aluminium flakes on a shredder-fungal-leaf decomposition system. *Freshwater Biology*, *61*(12), 2013-2025.

Padmaja, K., Prasad, D. D. K., & Prasad, A. R. K. (1990). Inhibition of chlorophyll synthesis in *Phaseolus vulgaris* L. seedlings by cadmium acetate. *Photosynthetica*, *24*(3), 399-405.

Padoan, M., Garzanti, E., Harlavan, Y., & Villa, I. M. (2011). Tracing Nile sediment sources by Sr and Nd isotope signatures (Uganda, Ethiopia, Sudan). *Geochimica et Cosmochimica Acta*, *75*(12), 3627-3644.

Palleiro, L., Patinha, C., Rodríguez-Blanco, M.L., Taboada-Castro, M.M. & Taboada-Castro, M.T. (2017). Aluminum fractionation in acidic soils and river sediments in the Upper Mero basin (Galicia, NW Spain). *Environmental Geochemistry and Health*, 1-13.

Parker, A. (1970). An index of weathering for silicate rocks. *Geological Magazine*, *107*(6), 501-504.

Parvaresh, H., Abedi, Z., Farshchi, P., Karami, M., Khorasani, N., & Karbassi, A. (2011). Bioavailability and concentration of heavy metals in the sediments and leaves of grey mangrove, *Avicennia marina* (Forsk.) Vierh, in Sirik Azini creek, Iran. *Biological Trace Element Research*, *143*(2), 1121–1130.

Passos, E.A., Alves, J.C., Santos, I.S., Alves, J.P., Garcia, C.A.B., & Costa, A.C.S.(2010). Assessment of trace metals contamination in estuarine sediments using a sequential extraction technique and principal component analysis. *Microchemical Journal*, *96*(1), 50-57

Paucot, H., & Wollast, R. (1997). Transport and transformation of trace metals in the Scheldt estuary. *Marine Chemistry*, *58*(1–2), 229–244.

Pekey, H. (2006). The distribution and sources of heavy metals in Izmit Bay surface sediments affected by a polluted stream. *Marine Pollution Bulletin*, *52*(10), 1197–1208.

Pekey, H., Karakaş, D., Ayberk, S., Tolun, L., & Bakoğlu, M. (2004). Ecological risk assessment using trace elements from surface sediments of Izmit Bay (Northeastern Marmara Sea) Turkey. *Marine Pollution Bulletin*, *48*(9), 946-953.

Perin, G., Craboledda, L., Lucchese, M., Cirillo, R., Dotta, L., Zanette, M. L., & Orio, A. A. (1985). Heavy metal speciation in the sediments of northern Adriatic Sea. A new approach for environmental toxicity determination. *Heavy Metals in the Environment*, *2*(1), 454-456.

Perret, D., Gaillard, J. F., Dominik, J., & Atteia, O. (2000). The diversity of natural hydrous iron oxides. *Environmental Science and Technology*, *34*(17), 3540-3546.

Peters, E. C., Gassman, N. J., Firman, J. C., Richmond, R. H., & Power, E. a. (1997). Ecotoxicology of tropical marine ecosystems. Environmental Toxicology and Chemistry, 16(1), 12–40.

Phaenark, C., Pokethitiyook, P., Kruatrachue, M. & Ngernsansaruay, C.(2009). Cd and Zn accumulation in plants from the Padaeng zinc mine area. *International Journal of Phytoremediation*,*11*, 479–95.

Pickering, W. F. (1986). Metal ion speciation—soils and sediments (a review). *Ore Geology Reviews*, *1*(1), 83-146.

Pilon-Smits, E. (2005). Phytoremediation. *Annuual Review of Plant Biology*, *56*, 15-39.

Pizarro, J., Rubio, M. A., & Castillo, X. (2003). Study of chemical speciation in sediments: An approach to vertical metals distribution in Rapel reservoir (Chile). *Journal of the Chilean Chemical Society*, *48*(3), 45-50.

Pohl, C., & Hennings, U. (1999). The effect of redox processes on the partitioning of Cd, Pb, Cu, and Mn between dissolved and particulate phases in the Baltic Sea. *Marine Chemistry*, *65*(1), 41-53.

Potter, P. E. (1978). Petrology and chemistry of modern big river sands. *The Journal of Geology*, *86*(4), 423-449.

Potter, P. E., Maynard, J. B., & Depetris, P. J. (2005). *Mud and mudstones: Introduction and overview*. Springer Science and Business Media.

Prabakaran, K., Nagarajan, R., Franco, F. M., & Kumar, A. A. (2017). Biomonitoring of Malaysian aquatic environments: A review of status and prospects. *Ecohydrology & Hydrobiology*.https://doi.org/10.1016/j.ecohyd.2017.03.001.

Prasad, M. N. V. (1995). Cadmium toxicity and tolerance in vascular plants. *Environmental and Experimental Botany*, *35*(4), 525-545.

Prasad, M. N. V., & Strzałka, K. (1999). Impact of heavy metals on photosynthesis. In *Heavy Metal Stress in Plants* (pp. 117-138). Springer Berlin Heidelberg.

Preda, M., & Cox, M.E. (2002). Trace metal occurrence and distribution in sediments and mangroves, Pumicestone region, southeast Queensland, Australia. *Environment International,* 28, 433–449.

Price R., Velbel, J., & Michael, A. (2003). Chemical weathering indices applied to weathering profiles developed on heterogeneous felsic metamorphic parent rocks. *Chemical Geology*, *202*(3), 397-416.

Pritchard, D. W. (1952). Estuarine hydrography. *Advances in geophysics*, *1*, 243-280.

Pritchard, D. W. (1955). Estuarine circulation patterns. *Proceedings of the American Society of Civil Engineers*,*81* (717), 1 - 11.

Pritchard, D.W. (1967). What Is an Estuary: Physical Viewpoint. In *Estuaries*. American Association for the Advancement of Science, Washington DC

Qiu, Y. W., Yu, K. F., Zhang, G., & Wang, W. X. (2011). Accumulation and partitioning of seven trace metals in mangroves and sediment cores from three estuarine wetlands of Hainan Island, China. *Journal of Hazardous Materials*, *190*(1–3), 631–638.

Quevauviller, P. (1998). Operationally defined extraction procedures for soil and sediment analysis I. Standardization. *TrAC Trends in Analytical Chemistry*, *17*(5), 289-298.

Rahman, S. (2016). *Cosmogenic Silicon-32 reveals extensive authigenic clay formation*

in deltaic systems and constrains the marine silica budget (Doctoral dissertation, State University of New York at Stony Brook).

Ramanathan, A. L., Subramanian, V., Ramesh, R., Chidambaram, S., & James, A. (1999). Environmental geochemistry of the Pichavaram mangrove ecosystem (tropical), southeast coast of India. *Environmental Geology*, *37*(3), 223-233.

Ramos E Silva, C. A., Da Silva, A. P., & De Oliveira, S. R. (2006). Concentration, stock and transport rate of heavy metals in a tropical red mangrove, Natal, Brazil. *Marine Chemistry*, *99*(1), 2-11.

Ramos, L., Gonzalez, M. J., & Hernandez, L. M. (1999). Sequential extraction of copper, lead, cadmium, and zinc in sediments from Ebro River (Spain): relationship with levels detected in earthworms. *Bulletin of Environmental Contamination and toxicology*, *62*(3), 301-308.

Ramos, L., Hernandez, L. M., & Gonzalez, M. J. (1994). Sequential fractionation of copper, lead, cadmium and zinc in soils from or near Donana National Park. *Journal of Environmental Quality*, *23*(1), 50-57.

Rao, C. K., Chinnaraj, S., Inamdar, S. N., & Untawale, A. G. (1991).Aarsenic content in certain marine brown-algae and mangroves from goa coast. *Indian Journal of Marine Sciences*, *20*(4), 283–285.

Rao, C. R. M., Sahuquillo, A., & Sanchez, J. L. (2008). A review of the different methods applied in environmental geochemistry for single and sequential extraction of trace elements in soils and related materials. *Water, Air, and Soil Pollution*, *189*(1-4), 291-333.

Ratcliffe, K. T., Wright, A. M., Hallsworth, C., Morton, A., Zaitlin, B. A., Potocki, D., & Wray, D. S. (2004). An example of alternative correlation techniques in a low-accommodation setting, nonmarine hydrocarbon system: The (Lower Cretaceous) Mannville Basal Quartz succession of southern Alberta. *AAPG bulletin*, *88*(10), 1419-1432.

Rath, P., Panda, U. C., Bhatta, D., & Sahu, K. C. (2009). Use of sequential leaching, mineralogy, morphology and multivariate statistical technique for quantifying metal pollution in highly polluted aquatic sediments-A case study: Brahmani and Nandira Rivers, India. *Journal of Hazardous Materials*, *163*(2–3), 632–644.

Rauret, G. (1998). Extraction procedures for the determination of heavy metals in contaminated soil and sediment. *Talanta*, *46*(3), 449–455.

Rauret, G., López-Sánchez, J. F., Sahuquillo, A., Rubio, R., Davidson, C., Ure, A., & Quevauviller, P. (1999). Improvement of the BCR three step sequential extraction procedure prior to the certification of new sediment and soil reference materials. *Journal of Environmental Monitoring*, *1*(1), 57-61.

Raymond, P. A, & Bauer, J. E. (2001). Riverine export of aged terrestrial organic matter to the North Atlantic Ocean. *Nature*, *409*(6819), 497–500.

Rimmer, S. M. (2004). Geochemical paleoredox indicators in Devonian–Mississippian black shales, central Appalachian Basin (USA). *Chemical Geology*, *206*(3), 373-391.

Robertson, A. I., & Duke, N. C. (1990). Mangrove fish-communities in tropical Queensland, Australia: Spatial and temporal patterns in densities, biomass and community structure. *Marine Biology*, *104*(3), 369–379.

Rollinson, H. R. (2014). *Using geochemical data: evaluation, presentation, interpretation*. Routledge.

Roser, B. P., Cooper, R. A., Nathan, S., & Tulloch, A. J. (1996). Reconnaissance sandstone geochemistry, provenance, and tectonic setting of the lower Paleozoic terranes of the West Coast and Nelson, New Zealand. *New Zealand Journal of Geology and Geophysics*, *39*(1), 1-16.

Roser, B.P., & Korsch, R.J. (1988). Provenance signatures of sandstone - mudstone suites determine using discriminant function analysis of major-element data. *Chemical Geology*, *67*,119–139

Rubio, B., Nombela, M. A., & Vilas, F. (2000). Geochemistry of major and trace elements in sediments of the Ria De Vigo (NW Spain): an assessment of metal pollution. *Marine Pollution Bulletin*, *40*(11), 968-980.

Saenger, P.,& Bellan, M.(1995).*The mangrove vegetation of the Atlantic Coast of Africa: a review*. Université de Toulouse, Toulouse, France.

Sakan, S. M., Đorđević, D. S., Manojlović, D. D., & Predrag, P. S. (2009). Assessment of heavy metal pollutants accumulation in the Tisza river sediments. *Journal of environmental management*, *90*(11), 3382-3390.

Sakan, S., Dević, G., Relić, D., Anđelković, I., Sakan, N., & Đorđević, D. (2015). Risk assessment of trace element contamination in river sediments in Serbia using pollution indices and statistical methods: a pilot study. *Environmental Earth Sciences*, *73*(10), 6625-6638.

Salomons, W., & Förstner, U. (1984). Sediments and the transport of metals. In *Metals in the Hydrocycle* (pp. 63-98). Springer Berlin Heidelberg.

Sánchez-España, J., Yusta, I., Gray, J., & Burgos, W. D. (2016). Geochemistry of dissolved aluminum at low pH: Extent and significance of Al–Fe (III) co-precipitation below pH 4.0. *Geochimica et Cosmochimica Acta*, *175*, 128-149.

Sandal, G. M., Vaernes, R., Bergan, T., Warncke, M., & Ursin, H. (1996). Psychological reactions during polar expeditions and isolation in hyperbaric chambers. *Aviation, Space, and Environmental Medicine*, *67*(3), 227-234.

Sandilyan, S., & Kathiresan, K. (2015). Mangroves as bioshield: An undisputable fact. *Ocean and Coastal Management*, *103*, 94–96.

Santschi, P. H., Lenhart, J. J., & Honeyman, B. D. (1997). Heterogeneous processes affecting trace contaminant distribution in estuaries: the role of natural organic matter. *Marine chemistry*, *58*(1), 99-125.

Sappal, S. M. ., Ramanathan, A. ., Ranjan, R. K. ., Singh, G. ., & Kumar, A. (2014). Rare earth elements as biogeochemical indicators in mangrove ecosystems (Pichavaram, Tamilnadu, India). *Journal of Sedimentary Research*, *84*(9), 781–791.

Saulnier, I., & Mucci, A. (2000). Trace metal remobilization following the resuspension of estuarine sediments: Saguenay Fjord, Canada. *Applied Geochemistry*, *15*(2), 191-210.

Schintu, M., Marrucci, A., Marras, B., Galgani, F., Buosi, C., Ibba, A., & Cherchi, A. (2016). Heavy metal accumulation in surface sediments at the port of Cagliari (Sardinia, western Mediterranean): Environmental assessment using sequential extractions and benthic foraminifera. *Marine pollution bulletin*, *111*(1), 45-56.

Schmidt, M. W., Vielzeuf, D., & Auzanneau, E. (2004). Melting and dissolution of subducting crust at high pressures: the key role of white mica. *Earth and Planetary Science Letters*, *228*(1), 65-84.

Schneider, S., Hornung, J., Hinderer, M., & Garzanti, E. (2016). Petrography and geochemistry of modern river sediments in an equatorial environment (Rwenzori Mountains and Albertine rift, Uganda)—Implications for weathering and provenance. *Sedimentary Geology*, *336*, 106-119.

Schramel, O., Michalke, B., & Kettrup, A. (2000). Study of the copper distribution in contaminated soils of hop fields by single and sequential extraction procedures. *Science of the Total Environment*, *263*(1), 11-22.

Scott, J. A., & Abumoghli, I. (1995). Modelling nitrification in the river Zarka of Jordan. *Water Research*, *29*(4), 1121-1127.

Segura, R., Arancibia, V., Zúñiga, M. C., & Pastén, P. (2006). Distribution of copper, zinc, lead and cadmium concentrations in stream sediments from the Mapocho River in Santiago, Chile. *Journal of Geochemical Exploration*, *91*(1–3), 71–80.

Selvaraj, K., & Chen, C. T. A. (2006). Moderate chemical weathering of subtropical Taiwan: constraints from solid-phase geochemistry of sediments and sedimentary rocks. *The Journal of Geology*, *114*(1), 101-116.

Selvaraj, K., Lin, B. Z., Lou, J. Y., Xia, W. L., Huang, X. T., & Chen, C. T. A. (2016). Lacustrine sedimentological and geochemical records for the last 170 years of climate and environmental changes in southeastern China. *Boreas*, *45*(1), 165-179.

Shafie, N. A., Aris, A. Z., & Haris, H. (2014). Geoaccumulation and distribution of heavy metals in the urban river sediment. *International Journal of Sediment Research*, *29*(3), 368-377.

Shaw, D. M. (1968). A review of K-Rb fractionation trends by covariance analysis. *Geochimica et Cosmochimica Acta*, *32*(6), 573-601.

Sheikh, J. A., Jeelani, G., Gavali, R. S., & Shah, R. A. (2014). Weathering and anthropogenic influences on the water and sediment chemistry of Wular Lake, Kashmir Himalaya. *Environmental Earth Sciences*, *71*(6), 2837-2846.

Sheoran, I. S., Singal, H. R., & Singh, R. (1990). Effect of cadmium and nickel on photosynthesis and the enzymes of the photosynthetic carbon reduction cycle in pigeonpea (*Cajanus cajan*L.). *Photosynthesis Research*, *23*(3), 345-351.

Shiller, A. M. (1997). Dissolved trace elements in the Mississippi River: Seasonal, interannual, and decadal variability. *Geochimica et Cosmochimica Acta*, *61*(20), 4321–4330.

Shiller, A. M., & Boyle, E. (1985). Dissolved zinc in rivers. *Nature*, *317*(6032), 49-52.

Shiller, A. M., & Boyle, E. A. (1987). Variability of dissolved trace metals in the mississippi river. *Geochimica et Cosmochimica Acta*, *51*(12), 3273–3277.

Shiller, A. M., & Boyle, E. A. (1991). Trace elements in the Mississippi River Delta outflow region: Behavior at high discharge. *Geochimica et Cosmochimica Acta*, *55*(11), 3241–3251.

Sholkovitz, E. R. (1978). The flocculation of dissolved Fe, Mn, Al, Cu, Ni, Co and Cd during estuarine mixing. *Earth and Planetary Science Letters*, *41*(1), 77–86.

Sholkovitz, E. R. (1979). Chemical and physical processes controlling the chemical composition of suspended material in the River Tay Estuary. *Estuarine and Coastal Marine Science*, *8*(6), 523-545.

Sholkovitz, E. R., & Copland, D. (1981). The coagulation, solubility and adsorption properties of Fe, Mn, Cu, Ni, Cd, Co and humic acids in a river water. *Geochimica et Cosmochimica Acta*, *45*(2), 181–189.

Sholkovitz, E.R., Boyle, E.A. & Price, N.B.(1978). The removal of dissolved humic acids and iron during estuarine mixing. *Earth and Planetary Science Letters*, 40(1), 130-136.

Sia, S. G., & Abdullah, W. H. (2012). Enrichment of arsenic, lead, and antimony in Balingian coal from Sarawak, Malaysia: Modes of occurrence, origin, and partitioning behaviour during coal combustion. *International Journal of Coal Geology*, *101*, 1-15.

Sial, A. N., Bettencourt, J. S., De Campos, C. P., & Ferreira, V. P. (2011). Granite-related ore deposits: an introduction. *Geological Society, London, Special Publications*, *350*(1), 1-5.

Siegel, F. R. (2002). *Environmental Geochemistry of Potentially Toxic Metals* (Vol. 32). Berlin: Springer.

Silva, C. A. R., Lacerda, L. D., & Rezende, C. E. (1990). Metals reservoir in a red mangrove forest. *Biotropica*, 339-345.

Simons, B., Andersen, J. C., Shail, R. K., & Jenner, F. E. (2017). Fractionation of Li, Be, Ga, Nb, Ta, In, Sn, Sb, W and Bi in the peraluminous Early Permian Variscan granites of the Cornubian Batholith: precursor processes to magmatic-hydrothermal mineralisation. *Lithos*, *278*, 491-512.

Singh, A. K., Hasnain, S. I., & Banerjee, D. K. (1999). Grain size and geochemical partitioning of heavy metals in sediments of the Damodar River - a tributary of the lower Ganga, India. *Environmental Geology*, *39*(1), 90–98.

Singh, K. P., Mohan, D., Singh, V. K., & Malik, A. (2005). Studies on distribution and fractionation of heavy metals in Gomti river sediments—a tributary of the Ganges, India. *Journal of hydrology*, *312*(1), 14-27.

Singh, M., Sharma, M., & Tobschall, H. J. (2005). Weathering of the Ganga alluvial plain, northern India: Implications from fluvial geochemistry of the Gomati River. *Applied Geochemistry*, *20*(1), 1–21.

Singh, S. K., Subramanian, V., & Gibbs, R. J. (1984). Hydrous Fe and Mn oxides—scavengers of heavy metals in the aquatic environment. *Critical Reviews in Environmental Control*, *14*(1), 33-90.

Song, Y. H., & Choi, M. S. (2009). REE geochemistry of fine-grained sediments from major rivers around the Yellow Sea. *Chemical Geology*, *266*(3), 328-342.

Sousa, A. I., Caçador, I., Lillebø, A. I., & Pardal, M. A. (2008). Heavy metal accumulation in *Halimione portulacoides*: intra-and extra-cellular metal binding sites. *Chemosphere*, *70*(5), 850-857.

Spalding, M. (2010). *World atlas of Mangroves*. Routledge.

Spalding, M. D., Blasco, E., & Field, C. D. (1997). *World Mangrove Atlas*. The International Society for Mangrove Ecosystems.

Stallard, R. F., & Edmond, J. M. (1983). Geochemistry of the Amazon: 2. The influence of geology and weathering environment on the dissolved load. *Journal of Geophysical Research: Oceans*, *88*(C14), 9671–9688.

Staub, J. R., & Esterle, J. S. (1994). Peat-accumulating depositional systems of Sarawak, East Malaysia. *Sedimentary Geology*, *89*(1-2), 91-106.

Stolpe, B., & Hassellöv, M. (2010). Nanofibrils and other colloidal biopolymers binding trace elements in coastal seawater: significance for variations in element size distributions. *Limnology and Oceanography*, *55*(1), 187-202.

Stommel, H. M., & Former, H. G. (1952). *On the nature of estuarine circulation: part I (chapters 3 and 4)*. Woods Hole Oceanographic Institution.

Stommel, H., & Farmer, H. G. (1953). Control of salinity in an estuary by a transition. *Journal of Marine Research*, *12*(1), 13-20.

Stone, M., & Droppo, I. G. (1996). Distribution of lead, copper and zinc in size-fractionated river bed sediment in two agricultural catchments of southern Ontario, Canada. *Environmental Pollution*, *93*(3), 353–362

Straub, K. M., & Mohrig, D. (2009). Constructional Canyons Built by Sheet-Like Turbidity Currents: Observations from Offshore Brunei Darussalam. *Journal of Sedimentary Research*, *79*(1), 24–39.

Strauss, E.A., Richardson, W.B., Bartsch, L.A., Cavanaugh, J.C., Bruesewitz, D.A., Imker, H., Heinz, J.A. & Soballe, D.M.(2004). Nitrification in the Upper Mississippi River: patterns, controls, and contribution to the NO3− budget. *Journal of the North American Benthological Society*, *23*(1), 1-14.

Stumm, W., & Morgan, J. J. (1981). *Aquatic chemistry: an introduction emphasizing chemical equilibria in natural waters*. John Wiley and Sons.

Suda, A. & Makino, T. (2016). Functional effects of manganese and iron oxides on the dynamics of trace elements in soils with a special focus on arsenic and cadmium: a review. *Geoderma*, 270, 68-75.

Sultan, K., Shazili, N. A., & Peiffer, S. (2011). Distribution of Pb, As, Cd, Sn and Hg in soil, sediment and surface water of the tropical river watershed, Terengganu (Malaysia). *Journal of Hydro-environment Research*, *5*(3), 169-176.

Sun, S. S., & McDonough, W. S. (1989). Chemical and isotopic systematics of oceanic basalts: implications for mantle composition and processes. *Geological Society, London, Special Publications*, *42*(1), 313-345.

Sundaray, S. K., Nayak, B. B., Lin, S., & Bhatta, D. (2011). Geochemical speciation and risk assessment of heavy metals in the river estuarine sediments—a case study: Mahanadi basin, India. *Journal of Hazardous Materials*, *186*(2), 1837-1846.

Sundby, B., Anderson, L.G., Hall, P.O., Iverfeldt, Å., van der Loeff, M.M.R. & Westerlund, S.F., (1986). The effect of oxygen on release and uptake of cobalt, manganese, iron and phosphate at the sediment-water interface. *Geochimica et Cosmochimica Acta*, *50*(6), pp.1281-1288.

Sungur, A., Soylak, M., Yilmaz, E., Yilmaz, S., & Ozcan, H. (2015). Characterization of heavy metal fractions in agricultural soils by sequential extraction procedure: the relationship between soil properties and heavy metal fractions. *Soil and Sediment Contamination: An International Journal*, *24*(1), 1-15.

Šurija, B., & Branica, M. (1995). Distribution of Cd, Pb, Cu and Zn in carbonate sediments from the Krka river estuary obtained by sequential extraction. *Science of the Total Environment*, *170*(1-2), 101-118.

Sutherland, R. A. (2010). BCR®-701: A review of 10-years of sequential extraction analyses. *Analytica Chimica Acta*, *680*(1), 10-20.

Tam, N. F. ., & Wong, Y. (2000). Spatial variation of heavy metals in surface sediments of Hong Kong mangrove swamps. *Environmental Pollution*, *110*(2), 195–205.

Tam, N. F. Y., & Wong, Y. S. (1993). Retention of nutrients and heavy metals in mangrove sediment receiving wastewater of different strengths. *Environmental Technology*, *14*(8), 719–729.

Tam, N. F. Y., & Wong, Y. S. (1995). Spatial and temporal variations of heavy metal contamination in sediments of a mangrove swamp in Hong Kong. *Marine Pollution Bulletin*, *31*(4–12), 254–261.

Tam, N. F. Y., & Wong, Y. S. (1996). Retention and distribution of heavy metals in mangrove soils receiving wastewater. *Environmental Pollution*, *94*(3), 283–291.

Tate, R. B. (2001). *The Geology of Borneo Island*. Geological Society of Malaysia.
Taylor, S. R., & McLennan, S. M. (1985). *The continental crust: its composition and evolution*.Blackwell Scientific Publications, Oxford

Tessier, A, Campbell, P. G. C., & Bisson, M. (1979). Sequential Extraction Procedure for the Speciation of Particulate Trace Metals. *Analytical Chemistry*, *51*(7), 844–851.

Tessier, A., & Campbell, P. G. C. (1987). Partitioning of trace metals in sediments: Relationships with bioavailability. *Hydrobiologia*, *149*(1), 43–52.

Tessier, A., & Campbell, P. G. C. (1991). Comment on Pitfalls of Sequential Extractions. *Water Resources*, 25(1), 115–117.

Tessier, A., Campbell, P. G., & Bisson, M. (1979). Sequential extraction procedure for the speciation of particulate trace metals. *Analytical chemistry*, *51*(7), 844-851.

Thomas, G., & Fernandez, T. V. (1997). Incidence of heavy metals in the mangrove flora and sediments in Kerala, India. *Hydrobiologia*, *352*, 77–87.

Tiemann, J. S., Gillette, D. P., Wildhaber, M. L., & Edds, D. R. (2004). Effects of lowhead dams on riffle-dwelling fishes and macroinvertebrates in a midwestern river. *Transactions of the American Fisheries Society*, *133*(3), 705-717.

Tiihonen, R.(2016). The distribution of iron and manganese in coastal sediments of the Gulf of Finland.https://helda.helsinki.fi/handle/10138/165595.

Tipping, E. & Heaton, M.J.(1983). The adsorption of aquatic humic substances by two oxides of manganese. *Geochimica et Cosmochimica Acta*, *47*(8), 1393-1397.

Tipping, E. (2004). *Cation Binding by Humic Substances.* Cambridge Environmental Chemistry Series.

Tomlinson, D. L., Wilson, J. G., Harris, C. R., & Jeffrey, D. W. (1980). Problems in the assessment of heavy-metal levels in estuaries and the formation of a pollution index. *Helgoländer Meeresuntersuchungen*, *33*(1), 566.

Totten, M. W., Hanan, M. A., & Weaver, B. L. (2000). Beyond whole-rock geochemistry of shales: The importance of assessing mineralogic controls for revealing tectonic discriminants of multiple sediment sources for the Ouachita Mountain flysch deposits. *Geological Society of America Bulletin*, *112*(7), 1012-1022.

Tovar-Sánchez, A., Sañudo-Wilhelmy, S.A. & Flegal, A.R. (2004). Temporal and spatial variations in the biogeochemical cycling of cobalt in two urban estuaries: Hudson River Estuary and San Francisco Bay. Estuarine, *Coastal and Shelf Science*, *60*(4), 717-728.

Tranvik, L. J., & von Wachenfeldt, E. (2009). Interactions of Dissolved Organic Matter and Humic Substances. *Encyclopedia of Inland Waters*, 754–760.

Tribovillard, N., Algeo, T. J., Lyons, T., & Riboulleau, A. (2006). Trace metals as paleoredox and paleoproductivity proxies: an update. *Chemical Geology*, *232*(1), 12-32.

Truzzi, C., Annibaldi, A., Illuminati, S., Mantini, C., & Scarponi, G. (2017). Chemical fractionation by sequential extraction of Cd, Pb, and Cu in Antarctic atmospheric particulate for the characterization of aerosol composition, sources, and summer evolution at Terra Nova Bay, Victoria Land. *Air Quality, Atmosphere and Health*, 1-16.

Turner, A. (1996). Trace-metal partitioning in estuaries: importance of salinity and particle concentration. *Marine Chemistry*, *54*(1-2), 27-39.

Turner, A., Millward, G. E., & Le Roux, S. M. (2004). Significance of oxides and particulate organic matter in controlling trace metal partitioning in a contaminated estuary. *Marine Chemistry*, *88*(3), 179-192.

Twilley, R. R., & Day, J. W. (2012). Mangrove wetlands. *Estuarine Ecology, Second Edition*, 165-202.

Underwood, G. J. C., & Kromkamp. J. (1999). Primary production by phytoplankton and microphytobenthos in estuaries. *Advances in Ecological Research*, *29*, 93-153.

United States Environmental Protection Agency (USEPA) (2001). The role of screeninglevel risk assessments and refining contaminants of concern in Baseline ecological risk assessments, Publication 9345 0-14, EPA 540/F-01/14, June, 2001.

Ure, A.M., Quevauviller, Ph., Muntau, H., & Griepink, B.(1992). B. *EUR report*. CEC Brussels, 14763, 1992, 85.

Usman, A. R., Alkredaa, R. S., & Al-Wabel, M. I. (2013). Heavy metal contamination in sediments and mangroves from the coast of Red Sea: *Avicennia marina* as potential metal bioaccumulator. *Ecotoxicology and environmental safety*, *97*, 263-270.

Valiela, I., Bowen, J. L., & York, J. K. (2001). Mangrove Forests: One of the World's Threatened Major Tropical Environments. *BioScience*, *51*(10), 807.

Van Hattum, M. W. A., Hall, R., Pickard, A. L., & Nichols, G. J. (2013). Provenance and geochronology of Cenozoic sandstones of northern Borneo. *Journal of Asian Earth Sciences*, *76*, 266-282.

Van Hees, P.A.W., Jones, D.L., Jentschke, G. & Godbold, D.L.(2004). Mobilization of aluminium, iron and silicon by *Picea abies* and ectomycorrhizas in a forest soil. *European Journal of Soil Science*, *55*(1), 101-112.

Vangronsveld, J., & Clijsters, H. (1994). Toxic effects of metals. *Plants and the chemical elements. Biochemistry, uptake, tolerance and toxicity*, 150-177.

Vannucci, M. (2001). What is so special about mangroves? *Brazilian Journal of Biology*, *61*(4), 599-603.

Varol, M. (2011). Assessment of heavy metal contamination in sediments of the Tigris River (Turkey) using pollution indices and multivariate statistical techniques. *Journal of Hazardous Materials*, *195*, 355-364.

Viers, J., Dupre, B., & Gaillardet, J. (2009). Chemical composition of suspended sediments in World Rivers: New insights from a new database. *Science of the Total Environment*, *407*(2), 853–868.

Walters, B. B., Rönnbäck, P., Kovacs, J. M., Crona, B., Hussain, S. A., Badola, R., ...& Dahdouh-Guebas, F. (2008). Ethnobiology, socio-economics and management of mangrove forests: a review. *Aquatic Botany*, *89*(2), 220-236.

Walther, J.V.(1996). Relation between rates of aluminosilicate mineral dissolution, pH, temperature, and surface charge. *American Journal of Science*, *296*(7), 693-728.

Wang, H., Liu, Z. F., Sathiamurthy, E., Colin, C., Li, J. R., & Zhao, Y. L. (2011). Chemical weathering in Malay Peninsula and North Borneo: Clay mineralogy and element geochemistry of river surface sediments. *Science China Earth Sciences*, *54*(2), 272–282.

Wang, S., Jia, Y., Wang, S., Wang, X., Wang, H., Zhao, Z., & Liu, B. (2010). Fractionation of heavy metals in shallow marine sediments from Jinzhou Bay, China. *Journal of Environmental Sciences*, *22*(1), 23-31.

Wang, Y., Qiu, Q., Xin, G., Yang, Z., Zheng, J., Ye, Z., & Li, S. (2013). Heavy metal contamination in a vulnerable mangrove swamp in South China. *Environmental Monitoring and Assessment*, *185*(7), 5775-5787.

Wattayakorn, G., Wolanski, E., & Kjerfve, B. (1990). Mixing, trapping and outwelling in the Klong Ngao mangrove swamp, Thailand. *Estuarine, Coastal and Shelf Science*, *31*(5), 667–688.

Wellburn, A.L.(1984). The spectral determination of chlorophylls a and b, as well as total carotenoids, usingvarious solvents with spectrophotometers of different resolution. *Journal of Plant Physiology*,*144*, 307–313.

Weltje, G. J., & von Eynatten, H. (2004). Quantitative provenance analysis of sediments: review and outlook. *Sedimentary Geology*, *171*(1), 1-11.

Wen, L. S., Santschi, P., Gill, G., & Paternostro, C. (1999). Estuarine trace metal distributions in Galveston Bay: importance of colloidal forms in the speciation of the dissolved phase. *Marine Chemistry*, *63*(3), 185-212.

Widerlund, A.(1996). Early diagenetic remobilization of copper in near-shore marine sediments: a quantitative pore-water model. *Marine Chemistry*, *54*(1-2),.41-53.

Wierzbicka, M. (1995). How lead loses its toxicity to plants. *Acta Societatis Botanicorum Poloniae*, *64*(1), 81-90.

Wigginton, N.S., Haus, K.L. & Hochella Jr, M.F.(2007). Aquatic environmental nanoparticles. *Journal of Environmental Monitoring*, *9*(12), 1306-1316.

Wilford, G. E. (1966). A peat landslide in Sarawak, Malaysia, and its significance in relation to washouts in coal seams. *Journal of Sedimentary Research*, *36*(1), 244-247.

Williams, P. R., Johnston, C. R., Almond, R. A., & Simamora, W. H. (1988). Late Cretaceous to early Tertiary structural elements of West Kalimantan. *Tectonophysics*, *148*(3-4), 279-297.

Witts, D., Hall, R., Nichols, G., & Morley, R. (2012). A new depositional and provenance model for the Tanjung Formation, Barito Basin, SE Kalimantan, Indonesia. *Journal of Asian Earth Sciences*, *56*, 77-104.

Wong, Y. S., Lam, H. M., Dhillon, E., Tam, N. F. Y., & Leung, W. N. (1988). Physiological effects and uptake of cadmium in *Pisum sativum*. *Environment international*, *14*(6), 535-543.

Woodroffe, C. D. (1990). The impact of sea-level rise on mangrove shorelines. *Progress in Physical Geography*, *14*(4), 483-520.

Woodroffe, C. D. (1992). Tropical mangrove ecosystems. *Coastal and Estuarine Studies*, *41*, 7–41.

Wu, Q., Tam, N. F., Leung, J. Y., Zhou, X., Fu, J., Yao, B. & Xia, L. (2014). Ecological risk and pollution history of heavy metals in Nansha mangrove, South China. *Ecotoxicology and Environmental Safety*, *104*, 143-151.

Wu, W., Xu, S., Lu, H., Yang, J., Yin, H., & Liu, W. (2011). Mineralogy, major and trace element geochemistry of riverbed sediments in the headwaters of the Yangtze, Tongtian River and Jinsha River. *Journal of Asian Earth Sciences*, *40*(2), 611–621.

Yarincik, K. M., Murray, R. W., & Peterson, L. C. (2000). Climatically sensitive eolian and hemipelagic deposition in the Cariaco Basin, Venezuela, over the past 578,000 years: Results from Al/Ti and K/Al. *Paleoceanography*, *15*(2), 210-228.

Yiğiterhan, O., Murray, J. W., & Tuğrul, S. (2011). Trace metal composition of suspended particulate matter in the water column of the Black Sea. *Marine Chemistry*, *126*(1–4), 207–228.

Yoon, J. M., Aken, B. V., & Schnoor, J. L. (2006). Leaching of contaminated leaves following uptake and phytoremediation of RDX, HMX, and TNT by poplar. *International Journal of Phytoremediation*, *8*(1), 81-94.

Yuan, C. G., Shi, J. B., He, B., Liu, J. F., Liang, L. N., & Jiang, G. B. (2004). Speciation of heavy metals in marine sediments from the East China Sea by ICP-MS with sequential extraction. *Environment International*, *30*(6), 769-783.

Zabetoglou, K., Voutsa, D., & Samara, C. (2002). Toxicity and heavy metal contamination of surficial sediments from the Bay of Thessaloniki (Northwestern Aegean Sea) Greece. *Chemosphere*, *49*(1), 17–26.

Zan, Q., Wang, Y., & Wang, B. (2002). Accumulation and cycle of heavy metals in *Sonneratia Apetala* and *S. caseolaris* mangrove community at Futian of Shenzhen, China. *Environmental Sciences*, *23*, 81–88 (in Chinese)

Zarcinas, B. A., & Rogers, S. L. (2002). Copper, lead and zinc mobility and bioavailability in a river sediment contaminated with paint stripping residue. *Environmental geochemistry and health*, *24*(3), 191-203.

Zhang, J. (1999). Heavy metal compositions of suspended sediments in the Changjiang (Yangtze River) estuary: significance of riverine transport to the ocean. *Continental Shelf Research*, *19*(12), 1521-1543.

Zhang, J., & Huang, W. W. (1993). Dissolved trace metals in the Huanghe: the most turbid large river in the world. *Water Research*, *27*(1), 1-8.

Zhang, J., Huang, W. W., & Martin, J. M. (1988). Trace metals distribution in Huanghe (Yellow River) estuarine sediments. *Estuarine, Coastal and Shelf Science*, *26*(5), 499-516.

Zhang, J., Huang, W. W., & Wang, J. H. (1994). Trace-metal chemistry of the Huanghe (Yellow River), China — Examination of the data from in situ measurements and laboratory approach. *Chemical Geology*, *114*(1–2), 83–94.

Zhang, J., Yu, Z.G., Liu, S.M., Xu, H. & Liu, M.G.(1997). Dynamics of nutrient elements in three estuaries of North China: the Luanhe, Shuangtaizihe, and Yalujiang. *Estuaries and Coasts*, *20*(1), 110-123.

Zhang, Z. W., Xu, X. R., Sun, Y. X., Yu, S., Chen, Y. S., & Peng, J. X. (2014). Heavy metal and organic contaminants in mangrove ecosystems of China: a review. *Environmental Science and Pollution Research*, *21*(20), 11938-11950.

Zhao, G., Li, K., Zhou, H., Liu, X., Zhang, P., Wen, W. & Yuan, H. (2013). Polyhalogenated aromatic hydrocarbons in surface sediments from Three Gorges Reservoir. *Journal of Environmental Science and Health, Part A*, *48*(2), 136-144.

Zhao, M. Y., & Zheng, Y. F. (2015). The intensity of chemical weathering: geochemical constraints from marine detrital sediments of Triassic age in South China. *Chemical Geology*, *391*, 111-122.

Zhong, H. & Wang, W.X.(2008). Effects of sediment composition on inorganic mercury partitioning, speciation and bioavailability in oxic surficial sediments. *Environmental Pollution*, *151*(1),222-230.

Zhou, Y. W., Peng, Y. S., Li, X. L., & Chen, G. Z. (2011). Accumulation and partitioning of heavy metals in mangrove rhizosphere sediments. *Environmental Earth Sciences*, *64*(3), 799-807.

Zwolsman, J. J., & Van Eck, G. T. (1999). Geochemistry of major elements and trace metals in suspended matter of the Scheldt estuary, southwest Netherlands. *Marine Chemistry*, *66*(1), 91-111.

Appendix 1: Paired Samples T- Test for surface water data

Pairs	Parameters	Paired Differences					t	df	Sig. (2-tailed)
					95% Confidence Interval of the Difference				
		Mean	Std. Deviation	Std. Error Mean	Lower	Upper			
Pair 1	Temperature_MON - Temperature_POM	-3.428	0.972	0.172	-3.778	-3.078	-19.959	31.000	**0.000**
Pair 2	pH_MON - pH_POM	-1.011	0.470	0.083	-1.180	-0.841	-12.173	31.000	**0.000**
Pair 3	DO_MON - DO_POM	-0.473	0.669	0.118	-0.714	-0.232	-3.999	31.000	**0.000**
Pair 4	EC_MOJ - EC_POM	-3134.489	3382.750	597.991	-4354.100	-1914.877	-5.242	31.000	**0.000**
Pair 5	TDS_MON - TDS_POM	-1535.906	1657.639	293.032	-2133.549	-938.264	-5.241	31.000	**0.000**
Pair 6	Salinity_MON - Salinity_POM	-1.634	1.873	0.331	-2.310	-0.959	-4.937	31.000	**0.000**
Pair 7	Resistivity_MON - Resistivity_POM	3.141	17.673	3.124	-3.230	9.513	1.006	31.000	0.322
Pair 8	Turbidity_MON - Turbidity_POM	509.796	223.241	42.189	423.233	596.360	12.084	27.000	**0.000**
Pair 9	Redox_MON - Redox_POM	49.906	24.969	4.414	40.904	58.909	11.306	31.000	**0.000**
Pair 10	Chloride_MON - Chloride_POM	-954.375	1094.944	193.561	-1349.144	-559.606	-4.931	31.000	**0.000**
Pair 12	Bicarbonate_MON - Bicarbonate_POM	5.052	11.816	2.089	0.792	9.312	2.419	31.000	**0.022**
Pair 13	Sodium_MON - Sodium_POM	-371.481	436.214	77.112	-528.753	-214.209	-4.817	31.000	**0.000**
Pair 14	Potassium_MON - Potassium_POM	-56.804	78.765	13.924	-85.201	-28.406	-4.080	31.000	**0.000**
Pair 15	Calcium_MON - Calcium_POM	-32.561	60.637	10.719	-54.423	-10.699	-3.038	31.000	**0.005**
Pair 16	Magnesium_MON - Magnesium_POM	-73.268	101.373	17.920	-109.817	-36.720	-4.089	31.000	**0.000**
Pair 17	Orthophosphate_MON - Orthophosphate_POM	0.012	0.311	0.055	-0.100	0.124	0.222	31.000	0.826

Pairs	Parameters	Paired Differences					t	df	Sig. (2-tailed)
					95% Confidence Interval of the Difference				
		Mean	Std. Deviation	Std. Error Mean	Lower	Upper			
Pair 18	Sulfate_MON - Sulfate_POM	-129.813	143.963	25.449	-181.717	-77.908	-5.101	31.000	**0.000**
Pair 19	Ammoniacalnitrogen_MON - Ammoniacalnitrogen_POM	-0.009	0.053	0.009	-0.028	0.010	-1.000	31.000	0.325
Pair 20	Nitrate_MON - Nitrate_POM	-0.038	0.051	0.009	-0.056	-0.019	-4.140	31.000	**0.000**
Pair 21	Boron_MON - Boron_POM	-0.466	0.486	0.086	-0.641	-0.290	-5.416	31.000	**0.000**
Pair 22	Pb_MON - Pb_POM	-0.009	0.023	0.004	-0.017	0.000	-2.141	31.000	**0.040**
Pair 23	Zn_MON - Zn_POM	0.054	0.082	0.014	0.025	0.084	3.760	31.000	**0.001**
Pair 24	Mn_MON - Mn_POM	0.303	0.513	0.091	0.117	0.488	3.334	31.000	**0.002**
Pair 25	Fe_MON - Fe_POM	10.679	12.209	2.158	6.277	15.081	4.948	31.000	**0.000**
Pair 26	Ni_MON - Ni_POM	-0.003	0.030	0.005	-0.014	0.008	-0.517	31.000	0.609
Pair 27	Cu_MON - Cu_POM	-0.002	0.028	0.005	-0.012	0.008	-0.502	31.000	0.619
Pair 28	Cr_MON - Cr_POM	0.084	0.105	0.019	0.047	0.122	4.552	31.000	**0.000**
Pair 29	Cd_MON - Cd_POM	-0.001	0.003	0.001	-0.002	0.000	-1.555	31.000	0.130
Pair 30	Co_MON - Co_POM	-0.002	0.020	0.004	-0.009	0.005	-0.528	31.000	0.601
Pair 31	Hg_MON - Hg_POM	0.000	0.000	0.000	0.000	0.000	1.593	31.000	0.121
Pair 32	Al_MON - Al_POM	14.783	23.595	4.171	6.276	23.291	3.544	31.000	**0.001**

Appendix 2: Paired Samples T- Test for surface sediments data									
Pairs	**Parameters**	Paired Differences					t	df	Sig. (2-tailed)
					95% Confidence Interval of the Difference				
		Mean	Std. Deviation	Std. Error Mean	Lower	Upper			
Pair 1	Si_MON - Si_POM	248.328	30467.606	5385.963	-10736.416	11233.071	0.046	31.000	0.964
Pair 2	Al_MON - Al_POM	79.388	15359.590	2715.218	-5458.335	5617.110	0.029	31.000	0.977
Pair 3	Fe_MON - Fe_POM	-194.529	6949.068	1228.433	-2699.935	2310.877	-0.158	31.000	0.875
Pair 4	Mn_MON - Mn_POM	-0.968	141.794	25.066	-52.090	50.154	-0.039	31.000	0.969
Pair 5	Mg_MON - Mg_POM	-62.195	1244.264	219.957	-510.800	386.410	-0.283	31.000	0.779
Pair 6	Ca_MON - Ca_POM	140.707	719.178	127.134	-118.585	399.998	1.107	31.000	0.277
Pair 7	Na_MON - Na_POM	-122.871	728.971	128.865	-385.693	139.952	-0.953	31.000	0.348
Pair 8	K_MON - K_POM	313.904	4021.241	710.862	-1135.908	1763.716	0.442	31.000	0.662
Pair 9	Ti_MON - Ti_POM	58.640	805.511	142.396	-231.778	349.057	0.412	31.000	0.683
Pair 10	P_MON - P_POM	-13.638	95.639	16.907	-48.120	20.843	-0.807	31.000	0.426
Pair 11	Sc_MON - Sc_POM	0.125	2.485	0.439	-0.771	1.021	0.284	31.000	0.778
Pair 12	Be_MON - Be_POM	0.250	0.762	0.135	-0.025	0.525	1.856	31.000	0.073
Pair 13	V_MON - V_POM	-0.813	19.458	3.440	-7.828	6.203	-0.236	31.000	0.815
Pair 14	Ba_MON - Ba_POM	0.063	47.279	8.358	-16.984	17.109	0.007	31.000	0.994
Pair 15	Sr_MON - Sr_POM	0.594	10.475	1.852	-3.183	4.371	0.321	31.000	0.751
Pair 16	Y_MON - Y_POM	1.781	4.141	0.732	0.288	3.274	2.434	31.000	**0.021**
Pair 17	Zr_MON - Zr_POM	28.781	144.361	25.520	-23.267	80.829	1.128	31.000	0.268
Pair 18	Cr_MON - Cr_POM	-14.375	12.165	2.150	-18.761	-9.989	-6.685	31.000	**0.000**
Pair 19	Co_MON - Co_POM	-0.938	2.699	0.477	-1.911	0.036	-1.965	31.000	0.058
Pair 20	Ni_MON - Ni_POM	-11.563	11.943	2.111	-15.868	-7.257	-5.477	31.000	**0.000**
Pair 21	Cu_MON - Cu_POM	86.563	114.684	20.273	45.215	127.910	4.270	31.000	**0.000**
Pair 22	Zn_MON - Zn_POM	44.688	53.339	9.429	25.457	63.918	4.739	31.000	**0.000**
Pair 23	Ga_MON - Ga_POM	-0.875	3.260	0.576	-2.050	0.300	-1.518	31.000	0.139
Pair 24	Ger_MON - Ger_POM	-0.063	0.504	0.089	-0.244	0.119	-0.701	31.000	0.488
Pair 25	As_MON - As_POM	-2.344	4.005	0.708	-3.788	-0.900	-3.310	31.000	**0.002**
Pair 26	Rb_MON - Rb_POM	-3.219	21.476	3.796	-10.962	4.524	-0.848	31.000	0.403

Pairs	Parameters	Paired Differences					t	df	Sig. (2-tailed)
					95% Confidence Interval of the Difference				
		Mean	Std. Deviation	Std. Error Mean	Lower	Upper			
Pair 27	Nb_MON - Nb_POM	0.156	2.567	0.454	-0.769	1.082	0.344	31.000	0.733
Pair 28	Mo_MON - Mo_POM	0.188	0.780	0.138	-0.094	0.469	1.359	31.000	0.184
Pair 29	Ag_MON - Ag_POM	0.434	0.619	0.109	0.211	0.657	3.971	31.000	**0.000**
Pair 30	Sn_MON - Sn_POM	0.813	2.389	0.422	-0.049	1.674	1.924	31.000	0.064
Pair 31	Sb_MON - Sb_POM	-1.084	0.348	0.062	-1.210	-0.959	-17.608	31.000	**0.000**
Pair 32	Cs_MON - Cs_POM	-0.316	1.777	0.314	-0.956	0.325	-1.005	31.000	0.323
Pair 33	La_MON - La_POM	-0.172	4.802	0.849	-1.903	1.560	-0.202	31.000	0.841
Pair 34	Ce_MON - Ce_POM	0.203	9.873	1.745	-3.356	3.763	0.116	31.000	0.908
Pair 35	Pr_MON - Pr_POM	-0.157	1.089	0.192	-0.550	0.235	-0.817	31.000	0.420
Pair 36	Nd_MON - Nd_POM	-0.153	4.223	0.746	-1.676	1.369	-0.205	31.000	0.839
Pair 37	Sm_MON - Sm_POM	-0.131	0.883	0.156	-0.450	0.187	-0.841	31.000	0.407
Pair 38	Eu_MON - Eu_POM	0.028	0.184	0.033	-0.038	0.095	0.873	31.000	0.390
Pair 39	Gd_MON - Gd_POM	-0.012	0.815	0.144	-0.307	0.282	-0.087	31.000	0.931
Pair 40	Tb_MON - Tb_POM	-0.016	0.137	0.024	-0.065	0.034	-0.645	31.000	0.524
Pair 41	Dy_MON - Dy_POM	-0.012	0.692	0.122	-0.262	0.237	-0.102	31.000	0.919
Pair 42	Ho_MON - Ho_POM	-0.006	0.141	0.025	-0.057	0.045	-0.250	31.000	0.804
Pair 43	Er_MON - Er_POM	-0.075	0.424	0.075	-0.228	0.078	-1.002	31.000	0.324
Pair 44	Tm_MON - Tm_POM	-0.020	0.059	0.010	-0.041	0.001	-1.926	31.000	0.063
Pair 45	Yb_MON - Yb_POM	-0.044	0.433	0.077	-0.200	0.112	-0.571	31.000	0.572
Pair 47	Hf_MON - Hf_POM	0.309	3.306	0.584	-0.883	1.501	0.529	31.000	0.600
Pair 48	Ta_MON - Ta_POM	0.009	0.184	0.032	-0.057	0.076	0.289	31.000	0.775
Pair 49	W_MON - W_POM	-2.969	1.675	0.296	-3.573	-2.365	-10.026	31.000	**0.000**
Pair 50	Tl_MON - Tl_POM	-0.203	0.128	0.023	-0.249	-0.157	-8.961	31.000	**0.000**
Pair 51	Pb_MON - Pb_POM	12.750	23.927	4.230	4.123	21.377	3.014	31.000	**0.005**
Pair 52	Th_MON - Th_POM	-0.375	1.946	0.344	-1.077	0.327	-1.090	31.000	0.284
Pair 53	U_MON - U_POM	-0.059	0.427	0.076	-0.213	0.095	-0.786	31.000	0.438

Appendix 3: Correlation Matrixfor the Long core sediments (BM-140)

	SiO2	Al2O3	Fe2O3	MnO	MgO	CaO	Na2O	K2O	TiO2	P2O5	LOI	Sc	V	Ba	Sr	Y	Zr	Cr	Co	Ni	Cu	Zn	Ga	As	Rb	Nb	Sn	Cs	La	Ce	Pr	Nd	Sm	Eu	Gd	Tb	Dy	Ho	Er	Tm	Yb	Lu	Hf	Ta	Pb	Th	U	CIA	PIA	WIP	CIA/W	LREE	HREE	TREE
SiO2	1																																																					
Al2O3	**-0.95**	1																																																				
Fe2O3	**-0.93**	**0.93**	1																																																		
MnO	**-0.54**	**0.57**	**0.75**	1																																																	
MgO	**-0.92**	**0.96**	**0.95**	**0.63**	1																																																	
CaO	**-0.81**	**0.85**	**0.92**	**0.74**	**0.91**	1																																																	
Na2O	0.35	-0.23	-0.44	-0.41	-0.24	-0.37	1																																															
K2O	**-0.92**	**0.97**	**0.95**	**0.66**	**0.98**	**0.89**	-0.24	1																																														
TiO2	**-0.54**	**0.61**	0.45	0.31	**0.52**	0.32	0.17	**0.56**	1																																													
P2O5	-0.37	0.46	0.49	0.40	**0.57**	**0.62**	-0.05	**0.53**	0.08	1																																												
LOI	**-0.90**	**0.92**	**0.93**	**0.58**	**0.95**	**0.91**	-0.27	**0.92**	0.38	**0.58**	1																																											
Sc	**-0.92**	**0.91**	**0.93**	**0.73**	**0.89**	**0.84**	-0.34	**0.91**	**0.56**	0.39	**0.85**	1																																									
V	**-0.89**	**0.93**	**0.96**	**0.69**	**0.97**	**0.91**	-0.36	**0.96**	0.43	**0.60**	**0.94**	**0.88**	1																																								
Ba	**-0.89**	**0.90**	**0.92**	**0.74**	**0.88**	**0.78**	-0.32	**0.93**	**0.60**	0.30	**0.79**	**0.94**	**0.85**	1																																							
Sr	**-0.96**	**0.96**	**0.88**	0.48	**0.91**	**0.76**	-0.23	**0.91**	**0.64**	0.31	**0.86**	**0.90**	**0.84**	**0.89**	1																																							
Y	-0.30	0.24	0.22	0.09	0.23	0.11	0.18	0.21	0.47	-0.23	0.21	0.32	0.11	0.33	0.37	1																																							
Zr	**0.91**	**-0.88**	**-0.86**	**-0.59**	**-0.89**	**-0.75**	0.21	**-0.88**	**-0.58**	-0.31	**-0.82**	**-0.91**	**-0.83**	**-0.89**	**-0.89**	-0.40	1																																						
Cr	**-0.55**	**0.60**	**0.63**	0.43	**0.64**	**0.68**	-0.22	**0.63**	0.17	**0.66**	**0.68**	0.49	**0.67**	0.42	**0.52**	-0.11	-0.42	1																																						
Co	**-0.73**	**0.72**	**0.82**	**0.73**	**0.72**	**0.74**	-0.38	**0.73**	**0.51**	0.35	**0.71**	**0.80**	**0.74**	**0.77**	**0.73**	0.37	**-0.66**	0.63	1																																				
Ni	-0.11	0.12	0.14	0.09	0.09	0.03	-0.06	0.11	0.17	-0.01	0.07	0.13	0.13	0.12	0.16	-0.08	-0.17	0.23	0.19	1																																				
Cu	**0.75**	**-0.78**	**-0.77**	**-0.62**	**-0.78**	**-0.76**	0.21	**-0.73**	-0.33	-0.36	**-0.75**	**-0.78**	**-0.76**	**-0.74**	**-0.77**	-0.19	**0.70**	-0.43	**-0.67**	-0.06	1																																				
Zn	**0.64**	**-0.70**	**-0.69**	**-0.62**	**-0.69**	**-0.72**	0.21	**-0.65**	-0.27	-0.36	**-0.65**	**-0.71**	**-0.66**	**-0.68**	**-0.67**	-0.07	**0.58**	-0.40	**-0.62**	-0.05	**0.95**	1																																			
Ga	**-0.85**	**0.86**	**0.92**	**0.68**	**0.88**	**0.86**	-0.43	**0.88**	0.45	**0.54**	**0.89**	**0.87**	**0.93**	**0.80**	**0.80**	0.14	**-0.73**	**0.71**	**0.82**	0.16	**-0.70**	**-0.64**	1																																			
As	**-0.64**	**0.55**	**0.60**	0.42	**0.54**	**0.56**	-0.41	**0.55**	0.25	0.26	**0.53**	**0.62**	**0.56**	**0.54**	**0.59**	0.16	**-0.57**	**0.51**	**0.57**	0.18	-0.44	-0.37	**0.65**	1																																	
Rb	**-0.87**	**0.91**	**0.94**	**0.67**	**0.94**	**0.89**	-0.36	**0.93**	**0.51**	**0.56**	**0.92**	**0.86**	**0.96**	**0.82**	**0.83**	0.13	**-0.80**	**0.70**	**0.77**	0.19	**-0.69**	**-0.61**	**0.96**	**0.62**	1																																
Nb	-0.41	**0.52**	**0.58**	**0.67**	**0.55**	**0.60**	-0.12	**0.58**	0.26	0.48	**0.54**	**0.51**	**0.62**	**0.51**	0.38	-0.10	-0.35	**0.56**	**0.56**	0.14	-0.45	-0.47	**0.66**	0.37	**0.64**	1																															
Sn	-0.09	0.20	0.12	-0.04	0.18	0.14	0.17	0.20	-0.01	0.17	0.21	0.05	0.18	0.07	0.13	-0.24	-0.10	0.22	-0.09	0.37	-0.15	-0.14	0.14	-0.08	0.20	0.12	1																													
Cs	**-0.91**	**0.89**	**0.86**	0.43	**0.83**	**0.73**	-0.42	**0.86**	0.48	0.28	**0.81**	**0.83**	**0.80**	**0.85**	**0.91**	0.18	**-0.80**	0.47	**0.64**	0.15	**-0.67**	**-0.60**	**0.77**	**0.51**	**0.80**	0.33	0.26	1																													
La	**-0.87**	**0.78**	**0.78**	0.39	**0.74**	**0.62**	-0.37	**0.75**	**0.53**	0.15	**0.72**	**0.83**	**0.70**	**0.79**	**0.87**	0.45	**-0.79**	0.41	**0.71**	0.15	**-0.57**	-0.48	**0.75**	**0.72**	**0.74**	0.27	-0.07	**0.84**	1																													
Ce	**-0.88**	**0.80**	**0.77**	0.34	**0.74**	**0.62**	-0.36	**0.74**	**0.54**	0.16	**0.73**	**0.81**	**0.68**	**0.77**	**0.89**	0.44	**-0.78**	0.41	**0.69**	0.13	**-0.61**	**-0.52**	**0.74**	**0.69**	**0.73**	0.21	-0.01	**0.87**	**0.98**	1																													
Pr	**-0.82**	**0.72**	**0.68**	0.22	**0.65**	0.49	-0.33	**0.65**	0.46	0.07	**0.65**	**0.73**	**0.58**	**0.69**	**0.84**	0.45	**-0.73**	0.30	**0.60**	0.12	**-0.54**	-0.43	**0.62**	**0.65**	**0.61**	0.10	-0.03	**0.82**	**0.95**	**0.97**	1																												
Nd	**-0.86**	**0.76**	**0.75**	0.34	**0.70**	**0.57**	-0.35	**0.70**	**0.51**	0.13	**0.69**	**0.78**	**0.65**	**0.74**	**0.87**	0.43	**-0.75**	0.39	**0.67**	0.19	**-0.59**	**-0.50**	**0.70**	**0.71**	**0.69**	0.18	-0.03	**0.83**	**0.96**	**0.97**	**0.97**	1																												
Sm	**-0.85**	**0.77**	**0.76**	0.33	**0.71**	**0.59**	-0.39	**0.71**	0.46	0.16	**0.72**	**0.77**	**0.66**	**0.74**	**0.85**	0.38	**-0.78**	0.40	**0.68**	0.15	**-0.57**	-0.49	**0.69**	**0.59**	**0.69**	0.17	0.00	**0.87**	**0.94**	**0.95**	**0.95**	**0.95**	1																											
Eu	**-0.85**	**0.80**	**0.79**	0.40	**0.77**	**0.66**	-0.34	**0.76**	**0.54**	0.24	**0.74**	**0.80**	**0.71**	**0.78**	**0.85**	0.42	**-0.79**	0.40	**0.67**	-0.01	**-0.60**	**-0.52**	**0.72**	**0.62**	**0.73**	0.20	-0.04	**0.84**	**0.91**	**0.92**	**0.87**	**0.88**	**0.88**	1																										
Gd	**-0.82**	**0.69**	**0.72**	0.36	**0.64**	**0.55**	-0.37	**0.63**	0.42	0.06	**0.66**	**0.74**	**0.59**	**0.69**	**0.81**	0.47	**-0.72**	0.37	**0.71**	0.10	**-0.58**	**-0.50**	**0.64**	**0.60**	**0.63**	0.13	-0.08	**0.77**	**0.90**	**0.91**	**0.91**	**0.93**	**0.93**	**0.86**	1																										
Tb	**-0.75**	**0.67**	**0.66**	0.22	**0.63**	**0.53**	-0.22	**0.62**	0.36	0.18	**0.69**	**0.63**	**0.59**	**0.58**	**0.72**	0.42	**-0.67**	0.40	**0.54**	-0.01	-0.42	-0.30	**0.59**	0.51	**0.62**	0.06	-0.03	**0.69**	**0.83**	**0.84**	**0.82**	**0.82**	**0.87**	**0.81**	**0.83**	1																								
Dy	**-0.73**	**0.62**	**0.59**	0.26	**0.54**	0.43	-0.25	**0.54**	**0.52**	-0.12	**0.54**	**0.66**	0.48	**0.63**	**0.75**	**0.58**	**-0.63**	0.21	**0.58**	0.03	-0.48	-0.41	**0.56**	**0.56**	0.53	0.02	-0.19	**0.66**	**0.85**	**0.87**	**0.86**	**0.89**	**0.81**	**0.81**	**0.90**	**0.77**	1																							
Ho	**-0.58**	0.43	0.44	0.23	0.37	0.28	-0.23	0.36	0.45	-0.15	0.39	**0.57**	0.30	0.49	**0.59**	**0.66**	**-0.56**	0.19	**0.61**	0.07	-0.31	-0.27	0.42	0.48	0.35	0.03	-0.35	0.49	**0.77**	**0.75**	**0.76**	**0.76**	**0.76**	**0.67**	**0.81**	**0.69**	**0.81**	1																						
Er	**-0.55**	0.38	0.39	0.09	0.32	0.21	-0.21	0.30	0.41	-0.29	0.34	0.47	0.25	0.44	**0.57**	**0.69**	-0.46	0.06	0.48	0.05	-0.33	-0.23	0.35	0.39	0.32	-0.19	-0.25	**0.50**	**0.74**	**0.76**	**0.77**	**0.78**	**0.72**	**0.68**	**0.83**	**0.70**	**0.90**	**0.86**	1																					
Tm	**-0.52**	0.37	0.35	0.01	0.30	0.18	-0.21	0.27	0.39	-0.27	0.34	0.45	0.22	0.36	**0.56**	**0.58**	-0.44	0.09	0.45	0.09	-0.27	-0.21	0.37	0.40	0.29	-0.16	-0.22	0.48	**0.75**	**0.76**	**0.79**	**0.79**	**0.75**	**0.66**	**0.81**	**0.69**	**0.87**	**0.88**	**0.92**	1																			
Yb	**-0.54**	0.42	0.43	0.19	0.36	0.29	-0.23	0.37	0.40	-0.25	0.34	**0.53**	0.28	**0.50**	**0.56**	**0.52**	-0.46	0.08	0.49	0.04	-0.31	-0.30	0.40	0.48	0.36	0.04	-0.21	**0.53**	**0.76**	**0.74**	**0.76**	**0.77**	**0.71**	**0.70**	**0.80**	**0.59**	**0.88**	**0.78**	**0.84**	**0.87**	1																		
Lu	-0.43	0.26	0.29	0.12	0.19	0.14	-0.22	0.19	0.28	-0.38	0.21	0.42	0.12	0.37	0.44	**0.61**	-0.38	-0.02	0.45	0.05	-0.25	-0.20	0.24	0.41	0.19	-0.17	-0.32	0.38	**0.67**	**0.67**	**0.70**	**0.71**	**0.68**	**0.57**	**0.78**	**0.65**	**0.83**	**0.87**	**0.89**	**0.85**	**0.82**	1																
Hf	**0.57**	-0.45	-0.39	-0.05	-0.40	-0.18	0.14	-0.43	-0.41	0.22	-0.31	-0.47	-0.30	**-0.56**	**-0.60**	-0.40	**0.64**	0.05	-0.23	-0.10	0.30	0.20	-0.18	-0.19	-0.26	0.29	0.08	**-0.61**	**-0.61**	**-0.61**	**-0.67**	**-0.63**	**-0.66**	**-0.58**	**-0.62**	**-0.54**	**-0.61**	**-0.53**	**-0.63**	**-0.56**	**-0.52**	**-0.53**	1												
Ta	-0.33	0.19	0.11	-0.16	0.08	-0.08	-0.05	0.12	0.22	-0.28	0.07	0.27	0.00	0.26	0.39	0.21	-0.24	-0.08	0.15	0.07	-0.16	-0.12	0.06	0.26	0.01	-0.22	-0.09	0.44	**0.51**	**0.53**	**0.63**	**0.59**	**0.54**	0.43	**0.57**	0.35	**0.53**	**0.51**	**0.58**	**0.58**	**0.56**	**0.59**	**-0.64**	1										
Pb	**-0.49**	0.47	0.41	0.12	0.49	0.48	0.10	0.43	0.18	0.29	**0.50**	0.41	0.40	0.38	**0.53**	0.15	-0.49	0.19	0.22	-0.09	**-0.57**	-0.47	0.24	0.27	0.33	-0.13	0.20	0.46	0.36	0.43	0.45	0.44	0.42	**0.51**	0.44	0.44	0.38	0.14	0.28	0.22	0.25	0.18	-0.42	0.28	1									
Th	**-0.73**	**0.62**	**0.57**	0.12	**0.51**	0.39	-0.34	**0.54**	0.42	-0.04	**0.50**	**0.63**	0.44	0.63	**0.77**	0.38	**-0.61**	0.21	0.53	0.18	-0.47	-0.42	0.48	**0.55**	0.47	-0.04	0.01	**0.81**	**0.87**	**0.91**	**0.93**	**0.90**	**0.90**	**0.81**	**0.87**	**0.72**	**0.80**	**0.71**	**0.75**	**0.74**	**0.74**	**0.71**	**-0.72**	**0.72**	0.44	1							
U	**-0.66**	**0.52**	0.46	-0.09	0.43	0.29	-0.32	0.42	0.31	-0.01	0.46	0.47	0.37	0.44	**0.68**	0.29	-0.48	0.26	0.41	0.16	-0.33	-0.25	0.44	**0.52**	0.41	-0.12	-0.03	**0.71**	**0.80**	**0.85**	**0.90**	**0.86**	**0.84**	**0.75**	**0.82**	**0.75**	**0.78**	**0.66**	**0.75**	**0.78**	**0.70**	**0.66**	**-0.62**	**0.71**	0.41	**0.92**	1						
CIA	**-0.62**	**0.60**	0.45	0.06	0.42	0.23	-0.38	0.41	0.45	-0.11	0.40	0.48	0.40	0.46	**0.67**	0.14	-0.47	0.17	0.33	0.15	-0.45	-0.38	0.43	0.33	0.40	0.00	0.04	**0.65**	**0.60**	**0.66**	**0.68**	**0.66**	**0.66**	**0.57**	**0.61**	0.49	**0.62**	0.47	**0.52**	**0.57**	0.44	0.40	-0.49	0.43	0.21	**0.67**	**0.69**	1					
PIA	**-0.74**	**0.71**	**0.64**	0.27	**0.57**	0.38	**-0.54**	**0.60**	0.46	0.01	0.53	**0.63**	**0.58**	**0.66**	**0.74**	0.13	**-0.62**	0.24	0.46	0.15	-0.49	-0.41	**0.59**	0.42	**0.57**	0.15	0.04	**0.78**	**0.71**	**0.73**	**0.74**	**0.72**	**0.74**	**0.67**	**0.66**	**0.55**	**0.62**	0.48	0.48	**0.51**	0.44	0.38	**-0.57**	0.39	0.15	**0.71**	**0.66**	**0.92**	1				
WIP	**-0.95**	**0.97**	**0.93**	**0.58**	**0.97**	**0.86**	-0.18	**0.99**	**0.58**	**0.51**	**0.93**	**0.92**	**0.93**	**0.91**	**0.94**	0.27	**-0.91**	**0.61**	**0.72**	0.10	**-0.74**	**-0.65**	**0.86**	**0.58**	**0.91**	**0.52**	0.19	**0.87**	**0.79**	**0.79**	**0.71**	**0.75**	**0.76**	**0.80**	**0.69**	**0.68**	**0.60**	0.44	0.38	0.35	0.42	0.27	-0.48	0.21	**0.50**	**0.61**	**0.51**	0.45	**0.60**	1			
CIA/WI	**0.91**	**-0.94**	**-0.91**	**-0.60**	**-0.95**	**-0.84**	0.11	**-0.96**	**-0.56**	**-0.52**	**-0.90**	**-0.91**	**-0.91**	**-0.90**	**-0.90**	-0.28	**0.89**	**-0.58**	**-0.70**	-0.12	**0.74**	**0.62**	**-0.82**	**-0.57**	**-0.88**	**-0.53**	-0.22	**-0.83**	**-0.75**	**-0.75**	**-0.68**	**-0.71**	**-0.70**	**-0.75**	**-0.65**	**-0.63**	**-0.56**	-0.39	-0.35	-0.29	-0.39	-0.24	0.45	-0.22	**-0.52**	**-0.57**	-0.46	-0.38	**-0.53**	**-0.98**	1		
LREE	**-0.88**	**0.79**	**0.77**	0.35	**0.73**	**0.61**	-0.37	**0.74**	**0.53**	0.15	**0.72**	**0.81**	**0.68**	**0.77**	**0.89**	0.44	**-0.78**	0.40	**0.69**	0.15	**-0.60**	**-0.50**	**0.73**	**0.70**	**0.72**	0.21	-0.03	**0.86**	**0.99**	**1.00**	**0.98**	**0.98**	**0.96**	**0.91**	**0.93**	**0.84**	**0.88**	**0.77**	**0.77**	**0.77**	**0.76**	**0.69**	**-0.63**	**0.55**	0.42	**0.91**	**0.85**	**0.65**	**0.73**	**0.79**	**-0.74**	1	
HREE	**-0.72**	**0.58**	**0.58**	0.24	**0.51**	0.41	-0.29	**0.50**	0.46	-0.13	**0.52**	**0.65**	0.44	**0.60**	**0.73**	**0.60**	**-0.62**	0.22	**0.61**	0.06	-0.46	-0.38	**0.53**	**0.55**	**0.50**	0.00	-0.19	**0.66**	**0.87**	**0.88**	**0.89**	**0.90**	**0.86**	**0.82**	**0.94**	**0.80**	**0.97**	**0.88**	**0.94**	**0.92**	**0.91**	**0.88**	**-0.63**	**0.58**	0.36	**0.85**	**0.82**	**0.59**	**0.59**	**0.57**	**-0.53**	**0.89**	1	
TREE	**-0.87**	**0.78**	**0.76**	0.34	**0.71**	**0.59**	-0.36	**0.72**	**0.53**	0.12	**0.71**	**0.80**	**0.66**	**0.76**	**0.88**	0.47	**-0.77**	0.39	**0.69**	0.14	**-0.59**	**-0.50**	**0.72**	**0.69**	**0.71**	0.19	-0.05	**0.85**	**0.99**	**0.99**	**0.98**	**0.99**	**0.96**	**0.91**	**0.94**	**0.85**	**0.90**	**0.79**	**0.79**	**0.80**	**0.78**	**0.71**	**-0.63**	**0.56**	0.42	**0.91**	**0.86**	**0.65**	**0.73**	**0.77**	**-0.73**	**1.00**	**0.92**	1

Appendix 4: Analysis of variance (ANOVA) of metal levels between all tissues and all sites

ANOVA - Single Factor-Cd-All tissues-All sites						
Alpha	0.05					
Groups	Count	Sum	Mean	Variance		
Leaves	5	0.433162	0.086632	0.00012		
Bark	6	0.593272	0.098879	2.45E-05		
Roots	6	0.991009	0.165168	0.003272		
Source of Variation	SS	df	MS	F	P-value	F critical
Between Groups	0.020455	2	0.010227	8.439201	0.003938	3.738892
Within Groups	0.016966	14	0.001212			
Total	0.037421	16				

ANOVA - Single Factor-Cu-All tissues-All sites						
Alpha	0.05					
Groups	Count	Sum	Mean	Variance		
Leaves	6	19.67669	3.279448	0.266951		
Bark	6	11.02776	1.83796	0.976401		
Roots	6	29.18988	4.864979	5.454055		
Source of Variation	SS	df	MS	F	P-value	F critical
Between Groups	27.50928	2	13.75464	6.161177	0.011138	3.68232
Within Groups	33.48704	15	2.232469			
Total	60.99632	17				

ANOVA - Single Factor-Cu-All tissues-All sites						
Alpha	0.05					
Groups	Count	Sum	Mean	Variance		
Leaves	6	19.67669	3.279448	0.266951		
Bark	6	11.02776	1.83796	0.976401		
Roots	6	29.18988	4.864979	5.454055		
Source of Variation	SS	df	MS	F	P-value	F critical
Between Groups	27.50928	2	13.75464	6.161177	0.011138	3.68232
Within Groups	33.48704	15	2.232469			
Total	60.99632	17				

ANOVA - Single Factor-Fe-All tissues-All sites						
Alpha	0.05					
Groups	Count	Sum	Mean	Variance		
Leaves	6	2035.472	339.2454	9740.802		
Bark	6	1234.042	205.6737	2345.763		
Roots	6	11279.78	1879.963	7156888		
Source of Variation	SS	df	MS	F	P-value	F critical
Between Groups	10389800	2	5194900	2.173909	0.148233	3.68232
Within Groups	35844871	15	2389658			
Total	46234671	17				

ANOVA - Single Factor-Mn-All tissues-All sites						
Alpha	0.05					
Groups	Count	Sum	Mean	Variance		
Leaves	6	900.9036	150.1506	6161.516		
Bark	6	608.9589	101.4931	1403.342		
Roots	6	1182.166	197.0276	7218.564		
Source of Variation	SS	df	MS	F	P-value	F critical
Between Groups	27383.69	2	13691.84	2.778486	0.094079	3.68232
Within Groups	73917.11	15	4927.807			
Total	101300.8	17				

ANOVA - Single Factor-Zn-All tissues-All sites						
Alpha	0.05					
Groups	Count	Sum	Mean	Variance		
Leaves	6	54.79026	9.13171	1.890187		
Bark	6	103.4578	17.24297	1190.193		
Roots	6	79.67197	13.27866	79.86252		
Source of Variation	SS	df	MS	F	P-value	F critical
Between Groups	197.4109	2	98.70544	0.232806	0.795117	3.68232
Within Groups	6359.729	15	423.9819			
Total	6557.14	17				

ANOVA - Single Factor-Zn-All tissues-All sites						
Alpha	0.05					
Groups	Count	Sum	Mean	Variance		
Leaves	6	6.650404	1.108401	0.059811		
Bark	6	8.251162	1.375194	1.740792		
Roots	6	16.05143	2.675238	2.385304		
Source of Variation	SS	df	MS	F	P-value	F critical
Between Groups	8.432542	2	4.216271	3.021762	0.07894	3.68232
Within Groups	20.92954	15	1.395302			
Total	29.36208	17				

Appendix 5: Analysis of variance between (ANOVA) of BCF based on total metal concentrations between all tissues and all sites

ANOVA - Single Factor-Fe total-BCF-All tissues-All sites						
Alpha	0.05					
Groups	Count	Sum	Mean	Variance		
Leaves	6	0.41	0.06833	0.00951		
Bark	6	0.045	0.0075	3.5E-06		
Roots	6	0.074	0.01233	1.4E-05		
Source of Variation	SS	df	MS	F	P-value	F critical
Between Groups	0.01372	2	0.00686	2.15932	0.14992	3.68232
Within Groups	0.04765	15	0.00318			
Total	0.06137	17				

ANOVA - Single Factor-Mn total-BCF-All tissues-All sites						
Alpha	0.05					
Groups	Count	Sum	Mean	Variance		
Leaves	6	4.416	0.736	0.10079		
Bark	6	2.275	0.37917	0.01962		
Roots	6	3.365	0.56083	0.08598		
Source of Variation	SS	df	MS	F	P-value	F critical
Between Groups	0.38203	2	0.19102	2.77647	0.09422	3.68232
Within Groups	1.03197	15	0.0688			
Total	1.41401	17				

ANOVA - Single Factor-Cu total-BCF-All tissues-All sites						
Alpha	0.05					
Groups	Count	Sum	Mean	Variance		
Leaves	6	0.507	0.0845	0.00164		
Bark	6	0.191	0.03183	0.0003		
Roots	6	0.342	0.057	7.7E-05		
Source of Variation	SS	df	MS	F	P-value	F critical
Between Groups	0.00833	2	0.00416	6.17938	0.01103	3.68232
Within Groups	0.01011	15	0.00067			
Total	0.01843	17				

ANOVA - Single Factor-Zn total-BCF-All tissues-All sites						
Alpha	0.05					
Groups	Count	Sum	Mean	Variance		
Leaves	6	0.996	0.166	0.0125		
Bark	6	1.293	0.2155	0.18586		
Roots	6	0.685	0.11417	0.0003		
Source of Variation	SS	df	MS	F	P-value	F critical
Between Groups	0.03081	2	0.01541	0.23265	0.79524	3.68232
Within Groups	0.99327	15	0.06622			
Total	1.02408	17				

ANOVA - Single Factor-Pb total-BCF-All tissues-All sites						
Alpha	0.05					
Groups	Count	Sum	Mean	Variance		
Leaves	6	1.112	0.18533	0.01143		
Bark	6	0.571	0.09517	0.00833		
Roots	6	0.46	0.07667	0.00029		
Source of Variation	SS	df	MS	F	P-value	F critical
Between Groups	0.04056	2	0.02028	3.03545	0.07817	3.68232
Within Groups	0.10022	15	0.00668			
Total	0.14078	17				

Appendix 6: Analysis of variance between (ANOVA) of BCF based on mobile metal concentrations between all tissues and all sites

ANOVA - Single Factor-Fe mobile-BCF-All tissues-All sites						
Alpha	0.05					
Groups	Count	Sum	Mean	Variance		
Leaves	6	1.01723	0.16954	0.0582		
Bark	6	0.11129	0.01855	1.9E-05		
Roots	6	0.18356	0.03059	7.9E-05		
Source of Variation	SS	df	MS	F	P-value	F critical
Between Groups	0.0845	2	0.04225	2.17391	0.14823	3.68232
Within Groups	0.29151	15	0.01943			
Total	0.37601	17				

ANOVA - Single Factor-Mn mobile-BCF-All tissues-All sites						
Alpha	0.05					
Groups	Count	Sum	Mean	Variance		
Leaves	6	5.212	0.86867	0.14039		
Bark	6	2.685	0.4475	0.0273		
Roots	6	3.973	0.66217	0.11961		
Source of Variation	SS	df	MS	F	P-value	F critical
Between Groups	0.53221	2	0.26611	2.77863	0.09407	3.68232
Within Groups	1.43653	15	0.09577			
Total	1.96874	17				

ANOVA - Single Factor-Co mobile-BCF-All tissues-All sites						
Alpha	0.05					
Groups	Count	Sum	Mean	Variance		
Leaves	5	0.992	0.1984	0.0098		
Roots	0	0	-	-		
Source of Variation	SS	df	MS	F	P-value	F critical
Between Groups	-	1	-	-	-	10.128
Within Groups	-	3	-			
Total	0.03919	4				

ANOVA - Single Factor-Cu mobile-BCF-All tissues-All sites						
Alpha	0.05					
Groups	Count	Sum	Mean	Variance		
Leaves	6	0.609	0.1015	0.00238		
Bark	6	0.23	0.03833	0.00043		
Roots	6	0.41	0.06833	0.00011		
Source of Variation	SS	df	MS	F	P-value	F critical
Between Groups	0.01198	2	0.00599	6.1541	0.01118	3.68232
Within Groups	0.0146	15	0.00097			
Total	0.02658	17				

ANOVA - Single Factor-Zn mobile-BCF-All tissues-All sites						
Alpha	0.05					
Groups	Count	Sum	Mean	Variance		
Leaves	6	1.504	0.25067	0.02842		
Bark	6	1.952	0.32533	0.42416		
Roots	6	1.033	0.17217	0.00067		
Source of Variation	SS	df	MS	F	P-value	F critical
Between Groups	0.07039	2	0.0352	0.23297	0.79499	3.68232
Within Groups	2.26626	15	0.15108			
Total	2.33665	17				

ANOVA - Single Factor-Pb mobile-BCF-All tissues-All sites						
Alpha	0.05					
Groups	Count	Sum	Mean	Variance		
Leaves	6	1.441	0.24017	0.01925		
Bark	6	0.741	0.1235	0.01407		
Roots	6	0.597	0.0995	0.00049		
Source of Variation	SS	df	MS	F	P-value	F critical
Between Groups	0.06795	2	0.03397	3.01515	0.07931	3.68232
Within Groups	0.16902	15	0.01127			
Total	0.23697	17				

ANOVA - Single Factor-Cd mobile-BCF-All tissues-All sites						
Alpha	0.05					
Groups	Count	Sum	Mean	Variance		
Leaves	6	4.15	0.69167	0.05738		
Bark	6	2.482	0.41367	0.00043		
Roots	5	1.813	0.3626	0.00213		
Source of Variation	SS	df	MS	F	P-value	F critical
Between Groups	0.35935	2	0.17968	8.45355	0.00391	3.73889
Within Groups	0.29756	14	0.02125			
Total	0.65692	16				

Appendix 7: Analysis of variance (ANOVA) between BCF values based on surface sediments and Short core sediments

ANOVA - Single Factor – BCF-Fe-Root-Surface –BSC 01						
Alpha	0.05					
Groups	Count	Sum	Mean	Variance		
Surface sediments	6	0.41	0.06833	0.00951		
BSC 01	9	0.94363	0.10485	0.00101		
Source of Variation	SS	df	MS	F	P-value	F critical
Between Groups	0.0048	1	0.0048	1.12098	0.30898	4.66719
Within Groups	0.05567	13	0.00428			
Total	0.06047	14				

ANOVA - Single Factor-BCF-Fe-Root – Surface - BSC 06						
Alpha	0.05					
Groups	Count	Sum	Mean	Variance		
Surface sediments	6	0.41	0.06833	0.00951		
BSC 06	9	0.2134	0.02371	2.4E-06		
Source of Variation	SS	df	MS	F	P-value	F critical
Between Groups	0.00717	1	0.00717	1.9582	0.18511	4.66719
Within Groups	0.04759	13	0.00366			
Total	0.05475	14				

ANOVA - Single Factor-BCF-Fe-Bark –Surface- BSC 01						
Alpha	0.05					
Groups	Count	Sum	Mean	Variance		
Surface sediments	6	0.045	0.0075	3.5E-06		
BSC 01	9	0.43622	0.04847	0.00022		
Source of Variation	SS	df	MS	F	P-value	F critical
Between Groups	0.00604	1	0.00604	44.9376	1.5E-05	4.66719
Within Groups	0.00175	13	0.00013			
Total	0.00779	14				

ANOVA - Single Factor-BCF-Fe-Bark –Surface- BSC 06						
Alpha	0.05					
Groups	Count	Sum	Mean	Variance		
Surface sediments	6	0.045	0.0075	3.5E-06		
BSC 06	9	0.07049	0.00783	2.6E-07		
Source of Variation	SS	df	MS	F	P-value	F critical
Between Groups	4E-07	1	4E-07	0.26444	0.61571	4.66719
Within Groups	2E-05	13	1.5E-06			
Total	2E-05	14				

ANOVA - Single Factor-Fe-Leaves-Surface- BSC 01						
Alpha	0.05					
Groups	Count	Sum	Mean	Variance		
Surface sediments	6	0.074	0.01233	1.4E-05		
BSC 01	9	0.36987	0.0411	0.00016		
Source of Variation	SS	df	MS	F	P-value	F critical
Between Groups	0.00298	1	0.00298	29.4789	0.00012	4.66719
Within Groups	0.00131	13	0.0001			
Total	0.00429	14				

ANOVA - Single Factor-Fe-Leaves-Surface- BSC 06						
Alpha	0.05					
Groups	Count	Sum	Mean	Variance		
Surface sediments	6	0.074	0.01233	1.4E-05		
BSC 06	9	0.10316	0.01146	5.5E-07		
Source of Variation	SS	df	MS	F	P-value	F critical
Between Groups	2.7E-06	1	2.7E-06	0.48164	0.4999	4.66719
Within Groups	7.4E-05	13	5.7E-06			
Total	7.6E-05	14				

ANOVA - Single Factor-Mn-Root-Surface- BSC 01						
Alpha	0.05					
Groups	Count	Sum	Mean	Variance		
Surface sediments	6	4.416	0.736	0.10079		
BSC 01	9	11.2488	1.24986	0.25852		
Source of Variation	SS	df	MS	F	P-value	F critical
Between Groups	0.9506	1	0.9506	4.8046	0.04719	4.66719
Within Groups	2.57209	13	0.19785			
Total	3.52269	14				

ANOVA - Single Factor-Mn-Root-Surface- BSC 06						
Alpha	0.05					
Groups	Count	Sum	Mean	Variance		
Surface sediments	6	4.416	0.736	0.10079		
BSC 06	9	5.66629	0.62959	0.01254		
Source of Variation	SS	df	MS	F	P-value	F critical
Between Groups	0.04076	1	0.04076	0.877	0.3661	4.66719
Within Groups	0.60426	13	0.04648			
Total	0.64503	14				

ANOVA - Single Factor-Mn-Bark-Surface- BSC 01						
Alpha	0.05					
Groups	Count	Sum	Mean	Variance		
Surface sediments	6	2.275	0.37917	0.01962		
BSC 01	9	9.04795	1.00533	0.16726		
Source of Variation	SS	df	MS	F	P-value	F critical
Between Groups	1.41148	1	1.41148	12.7765	0.00339	4.66719
Within Groups	1.43618	13	0.11048			
Total	2.84766	14				

ANOVA - Single Factor-Mn-Bark-Surface- BSC 06						
Alpha	0.05					
Groups	Count	Sum	Mean	Variance		
Surface sediments	6	2.275	0.37917	0.01962		
BSC 06	9	2.81604	0.31289	0.0031		
Source of Variation	SS	df	MS	F	P-value	F critical
Between Groups	0.01581	1	0.01581	1.67248	0.21844	4.66719
Within Groups	0.1229	13	0.00945			
Total	0.13872	14				

ANOVA - Single Factor-Mn-Leaves-Surface- BSC 01						
Alpha	0.05					
Groups	Count	Sum	Mean	Variance		
Surface sediments	6	3.365	0.56083	0.08598		
BSC 01	9	6.68028	0.74225	0.09117		
Source of Variation	SS	df	MS	F	P-value	F critical
Between Groups	0.11849	1	0.11849	1.32867	0.2698	4.66719
Within Groups	1.15932	13	0.08918			
Total	1.2778	14				

ANOVA - Single Factor-Mn-Leaves-Surface- BSC 06						
Alpha	0.05					
Groups	Count	Sum	Mean	Variance		
Surface sediments	6	3.365	0.56083	0.08598		
BSC 06	9	3.91351	0.43483	0.00598		
Source of Variation	SS	df	MS	F	P-value	F critical
Between Groups	0.05715	1	0.05715	1.55507	0.23439	4.66719
Within Groups	0.47778	13	0.03675			
Total	0.53493	14				

ANOVA - Single Factor-Cu-Root-Surface- BSC 01						
Alpha	0.05					
Groups	Count	Sum	Mean	Variance		
Surface sediments	6	0.507	0.0845	0.00164		
BSC 01	9	0.11786	0.0131	0.00024		
Source of Variation	SS	df	MS	F	P-value	F critical
Between Groups	0.01835	1	0.01835	23.5159	0.00032	4.66719
Within Groups	0.01015	13	0.00078			
Total	0.0285	14				

ANOVA - Single Factor-Cu-Root-Surface- BSC 06						
Alpha	0.05					
Groups	Count	Sum	Mean	Variance		
Surface sediments	6	0.507	0.0845	0.00164		
BSC 06	9	0.11755	0.01306	1.6E-05		
Source of Variation	SS	df	MS	F	P-value	F critical
Between Groups	0.01837	1	0.01837	28.6184	0.00013	4.66719
Within Groups	0.00835	13	0.00064			
Total	0.02672	14				

ANOVA - Single Factor-Cu-Bark-Surface- BSC 01						
Alpha	0.05					
Groups	Count	Sum	Mean	Variance		
Surface sediments	6	0.191	0.03183	0.0003		
BSC 01	9	0.05627	0.00625	5.5E-05		
Source of Variation	SS	df	MS	F	P-value	F critical
Between Groups	0.00236	1	0.00236	15.7445	0.00161	4.66719
Within Groups	0.00195	13	0.00015			
Total	0.0043	14				

ANOVA - Single Factor-Cu-Bark-Surface- BSC 06						
Alpha	0.05					
Groups	Count	Sum	Mean	Variance		
Surface sediments	6	0.191	0.03183	0.0003		
BSC 06	9	0.04059	0.00451	1.9E-06		
Source of Variation	SS	df	MS	F	P-value	F critical
Between Groups	0.00269	1	0.00269	22.9814	0.00035	4.66719
Within Groups	0.00152	13	0.00012			
Total	0.00421	14				

ANOVA - Single Factor-Cu-Leaves-Surface- BSC 01						
Alpha	0.05					
Groups	Count	Sum	Mean	Variance		
Surface sediments	6	0.342	0.057	7.7E-05		
BSC 01	9	0.09067	0.01007	0.00014		
Source of Variation	SS	df	MS	F	P-value	F critical
Between Groups	0.00793	1	0.00793	67.3974	1.7E-06	4.66719
Within Groups	0.00153	13	0.00012			
Total	0.00946	14				

ANOVA - Single Factor-Cu-Leaves-Surface- BSC 06						
Groups	Count	Sum	Mean	Variance		
Surface sediments	6	0.342	0.057	7.7E-05		
BSC 06	9	0.11568	0.01285	1.6E-05		
Source of Variation	SS	df	MS	F	P-value	F critical
Between Groups	0.00702	1	0.00702	178.078	5.8E-09	4.66719
Within Groups	0.00051	13	3.9E-05			
Total	0.00753	14				

ANOVA - Single Factor-Zn-Root-Surface- BSC 01						
Alpha	0.05					
Groups	Count	Sum	Mean	Variance		
Surface sediments	6	0.996	0.166	0.0125		
BSC 01	9	0.58226	0.0647	0.00426		
Source of Variation	SS	df	MS	F	P-value	F critical
Between Groups	0.03695	1	0.03695	4.97076	0.04404	4.66719
Within Groups	0.09662	13	0.00743			
Total	0.13357	14				

ANOVA - Single Factor-Zn-Root-Surface- BSC 06						
Alpha	0.05					
Groups	Count	Sum	Mean	Variance		
Surface sediments	6	0.996	0.166	0.0125		
BSC 06	9	0.42721	0.04747	7.1E-05		
Source of Variation	SS	df	MS	F	P-value	F critical
Between Groups	0.05058	1	0.05058	10.4247	0.00659	4.66719
Within Groups	0.06307	13	0.00485			
Total	0.11365	14				

ANOVA - Single Factor-Zn-Bark-Surface- BSC 01						
Alpha	0.05					
Groups	Count	Sum	Mean	Variance		
Surface sediments	6	1.293	0.2155	0.18586		
BSC 01	9	0.32281	0.03587	0.00131		
Source of Variation	SS	df	MS	F	P-value	F critical
Between Groups	0.11616	1	0.11616	1.60692	0.22716	4.66719
Within Groups	0.93977	13	0.07229			
Total	1.05593	14				

ANOVA - Single Factor-Zn-Bark-Surface- BSC 06						
Alpha	0.05					
Groups	Count	Sum	Mean	Variance		
Surface sediments	6	1.293	0.2155	0.18586		
BSC 06	9	0.04059	0.00451	1.9E-06		
Source of Variation	SS	df	MS	F	P-value	F critical
Between Groups	0.16026	1	0.16026	2.2419	0.1582	4.66719
Within Groups	0.9293	13	0.07148			
Total	1.08956	14				

ANOVA - Single Factor-Zn-Leaves-Surface- BSC 01						
Alpha	0.05					
Groups	Count	Sum	Mean	Variance		
Surface sediments	6	0.685	0.11417	0.0003		
BSC 01	9	0.48282	0.05365	0.00293		
Source of Variation	SS	df	MS	F	P-value	F critical
Between Groups	0.01319	1	0.01319	6.871	0.02114	4.66719
Within Groups	0.02495	13	0.00192			
Total	0.03813	14				

ANOVA - Single Factor-Zn-Leaves-Surface- BSC 06						
Alpha	0.05					
Groups	Count	Sum	Mean	Variance		
Surface sediments	6	0.685	0.11417	0.0003		
BSC 06	9	0.43485	0.04832	7.4E-05		
Source of Variation	SS	df	MS	F	P-value	F critical
Between Groups	0.01561	1	0.01561	97.644	2.1E-07	4.66719
Within Groups	0.00208	13	0.00016			
Total	0.01769	14				

ANOVA - Single Factor-Pb-Root-Surface- BSC 01						
Alpha	0.05					
Groups	Count	Sum	Mean	Variance		
Surface sediments	6	1.112	0.18533	0.01143		
BSC 01	9	1.19196	0.13244	0.00333		
Source of Variation	SS	df	MS	F	P-value	F critical
Between Groups	0.01007	1	0.01007	1.56265	0.23331	4.66719
Within Groups	0.08379	13	0.00645			
Total	0.09386	14				

ANOVA - Single Factor-Pb-Root-Surface- BSC 06						
Alpha	0.05					
Groups	Count	Sum	Mean	Variance		
Surface sediments	6	1.112	0.18533	0.01143		
BSC 06	9	0.89066	0.09896	0.00022		
Source of Variation	SS	df	MS	F	P-value	F critical
Between Groups	0.02686	1	0.02686	5.92649	0.03008	4.66719
Within Groups	0.05891	13	0.00453			
Total	0.08577	14				

ANOVA - Single Factor-Pb-Bark-Surface- BSC 01						
Alpha	0.05					
Groups	Count	Sum	Mean	Variance		
Surface sediments	6	0.571	0.09517	0.00833		
BSC 01	9	0.50962	0.05662	0.00061		
Source of Variation	SS	df	MS	F	P-value	F critical
Between Groups	0.00535	1	0.00535	1.49438	0.24324	4.66719
Within Groups	0.04652	13	0.00358			
Total	0.05187	14				

ANOVA - Single Factor-Pb-Bark-Surface- BSC 06						
Alpha	0.05					
Groups	Count	Sum	Mean	Variance		
Surface sediments	6	0.571	0.09517	0.00833		
BSC 06	9	0.33921	0.03769	3.2E-05		
Source of Variation	SS	df	MS	F	P-value	F critical
Between Groups	0.01189	1	0.01189	3.68919	0.07697	4.66719
Within Groups	0.04191	13	0.00322			
Total	0.0538	14				

ANOVA - Single Factor-Pb-Leaves-Surface- BSC 01						
Alpha	0.05					
Groups	Count	Sum	Mean	Variance		
Surface sediments	6	0.46	0.07667	0.00029		
BSC 01	9	0.66016	0.07335	0.00102		
Source of Variation	SS	df	MS	F	P-value	F critical
Between Groups	4E-05	1	4E-05	0.05347	0.82073	4.66719
Within Groups	0.00962	13	0.00074			
Total	0.00966	14				

ANOVA - Single Factor-Pb-Leaves-Surface-BSC 06						
Alpha	0.05					
Groups	Count	Sum	Mean	Variance		
Surface sediments	6	0.46	0.07667	0.00029		
BSC 06	9	0.38484	0.04276	4.2E-05		
Source of Variation	SS	df	MS	F	P-value	F critical
Between Groups	0.00414	1	0.00414	30.2554	0.0001	4.66719
Within Groups	0.00178	13	0.00014			
Total	0.00592	14				

Appendix 8: Analysis of variance (ANOVA) between BCF values based on surface water and Short core sediments

ANOVA - Single Factor-Fe- Root-Surface water-BSC 01						
Alpha	0.05					
Groups	Count	Sum	Mean	Variance		
Surface water	6	2480.8253	413.47088	346190.6		
BSC 01	9	0.943633	0.1048481	0.001012		
Source of Variation	SS	df	MS	F	P-value	F critical
Between Groups	615137.3	1	615137.3	4.619875	0.051013	4.667193
Within Groups	1730952.8	13	133150.22			
Total	2346090.1	14				

ANOVA - Single Factor-Fe- Root-Surface water-BSC 06						
Alpha	0.05					
Groups	Count	Sum	Mean	Variance		
Surface water	6	2480.8253	413.47088	346190.6		
BSC 06	9	0.2134045	0.0237116	2.36E-06		
Source of Variation	SS	df	MS	F	P-value	F critical
Between Groups	615378.81	1	615378.81	4.621688	0.050974	4.667193
Within Groups	1730952.8	13	133150.22			
Total	2346331.6	14				

ANOVA - Single Factor-Fe- Bark-Surface water-BSC 01						
Alpha	0.05					
Groups	Count	Sum	Mean	Variance		
Surface water	6	271.4097	45.23496	113.4684		
BSC 01	9	0.43622	0.048469	0.000216		
Source of Variation	SS	df	MS	F	P-value	F critical
Between Groups	7350.547	1	7350.547	168.4289	8.12E-09	4.667193
Within Groups	567.3439	13	43.64184			
Total	7917.891	14				

ANOVA - Single Factor-Fe- Bark-Surface water-BSC 06						
Alpha	0.05					
Groups	Count	Sum	Mean	Variance		
Surface water	6	271.4097	45.23496	113.4684		
BSC 06	9	0.070492	0.007832	2.58E-07		
Source of Variation	SS	df	MS	F	P-value	F critical
Between Groups	7363.774	1	7363.774	168.7325	8.03E-09	4.667193
Within Groups	567.3422	13	43.64171			
Total	7931.116	14				

ANOVA - Single Factor-Fe- Leaves-Surface water-BSC 01						
Alpha	0.05					
Groups	Count	Sum	Mean	Variance		
Surface water	6	447.6728	74.61214	471.1788		
BSC 01	9	0.369872	0.041097	0.000156		
Source of Variation	SS	df	MS	F	P-value	F critical
Between Groups	20019.02	1	20019.02	110.4664	1.01E-07	4.667193
Within Groups	2355.895	13	181.2227			
Total	22374.92	14				

ANOVA - Single Factor-Fe- Leaves-Surface water-BSC 06						
Alpha	0.05					
Groups	Count	Sum	Mean	Variance		
Surface water	6	447.6728	74.61214	471.1788		
BSC 06	9	0.103159	0.011462	5.52E-07		
Source of Variation	SS	df	MS	F	P-value	F critical
Between Groups	20034.94	1	20034.94	110.5543	1E-07	4.667193
Within Groups	2355.894	13	181.2226			
Total	22390.83	14				

ANOVA - Single Factor-Mn- Roots-Surface water-BSC 01						
Alpha	0.05					
Groups	Count	Sum	Mean	Variance		
Surface water	6	8433.285	1405.547	367356.4		
BSC 01	9	11.24878	1.249864	0.25852		
Source of Variation	SS	df	MS	F	P-value	F critical
Between Groups	7099386	1	7099386	50.24653	8.19E-06	4.667193
Within Groups	1836784	13	141291.1			
Total	8936170	14				

ANOVA - Single Factor-Mn- Roots-Surface water-BSC 06						
Alpha	0.05					
Groups	Count	Sum	Mean	Variance		
Surface water	6	8433.285	1405.547	367356.4		
BSC 06	9	5.666294	0.629588	0.012541		
Source of Variation	SS	df	MS	F	P-value	F critical
Between Groups	7105659	1	7105659	50.29099	8.15E-06	4.667193
Within Groups	1836782	13	141290.9			
Total	8942441	14				

ANOVA - Single Factor-Mn- Bark-Surface water-BSC 01						
Alpha	0.05					
Groups	Count	Sum	Mean	Variance		
Surface water	6	4344.165	724.0275	71416.77		
BSC 01	9	9.047953	1.005328	0.167257		
Source of Variation	SS	df	MS	F	P-value	F critical
Between Groups	1881940	1	1881940	68.51368	1.54E-06	4.667193
Within Groups	357085.2	13	27468.09			
Total	2239025	14				

ANOVA - Single Factor-Mn- Bark-Surface water-BSC 06						
Alpha	0.05					
Groups	Count	Sum	Mean	Variance		
Surface water	6	4344.165	724.0275	71416.77		
BSC 06	9	2.816039	0.312893	0.003098		
Source of Variation	SS	df	MS	F	P-value	F critical
Between Groups	1885546	1	1885546	68.64523	1.52E-06	4.667193
Within Groups	357083.9	13	27467.99			
Total	2242630	14				

ANOVA - Single Factor-Mn- Leaves-Surface water-BSC 01						
Alpha	0.05					
Groups	Count	Sum	Mean	Variance		
Surface water	6	6426.828	1071.138	313562.6		
BSC 01	9	6.680284	0.742254	0.091174		
Source of Variation	SS	df	MS	F	P-value	F critical
Between Groups	4124690	1	4124690	34.20111	5.7E-05	4.667193
Within Groups	1567814	13	120601.1			
Total	5692504	14				

ANOVA - Single Factor-Mn- Leaves-Surface water-BSC 06						
Alpha	0.05					
Groups	Count	Sum	Mean	Variance		
Surface water	6	6426.828	1071.138	313562.6		
BSC 06	9	3.91351	0.434834	0.005982		
Source of Variation	SS	df	MS	F	P-value	F critical
Between Groups	4127059	1	4127059	34.22077	5.69E-05	4.667193
Within Groups	1567813	13	120601			
Total	5694873	14				

ANOVA - Single Factor-Cu- Root-Surface water-BSC 01						
Alpha	0.05					
Groups	Count	Sum	Mean	Variance		
Surface water	6	553.7375	92.28958	1962.741		
BSC 01	9	0.117862	0.013096	0.000241		
Source of Variation	SS	df	MS	F	P-value	F critical
Between Groups	30653.82	1	30653.82	40.60644	2.45E-05	4.667193
Within Groups	9813.705	13	754.9004			
Total	40467.52	14				

ANOVA - Single Factor-Cu- Root-Surface water-BSC 06						
Alpha	0.05					
Groups	Count	Sum	Mean	Variance		
Surface water	6	553.7375	92.28958	1962.741		
BSC 06	9	0.117551	0.013061	1.63E-05		
Source of Variation	SS	df	MS	F	P-value	F critical
Between Groups	30653.84	1	30653.84	40.60648	2.45E-05	4.667193
Within Groups	9813.703	13	754.9002			
Total	40467.54	14				

ANOVA - Single Factor-Cu- Bark-Surface water-BSC 01						
Alpha	0.05					
Groups	Count	Sum	Mean	Variance		
Surface water	6	209.1987	34.86646	351.3757		
BSC 01	9	0.056274	0.006253	5.5E-05		
Source of Variation	SS	df	MS	F	P-value	F critical
Between Groups	4374.842	1	4374.842	32.37158	7.42E-05	4.667193
Within Groups	1756.879	13	135.1445			
Total	6131.72	14				

ANOVA - Single Factor-Cu- Bark-Surface water-BSC 06						
Alpha	0.05					
Groups	Count	Sum	Mean	Variance		
Surface water	6	209.1987	34.86646	351.3757		
BSC 06	9	0.040587	0.00451	1.94E-06		
Source of Variation	SS	df	MS	F	P-value	F critical
Between Groups	4375.279	1	4375.279	32.37483	7.42E-05	4.667193
Within Groups	1756.878	13	135.1445			
Total	6132.157	14				

ANOVA - Single Factor-Cu- Leaves-Surface water-BSC 01						
Alpha	0.05					
Groups	Count	Sum	Mean	Variance		
Surface water	6	373.2705	62.21175	96.0672		
BSC 01	9	0.090672	0.010075	0.000143		
Source of Variation	SS	df	MS	F	P-value	F critical
Between Groups	13928.57	1	13928.57	376.9675	5.52E-11	4.667193
Within Groups	480.3371	13	36.94901			
Total	14408.91	14				

ANOVA - Single Factor-Cu- Leaves-Surface water-BSC 06						
Alpha	0.05					
Groups	Count	Sum	Mean	Variance		
Surface water	6	373.2705	62.21175	96.0672		
BSC 06	9	0.11568	0.012853	1.58E-05		
Source of Variation	SS	df	MS	F	P-value	F critical
Between Groups	13927.33	1	13927.33	376.9346	5.52E-11	4.667193
Within Groups	480.3361	13	36.94893			
Total	14407.67	14				

ANOVA - Single Factor-Zn- Roots-Surface water-BSC 01						
Alpha	0.05					
Groups	Count	Sum	Mean	Variance		
Surface water	6	2136.796	356.1327	57445.77		
BSC 01	9	0.582259	0.064695	0.004265		
Source of Variation	SS	df	MS	F	P-value	F critical
Between Groups	456423.9	1	456423.9	20.65778	0.00055	4.667193
Within Groups	287228.9	13	22094.53			
Total	743652.8	14				

ANOVA - Single Factor-Zn- Roots-Surface water-BSC 06						
Alpha	0.05					
Groups	Count	Sum	Mean	Variance		
Surface water	6	2136.796	356.1327	57445.77		
BSC 06	9	0.42721	0.047468	7.14E-05		
Source of Variation	SS	df	MS	F	P-value	F critical
Between Groups	456468	1	456468	20.65978	0.00055	4.667193
Within Groups	287228.8	13	22094.53			
Total	743696.9	14				

ANOVA - Single Factor-Zn- Bark-Surface water-BSC 01						
Alpha	0.05					
Groups	Count	Sum	Mean	Variance		
Surface water	6	2774.73	462.4551	856115.7		
BSC 01	9	0.322807	0.035867	0.001311		
Source of Variation	SS	df	MS	F	P-value	F critical
Between Groups	769793.5	1	769793.5	2.337842	0.150226	4.667193
Within Groups	4280579	13	329275.3			
Total	5050372	14				

ANOVA - Single Factor-Zn- Bark-Surface water-BSC 06						
Alpha	0.05					
Groups	Count	Sum	Mean	Variance		
Surface water	6	2774.73	462.4551	856115.7		
BSC 06	9	0.040587	0.00451	1.94E-06		
Source of Variation	SS	df	MS	F	P-value	F critical
Between Groups	769897.9	1	769897.9	2.338159	0.1502	4.667193
Within Groups	4280579	13	329275.3			
Total	5050477	14				

ANOVA - Single Factor-Zn- Leaves-Surface water-BSC 01						
Alpha	0.05					
Groups	Count	Sum	Mean	Variance		
Surface water	6	1469.471	244.9118	1359.628		
BSC 01	9	0.48282	0.053647	0.002933		
Source of Variation	SS	df	MS	F	P-value	F critical
Between Groups	215839.8	1	215839.8	412.7465	3.12E-11	4.667193
Within Groups	6798.161	13	522.9355			
Total	222637.9	14				

ANOVA - Single Factor-Zn- Leaves-Surface water-BSC 06						
Alpha	0.05					
Groups	Count	Sum	Mean	Variance		
Surface water	6	1469.471	244.9118	1359.628		
BSC 06	9	0.434849	0.048317	7.39E-05		
Source of Variation	SS	df	MS	F	P-value	F critical
Between Groups	215849.2	1	215849.2	412.7658	3.12E-11	4.667193
Within Groups	6798.138	13	522.9337			
Total	222647.3	14				

ANOVA - Single Factor-Pb- Roots-Surface water-BSC 01						
Alpha	0.05					
Groups	Count	Sum	Mean	Variance		
Surface water	6	1190.515	198.4192	13121.58		
BSC 01	9	1.191962	0.13244	0.003333		
Source of Variation	SS	df	MS	F	P-value	F critical
Between Groups	141543.4	1	141543.4	28.04638	0.000145	4.667193
Within Groups	65607.93	13	5046.764			
Total	207151.4	14				

ANOVA - Single Factor-Pb- Roots-Surface water-BSC 06						
Alpha	0.05					
Groups	Count	Sum	Mean	Variance		
Surface water	6	1190.515	198.4192	13121.58		
BSC 06	9	0.890661	0.098962	0.000223		
Source of Variation	SS	df	MS	F	P-value	F critical
Between Groups	141591.2	1	141591.2	28.05586	0.000145	4.667193
Within Groups	65607.9	13	5046.762			
Total	207199.2	14				

ANOVA - Single Factor-Pb- Bark-Surface water-BSC 01						
Alpha	0.05					
Groups	Count	Sum	Mean	Variance		
Surface water	6	611.9788	101.9965	9576.116		
BSC 01	9	0.339213	0.03769	3.23E-05		
Source of Variation	SS	df	MS	F	P-value	F critical
Between Groups	37424.13	1	37424.13	10.16098	0.007136	4.667193
Within Groups	47880.58	13	3683.121			
Total	85304.71	14				

ANOVA - Single Factor-Pb- Bark-Surface water-BSC 06						
Alpha	0.05					
Groups	Count	Sum	Mean	Variance		
Surface water	6	611.9788	101.9965	9576.116		
BSC 06	9	0.339213	0.03769	3.23E-05		
Source of Variation	SS	df	MS	F	P-value	F critical
Between Groups	37424.13	1	37424.13	10.16098	0.007136	4.667193
Within Groups	47880.58	13	3683.121			
Total	85304.71	14				

ANOVA - Single Factor-Pb- Leaves-Surface water-BSC 01						
Alpha	0.05					
Groups	Count	Sum	Mean	Variance		
Surface water	6	493.2525	82.20875	329.0232		
BSC 01	9	0.660157	0.073351	0.001022		
Source of Variation	SS	df	MS	F	P-value	F critical
Between Groups	24286.4	1	24286.4	191.9146	3.67E-09	4.667193
Within Groups	1645.124	13	126.548			
Total	25931.53	14				

ANOVA - Single Factor-Pb- Leaves-Surface water-BSC 06						
Alpha	0.05					
Groups	Count	Sum	Mean	Variance		
Surface water	6	493.2525	82.20875	329.0232		
BSC 06	9	0.384836	0.04276	4.16E-05		
Source of Variation	SS	df	MS	F	P-value	F critical
Between Groups	24304.5	1	24304.5	192.0585	3.65E-09	4.667193
Within Groups	1645.116	13	126.5474			
Total	25949.61	14				